Journal of
Geophysical Research

UME 66 AUGUST 1961 NUMBER 8

PUBLISHED BY

THE AMERICAN GEOPHYSICAL UNION

Journal of Geophysical Research

An International Scientific Publication

OFFICERS OF THE UNION

THOMAS F. MALONE, *President*
GEORGE P. WOOLLARD, *Vice President*
A. NELSON SAYRE, *General Secretary*
WALDO E. SMITH, *Executive Secretary*

OFFICERS OF THE SECTIONS

Geodesy
FLOYD W. HOUGH, *President*
CHARLES A. WHITTEN, *Vice President*
BUFORD K. MEADE, *Secretary*

Seismology
JAMES A. PEOPLES, JR., *President*
JACK E. OLIVER, *Vice President*
BENJAMIN F. HOWELL, JR., *Secretary*

Meteorology
MORRIS NEIBURGER, *President*
HENRY G. HOUGHTON, *Vice President*
WOODROW C. JACOBS, *Secretary*

Geomagnetism and Aeronomy
C. T. ELVEY, *President*
E. H. VESTINE, *Vice President*
J. HUGH NELSON, *Secretary*

Oceanography
DONALD W. PRITCHARD, *President*
ROBERT S. ARTHUR, *Vice President*
ARTHUR E. MAXWELL, *Secretary*

Volcanology, Geochemistry, and Petrology
HATTEN S. YODER, JR., *President*
EDWARD D. GOLDBERG, *Vice President*
DAVID R. WONES, *Secretary*

Hydrology
WILLIAM C. ACKERMANN, *President*
DAVID K. TODD, *Vice President*
RALPH N. WILSON, *Secretary*

Tectonophysics
LOUIS B. SLICHTER, *President*
DAVID T. GRIGGS, *Vice President*
IRIS BORG, *Secretary*

BOARD OF EDITORS

Editors: PHILIP H. ABELSON and J. A. PEOPLES, JR.

ASSOCIATE EDITORS

1959–1961

HENRI BADER
K. E. BULLEN
CONRAD P. MOOK
WALTER H. MUNK
T. NAGATA
FRANK PRESS
A. NELSON SAYRE
MERLE A. TUVE
JAMES A. VAN ALLEN

1960–1962

JULIUS BARTELS
V. V. BELOUSSOV
E. G. BOWEN
JOHN E. CHAPPELEAR
G. D. GARLAND
GORDON J. F. MACDONALD
L. A. MANNING
TOR J. NORDENSON
E. N. PARKER
GEORGE P. RIGSBY
WALTER O. ROBERTS
C. N. TOUART
JAMES R. WAIT

1961–1963

FRANKLIN I. BADGLEY
HENRY G. BOOKER
JOSEPH W. CHAMBERLAIN
HERBERT FRIEDMAN
MARK F. MEIER
ROBERT O. REID
BRUNO ROSSI
GEORGE H. SUTTON
DAVID K. TODD
VICTOR VACQUIER
ARTHUR H. WAYNICK

The Editors of the *Journal of Geophysical Reseac* welcome original scientific contributions on the phy of the earth and its environment.

Manuscripts should be submitted in triplicate J. A. Peoples, Jr., Department of Geology, Univers of Kansas, Lawrence, Kansas. Authors' institutio if in the United States or Canada, are requested pay a publication charge of $25 per page, which honored, entitles them to 100 free reprints.

Subscriptions to the *Journal of Geophysical search* and *Transactions, AGU*, are included in me bership dues.

Nonmember subscriptions, *Journal of Geophys Research*..$30 for back volume of 1959, $42 back volume of 1960, $4 for this issue; $20 the calendar year 1961.

Nonmember subscriptions, *Transactions, AGU*..$4 per calendar year, $1.25 per co

Subscriptions, renewals, and orders for back numb should be addressed to American Geophysical Uni 1515 Massachusetts Ave., Northwest, Washingto D. C. Suggestions to authors are available on requ

Advertising Representative: Howland and Howla Inc., 230 Park Ave., New York 17, N. Y.

Since January 1959 (Vol. 64, No. 1) the *Journal of Geophysical Research* has been publis monthly by the American Geophysical Union, the U. S. National Committee of the International Un of Geodesy and Geophysics organized under the National Academy of Sciences-National Research Cou as the U. S. national adhering body. Publication of this journal is supported by the National Science Fo dation and the Carnegie Institution of Washington. The new monthly combines the type of scien material formerly published in the bi-monthly *Transactions, American Geophysical Union*, and the quart *Journal of Geophysical Research*. The *Transactions, American Geophysical Union* will continue as a quart publication for Union business and items of interest to members of the Union.

Published monthly by the American Geophysical Union from 1407 Sherwood Avenue, Richmond, Virgi Second class postage paid at Richmond, Virginia.

Physicists

The Hughes Research Laboratories offer an outstanding professional environment to Scientists with an interest in basic and applied research. At these exceptional facilities you can realize maximum professional growth through programs including:

SOLID STATE PHYSICS RESEARCH
Microwave and millimeter wave magnetic resonance
Optical and infrared spectroscopy
Solid state masers
Semiconductor physics

MATERIALS RESEARCH
Crystal growing
Crystal growth mechanisms
Crystal perfection

SURFACE PHYSICS
Low work function surfaces
Thermionic electron emission
Thermionic ion emission

MATERIALS STUDIES
Molecular design
Chemical synthesis

PLASMA PHYSICS
Thermionic energy conversion
Microwave plasma devices

ION PROPULSION

The facilities of the Hughes Research Laboratories are located in Malibu, California, overlooking the Pacific Ocean—immediately adjacent to major academic institutions—with programs of academic support and participation. These facilities were specifically designed for effective research efforts with private offices and complete research laboratories. In this uniquely creative atmosphere, Hughes scientists are continually adding to their record of accomplishments in electronics and physics research.

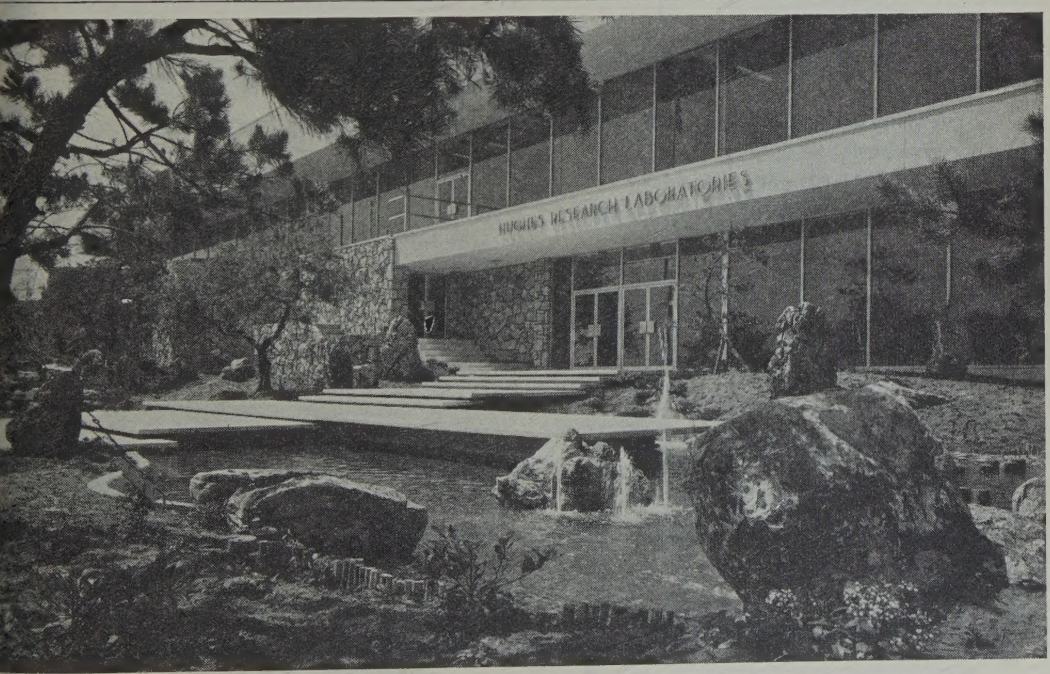
Your inquiry may be directed in strict confidence to: Mr. D. A. Bowdoin, Hughes Research Laboratories, Malibu, California.

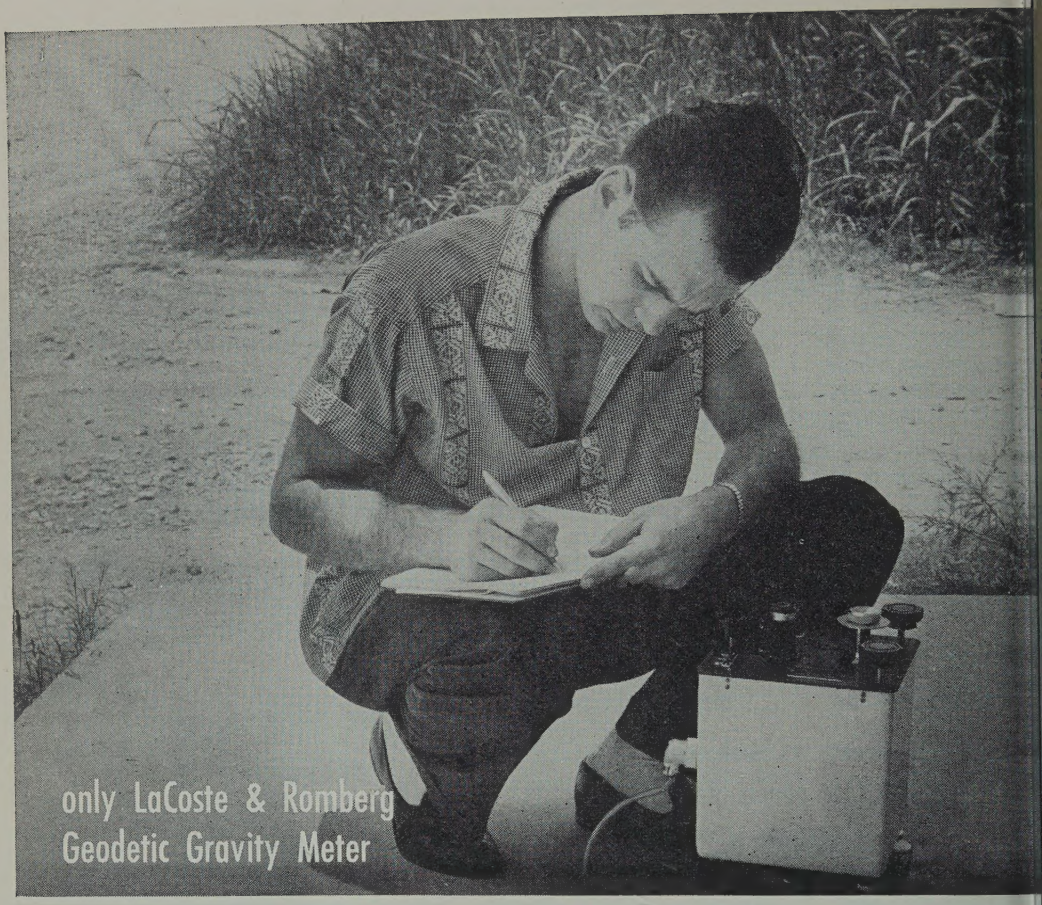
All qualified applicants will receive consideration for employment without regard to race, creed, color or national origin.

creating a new world with electronics

HUGHES

HUGHES AIRCRAFT COMPANY
RESEARCH LABORATORIES





gives you **thermal controlled accuracy in a 7-pound meter**

- world survey without resetting
- never requires recalibrating
- less than 0.5 mgl drift per month
- no "sets" or "tares" under normal operation

This new miniaturized Geodetic Gravity Meter retains all the accuracy and dependability of the standard model introduced by LaCoste & Romberg in 1956, yet it weighs only 7 pounds. (Complete with battery and luggage-type carrying case, it weighs less than 17 pounds). With a world-wide range of over 6,000 mgl., this instrument has a repeatability of 0.01 mgl. Actual field tests over the complete gravity range have shown an accuracy better than 0.04 mgl.

Exceptionally high sensitivity of the LaCoste & Romberg meter is attained by a zero length spring suspension (U. S. Patent No. 2,293,437). Calibration is stabilized by means of patented lever systems that act on the main spring rather than on weak measuring springs. And by thermostating, drift is normally reduced to less than 0.5 milligal per month.

Rugged and dependable, the LaCoste & Romberg Geodetic Meter requires practically no maintenance in the field. Its gravity responsive system is completely suspended by springs and will therefore withstand any shock that will not damage the housing supporting it. It is specifically designed to provide a lightweight meter with higher accuracy and lower drift than can be attained in any other geodetic gravity meter. For complete information, write for *Miniature Geodetic Gravity Meter Bulletin.*



LaCoste & Romberg | 6606 NORTH LAMAR | AUSTIN, TEX



IONOSPHERIC PROPAGATION AND HF COMMUNICATIONS

If you have the background, the imagination and the desire to contribute to important programs in these fields, you are invited to join a carefully selected team of outstanding scientists and engineers now contributing significantly to current knowledge through advanced research.

Our present needs are for:

SENIOR IONOSPHERIC PHYSICISTS

Ph.D. preferred, with several years' experience in the study of Ionospheric phenomena. Should be familiar with present knowledge of upper atmosphere physics and possess an understanding of current programs using rockets and satellites for studies in F-region and beyond. Qualified individuals with supervisory abilities will have an exceptional opportunity to assume project leadership duties on HF projects already under way involving F-layer propagation studies backed by a substantial experimental program.

SENIOR DEVELOPMENT PHYSICISTS

Advanced degree in Physics or E. E. preferred. Must be familiar with latest techniques in the design of advanced HF receivers and transmitters and possess working knowledge of modern HF networks employing ferrites and metallic tape cores. Strong theoretical background in modern linear circuit theory desired. Will carry out laboratory development and implementation of new HF communications systems.

SENIOR ELECTRONIC ENGINEERS

Advanced degree in E.E. preferred. Must be familiar with conventional pulse circuit designs and applications. Technical background should include substantial experience in data process and data recovery systems using both analog and digital techniques. Knowledge of principles and application of modern information theory including correlation techniques helpful. Will be responsible for the design of sub-systems.

These programs are being conducted at our ELECTRO-PHYSICS LABORATORIES in the suburban Washington, D.C. area, ideally located from the viewpoint of advanced study which may be conducted at one of several nearby universities; for readily available housing in pleasant residential neighborhoods; and for the general amenities of living offered by this important Metropolitan center.

All qualified applicants will receive consideration for employment without regard to race, creed, color or national origin.

For a prompt reply to your inquiry, please forward resume in confidence to:

W. T. WHELAN
Director of Research & Development

ACF ELECTRONICS
DIVISION

ACF INDUSTRIES

HYATTSVILLE, MARYLAND

Journal of Geophysical Research

BACK ISSUES AVAILABLE

Volume 64, 1959 Total 2488 pages		Volume 65, 1960 Total 4248 pages	
Complete Volume	$30.00	Complete Volume	$42.00
January, 132 pp.	$2.00	January, 384 pp.	$5.00
February, 138 pp.	$2.00	February, 414 pp.	$5.00
March, 112 pp.	$2.00	March, 284 pp.	$4.00
April, 106 pp.	$2.00	April, 248 pp.	$4.00
May, 98 pp.	$2.00	May, 314 pp.	$4.00
June, 110 pp.	$2.00	June, 220 pp.	$4.00
July, 168 pp.	$2.00	July, 348 pp.	$4.00
August, 268 pp.	$4.00	August, 350 pp.	$4.00
September, 230 pp.	$3.00	September, 462 pp.	$6.00
October, 284 pp.	$4.00	October, 490 pp.	$6.00
November, 390 pp.	$5.00	November, 344 pp.	$4.00
December, 452 pp.	$6.00	December, 390 pp.	$5.00

SYMPOSIA REPRINTED from JGR

International Symposium on Electronic Distance-Measuring Techniques (144-page Symposium reprinted from the February 1960 issue) $3.50

Symposium on Sferics and Thunderstorm Electricity (102-page Symposium reprinted from the July 1960 issue) $3.50

Symposium on the Exosphere and Upper *F* Region (74-page Symposium reprinted from the September 1960 issue) $2.50

Scientific Effects of Artificially Introduced Radiations at High Altitudes (74-page Symposium reprinted from the August 1959 issue) $1.50

International Symposium on Fluid Mechanics in the Ionosphere (202-page Symposium reprinted from the December 1959 issue) $4.50

AMERICAN GEOPHYSICAL UNION

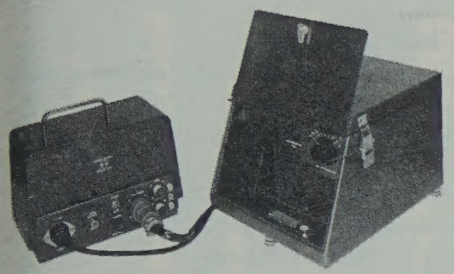
1515 Massachusetts Avenue, N.W., Washington 5, D. C.

To obtain back issues for 1958 and earlier years, write to Walter J. Johnson, Inc., 111 Fifth Avenue, New York 3, New York.

GEOTECH

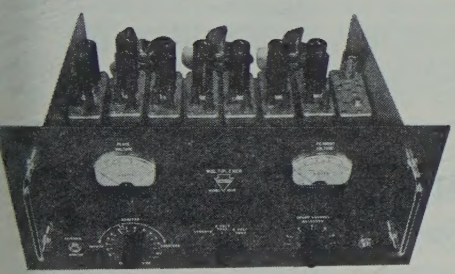
PRECISION INSTRUMENTS for SEISMOLOGY—GEOPHYSICS

ULTRA-LOW LEVEL AMPLIFIERS



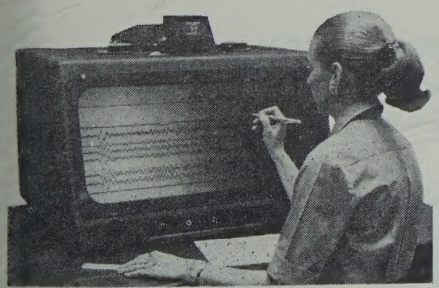
Ultra-low level signals of low frequency can be amplified faithfully with these galvanometer-phototube amplifiers. They are designed for trouble-free, long-term use. They are sealed, and contain a band-pass filter for effective reduction of DC drift. Model 4300 shown at left amplifies .01 to 5 cps data with an output noise level down to 5 mv p-p and a voltage gain up to ¼-million. Model 5240 amplifies .001 to .04 cps data with an output noise level down to 5 mv p-p and a gain up to 1-million. Dynamic range is at least 65 db. Power consumption is less than 7 watts. These amplifiers have seen extensive field service.

DATA TRANSMISSION — TELEMETRY EQUIPMENT



This is economical transmitting and receiving terminal equipment for telemetering one or more channels of analog data over a single radio or telephone circuit, coast to coast if necessary. These circuits are often leased. Only as many components need be obtained as there are channels required, up to a maximum of 7 channels. The multiplexer shown at left contains 1 to 7 Geotech FM subcarrier oscillators. It accepts the analog voltage outputs of 1 to 7 transducers and amplifiers, converts the data to FM, and "transmits" a composite signal over the voice-frequency circuit. At the receiving end, one Geotech subcarrier discriminator per channel is required to demodulate and amplify the data for analog recording. A transmission accuracy of ±1% is often obtained. The first equipment delivered has now operated 24 hours a day for several years.

WIDE-SCREEN FILM VIEWER



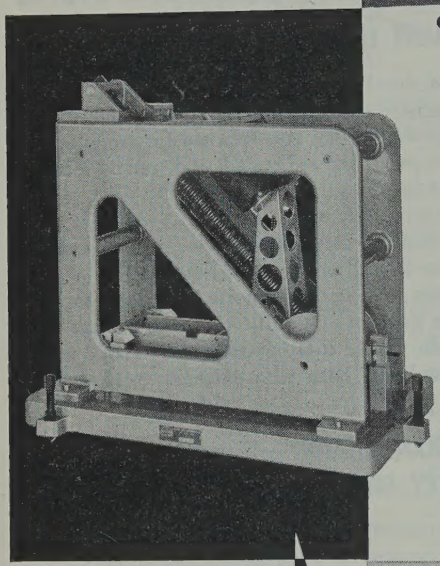
This 16 mm film viewer features a motorized film drive, a remote operator control, and data magnified 20 times on a 27.5" x 11.5" viewscreen. Data of interest can be located quickly by using a push-button to traverse the film in either direction at 120 cm/sec. Data can be studied in detail by varying the film speed from 1.3 to 0 cm/sec. The remote control permits operation up to 10 feet from the viewer. The case is cast aluminum. Distortion is not more than ±1%.

For detailed specifications, price, or delivery, write to:

THE GEOTECHNICAL CORP.

1 SHILOH ROAD **GARLAND, TEXAS**

SPRENGNETHER LONG PERIOD VERTICAL SEISMOMETER



GENERAL SPECIFICATIONS:

- Period Range: 6 to 70 seconds.
- Magnification: Up to 15,000, depending on operating period.
- Damping: Electromagnetic.
- Transducer-moving coils in circular magnetic gaps.
- Boom centering adjustment visible through sealed windows to facilitate adjustment.
- Coils approximately 500 ohms. or to your specifications.
- Pendulum steady mass weight 22 lbs.
- Invar spring for thermal stability.
- Airtight metal cover is provided to prevent recording of microbarometric oscillations.

PHYSICAL SPECIFICATIONS:

Length.....26″ Width.....14″ Height.....
Net Weight.....120 lbs. Shipping Weight.....175

To compliment this instrument, a long period horizontal seismometer is also available.

WRITE FOR DETAILED INFORMATION ON THESE INSTRUMENTS.

Internationally Known Mfrs. of Seismological, Geophysical Instruments.

W. F. SPRENGNETHER INSTRUMENT CO., INC.

4567 SWAN AVENUE • ST. LOUIS 10, MO.

GEODESY AND CARTOGRAPHY, 1959 and 1960

(Geodezia i Kartografiya)

The leading monthly journal of Geodesy and Cartography in the USSR is being translated and published in an English edition, *for the years 1959 and 1960,* by the American Geophysical Union, aided by a grant from the National Science Foundation.

Subscription price, $20.00 for each volume of 12 numbers

Send subscription requests to

AMERICAN GEOPHYSICAL UNION

1515 Massachusetts Avenue, N.W.

Washington 5, D. C., U.S.A.

Other publications of the AGU include

—JOURNAL OF GEOPHYSICAL RESEARCH (monthly), 4800 pages anticipated for 1961, subscription $20.00

—TRANSACTIONS (quarterly), $4.00 per calendar year

—GEOPHYSICAL MONOGRAPH SERIES (occasional volumes), No. 5 (issued in 1960) *Physics of Precipitation* (proceedings of the Cloud Physics Conference, Woods Hole, Massachusetts, June 3-5, 1959), 435 pp., $12.50

—IZVESTIYA, Academy of Sciences, USSR, Geophysics series, English edition (monthly), $25.00 per calendar year, available for 1957, 1958, 1959, 1960, and 1961.

BREADTH

A new facility, a new scientific community, and new and ambitious scientific goals—this is the Sperry Rand Research Center. Here academic curiosity, scientific objectivity and true interdisciplinary exchange will combine to fill broad and varied basic research needs of the many divisions of Sperry Rand Corporation in the following areas: Materials Sciences including solids, mechanics, magnetics, and physical chemistry; Radiation Sciences including microwave physics, plasmas, infrared, optics, energy conversion, and communications; Applied Mathematics and Theoretical Physics; Earth and Life Sciences.

Our immediate needs for top scientific talent are in the areas of:

- Seismology
- Oceanography
- Geomagnetism
- Atmospheric Physics

If you are interested in fundamental research in any of the above fields, direct your communication in confidence to: Frederick M. Swope, Jr., Sperry Rand Research Center, North Road, Sudbury, Massachusetts

an important word at the new

SPERRY RAND RESEARCH CENTER

SUDBURY, MASSACHUSETTS

Space Physics at

AEROSPACE CORPORATION

The scientists and engineers of Aerospace Corporation are the critical civilian link uniting government and the scientific-industrial team developing space systems and advanced ballistic missiles. These men, highly skilled in at least one discipline, are also knowledgeable in inter-disciplinary problem solving.

In space physics their specific activities include extensive studies of particle measurement in auroral zones; space plasma physics; solar physics and solar-terrestrial interactions; Van Allen belts and solar flares; magnetic and electric field measurements; analysis of planetary atmospheres, surfaces and magnetic fields; micrometeorite investigations; space probe instrumentation; and space data processing and evaluation.

These studies, conducted in close association with Air Force space and missile experimental flight programs, are enhanced by the stimulating environment made possible by Aerospace Corporation's stable funding.

Today more men of superior ability and advanced education are needed to meet Aerospace Corporation's growing responsibilities in the area of space physics. Immediate assignments exist for qualified physicists interested in theoretical and experimental investigations of the space environment.

Such men are urged to contact Mr. George Herndon (OSborne 9-4661, Extension 1171), Aerospace Corporation, Room 193, P.O. Box 95081, Los Angeles 45, Calif. All qualified applicants will receive consideration for employment without regard to race, creed, color or national origin.



AEROSPACE CORPORATION

Organized in the public interest and dedicated to providing objective leadership in the advancement and application of space science and technology for the United States Government.

Journal of
GEOPHYSICAL RESEARCH

OLUME 66 AUGUST 1961 No. 8

Intensity Variations in Outer Van Allen Radiation Belt

S. E. FORBUSH,[1] D. VENKATESAN, AND C. E. MCILWAIN

Department of Physics and Astronomy, State University of Iowa Iowa City, Iowa

Abstract. Using data from Explorer VII, the changes in the intensity of the outer Van Allen radiation belt were investigated in detail over the period October 26, 1959 to December 9, 1959. To relate the intensities to location in the belt, the parameter L was used. L is defined as a function of the integral invariant I and scalar magnetic field B, such that everywhere on the shell described by the motion of a trapped particle in the earth's magnetic field, L closely approximates the equatorial radius of the shell. For the period under study, the intensity variations at selected values of L were negatively correlated with geomagnetic activity. However, an analysis of data over a much longer period is required to determine whether this correlation is statistically significant.

For the period studied, the decrease in measured intensity during periods of magnetic storms (large a_p) is consistent with the idea that some of the particles are 'dumped' into the auroral and subauroral zones where they may partly contribute to the auroral zone currents that account for a_p. In addition, the reduction in intensity generally occurred in the outer part of the zone. The low values of intensity, for $L = 3.5$, 4.1, and 4.7, occurred in the interval November 22 to December 9, at times when the equatorial ring current field, U (southward on the earth at the equator), was large. Thus, U cannot be due to the westward current due to the longitudinal drift of measured trapped particles in the region for which L is greater than 3.5, since a decrease in particle density therein would diminish the westward drift current with a consequent decrease in U, which is opposite to what is observed. This result indicates that the site of the ring current is either elsewhere, or that the principal contribution to it comes from drifting particles having energies below the detection thresholds of Explorer VII equipment. The phenomena were investigated over a longer period, using daily averages of the maximum counting rates. This procedure had serious limitations.

ntroduction. A study of the temporal fluctions of the intensity of the outer Van Allen iation belt and its association with magnetic ms is of importance [*Rothwell and McIlwain,* 0; *Arnoldy, Hoffman and Winckler,* 1960; *Allen and Lin,* 1960]. The present study s data from Explorer VII and covers in de- the period from October 26 to December 9, 9.

ounting rates are available as a function of e since October 1959 from passes of Explorer VII through the outer Van Allen radiation belt. The equipment was prepared by the Department of Physics and Astronomy of the State University of Iowa. The details of the equipment and the characteristics of the counters have been described earlier [*Ludwig and Whelpley,* 1960]. The approximate detection thresholds for the 112 Geiger counter are 30 Mev for protons, 2.5 Mev for electrons, and 80 kev for X rays (5 per cent transmission), and for the 302 Geiger counter the corresponding values are respectively 18 Mev, 1.1 Mev, and 30 kev. The counting-rate data for the 302 and 112 counters, corrected for dead time, are available for each pass as a func-

[1] Visiting Professor from the Department of Terrial Magnetism, Carnegie Institution, Washing- D. C.

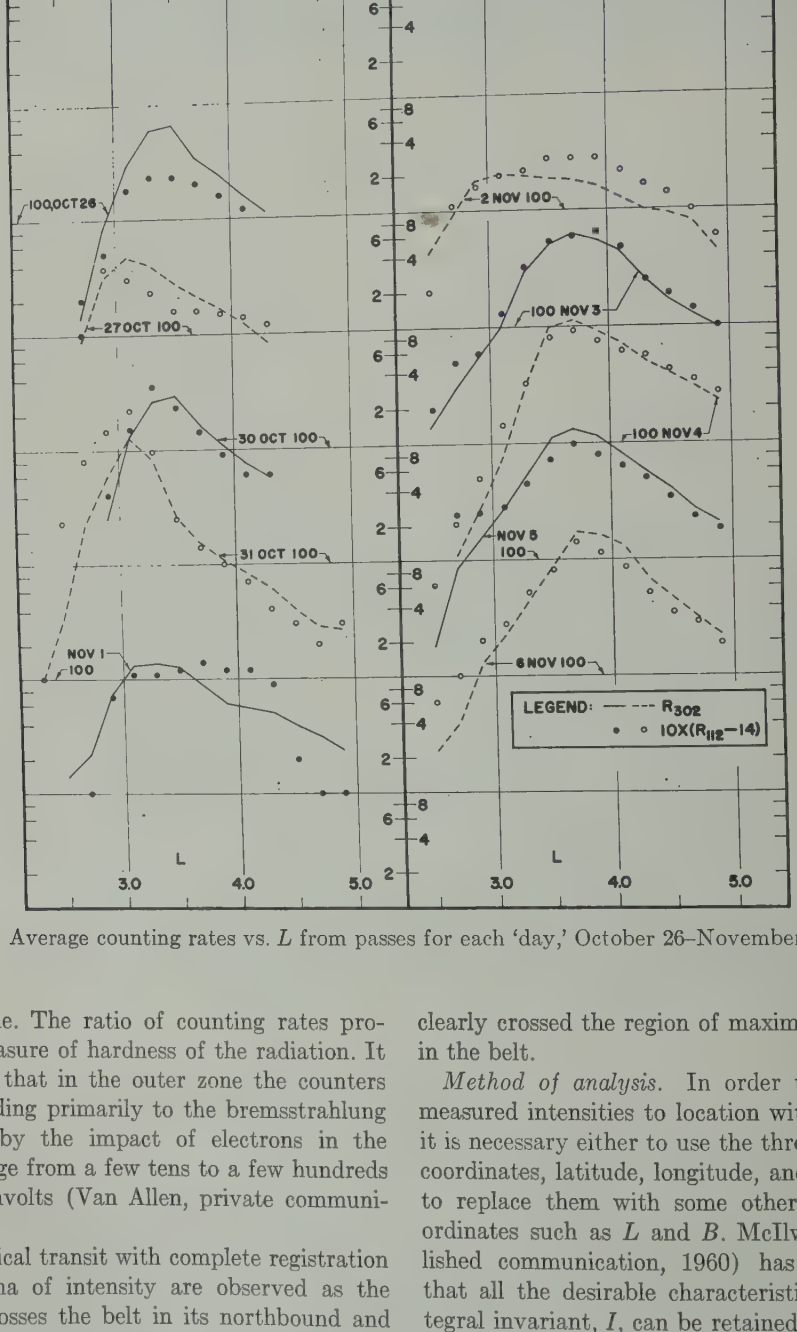


Fig. 1. Average counting rates vs. L from passes for each 'day,' October 26–November 6, 1959.

tion of time. The ratio of counting rates provides a measure of hardness of the radiation. It is believed that in the outer zone the counters are responding primarily to the bremsstrahlung generated by the impact of electrons in the energy range from a few tens to a few hundreds kiloelectronvolts (Van Allen, private communication).

In a typical transit with complete registration two maxima of intensity are observed as the satellite crosses the belt in its northbound and southbound passes. All the data used in the analysis were principally recorded by receivers at SUI, Iowa City, Iowa, and Blossom Point, Maryland, with occasional additional recordings from San Diego, California, and Ottawa, Canada. Data were used only for those passes that clearly crossed the region of maximum inten in the belt.

Method of analysis. In order to relate measured intensities to location within the it is necessary either to use the three geogra coordinates, latitude, longitude, and altitud to replace them with some other suitable ordinates such as L and B. McIlwain (unp lished communication, 1960) has pointed that all the desirable characteristics of the tegral invariant, I, can be retained by a par eter L which is nearly constant along a lin force in the earth's magnetic field. L is def as a function of the integral invariant I [*Ne rup and Teller*, 1960; *Vestine and Sibley*, 1 and scalar magnetic field B, such that everyw on the shell described by the motion of a tra

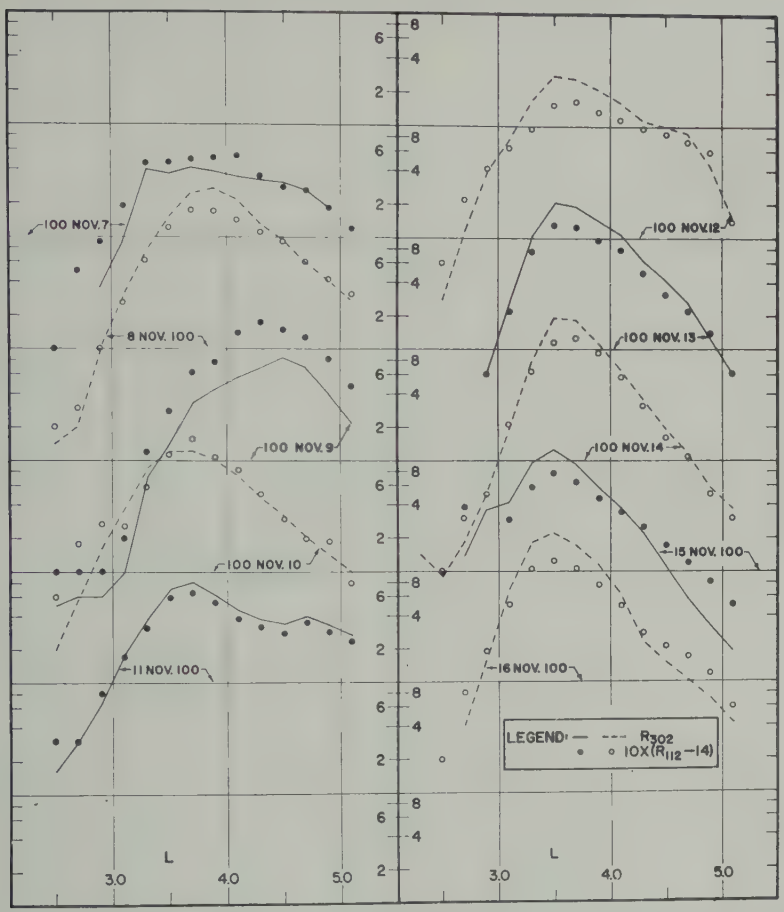


Fig. 2. Average counting rates vs. L from passes for each 'day,' November 7–16, 1959.

harged particle in the earth's magnetic field, L osely approximates the equatorial radius of the ield. The computation of L was supervised by IcIlwain; L is derived on the basis that the arth's field for epoch 1955 is represented by the x spherical harmonics obtained by *Finch and caton* [1957]. Because of the strong intensity ariations with time, it has not as yet been posble to determine the dependence of intensity pon B. As a result, it has been necessary to igore this important effect.

For a constant L, the intensity should depend ily on B, which in turn will depend on the altiude and longtitude at which the satellite crosses ie zone. In addition there may be absorption ffects resulting in additional intensity variations ith altitude. The motion of the satellite is such hat the altitude, B, and the longitude for the ame L, all vary systematically rather than randomly and independently. As a consequence, to determine the effect of each of these parameters upon the intensity, a much longer sequence of observations is required than would be the case if the consecutive values of these variables were both random and independent. These effects, together with relatively large and rapid time variations of intensity associated with magnetic disturbances, indicate that a systematic analysis of data over a long period of time is required to reveal quantitatively the effects of the individual parameter with a reasonable degree of certainty.

In general, all passes for which the data were received by the tracking stations listed above occurred within successive intervals of about 10 hours or less, which were interspersed with intervals of 14 hours or so, when no data could be recorded. The intensities for the same values of L were averaged for the passes in the 10-hour

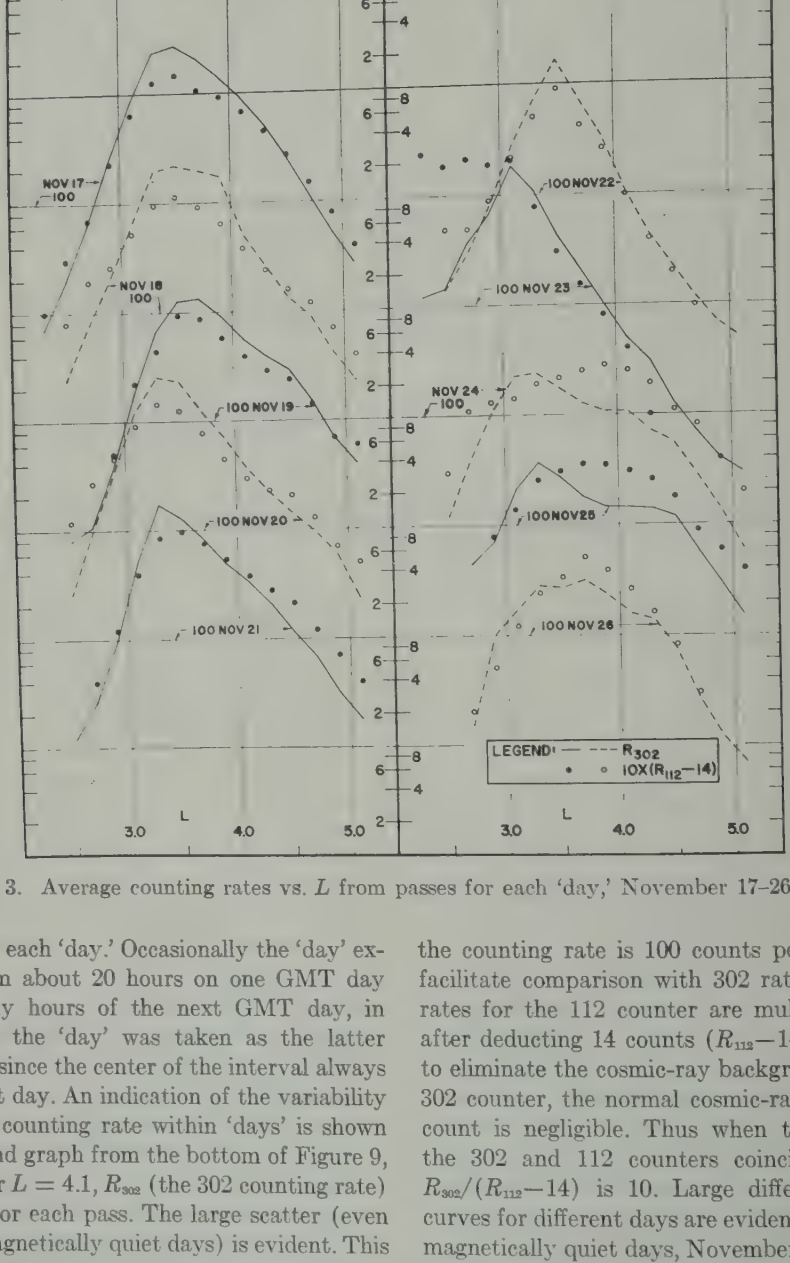


Fig. 3. Average counting rates vs. L from passes for each 'day,' November 17–26, 1959.

interval for each 'day.' Occasionally the 'day' extended from about 20 hours on one GMT day to the early hours of the next GMT day, in which case the 'day' was taken as the latter GMT day, since the center of the interval always was on that day. An indication of the variability of the 302 counting rate within 'days' is shown in the second graph from the bottom of Figure 9, in which for $L = 4.1$, R_{302} (the 302 counting rate) is plotted for each pass. The large scatter (even on some magnetically quiet days) is evident. This scatter is more or less typically similar to that at other values of L.

Average intensity for each 'day' as function of L. Figures 1 to 5 show for each 'day' the average intensity as a function of L. The counting-rate scale is logarithmic. The curve for each day is indicated together with the horizontal line that shows where, on the curve for that day, the counting rate is 100 counts per second. T facilitate comparison with 302 rates (R_{302}), t rates for the 112 counter are multiplied by after deducting 14 counts ($R_{112}-14$) per seco to eliminate the cosmic-ray background. For t 302 counter, the normal cosmic-ray backgrou count is negligible. Thus when the points the 302 and 112 counters coincide, the ra $R_{302}/(R_{112}-14)$ is 10. Large differences in t curves for different days are evident. Even on t magnetically quiet days, November 9, 11, and 1959, there were considerable differences in t curves for the individual passes.

Figures 6 and 7 show the counting rates individual passes as a function of L for Nove ber 23 and 28, 1959, which were days of la magnetic disturbance. Shown also for comp son are the average curves for each day prec ing and following those dates. Within each

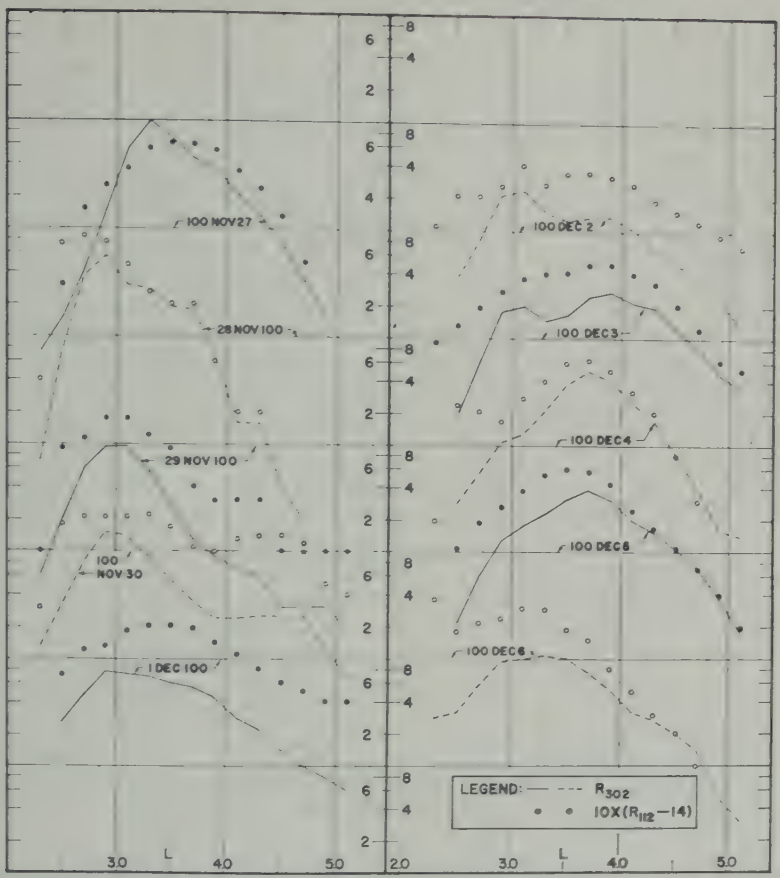


Fig. 4. Average counting rates vs. L from passes for each 'day,' November 27–December 6, 1959.

se 4 days the curves for the individual passes re quite similar. The curves for 3.6 hours UT l 3.8 hours UT on November 28, 1959, corre- nd to those in the center part of Figure 1, cussed by *O'Brien, Van Allen, Roach, and rtlein* [1960], who showed that low-latitude ora occurred at a location that corresponds the L for the maximum rate near these times. e curves on November 28 at 3.6 and 3.8 hours show that for $L > 3.6$ the counting rates are ntially zero, although the maximum counting es for these two passes are at least as high on November 27, before the start of the rm. Incidentally, the curve in Figure 7 for 1.9 rs UT on November 28, 1959, was obtained ing the initial phase of the storm. (The sud- commencement was at 2351 UT, November) This curve is not very different (except per- s for $L > 4.4$) from the average curve for vember 27; the curve for 3.6 hours UT, November 28, 1959, however, is markedly different. It should be noted that the value of 8o for K_p (corresponding to $a_p = 414$ gammas) for the interval 3 to 6 hours UT was one of the two highest for any 3-hour interval during the entire period October 26 to December 9, 1959. The other case was 18 to 21 hours UT, December 5, 1959, for which K_p was 8- (corresponding to $a_p = 358$ gammas). The values for U for the two corresponding cases were respectively 149 and 194 gammas.

The curves for the individual passes on November 23 differ less from the average for the previous day than do those for November 28. On November 23 the maximum value of K_p for any 3-hour interval in which one or more passes occurred was 6- ($a_p = 134$); also, it may be noted that the beginning of the storm of November 28 was marked by a sudden commencement, whereas that of November 23 was not.

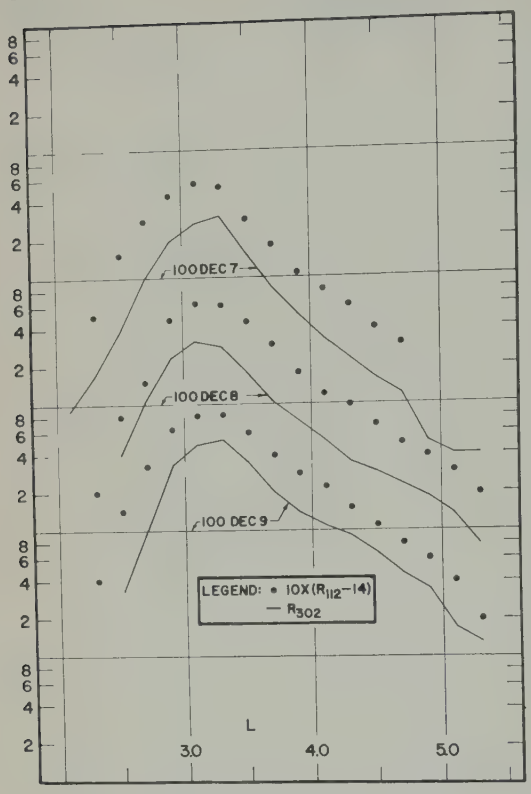


Fig. 5. Average counting rates vs. L during December 7–9, 1959.

Which, if any, of these factors was connected with the difference in the counting-rate curves for November 23 and 28 is uncertain.

The magnetic storm on December 5, 1959, with a 3-hour value for U and K_p as high as 194 gammas and 8- (corresponding $a_p = 358$ gammas), and with sudden commencement at 0659 UT, was preceded closely by two other moderate storms on November 30 and December 3 wi 3-hour values of K_p of 6o. This complicates t study of storm of December 5. The individu passes on that day, which occur just before t sudden commencement, are similar to the curv on December 4. Unfortunately, the next ava able pass is 16 hours after sudden commen ment. However, this pass reveals a reduction intensity, especially for $L > 3.4$, which is o served in the early hours of the next day also recovery to higher intensities is observed sta ing from the pass at ~ 2230 UT on December

Another storm in the beginning of the peri —namely, October 29—with sudden commen ment at 2347 UT initiates a disturbance lasti up to November 4, with the peak disturban being around November 1-2. It can definit be stated that the intensity on these 2 days w the lowest, and that recovery was observed fr November 3.

Further analysis of data over long periods essential before one can answer whether t counting rate always decreases with storms, a if so, whether the decrease occurs only during t main phase, and whether a quantitative relati between the decrease in intensity and so characteristic parameter of the geomagnetic d turbance can be derived.

To get an average picture of intensity chan during magnetic disturbances, the four stor were considered together. The days—nam November 1, 23, and 28, and December 6, wh U was the highest—were chosen as the 'O' da The average variation of the intensity of the counter (R_{302}) plotted as a function of L shown in Figure 8 from (−4) day to (+5) d The values are also given in Table 1.

TABLE 1. Average Counting Rate R_{302} Vs. L for Chosen Epoch Days. '0' Days are November 1, and 28, and December 6, 1959.

Designation of Day	$L \rightarrow$ 2.5	2.7	2.9	3.1	3.3	3.5	3.7	3.9	4.1	4.3	4.5	4.7	4.9	5.1 5
−4	8	11	41	182	670	1281	1305	910	560	392	291	152	70	40
−3	23	69	197	544	1028	919	563	373	245	185	130	75	45	24
−2	22	32	105	275	649	796	707	497	303	215	121	61	32	18
−1	22	86	235	563	664	640	388	258	142	96	59	35	22	12
0	64	202	352	597	538	287	140	70	39	32	19	14	9	3
+1	29	72	143	197	200	137	104	84	70	51	42	31	17	4
+2	22	65	128	194	266	252	242	204	169	117	86	59	40	12
+3	15	44	133	200	296	418	426	337	254	190	138	98	71	49
+4	25	76	184	242	287	366	566	519	373	274	192	126	92	24
+5	22	52	155	216	308	536	1010	967	768	444	298	200	138	

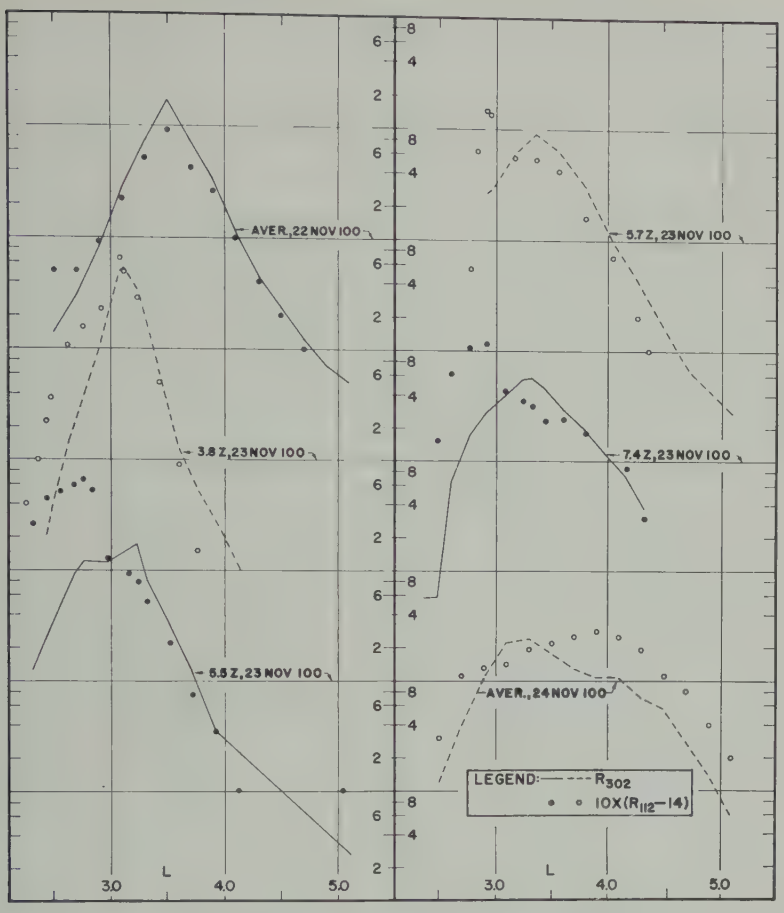


Fig. 6. Counting rates vs. L for individual passes, November 23, 1959. Average counting rates vs. L from passes on November 22 and 24, 1959.

The number of storms considered, namely, ur, is not sufficient for drawing any quantita- ve conclusions. Nevertheless it can be seen om the figure that the intensity decreases to a inimum value on day (+1) and gradually re- vers from day (+2). It should also be noted at the maximum intensity apparently shifts to lower value of L, and subsequently recovers adually to its original value of $L \sim 3.7$. Par- ularly noticeable are the large changes in in- nsity, especially at the higher L values.

Time variations of intensity at fixed values of

During the period October 26 to December 1959, the average counting rates for each ay' for the 302 and 112 counters, at $L = 2.9$, 5, 4.1, and 4.7, are given in Table 2 and otted in Figure 9. As pointed out earlier, the te for the 112 counter, after subtracting 14 for cosmic-ray background, is multiplied by 10 before plotting. The table also gives ρ, the ratio $R_{302}/(R_{112}-14)$. The GMT time in hours refers to the middle of the pass. The U and a_p values are computed for the 3-hour intervals in which the passes occur.

At $L = 2.9$, the counting rates show large fluctuations from day to day. Indeed, within days, at $L = 2.9$, the fluctuations were often larger than at larger L values. The curve at $L = 2.9$ for the whole period of study shows no correspondence with those for larger values of L. However, the curves at $L = 3.5$, 4.1, and 4.7 exhibit a similar variation during this period. Figures 10 and 11 show that for the period October 26 to December 9, the average counting rates for each 'day' at $L = 3.5$ are about 2.0 times those at $L = 4.1$, and the average count-

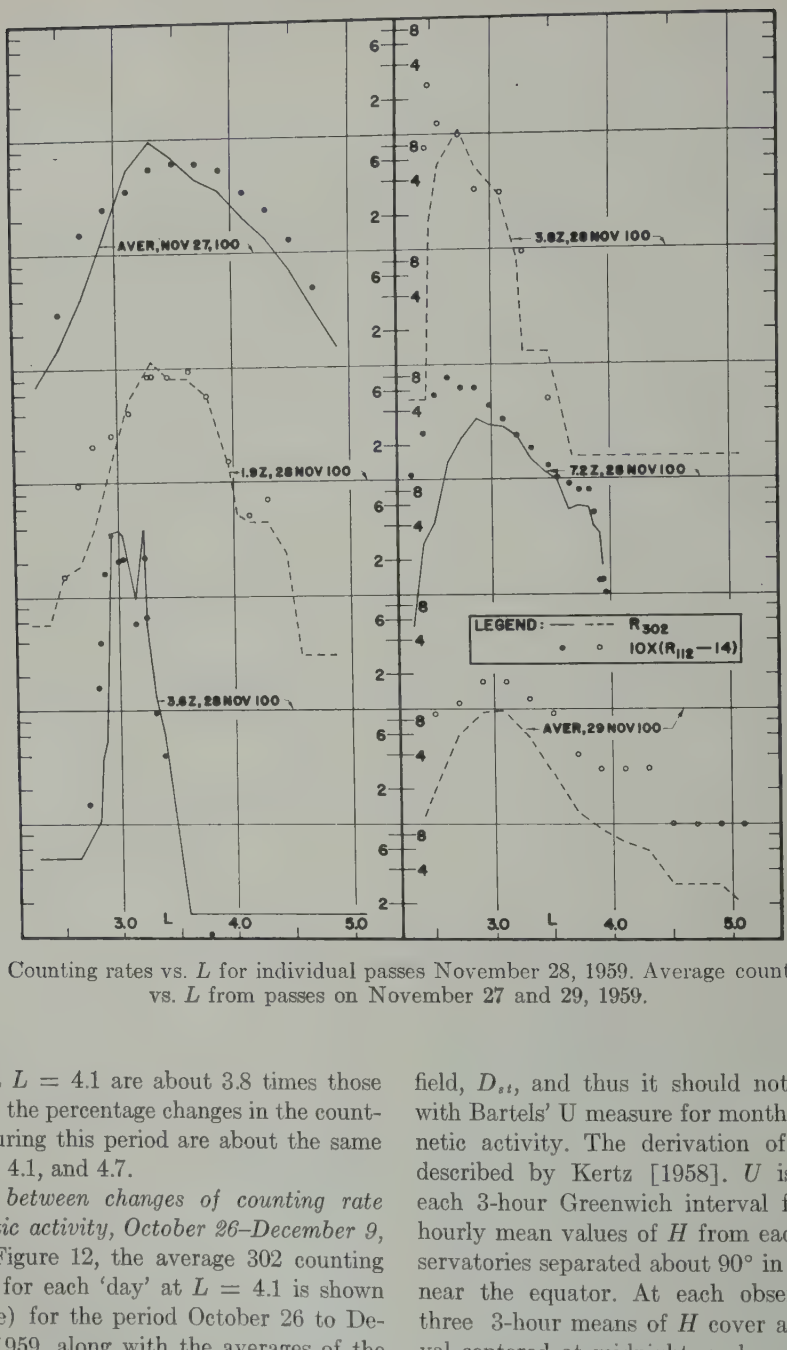


Fig. 7. Counting rates vs. L for individual passes November 28, 1959. Average counting rates vs. L from passes on November 27 and 29, 1959.

ing rates at $L = 4.1$ are about 3.8 times those at 4.7. Thus the percentage changes in the counting rates during this period are about the same at $L = 3.5$, 4.1, and 4.7.

Relation between changes of counting rate and magnetic activity, October 26–December 9, 1959. In Figure 12, the average 302 counting rate (R_{302}) for each 'day' at $L = 4.1$ is shown (solid curve) for the period October 26 to December 9, 1959, along with the averages of the values of U (dashed curve) and of the a_p (crosses) values for the 3-hour intervals in which the individual passes occurred. U is the southward geomagnetic component, in gammas, of the equatorial ring current, ERC (primary plus induced). U is thus a measure of the storm-time field, D_{st}, and thus it should not be confuse with Bartels' U measure for monthly mean mag netic activity. The derivation of U was firs described by Kertz [1958]. U is derived fo each 3-hour Greenwich interval from three 3 hourly mean values of H from each of four ob servatories separated about 90° in longitude an near the equator. At each observatory thes three 3-hour means of H cover a 9-hour inte val centered at midnight, and are consequentl unaffected by the ordinary diurnal variation, S and it variability. By taking advantage of th antisymmetry, about local midnight, of the di turbance diurnal variation, S_D in H, the effect S_D can be effectively eliminated. In addition, th secular variation is removed to permit compar

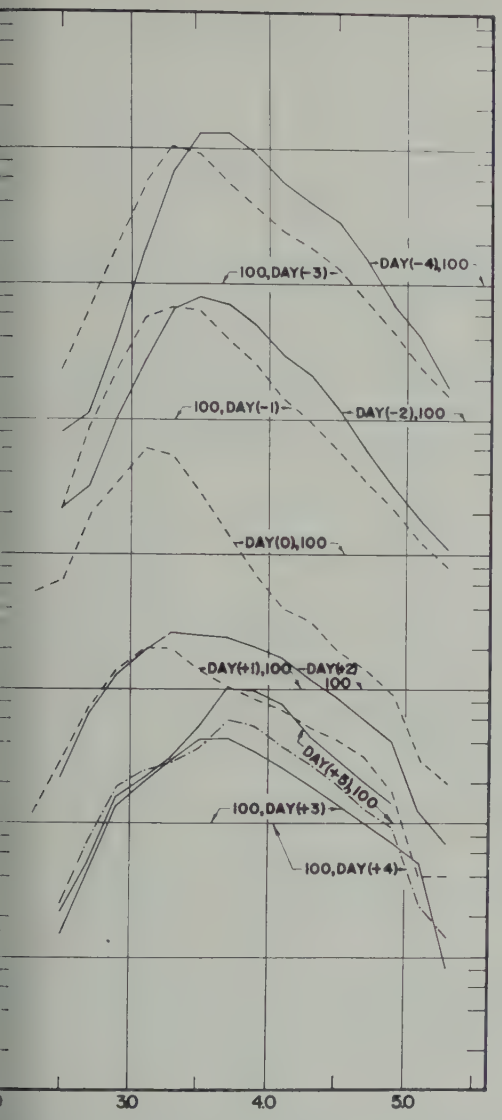


Fig. 8.- Average counting rates (R_{302}) vs. L dur- four magnetic storms in period October 26– ecember 9, 1959. 'O' days: November 1, 23, 28, d December 6, 1959.

n of U values separated by long periods of ne.

The correspondence between the changes in $_{02}$ and those in U and a_p [*Annals IGY*, 1957; *PPL*, 1960] is shown in Figure 12. During this riod the higher counting rates at $L = 4.1$ ur for the periods when U and a_p are small- , that is, during magnetically quiet periods. e decrease in the counting rate R_{302} and R_{112} ring the storms on November 23, November 28, and December 6 is notable as is the similarity in the 'recovery' of the counting rate and of U and of a_p during the post-perturbation period of the storms. The similarity in the 'recovery' part of the earlier storm on November 1 can also be seen. It is not possible from the study to say which of the two parameters U and a_p is to be preferred.

For a geophysical phenomenon that is affected through some link with solar activity, experience dictates that it would be thoroughly unjustified on any statistical basis (or otherwise) to conclude from such a very limited sample of data that the same relationships shown in Figure 12 would apply to subsequent data. It must be emphasized that the similarity between counting rate, U, and a_p shown in Figure 12, has been maximized by the choice of base values and of scales. Although these results are suggestive, it is essential to apply the analysis to additional data over a much longer period before accepting the conclusions suggested by this analysis. For this period, the decrease in measured intensity during periods of magnetic storms (large a_p) is consistent with the idea that some of the particles are 'dumped' into the auroral zone where they may partly contribute to the auroral zone currents that account for a_p. In addition, the reduction in intensity generally occurred in the outer part of the zone. The low values of intensity, for $L = 3.5$, 4.1, and 4.7, occurred in the interval November 22 to December 9, at times when the equatorial ring current field, U (southward on the earth at the equator), was large. Thus, U cannot be due to the westward current due to the longitudinal drift of the trapped particles measured by the equipment of Explorer VII, in the region for which L is greater than 3.5, since a decrease in particle density therein would diminish the westward drift current with a consequent decrease in U, which is opposite to what is observed. This result indicates that the site of the ring current is either elsewhere, or that the principal contribution to it comes from drifting particles having energies below the detection thresholds of Explorer VII equipment.

Analysis of the maximum counting rates for passes. Since values of L were not yet computed for the period after December 9, 1959, an alternative procedure was adopted on which the average of the maximum counting rates for all the passes in the day was derived. For the period

TABLE 2. Average Counting Rates R_{302} and $(R_{112}-14)$ at $L=2.9$, 3.5, 4.1, and 4.7 for the Period Oct. 26 to Dec. 9, 1959. ρ is the Ratio $R_{302}/(R_{112}-14)$

Date, month, day	Time GMT, hours	U gammas	A_p	$L=2.9$ R_{302}	$R_{112}-14$	ρ	$L=3.5$ R_{302}	$R_{112}-14$	ρ	$L=4.1$ R_{302}	$R_{112}-14$	ρ	$L=4.7$ R_{302}	$R_{112}-14$	ρ
Oct. 26	12.6	72	112	82	5	16.4	650	33	20.3	165	12	13.8	...	...	...
27	12.2, 17.5	59	18	315	37	8.5	285	16	17.8	126	14	9.0	...	...	...
30	11.1	27	18	(25)	4	6.2	295	23	12.8	76	6	12.6	...	...	...
31	12.4	97	64	590	146	4.0	265	25	10.6	85	7	12.1	29	2	14.5
Nov. 1	12.1	116	112	75	7	10.7	130	12	10.8	56	12	4.8	32	1	32.0
2	10.0, 11.7, 13.5	95	109	181	16	11.4	190	28	6.8	132	22	6.0	82	10	8.2
3	9.6, 11.3	86	96	56	6	9.3	520	52	10.0	455	48	9.5	130	14	9.3
4	11.0, 14.4	74	80	27	5	5.4	1000	80	12.5	725	60	12.1	310	34	9.1
5	8.8, 10.6, 12.3, 14.1	84	64	158	25	6.3	1102	71	15.6	805	63	12.8	270	23	11.7
6	8.4, 10.2	70	54	132	20	6.6	905	82	11.0	1325	85	15.6	330	29	11.4
7	9.8, 16.6	56	13	35	9	3.9	370	46	8.0	348	53	6.6	265	26	10.2
8	7.6, 9.4, 11.2	55	32	98	10	9.8	1500	121	12.4	2200	141	15.7	600	60	10.0
9	9.0, 10.8, 12.6	34	8	6	1	6.0	139	28	5.0	556	140	4.0	687	128	5.3
10	6.9, 8.7, 10.5	41	15	160	27	5.9	1214	115	10.5	740	82	9.0	210	20	10.5
11	8.3, 11.8, 10.1	44	10	68	8	8.5	727	59	12.3	460	38	12.1	407	35	11.7
12	6.2, 8.0, 9.7, 11.5	39	8	400	42	9.5	2837	156	18.2	1613	115	14.0	894	73	12.2
13	5.9, 9.4, 11.1	41	13	60	6	10.0	2090	131	15.9	1080	78	13.8	260	22	11.8
14	5.5, 7.2, 9.0, 10.8	55	58	52	5	10.4	1958	115	17.0	665	56	11.9	119	11	10.8
Nov. 15	6.9, 8.5, 10.3	31	11	360	46	7.8	1245	77	16.2	369	34	10.9	56	12	4.7
16	4.7, 6.5, 8.2	31	9	161	19	8.5	2233	126	18.6	605	49	12.3	106	17	6.2
17	6.1, 7.9, 9.5	52	24	252	23	11.0	2727	147	18.6	913	67	13.6	117	15	7.8
18	5.7, 7.4, 9.2	63	18	214	26	8.2	2132	112	19.2	515	38	13.6	90	12	7.5
19	5.2, 7.1, 8.8	54	37	41	5	8.2	1281	92	14.0	560	39	14.4	152	14	10.7
20	4.9, 6.6, 8.4	48	11	343	46	7.5	2313	124	18.7	378	30	12.3	98	13	7.5
21	4.5, 6.3, 8.1	43	15	104	12	8.7	1739	97	17.9	496	38	13.1	116	12	9.7
22	2.5, 4.2, 6.0	62	48	67	9	7.4	1282	91	14.1	76	10	7.6	10	1	10.0
23	3.8, 5.6, 7.4	117	127	672	187	3.6	440	30	14.7	50	4	12.2	7	0	...
24	3.4, 5.2, 6.9	60	13	106	13	8.2	174	22	7.9	107	25	4.3	28	8	3.5
25	3.1, 3.9, 6.6	45	11	71	8	8.9	276	31	9.0	145	31	4.7	58	9	6.4
26	2.7, 4.5, 6.2	47	23	102	5	20.0	272	33	8.2	158	26	6.1	26	3	8.7
27	0.5, 2.3, 4.0, 5.8	54	31	155	26	6.0	720	63	11.4	240	32	7.5	32	7	4.7
28	1.9, 3.7, 5.4, 7.2	119	324	563	75	7.5	189	20	9.4	16	2	8.0	2	0	...
29	1.6, 3.3, 5.1, 6.9	102	26	91	17	5.3	28	9	3.1	7	3	2.3	3	1	3.0
30	1.2, 2.9, 4.8	76	22	150	21	7.1	55	17	3.2	24	13	1.9	25	12	2.1
Dec. 1	2.6, 4.3	83	80	76	13	5.8	60	20	3.0	28	11	2.5	10	5	2.0
2	2.2	70	36	215	26	8.3	128	34	3.8	104	27	4.2	38	12	3.2
3	0.1, 1.8, 3.6, 5.3	77	87	178	27	6.6	168	41	4.1	212	39	5.4	70	12	5.8
4	−0.3, 1.4, 3.2, 4.9	59	64	108	17	6.4	378	59	6.4	256	32	8.0	41	3	13.7
5	−0.7, 1.1, 2.8, 4.5	56	5	131	27	4.9	325	61	5.3	200	25	8.0	72	7	10.3
6	−1.1, 0.7, 2.5, 4.2	118	78	95	24	4.0	101	19	5.3	32	5	6.4	14	1	14.0
7	−1.1, 0.3, 2.0, 3.8	80	28	194	44	4.4	156	29	5.4	33	8	4.1	12	3	4.0

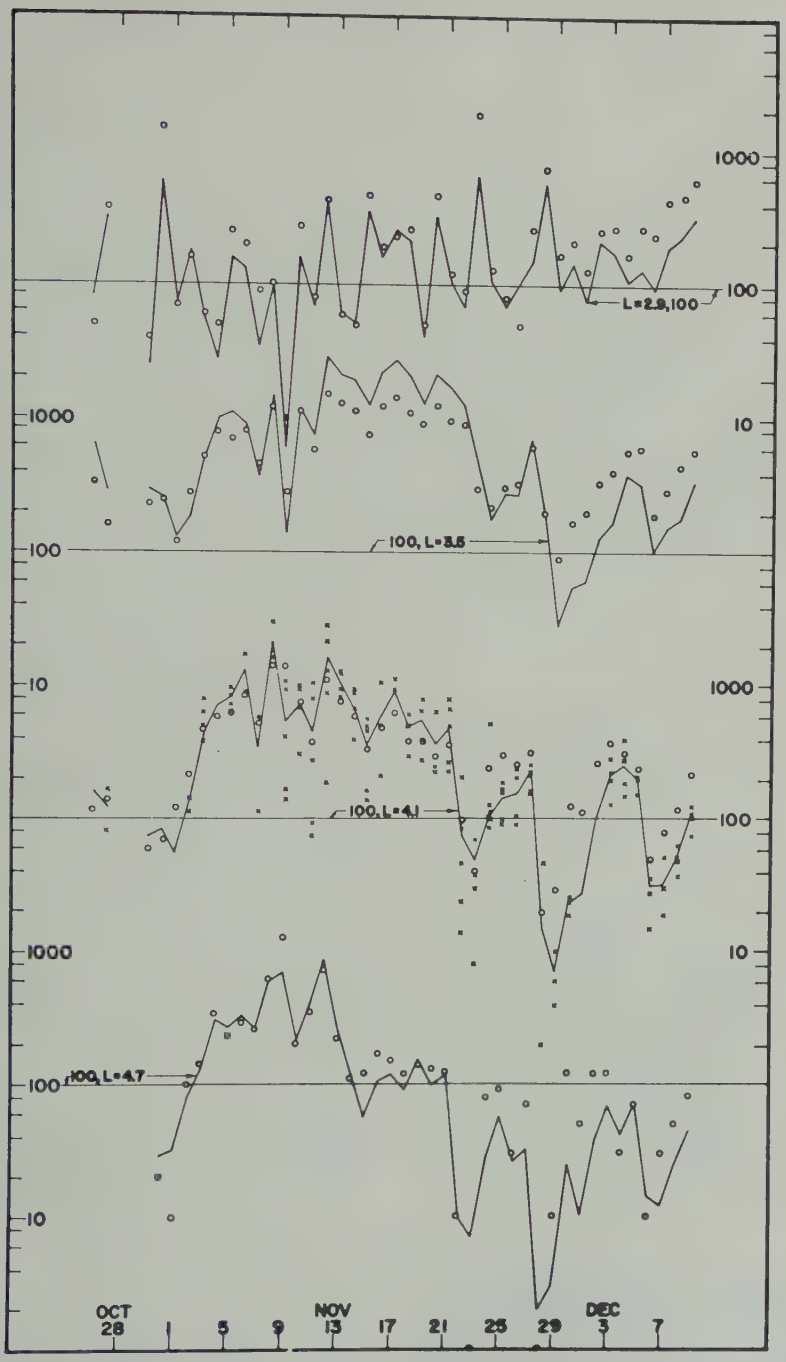


Fig. 9. Average counting rates from passes for each 'day,' October 26–December 9, 1959, at $L = 2.9$, 3.5, 4.1, and 4.7, and rates from individual passes at $L = 4.1$.

ctober 26 to December 9, 1959, these daily erages of maximum counting rates fell on a rve quite similar to that for $L = 4.1$ in Figure . This indicated that such averages of 'intensity maxima" for the passes of the day might be used to determine the effect of magnetic disturbance. However, it was anticipated from the graph for $L = 2.9$, in Figure 9, that if the in-

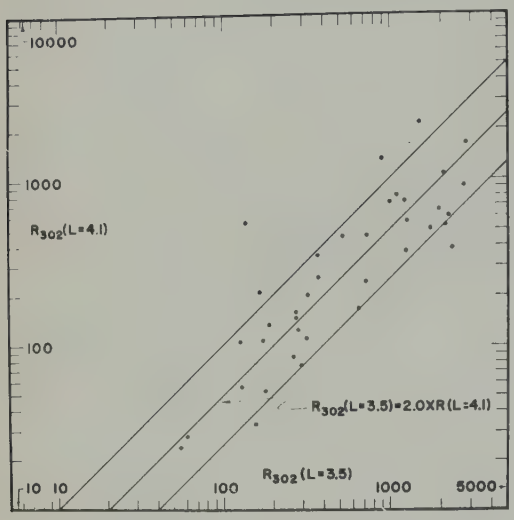


Fig. 10. R_{302} ($L = 4.1$) vs. R_{302} ($L = 3.5$) from daily averages, October 26–December 9, 1959.

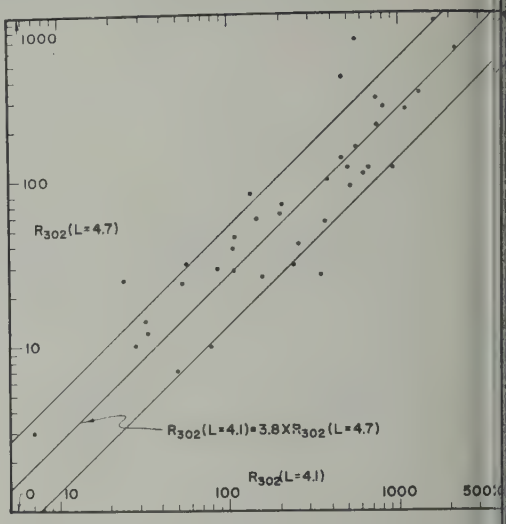


Fig. 11. R_{302} ($L = 4.7$) vs. R_{302} ($L = 4.1$) fr daily averages, October 26–December 9, 1959.

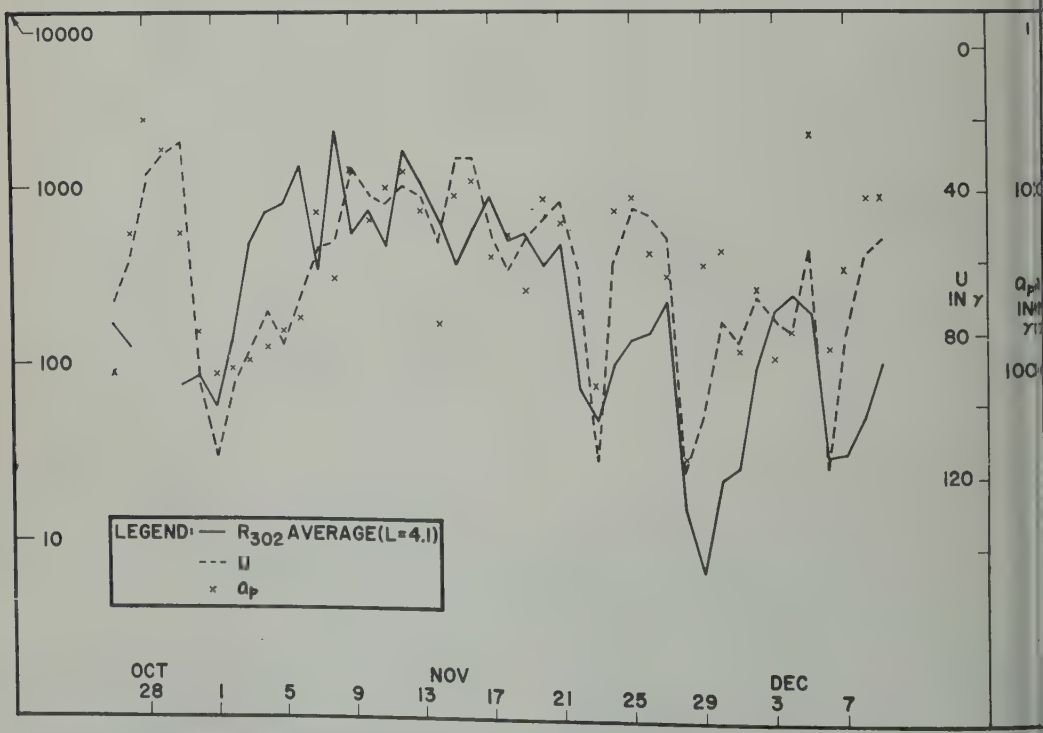


Fig. 12. Average counting rate, R_{302} at $L = 4.1$ from passes for each 'day,' equatorial ring current measure U, and magnetic activity a_p, October 26–December 9, 1959.

nsity maxima occurred at values of L of about 9 or so, then these intensity maxima would not e likely to show a consistent effect of magnetic sturbance. Except during April and May 1960, ie departures from their monthly means of iese averages of 'intensity maxima' for the daily asses indicated some negative correlation with ie corresponding departures for magnetic ac- vity. During April and May 1960, a rough valuation reveals many cases of maxima of in- nsity occurred at values of L less than about 0, which possibly may account for the absence any consistent correspondence btween the 'in- nsity maxima' and magnetic activity; if so, ie use of these average maximum counting tes for long-term investigations is of dubious lue.

Between the departures of the average maxi- um counting rates for the day, from their ean over the interval October 26, 1959, to July 1960, and the corresponding departures in U, e correlation is of doubtful significance. There e indications, however, that this may be due an effect of altitude on counting rate, although is cannot be reliably determined before all the ta are examined.

Ratio of counting rate for the 302 counter to at for the 112 counter. From Figure 9, for tober 26 to December 9 (for $L = 3.5$, 4.1, d 4.7) the ratio $\rho = R_{302}/(R_{112}-14)$ is gen- ally seen to be greater for periods when R_{302} high, although the rates for both counters ry somewhat similarly. This shows that the diation is softer (i.e., more easily absorbed by e lead shield of the 112) at times of high tensity.

Acknowledgment. Work for this paper was as- ted by the joint program of the Office of Naval search and Atomic Energy Commission under ntract N9onr—93803.

References

Annals of the International Geophysical Year, 4, Parts IV–VII, Pergamon Press, 1957.

Arnoldy, R., R. Hoffman, and J. R. Winckler, Observation of the Van Allen Radiation Regions during August and September 1959, Part I, *J. Geophys. Research, 65,* 1361–1375, 1960.

CRPL—F, Part B, January, February, 1960. Publication of the U. S. Department of Commerce National Bureau of Standards Central Radio Propagation Laboratory, Boulder, Colorado, 1960.

Finch, H. F., and B. R. Leaton, The earth's main magnetic field—Epoch 1955·0, *Mon. Not. Roy. Astronom. Soc.* (Geophys. Suppl.) *7* (6), 314–317, 1957.

Kertz, Walter, Ein Neues Mass für die Feldstärke des Erdmagnetischen Äquatorialen Ringstroms Abhandlungen. der Akademie der Wissenschaften in Göttingen Mathematisch Physikalische Klasse Beiträge zum Internationalen Geophysikalischen Jahr Heft *2,* Göttingen Vandenhoeck and Ruprecht, 1958.

Ludwig, G. H., and W. A. Whelpley, Corpuscular radiation experiment of Satellite 1959 Iota (Explorer VII), *J. Geophys. Research, 65,* 1119–1124, 1960.

Northrup, T. G., and E. Teller, Stability of the adiabatic motion of charged particles in the earth's field, *Phys. Rev., 117,* 215–225, 1960.

O'Brien, B. J., J. A. Van Allen, F. E. Roach, and C. W. Gartlein, Correlation of an auroral arc and a subvisible monochromatic 6300 A arc with outer-zone radiation on November 28, 1959, *J. Geophys. Research, 65,* 2759–2766, 1960.

Rothwell, P., and C. McIlwain, Magnetic storms and the Van Allen radiation belts: Observations with satellite 1958ε (Explorer IV), *J. Geophys. Research, 65,* 799–806, 1960.

Van Allen, J. A., and Wei Ching Lin, Outer radiation belt and solar proton observations with Explorer VII during March–April 1960, *J. Geophys. Research, 65,* 2998–3003, 1960.

Vestine, E. H., and W. L. Sibley, The geomagnetic field in space, ring currents and auroral isochasms, *J. Geophys. Research, 65,* 1967–1979, 1960.

(Manuscript received June 2, 1961.)

Some Effects of Diamagnetic Ring Currents on Van Allen Radiation[1]

A. J. DESSLER

Lockheed Missiles and Space Division
Palo Alto, California

ROBERT KARPLUS[2]

University of Vienna, Vienna, Austria

Abstract. The distortion of the geomagnetic field by diamagnetic ring currents (such as the magnetic storm main phase ring current) is calculated quantitatively. It is shown that these distortions cause changes in the energy of the trapped electrons in the outer zone of the Van Allen radiation belt. The changes are brought about by betatron acceleration and deceleration of the trapped radiation as the distortions move the radiation from one field strength region into another. A model is presented involving a system of two diamagnetic ring currents for which there is some observational evidence. In this model part of the geomagnetic storm energy is temporarily transferred to the Van Allen radiation. It is proposed that such a mechanism contributes, in part, to the major fluctuations in the observed intensities of the outer zone of the radiation belt because (1) the changes in particle energy cause changes in the counting rate of radiation instruments flown through the belt, and (2) the Van Allen electron number density is a steep function of radial distance so that distortions of the geomagnetic field can cause changes in particle flux.

Introduction. The Van Allen radiation is a elt of energetic particle radiation that is rapped in the geomagnetic field. Observations *Vernov, Chudakov, Vakulov, and Logachev,* 959; *Walt, Chase, Cladis, Imhof, and Knecht,* 960; *Fan, Meyer, and Simpson,* 1960] have hown that beyond about 2 earth radii geocenric distance, the penetrating radiation consists holly of energetic electrons. The source of this adiation has not been established. It has been ointed out that the results of the radiation elt observations made with Explorer IV and Explorer VI satellite systems showed that direct olar injection could not be the source of the lectrons in the outer zone of the radiation belt *Dessler and Karplus,* 1960]. This conclusion was onfirmed by the results obtained with the space robe Pioneer V [*Arnoldy, Hoffman, and Winc-ler,* 1960]. Two theories are currently put forth o account for the electrons observed in the outer one: (*a*) the local acceleration hypothesis [*Van llen,* 1959; *Arnoldy, Hoffman, and Winckler,* 1960; *Helliwell and Bell,* 1960] in which it is proposed that the outer zone electrons are accelerated up to their observed energies within the geomagnetic field, and (*b*) the neutron decay hypothesis [*Dessler and Karplus,* 1960; *Hess,* 1960] in which it is argued that the decay of neutrons produced by the interaction of cosmic radiation (galactic and solar flare) with nuclei of atmospheric nitrogen and oxygen is the source of the energetic electrons in both zones of the radiation belt. This latter point of view has been seriously questioned by *Kellogg* [1960]. However, the interpretation of the experimental evidence on which his arguments are based is ambiguous [*Hess,* 1960; *Dessler,* 1960] so that further investigation of the neutron-albedo-origin hypothesis is warranted.

In our earlier analysis [*Dessler and Karplus,* 1960] it was suggested that magnetic-storm-induced changes in the geomagnetic field might account for the relatively rapid ($\sim 10^5$ sec) fluctuations in outer-zone intensity as observed by radiation instruments aboard Explorer VI. (The time scale of these changes must be considered in the light of the long electron lifetime ($\sim 10^9$ sec) needed to make the weak neutron decay source an adequate one.) It was proposed that it is the magnetic field changes rather than

[1] Presented at the meeting of the American Geophysical Union, April 18-21, 1961, Washington, D. .

[2] Fulbright Research Scholar and John Simon uggenheim Fellow on leave from the University f California, Berkeley, California.

changes in the number of trapped particles that give rise to the varying counting rates.

However, the recent analysis of Explorer VI results carried out by *Rosen and Farley* [1961] shows that a simple reversible betatron acceleration and deceleration, such as mentioned above, can not account for all the observed counting rate changes. The reversible, magnetic-storm-induced changes that will be described in this paper, therefore, can only be a part of the over-all mechanism that produced the counting rate fluctuation associated with a geomagnetic storm; an irreversible modulation mechanism is also required.

Distortion of geomagnetic field by diamagnetic ring current. In this section, we will describe quantitatively the displacement of the lines of force of the geomagnetic field due to the perturbing action of a belt of trapped radiation that constitutes a diamagnetic ring current. Two illustrative cases will be considered to show what particle effects result from the following ring currents: (*a*) a belt of trapped particles with peak energy density near 4 earth radii, and (*b*) a belt with peak particle energy density near 9 earth radii. Case (*a*) is thought to represent the ring current which produces the main phase of geomagnetic storms [*Dessler and Parker,* 1959]. Case (*b*) is based on the quiet-day ring current postulated by *Smith, Coleman, Judge, and Sonett* [1960], and the observation [*Gringauz, Kurt, Moroz, and Shklovskii,* 1960] of a belt of soft radiation trapped between about 8 and 11 earth radii. Although the Van Allen radiation itself is a diamagnetic ring current, it is probably too weak to significantly affect the geomagnetic field. It is estimated that the total energy stored in the Van Allen radiation is less than 10^{13} joules, which is small compared with the ring current energies assumed in this paper [*Dessler and Vestine,* 1960; *Dessler,* 1961, p. 69]. Therefore, the two ring currents to be considered in our model completely control the displacement of the geomagnetic field lines and the Van Allen radiation trapped on those field lines.

The displacement of the dipole geomagnetic field lines is calculated from the relationship

$$\Phi = 2\pi \int_{R_e}^{r_1} rB(r)\, dr = 2\pi \int_{R_e}^{r_2} r[B(r) + \Delta B(r)]\, dr \qquad (1)$$

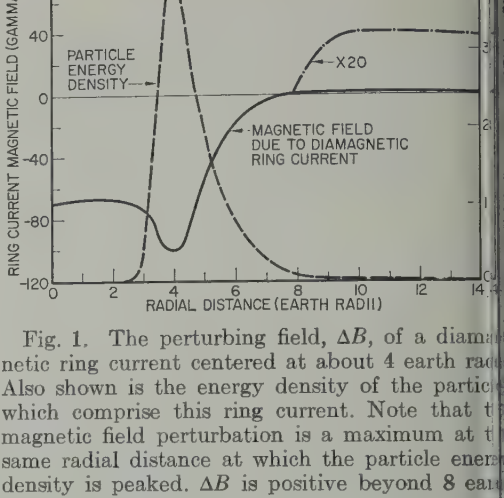


Fig. 1. The perturbing field, ΔB, of a diamagnetic ring current centered at about 4 earth radii. Also shown is the energy density of the particles which comprise this ring current. Note that the magnetic field perturbation is a maximum at the same radial distance at which the particle energy density is peaked. ΔB is positive beyond 8 earth radii and has been multiplied by 20 to be conveniently shown on this graph [after *Apel,* 1961].

where Φ is the magnetic flux through the equatorial plane inside a circle of radius r_1 when there is no ring current present, and through a circle of radius r_2 when a diamagnetic ring current is present that produces a magnetic perturbation $\Delta B(r)$. $B(r)$ is the unperturbed dipole field strength and R_e is the radius of the earth.

The linear solution (mutual interaction of the particles making up the ring current, is neglected) of the magnetic perturbation in the equatorial plane due to a specific diamagnetic ring current configuration is given by *Apel* [1960]. The values for $B(r)$ used in this paper have been scaled from Apel's work.

Case (a) is that of the magnetic storm main phase ring current. Equation 1 is used to calculate the distention of the geomagnetic field due to a diamagnetic ring current located at about 4 earth radii (see Fig. 1). This location is consistent with the magnetic storm observations made with Explorer VI [*Smith and Rose,* 1960]. The results are shown in Table 1 for two ring currents that cause a nominal main phase decrease at the earth's surface of 70 γ and 90 γ, respectively. *Case (b)* is the quiet-day ring current. For this case it is assumed that the magnetic field is normally distended by a diamagnetic ring current flowing near 9 earth radii. Equation 1 is used to calculate how far the field lines move inward to return to an unstressed configuration when this ring current is removed, by a magne-

TABLE 1. Distortion of geomagnetic field lines due to main phase diamagnetic ring current. r_i is the ocentric distance of a field line before the ring current is established, B_i is the unperturbed dipole field ength at r_i, ΔB is the perturbing field of the ring current, r_f is the final or distended geocentric distance the field line, and B_f is the magnetic field at the position r_f. B_f is the vector sum of ΔB and the unrturbed dipole field strength at r_f. Two examples are given, one in which the magnetic storm main-phase crease is 70γ and the other in which it is 90γ.

r_i arth adii	70 γ Main-Phase Decrease				90 γ Main-Phase Decrease		
	B_i gamma	ΔB gamma	r_f earth radii	B_f gamma	ΔB gamma	r_f earth radii	B_f gamma
		−70	0		−90	0	
	3.2×10^4	−69	1.0011	3.18×10^4	−88	1.0014	3.18×10^4
.5	9.5×10^3	−68	1.505	9.31×10^3	−87	1.507	9.26×10^3
	4.0×10^3	−68	2.017	3.83×10^3	−87	2.022	3.78×10^3
.5	2.0×10^3	−69	2.542	1.88×10^3	−89	2.555	1.83×10^3
	1.18×10^3	−74	3.090	1.008×10^3	−95	3.117	958
.5	746	−91	3.678	547	−117	3.733	489
	500	−100	4.340	300	−129	4.448	253
.5	351	−84	5.091	193	−108	5.288	164
.5	256	−54	5.914	135	−69	6.24	114
	192	−32	6.78	95.5	−41	7.27	80.4
	148	−18	7.69	70.4	−23	8.36	56.3
.5	116	−10	8.62	51.2	−12.8	9.52	39.7
	93.3	−4	9.62	37.9	−5.1	10.8	28.5
	62.5	1.0	11.6	23.0	1.3	13.3	16.6
	43.9	1.5	13.8	14.7	1.9	16.2	10.5
	32.0	2.0	16.1	10.6	2.6	19.5	7.3

rm, for instance. Hence, now r_2 is the initial dius r_i, and r_1 is the final radius r_f of the field e at the equator.

The six space vehicles (Pioneer I, Mechta, nik, Explorer VI, Pioneer V, and Explorer X) at to date have carried magnetometers far m the earth do not agree on any deviation m a dipole-like magnetic field that would consively demonstrate the existence of a quiet-y ring current. For example, the magnetic perbations observed at apogee by Explorer VI *nett, Smith, Judge, and Coleman,* 1960] ve been interpreted as a 5 x 10^6 amp current wing at about 10 earth radii. Such a ring curnt would produce a 60-γ increase in the geognetic field at 12.5 earth radii. However, Pioer I showed that the geomagnetic field in this ion was within 15 γ of that predicted by an perturbed dipole [*Sonett, Judge, Sims, and lso,* 1960]. Preliminary results of Explorer X icate that at 6.5 earth radii the geomagnetic d strength is within about 3 γ of that pre-ted by the spherical harmonic analysis [*Hepp-, Skillman, Scearce, and Ness,* 1961]. Furtherre, the Explorer VI results are not compatible h the trapped soft-radiation belt reported by *Gringauz, Kurt, Moroz, and Shklovskii* [1960]. The soft-radiation belt was observed to be between 8 and 11 earth radii, and therefore would produce a maximum magnetic perturbation in this region (Fig. 1 shows that the maximum magnetic deviation occurs where the particle energy density is a maximum) whereas the maximum magnetic perturbation as observed by Explorer VI occurred at about 7 earth radii.

The purpose of this section is simply to illustrate the effect of a quiet-day ring current on the Van Allen radiation. Therefore, in order to present the most meaningful examples, the quiet-day ring currents chosen are based on the observations of *Sonett, Smith, Judge, and Coleman,* [1960] and *Gringauz, Kurt, Moroz, and Shklovskii* [1960] even though the measurements do not appear mutually consistent.

The observations of Gringauz and his coworkers were interpreted as due to a belt of trapped electrons with a flux of 2 x 10^8 electrons/cm^2-sec for electron energies above 200 ev. Since this belt has not been detected with other radiation instruments, the electron energy must be less than about 20 kev. Assuming that electrons have an energy of 10 kev, leads to a total

TABLE 2. Calculations of the distortion of geomagnetic field lines by quiet-day ring current. r_i is th geocentric distance of a field line while it is being distended by the soft radiation belt (which constitut a diamagnetic ring current). ΔB is the perturbing field of the ring current, B_i is the net magnetic field r_i and is the vector sum of ΔB and the unperturbed dipole field strength, r_f is the final or undistort position of the field line after the quiet-day ring current is removed, and B_f is the unperturbed dipo field strength at r_f. Two examples are given: one is a diamagnetic ring current with peak particle ener density at 9 earth radii and a total energy of approximately 5×10^{14} joules; the other has its peak partic energy density at 7.5 earth radii, and contains approximately 8×10^{14} joules.

	Peak Particle Energy Density at 9 Earth Radii				Peak Particle Energy Density at 7.5 Earth Ra			
r_i earth radii	B_i gamma	ΔB gamma	r_f earth radii	B_f gamma	B_i gamma	ΔB gamma	r_f earth radii	B_f gamma
0		17.5	0			26.2	0	
1	3.198×10^4	17.2	0.9997	3.203×10^4	3.197×10^4	26.0	0.9996	3.204×10
2	3.98×10^3	17.0	1.996	4.02×10^3	3.97×10^3	25.8	1.99	4.04×10^3
3	1.17×10^3	17.0	2.978	1.21×10^3	1.16×10^3	25.6	2.97	1.22×10^3
4	483	17.0	3.93	526	474	25.6	3.90	539
5	239	17.0	4.84	282	230	26.2	4.76	297
6	131	17.5	5.67	175	119	29.2	5.51	191
7	74.5	18.8	6.42	121	57.3	36.0	6.10	141
8	39.8	22.7	6.99	93.8	26.5	36.0	6.44	120
9	18.9	25.0	7.37	79.8	16.9	27.0	6.67	108
10	9.4	22.6	7.59	73	15.9	16.1	6.90	97
11	7.5	16.5	7.74	69	15.0	9.0	7.15	87
12	7.8	10.7	7.91	65	13.6	4.9	7.43	78
13	7.8	6.8	8.10	60		3.8		
14	7.7	4.0	8.33	55	11	0.75	7.97	63

trapped particle energy of approximately 2 x 10^{13} joules in a magnetic shell having a volume of 4 x 10^{22} m^3. This amount of trapped particle energy is inadequate to distort the geomagnetic field in an important way. Therefore, for this calculation, we have assumed that the total energy in this radiation band is about 25 times greater than calculated, or about 5 x 10^{14} joules, which is about as much as the magnetic field between 8 and 11 earth radii can hold without overloading the field (i.e., the particle kinetic energy density is about equal to the magnetic field energy density). This assumption implies that an important component of the trapped electron flux has energies of less than 200 ev [following *Gringauz and Rytov*, 1960] and/or that the protons in this region have energies of the order of 10 ev. The results of the calculation are given in Table 2. In addition the results are given for a second calculation where the peak particle energy density of the ring current has been moved in to 7.5 earth radii and the total particle energy increased to approximately 8 x 10^{14} joules in order to represent the field perturbation observed by Explorer VI [*Sonett, Smith, Judge, and Coleman*, 1960].

Effects of geomagnetic field distortion on V Allen radiation. As indicated in Table 1, the troduction of a diamagnetic ring current cau the geomagnetic field to be distended so that it is everywhere less than B_i. (The subscripts i a f refer to initial and final conditions, resp tively.) Table 2 gives the motion and change field strength associated with geomagnetic fi lines when a diamagnetic ring current is moved. If the field lines are introduced and moved slowly enough (i.e., times greater th about 1 hour) so that the third invariant (flux invariant) is not violated, the Van Al radiation will follow the motion of the lines force [*Northrup and Teller*, 1960]. For such sl field changes, the magnetic moment of the pa cle, $E_\perp/B$, will remain constant. Here, $E_\perp$ is component of particle energy perpendicular the magnetic field at a point where the fi strength is B. Thus, if a diamagnetic ring curr is introduced or removed, $E_\perp$ changes in the ra B_f/B_i. This phenomenon is often called 'betat acceleration' or 'deceleration.'

The effects of the ring currents, descri above as cases (*a*) and (*b*), on $E_\perp$ are given Table 3. The deceleration due to the main ph

TABLE 3. Effect of distortion of geomagnetic field by diamagnetic ring currents on the perpendicular ergy component of trapped radiation. Case (*a*) shows the deceleration due to a magnetic storm, diamagtic ring current which moves the particles from r_i to r_f. Two examples are shown, one in which the agnetic storm main-phase decrease is 70 γ and one in which it is 90 γ. Case (*b*) shows the acceleration e to the removal of a ring current. Two examples are shown, in one the ring current is located near 9 rth radii, and in the other the ring current is near 7.5 earth radii. The acceleration and deceleration own here are for particles with 90° pitch angle (i. e., particles constrained to move along the integral variant equator). For an isotropic pitch angle distribution, since $E_\perp$ is 2/3 of the total particle energy, e acceleration and deceleration factors are given by $1/3 + (2/3)B_f/B_i$.

	Case (*a*)				Case (*b*)				
	70 γ Main-Phase		90 γ Main-Phase			9 Earth Radii		7.5 Earth Radii	
r_i: earth radii	r_f earth radii	Deceleration B_f/B_i	r_f earth radii	Deceleration B_f/B_i	r_i earth radii	r_f earth radii	Acceleration B_f/B_i	r_f earth radii	Acceleration B_f/B_i
1	1.0011	0.995	1.0014	0.993	1	0.9997	1.0013	0.9996	1.002
1.5	1.505	0.982	1.507	0.977	2	1.996	1.010	1.99	1.016
2	2.017	0.958	2.022	0.946	3	2.978	1.038	2.97	1.056
2.5	2.542	0.917	2.555	0.894	4	3.93	1.089	3.90	1.137
3	3.090	0.851	3.117	0.808	5	4.84	1.180	4.76	1.291
3.5	3.678	0.733	3.733	0.655	6	5.67	1.342	5.51	1.61
4	4.340	0.600	4.448	0.506	7	6.42	1.63	6.10	2.47
4.5	5.091	0.550	5.288	0.467	8	6.99	2.36	6.44	4.51
5	5.914	0.526	6.24	0.444	9	7.37	4.22	6.67	6.37
5.5	6.78	0.497	7.27	0.418	10	7.59	7.78	6.90	6.12
6	7.69	0.475	8.36	0.380	11	7.74	9.19	7.15	5.83
6.5	8.62	0.440	9.52	0.341	12	7.91	8.29	7.43	5.75
7	9.62	0.406	10.8	0.31					
8	11.6	0.37	13.3	0.27					

ng current, case (*a*), is illustrated graphically Figure 2.

Discussion of specific model. The model prented in this section illustrates how distortions the geomagnetic field by diamagnetic ring rrents can cause changes in the counting rate radiation instruments flown through the lt. However, as mentioned in the introduction, osen and Farley have presented convincing guments which indicate that betatron mechasms alone can not account for all the observed unting rate changes. Therefore, the calculaons carried out in this paper—a quantitative timate of the effect of observed diamagnetic g currents on the Van Allen radiation—should regarded as part of a more complex mechasm.

If we assume that the total energy of the rticles trapped between 6 and 11 earth radii sufficiently high to cause the field distortion ven in Table 2, then neutron decay electrons at are trapped in outer zone have, in general, en deposited in a region where the geomagnetic ld is normally distended. *Johnson* [1960] has gued that the geomagnetic field will be distorted into a teardrop shape by the solar wind. During magnetically disturbed times, the leading edge of this teardrop will move in to about 6 earth radii. No radiation can then remain trapped in the tail of the teardrop since the magnetic shells (i.e., the surfaces on which the trapped particles move) in this region can not form a closed surface around the earth. Rather, the magnetic shells intersect the boundary between the geomagnetic field and interplanetary space; when a trapped particle drifts to the boundary, the particle will be lost into interplanetary space. We conclude that during the violent phase of a geomagnetic storm (high K index) the belt of low-energy radiation beyond 6 earth radii is lost from the geomagnetic field, and thus the stresses produced in the geomagnetic field by this radiation are removed. The geomagnetic field would then collapse back to an unstressed equilibrium configuration if it were not for the main phase diamagnetic ring current which flows at this same time at about 4 earth radii [*Smith and Rosen,* 1960]. However, after about a day, the main phase ring current will decay, and the geomagnetic field will shrink

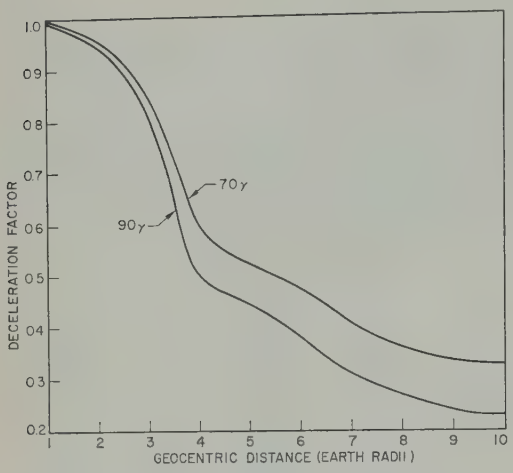


Fig. 2. Factor by which the perpendicular energy of a trapped particle is reduced owing to the establishment of the magnetic storm main phase diamagnetic ring current. Two examples are shown: ring currents producing nominal main-phase decreases of 90 γ and 70 γ at the earth's surface. The reduction of particle energy is due to betatron deceleration; the main contribution to this effect in the displacement of the trapped radiation into a region of weaker magnetic field.

to an unstressed state. The field configuration changes slowly enough so that the invariants of motion of trapped particles are conserved, and the Van Allen radiation will move with the geomagnetic field lines. The inward displacement of the field lines and the accompanying compression (betatron acceleration) of the trapped particles will increase the component of particle energy perpendicular to the geomagnetic field line. This compression and increase in particle energy increases the counting rate of instruments flown through the belt in the following 3 ways: (1) previously unobservable particles (in an unknown number) will pass the detector threshold or, equivalently, particles which had previously been counted with low efficiency will be counted with much greater efficiency as their energy increases; (2) the compression will increase the trapped particle number density and hence the particle flux; and (3) the increase in energy corresponds to an increase in the velocity of the nonrelativistic component of the trapped electrons; the velocity increase will result in a proportionate change of the electron flux.

The decrease in counting rate or apparent 'dumping' of radiation [*Fan, Meyer, and Simpson,* 1960; *Arnoldy, Hoffman, and Winckler,* 1960] during the active part of the magne storm is explained by the diamagnetism of t magnetic storm ring current. The diamagneti temporarily reduced the magnetic field streng in the region where the ring current partic are trapped (i.e., approximately 4 earth rad [*Smith and Rosen,* 1960] The reduction in fi strength results in a decrease in counting ra by just the inverse of the three effects describ above.

The following sequence of events is theref proposed as a partial explanation of the obser changes in the outer zone of the Van Allen ra ation belt: (1) The geomagnetic field in the gion of the outer zone of the Van Allen radiati belt is normally distended by a band of trapp low-energy radiation between 6 and 11 ea radii. Electrons from neutron decay are dep ited throughout the entire geomagnetic field w a trapping time of the order of 10^9 seconds. The arrival of plasma from the sun causes a g magnetic storm with a diamagnetic current ri set up in the 3-5 earth radii region. The red tion in field strength in this region due to diamagnetism causes a deceleration of trapped radiation and a resultant decrease counting rate in instruments flown through outer zone. (3) The distortion of the geom netic field due to the geomagnetic storm cau the low-energy radiation, which is normally pr ent between about 6 to 11 earth radii, to be l into interplanetary space. Therefore, after decay of the magnetic storm ring current, magnetic field will contract beyond its presto configuration. This 'adiabatic compression' the trapped Van Allen electron 'gas' will caus 'heating' or increase in energy, and hence an crease in counting rate. The recovery of Van Allen radiation to its prestorm condition then ascribed to the replenishment of the l energy radiation found between 6 and 11 ea radii.

Acknowledgment. We wish to thank Mr. W Francis for performing the calculations given Tables 1, 2, and 3. We are also indebted to Mr Apel for sending us a copy of his thesis in adva of publication, and to Dr. E. N. Parker several comments helpful in the preparation of t paper.

This work was supported in part by the G physics Research Directorate of the Air Fo Cambridge Research Laboratories under contr AF 19(604)-7989.

References

el, J. R., Geomagnetic field perturbations due to rapped particles, Masters thesis, University of Maryland, 1961.

noldy, R. L., R. A. Hoffman, and J. R. Winckle, Observations of the Van Allen radiation regions during August and September, 1959. Part I, *J. Geophys. Research, 65,* 1361–1376, 1960.

ssler, A. J., Discussion of paper by R. L. Arnold, R. A. Hoffman, and J. R. Winckler, 'Observations of the Van Allen radiation regions during August and September, 1959, Part I,' *J. Geophys. Research, 65,* 3487–3490, 1960.

ssler, A. J., Penetrating radiation, *Satellite Environment Handbook,* edited by F. S. Johnson, Stanford University Press, Stanford, 168 pp., 1961.

ssler, A. J., and R. Karplus, Some properties of the Van Allen Radiation, *Phys. Rev. Letters, 4,* 271–274, 1960.

ssler, A. J., and E. N. Parker, Hydromagnetic theory of geomagnetic storms, *J. Geophys. Research, 64,* 2239–2252, 1959.

ssler, A. J., and E. H. Vestine, Maximum total energy of the Van Allen radiation belt, *J. Geophys. Research, 65,* 1069–1071, 1960.

n, C. Y., P. Meyer, and J. A. Simpson, Trapped and cosmic radiation measurements from Explorer VI, *Space Research,* edited by H. K. Kallmann Bijl, North Holland Publishing Company, Amsterdam, pp. 951–966, 1960.

ingauz, K. I., V. G. Kurt, V. I. Moroz, and I. S. Shklovskii, The ionized gas and fast electrons in the vicinity of the earth and in interplanetary space, *Doklady Akad, Nauk, 132,* 1062–1065, 1960 (translation in *Physics Express,* October 1960, pp. 5–9).

ingauz, K. I., and S. M. Rytov, On the connection between the results of measurements by means of charged particle traps on the Soviet space rockets, and measurements of the magnetic field on the American Explorer VI and Pioneer V vehicles, *Doklady Akad. Nauk, 135,* 48–51, 1960.

lliwell, R. A., and R. F. Bell, A new mechanism for accelerating electrons in the outer ionosphere, *J. Geophys. Research, 65,* 1839–1842, 1960.

ppner, J., T. L. Skillman, C. S. Scearce, and N. Ness, Preliminary magnetic field results from Explorer X, presented at meeting of American Geophysical Union, April 18-21, 1961, Washington, D. C.

Hess, W. N., The radiation belt produced by neutrons leaking out of the atmosphere of the earth, *J. Geophys. Research, 65,* 3107–3115, 1960.

Hess, W. N., E. H. Canfield, and R. E. Lingenfelter, Cosmic ray neutron demography, *J. Geophys. Research, 66,* 665–677, 1961.

Johnson, F. S., The gross character of the geomagnetic field in the solar wind, *J. Geophys. Research, 65,* 3049–3051, 1960.

Kellogg, P. J., Electrons of the Van Allen radiation, *J. Geophys. Research, 65,* 2705–2713, 1960.

Northrup, T. G., and E. Teller, Stability of the adiabatic motion of charged particles in the earth's field, *Phys., Rev., 117,* 215–225, 1960.

Rosen, A., and T. Farley, Characteristics of the Van Allen radiation zones as measured by the scintillation counter on Explorer VI, *J. Geophys. Research, 66,* 2013–2028, 1961.

Smith, E. J., P. J. Coleman, D. L. Judge, and C. P. Sonett, Characteristics of the extraterrestrial current system; Explorer VI and Pioneer V, *J. Geophys. Research, 65,* 1858–1861, 1960.

Smith, E. J., and A. Rosen, The scientific results of the satellite Explorer VI, *Ballistic Missile and Space Technology, III,* Academic Press, New York, 450 pp., 405–443, 1960.

Sonett, C. P., E. J. Smith, D. L. Judge, and P. J. Coleman, Jr., Current systems in the vestigial geomagnetic field: Explorer VI, *Phys. Rev. Letters, 4,* 161–163, 1960.

Sonett, C. P., D. L. Judge, A. R. Sims and J. M. Kelso, A radial rocket survey of the distant geomagnetic field, *J. Geophys. Research, 65,* 55–68, 1960.

Van Allen, J. A., The geomagnetically trapped corpuscular radiation, *J. Geophys. Research, 64,* 1683–1689, 1959.

Vernov, S. N., A. E. Chudakov, P. V. Vakulov and Yu. I. Logachev, Study of terrestrial corpuscular radiation and cosmic rays during the flight of a cosmic rocket, *Soviet Phys. Doklady, 4,* 338–342, 1959.

Walt, M., L. F. Chase, Jr., J. B. Cladis, W. L. Imhof, and D. J. Knecht, Energy, spectra and altitude dependence of electrons trapped in the earth's magnetic field, *Space Research,* edited by H. K. Kallman Bijl, North Holland Publishing Company, Amsterdam, pp. 910–920, 1960.

(Manuscript received May 31, 1961.)

Energy Spectrum and Angular Distributions of Electrons Trapped in the Geomagnetic Field

J. B. CLADIS, L. F. CHASE, JR., W. L. IMHOF

Lockheed Aircraft Corporation, Missiles and Space Division
Sunnyvale, California

D. J. KNECHT

Air Force Special Weapons Center, Kirtland AFB, New Mexico

Abstract. The energy spectrum and the pitch-angle distribution of the electrons near the lower edge of the outer radiation zone were measured by means of a collimated magnetic-deflection spectrometer carried in a Javelin rocket. The rocket was launched from Wallops Island, Virginia, and reached an altitude of 1045 km. Along the ascent trajectory, the rocket followed closely a geomagnetic line of force, permitting measurements of the electron flux to be made along the reflection points of the electrons. The pitch-angle distributions of the electrons were found to be symmetrical about 90° and to have widths that increased as the rocket moved up the magnetic field line. The widths of these distributions at half-height were found to be 31.2° at 750 km and 41.6° at 920 km. The spectrometer data yield a spectrum which can be fitted well by the form $E^p \exp(-qE)$, where $p = 1.60\ ^{+0.74}_{-0.44}$, $q = 0.022\ ^{+0.0025}_{-0.0019}$ kev^{-1}, for $E > 50$ kev. Within the accuracy of the measurements, no change in spectrum shape was observed at altitudes greater than about 600 km. At apogee the omnidirectional intensity of electrons of energies greater than 50 kev was found to be $4.2 \pm 0.8 \times 10^6$ electrons/cm^2-sec.

INTRODUCTION

Initial information on the trapping of charged rticles by the earth's magnetic field was ob-ined by *Van Allen, Ludwig, Ray, and McIl-ain* [1958], *Van Allen, McIlwain, and Ludwig* 959], *Rosen, Sonett, Coleman, and McIlwain* 959], *Van Allen and Frank* [1959*a*, *b*], and *an Allen* [1959]. The detailed spatial distribu-ons of the radiation obtained by these investi-tors revealed the approximate symmetry of e flux about the magnetic dip equator and owed the existence of two zones of radiation n inner and an outer zone).

Later measurements yielded information on e nature of the particles in these zones. The netrating radiation of the outer zone was ind to consist predominantly of electrons *ernov, Chudakov, Vakulov, and Logacher,* 59; *Vernov and Chudakov,* 1960]. At low lat-ides, the intensity distribution of these elec-ons extends from an altitude of about 600 km an altitude of 8 or more earth radii, with the aximum occurring near an altitude of 16,000 [*Fan, Meyer, and Simpson,* 1960; *Rosen, rley, and Sonett,* 1960; *Arnoldy, Hoffman,* and *Winckler,* 1960; and *Holly and Johnson,* 1960]. A measurement of the integral spectrum of these electrons made by *Vernov, Chudakov, Vakulov, and Logacher* [1959] indicates that this spectrum drops off as the fifth power of the energy above the minimum threshold energy of their detectors (about 50 kev). The inner zone contains very high energy protons [*Freden and White,* 1959] in addition to the electrons described above. The intensity distribution of the protons in the region near the equatorial plane extends in altitude from about 900 to about 8300 km, with the maximum occurring near 3800 km [*Fan, Meyer, and Simpson,* 1960].

In this report we present information obtained with a Javelin sounding rocket. This was a four-stage, solid-propellant rocket (XM-20, XM-45, XM-45, X-248), which was launched from Wallops Island, Virginia, on July 7, 1959, and reached an altitude of 1045 km. Preliminary data obtained from this flight were presented at the First International Space Science Symposium at Nice, France, [*Walt, Chase, Cladis, Imhof, and Knecht,* 1960] and at the American Physical Society Meeting in New York [*Cladis, Chase,*

Imhof, and Knecht, 1960]. The ascent trajectory of this rocket generally followed a magnetic line of force which extends to a geocentric distance of 2.4 earth radii (altitude of 8900 km) in the equatorial plane, as shown in Figure 1. Along this portion of the flight, measurements were made as the rocket passed the reflection points of the particles trapped in the outer zone. Along the descent trajectory, measurements of the radiation were made as the rocket crossed magnetic lines of force. For a period of 1 week before the flight, the K_p magnetic index never exceeded 5. This index was equal to 3 during the flight.

Following burnout of the final stage of the rocket, the nose cone was ejected to expose the instruments directly to the radiation. Data from the instruments were telemetered to ground stations by a standard FM-FM system. This telemetering unit was designed and manufactured by United Electrodynamics, Inc., Pasadena, California. Telemetry ground stations were located at Wallops Island, Virginia; at Cape Canaveral, Florida; and at Antigua Island, British West Indies. The trajectory of the vehicle was computed from elevation and azimuth readings of the tracking antennas at these stations.

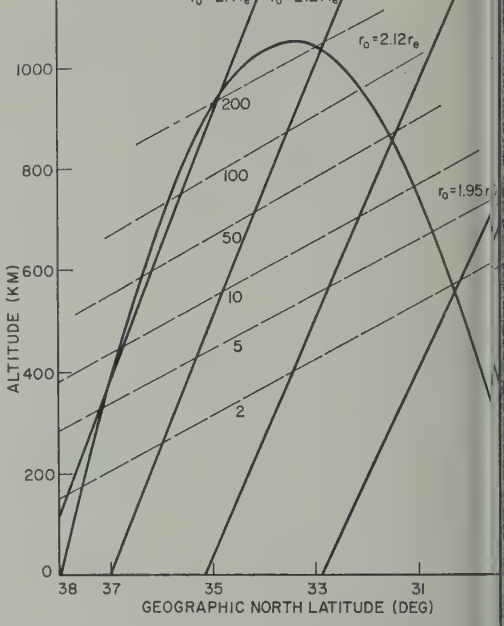


Fig. 1. Rocket trajectory. The dashed li represent approximate isocount contours. Seve geomagnetic lines of force are also shown; th geocentric distances at the magnetic equator given in earth radii.

Instrumentation

The principal radiation instrument carried by the rocket was a magnetic-deflection spectrometer shown in Figure 2. Electrons passing through the collimator were deflected (upward in the figure) by the field of a permanent magnet into the four end-window Geiger tubes; the lowest energy electrons passed into tube 5 while higher energy electrons fell successively into tubes 4, 3, and 2. Very energetic electrons (greater than 1.5 Mev) and protons (greater than 1 Mev) passed essentially undeflected into tube 1. The spectrometer was shielded by 10 g/cm^2 of brass.

A second detector was an Anton-302 Geiger tube, placed in the package with no deliberate shielding. Its purpose was largely to correlate the present data with those of Explorer IV which carried an identical Geiger tube.

A Schonstedt flux gate magnetometer, a commercially available device which measures the component of the field along the axis of the magnetometer probe, was included to yield information on vehicle orientation with respect to the magnetic field.

The spectrometer was calibrated with monoenergetic electrons from a 180° beta-ray sp trometer. By varying the energy of the sou electrons, the energy sensitivity of each coun channel in the spectrometer was obtained. Th data were taken with electrons incident fro number of angles. By integrating directio data over the view solid angle of the spectro ter, the response functions were obtained an incident flux isotropic over the aperture the collimator. Figure 3 shows these respo functions for the individual Geiger tubes. T counting rate of tube k in a flux that is isotro within the view solid angle of the collimato given by

$$C_k = \int g_k(E) f(E)\, dE$$

where $g_k(E)$ is the appropriate function of Fig 3 and $f(E)$ is the flux of electrons in units number·cm^{-2}·sec^{-1}·kev^{-1}·steradian^{-1}. The sponse functions obtained in this way w verified by exposing the spectrometer to c brated sources of W^{185}, Tl^{204}, and $Sr^{90}Y^{90}$. T were also verified analytically by computing

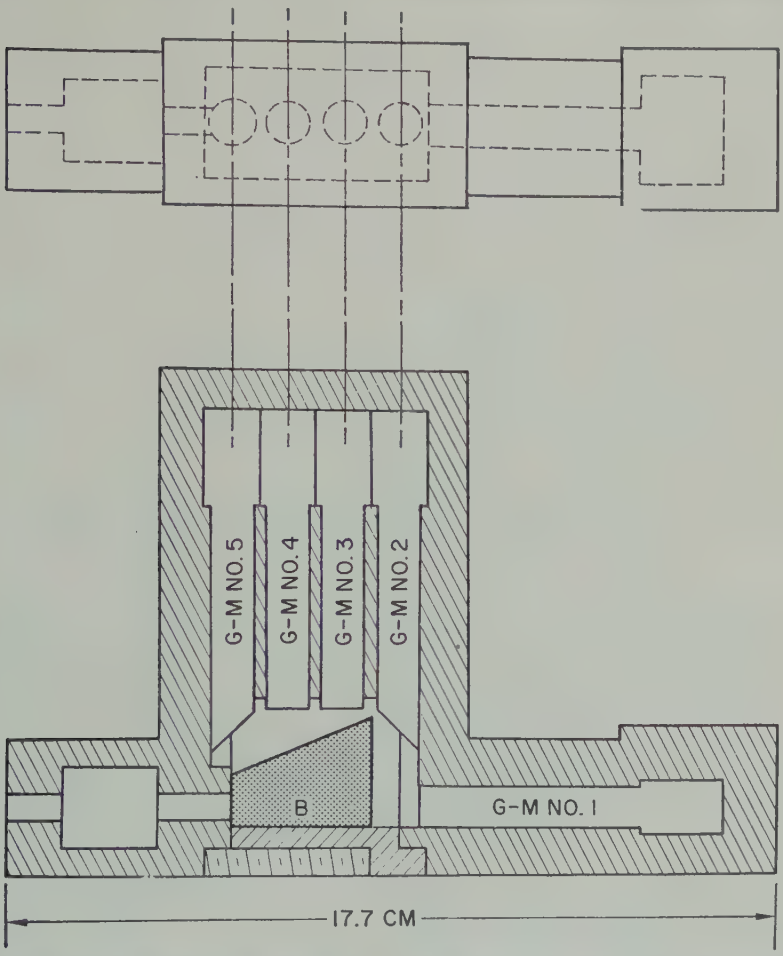


Fig. 2. Diagram of magnetic spectrometer. The electrons entered from the left, were bent upward by the magnetic field B, and were detected by the end-window Geiger counters.

nergy-dependent geometric functions of the ounter channels and multiplying these functions y the transmission of the Geiger tube windows. Since the spectrometer was well collimated nd the vehicle was designed to spin about its ongitudinal axis, the following information ould be expected from these instrumentations:

1. The intensity, the direction, and the energy spectrum of electrons between about 50 kev and 1 Mev.
2. The correlation of the directional measurements with the direction of the magnetic field.
3. The total flux and direction of higher energy particles (greater than 1.5 Mev for electrons and 1.0 Mev for protons).

The instrumentation also permitted a rough correlation of intensities with those of the Explorer IV measurements and a rough measure of the magnetic-field intensity.

Analysis of Orientation Data

The output of the flux gate magnetometer was a linear function of the component of the magnetic field intensity along its probe axis. The probe was mounted at a known angle with the vehicle axis so that if the vehicle spun around its axis, the output signal would be an oscillating voltage unless the vehicle happened to be aligned with the field. A sample of the signal actually obtained is shown in the lower part of Figure 4. The short-period oscillation corresponds to the

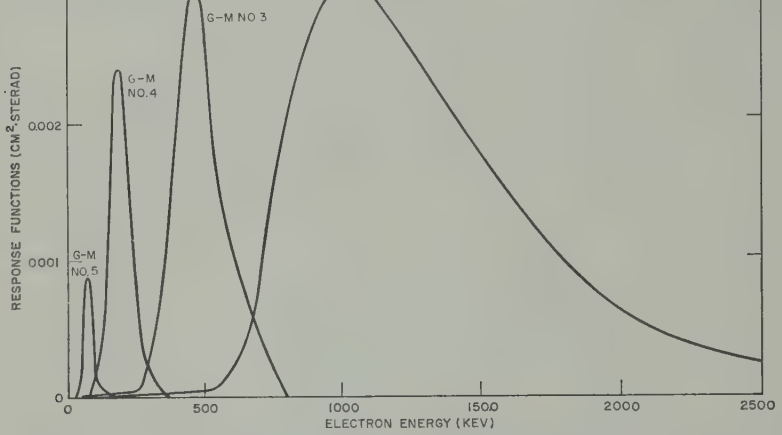


Fig. 3. Response functions of Geiger tubes. The counting rate of the kth tube is given by the integral $C_k = \int f(E)\, g_k(E)\, dE$, where $f(E)$ is the electron flux.

spinning of the vehicle whereas the longer-period oscillation forming the envelope indicates a precession. The vehicle behaved like a simple top, as shown in the upper part of Figure 4. The probe **P** rotated in a cone about the vehicle spin axis **S**, while the spin axis precessed in a cone about an axis of constant angular momentum Z. This in turn was inclined to the field direction $\mathbf{B}_0$.

A mathematical expression for the time-varying signal in terms of the various angles involved is given in Appendix A. This appendix also contains a description of two simplified analytical methods of deducing the vehicle orientation angles from the magnetometer signal. The first method is based on the maxima and minima of the signal envelope; the second, on the frequency change of the signal within a precession period of the rocket. The first method gave the more accurate results; the second proved difficult to apply because of the relatively large frequency change per cycle which occurred over regions of the precession cycle about the points marked B_M, and B_m, in the lower part of Figure 4. Accurate orientation angles were obtained by use of the first method. Substantially the same results were obtained by making a least-squares fit of the expression given in Appendix A to the raw signal (instead of the envelope only) using a digital computer. It was found that the vehicle precessed in a cone of 31.5° half-angle (angle between **S** and Z), while the magnetic field intensity $\mathbf{B}_0$ varied in inclin tion to the constant angular momentum vect (along Z) from 36.8° to 40°, in a way consista with the motion of the vehicle through the fiel The angle between the probe **P** and the sp axis **S** was found to be 51.4°, as compared wi the intended preset value of 54.7° with t vehicle axis. These angles (except that betwe $\mathbf{B}_0$ and Z) remained constant within maximu individual deviations of about ±0.5° over t duration of the flight, and knowledge of th values allows an unambiguous interpretation the data on directional intensities.

Analysis of Spatial Distribution Data

A first result from the spectrometer data is measure of counting rate as a function of altitud The essential features are shown in Figure In this figure, a trajectory is projected onto meridian plane; the dashed lines drawn acr the trajectory connect points on ascent a descent where counting rates were equal, a are thus an approximation to the isocou contours in this vicinity. The numbers indic the counting rate (counts per second) of Gei tube 4. (In view of the results to follow, all f tubes would give the same shape of isocou lines.) The tilt of these lines indicates hig counting rates at higher latitude; that is, t the trajectory falls on a magnetic line of fo which lies on the inner edge of the outer zo This is indeed the case; the line followed

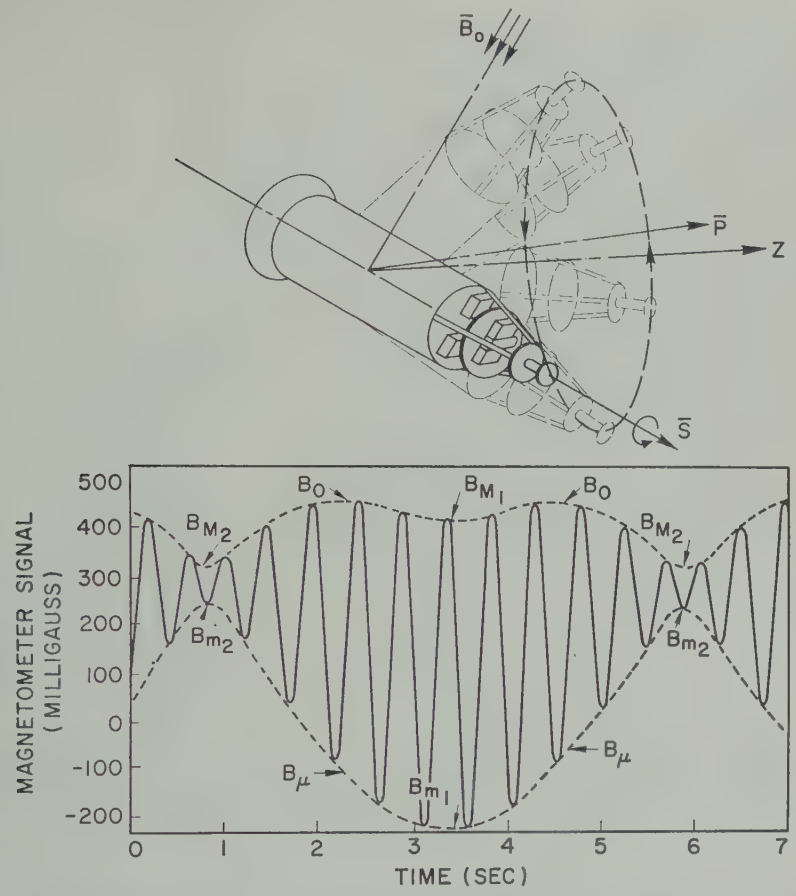


Fig. 4. Body motion of rocket in flight and sample of magnetometer output.

cent reaches an altitude of 8900 km in the ane of the geomagnetic equator[1] while lunar obe and satellite data show the lowest maxi- um of the outer belt to lie at about 11,000 km *an, Meyer, and Simpson*, 1960; and *Arnoldy, offman, and Winckler*, 1960].

NALYSIS OF DIRECTIONAL DISTRIBUTION DATA

The spin and precession of the vehicle offered opportunity to measure the distribution in gle of the particle velocities with respect to e local geomagnetic field vector. At certain ints in the precessional period, the vehicle n caused the collimator axis to cut quite squarely through the plane perpendicular to the geomagnetic field, yielding a profile of counting rate as a function of angular displacement. (The collimator axis was perpendicular to the vehicle axis.) Since the orientation of the collimator axis with respect to the magnetometer probe was known, the angular displacement α of the collimator axis from the local magnetic field lines was easily related to the magnetometer signal. The electron intensity was then correlated with the angle α by recording the Geiger tube counts which occurred in certain phase intervals of the magnetometer signal.

Not all of the Geiger tube counts could be used to determine the angular distribution of the electrons. The counting-rate information from each channel was obtained on telemetry subcarriers as a stair-step-level signal indicating the states of binary scalers. Therefore, only the

[1] The altitude of the magnetic line of force in e plane of the geomagnetic equator was obtained m the 512-term, spherical harmonic expansion the geomagnetic field [*Jensen, Murray, and elch*, 1960].

counts which produced a change in the level of the stair-step signal could be used to determine the distribution. The times at which other counts occurred were unknown, and therefore could not be correlated with the phase of the magnetometer signal.

The scaling of the Geiger tube pulses and the rather rapid spin of the vehicle required the superposition of data from many cuts through the normal plane taken at corresponding points in consecutive precession periods in order to obtain adequate statistics. Even so, statistically significant distributions were obtained only for electrons detected by Geiger tubes 4 and 5 (energy groups centered about 185 and 75 kev, respectively); the counting rates of the other Geiger tubes were too low. Within the accuracy of these measurements, the distributions of the electrons of these two energy groups were found to be identical to each other and symmetrical about the plane perpendicular to the magnetic field, $\alpha = 90°$.

The angular distribution data obtained at 750 and at 920 km are given by the rectangles in Figures 5 and 6, respectively. These results were obtained by combining the counts of Geiger tubes 4 and 5. The counts were accumulated over an altitude range of ± 100 km about the 750-km level and over a range of ± 50 km about 920 km. Moreover, counts occurring at angles $\pi - \alpha$ were combined with counts occurring at α to improve the statistics. Finally, although counts were recorded in 3° intervals of α, counts in adjacent intervals were combined as shown by the widths of the rectangles depicting the data. The heights of these rectangles give the probable errors of the measurements. A similar analysis made for altitudes of 690, 845, and 1035 km yielded similar results with the distribution width becoming narrower for lower altitudes.

For the time intervals used in the accumulation of the distribution data, the total number of counts of Geiger tubes 4 and 5 (not just counts required to change scaler levels) were also recorded. This information was used to obtain the directional distribution in units of $(I_4 + I_5)$, as indicated on the ordinate scale used in the figures. The symbols I_4 and I_5 represent integrations of the energy spectrum of the electrons over the response functions of Geiger tubes 4 and 5, respectively. This normalization of the data is described in section 1 of Appendix B.

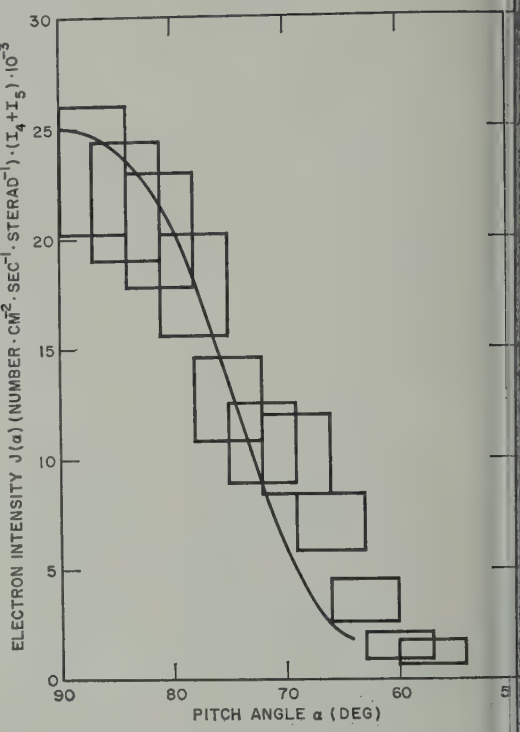
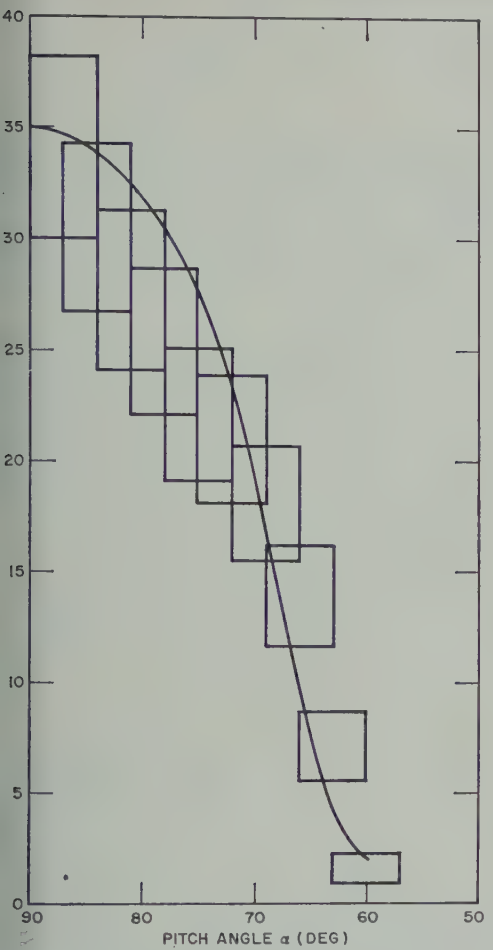


Fig. 5. Pitch-angle distribution of electrons a 750 km. The rectangles represent the direct meas urements of the distribution obtained by correla ing the counting rates of the Geiger tubes with th angle the collimator made with the local geoma netic field vector. The curve in the figure is th distribution computed from the measurements the mirror-point values of the flux along the geo magnetic field line at lower altitudes.

The directional distributions that are show as solid curves in Figures 5 and 6 were obtaine by an entirely different method. They we computed from the counting rates of Geig tubes 4 and 5 at lower altitudes during th ascent of the rocket along the magnetic line force. The computation was based on the fo lowing characteristics of geomagnetically trapp particles.

1. A particle which has a pitch angle α_1 wi respect to the field line at an altitude where th magnetic field intensity is B_1 will have a larg pitch angle α_2 at a lower altitude along th field line where the field intensity is B_2, accordi to the equation

$$\frac{\sin^2 \alpha_2}{B_2} = \frac{\sin^2 \alpha_1}{B_1} \qquad (1$$



. 6. Pitch-angle distribution of electrons at 920 km. (For explanation, see Fig. 5.)

is equation follows directly from the adiabatic ariance of the magnetic moment of a spiraling rged particle. Hence, as the particle spirals und a magnetic field line towards lower tudes, its pitch angle continually increases. e particle becomes 'reflected' at the position ng the field line where its pitch angle reaches limiting value $\pi/2$. The magnetic field nsity at the mirror point of the particle is refore given by the equation

$$B_m = B_1/\sin^2 \alpha_1$$

. The second characteristic follows from uville's theorem which states that the density particles in phase space is a constant of the ion where particle and electromagnetic inter- ons are unimportant. This theorem leads to the following relationship between the electron flux at a position where the magnetic field intensity is B_1 and the flux at another position along the same field line where the field intensity is B_2:

$$f(B_1, \alpha_1) = f(B_2, \alpha_2) \tag{3}$$

where the flux is measured for the directions α_1 and α_2 so that these parameters satisfy equation 2. The flux f is defined in the usual way, with units of number·(solid angle)$^{-1}$·(unit area)$^{-1}$·(unit time)$^{-1}$·(unit energy interval)$^{-1}$.

From the above equations it follows that

$$f(B_1, \alpha_1) = f(B_m, \pi/2) \tag{4}$$

where

$$B_m = \frac{B_1}{\sin^2 \alpha_1} \tag{5}$$

The directional distribution of electrons at the altitude where $B = B_1$ was obtained by using equation 4 to calculate $f(B_1, \alpha_1)$* for various values of α_1, with values of $f(B_m, \pi/2)$ computed from the counting-rate data as shown in section 2 of Appendix B. For each value of α_1, the flux value at $\pi/2$ was taken for an altitude corresponding to B_m as given by equation 5. (The magnetometer data were used to correlate the counting rates with the local magnetic field intensity.) In order to compare the directional flux distributions given by this method with those measured directly at the central altitudes of 750 and 920 km, the counting rates of Geiger tubes 4 and 5 were combined, as shown in section 2, Appendix B.

The results given in Figures 5 and 6 show that the directional distributions obtained by these two independent methods are in fairly good agreement, both in form and in absolute magnitude. Somewhat better agreement would have been obtained if the direct measurements, given by rectangles in the figures, had been corrected for the finite angular aperture of the collimator. This correction was not computed in detail because it does not appreciably affect the width at half-maximum. (Roughly, one can see that this correction would have raised the peak value of these distributions about 4 per cent and reduced the tails about 3°.) The distributions computed from the mean counting rates of the Geiger tubes are not appreciably influenced by the finite aperture of the collimator.

The observed distribution at 1035 km is appreciably different from that computed by the latter method, being about 9° narrower. This is to be expected, however, since at this point the trajectory has departed from the field line along which the quantities $f(B_m, \pi/2)$ were observed, and is crossing a field line which lies away from the peak of the outer zone.

Analysis of Energy Spectrum Data

The third and most important result from the spectrometer is the measurement of electron energy spectra and intensities. Following equation 1 the instantaneous counting rate in Geiger tube k can be expressed by

$$C_k(\alpha) = \int g_k(E) f(E, \alpha)\, dE \qquad (6)$$

where the angle α is the angular displacement of the collimator axis from the direction of the local geomagnetic line of force. In this equation, as well as in the analysis which follows, the angle α is also used to designate the pitch angle of the electrons. This should lead to no confusion, however, because the flux $f(E, \alpha)$ was taken to be constant over the angular aperture of the collimator; that is, separate integrations over solid angle were not performed.

In order to obtain the counting rates of the detectors with good statistical accuracy, it was necessary to average the counting rates over a time interval that was large in comparison with the precession period of the rocket. We therefore define an average flux $f_p(E)$ which is measured over one full precession period T_p of the rocket as follows:

$$f_p(E) = \frac{1}{T_p} \int_0^{T_p} f(E, \alpha)\, dt$$

This can also be written as

$$f_p(E) = \int_{\alpha_{min}}^{\pi/2} f(E, \alpha) w(\alpha)\, d\alpha \qquad (7)$$

where

$w(\alpha)\, d\alpha$ = fraction of each precession period during which collimator is directed between α and $\alpha + d\alpha$. (Symmetry of $f(E, \alpha)$ about $\alpha = \pi/2$ is assumed.)

α_{min} = minimum angular displacement of collimator from magnetic field line during body motion of rocket ($\alpha_{min} \simeq 21°$).

The weighting function

$$w(\alpha) = \frac{2}{T_p} \left\langle \frac{dt}{d\alpha} \right\rangle$$

was computed by differentiating the time dependent mathematical expression for α (equation 32, Appendix A) and averaging the reciprocal of this expression over all phase angles of rocket-spin motion within the precession cycle. This weighting function is shown in Figure 7.

The energy spectrum will be given in terms of still another flux, the omnidirectional flux $F_0(E)$, which is the flux that passes through a sphere of unit cross-sectional area (that is, an omnidirectional detector). This flux has the units: number · (unit area)$^{-1}$ · (unit time)$^{-1}$ · (unit energy interval)$^{-1}$. It is the flux per differential solid angle, $f(E, \alpha)$, integrated over 4π:

$$F_0(E) = 2 \int_0^{\pi/2} f(E, \alpha) 2\pi \sin \alpha\, d\alpha$$

Thus, equations 7 and 8 give

$$F_0(E) = \left[4\pi \frac{\int_0^{\pi/2} f(E, \alpha) \sin \alpha\, d\alpha}{\int_{\alpha_{min}}^{\pi/2} f(E, \alpha) w(\alpha)\, d\alpha} \right] f_p(E)$$

$$= K f_p(E) \qquad (8)$$

The quantity within brackets termed K is computed by using the angular distribution given by the curves of Figures 5 and 6. Its value is $K = 9.9$, and it is not appreciably different for distributions narrower than those shown in the figures.

Now, following equation 6, the mean counting rate of a Geiger tube over a precession period of the rocket can be written as

$$\langle C_k \rangle = \int g_k(E) f_p(E)\, dE$$

or

$$\langle C_k \rangle = \frac{1}{K} \int g_k(E) F_0(E)\, dE \qquad (9)$$

If each tube is sensitive to only a very narrow energy interval ($E \simeq E_k$) or if the energy spectrum is relatively flat within that interval, we may write the approximation

$$K \langle C_k \rangle \simeq F_0(E_k) \int g_k(E)\, dE$$

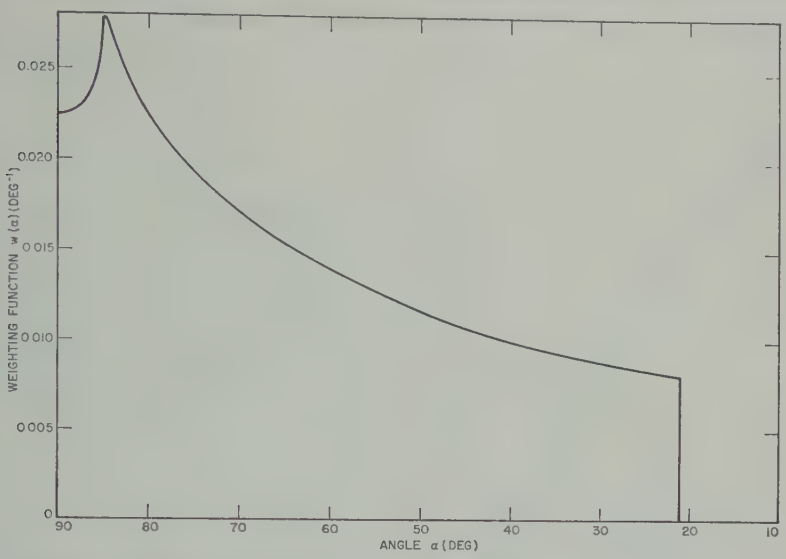


Fig. 7. The function $w(\alpha)\ d\alpha$ represents the fraction of each precession period that the collimator is directed along α in the interval $d\alpha$. The angle α is measured from the direction of the geomagnetic field vector.

$$F_0(E_k) \simeq \frac{K\langle C_k\rangle}{G_k} \qquad (12)$$

ere G_k represents the integral over energy of response function of the tube. The counting es $\langle C_k\rangle$, of course, are the values obtained er corrections are made for cosmic ray back- und. This background was determined when rocket was at low altitudes, below the oped radiation, both on the ascent and descent tions of the trajectory. It is apparent from ure 3 that the approximation equation 12 is ly good for Geiger tube 5, but it becomes gressively worse for Geiger tubes that detect ier-energy electrons. Nevertheless, this pro- ure serves as a first step in the iterative edure to find the true spectrum.

t the altitude of 920 km during ascent, the roximate values of the flux detected by Geiger es 3, 4, and 5, as computed by means of ation 12, are described by the rectangles in ure 8. The heights of these rectangles reflect probable errors of the counting-rate data, the horizontal extent of the rectangles esent the energy regions within the half- ht values of the response function of the es.

he flux detected by Geiger tube 2 cannot be computed in this way, not only because of the extreme width of the response function of that tube, but principally because of a long low-energy tail which exists in that response function owing to the scattering of low-energy electrons in the spectrometer. The height of the function in this low-energy region is quite small, as is shown in Figure 3. Nevertheless, because of the steep spectrum, the integration of equation 11 over this portion of the response function, using the values of $F_0(E)$ indicated by the rectangles in Figure 8, yields a counting rate that is essentially the same as that observed by the tube after correction for cosmic-ray background. (The counting rate of the tube at apogee was less than four times cosmic-ray background.) The uncertainty in this highest-energy point therefore is very large, and it serves more or less as an upper limit on this point of the spectrum. (That portion of the response functions arising from the scattering of low-energy electrons into tubes 1, 2, and 3 were computed subsequent to the presentation of the preliminary results [*Walt, Chase, Cladis, Imhof, and Knecht*, 1960] from calibration data taken with the 180° beta-ray spectrometer.)

Several iterations of the spectrum shape using equation 11 indicated that a good fit to the data could be obtained by using the mathematical form

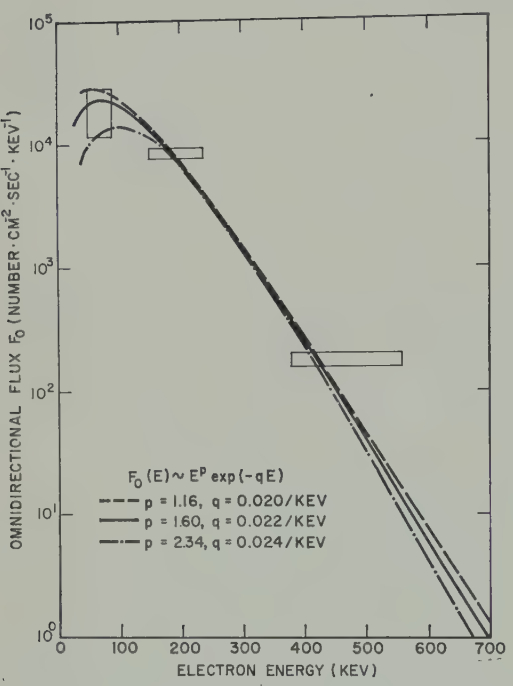


Fig. 8. Omnidirectional electron flux at 920 km. The rectangles give the first approximation to the spectrum; the heights of the rectangles designate probable errors of the measurements; and the horizontal extents of the rectangles represent the energy-sensitive regions of the Geiger tubes (half-height values of response functions). The solid-line curve gives the best fit of the mathematical form $E^p \exp(-qE)$ to the data. This best-fit curve was obtained for $p = 1.60$, $q = 0.022$/kev. The dashed lines give the extreme spectrum shapes that fit the data with a probability of $1/e$ that of the best fit.

$$F_0(E) = AE^p \exp(-qE) \qquad (13)$$

Hence, a digital computer was programmed to integrate equation 11 repeatedly for certain ranges of the parameters A, p, and q. For each set of these parameters, the computer printed out the counting rate given by each integration and a 'fit index' I given by the following equation:

$$I = \sum_{k=2}^{5} h_k^2[(\langle C_k \rangle)_c - (\langle C_k \rangle)_m]^2 \qquad (14)$$

where

$(\langle C_k \rangle)_c$ = computed counting rate of Geiger tube k.

$(\langle C_k \rangle)_m$ = measured counting rate of tube k minus cosmic-ray background.

h_k = precision index of measurem made by Geiger tube k. (Er due to counting statistics, m urements of response functi and scattering corrections are cluded here.)

The best fit (minimum value obtained for I 0.214) resulted from $p = 1.6$ and $q = 0.$ kev^{-1}. (The parameter A was chosen to malize to the observed counting rate of tube This spectrum is shown as a solid line in Figu At the altitude of 920 km, the computed coun rates of the tubes, based on this spectrum, the measured counting rates above cosmic background compare as follows:

(Counting rates are given in number per seco

	2	3	4	
$(\langle C_k \rangle)_m$	5.18	17.4	202	7
$(\langle C_k \rangle)_c$	4.87	17.2	202	8

The range in the shape of the spectrum ca investigated by plotting the parameter p aga q for constant values of I. Such curves resen concentric elongated ellipses with the long generally along the direction of increasing va of p and q. Each ellipse is the locus of po (p, q) which define a family of spectrum sha that fit the data with a probability proporti to e^{-I}. Hence, by selecting the extreme va of p and q which fall on the ellipse for $I_{\min} +$ one obtains the spectrum curves which are limiting envelope of all spectra that fit data with a probability no less than $1/e$ of the best fit. These limiting curves re from $p = 1.16$, $q = 0.020$/kev and $p = 2$ $q = 0.024$/kev and are plotted as dashed cu in Figure 8. Here, the spectra were arbitra normalized to the best fit spectrum at 200

The data of *Vernov, Chudakov, Vakulov, Logacher* [1959] indicate that the differe spectrum of the electrons in the outer radia zone drops off as E^{-6} above about 50 kev. best-fit spectrum given above, namely:

$$F_0(E) \sim E^{1.6} \exp(-0.022E)$$

has the same slope as E^{-6} only in the re near 350 kev.

The shape of the spectrum remained essent unchanged throughout the spatial regions of investigations. Spectrum shapes as a functio the position of the rocket were compared plotting the counting rate ratios $C_k/C_4 (k \neq$ as a function of time.

The omnidirectional intensity of electrons ve 50 kev at 920 km is given by the integral

>50 kev)

$$\int_{50\text{ kev}}^{\infty} AE^{1.6} \exp(-0.022E)\, dE \qquad (15)$$

$(3.4 \pm 0.7) \times 10^6$ electrons/cm^2·sec

ce the omnidirectional flux is not very sensitive the angular distribution of the electrons and change in the spectrum as a function of tude was not observed, the omnidirectional nsity $\Phi(>50$ kev) for other positions along trajectory of the rocket is merely pro- tional to the counting rates of the detectors. is intensity as a function of altitude along ascent and descent paths of the rocket is wn in Figure 9. At low altitudes the vertical s at the data points are standard deviations to counting statistics. Near apogee, these s include estimates of tape-reading errors.

Estimate of the Proton Content

The straight-through counter, tube 1, detected trons of energy greater than about 1.5 Mev protons of energy greater than 1 Mev. e lower limit on proton energy results from thickness of the window.) After subtracting cosmic-ray background (1.8/sec) and the tron-scattering correction (3.8/sec), the re- ning counting rate of this tube at 920 km 0.5 ± 0.6 count per second. By dividing this nting rate by the geometric factor of the nter channel and multiplying by K (see ation 10) and assuming that the high-energy has an angular distribution which is similar hat of the lower-energy electrons, the omni- ctional intensity above 1 Mev becomes

>1 Mev) $= (3.8 \pm 5.0) \times 10^3$/cm^2·sec

ce, the ratio of particle intensity obtained tube 1 to the electron intensity given by ation 15 is $(1.1 \pm 1.3) \times 10^{-3}$. We can efore conclude that the intensity of protons energies greater than 1 Mev must be ller than the electron intensity above 50 by at least a factor of 500.

Analysis of the 302 Geiger Tube Data

t 920 km, the Anton-302 tube had a counting of 11.4/sec above cosmic-ray background 3/sec). This tube was approximately an

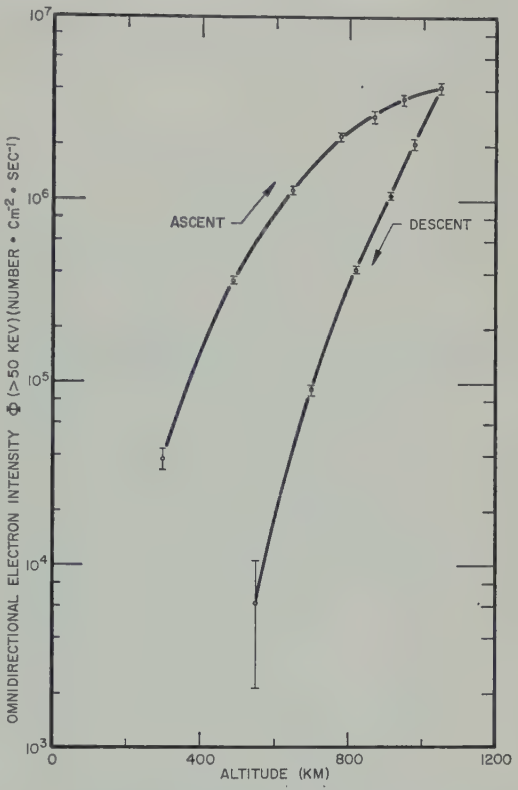


Fig. 9. Omnidirection intensity of electrons having energies greater than 50 kev vs. altitude.

omnidirectional detector of 0.42 cm^2 cross-sectional area, except that it was shielded over about half the full solid angle. Also, the efficiency for counting electrons was never more than 50 per cent; it fell to 40 per cent at 1600 kev and 5 per cent at 1000 kev. Its threshold, owing to wall thickness, was at 600 kev for electrons and about 15 Mev for protons.

It was therefore hoped that this tube would give additional information concerning the intensity of electrons above 600 kev. Unfortunately, the 302 counting rate probably resulted entirely from bremsstrahlung. A computation of the counting rate of the tube due to the detection of the bremsstrahlung produced in the walls of the counter by the electron flux given in Figure 8, for $E < 600$ kev, yields a value which is not significantly different from the measured counting rate of the tube above cosmic-ray background. If the bremsstrahlung contribution had been small, then the counting rate of the 302 tube would have required a somewhat higher tail of

the electron spectrum shown in Figure 8, since the flux in Figure 8 yields the counting rate

$$\langle C_{302} \rangle \simeq 2\pi(0.42) \cdot \int_{600\ \mathrm{kev}}^{\infty} \eta(E) F_0(E)\, dE \simeq 0.5/\mathrm{sec}$$

where η is the counting efficiency.

Comparison of Results with Explorer IV Data

The contours of constant counting rate of the 'unshielded' 302 Geiger tube used in the Explorer IV satellite, as given by *Van Allen, McIlwain, and Ludwig* [1959], reveal that the counting rate of that detector averaged over the data obtained from July 26 to August 26, 1958, was 30 counts/sec at a spatial position 160 km above apogee of the Javelin rocket. The counting rate of the 302 Geiger tube used in the Javelin experiment was about 14 counts/sec at apogee. These counting rates are essentially the same when corrections are made for the altitude difference and for the somewhat different geometric factors and absorber thicknesses, assuming that both 302 tubes were detecting bremsstrahlung alone. Hence, we may infer that the intensity of the electrons ($E \gtrsim 80$ kev) in this region of the outer zone was not unusually high or low at the time of our measurements, but was representative of the intensity prevalent during the Explorer IV observations.

Appendix A: Determination of the Body Motion of the Rocket from the Magnetometer Signal

Method 1. The analysis of the body motion of the rocket during the flight will be described with reference to Figure 10. Here, the origin of the coordinate system X, Y, Z is considered to be located at the center of mass of the rocket, with the Z axis aligned with the constant angular momentum vector, the vector which remains fixed in direction throughout the flight. The X axis is directed so that the geomagnetic field vector $\mathbf{B}_0$ lies in the X-Z plane. The vector $\mathbf{P}$ depicts a unit vector aligned with the axis of the Schonstedt probe. It forms an angle μ with the unit vector $\mathbf{S}$ which is aligned with the spin axis of the rocket and rotates in a cone about S with the angular velocity $d\varphi/dt$ (spin rate). The vector S forms an angle θ with the Z axis and rotates in a cone about the Z axis with the angular

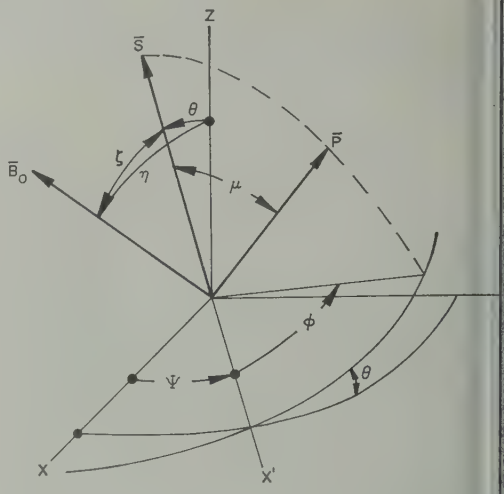


Fig. 10. Coordinate system used to describe output of the flux-gate magnetometer.

velocity $d\psi/dt$ (precession rate). The angl and ψ are the usual Euler angles.

Now, if η denotes the angle between $\mathbf{B}_0$ the Z axis, and β the angle between $\mathbf{B}_0$ an the signal from the aspect magnetomete proportional to

$$B = B_0 \cos\beta$$

where

$$\cos\beta = \sin\eta \sin\mu (\cos\psi \cos\varphi - \cos\theta \sin\psi \sin\varphi) + \sin\eta \cos\mu \sin\theta \sin\psi + \cos\eta \sin\mu \sin\theta \sin\varphi + \cos\eta \cos\mu \cos\theta$$

A sample of the signal obtained is show the lower part of Figure 4. The rapid oscillat are due to the spin of the rocket about longitudinal axis, and the modulation is ca by the precession of this axis about the cons angular momentum vector.

Certain points on the envelope of the os tions correspond to the special cases in whic of the vectors $\mathbf{B}_0$, $\mathbf{Z}$, $\mathbf{S}$, and $\mathbf{P}$ lie in a plan more accurately, are extrapolated to this co tion by drawing the envelope), and the ang is a simple addition or subtraction of η, θ, a These cases occur when φ and ψ are $\pm \pi/2$, equation (17) simplifies accordingly. At points on the envelope marked B_{M_1} and B

gure 4, the spin axis S was the farthest removed
om the direction of the magnetic field vector
. Here $\psi = -\pi/2$, and equations 16 and 17
come

$$_{M_1} = B_0 \cos(\eta + \theta - \mu) \quad \text{for } \varphi = \pi/2 \quad (18)$$

d

$$_{m_1} = B_0 \cos(\eta + \theta + \mu) \quad \text{for } \varphi = -\pi/2 \quad (19)$$

the points marked B_{M_1} and B_{m_1} in Figure 4,
e spin axis reached its nearest proximity to $\mathbf{B}_0$.
ere, $\psi = \pi/2$, and equations 16 and 17 become

$$_{M_2} = B_0 \cos(\eta - \theta - \mu) \quad \text{for } \varphi = -\pi/2 \quad (20)$$

d

$$_{m_2} = B_0 \cos(\eta - \theta + \mu) \quad \text{for } \varphi = \pi/2 \quad (21)$$

The four equations, 18, 19, 20, and 21, can be
ed to evaluate the four unknowns B_0, η, θ,
d μ at any time t during the flight if values of
$_{M_1}$, B_{m_1}, B_{M_2}, and B_{m_2} are interpolated to the
me time t. This can be done by reading these
lues off the entire trace obtained during the
ght, plotting them on a graph against their
ividual times of occurrence, and drawing a
ooth curve through the data.

Two other points on the envelope, marked B_0
d B_μ in Figure 4, correspond to another
ecial case where all vectors are not coplanar
t where the cone described by **P** about **S** has
ecessed to the point at which it contains the
ld vector $\mathbf{B}_0$. Then, only $\mathbf{B}_0$, **S**, and **P** are
planar and **P** either lies along $\mathbf{B}_0$ (point B_0)
makes an angle of 2μ with B_0. Equations 16
d 17 then become

$$B_0 = B_0 \quad (22)$$

d

$$B_\mu = B_0 \cos 2\mu \quad (23)$$

ese provide an independent measure of B_0
d μ.

Method 2. The orientation angles of η and θ
n also be determined from the frequency
riation of the signal within a precession cycle
the rocket. If γ denotes the angle between the
nes **S**, X' and **S**, $\mathbf{B}_0$, and ζ denotes the angle
tween **S** and $\mathbf{B}_0$, then equation 17 can be
itten as

$$\cos\beta = \cos\mu\cos\zeta + \sin\mu\sin\zeta\cos(\gamma + \varphi) \quad (24)$$

where

$$\cos\zeta = \cos\eta\cos\theta - \sin\eta\sin\theta\sin\psi \quad (25)$$

and

$$\tan\gamma = \frac{\sin\eta\cos\theta\sin\psi - \cos\eta\sin\theta}{\sin\eta\cos\psi} \quad (26)$$

Then, by differentiating equation 26 with respect to time, the angular velocity of the signal becomes

$$\omega_s = \dot{\varphi} + \dot{\gamma} = \dot{\varphi} + \dot{\psi}\frac{\cos\theta - \cos\eta\cos\zeta}{\sin^2\zeta} \quad (27)$$

By determining the time duration of a precession cycle, $\dot{\psi}$ can be obtained directly from the magnetometer signal, and $\dot{\varphi}$ can be determined from the equation

$$\dot{\varphi} = \langle\omega_s\rangle_p \quad \text{for} \quad \theta > \eta \quad (28)$$

or

$$\dot{\varphi} = \langle\omega_s\rangle_p - \dot{\psi} \quad \text{for} \quad \theta < \eta \quad (29)$$

where $\langle\omega_s\rangle_p$ represents the mean value of the angular velocity of the magnetometer signal over a precession period of the rocket. (Equations 28 and 29 can easily be verified by integrating equation 27 over a precession period.)

Equation 27 shows that ω_s has its extreme values when $\zeta = \eta + \theta$ and when $\zeta = |\eta - \theta|$; the former occur at $\psi = -\pi/2$ (points marked B_{M_1}, B_{m_1} in Fig. 4), and the latter occur at $\psi = \pi/2$ (points marked B_{M_2}, B_{m_2} in Fig. 4). At these locations, the extreme values of ω_s are

$$\omega_s(\eta + \theta) = \dot{\varphi} + \dot{\psi}\frac{\sin\eta}{\sin(\eta + \theta)} \quad (30)$$

and

$$\omega_s(|\eta - \theta|) = \dot{\varphi} + \dot{\psi}\frac{\sin\eta}{\sin|\eta - \theta|} \quad (31)$$

These equations immediately yield which of angles η and θ is larger, η is greater than θ if $\omega_s(\eta + \theta)$ is found to be less than $\omega_s(|\eta - \theta|)$, and conversely, η is less than θ if $\omega_s(\eta - \theta)$ is greater than $\omega_s(|\eta - \theta|)$. Hence, estimates of the extreme values of the frequency of the signal

specified whether equation 28 or 29 should be used to determine $\dot{\varphi}$, the spin rate of the rocket. If the extreme values of ω_s can be measured accurately, then equations 30 and 31 can actually be used to determine the magnitudes of η and θ.

The angle α between the collimator of the spectrometer and the direction of the geomagnetic field is given by the equation

$$\cos\alpha = \sqrt{\cos^2\xi + \sin^2\xi\sin^2(\theta - \lambda)} \cdot \sin(\psi + \nu + \delta) \qquad (32)$$

where

$\cos\xi = \sin\eta\cos\psi.$
$\sin\lambda = \sin\eta\csc\xi\sin\psi.$
$\tan\delta = \operatorname{ctn}\xi\csc(\theta - \lambda).$
ν = angular displacement of collimator axis from plane containing vectors **S** and **P**.

Appendix B: Directional Distribution of Electron Flux

1. *Normalization of distribution data.* Normalization of distribution data is taken by correlating counting rates of Geiger tubes with the angular displacement of the collimator axis from the direction of the geomagnetic line of force. The instantaneous counting rate of Geiger tube k is given by equation 6 as

$$C_k(\alpha) = \int g_k(E) f(E, \alpha)\, dE$$

But since an energy dependence of the angular distribution data was not evident, we will put

$$f(E, \alpha) = N(E) J(\alpha) \qquad (33)$$

Then

$$C_k(\alpha) = I_k J(\alpha) \qquad (34)$$

where

$$I_k = \int g_k(E) N(E)\, dE \qquad (35)$$

Now let $\langle q_k \rangle$ represent the number of true counts of Geiger tube k per rotation of the collimator through the normal plane, averaged over the altitude interval over which the distribution data were accumulated. Also, let $Q_k(\alpha_i)$ denote the number of scaler-level changes which were recorded while the collimator was along α_i within the interval $\Delta\alpha_i$. Evidently

$$J(\alpha_i)\frac{\Delta\alpha_i}{\dot{\alpha}_i} = A Q_k(\alpha_i)\,\Delta\alpha_i$$

where A is a proportionality constant given the equations:

$$\langle q_k \rangle = I_k \int J(\alpha)\frac{d\alpha}{\dot{\alpha}} \simeq I_k A \sum_i Q_k(\alpha_i)\,\Delta$$

Hence,

$$J(\alpha_i) = \frac{\langle q_k \rangle \dot{\alpha}_i Q_k(\alpha_i)}{I_k \sum_i Q_k(\alpha_i)\,\Delta\alpha_i}$$

By combining the counts of tubes 4 and 5, we

$$J(\alpha_i) = \frac{[\langle q_4 \rangle + \langle q_5 \rangle]\dot{\alpha}_i[Q_4(\alpha_i) + Q_5(\alpha_i)}{(I_4 + I_5)\sum_i [Q_4(\alpha_i) + Q_5(\alpha_i)]}$$

The angular distribution function $J(\alpha)$ in u of $(I_4 + I_5)$ is plotted in Figures 5 and 6.

2. *Computation of the angular distribution electron flux.* The angular distribution of e tron flux is computed from counting rates Geiger tubes during the ascent through lo altitudes along a magnetic line of force. It again be convenient to separate the energy angular dependence of the flux as in equation

$$f(E, \alpha) = N(E) J(\alpha)$$

The desired angular distribution of the flux an altitude where $B = B_1$ is given by the equat

$$J(B_1, \alpha_1) = J(B_m, \pi/2) \qquad (36)$$

where

$$B_m = \frac{B_1}{\sin^2\alpha_1}$$

as noted earlier in the text. Remaining to found from measured counting rates is t fraction of the flux $J(B_m, \pi/2)$, which mirror the altitude where $B = B_m$. The procedure u was to break up the ascent trajectory int number of intervals, and to assume that flux mirroring in any interval was equal to total flux measured in that interval minus sum of all flux encountered at lower altitu The equation for the counting rate of the tube, averaged over a precession period at altitude where the magnetic field magnitud B_1 is

$$\langle C_k(B_1) \rangle = I_k \int_{\alpha_{min}}^{\pi/2} J(B_1, \alpha) w(\alpha)\, d\alpha \qquad (37)$$

where the weighting function $w(\alpha)$ is defi below equation 7. This can be expanded as

$$C_k(B_1)\rangle = I_k\Big\{J(B_1, \pi/2)w(\pi/2)\ \Delta\alpha_1$$

$$+ J(B_1, \pi/2 - \Delta\alpha_1)w(\pi/2 - \Delta\alpha_1)\ \Delta\alpha_2$$

$$+ \cdots + J\Big(B_1, \pi/2 - \sum_{i=1}^{N}\Delta\alpha_i\Big)$$

$$\cdot w\Big(\pi/2 - \sum_{i=1}^{N}\Delta\alpha_i\Big)\ \Delta\alpha_N\Big\} \qquad (38)$$

ut from equation 36,

$$J(B_1, \pi/2 - \Delta\alpha_1) = J(B_2, \pi/2)$$

$$J(B_1, \pi/2 - \Delta\alpha_1 - \Delta\alpha_2) = J(B_3, \pi/2)$$

$$\cdots \text{ etc.}$$

here

$$\Delta\alpha_1 = \pi/2 - \sin^{-1}\sqrt{\frac{B_1}{B_2}}$$

$$\Delta\alpha_2 = \sin^{-1}\sqrt{\frac{B_1}{B_2}} - \sin^{-1}\sqrt{\frac{B_1}{B_3}} \cdots \text{ etc.}$$

hus, the counting rate $\langle C_k(B_1)\rangle$ can be expressed as a series in which successive terms ontain the mirror-point flux values at successively lower altitudes along the field line

$$C_k(B_1)\rangle = I_k \sum_{i=1}^{N} J(B_i, \pi/2)w\Big(\sin^{-1}\sqrt{\frac{B_1}{B_i}}\Big)$$

$$\cdot\Big[\sin^{-1}\sqrt{\frac{B_1}{B_i}} - \sin\sqrt{\frac{B_1}{B_{i+1}}}\Big] \qquad (39)$$

here B_1 will now be taken to be the value of he field intensity at the highest altitude (about 20 km) at which the rocket remains along the eld line; and B_N represents the field intensity t the lowest altitude of the rocket at which the ectron flux is encountered (where the counting ate just exceeds cosmic-ray background). By riting equation 37 for the counting rate $C_k(B_n)\rangle$, where $B_1 \leq B_n \leq B_N$, and solving he equation for the mirror-point value of the ux at that location, we get

$$(B_n, \pi/2) = \frac{1}{w(\pi/2)\Big[\pi/2 - \sin^{-1}\sqrt{\frac{B_n}{B_{n+1}}}\Big]}$$

$$\cdot\Big\{\frac{\langle C_k(B_n)\rangle}{I_k} - \sum_{i=n+1}^{N} J(B_i, \pi/2)w\Big(\sin^{-1}\sqrt{\frac{B_n}{B_i}}\Big)$$

$$\cdot\Big[\sin^{-1}\sqrt{\frac{B_n}{B_i}} - \sin^{-1}\sqrt{\frac{B_n}{B_{i+1}}}\Big]\Big\} \qquad (40)$$

The mirror-point values of the flux along the field line were computed by means of this equation starting at the lowest altitude interval with the expression

$$J(B_N, \pi/2) = \frac{\langle C_k(B_N)\rangle}{I_k w(\pi/2)\sqrt{\frac{B_N - B_{N-1}}{B_N}}}$$

The spacing of the altitude intervals was chosen so that the flux computed to be mirroring in that interval fell in the range 90° ± 7°. Again, by combining the counting rates of Geiger tubes 4 and 5, the flux is given in units of $(I_4 + I_5)$ as before. The results of this computation are shown by the solid curves in Figures 5 and 6.

Acknowledgments. We wish to thank Martin Walt of the Lockheed Missiles and Space Division for his valuable contributions in all phases of this work. The Air Force Special Weapons Center provided the central coordination of the experiment under the leadership of Lew Allen, Jr., and J. A. Welch, Jr. A. J. Meyerott, R. J. Sorenson, and E. N. Perry of LMSD performed the engineering work associated with the design and assembly of the instrumentation package. F. E. Holly, R. H. Beene, Jr., and J. L. Dennis of AFSWC assisted in the fielding and supervision of the project. Thanks are due many others both at LMSD and at AFSWC who assisted in the reduction of the data.

The AFSWC Special Projects Division, under the leadership of J. L. Beavers, II, is to be congratulated on the successful design and launching of the Javelin rocket. Financial support for the LMSD study contract which led to the design of the experiment, as well as for the development and construction of the instruments used, was furnished by AFSWC.

References

Arnoldy, R. L., R. A. Hoffman, and J. R. Winckler, Observations of the Van Allen radiation regions during August and September 1959, Part 1, *J. Geophys. Research, 65,* 1361–1376, 1960.

Cladis, J. B., L. F. Chase, W. L. Imhof, and D. J. Knecht, Energy spectra and spatial distributions of electrons trapped in the earth's magnetic field, *Bull. Am. Phys. Soc., 5* [2], Paper N4, January 27, 1960.

Fan, C. Y., P. Meyer, and J. A. Simpson, Trapped and cosmic radiation measurements from Explorer VI, in *Space Research,* edited by H. Kallman Bijl, North Holland, Amsterdam, pp. 951–966, 1960.

Freden, S. C., and R. S. White, Protons in the earth's magnetic field, *Phys. Rev. Letters, 3,* 9, 1959.

Holly, F. E., and R. G. Johnson, Measurements of

radiation in the lower Van Allen belt, *J. Geophys. Research, 65,* 771–772, 1960.

Jensen, D. C., R. W. Murray, and J. A. Welch, Jr., *Tables of Adiabatic Invariants for Geomagnetic Field 1955.0,* AFSWC-TN-60-8, Kirtland Air Force Base, New Mexico, 1960.

Rosen, A., C. P. Sonett, P. J. Coleman, Jr., and C. E. McIlwain, Ionizing radiation at altitudes of 3,500 to 36,000 kilometers, Pioneer I, *J. Geophys. Research, 64,* 709–712, 1959.

Rosen, A., T. A. Farley, and C. P. Sonett, Soft radiation measurements on Explorer VI earth satellite; in *Space Research,* edited by H. Kallman Bijl, North Holland, Amsterdam, pp. 938–950, 1960.

Van Allen, J. A., The geomagnetically trapped corpuscular radiation, *J. Geophys. Research, 64,* 1683–1689, 1959.

Van Allen, J. A., C. H. Ludwig, E. C. Ray, and C. E. McIlwain, Observation of high-intensity radiation by satellites 1958 α and γ, *Jet Propul., 28,* 588–592, 1958.

Van Allen, J. A., C. E. McIlwain, and G. H. Ludwig, Radiation observations with satellite 1958ϵ, *J. Geophys. Research, 64,* 271–286, 1959.

Van Allen, J. A., and L. Frank, Radiation around the earth to a radical distance of 107,400 km, *Nature, 183,* 430–434, 1959*a*.

Van Allen, J. A., and L. Frank, Radiation to 658,300 km with Pioneer IV, *Nature, 184,* 219–224, 1959*b*.

Vernov, S. N., A. E. Chudakov, P. V. Vakulov, and Yu I. Logacher, Study of terrestrial corpuscular radiation and cosmic rays during the flight of a cosmic rocket, *Soviet Physics Doklady, 4,* 338–342, 1959.

Vernov, S. H., and A. E. Chudakov, Terrestrial corpuscular and cosmic rays, in *Space Research,* edited by H. Kallman Bijl, North Holland, Amsterdam, pp. 751–796, 1960.

Walt, M., L. F. Chase, Jr., J. B. Cladis, W. L. Imhof, and D. J. Knecht, Energy spectra and altitude dependence of electrons trapped in Earth's magnetic field, in *Space Research,* edited by H. Kallman Bijl, North Holland, Amsterdam, pp. 910–920, 1960.

(Manuscript received April 13, 1961.)

The Observed Outer-Belt Electron Distribution and the Neutron Decay Hypothesis

W. N. HESS AND J. KILLEEN

Lawrence Radiation Laboratory, University of California
Livermore, California

C. Y. FAN, P. MEYER, AND J. A. SIMPSON

Enrico Fermi Institute for Nuclear Studies
University of Chicago
Chicago 37, Illinois

Abstract. Measurements of electron flux along a line of force in the outer radiation belt are compared with calculations that assume that all electrons are injected by neutron decay. The comparison shows that the two distributions are quite different at intermediate and low latitudes where corrections are unimportant. It is concluded that other processes, in addition to electron injection by neutron decay, are necessary to explain the experimentally observed flux distribution along a line of force.

Theories for the sources and losses of electrons in the outer radiation belt must take into account not only electron flux and energy spectrum but also the spatial distribution of electron mirror points along a line of force in the geomagnetic field. Different sources lead to different distributions [*Killeen and Boer*, 1960]. The theory that the outer belt is entirely due to β-decay electrons from neutrons leaking out of the terrestrial atmosphere requires that low-altitude electron injection be dominant [*Hess, Canfield, and Lingenfelter*, 1961]. Therefore, it is of interest to compare the predicted distribution for the neutron decay hypothesis (Hess and Killeen, to be published) with a recent experiment [*Fan, Meyer, and Simpson*, 1961] which shows the electron intensity along lines of force can be obtained directly from Explorer VI satellite measurements using a detector sensitive to bremsstrahlung principally from electrons above 100-kev energy. This is an energy range suitable for comparison with the energy spectrum from neutron decay. Since the calculated distribution of electrons at intermediate and low latitudes in the outer radiation belt is determined more by the source distribution—which is well known—than by the details of the loss mechanism, a comparison of experiment and theory is a valid test of the neutron decay hypothesis.

There are three equivalent ways to represent the electron distribution along a line of force; namely, the flux, or the mirror point distributions along a line of force, or the pitch angle distribution at the equator of particles trapped along a line of force [*Fan, Meyer, and Simpson*, 1961]. In this paper all results are expressed as an electron flux along a line of force through the maximum intensity of the E_3 region of the outer belt. For both the experimental results and the calculations, the geomagnetic field is assumed to be a dipole field. This has been found experimentally to be a good representation for the outer electron belt [*Fan, Meyer, and Simpson*, 1960].

The measured electron intensity along a dipole line of force passing through the equator at the geocentric range $R_0 = 21{,}000$ km, or intersecting the earth at the geomagnetic latitude $\lambda = 57°$, is shown in Figure 1. B_0 is the geomagnetic field intensity at the equator, and B is the field intensity at any latitude λ. This is also the line of force through the maximum intensity of the E_3 region in the outer belt [*Fan, Meyer, and Simpson*, 1961]. These measurements were obtained in a period free from large-scale temporal changes of electron intensity or magnetic field intensity, and represent the prevailing electron flux along a line of force at this range.

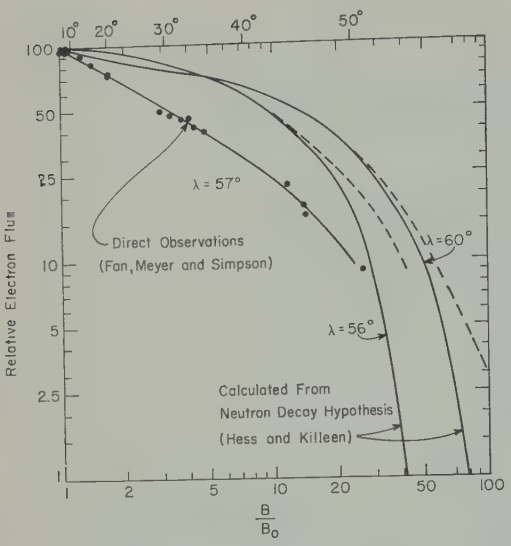


Fig. 1. Relative electron flux measured along a geomagnetic dipole line of force whose range at the equator is $R_0 = 21{,}000$ km [*Fan, Meyer, and Simpson,* 1961]. For comparison the calculated electron flux distributions assuming only β decay electrons from neutrons escaping from the terrestrial atmosphere are shown for nearby lines of force (Hess and Killeen, to be published). (B_0 is the magnetic field intensity at the geomagnetic equator.)

Since the electron fluxes are derived from bremsstrahlung measurements, it is especially important to note that the change in electron spectrum along the line of force through E_3 maximum was found to be negligible (Fan, Meyer, and Simpson, to be published).

It has been shown that the measured electron intensity I along a line of force may be well represented at intermediate and low latitudes by $I = I_0 (B/B_0)^{-x}$, where I_0 is the equatorial intensity (Fan, Meyer, and Simpson, to be published). Thus, changes in x reflect changes in electron pitch angle distribution. The smallest values of x are found during undisturbed periods and have the value $x \approx 0.5$ as derived from Figure 1. During geomagnetic disturbances, x may increase in value to ~ 1.2.

The calculated electron flux along lines of force intersecting the earth at $\lambda = 56°$ and $\lambda = 60°$ are also shown in Figure 1, normalized to the experimental curve at the equator (Hess and Killeen, to be published). These calculations assume injection by neutron decay electrons with energies greater than 100 kev. This represents nearly all the electrons in the neutron decay spectrum. Two loss processes were considered. First, trapped electrons are slowed down by collisions with thermal electrons—this is the dominant loss mechanism at high altitudes for electrons with energies greater than 100 kev. Second, at altitudes below a few thousand kilometers where the exosphere becomes principally oxygen and nitrogen, instead of hydrogen, the dominant loss process becomes Coulomb scattering.

The inclusion of scattering losses only changes the calculated flux distribution along a line of force at high latitudes, as indicated by the uncorrected curves drawn by dotted lines in Figure 1. This will not affect the low latitude calculations where the comparison with experiment is valid.

A comparison of the exponents x in Figure 1 proves that $x < 0.23$ for the neutron decay hypothesis lies below the possible range of x values ($x \geq 0.5$) found by direct measurements in the outer radiation belt. Thus, there are relatively more electrons with mirror points at low latitudes than predicted by the neutron decay hypothesis.

Therefore, other processes in addition to electron injection by neutron decay are necessary to explain the experimentally observed flux distribution along a line of force in the outer electron belt.

Acknowledgment. The calculations of Hess and Killeen were supported by the U. S. Atomic Energy Commission. The work of Fan, Meyer, and Simpson was supported in part by the National Aeronautics and Space Administration and in part by the U. S. Air Force Office of Scientific Research, contract AF 18 (600)-666.

References

Fan, C. Y., P. Meyer, and J. A. Simpson, Trapped and cosmic radiation measurements from Explorer VI, *Space Research,* edited by H. Kallmann-Bijl, North Holland Publishing Company, Amsterdam, pp. 951–966, 1960.

Fan, C. Y., P. Meyer, and J. A. Simpson, The equatorial pitch angle distributions of electrons in the outer radiation belt, EFINS–61–20, Second International Meeting of COSPAR, Florence, Italy, April 1961. (To be published.)

Hess, W. N., E. Canfield, and R. E. Lingenfelter, Cosmic-ray neutron demography, *J. Geophys. Research, 66,* 665–677, 1961.

Killeen, J., and G. Boer, Densities of particles trapped by the geomagnetic field, *Bull. Am. Phys. Soc.* [2], *5,* 312, 1960.

(Manuscript received May 19, 1961.)

Three-Frequency Measurements of Auroral Absorption

SYED ZIAUDDIN[1] AND P. A. FORSYTH

Institute of Upper Atmospheric Physics, University of Saskatchewan
Saskatoon, Canada

Abstract. Measurements of the effective height of the regions responsible for VHF radio wave absorption have been carried out during auroral disturbances. The technique depends upon measurements of the cosmic noise level at three closely spaced frequencies using a single antenna with a very broad sensitivity pattern. The absorbing region is usually above 70 km in height except during intense disturbances when there is an interesting sequence of separate events which progress toward lower heights, sometimes apparently reaching a level as low as 50 km.

troduction. Since the IGY the use of radio es of extraterrestrial origin (cosmic noise) tudies of the lower ionosphere has increased tly. The usual technique follows the earlier k of *Mitra and Shain* [1953] and of *Little* 4], who used stable receivers to make care- measurements of the variations in cosmic e level in order to deduce the amount of rption suffered by the radio waves in passing ugh the ionosphere. Absorption measure- ts at a single frequency give no direct evi- e of the height at which the absorption is ng place, although indirect reasoning was by Mitra and Shain to deduce that the ter part of the absorption observed at 18.3 s was taking place in the *D* region. *Chap- and Little* [1957] used theoretical argu- s to place the region responsible for ab- nal absorption in the height range of 70 to m.

should be possible to use multiple-frequency urements to gain information about the t of the active region, since the frequency ndence of absorption is governed by the of the wave frequency to the local elec- e collisional frequency in the absorbing re- Some work using two widely spaced fre- cies has been reported by *Little and Lein-* [1958] and by *Hartz* [1960]. Although measurements appear to be effective when bsorption is taking place in a homogeneous of large horizontal extent, there are difficul- when the technique is applied to the patchy abnormal absorption associated with aurora. These difficulties arise from the uncertainty regarding the geometric equivalence of the two receiving systems. This paper describes an experiment in which an attempt was made to overcome the difficulties by using three closely spaced frequencies.

Experimental arrangements. The receiving system consisted of three receivers and associated moving chart recorders of conventional design. The receivers, operating at frequencies of 30.0, 32.8, and 34.8 Mc/s with IF bandwidths of 8 kc/s, were connected through a single broadband preamplifier to the antenna. The antenna consisted of a single half-wave dipole of cage construction mounted at a height of one-quarter wavelength above the ground. The resulting very broad coverage (amounting to nearly the whole sky) was chosen in order to minimize the variation of coverage with frequency. The absolute sensitivity of such a system to localized absorbing regions is correspondingly reduced from that of a narrow-beam system, but this is not an important consideration when relative absorption at the different frequencies is being determined.

Since the investigation was concerned primarily with abnormal absorption events of large magnitude and relatively short duration, lasting from a few minutes to an hour or two, it was not necessary to stabilize the gain of the receivers, although the system was calibrated at frequent intervals in order to maintain the accuracy of scaling.

Theoretical considerations. The absorption suffered by a radio wave of frequency well above the ionospheric critical frequency, and well above

t present the holder of a post-doctoral fellow- National Research Council, Ottawa, Canada.

the magnetic gyro frequency, in passing through the lower ionosphere is given with sufficient accuracy by the expression,

$$A(\text{db}) = 0.46 \int \frac{N\nu}{\omega^2 + \nu^2} ds$$

where N is the local electronic density (cm^{-3}), ν the electronic collisional frequency, and ω the angular frequency of the radio wave. The integral is taken along the radio wave path s measured in centimeters. For absorbing regions located at heights where the electronic collisional frequency is much less than the wave frequency, the absorption will vary inversely as the square of the wave frequency. For much lower absorbing regions, where the collisional frequency greatly exceeds the wave frequency, the absorption becomes independent of frequency. For heights between these two extremes, the ratio of the absorptions suffered at two frequencies may be used as a measure of the collisional frequency in the absorbing region, and hence as a measure of the height of the region. Implied in this statement are the assumptions that the absorbing region consists of a single relatively thin layer for which a single electronic collisional frequency can be specified, and that there is a constant relationship between height and collisional frequency. Neither of these assumptions is likely to be satisfied in any exact sense but both seem to be sufficiently accurate for the present purpose. Certainly, if the variation of electronic density with height is either monotonic or single peaked, the resulting variation of absorption with height will have a single fairly sharp maximum. In the absence of detailed knowledge of the electronic density distribution, it is still valid to consider an effective height which is the height of the thin layer that would produce the observed variation of absorption with frequency.

The variation of absorption ratio with height of the absorbing region is shown in Figure 1 for each of two combinations of the three frequencies used in this investigation. The computations are based upon the collisional frequencies adopted by Chapman and Little. It is possible that for the particular conditions of some of the measurements the effective collisional frequencies were greater than these equilibrium values [see, for example, *Kane*, 1960], but this effect would only cause the absolute heights to be underestimated by not more than a scale height, and

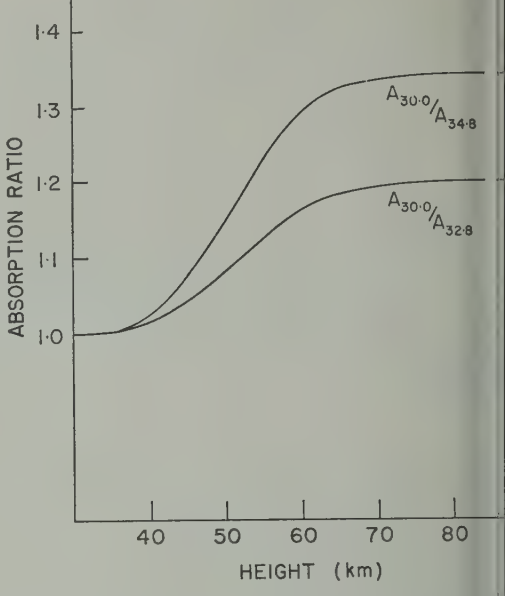


Fig. 1. The variation of absorption ratio w height for two pairs of frequencies. In each c the subscript indicates the frequency in megacyc

would not affect the observations regarding p gressive changes of height.

Observations. Most of the observations late to auroral absorption events of the kind t were designated 'Type II' by *Reid and Coll* [1959]. Figure 2 shows the appearance of record for one frequency during (*a*), a period weak auroral activity, and (*b*), a period of tense activity. The second, (*b*), period is ch acterized by a number of separate sudden currences, each occurrence presumably cor sponding to the nearly instantaneous creation a patch of ionization in the atmosphere. For t reason, each such event (marked *AB* in the F ure) has been treated as a separate occurrenc

The magnitude of the absorption measu was generally in the range of 1 to 5 decib with an accuracy of measurement of 0.1 db. use of three frequencies served to elimin spurious events and also improved the accur of the derived heights so that the effective hei was probably determined to within one s height.

The behavior of the absorption during th separate auroral disturbances is shown in Fig 3. For each event the derived height is sho In Figure 3*a* and 3*b* there is a trend in wh

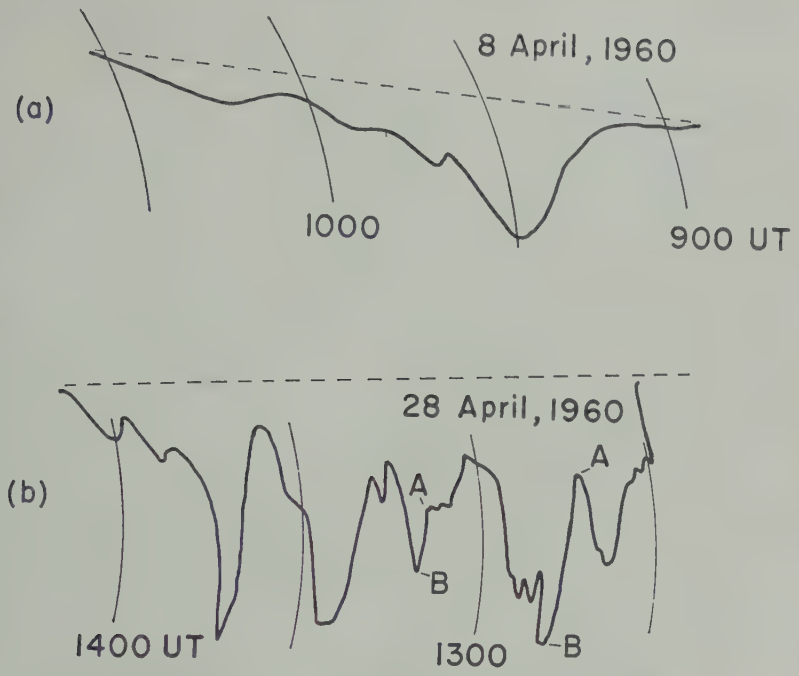


Fig. 2. The appearance of the absorption record during (*a*) a weak auroral disturbance, and (*b*) an intense auroral disturbance. The records for only one frequency (30 Mc/s) are shown, and time increases from right to left. The broken line indicates the normal level of cosmic noise in the absence of absorption.

cessive events occur lower in the atmosphere. s seemed to be true of most of the intense urbances. Whenever several events followed another in rapid succession, each succeeding nt occurred at a lower level. If, however, re was a significant recovery (decrease of ab- ption), the next following event might be at reater height. The records were examined in e detail to see if this effect was instrumental related to the total amount of absorption. progression seems to be real and is not di- ly dependent upon the amount of absorp- present.

dicated heights below 50 km were found rarely (less than 4 per cent of the observa- s) and then only when the absorption was than 1.5 db. The frequency of occurrence arious absorption ratios found during intense ral disturbances is shown in Figure 4, for ratio $A_{30}/A_{34.8}$ and also for the ratio $A_{30}/A_{32.8}$. effect of the limited accuracy of measure- t (± 0.1 db) is to introduce an uncertainty each derived height. This uncertainty is test for the smaller absorption values and the greater heights, where the use of the second ratio does little to improve the accuracy. Nevertheless, the strong grouping of the ratios about values representing the inverse square frequency dependence, leaves little doubt that the absorbing region is most frequently near or above the 70-km level. It is apparent that the lower heights are comparatively rare and, presumably, are associated with the most intense disturbances.

In Figure 4 some ratios shown are in excess of that corresponding to the inverse square frequency dependence. Most of these occurrences could be due to the limited accuracy of the individual measurements. On two occasions, during intense auroral displays that followed solar flares, the absorption ratio, $A_{30}/A_{34.8}$, exceeded 1.4 when the magnitude of the absorption was sufficiently large (7 db) to make the measurement fairly reliable. There seems to be no simple way to account for these observations. It is tempting to suggest that the ionization was sufficiently intense to reflect the incoming radio waves at the lower frequency, but this would require that ionization corresponding to an electronic density

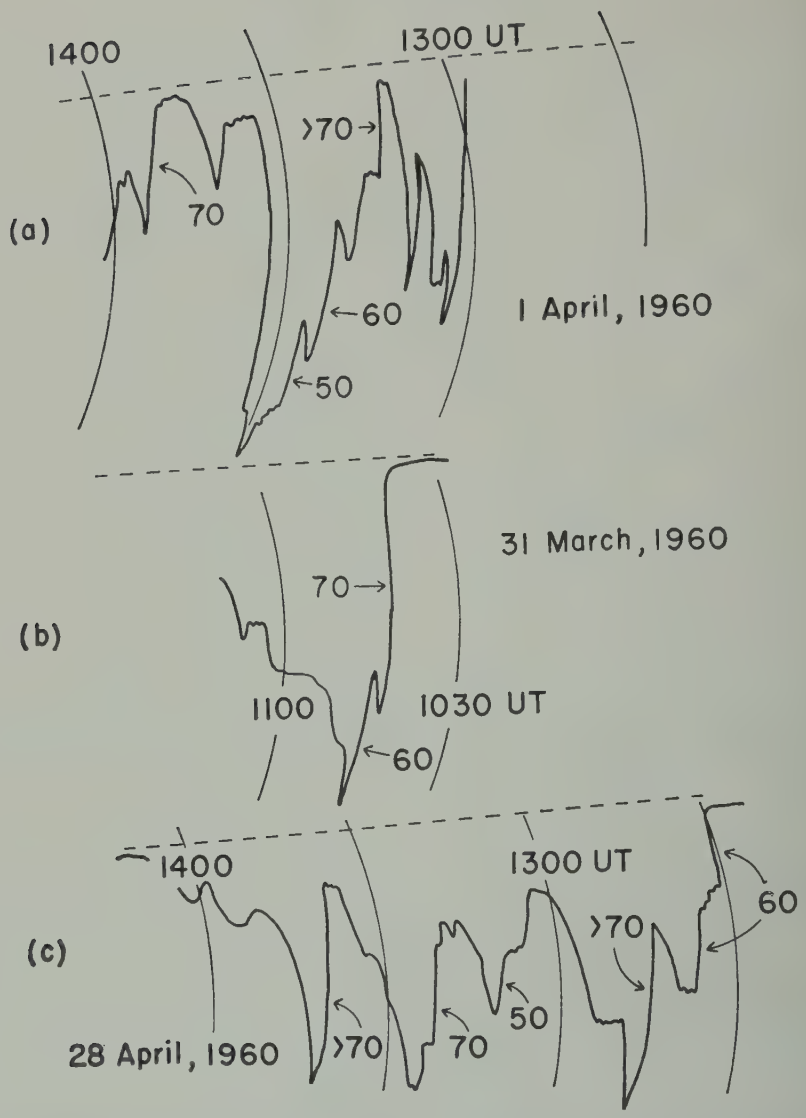


Fig. 3. Examples of the behavior of absorption during three separate auroral disturbances. The derived height of the absorbing region for each separate event is shown. The disturbances (*a*) and (*b*) show the typical trend toward lower heights, while (*c*) shows a series of apparently independent events.

approaching 10^7 cm^{-3} existed over a sufficient area to cover effectively the whole sky. Radar measurements of aurora indicate that electronic densities somewhat in excess of this value do exist during intense auroral displays, but only in very localized regions.

For the weaker auroral disturbances (see Fig. 2*a*) the records showed no sudden change but only slow irregularly varying absorption 'bays,' sometimes extending over 2 or 3 hours. At t times, the absorption was always inversely portional to the square of the frequency, ind ing heights in excess of 70 km.

In contrast to the auroral events, the ion tion produced during solar flares seems to tend characteristically to lower levels. Figu shows the record obtained during the su cosmic noise absorption event (SCNA) as

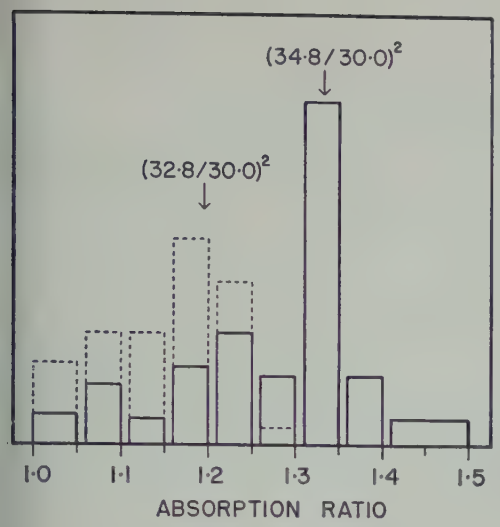


Fig. 4. Histograms of the distribution of frequency of occurrence of various absorption ratios. The solid line is for $A_{30.0}/A_{34.8}$ and the broken line for $A_{30.0}/A_{32.8}$

ed with the solar flare of March 30, 1960. he absorption in this case was independent of equency, indicating an effective height of less an 50 km.

Discussion. The purpose of the experiment s primarily to explore a technique. The occrrence during intense auroral disturbances of a quence of separate events, each succeeding ent representing a penetration of the auroral ization to a lower depth in the atmosphere, of interest. Before any detailed interpretation this phenomenon is attempted, however, a re extensive morphological study is needed in ich the indicated height of the absorbing reon is compared directly with contemporaneous ents in other aspects of the auroral process. he possible association of these events with inidual features in the visible aurora might well investigated. Comparison of the height of the sorbing region with the energy spectrum of rays observed at balloon heights beneath the rora would likely be rewarding. In any event, e use of simple equipment and closely spaced quencies appears to introduce no significant ficulties. In this regard it is worth noting that

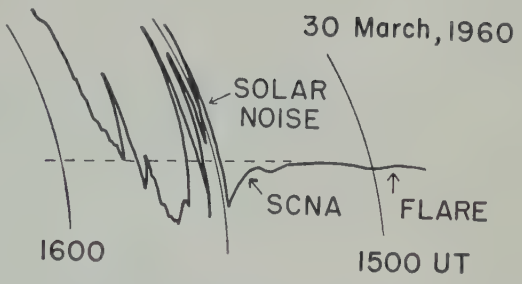


Fig. 5. The absorption record during a solar flare and subsequent Sudden Cosmic Noise Absorption event (SCNA).

the equipment could be arranged to record directly the effective height of the absorbing region.

Acknowledgments. The material on which this paper is based forms part of a doctoral thesis presented by one of the authors (S.Z.) to the Graduate Faculty, University of Saskatchewan. Work was supported in part by the Defence Research Board of Canada under grant 9511-25 and in part by the National Research Council under grant T-123.

References

Chapman, S., and C. G. Little, The nondeviative absorption of high-frequency radio waves in auroral latitudes, *J. Atmospheric and Terrest. Phys., 10,* 20, 1957.

Hartz, T. R., Unpublished investigation of absorption using two frequencies, reported to URSI-IRE Spring Meeting, Washington, 1960.

Kane, J. A., Reevaluation of ionospheric electron densities and collision frequencies derived from rocket measurements of refractive index and attenuation, *NASA Tech. Note D-503,* 1960.

Little, C. G., High latitude ionospheric observations using extra-terrestrial radio waves, *Proc. IRE 42,* 1700, 1954.

Little, C. G., and H. Leinbach, Some measurements of high-latitude absorbtion using extra-terrestrial radio waves, *Proc. IRE, 46,* 334, 1958.

Mitra, A. P., and C. A. Shain, The measurement of ionospheric absorption using observations of 18.3 Mc/s cosmic radio noise, *J. Atmospheric and Terrest. Phys., 4,* 204, 1953.

Reid, G. C., and C. Collins, Observations of abnormal VHF radio wave absorption at medium and high latitudes, *J. Atmospheric and Terrest. Phys., 14,* 63, 1959.

(Manuscript received April 6, 1961; revised May 15, 1961.)

The Analysis of Transient Modes of Propagation across the Auroral Zone

B. J. FULTON AND L. E. PETRIE

Defence Research Telecommunications Establishment
Ottawa, Ontario, Canada

Abstract. A model of propagation by scatter and ionospheric reflection is proposed to explain transient modes of propagation across the auroral zone. The parameters of the trace that is identified as a transient mode on sweep-frequency oblique-incidence records are used to calculate the position of the irregularity or cloud of ionization that acts as the scattering source. These parameters are also sufficient to establish the self-consistency of the model.

Introduction. Transient modes of high-frequency radio-wave propagation between Winnipeg (49.9°N, 97.4°W) and Resolute Bay (74.7°N, 94.9°W) have been observed on sweep-frequency oblique-incidence sounding records for this circuit. The occurrence of these modes and a model of propagation by scatter and reflection have been reported earlier [*Fulton, Petrie, and Ward,* 1959].

The transient modes appear on the ionogram as extra traces which have the same general structure as fragments of the trace produced by regular ionospheric reflections. To interpret these traces, it is proposed that the ray is scattered by clouds of ionization either before or after ionospheric reflection. The position of the cloud of ionization that is associated with the transient mode on any particular ionogram can be calculated in one of four positions by a method given in this paper. The coordinates calculated are the heights, the horizontal distance from either the transmitter or receiver, and the lateral deviation from the great-circle path between the two stations.

The frequency sweep 1–49 Mc/s is recorded twice an hour on the Winnipeg–Resolute Bay circuit. The ionospheric sounder is described in a recent report [*Southern,* 1961]. From the records taken on these regular soundings, a study was made on the percentage occurrence of transient modes during December 1958 to December 1959. The sweep was repeated continuously at certain times in order to study the duration of the transient modes. The velocity of the cloud of ionization is estimated from three or more successive records.

Occurrence. The percentage occurrence of the transient modes was found as a function of time of day for each of the eleven months: December 1958 to June 1959, and September 1959 to December 1959. No records were taken on this circuit for July and August 1959 because of equipment failure. The percentage occurrence of transient modes for a specific time is the percentage of records that show these traces out of the total number of records showing regular traces. The percentage is almost constant during the night and morning hours, but starts to rise around noon and peaks at about 13:30 to 15:30 hours for the months January to March and September to December. Figure 1 shows the diurnal variation of occurrences for January, March, and November, 1959. A smoothed curve has been drawn by taking a 3-hour running average in each case. The plotted points for the other 5 months are scattered approximately the same amount as those points shown in Figure 1. The smoothed maximum occurrences are:

December (1958)	35%	September	16%
January	36	October	24
February	28	November	44
March	29	December (1959)	33

During April, May, and June, the occurrences are evenly distributed throughout the day and are few in comparison with the other months. The mean occurrences are 7, 3.3, and 1.5 per

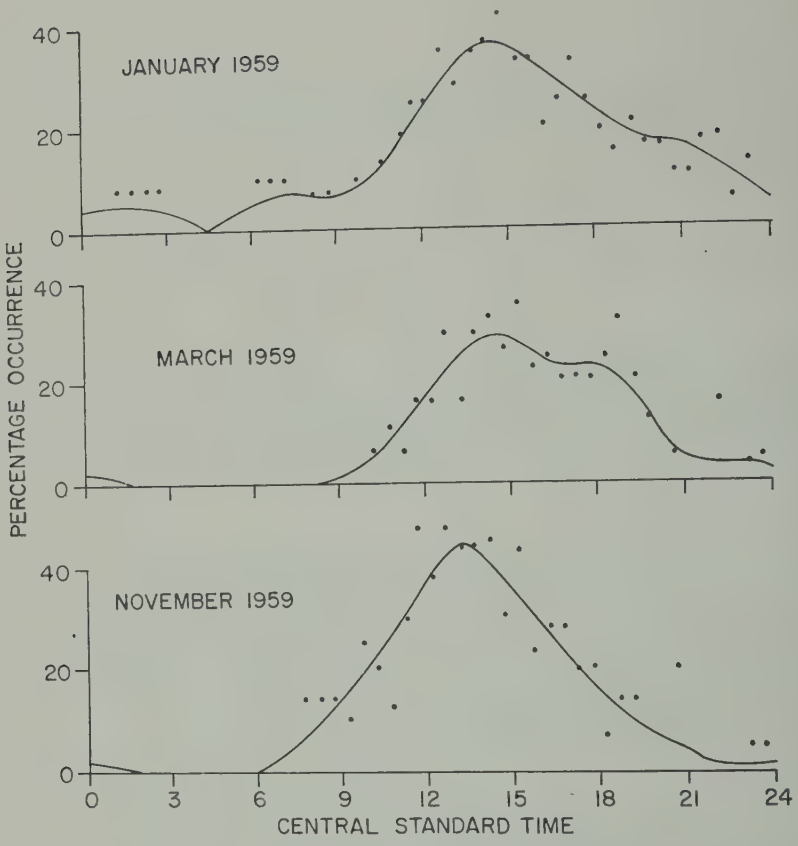


Fig. 1. Diurnal variation of the percentage occurrence of transient modes on the Winnipeg-Resolute Bay circuit.

cent for April, May, and June, respectively.

The percentage occurrence of transient modes was correlated with the average values of magnetic K index from Meanook (54.6°N, 113.3°W) for each of the eleven months. It was found that the average correlation coefficient for April, May, and June 1959, is +0.2. For the 8 months, December 1958 to March 1959, and September 1959 to December 1959, the average coefficient is −0.8. This negative coefficient may indicate that during disturbed conditions transient modes are not seen on the records because of enhanced scatter and absorption in the ionosphere.

Calculation of position. An irregularity situated in the E layer or at the bottom of the F layer can provide two possible paths involving scatter that deviate from the regular great-circle path between transmitter and receiver. The ray can be reflected from the F layer to the irregularity, from which the energy is scattered to the receiver; or the ray is transmitted directly to the irregularity, and the energy is scattered forward into an F-layer reflection before arriving at the receiver. For each of these deviate paths there may be a high- and low-angle ray path. When the position of the irregularity is such that the F layer supports high- and low-angle reflections for both paths, two extra traces would appear on the record. If the irregularity is located too close to the transmitter or receiver, the electron density of the F layer may support reflections on only one of these deviate paths, and only one extension is seen on the record. This is illustrated in Figure 2. When the irregularity is located within the F layer, direct ray reflections on the deviate path may be excluded by reflections at the bottom of the F layer, and only a high-angle ray trace would appear, as illustrated in Figure 3. The large increase in time delay of the extr

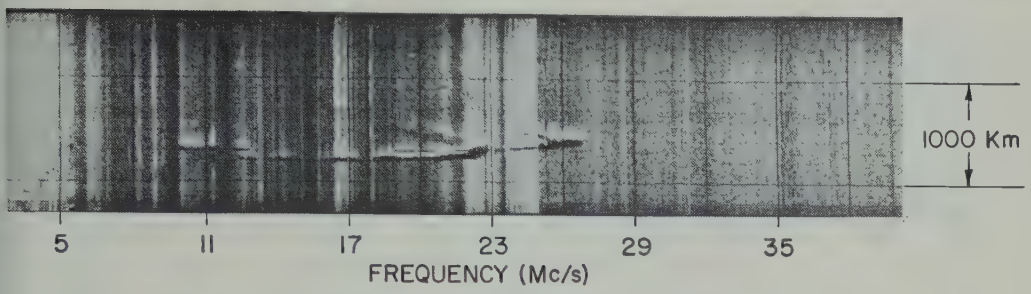


Fig. 2. Winnipeg–Resolute Bay; November 13, 1958, 11:40 CST.

ace over the regular one-hop trace ordinarily bserved on this circuit is mainly due to con-derable lateral deviation of the irregularity om the great-circle path.

Methods have been developed to calculate ie position of the irregularity for each of the pes of transient mode shown in Figures 2 and

The traces on the oblique-incidence ionogram id the corresponding vertical-incidence iono-am for the mid-point of the path are used. A ngle trace of either type on the ionogram is fficient for the calculation.

Let h_0 represent the height of the irregularity nd D_T the distance of the irregularity from the ansmitter or receiver. The following general uation is obtained from the geometry of Fig-e 4:

$$_T = R\left[\frac{\pi}{2} - \kappa - 2 \arcsin \frac{R \cos \kappa}{R + h'} + \arcsin \frac{R \cos \kappa}{R + h_0}\right] \quad (1)$$

here κ is the elevation angle and h' is the rtual height of reflection.

Two points on the transient mode trace which n be identified are the maximum usable fre-ency (MUF) and the lowest frequency for gh-angle-ray propagation (f_L). These give two rticular solutions of equation 1:

$$_T = R\left[\frac{\pi}{2} - \kappa_M - 2 \arcsin \frac{R \cos \kappa_M}{R + h'_M} + \arcsin \frac{R \cos \kappa_M}{R + h_0}\right] \quad (2)$$

$$_T = R\left[\frac{\pi}{2} - \kappa_L - 2 \arcsin \frac{R \cos \kappa_L}{R + h'_L} + \arcsin \frac{R \cos \kappa_L}{R + h_0}\right] \quad (3)$$

where subscripts M and L refer to the maximum usable frequency and lowest usable frequency (high-angle ray) respectively. When the four values κ_M, h'_M, κ_L, h'_L are obtained, they can be substituted in equations 2 and 3 to find h_0. The suitable vertical-incidence ionogram can be used with a transmission slider to obtain the angle of elevation κ and the height h' of the geometrical path for the reflection. The regular one-hop MUF for the Winnipeg-Resolute Bay circuit is first calculated from the vertical-incidence ionogram using the transmission slider for 2760 km taken from the set in CRPL Bulletin 462 [*National Bureau of Standards*, 1948]. If there is a difference between the calculated and observed MUF on the oblique-incidence ionogram, a correction must be applied to the observed limits for the extra trace before further calculations are made. The CRPL transmission slider consists of curves of constant κ (elevation angle) and constant D (distance) on the coordinates of h' and corrected secant ϕ values. When the index of the slider (sec $\phi = 1$) is placed on the vertical-incidence scale at the value of the MUF, there is found the constant D line that is tangent to the vertical incidence trace. The values of κ_M and h'_M at the point of tangency are noted, as well as the value of D.

The lower limit for high-angle propagation must be geometrically defined in order to find the corresponding κ and h'. The high-angle trace should cut off very sharply and not be obscured by absorption or a drop in equipment gain before the geometrical limit. For a certain path length D, it is possible to predict the high-angle lower-frequency limit using transmission sliders by finding a κ line tangent to the vertical incidence trace at the point of intersection with the curve for the distance D [*Fulton, Sandoz, and Warren*, 1960]. Inversely, if f_L is found from the

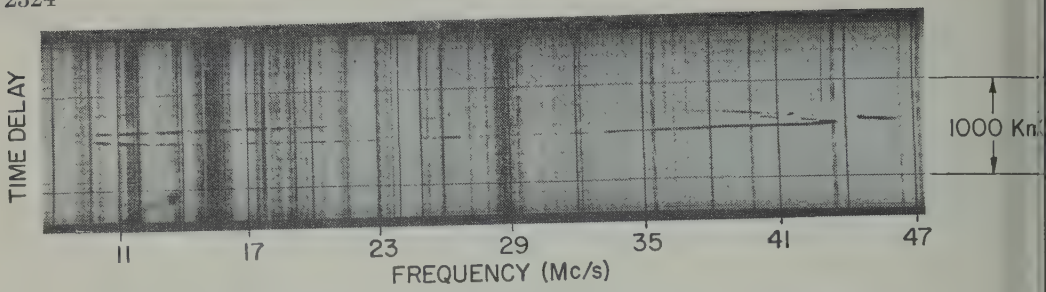


Fig. 3. Winnipeg–Resolute Bay; November 30, 1958, 13:41 CST.

Winnipeg–Resolute Bay record, the distance D, and also κ_L and h'_L, can be found by placing the index of the slider on the frequency f_L on the vertical-incidence record.

The details of the calculation for transient modes of the type illustrated in Figure 2 will now be described. The four values κ_M, h'_M, κ_L, h'_L are substituted in equations 2 and 3 which are solved to find h_0, the height of the irregularity. When the irregularity is situated in the E layer, or at the bottom of the F layer, h_0 can be taken as the real height. The horizontal distance of the irregularity from the transmitter or receiver, D_T, can now be found from equation 2 or 3. The azimuthal angle is not yet defined.

The absolute time delay P' at the high-angle lower limit can be found by examining ionograms taken at both ends of the circuit. The values for h_0, D_T, κ_L, and h'_L are used to calculate the time delay of the ray on the ionospheric reflection to or from the irregularity. The difference of this value from P', calculated from the records, is the time delay for the direct path to or from the irregularity. This difference value, and the values of h_0 and D_T, will give the horizontal distance of the irregularity, projected onto the great-circle path. The irregularity can be located in any one of four positions, because D_T is the distance from either transmitter or receiver and the lateral deviation can be either side of the great-circle path.

The total time delay for the MUF of the extra trace is calculated by using the ionograms from both ends of the circuit. The self-consistency of the model can be checked by comparing the calculated value of the MUF time delay to the value observed on the oblique-incidence ionogram.

When an extra trace shows only the high-angle mode, it is assumed that propagation at the maximum frequency occurs directly to the irregularity and back to the receiver. A graphical method is used to find the height of the irregularity for transient modes of the type illustrated in Figure 3.

Lejay and Lepechinsky [1950] have represented the locus of reflection points for a given frequency as a graph of corresponding values of apparent height and distance from the transmitter for plane earth and ionosphere. This reflectrix can also be constructed for a curved earth and ionosphere using corresponding values of κ and h'.

The maximum frequency on the extra trace is read from the oblique-incidence record; a reflectrix is then constructed for this frequency as shown in Figure 5. The lowest frequency on the extra trace gives a height h'_L and angle κ_L when the transmission slider method is applied. These values are used to plot the geometrical ray path as illustrated in Figure 5. A ray is scattered back to the receiver by an irregularity situated some

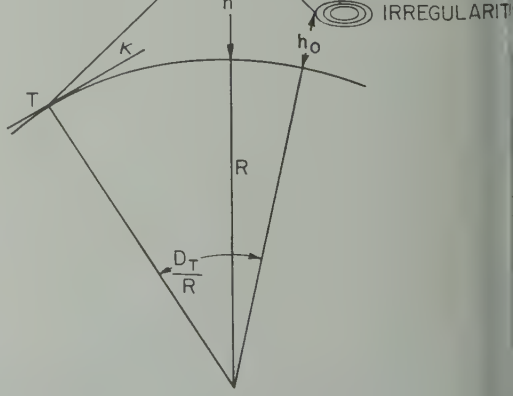


Fig. 4. The geometry used in the derivation of equation 1.

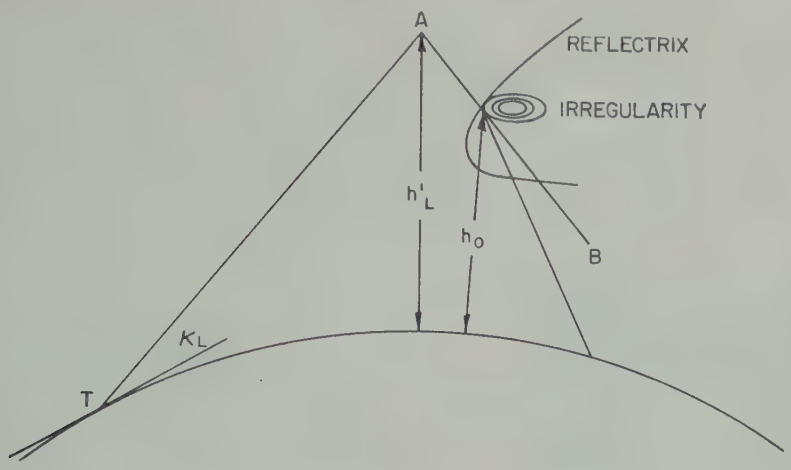


Fig. 5. The graphical method for the determination of the height of the irregularity h_o.

ere on the line AB. The point of intersection the line AB with the reflectrix will yield the ight h_o of the irregularity above the ground. int T in Figure 5 can alternatively represent receiver.

The distance of the irregularity from the nsmitter or receiver can be calculated from ıation 3 by substitution of values for h_o, h_L, d κ_L. The time delays for the maximum and nimum frequencies on the high-angle-ray trace then used to calculate the lateral deviation d check the model as described previously.

Seventeen Winnipeg–Resolute Bay ionograms owing transient mode traces were used to ck the self-consistency of the model. The culated time delay for the MUF of the extra ce was within 20 km of the value scaled from oblique-incidence ionogram for sixteen of cases. The time delay can be scaled with an uracy of 20 km. An error of 45 km was culated for the seventeenth case. Therefore, een out of the seventeen cases can be reason-y explained by the model, if it is assumed t the received signals are sufficiently strong be detected.

t was found that irregularities that produce es similar to those in Figure 2 are at heights 100 to 200 km and at horizontal distances up 900 km from the mid-point of the great-circle h. The irregularities that produce an extra h-angle-ray trace occur at heights up to 200 above the minimum height of the F layer and km from the mid-point of the path. The ximum lateral deviation of the irregularity from the great-circle path between the transmitter and receiver varied from 7 to 390 km, with one value of 695 km. For a deviation of 695 km, it is doubtful that the signals would be sufficiently strong to be recorded on the transmitting and receiving system. The azimuthal angles for the other cases have values up to 16° from the great circle path. Regular one-hop and two-hop signals are received on the Winnipeg–Resolute Bay circuit at elevation angles from 3° to 30°. These values were found from a consideration of the ray paths. Azimuthal directivity can be assumed to be approximately the same as, if not broader than, the vertical directivity.

Calculation of velocity. During two weeks in November 1959, continuous runs on the VHF range of the sounder (25–49 Mc/s) were made at the time the maximum occurrence of transient modes on the Winnipeg–Resolute Bay circuit was expected. Eleven consecutive 4-minute sweeps were obtained daily starting at 13 : 06 hours CST. The duration of the transient modes varied from a time less than 4 to about 35 minutes on these runs. Also, continuous 45-minute runs in the range 1–49 Mc/s were made daily from March 15 to April 15, 1960, starting at 13 : 06 and 15 : 06 hours CST. No transient modes were observed on the ionograms during this period.

Five consecutive ionograms taken November 9, 1959, starting at 13 : 12 CST are shown in Figure 6. Part of the VHF sweep, from 25 to 38 Mc/s, is illustrated. The regular MUF, which is

just visible on the 13 : 12 record, is increasing rapidly, and exceeds the transient mode MUF on the 13 : 24 record. There is no indication of the transient mode on the 13 : 28 record.

Consecutive ionograms were used in an attempt to determine the velocity and direction of travel of the irregularity associated with the transient mode. The position of the irregularity was calculated for each of the ionograms in Figure 6.

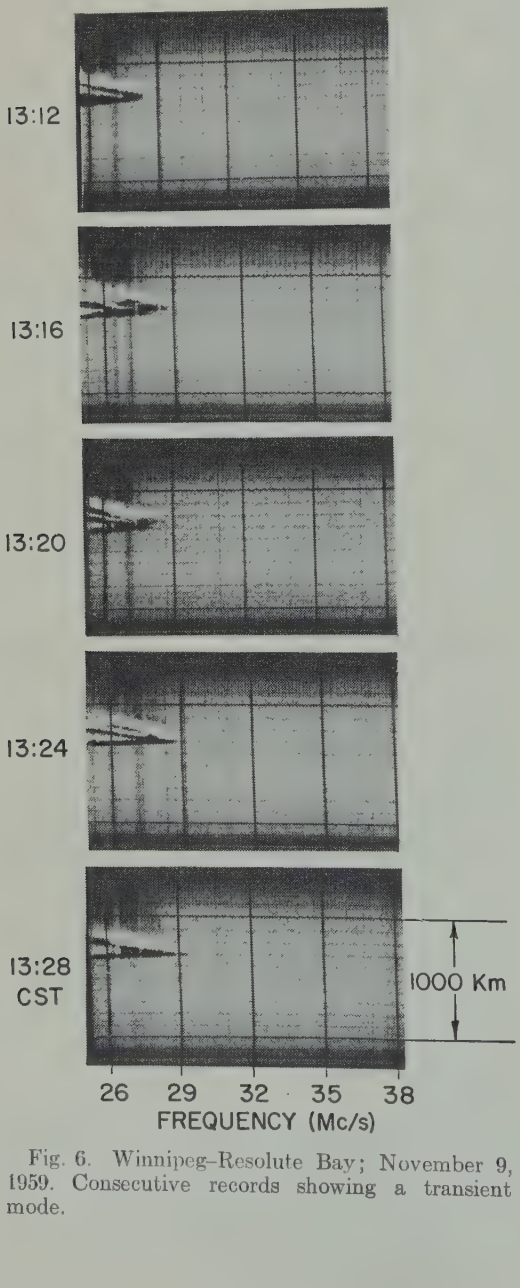


Fig. 6. Winnipeg–Resolute Bay; November 9, 1959. Consecutive records showing a transient mode.

Velocity and direction of travel are found from the calculated change of position between two consecutive records; however, the method of calculating the position is not sufficiently accurate that velocities less than 100 km/hr can be found with any reliability. The velocities calculated for the ionograms in Figure 6 are less than this upper limit, and therefore the direction cannot be resolved. The analysis of two other groups of records gave the same results. Only these three groups of consecutive records were suitable for calculation. Other transient modes that were observed on the records were either isolated instances or else the frequency limits were poorly defined.

Discussion of results. A method has been developed to calculate the heights of irregularities that are believed to be the cause of transient modes of propagation on the Winnipeg–Resolute Bay circuit.

Gradients along and across the great-circle path have been investigated as an alternative explanation for the occurrence of the transient modes. However, the model for which calculations have been presented is the only one that will explain the large time delays between the low-angle traces of the transient mode and the regular mode ordinarily observed on the ionogram. The time delay differences to be expected from gradients along the path were estimated to be only of the order of 10 km, whereas the observed time delay differences are up to 90 km. When the time delay differences were of the order of 10 km, the gradient in f_oF_2 (critical frequency of F_2 layer) along the Winnipeg–Resolute Bay path was investigated using data from Winnipeg, Churchill, Baker Lake, and Resolute Bay for the time the transient mode occurred. The gradient which could produce extra reflections of larger time delays and higher frequencies than the regular reflections is situated between Winnipeg and Churchill. However, the transient mode trace could not be produced because the earth intercepts the rays that would be reflected in the region of the gradient. Gradients across the path produced by diurnal variations of f_oF_2 at the time of occurrence of transient modes are such that they do not produce more than one reflection mode. Localized gradients could occur at these times but could not give the large time delay difference between the regular and transient modes.

ntinuous repetition of sweeps over certain ds have shown the duration of these modes. method which has been given for the cal- ion of the velocity of the clouds of ioniza- is not sufficiently accurate to determine ities less than 100 km/hr. Since the three each gave a velocity estimated to be less 100 km/hr, the velocity of transport of the ularities is probably the same as wind ities in the ionosphere.

knowledgments. We wish to express our ap- ation for the assistance and helpful criticism by Dr. E. S. Warren. The oblique-incidence ders on the Winnipeg-Resolute Bay circuit perated in cooperation with the Department ransport for the Defence Research Board.

References

Fulton, B. J., L. E. Petrie, and W. S. P. Ward, *J. Atmospheric and Terrest. Phys., 16,* 185, 1959.

Fulton, B., O. Sandoz, and E. Warren, *J. Geophys. Research, 65,* 177–183, 1960.

Lejay, P., and D. Lepechinsky, *Nature, 165,* 306, 1950.

National Bureau of Standards, Ionospheric radio propagation, *CRPL, Natl. Bur. Standards Circ. 462,* 74, June 25, 1948.

Southern, R. W., *DRTE Rept. 1058,* Defence Research Board, Department of National Defence, Canada, 1961.

(Manuscript received March 23, 1961; revised May 23, 1961.)

Effects of Corpuscular Emissions on the Polar Ionosphere Following Solar Flares

G. E. HILL

Research and Advanced Development Division, AVCO Corporation
Wilmington, Massachusetts

Abstract. The morphology of two polar absorption events, July 24–25 and September 18–22, 1957, representing different types of ionospheric disturbances, is presented. It was found that in both events the absorption was more intense in the sunlit portion of the polar cap than in the darkened portion by several megacycles, and that following the polar cap absorption event (PCA) of the September storm, strong auroral zone absorption occurred, a geomagnetic storm developed, and the F_2 layer critical frequency decreased markedly, whereas following the July PCA none of these additional disturbances appeared.

ntroduction. In recent studies of solar-ter-rial disturbances it has been found that fol-ing the occurrence of a solar flare energetic ticles enter the polar regions of the earth's osphere prior to a sudden commencement) of geomagnetic activity and cause en-ced ionization in the *D* region and in the tosphere. The energy of these particles is of order of 100 Mev [*Bailey,* 1959; *Anderson, oldy, Hoffman, Peterson, and Winckler,* 9; *Rothwell and McIlwain,* 1959]. These kers have shown that such particles are low-gy solar cosmic rays produced by flare ac-y. *Hakura, Takenoshita, and Otsuki,* [1958] e shown by analysis of f_{min} data (lowest uency observed by HF vertical-incidence ading) that the bombardment of the iono-ere by low-energy cosmic rays may occur he polar cap north of the auroral zone fol-ng a solar flare. This polar cap f_{min} disturb-begins near the pole and spreads outward he vicinity of the auroral zone.

llowing the SC of geomagnetic storms, au-l zone disturbances develop. In terms of rption this development constitutes the sec-phase of the storm. It has already been lished that particles associated with these ral zone disturbances generally possess h less energy than do particles causing r-cap absorption, i.e., of the order of 100 [*Chamberlain,* 1954; *Van Allen,* 1957].

the present paper the morphology of two al absorption events is presented. These events have been taken from a study of polar-cap absorption (PCA), and auroral zone absorption (AZA), covering the first 6 months of the IGY (Hill, 1961, unpublished). The first event is typical of the absorption produced by a high-energy solar cloud as described by *Obayashi and Hakura* [1960], and the second is typical of a mixed high- and low-energy solar cloud.

In a previous investigation [*Hill,* 1960] it was found that, following a solar flare, a region of absorption of HF radio signals was found near the pole and spread outward to about the auroral zone. In that study the ionospheric parameter f_{min} was used as a measure of absorption. After the SC of geomagnetic activity occurred, the f_{min} disturbance formed in a ring around the polar cap in the vicinity of the auroral zone, and at the same time the polar-cap f_{min} disturbance dissipated. This ring of enhanced f_{min} expanded outward from the auroral zone during the development of the main phase of geomagnetic activity. The development of the f_{min} ring in the vicinity of the auroral zone may be linked with the loss of trapped particles during the main phase of a geomagnetic storm. It is known that, during the main phase of a geomagnetic storm, particles trapped in the Van Allen belt are precipitated into the lower ionosphere near the auroral zone. This fact is derived mainly from satellite observations [*Arnoldy, Hoffman, and Winckler,* 1960]. However, these observations do not include pro-

tons having energy less than about 1 Mev. Whether these particles enter the atmosphere directly from space or become temporarily trapped in the earth's magnetic field is not yet established.

In either instance it is reasonable to explain the development of an f_{min} auroral ring by the presence of a solar cloud. If this is so, one would expect an f_{min} ring to develop subsequent to the occurrence of a SC of geomagnetic activity, provided that the solar cloud responsible was in the immediate vicinity of the earth. In addition, if the solar cloud was in the vicinity of the earth one would expect to observe a main phase geomagnetic storm and the usual large-middle latitude decrease in the F_2 layer critical frequency, f_oF_2.

Before proceeding to the discussion of particular cases, the basic data and method of analysis will be briefly described. The base map is a polar stereographic projection especially suitable for arctic work, and the data plotted on it became available through the international exchange program of IGY observations, which are published by the Central Radio Propagation Laboratory of the National Bureau of Standards. The f_{min} charts have been constructed for intervals of 3 hours, and during some periods, for intervals of 1 hour. Isopleths are drawn on the charts for every megacycle per second, starting with 2 Mc/s.

The storm of July 24–25, 1957. A class 3 solar flare occurred at 1712Z, July 24, with major radio noise outbursts. Within 6 hours enhanced absorption was found in polar regions. In accordance with riometer data from College, Alaska, *Reid and Leinbach* [1959] determined the starting time of the PCA to be at 2015Z on the 24th. The development of this PCA can clearly be seen by inspection of the f_{min} charts shown in Figure 1. On the first chart, 1800Z, July 24, a moderate SID is found. In addition, there is absorption taking place in the auroral zone in Alaska and in the Atlantic. At 2100Z auroral-zone absorption is found to have increased slightly. No substantial increase in absorption over the polar cap is found at this time. Within the next 3 hours high f_{min} and blackout conditions developed over most of the polar cap. It appears that the main increase in polar-cap absorption occurred between 2100 and 2400Z on July 24. Throughout most of the 25th, high f_{min} values persisted over the p cap. By a careful inspection of these chart is possible to recognize the effect of sunlig on the PCA. That is, in the sunlit portion the polar cap, f_{min} is found to be several m cycles higher than in the darkened port However, most of the polar-cap region is lit, so only a slight rotation of the f_{min} distu ance during the course of the storm is noticea

The time at which the PCA ended ca easily be given unless some particular crite for the existence of a PCA is chosen. For s general considerations an f_{min} value of 4 M or greater serves as this criterion. In the PCA, a value of 4 Mc/s was found as lat 1500Z on the 25th in a small region near North Pole. Following this time the PCA g ually diminished, with f_{min} values no hig than 2 Mc/s by the end of July 26.

From the time of the solar flare until the currence of a SC of geomagnetic activity 2000Z, July 27, the geomagnetic index, remained below 3. The geomagnetic disturba lasted about 5 hours without a main phase magnetic storm. The geomagnetic disturba was relatively weak, inasmuch as the hig value of the K_p index was 4. Values of observed on the 3-hourly maps and on *f* pl during this period of geomagnetic activity mained normal, except in a few isolated a where it increased to 3 or 4 Mc/s. There wa widespread increase in absorption in either auroral zone or in the polar-cap region.

The storm of September 18–22, 1957. solar flare responsible for the storm of Sept ber 18–22, 1957, is not readily identified bec there were several flares of class 2 and cla that occurred on the 17th and 18th. Howe methods have been developed by several w ers with the aid of solar radio noise data identify solar flares producing ionosph storms [*Denisse,* 1952; *Simon,* 1956; *Do and Hedeman,* 1958]. Application of their m ods to solar radio noise data published in IAU Bulletin (no. 119) led to the selectio a class 3+ flare beginning at 1722Z on S tember 18 as the one responsible for the P

To facilitate the discussion of the July

[1] The limit of the sunlit portion of the eart indicated on the charts by a broken line.

[2] An *f* plot is a diagram showing the meas ionospheric parameters at fifteen minute inter

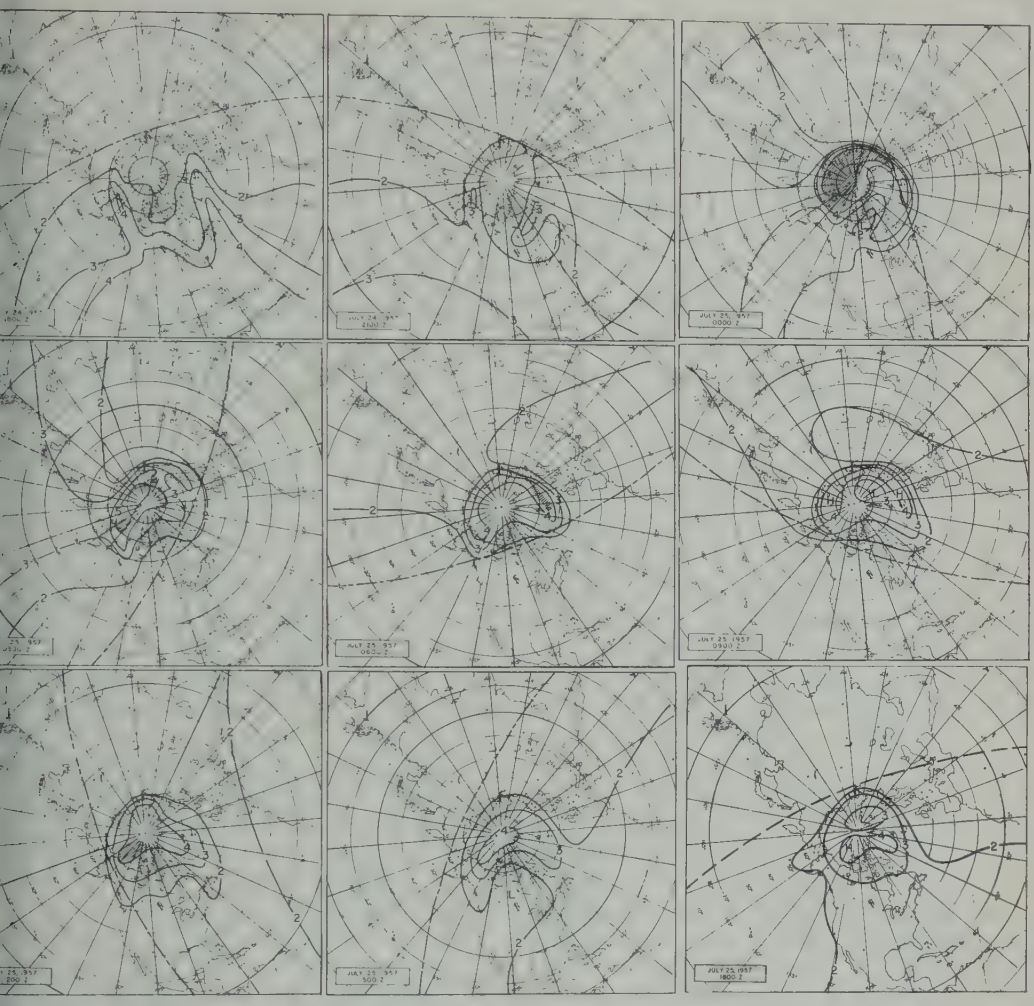


Fig. 1. Polar-cap absorption during July 24–25, 1957, storm. Minimum frequency in megacycles of signals returned vertically from the ionosphere.

ptember storms the basic geophysical paramrs are given in Table 1.

The development of the PCA up until 2 rs after the sudden commencement of geognetic activity is shown in Figure 2. Alugh charts were constructed for intervals 3 hours, only every other one is shown. The portant features of the PCA event are not tted as a result of this limited presentation. first chart in the series is at 1800Z September 18, at which time a remarkable SID is id.

s shown on the next chart, 0000Z September 19, the polar-cap region is relatively free n abnormal absorption, excepting that which may be attributed to flare effects, but on the subsequent charts the PCA is clearly evident.

Throughout September 19 the polar cap f_{min} disturbance remained relatively weak. The highest f_{min} value was around 4 Mc/s. Early on the 20th the PCA became more intense in the sunlit portion of the polar cap than in the dark portion, and for the remainder of the 20th this PCA pattern did not change. At 0000Z September 21, the disturbance is found to be somewhat weakened, and during the next 6 hours it continued to weaken as it rotated in the polar-cap region. The remaining disturbance is shown on the 0600Z chart.

TABLE 1. Basic Geophysical Parameters

Flare Time	July 24	1712Z	Sept. 18	1722Z
PCA start (approx)	July 25	0000Z	Sept. 19	0300Z
SC time	July 27	2000Z	Sept. 21	1005Z
K_p	4		7+	
AZA start	None		Sept. 21	1200Z
Δf_0F_2	+1 Mc/s		−5 Mc/s	

From an inspection of the f_{min} charts for this September storm, a rotation of the polar-cap f_{min} disturbance can be clearly seen. During the height of the PCA, on the sunlit portion of the polar cap, f_{min} is generally several megacycles higher than on the remaining portions. The rotation of the polar-cap f_{min} disturbance with the sun can be qualitatively explained on the basis of photo-detachment of negative ions [*Hultqvist and Ortner,* 1958; *Davies,* 1960]. Photo-detachment will cause a higher electron density in the sunlit portion of the polar cap than in the dark portion. It is not expected that this rotation would be so evident on the charts for the July storm because at that time of year most of the polar-cap region is sunlit. On the other hand, during the winter months the only portion of the polar cap that is sunlit is a region near the auroral zone around the local noon meridian. A winter PCA event would presumably be found with relatively high absorption confined to this small sunlit region. Since high polar-cap absorption would be confined to a region near the auroral zone during winter, it will be difficult to separate auroral-zone and polar-cap absorption unless the summer hemisphere data are used. Studies concerning the differential effects of sunlight vs. darkness on PCA events are best conducted for the equinoctial months, because at these times the differential effects are most pronounced.

After the ocurrence of the SC of geomagnetic activity at 1005Z, September 21, the geographic distribution of absorption changed markedly. The polar-cap disturbance located on the Eurasian side of the Arctic Ocean at 0600Z rotated to near the Greenwich Meridian by 1200Z, as would be expected from the sunlight effect on a PCA. The remaining portion of the PCA is merged with intense auroral-zone absorption that developed following the SC. This auroral-zone absorption took place at all longitudes with the nighttime f_{min} values being about high as the daytime values.

By 1500Z, September 21 (SC + 5 hour widespread blackout conditions were found ov the polar cap.[3] It was therefore impossible analyze reliably either the f_0F_2 or the f_{min} cha from 1500Z and afterward. The F_2 layer criti frequency decreased rapidly during the develo ment of the geomagnetic main phase stor This decrease in f_0F_2 was accompanied by increase in f_{min} over the polar cap apparen associated with another geomagnetic storm th occurred on the 22nd. A third geomagne storm occurred on the 23rd, so that the ion sphere remained disturbed for at least 2 da after the beginning of the first geomagne storm. Because of these complications, a discu sion of the first storm is carried only as far 1200Z, September 21.

Outstanding characteristics of the July a September ionospheric storms. Both the Ju and September storms are characterized by t development of a PCA within a few hours af the occurrence of the solar flare responsib The July PCA lasted about 1 day and the Se tember PCA about 2 days. This duration based on an f_{min} value of 4 Mc/s as a criteri for the existence of a PCA. However, both t beginning and end of a PCA may be gradu so that one particular f_{min} value cannot ve well represent the true picture.

In both events the PCA was more inte in the sunlit portion of the polar cap than the darkened portion by several megacyc This difference in absorption between the sun and darkened regions is more noticeable in September storm than in the July storm cause in September about half the polar reg is in sunlight and half is in darkness.

The main difference between the two abso tion events described is that in the July sto no auroral zone f_{min} disturbance develop whereas in the September storm an auro zone f_{min} disturbance did develop following SC of geomagnetic activity.

The behavior of both the geomagnetic f

[3] Widespread blackout conditions may devo when two ionospheric storms occur in close cession, because the f_0F_2 decreases in the la stages of the first storm (during the main pha and, at the same time, the f_{min} increases in early stage of the second storm (during the PC

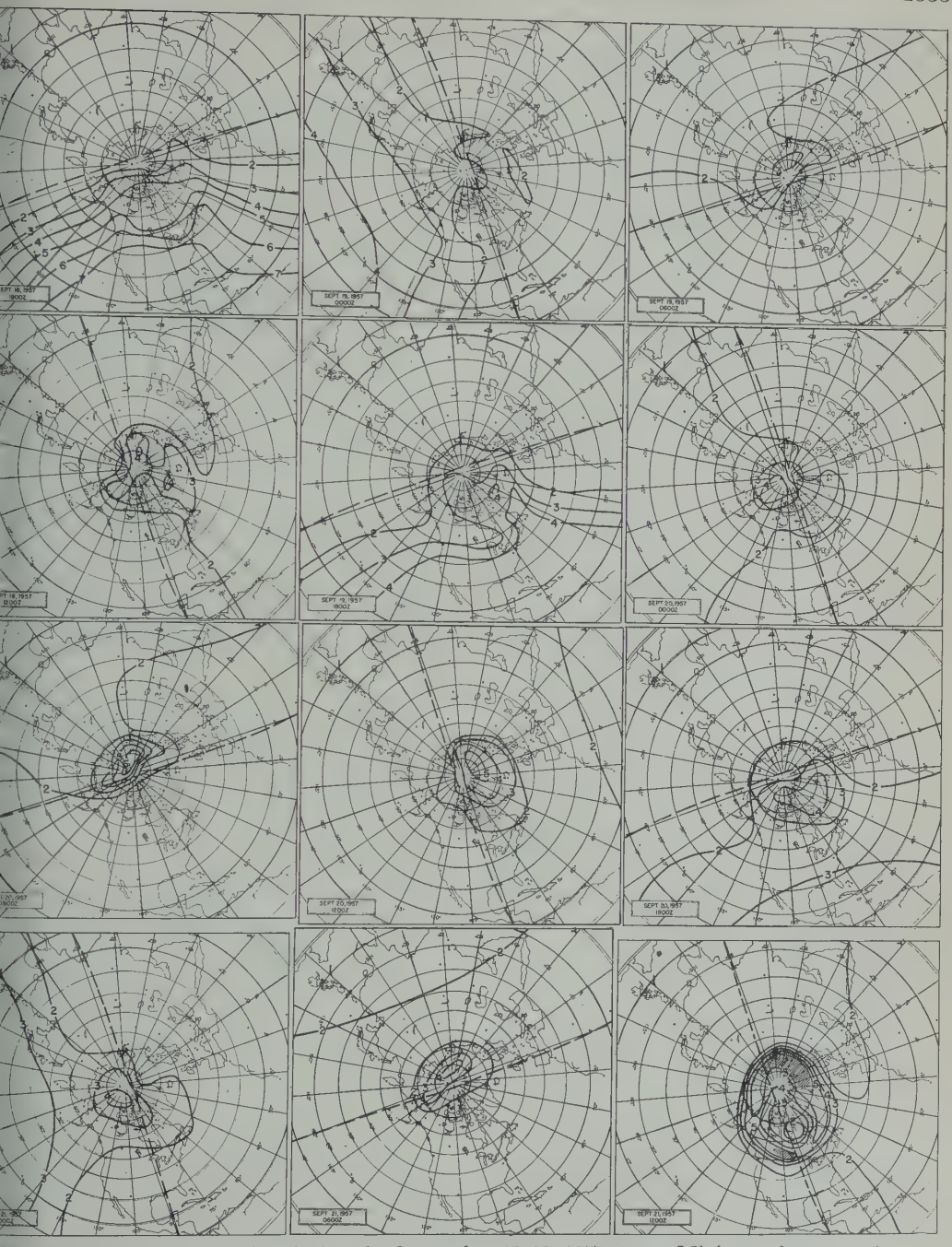


Fig. 2. Polar-cap absorption during the September 18–22, 1957 storm. Minimum frequency in megacycles of signals returned vertically from the ionosphere.

the F_2 layer critical frequency also showed sic difference in the period following the and September PCA events. The planetary x of geomagnetic activity, K_p, reached no higher than 4 during the whole week following the occurrence of the flare on July 24, whereas K_p reached 7+ a few hours after the sudden commencement on September 21. The increase

in K_p to 8+ on the 22nd appears to be associated with another geomagnetic storm that began at 1344Z on the 22nd.

It has already been suggested by *Obayashi and Hakura* [1960] that the solar plasma reaching the vicinity of the earth may be classified as high-energy or as low-energy clouds. The high-energy cloud causes polar-cap absorption, and the low-energy cloud causes auroral-zone absorption. Also, the solar cloud may be of a mixed type causing both PCA and AZA. According to this classification, the July storm was associated with a high-energy cloud and the September storm with a mixed high- and low-energy cloud. The July storm appears to have much the same character as the October 20–22, 1957, storm analyzed by Obayashi and Hakura.

It is suggested that the f_{min} auroral zone ring disturbance and the geomagnetic storm occur together. In the storm of July 24–25, 1957, both the f_{min} auroral zone ring disturbance and the main phase geomagnetic storm were absent. In the storm of October 20–22, 1957, some auroral-zone absorption occurred. No main phase geomagnetic storm occurred during this period of absorption, although around the time of the SC the K_p index reached 7−. In several other cases, September 11–14, 1957 [*Hill*, 1960], September 18–22, 1957 (present paper), and February 10–12, 1957 [*Hakura, Takenoshita, and Otsuki*, 1958] both the f_{min} auroral-zone disturbance and the main phase geomagnetic storm were present. However, it should be pointed out that f_{min} auroral-zone disturbances often occur without a main phase geomagnetic disturbance.

The difference in the behavior of f_oF_2 for the two storms was found to be similar to the K_p index. That is, relatively small departures of $f_o F_2$ from the normal value were found in the July storm, whereas large departures were found in the September storm. To show this, hourly values of f_oF_2 for a subauroral station are reproduced in Figure 3. The only significant f_oF_2 departure found that might be associated with the July solar-terrestrial disturbance is an increase of about 2 Mc/s above the normal value on the 27th. In the September storm the f_oF_2 decreased about 5 Mc/s below the normal value within 6 hours of the sudden commencement of geomagnetic activity. Similar differences in the behavior of f_oF_2 between the two storms are found at other stations.

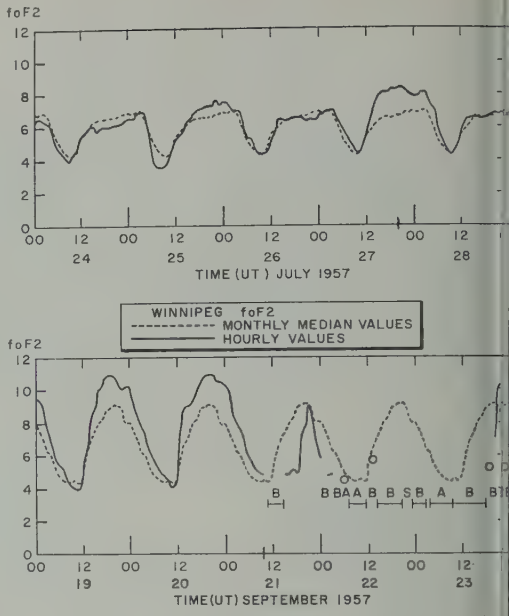


Fig. 3. F_2 layer critical frequency at Winnip for July 24–28 and September 19–23, 1957. (SC occurred at 2000Z July 27 and the first three SC's occurred at 1005Z September 21).

During the July and October storms, depa tures from the monthly medians of f_oF_2 mained less than about 2 Mc/s, whereas duri the storms with a geomagnetic main phase, t f_oF_2 fell at least 5 Mc/s below the month median. This difference in behavior of f_oF_2 tween the two types of ionospheric storms su stantiates the close connection between worl wide variations in the F-layer ionization a the earth's magnetic field.

Summary. The main features found to associated with the two storms analyzed are t following:

July 24–25, 1957. 1. A PCA event beg within about 6 hours of a class 3+ solar fla and lasted about a day with the PCA strong within 2 or 3 hours of its beginning.

2. The PCA was more intense in the su portion of the polar cap than in the darken portion by several megacycles.

3. Although a main phase geomagnetic sto did not develop, a SC of geomagnetic activ did occur 74 hours after the solar flare.

September 18–22, 1957. 1. A PCA event gan within 6 hours of a class 3 solar flare a lasted about 2 days. The most intense part the PCA occurred early on the second day

. The PCA was more intense in the sunlit tion of the polar cap than in the darkened tion by several megacycles.

. Sixty-four hours after the solar flare a SC geomagnetic activity occurred. It was fol- ed by a main phase geomagnetic storm with K_p index of 7+.

. Intense auroral zone absorption occurred owing the SC. The duration and behavior of AZA was not studied because a new iono- eric disturbance began shortly after the de- opment of the AZA.

. During the main phase geomagnetic storm F_2 layer critical frequency decreased by sev- l megacycles below its normal value.

n summary, the basic characteristics of the storms are that a PCA event began within ut 6 hours of the solar flare and remained stly in the sunlit portion of the polar cap, that following the PCA of the September m strong auroral-zone absorption occurred, eomagnetic storm developed, and the F_2 layer ical frequency decreased markedly; whereas owing the July PCA none of these additional urbances were found.

cknowledgment. The research in this docu- nt was supported by Air Force Cambridge Re- rch Laboratories under contract AF19(604)- 2. I am indebted to Mr. S. C. Coroniti and to R. B. Penndorf for their helpful advice and ussion.

References

lerson, K. A., R. Arnoldy, R. Hoffman, L. eterson, and J. R. Winckler, Observations of w-energy solar cosmic rays from the flare of ugust 22, 1958, *J. Geophys. Research, 64,* 1133–147, 1959.

oldy, R. L., R. A. Hoffman, and J. R. Winck- r, Observations of the Van Allen radiation re- gions during August and September 1959, Part I, *J. Geophys. Research, 65,* 1361–1376, 1960.

Bailey, D. K., Abnormal ionization in the lower ionosphere associated with cosmic ray flux enhancements, *Proc. IRE, 47,* 255–266, 1959.

Chamberlain, J. W., The excitation of hydrogen in aurorae, *Astrophys. J. 120,* 360–366, 1954.

Davies, K., A study of 2 Mc/s ionospheric absorption measurements at high latitudes, *J. Geophys. Research, 65,* 2285–2294, 1960.

Denisse, J. F., Relation entre l'activité géomagnetique et l'activité radioélectrique solaire, *Ann. géophys., 8,* 55, 1952.

Dodson, H. W., and E. K. Hedeman, Geomagnetic disturbances associated with solar flares with premaximum bursts at radio frequencies $\leq$200 Mc/s, *J. Geophys. Research, 63,* 77–96, 1958.

Hakura, Y., Y. Takenoshita, and T. Otsuki, Polar blackouts associated with severe geomagnetic storms on September 13th, 1957, and February 11th, 1958, *Rept. Ionosphere Research Japan, 12,* no. 4, 1958.

Hill, G. E., Ionospheric disturbances following a solar flare, *J. Geophys. Research, 65,* 3183–3207, 1960.

Hultqvist, B., and J. Ortner, Observations of intense ionization of long duration below 50 km altitude after some strong solar flares, *Nature, 183,* 1179–1180, 1958.

Obayashi, T., and Y. Hakura, Enhanced ionization in the polar ionosphere caused by solar corpuscular emissions, *J. Radio Research Lab., 7* (29), 27–66, 1960.

Reid, G. C., and H. Leinbach, Low-energy cosmic ray events associated with solar flares, *J. Geophys. Research, 64,* 1801–1805, 1959.

Rothwell, P., and C. McIlwain, Satellite observations of solar cosmic rays, *Nature, 184,* 138–140, 1959.

Simon, P., Activité géomagnetique et éruptions, *Ann. géophys., 12,* 167, 1956.

Van Allen, J. A., Rocket measurements of soft radiation, *IGY Rocket Rept.,* Ser. 1, 169–178, 1957.

(Manuscript received September 19, 1960; revised May 4, 1961.)

The Latitude Dependence of Radar Meteor Shower Observations

C. S. L. KEAY AND C. ELLYETT

Physics Department, University of Canterbury
Christchurch, New Zealand

Abstract. A simplified method of assessing the relative significance of meteor showers is discussed. The bias inherent in single-station rate measurements is largely eliminated and the importance of short-range echoes is emphasized. Comparison of results obtained from both hemispheres reveals a considerable measure of agreement between various surveys.

ntroduction. Radio echo observations of teors have greatly extended our knowledge of meteor streams intercepting the earth's or- and have revealed the main features of the tribution of sporadic meteors around the sun. servations of individual meteors can be made h considerable precision because it is possible calibrate radar equipments to a high degree accuracy [*Whipple and Hawkins,* 1959]. This cision, however, applies only to such factors radiant coordinate determination and ve- ty measurements.

Of great importance is the measurement of incident meteor flux of both shower and radic meteors, but unfortunately it is the st difficult to measure accurately, even though e measurements are readily obtained. Meteor es at a given observing station are very ngly dependent on the geographical location he station, as will be shown, and do not give liable indication of the relative particle fluxes n different meteor showers. These measure- nts are also dependent to a lesser extent on aerial configuration employed. In other ds, the hourly rates for radio observations ted in the literature [for example, *Whipple Hawkins,* 1959] are without meaning, un- it is understood that they apply only to a ticular observing station.

To be meaningful, rate measurements should converted to incident meteor flux measure- nts [*Kaiser,* 1960], but the conversion in- es experimental difficulties and laborious ulations. It has been attempted, for example, *Weiss* [1957], who obtains values for eight eor showers.

Kaiser [1960] has published a semigraphical method enabling the incident flux of shower meteors to be deduced from the observed rate. This method is considerably simpler than any previous one, but even so the amount of computation required may not be justified unless it is imperative that an absolute flux measurement be obtained.

However, for the purpose of establishing the relative importance of showers detected from any given observing station, and eliminating the long recognized tendency to emphasize those showers which transit close to the zenith, a simple plot of observed rate against declination can be most helpful, as will now be shown.

Theory. Expressions for the total radio echo rate of shower meteors detected by apparatus employing narrow-beam aerials have been derived by *Kaiser* [1955]. For a narrow aerial beam he obtains the following close approximation for the total echo rate, N:

$$N \cong A\Theta(\alpha_0/\cos\chi)F(\phi) \qquad (1)$$

where A is a function of the mass distribution parameter s, the aerial beam width, the mean height of the reflection points, and the atmospheric scale height. These will be regarded as constants for the purposes of this paper.

The flux function $\Theta(\alpha_0/\cos\chi)$ depends also on s and can be rewritten in the form $BN_i \cos^{s-1}\chi$, where B is a function of the minimum detectable line density α_0 in the direction of the beam maximum, i.e., it is an equipment parameter, and N_i is the incident meteor flux for the shower concerned. The angle χ is the zenith angle of the trajectory of a detectable meteor, which to a good approximation is also the zenith angle of the true meteor radiant.

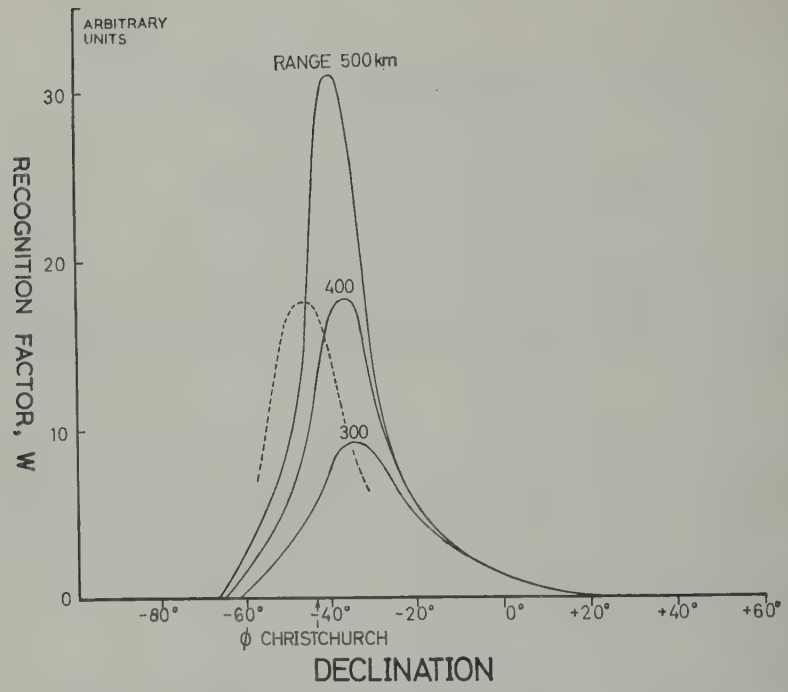


Fig. 1. Meteor shower recognition factor, W, plotted as a function of shower declination.

Following Kaiser, the remaining function $F(\phi)$ can be written

$$F(\phi) \cong \cos^{-2} \theta \sin^{-2} \chi \qquad (2)$$

where θ is the angle between the reflection point and the beam maximum. For narrow beam equipments the variation with θ can usually be neglected, and we have finally

$$N \cong CN_i \cos^{s-1} \chi \sin^{-2} \chi \qquad (3)$$

where C is a function independent of χ. Thus the above expression gives the observed echo rate as a function of the radiant zenith angle when the rate is at its maximum.

The *recognition* of a meteor shower of given flux when using methods essentially dependent on rate measurement is influenced by the radiant declination δ. The sharpness of a peak in the echo rate must depend on the speed with which a radiant moves across the sky, and is, therefore, dependent on the cosine of the radiant declination. Inclusion of the factor cos δ in equation 3 then leads to a simple expression showing how well a meteor shower may be recognized by using a given equipment at a given location:

$$W = \frac{\cos^{s-1} \chi \cos \delta}{\sin^2 \chi} \qquad (4)$$

where W may be termed the recognition factor.

The variation of recognition factor with declination is strongly dependent on the range R, at which echoes are received, since the zenith angle χ of a shower radiant at the time of maximum echo rate is itself a function of R. The variation with s and other parameters is relatively unimportant.

Figure 1 shows W plotted for various values of range in the case of an equipment located at latitude −43°31′ utilizing a narrow-beam aerial directed to a local azimuth of 112°30′E. The dotted curve (included for comparison only) is drawn for echoes received from a range of 400 km by an aerial directed to a local azimuth of 67°30′E.

It is evident from Figure 1 that any method of meteor shower detection that depends on the presence of long-range echoes will greatly favor radiants culminating near the zenith. To avoid this source of bias as far as possible, methods of meteor-shower delineation should utilize short-range echoes.

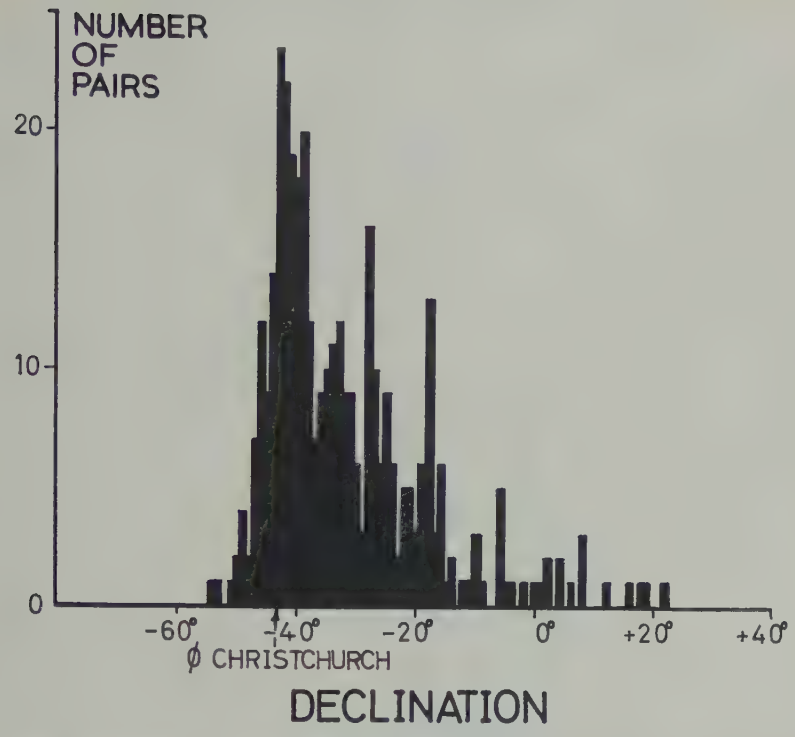


Fig. 2. Histogram showing number of pairs of peaks in measured rate plotted against the resulting value of declination.

xperimental verification. The curves drawn igure 1 have been verified experimentally, g results obtained from the radio echo pment at Christchurch, New Zealand [*Ell- and Keay,* 1956], during the last 5 months 956. During this period partial-rate curves *ay,* 1957] were plotted for echoes originat- etween 350- and 450-km range on each of aerials directed to local azimuths of 67°30′ 112°30′ east of north. The most prominent ma on the two partial-rate curves were d day by day to yield values of declination he mean radiants of the sudden increases in or flux causing the maxima. Significant or showers were sorted out by considering factors as the number of consecutive daily rrences of the same pair of maxima.

hen the total number of pairs of maxima plotted against declination, without apply- ny selection tests, the histogram shown in re 2 was obtained. This exhibits a sharp close to the value of declination corre- ding to the latitude of the station, or, rather, e value of declination where the solid and dotted curves of Figure 1 cross. The over-all shape of the histogram is closely similar to the curves of Figure 1.

Application to Christchurch results. During 1953 a survey of southern hemisphere meteor activity was carried out [*Ellyett and Roth,* 1955] and the results were analyzed by drawing envelopes enclosing meteors from specific radiants on daily range-time plots of meteor echoes [*Aspinall, Clegg, and Hawkins,* 1951]. The major showers detected by this survey, together with the significant meteor showers detected in 1956, are shown in Figure 3 in which the maximum hourly rate of each shower is plotted against the shower declination.

Superimposed on the shower plot are two curves representing the shower recognition factors for the two aerials of the system. These have been calculated on the assumption that the range of maximum occurrence of meteors (400 km) leads to fair values for the shower recognition factor in the case of meteors recorded over a wide-range interval as in the range-time plot method. For the partial-rate method, of course,

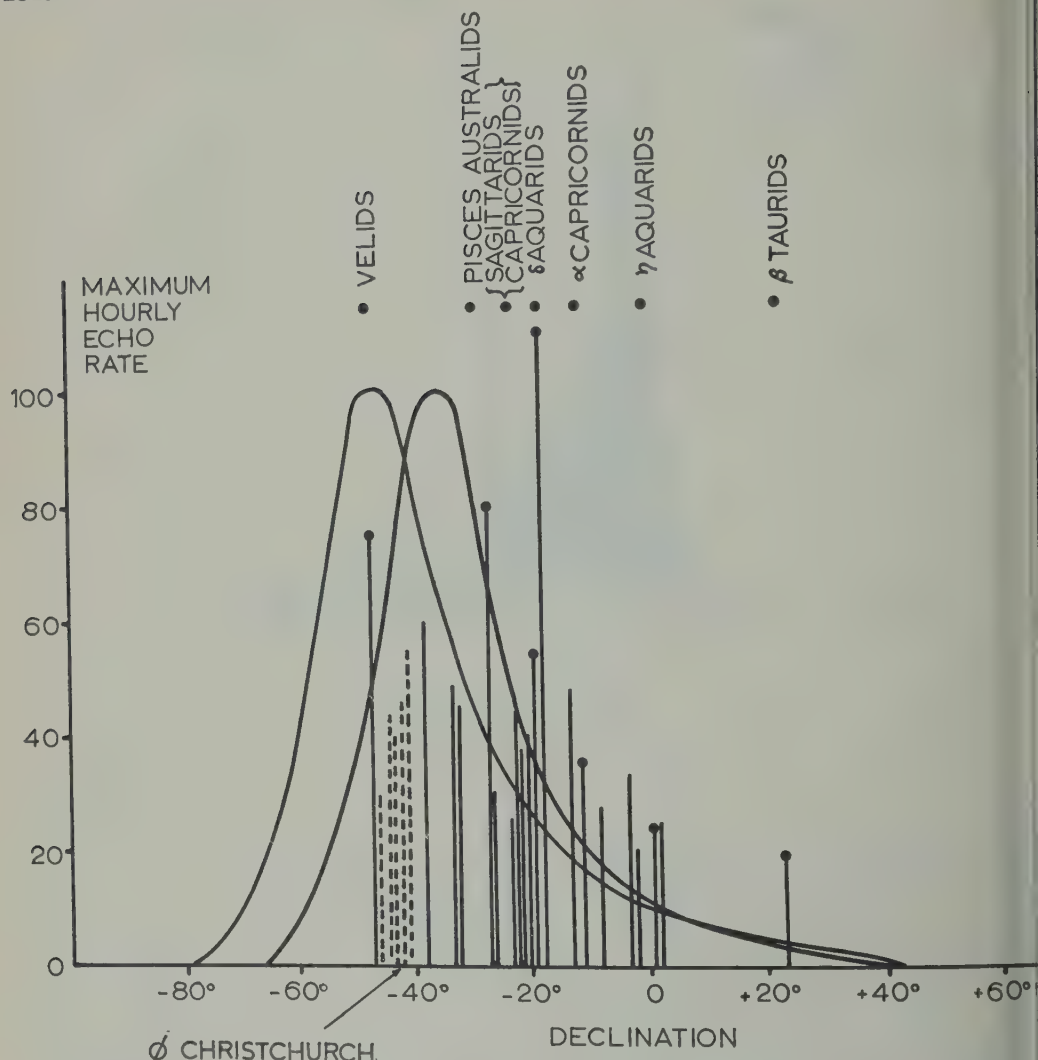


Fig. 3. Maximum hourly echo rates of meteor showers observed from Christchurch compared with the shower recognition factors for the two aerials employed.

it is perfectly valid since the range interval used was centered on 400 km.

In Figure 3 and subsequent figures the recognition curves have been normalized by making the peak value of W correspond to an hourly echo rate of 100. The showers of highest flux in Figure 3 are those which rise above the two recognition curves by the greatest amount. Examples are the δ-Aquarids and the β-Taurids.

Similarly, showers whose observed echo rates cause them to lie well below the recognition curve are of lowest flux. The showers shown dotted in Figure 3 yielded echo rates higher th many of the major showers shown, but it is vious from the figure that they are of much importance. (These particular showers did in fact, meet the requirements of consiste necessary for shower acceptance, and have b excluded from published lists.)

Application to other observing stations. S ilar calculations have been made for two ot observing stations which have used narrow-b dual-aerial systems for the delineation of teor radiants. For these two stations, nam

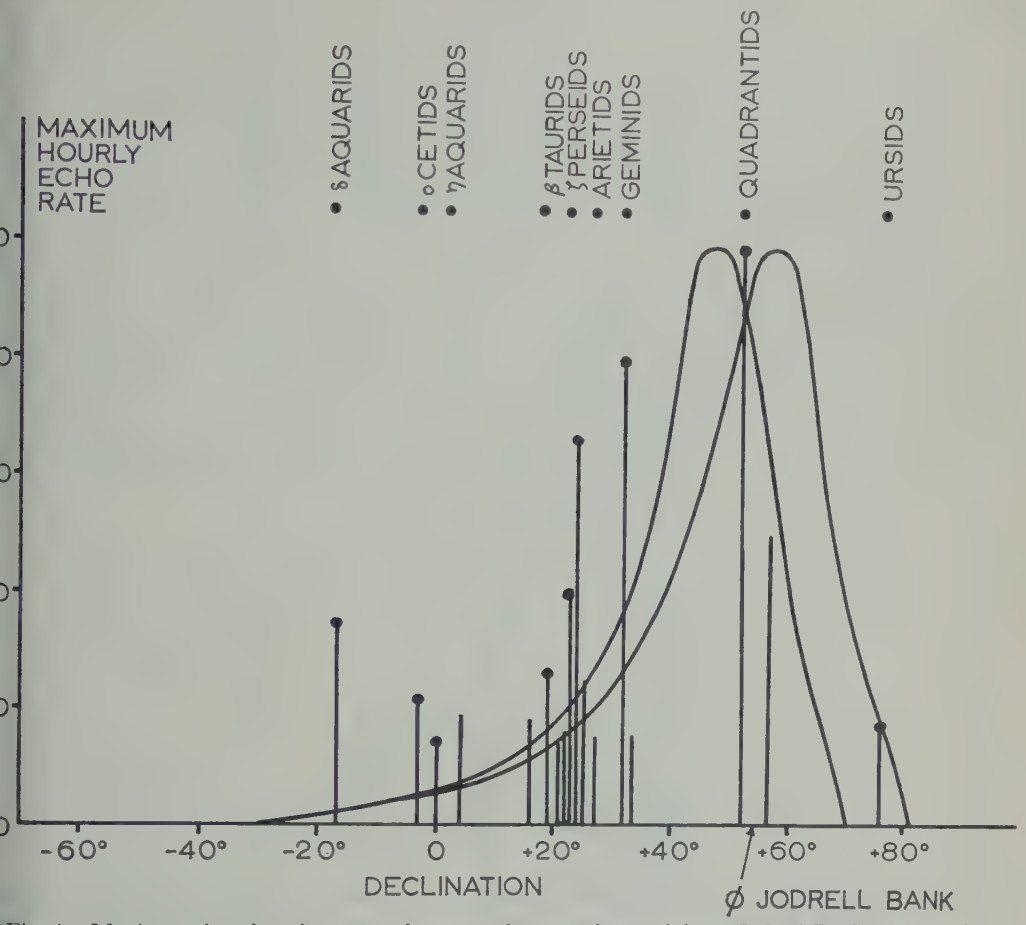


Fig. 4. Maximum hourly echo rates of meteor showers observed from Jodrell Bank compared with the estimated shower recognition factors for the two aerials employed.

rell Bank and Adelaide, meteor shower rec- tion curves are shown in Figures 4 and 5. curves are based on parameters published *Aspinall, Clegg, and Hawkins* [1951], and *ss* [1960], respectively. It must again be ssed that the height and sharpness of the in each curve depends on the way echoes selected to yield the transit times necessary determining radiant coordinates. However, form of the curves will be accurate enough qualitative discussion.

perimposed on the shower recognition curves gures 4 and 5 are the rates and declinations e main meteor showers observed at the two ons. [See *Hawkins and Almond,* 1952*a* and *lmond, Bullough, and Hawkins,* 1952; *Bul-*, 1954; and *Davidson,* 1956, for the Jodrell results, and *Weiss,* 1960, for the Adelaide results.] The showers shown dotted in Figure 5 are those classified by Weiss as possible showers, the others as accepted showers.

These figures are particularly illuminating if the Christchurch and Adelaide results are compared with those from Jodrell Bank. The relative importance of the different meteor showers is easily seen, and the results from both hemispheres agree well as far as the major low declination showers are concerned.

Showers which transit close to the zenith, such as the Quadrantid shower detected at Jodrell Bank, appear reduced in importance compared with showers such as the η-Aquarids, whose low observed rate from all three stations belies their true strength. The δ-Aquarids emerge as the strongest known meteor shower.

In each of the three figures it is seen that the

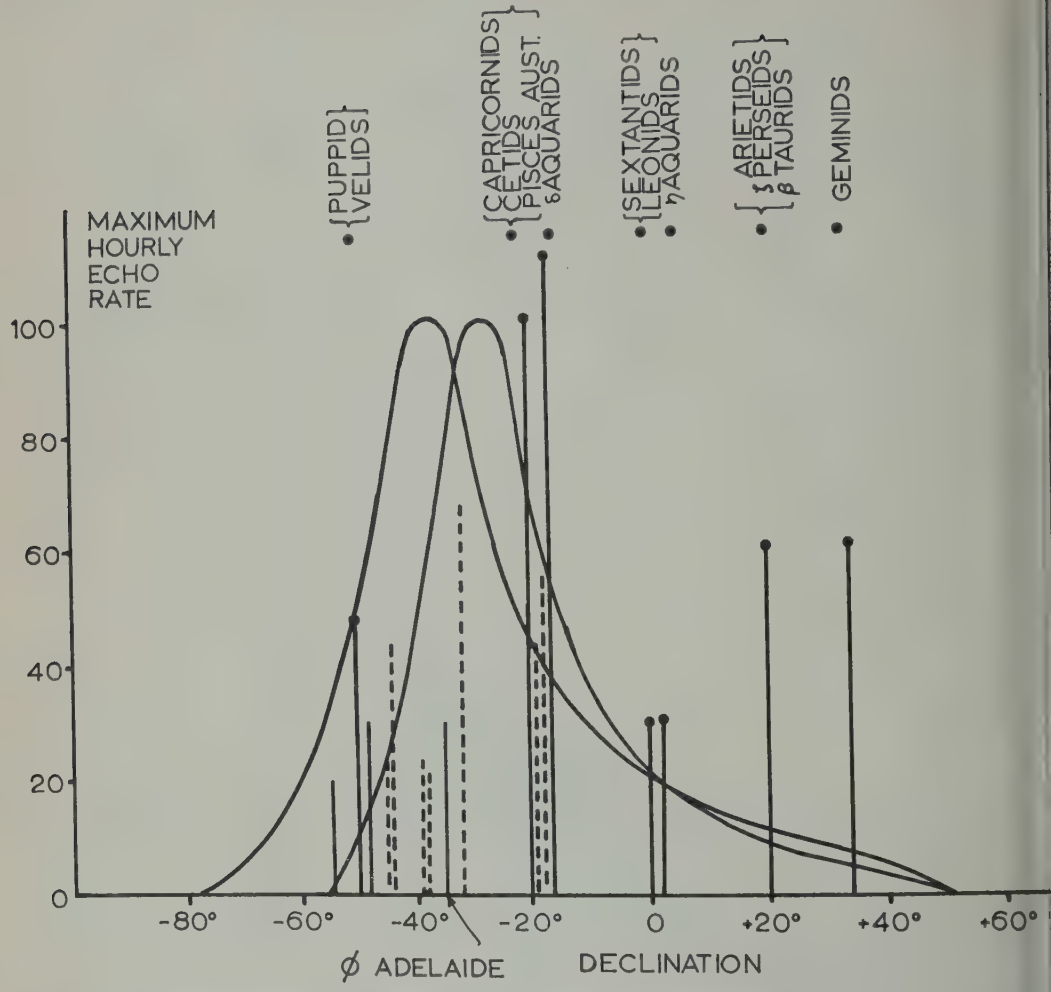


Fig. 5. Maximum hourly echo rates of meteor showers observed from Adelaide compared with the estimated shower recognition factors for the two aerials employed.

recognition curves give a reasonable fit to the plotted shower rates, except in the case of the Adelaide results where the Arietids, ζ-Perseids and β-Taurids are taken together, and where the Geminids appear to have produced a surprisingly high rate. The known low value of s for the Geminid shower does not entirely account for its observed rate of 60 per hour from Adelaide.

Conclusions. Most of the tables of meteor showers quoted in the literature give a false impression of the actual influx of meteoric shower particles into the earth's atmosphere, particularly when rate measurements are quoted. This may be avoided in two ways, either by quoting results from several observing stations in bo hemispheres or by presenting the information the form shown in Figures 3, 4, and 5.

Acknowledgment. This work has been su ported by grants from the New Zealand Depa ment of Scientific and Industrial Research, a contract assistance from the Electronics Resear Directorate of the Air Research and Developme Command, USAF, under contract AF64(500)-6.

References

Almond, Mary, K. Bullough, and G. S. Hawki Radio-echo observation of the daytime met streams, *Jodrell Bank Ann., 1,* 13–21, 1952.

Aspinall, A., J. A. Clegg, and G. S. Hawkins, Rad echo apparatus for the delineation of met radiants, *Phil. Mag., 42,* 504–514, 1951.

llough, K., Radio-echo observations of the day- and night-time meteor streams 1951 October to 1953 December, *Jodrell Bank Ann., 1,* 68–97, 1954.
vidson, T. W., Radio-echo observations of the day- and night-time meteor streams between 1954 January and 1955 August, *Jodrell Bank Ann., 1.,* 116–125, 1956.
yett, C. D., and C. S. L. Keay, Radio-echo observations of meteor activity in the southern hemisphere, *Australian J. Phys., 9,* 471–480, 1956.
yett, C. D., and K. W. Roth, The radar determination of meteor showers in the southern hemisphere, *Australian J. Phys., 8,* 390–401, 1955.
wkins, G. S., and Mary Almond, Radio-echo observations of the major night-time meteor streams, *Mon. Not. Roy. Astron. Soc., 112,* 219–233, 1952*a*.
wkins, G. S., and Mary Almond, Radio-echo observations of the daytime meteor streams in 1951, *Jodrell Bank Ann., 1,* 1–12, 1952*b*.
Kaiser, T. R., Meteors, *Supp. J. Atmospheric and Terrest., Phys. 2,* 119–130, 1955.
Kaiser, T. R., The determination of the incident flux of radio-meteors, *Mon. Not. Roy. Astron. Soc., 121,* 284–298, 1960.
Keay, C. S. L., Meteor radiant determination from high-echo-rate observations, *Australian J. Phys., 10,* 471–482, 1957.
Weiss, A. A., The incidence of meteor particles upon the earth, *Australian J. Phys., 10,* 397–411, 1957.
Weiss, A. A., Radio echo observations of southern hemisphere meteor shower activity from 1956 December to 1958 August, *Mon. Not. Roy. Astron. Soc., 120,* 387–403, 1960.
Whipple, F. L., and Hawkins, G. S., Meteors, in *Handbuch der Physik, 53,* 519–564, Springer-Verlag, Berlin, 1959.

(Manuscript received May 19, 1961.)

Theory of Electrostatic Fields in the Ionosphere at Equatorial Latitudes

JOHN R. SPREITER AND BENJAMIN R. BRIGGS

National Aeronautics and Space Administration
Ames Research Center, Moffett Field, California

Abstract. The properties of the elongated electrostatic fields that are required to provide the coupling mechanism in the dynamo-motor concept of the *E* and *F* regions of the ionosphere are examined theoretically for the conditions that prevail in equatorial latitudes. The analysis is developed for an electrostatic field of arbitrary horizontal scale in a horizontally stratified partly ionized gas subject to an imposed magnetic field having the form of a parabolic arch over the equator. The anisotropic character and continuous variation with height of the conductivity are retained throughout, and numerical solutions are determined for the attenuation of the electric field with distance along the field line.

The results are similar qualitatively to those found previously upon analysis of the corresponding problem for middle latitudes, but the attenuation of the electrostatic field with height is considerably greater. It develops, in particular, that the coupling between *E* and *F* regions is very small for fields having horizontal wavelengths of a few kilometers. It follows that the dynamo-motor concept could not be used to account for the presence of irregularities of this scale. On the other hand, it is found that almost all the attenuation occurs at heights near that of the *E* region. If an electrostatic field having a horizontal wavelength of a few kilometers could be produced at heights of, say 200 km or greater, it follows that it would be very elongated and extend with little change in amplitude from hemisphere to hemisphere. The results also indicate that effective coupling could be achieved for fields having horizontal wavelengths of the order of tens of kilometers, but the assumptions introduced to simplify the analysis may impair the quantitative reliability of the results for fields of this scale.

Introduction. The present study of electrostatic fields in the equatorial ionosphere represents a continuation of the investigations of *Farley* [1959, 1960] and *Spreiter and Briggs* [1961] that have been prompted by the desire to understand better the coupling mechanism that is required in the dynamo-motor concept of the *E* and *F* regions of the ionosphere. The original suggestion of this concept was made by *Martyn* [1955] in order to provide a satisfactory explanation for the presence of strong tidal flows in the F_2 region. It has been subsequently suggested by *Dagg* [1957] that a similar mechanism, operating on a much smaller scale, is responsible for the irregularities in electron density in and above the *F* region that are associated with the scintillation of radio stars.

Among the many questions that arise in a quantitative examination of Dagg's proposal is that of whether the conductivity along the magnetic lines is sufficiently greater than that in other directions to produce the elongated electric fields required for effective coupling between kilometer-scale motions in the dynamo and *F* regions. This fact was recognized by *Farley* [1959, 1960], who proceeded to develop a quantitative theory of electrostatic fields in a horizontally stratified ionized gas subject to an imposed magnetic field. *Spreiter and Briggs* [1961] showed, however, that the analysis for polar and middle latitudes contained certain inconsistencies. These were corrected, the resulting equations solved numerically, and a new set of results for the variation of the electrostatic field with height above the dynamo region was presented.

The results show that the electrostatic coupling necessary for the operation of the mechanism proposed by Dagg can be attained under conditions that can reasonably be expected to occur in the ionosphere. They also show that relatively small changes in the ionospheric conditions, well within the range of possibilities, can result in very substantial changes in the degree of coupling that can be associated with irregularities having a horizontal wavelength of the order of a few kilometers. A further property of the results that may be of great importance

is that there is almost no attenuation of the electrostatic field with height above the lower portions of the F region. If the mechanism described by Dagg is indeed responsible for all or some of the irregularities observed in the F region, it follows that these irregularities will not terminate at this level, but will extend for great distances along the magnetic lines. It is well known, of course, that the existence of such extremely elongated irregularities in the ionosphere is virtually required to account for the occurrence of whistler and related radio noise phenomena, and possibly also for the recent observations of radar echoes from the opposite hemisphere.

The results for polar and middle latitudes disclose that the attenuation with height of an electrostatic field having a given horizontal wavelength is least over the magnetic pole and increases continuously as the location of the source field is shifted toward the equator. The assumptions upon which the analysis is based gradually fail, however, as the equator is approached, and it is necessary to carry out a further investigation to obtain results of comparable quality for the equatorial regions.

Farley [1960] has derived the governing equations for the electrostatic field in the equatorial regions, and has presented a number of results determined by numerical solution of these equations. It is assumed in the determination of these solutions that the distribution of the electrostatic potential is symmetric about the equatorial plane. This condition corresponds to stating that no current flows across the equatorial plane, and requires that the generating mechanism operative in the dynamo region produces identical fields at conjugate points in the northern and southern hemispheres. This might be appropriate at certain times during the year for large-scale fields produced by tidal motions, but is clearly not appropriate for small-scale phenomena associated with turbulence or irregular winds in the dynamo region.

It is considered in the present investigation that the governing equations of Farley hold, but that the mechanisms that operate to generate the electrostatic fields at conjugate points function independently. The linearity of the equations then assures that the properties of the fields generated in each hemisphere can be treated separately, the appropriate boundary condition for the other hemisphere being that the current vanishes at the bottom of the ionosphere. Solutions are obtained by application of numerical techniques, and results are presented for a substantial number of representative cases.

Basic assumptions and equations. Except for the change in the boundary condition noted above, the basic assumptions and equations fundamental to the present study are the same as those given by *Farley* [1959, 1960]. It is assumed, first of all, that a relatively slow-moving mechanism, such as turbulence, irregular winds or internal gravity waves, exists in the dynamo region and generates an irregular electric field at a given level in the ionosphere. It is considered throughout that the phenomena are sufficiently slow moving that all time derivatives are negligible, and the governing equations reduce to those of electrostatics. The ionosphere is assumed to be a finitely conducting horizontally stratified medium with anisotropic conductivity due to the presence of the geomagnetic field. Simplification is achieved by confining attention to the equatorial region where the dip angle is small and to phenomena of sufficiently small scale that the earth may be considered to be flat, and the geomagnetic field lines to be parabolas situated symmetrically with respect to the magnetic equator.

It is convenient, as a result of the assumptions stated above, to introduce a Cartesian coordinate system as illustrated in Figure 1, in which the origin is placed at the magnetic equator, the x axis extends along the equator, and the z axis is vertical. The maximum height of any particular field line occurs over the equator, and is designated z_F. The height at which the electrostatic field is considered to be generated is designated z_I, and the value of y at which the field line that intersects the equatorial plane at height z_F is at height z_I is designated y_I, as indicated in the figure. The coordinates of the point in the opposite hemisphere at which the field line intersects the bottom of the ionosphere are designated y_{II}, z_{II}. The magnetic field vector B is situated in the yz plane, and is inclined at the dip angle I with respect to the y axis. The variation of the dip angle with latitude L is given, according to the dipole approximation to the earth's field, by the expression $\tan I = 2 \tan L$. For low latitudes, L is small and $\tan I$ can be approximated by y/R_0, thus

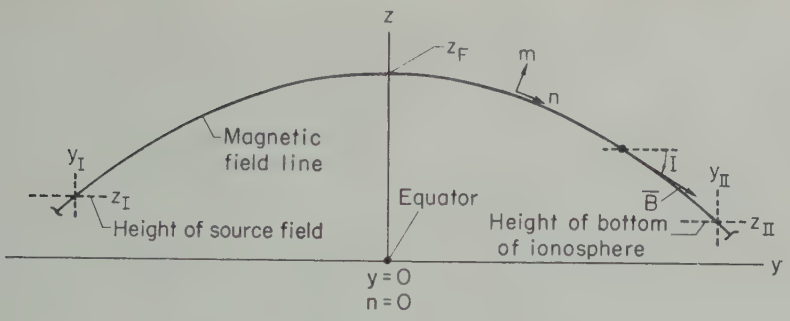


Fig. 1. View of coordinate systems.

$$\tan I = 2y/R_0 \qquad (1)$$

re R_0 is the earth's radius. The expression the coordinates for a magnetic field line can determined directly by integration upon acement of tan I by $-dz/dy$ and is the owing:

$$z = y^2/R_0 \quad \text{or} \quad z - z_I = \frac{y_I^2 - y^2}{R_0} \qquad (2)$$

n electric current $\mathbf{J}$ will flow in the ionosphere er the conditions described above and have rength given by

$$\sigma_0\mathbf{E}_0 + \sigma_1\mathbf{E}_1 + \sigma_2(\mathbf{B} \times \mathbf{E}_1)/|\mathbf{B}| \qquad (3)$$

re σ_0 and σ_1 are the electrical conductivities sured parallel and transverse to the mag- c field, σ_2 is the Hall conductivity, and $\mathbf{E}_0$ $\mathbf{E}_1$ are the components of the electric field $\mathbf{E}$ llel and transverse to the magnetic field. ibination of this relation with the assumption σ_0, σ_1, and σ_2 depend only on z, and not on d y, and that in the steady-state case

$$\text{div } \mathbf{J} = 0, \qquad \mathbf{E} = -\text{grad } \varphi \qquad (4)$$

ces to determine a single second-order linear ial differential equation for the electrostatic ntial φ.

asmuch as the governing equation is linear the principle of superposition applies, ition is confined to the analysis of the ition along a field line of the amplitude of Fourier component of an arbitrary hori- al potential distribution imposed in the ity of the point at which the field line sects the source field. Thus, the potential ibution in the vicinity of y_I and z_I is given by

$$A_I(y_I, z_I) \exp [ik_1x + ik_2(-y)] \qquad (5)$$

e k_1 and k_2 are wave numbers equal to $2\pi/\lambda_1$ and $2\pi/\lambda_2$, where λ_1 and λ_2 are the wavelengths in the x and y directions, A_I is the amplitude, and $i = \sqrt{-1}$. The anisotropic conductivity of the ionosphere associated with the much larger values for σ_0 than for σ_1 and σ_2 results in much smaller variations of the potential along the lines of the geomagnetic field than across these lines, and the potential at other heights is assumed to be given by

$$\varphi = A_I(\exp \{ik_1x + ik_2[(z - z_I)R_0 + y^2]^{1/2}\}) A(y, z) \qquad (6)$$

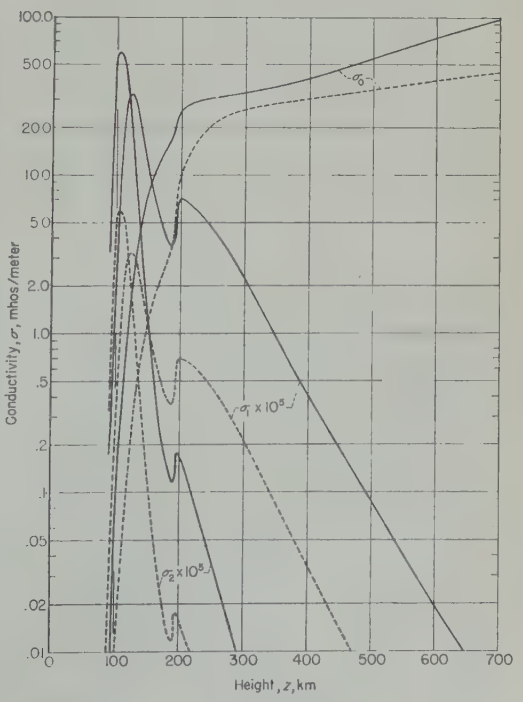


Fig. 2. Values for the longitudinal σ_0, transverse σ_1, and Hall σ_2 conductivities in the ionosphere.

where the amplitude distribution function $A(y, z)$ varies with y and z, but is normalized to equal unity at y_I, z_I.

Substitution into equations 3 and 4 leads to a two-dimensional partial differential equation for the amplitude distribution function having independent variables y and z. The equation as expressed does not lend itself readily to the introduction of approximations stemming from the anisotropic character of the conductivity, and it is convenient to introduce an alternative coordinate system in the yz plane in which m is measured transverse, and n parallel, to the magnetic field lines, as indicated in Figure 1. The resulting differential equation for $A(m, n)$ has been given by *Farley* [1960] and is as follows:

$$\frac{\sigma_0}{\sigma_1}\left[\frac{\partial^2 A}{\partial n^2} - \left(S\frac{\partial \ln \sigma_0}{\partial z} + \frac{2SC^2}{R_0}\right)\frac{\partial A}{\partial n}\right]$$
$$- \left(k_1^2 + \frac{k_2^2 C_I^2}{S_I^2 C^2}\right)A + \frac{\partial^2 A}{\partial m^2}$$
$$+ \left(C\frac{\partial \ln \sigma_1}{\partial z} + \frac{2C^3}{R_0}\right)\frac{\partial A}{\partial m} + \frac{2ik_2 C_I}{CS_I}\frac{\partial A}{\partial m}$$
$$+ \left\{\frac{2ik_2 C_I}{R_0 S_I}\left[1 - \frac{C_I^2}{S_I^2 C^2}(1 + C^2 S^2)\right]\right.$$
$$- \frac{ik_1 C\sigma_2}{\sigma_1}\left(\frac{\partial \ln \sigma_2}{\partial z} + \frac{2C^2}{R_0}\right)$$
$$\left. + \frac{ik_2 C_I}{S_I}\frac{\partial \ln \sigma_1}{\partial z}\right\}A = 0 \qquad (7)$$

where

$$C = \cos I, \qquad S = \sin I$$

and the subscript I on S and C indicates that $\sin I$ and $\cos I$ are to be evaluated at y_I, z_I.

Electrical conductivity of the ionosphere. The calculations to be presented in the following sections are based on the values for the conductivities given by *Spreiter and Briggs* [1961], and presented here in Figure 2. Two sets of results, indicated by solid and dashed lines, are presented in Figure 2. Both have been computed using the simple relations of mean-free-path theory given by *Farley* [1959], and more extensively by *Chapman* [1956], together with atmospheric data from 'The ARDC Model Atmosphere, 1959' [*Minzner, Champion, and Pond,* 1959]. It is assumed in the calculations that the magnetic intensity is 0.49 gauss, which corresponds, for instance, approximately to its value at 120 k over White Sands, and is hence somewhat larg than the appropriate value for the equator ionosphere. The solid lines represent the resu obtained using the values for the electron densi given in a recent summary by *Newell* [196 for conditions for summer noon at middle la tudes during a sunspot maximum. The dash lines represent the corresponding results obtain when the computations are performed with t values for the electron density arbitrarily minished by a factor of 10, as is indicated occur approximately at time of sunspot mi mum [*Newell,* 1960], and also at midnight time of sunspot maximum [*Handbook of G physics,* 1960]. Both sets of values for the c ductivities are thus more appropriate for te perate than for equatorial latitudes. The ferences should not be a decisive effect on results, however, and are, moreover, smaller th the diurnal and other variations at either l tude.

Simplification of differential equation. differential equation for A (m,n) given by eq tion 7 is exact within the framework of fundamental assumptions of the theory, bu very difficult to solve because it is a rather co plicated second-order partial differential eq tion and the dependent variable A is complex is therefore appropriate to seek further simp cation before proceeding to the solution. *Fa* [1960] has examined this point, and shown t it is usually permissible, above about 100 to introduce great simplifications on the basi the facts that σ_0/σ_1, σ_0/σ_2, and R_0 are very l numbers, the logarithmic derivatives of the ductivities are small, the derivatives of A generally small compared with A, and th derivatives of A are much smaller than th derivatives. Equation 7 can then be appr mated by

$$\frac{d^2 A}{dn^2} - S\frac{d \ln \sigma_0}{dz}\frac{dA}{dn}$$
$$- \frac{\sigma_1}{\sigma_0}\left(k_1^2 + k_2^2\frac{C_I^2}{S_I^2 C^2}\right)A = 0$$

in which it may be noted that the coefficie dA/dn is merely the logarithmic derivative in the n direction, and $k_2 C_I/S_I C$ is the number of the potential field in the m direc It is apparent that enormous simplification

achieved, since equation 8 is an ordinary rential equation and the dependent variable is a real rather than a complex quantity. llows that the results for A can be expressed nctions of the distance n along the field line igh y_I, z_I. Equation 8 is, moreover, of such m that solutions can be obtained by appli- n of simple numerical methods.

ie results given by *Farley* [1960] are those iated with the boundary conditions that A mmetric about $n = 0$. Thus, dA/dn is ymmetric, and it follows that dA/dn, which be continuous, is zero at $n = 0$. Farley sets $A(0)$ equal to a constant, solves equa- 8 by a step-by-step numerical integration, later normalizes so that A is unity at the for n corresponding to the point y_I, z_I; is, $A(n_I) = 1$.

ie boundary condition that $A(n_I) = 1$ is ned in the analysis to be given in the fol- ig sections, but the condition that A be netric about the equator is dropped and ced by the condition that no current flows the magnetic lines at the bottom of the phere at the end of the field line opposite associated with the source field. The appli- n of boundary conditions at both ends of eld line prohibits the use of the step-by-step ration method employed by Farley, but ifferential equation and boundary conditions f such a form that numerical solutions can btained by application of the iteration od described by *Spreiter and Briggs* [1961] ie solution of the corresponding electrostatic problem for the temperate and polar regions.

ration solution and further simplification of ential equation. The mathematical prob- provided by equation 8, together with the dary conditions that A is unity in the source in the dynamo region, and that no current low through the bottom of the ionosphere e opposite end of the field line, may be l briefly as follows:

$$\frac{}{i}\left(\sigma_0 \frac{dA}{dn}\right) = \sigma_1\left(k_1^2 + k_2^2 \frac{C_I^2}{S_I^2 C^2}\right) A \quad (9)$$

$$(A)_{nI} = 1, \quad \left(\sigma_0 \frac{dA}{dn}\right)_{nII} = 0 \quad (10)$$

lack of analytic expressions for σ_0 and σ_1 ides solution in analytic form. Numerical ons can be obtained, however, by applica- f an iteration scheme in which the $(i + 1)$ approximation is related to the ith approximation by

$$A_{i+1} = 1 - b_i \int_{nI}^{n} \frac{dn_1}{\sigma_0} \cdot \int_{n_1}^{nII} \sigma_1\left(k_1^2 + k_2^2 \frac{C_I^2}{S_I^2 C^2}\right) A_i \, dn_0 \quad (11)$$

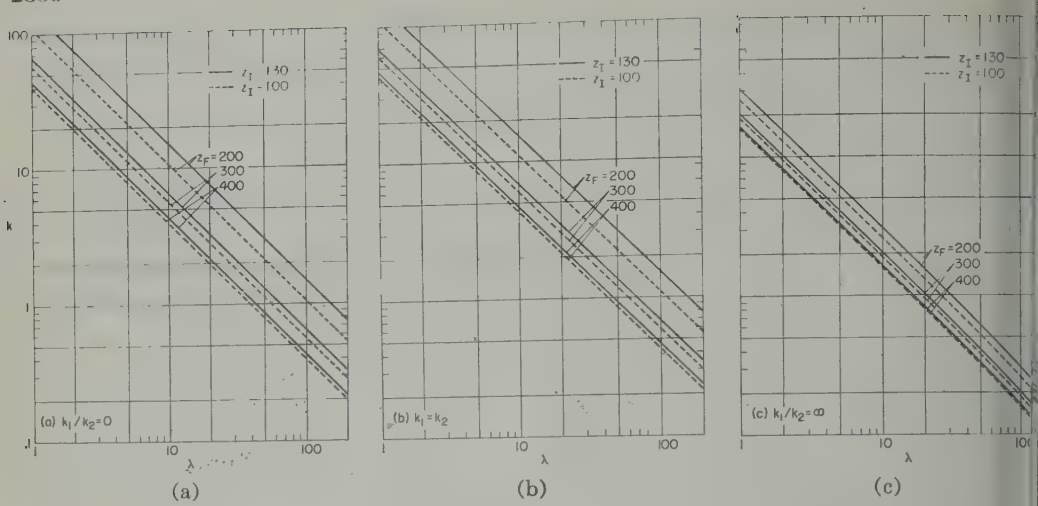
where the quantity b_i is a constant factor selected at each step of the iteration process so that

$$b_i(A_i)_{nII} = 1 - b_i \int_{nI}^{nII} \frac{dn_1}{\sigma_0} \cdot \int_{n_1}^{nII} \sigma_1\left(k_1^2 + k_2^2 \frac{C_I^2}{S_I^2 C^2}\right) A_i \, d\eta_0 \quad (12)$$

and the zeroth approximation for A_i is taken to be unity. Inclusion of the factor b_i assures that the values for A remain bounded between zero and unity at all stages in the iteration process. This has the effect of greatly extending the range of values for k_1 and k_2 for which the process converges, and of increasing the rate at which the process converges for any given values for these quantities. As in the earlier applications, the process converged satisfactorily in all cases, and the calculations were performed with repeated iterations until the differences between the values for A_i and A_{i+1} were less than 0.001 at all points. The values for b_i converged meanwhile to unity.

Although equation 8 is perfectly suitable for solution by the iteration method described above, the number of cases required to provide an adequate coverage of the interesting ranges of the various parameters is unnecessarily large when the variation of C or $\cos I$ with n is retained in the coefficient of A. The values for C vary, for instance, by only about 6 per cent along the portion above a height of 90 km of a field line passing through the equatorial plane at a height of 300 km, whereas the values for the conductivities σ_0 and σ_1 may vary through several powers of 10 along the same portion of the field line. It is therefore reasonable to disregard the variation of C with n and equate C to C_I. Thus, equations 11 and 12 simplify to

$$A_{i+1} = 1 - b_i k^2 S_I^2 \cdot \int_{nI}^{n} \frac{dn_1}{\sigma_0} \int_{n_1}^{\eta II} \sigma_1 A_i \, dn_0 \quad (13)$$



(a) (b) (c)

Fig. 3. Variation of effective wave number k with wavelength λ.

and

$$b_i(A_i)_{n\mathrm{II}} = 1 - b_i k^2 S_\mathrm{I}^2 \cdot \int_{n\mathrm{I}}^{n\mathrm{II}} \frac{dn_i}{\sigma_0} \int_{n_1}^{\eta\mathrm{II}} \sigma_1 A_1 \, dn_0 \qquad (14)$$

where k is an effective wave number related to k_1 and k_2 as follows:

$$k^2 = \frac{1}{S_\mathrm{I}^2}\left(k_1^2 + \frac{k_2^2}{S_\mathrm{I}^2}\right) \qquad (15)$$

The seemingly extraneous factor S_I^2 has been incorporated into this relation in order to make it conform to the corresponding expressi employed in the analysis of electrostatic fie in the ionosphere at polar and middle latitu [*Spreiter and Briggs*, 1961], and thereby facilitate comparison between the two sets results.

The variations of the effective wave num k with wavelength λ are shown in Figure 3 three families of electrostatic fields. The resu on part (*a*) are for $k_1/k_2 = 0$, which correspo to ripplelike source fields that vary along, not perpendicular to, the geomagnetic meridi The results on part (*b*) are for $k_1/k_2 = 1$, wh

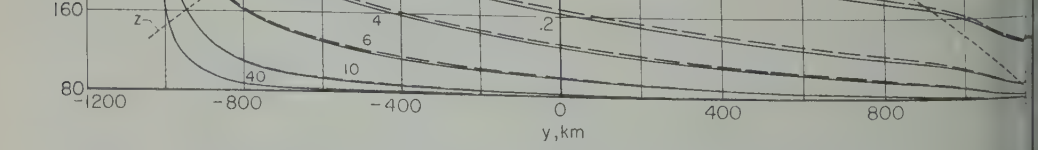


Fig. 4. Comparison of results obtained with variable and constant C for the variation of the amplitude A of the electrostatic potential along a geomagnetic field line; z_F = 300 km, z_I = 130 km, $k_1/k_2 = 0$.

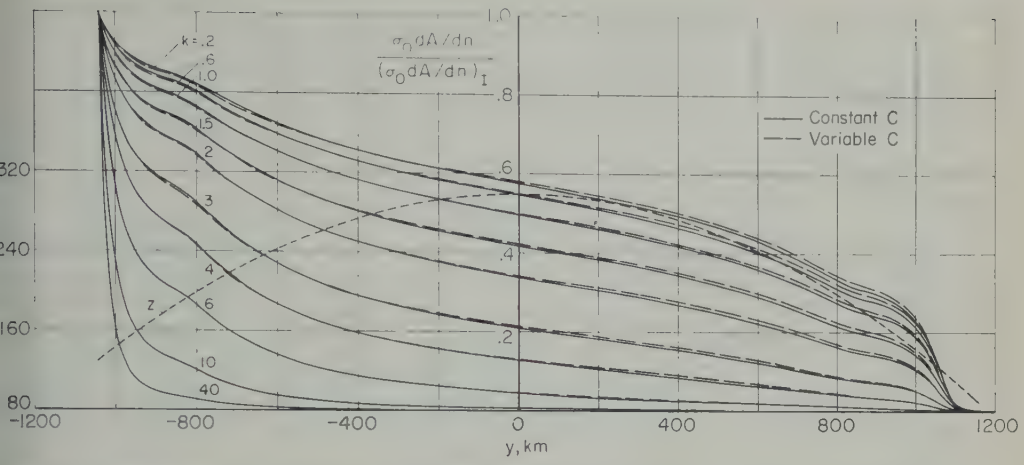


Fig. 5. Comparison of results obtained with variable and constant C for the variation of the current ratio $[\sigma_0(dA/dn)]/[\sigma_0(dA/dn)]_I$ along a geomagnetic field line; $z_F = 300$ km, $z_I = 130$ km, $k_1/k_2 = 0$.

esponds to checkerboardlike source fields have equal wavelengths both parallel and endicular to the meridians, and those on (c) are for $k_1/k_2 = \infty$ which corresponds to lelike source fields that vary along the endiculars to the meridians. In Figure 3 the bol λ without subscript represents whichever ntity, λ_1 or λ_2, is finite. Three pairs of lines shown on each part of the figure repre- ng conditions associated with field lines ing through the equatorial plane at heights 00, 300, and 400 km. Each pair consists of a line which indicates the relation between k and λ when the source field is at a height of 130 km, and a dashed line which indicates the relation when the source field is at a height of 100 km.

A comparison of a set of results for the variation of A along a field line obtained with variable and constant values for C is shown in Figure 4. The calculations were performed using the values for the electrical conductivities indicated by the solid lines in Figure 2. Results are shown for source fields having several different wavelengths, but with $k_1 = 0$ so that $k = k_2/S_I^2$ throughout. The difference between the two sets

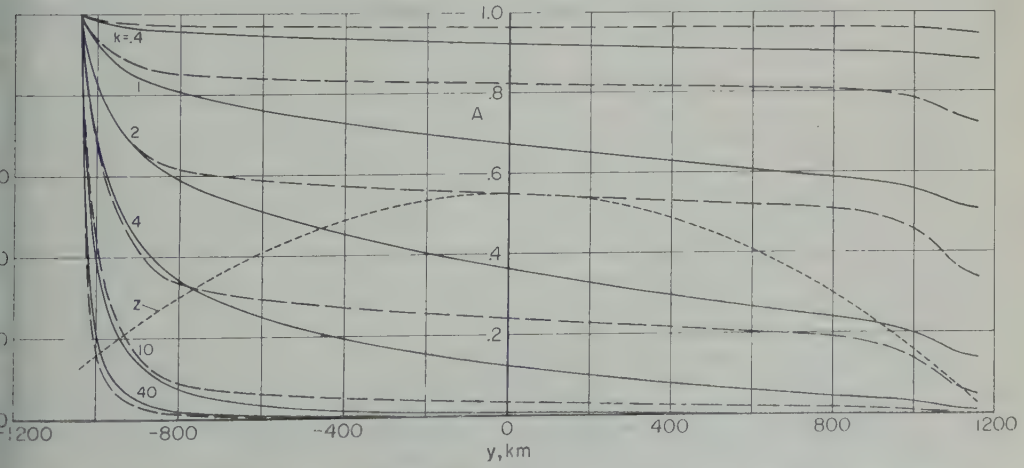


Fig. 6. Variation of amplitude of electrostatic field along a geomagnetic field line for several values for the effective wave number; $z_F = 300$ km, $z_I = 130$ km.

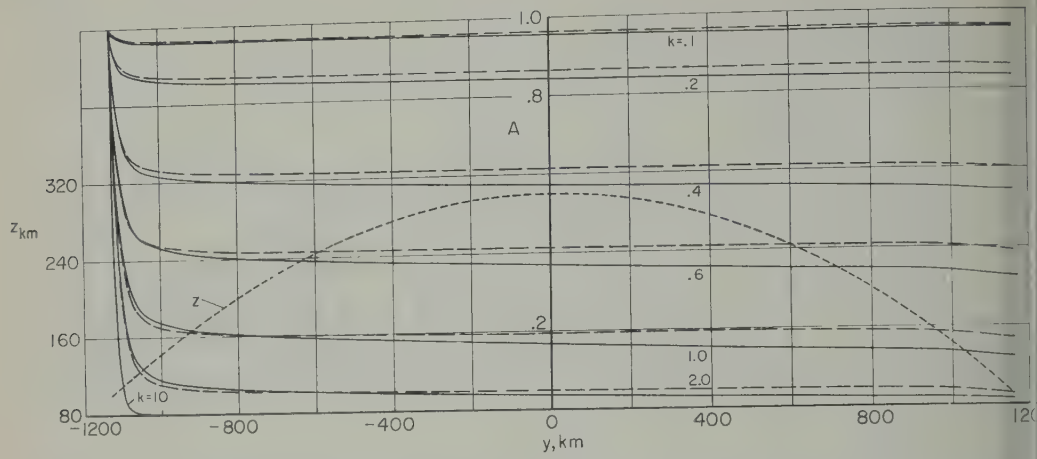


Fig. 7. Variation of amplitude of electrostatic field along a geomagnetic field line for several values for the effective wave number; z_F = 300 km, z_I = 100 km.

of results is then a maximum. The particular conditions selected for this comparison are those associated with a source field at a height of 130 km in the vicinity of one end of a field line that passes through the equatorial plane at a height of 300 km. The results show that the difference between the values for A obtained with variable and constant C is small, and, in view of the quantitative uncertainties in the numerical values for the electrical conductivities, of only minor importance for the present discussion.

The boundary condition associated with the vanishing of the current at the bottom of the ionosphere at the end of the field line opposite that of the source field is arbitrarily applied at 90 km in the preceding example, since the approximations fundamental to the reduction of equation 7 to the simpler form given by equati 8 begin to fail at lower altitudes. The exa height at which this boundary condition applied is not very important, provided it sufficiently low, since the conductivity is so sm in this vicinity that the quantity $\sigma_0(dA/dn)$ virtually zero for a considerable distance abo 90 km. This fact is illustrated in Figure 5 which is presented the variation of the curre ratio $[\sigma_0(dA/dn)]/[\sigma_0(dA/dn)]_I$ with y for t same conditions as considered in Figure 4.

As a consequence of the above considerati all results to be given in the following secti will be those obtained with equations 13 and that is, with C approximated by C_I, and w the boundary condition at the end of the fi line opposite the source field applied at 90 k

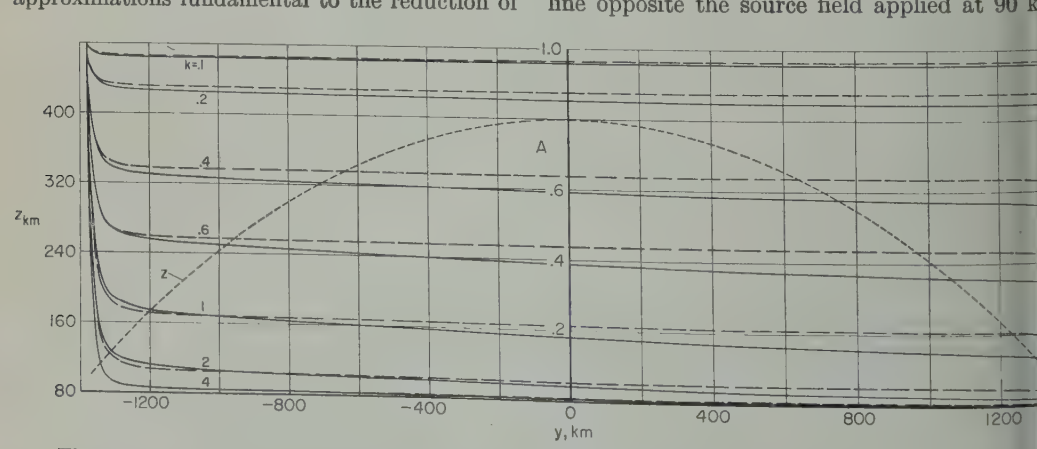


Fig. 8. Variation of amplitude of electrostatic field along a geomagnetic field line for several values for the effective wave number; z_F = 400 km, z_I = 100 km.

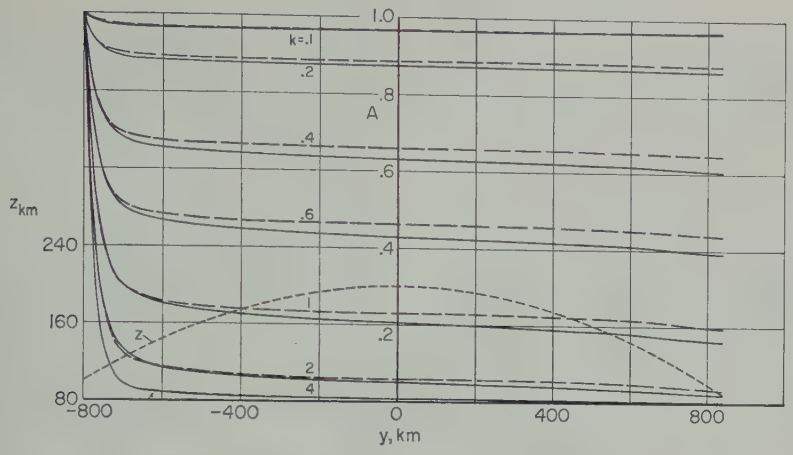


Fig. 9. Variation of amplitude of electrostatic field along a geomagnetic field line for several values for the effective wave number; $z_F = 200$ km, $z_I = 100$ km.

Results and conclusions. Numerical results the variation of A with distance along a field are presented in Figures 6 through 9 for a iety of combinations of k, z_I, and z_F. Two sets curves, solid and dashed, are shown on each re representing the results calculated using values for the conductivities indicated by the responding type of curve on Figure 2. The d lines are thus more indicative of results daytime conditions, and the dashed lines for ttime conditions. The results show that the nuation of the amplitude of the electrostatic l with distance from the source field is usu- less for nighttime conditions than for day- e conditions.

The results for an electric field generated at a ght of 130 km at such a latitude that the field through the source field passes over the ator at a height of 300 km are shown in ure 6. The range of wavelengths correspond- to values for k between about 0.4 and 4 is haps the most interesting from the point of v of the present discussion. The attenuation o small for values for k less than 0.4 that the olitude is essentially independent of distance the equipotential lines coincide with the geo- gnetic lines. On the other hand, the attenua- is so great for values for k greater than 4, icularly for daytime conditions, that the ibility of effective electrostatic coupling be- en the E and F regions is virtually nonex- nt.

f most significance from the point of view of the geophysical problem that prompted the present investigation is the fact that a value for k of 4 corresponds, as is illustrated in Figure 3, to a wavelength of about 5 km for the case of $k_1/k_2 = \infty$, that is, ripplelike fields that vary with longitude, but not with latitude. It thus appears that the electrostatic coupling required for the operation of the mechanism described by *Dagg* [1957] could possibly be obtained in equatorial latitudes. The possibility for effective coupling is very marginal, however, and virtually disappears when source fields with other ratios of k_1/k_2 are considered. For example, a wavelength of 5 km with k_1/k_2 equal to zero or unity corresponds to values for k of about 13, and Figure 6 shows that the attenuation of such an electrostatic field is so great that it is effectively terminated within a short distance of the source.

The electrostatic fields associated with values for k less than 0.4 provide the possibility of effective coupling not only between the equatorial E and F regions, but also along entire lines of force extending between conjugate points in opposite hemispheres. The wavelengths associated with such a value for k are very large, however, being about 50 km for fields with $k_1/k_2 = \infty$ and from about 140 to 170 km for fields with this ratio equal to zero or unity. Although it is evident that elongated fields must occur if the wavelength is permitted to grow to such large values, the precise study of the properties of these fields is not possible with the present the-

ory, since it is implicit in the analysis that the wavelength be small compared with other dimensions of the system.

The corresponding results associated with the same field line but with the height of the source field reduced to 100 km are shown in Figure 7. The curves are generally similar in form to those discussed above, but it should be observed that, for a given value for k, the attention of the amplitude A with distance from the source field is increased substantially. The slight possibility found previously for electrostatic coupling of kilometer-scale irregularities in the equatorial E and F regions thus disappears altogether as the height of the source field is reduced from 130 to 100 km. On the other hand, most of the attenuation occurs in the lower part of the ionosphere, and the possibility of effective electrostatic coupling of kilometer-scale irregularities extending great distances along a field line increases rapidly if the height of the source field increases to, say, 160 or 200 km. The effect of such changes can be ascertained from Figures 6 or 7 by simply dividing the values for A at all heights by the value for A at the assumed height of the source field. Consideration of the variation with height of the mobility of electrons and ions in the ionosphere, [*Ratcliffe*, 1959] indicates, however, that the possibility of the generation of an electric field by irregular winds is rather remote at such heights.

The effects of a change in latitude of the source field can be ascertained by comparing the results shown on Figure 7 with those on Figures 8 and 9. The height of the source field is maintained at 100 km in all three figures, but the latitude is selected so that the height z_F of the field line over the equator is 400 km for Figure 8 and 200 km for Figure 9, whereas it is 300 km for Figure 7. Although there are considerable differences in the position and length of the field lines associated with the various locations for the source field, the results reveal that remarkably small differences exist in the amplitude of the electrostatic fields beyond a short distance from the source. The results are qualitatively similar to those given previously by *Spreiter and Briggs* [1961] for low latitudes, although the present results indicate somewhat smaller values for the amplitude for any given combination of conditions. These differences are the consequence of the fact that the previous work is concerne primarily with conditions in the ionosphere i polar and middle latitudes, and effects of th curvature of the field lines are disregarded i the analysis. Thus, the quantity $S_1 dn$ that ap pears squared in equations 13 and 14 is replace by simply dz in the corresponding equations the previous analysis. The values for the ele trical conductivities are the same at any give height in the two investigations, but the valu for $S_1 dn$ are, of course, larger than those for d It follows that the deviations from unity of th amplitude A are larger in the present analysi It is clear, however, that such differences woul tend to disappear if similar calculations we made for higher latitudes, since the values f $S_1 dn$ would tend to approach dz throughout th effective thickness of the ionosphere.

References

Chapman, S., The electrical conductivity of th ionosphere: A review, *Nuovo Cimento, 4* supp (4), 1385–1412, 1956.

Dagg, M., The origin of the ionospheric irregular ties responsible for radio-star scintillations an spread-F, I, Review of existing theories; Turbulent motion in the dynamo region, *J. A mospheric and Terrest. Phys., 11,* 133–150, 1957

Farley, D. T., Jr., A theory of electrostatic field in a horizontally stratified ionosphere subject a constant, vertical magnetic field, *J. Geophy Research, 64,* 1225–1233, 1959.

Farley, D. T., Jr., A theory of electrostatic fields the ionosphere at nonpolar geomagnetic lat tudes, *J. Geophys. Research, 65,* 869–877, 1960.

Handbook of Geophysics, The Macmillan Co pany, New York, 662 pp., 1960.

Martyn, D. F., Interpretation of observed *F* 'winds' as ionization drifts associated with th magnetic variations, *Physics of the Ionospher* Physical Society, London, 163–165, 1955.

Minzner, R. A., K. S. W. Champion, and H. Pond, The ARDC model atmosphere, 195 *AFCRC TR-59-267,* Geophysics Research Dire torate, Air Force Cambridge Research Cent Bedford, Mass., 1959.

Newell, Homer E., Jr., The space environme *Science, 131,* 385–390, 1960.

Ratcliffe, J. A., Ionizations and drifts in the ion sphere, *J. Geophys. Research, 64,* 2102–2111, 195

Spreiter, John R., and Benjamin R. Briggs, Theo of electrostatic fields in the ionosphere at pol and middle geomagnetic latitudes, *J. Geophy Research, 66,* 1731–1744, 1961.

(Manuscript received April 13, 1961.)

Measurement of Ionospheric Drift by Radio-Star Observations

BRAULIO DUEÑO

University of Puerto Rico, Mayaguez, Puerto Rico

Abstract. Measurements of the fluctuations of the signals from the radio-star Cassiopeia have been made at Lajas, Puerto Rico. It has been found that there exists at this location a great increase in fluctuation activity during June and July which appears to be associated with the large-scale changes taking place in the F_2 layer during the presunrise period. No significant relationship between fluctuation activity and E_s or between fluctuations and spread F was observed. Measurements of drift velocities by means of three spaced interferometers have also been made. It has been found that drift is toward SE in the evening hours and toward NW in the morning with transitions occurring at noon and at midnight. About 75 per cent of all the drift measurements taken were easily analyzable by Putter's method. This is taken to mean that for 75 per cent of the cases the random changes in the shape of the irregularities were either very small or were taking place very slowly in time compared with that taken by the irregularity to drift along the three interferometers.

INTRODUCTION

Measurements of the fluctuations of the sig-
ls from the radio-star Cassiopeia have been
ade, on a routine basis, at Lajas, Puerto Rico,
2 years up to November 1959. From this
ne on routine measurements have been made
the drifts of the ionospheric irregularities that
e rise to the fluctuations of the radio-star
nals. The fluctuation data were obtained by
ans of a *Ryle-* [1952] type interferometer
erating at a frequency of 53.5 Mc/s. An
terline-Angus recorder was used in conjunc-
n with this equipment. For the drift measure-
nts three identical *Ryle-type* interferometers
re used, spaced on a right-angle triangle. A
ır-channel Sanborn recorder was used for dis-
ying the data. The spacing between the refer-
e interferometer and the south interfero-
ter was 1030 ft whereas that between the ref-
nce and west interferometer, was 950 ft.

A smooth ionosphere causes the radio waves
m a extraterrestrial source to undergo refrac-
n of a steady-state nature. On the other hand,
isturbed ionosphere, or one containing irregu-
ities or blobs with electron densities slightly
her or lower than the surrounding medium,
cause sizable variations in the refraction of
radio-star waves. It is now believed [*Spen-*
, 1955] that these irregularities are cigar-
ped and oriented along the magnetic field
es of the earth. According to *Maxwell* [1955]
extension in the north-south direction is of the order of 20 to 30 km, whereas that in the east-west direction is about 3.5 km.

Most of the workers in the field have found a strong relationship between spread F and the occurrence of fluctuations. This would tend to indicate that radio-star fluctuations and spread F have a common causative mechanism. On the other hand, the diurnal and seasonal variations of fluctuations and spread F are not similar. *Dagg* [1957*a*, *b*] has found that fluctuations occur, in general, 4 hours before the commencement of spread F, and that the seasonal variations of spread F are not obvious in radio-star fluctuations.

The height of the irregularities that cause radio-star fluctuations is not known. *Hewish* [1952] and *Maxwell* [1955] believe the height of the diffraction screen responsible for the radio-star fluctuations to be above the maximum of ionization of the F region. On the other hand, *Booker* [1956] has endeavored to explain scintillation phenomena in terms of turbulence in the ionosphere and has estimated that turbulence can occur at a level of approximately 140 km with a required turbulence power per unit mass of 1000 watts/kg. *Briggs* [1958*a*, *b*] has also presented arguments in favor of the view that irregularities that cause fluctuations are at a height less than 300 km.

Closely associated with the fluctuations in amplitude of the extraterrestial signal there exist changes in apparent position of the radio star.

It has been estimated by *Hewish* [1952] that the apparent position of the radio star may vary by about 5 minutes of arc at a wavelength of 8 meters, and that strong fluctuations are accompanied by large changes in the apparent position.

In the experiment reported here, all observations have been made on a fixed frequency of 53.5 Mc/s.

Fluctuation Data

At the geographic latitude of Puerto Rico (18° 12′) the radio-star Cassiopeia can be observed 5 hours per day with the antenna system used in this experiment which consists of an array of two four-element Yagis on each leg of the interferometer. At upper culmination the radio star makes an angle with the zenith of approximately 45 degrees. The point at which the radio waves emerge from the F_2 layer of the ionosphere is thus at a distance of approximately 1000 km when the signals are first recorded. This point approaches the point of observation to distance of approximately 300 km and then r cedes. The change in latitude involved in t process is of the order of 5 degrees.

Generally speaking, ionospheric conditions r lated to the F layer remain substantially co stant during the transit of Cassiopeia as o served here. On the other hand, the thickne of the layer involves changes in the ratio 3 to 1.4, or approximately 2.5 times. The slan height distances to irregularities will vary fro 1100 to 425 kms.

On certain occasions fluctuations of very lar amplitude were observed. When these large flu tuations occurred they were observed to ta place for a considerable interval of the to time of transit. The periods of these fluctuatio occur in the range from 1 to 5 minutes. Only very rare occasions did they assume values s 25 to 30 seconds. The amplitude of the fluctu tion quite often exceeded twice the value of t amplitude of an undisturbed trace.

To obtain an accurate measure of the fluctu

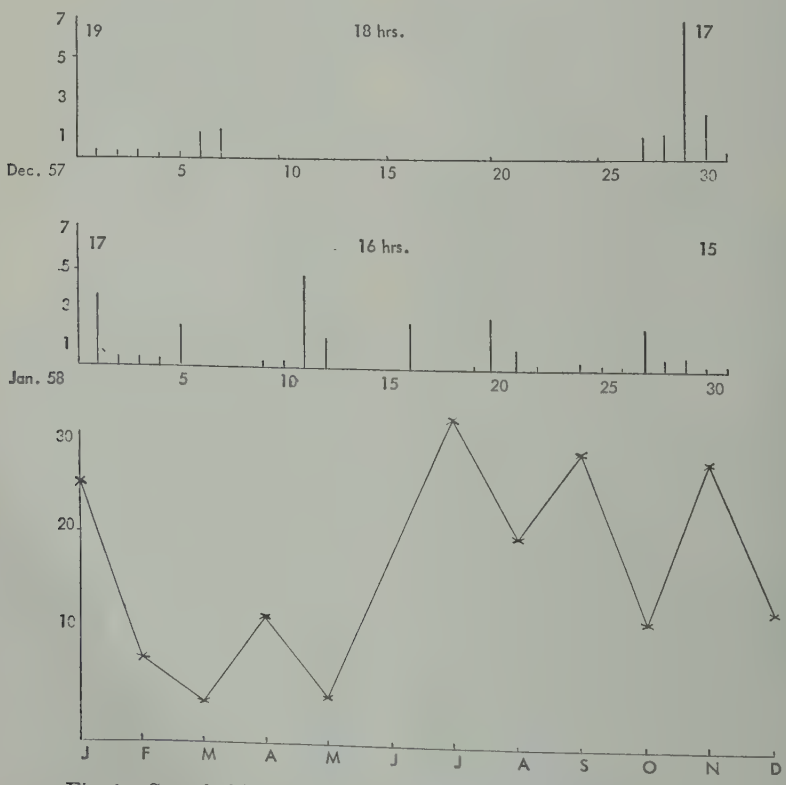


Fig. 1. Sample histograms for December 1957 and January 1958.

activity, the mean fluctuation amplitude tive to the undisturbed value was computed very day for which data were available dur- he period from November 1957 to July 1959. value was multiplied by the duration in rs of the fluctuation occurrence for the day. ples of the histograms obtained are shown Figure 1 for December 1957 and January 8. The hours during which transit of the o star is taking place at the beginning, mid- and end of the month is indicated in the ograms. From the diagrams obtained for he months in the 2-year period it was im- iately obvious that fluctuation activity picks considerably during the period from May to e. The absence of dots on the zero reference indicate outages.

he last of the drawings on Figure 1 sum- izes the information on the histograms. In drawing the vertical scale represents the of the average amplitude hours for the en- month. The minimum of fluctuation activity hus seen to occur during the months of ruary, March, April, and May. During these ths the radio-star transit occurs during the ight hours, namely from 1400 to 0800 hours. is the time when the ionosphere is more le. Likewise the large increase in fluctuation vity experienced in the period of May, June, July can be ascribed to the fact that the sit of Cassiopeia is now taking place from) to 0600 to 0400 hours, or during a period vhich the ionosphere is experiencing large nges in ionization with respect to time.

A possible relationship between large amplitude fluctuations and magnetic activity was sought. Agreement between large fluctuations and high values of K_p was found to be on the positive side by a factor of about 5 to 1. This result appears to be in contradiction with observations at higher latitudes by *Little and Maxwell* [1952]. On the other hand large values of K_p were found to be almost invariably accompanied by fluctuation periods of a minute or less. The result is in agreement with those at a higher latitude by *Little and Maxwell* [1952].

Comparison of these data with E_s data from a backscatter sounder operated at a frequency of 21.6 and 40.68 Mc/s at Mayaguez did not show any significant relationship between E_s and fluctuation activity, not even during June and July. During these months E_s occurrence is high and intense at this location, and the slant distances in both cases are compatible. On the other hand, the most intense forms of E_s do have a tendency to occur here around 1700 hours. During these 2 summer months the radio-star Cassiopeia is in transit from 06 to 04 hours.

It is of interest to point out here that *Dagg* [1957*b*] found in England positive correlation between large amplitude fluctuations and E_s in June and July of 1954.

No relationship between spread F and fluctuation activity was found. Furthermore, the incidence of spread F at this geomagnetic latitude is so light [*Singleton*, 1960] that the possibility of a relationship between the two is very unlikely.

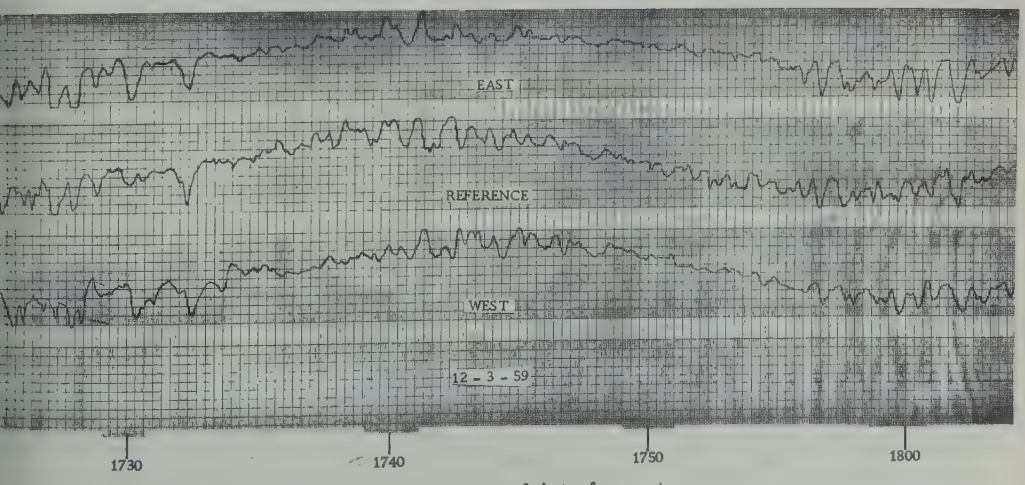


Fig. 2. Sample trace of interferometers.

Drift Measurements

Experimental setup. For the drift measurements three Ryle-type phase-switching interferometers were used. The output from the phase detectors of the east and south interferometers were brought, by means of a shielded cable, to the trailer which housed the reference interferometer and a four-channel Sanborn recorder. A chart speed of 3 cm/minute was used all through the experiment. The equipment was run 3 hours every day by means of a timer which turned on the recorder during the specified 3 hours per day that cover the time around transit of the Cassiopeia radio-star source.

Analysis of the data. Figure 2 shows a sample of the fluctuations recorded by three channels of the Sanborn instrument. The top trace corresponds to the east interferometer, and the middle and bottom traces are the reference and south traces. The great advantage of using three phase-switching interferometers is obvious from Figure 2. Only bonafide fluctuations will show in the same sense in the three traces. Noise or interference from the sun will normally show amplitudes with different phase displacement on the three traces.

These traces were scaled using a Sanborn Chart Inspector, and the time differences of the corresponding maxima between the different traces were recorded together with the time the fluctuation occurred. The amplitudes and the periods in seconds were also taken down for the fluctuations whose time delays were recorded. Only cases in which at least three successive points were observed on each trace were recorded.

The trace shown in Figure 2 shows very strong fluctuations. Notice that in the middle trace the fluctuations on two successive lobes have been clipped since their amplitude exceeded the pen travel allowed by the instrument. For small fluctuations the small pen travel allowed by the instrument is a disadvantage. Small fluctuations show off much better in an Esterline-Angus recorder than in one of these channels owing to the wider pen travel available in the former.

It is probable that the spacing between the interferometer stations were on the short side. The spacing between the east and reference stations was 850 ft (260 m) and between the south and reference stations was 1030 ft (314 m). However, a close inspection of Figure 2 will sho that on certain occasions the amplitude of a flu tuation is greater, say on the east trace, tha on the reference, whereas on other occasions t reverse is true. This can be due either to irregu larities whose change with respect to time faster than its drift velocity, or else to an i regularity whose line of maxima passes main over two of the interferometer stations but n the third. In either case, it is obvious that wider spacing between stations would only resu in decreasing the number of identifiable poin from all three traces. On the other hand, d creasing the spacing would decrease the magn tude of the time delays thus requiring a fast chart speed.

Putter's straight-line analysis. *Putter* [195 has developed a simple geometrical interpret

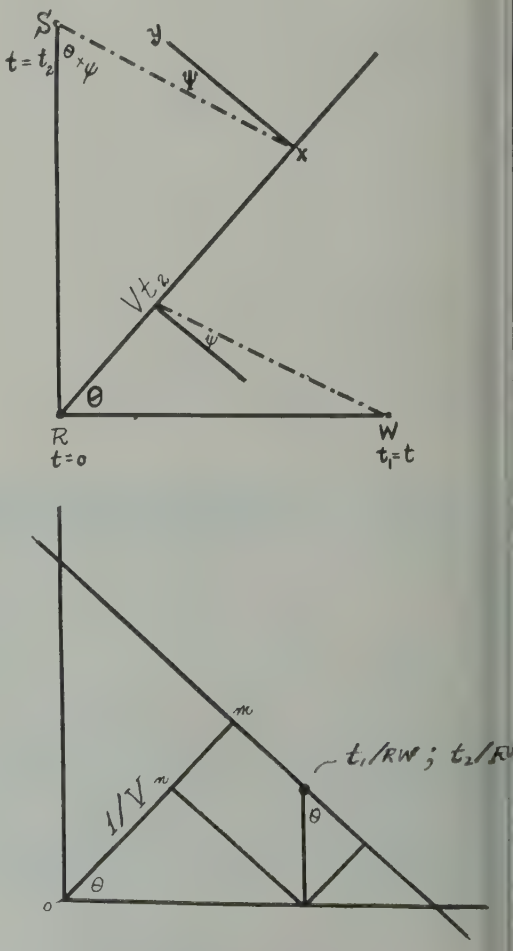


Fig. 3. Putter's straight-line analysis.

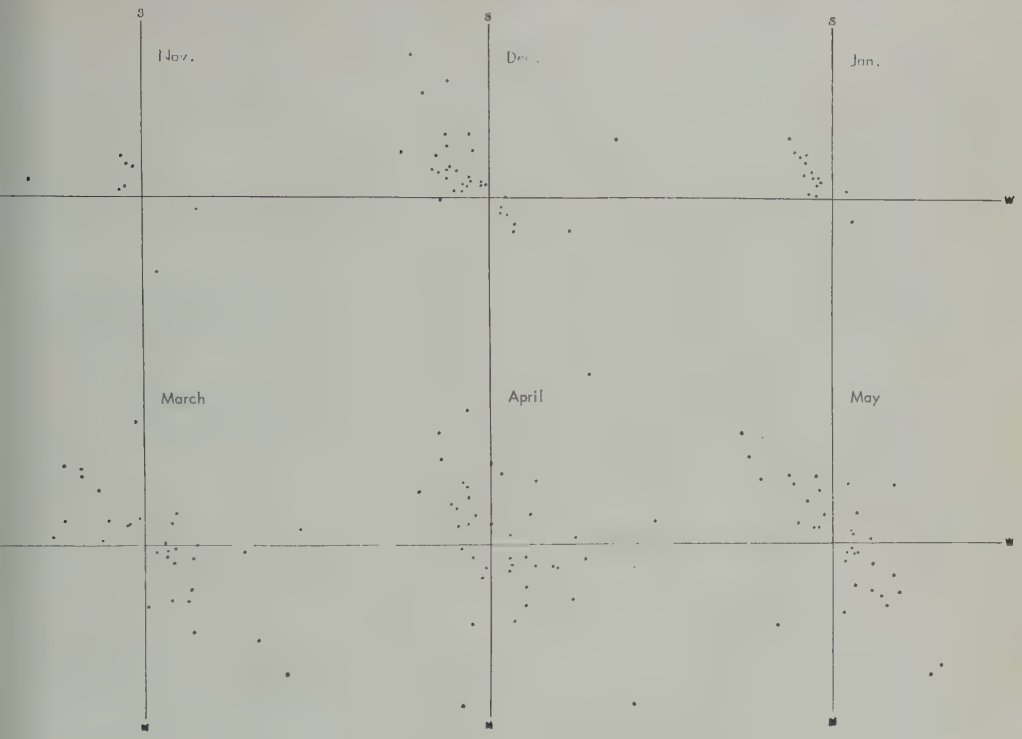


Fig. 4*a*. Polar plots of drift velocities for November 1959 to May 1960.

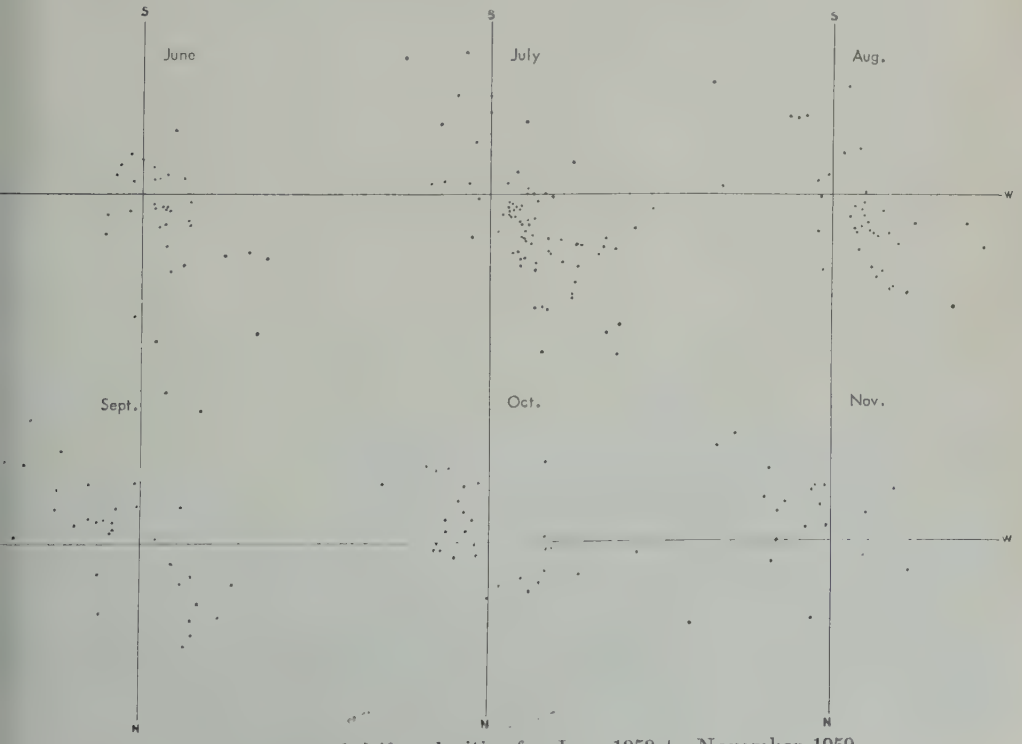


Fig. 4*b*. Polar plots of drift velocities for June 1959 to November 1959.

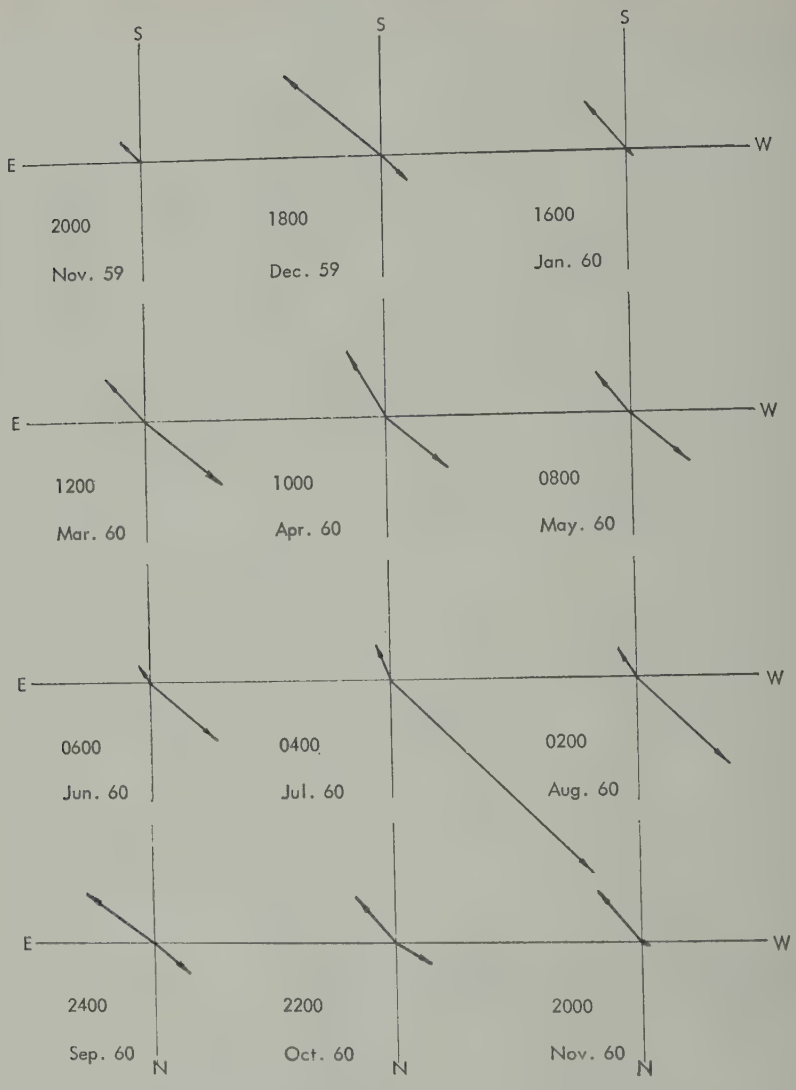


Fig. 5. Monthly average of the drift direction.

tion of the problem of drifts which is valid in absence of random changes in the irregularities. Putter straight-line technique has also been discussed by *Banerji* [1958]. Figure 3 shows the essentials of the geometry involved. In the top drawing the line RX represents the direction of the irregularity. SX is the line of maxima of the pattern at the ground which makes an angle ψ with the normal to the direction of the drift. The three dots R, S, and W represent positions of the three interferometer stations, and t_2 and t_1 are the observed time delays between the reference and west stations and between the reference a south station.

From this figure it is obvious that

$$Vt_2/\sin(\theta + \psi) = RS/\sin(90 - \psi)$$

$$Vt_1/\cos(\theta + \psi) = RW/\cos\psi$$

By eliminating ψ between these two equati it is found that

$$t_1 \cos\theta/RW + t_2 \sin\theta/RS = 1/v$$

The bottom drawing of Figure 3 shows t

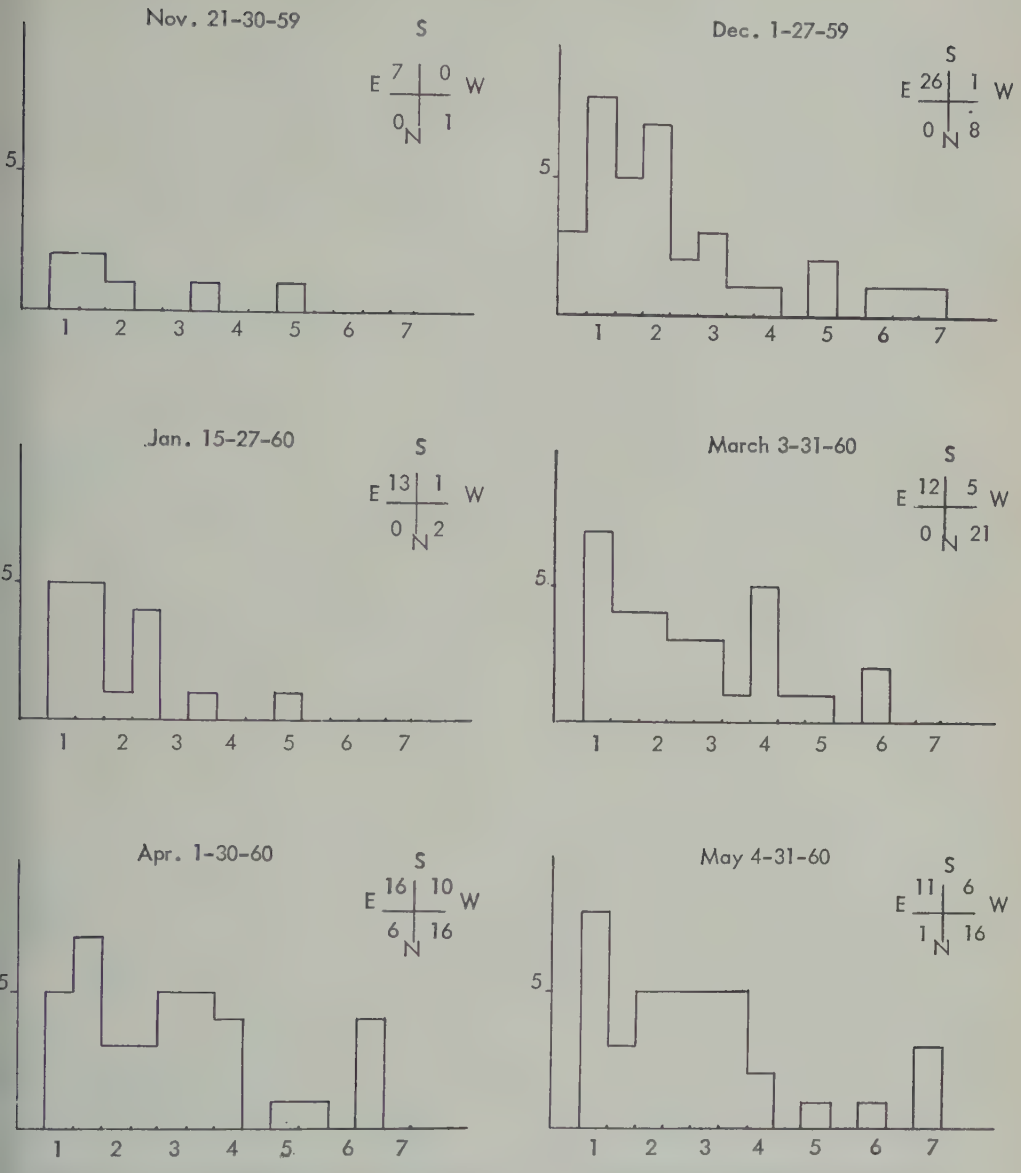


Fig. 6*a*. Monthly distributions of velocity of drift for November 1959 to May 1960.

rst and second left members of equation 3 qual to lengths n–o and n–m respectively. the points t_1/RW, t_2/RS, and t'_1/RW, S will actually determine a straight line. ormal from the origin to this line determines eciprocal velocity of drift and its direction eference to the east-west line. Since in this ment RW equals 850 ft and RS equals ft, the actual computing equation becomes

$$.97t_1 \cos \theta + .93t_2 \sin \theta = 1000/v \qquad (4)$$

The graphs were plotted on 20 by 20 to the inch K and E graph paper. Only points occurring within an interval of 1 to 2 minutes were used to determine a straight line. Instances in which less than 3 points for plotting occurred were rejected. The reason for these is as follows: in practice the points do not exactly plot out into a straight line. They show instead, a varying degree of scatter on the proximity of the ideal line. On the other hand, an error in reading the

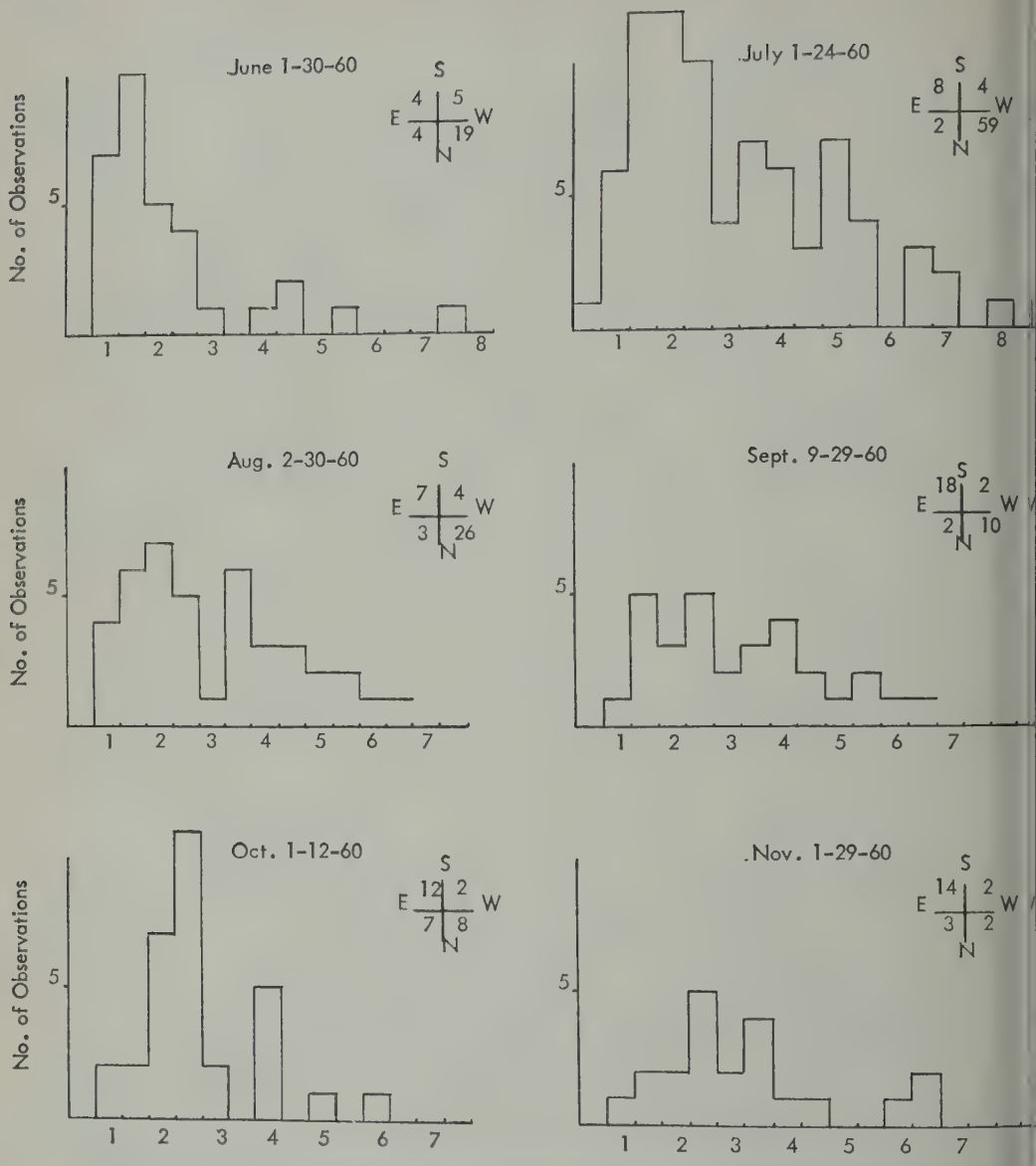


Fig. 6*b*. Monthly distributions of velocity of drift for June 1960 to November 1960.

time delays may have been made, the worst one being that of estimating incorrectly the three corresponding points on the three interferometer traces. Thus if four points plot reasonably well into a straight line, but a fifth is way off, then it appears logical that this fifth point should be eliminated.

It is interesting to point out here that of all the data available in this experiment only about 25 per cent showed too much scatter and had be discarded. The rest of the data were eas analyzable by Putter's method. This is taken mean that on 75 per cent of the occasions random changes in the shape of the irregularit were either very small or were taking place ve slowly in time compared to that taken by irregularity to drift along the three interferon ters.

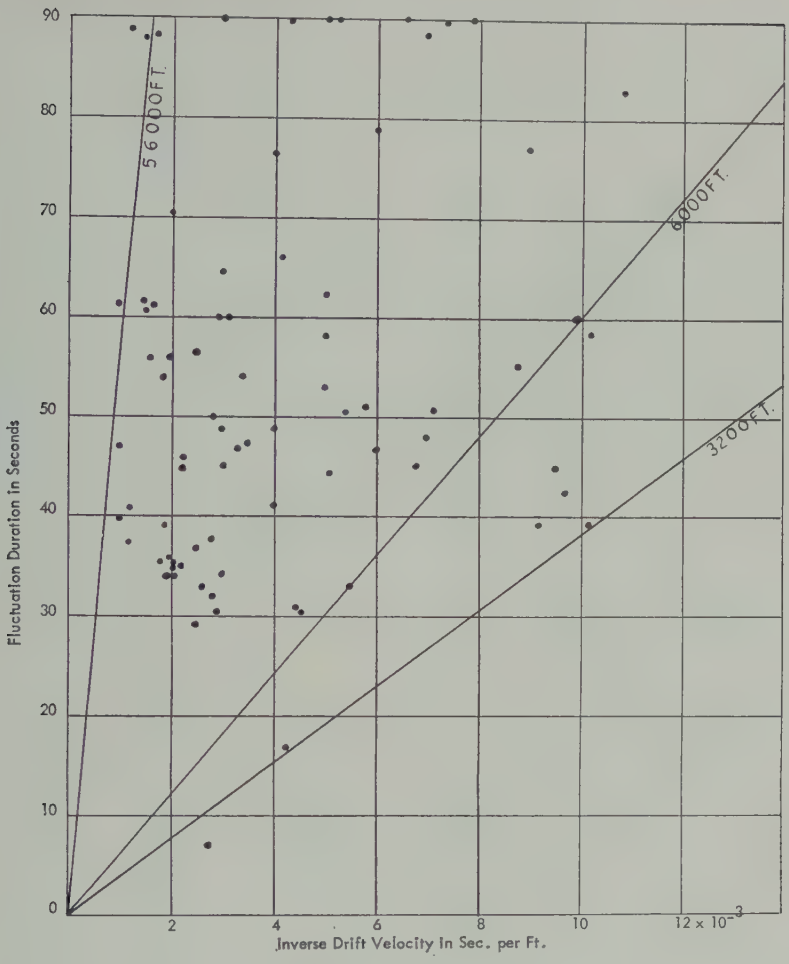


Fig. 7. Plot of inverse velocity vs. fluctuation duration for July 1960.

Results of the Measurements

e important disadvantage of the radio-star od as a technique for measuring ionospheric arises from the fact that the radio source transit for a limited number of hours each In this experiment only 3 consecutive hours ay were used for the drift measurements. ring these 3 hours Cassiopeia is substan- at the same elevation, so that these meas- ents relate to ionospheric irregularities slant-height distance remains substantially ant.

ereas with the radar method the height of regularities involved is easily determined, the radio-star method the height of the larities is not known, nor is the nature of regularities that give rise to fluctuations well understood. The only precise statement that can be made is that these irregularities arise in the *F* layer.

Since the Sanborn recorder was first placed in operation in the latter part of November 1959, the only data available for that month are for the last 9 days of the month.

Figures 4*a* and 4*b* show the measured drift velocities plotted on polar coordinates for the 12 months from November 1959 to November 1960. Because of equipment failure no data are available for the month of February. The direction data on Figures 4*b* are summarized in Figure 5 which shows the computed average direction of the drift velocity for each of the 12 months. In each instance the length of the vector is proportional to the number of measurements in the

quadrant. In this figure the small components of drift in the south-west and north-east quadrants have been ignored. From this figure it is seen that the drift appears to move toward the SE in the evening hours and toward the NW in the morning, with transitions occurring at noon and midnight.

It can be readily verified that the irregularities that give rise to these velocities of drift are predominantly elongated along the magnetic lines of force. This is done by referring back to the graphs from which the drift magnitude and sense were computed by Putter's method. If on a particular graph the south, reference, and west stations are marked down with the west point at the origin, and if an ellipse is moved in the computed direction, two time delays can be visualized that will determine a point in the graph. Shifting the ellipse upward along its major axis and again moving in the computed direction will determine another point. Shifting the ellipse downward will similarly determine another point. Only an ellipse with the proper orientation will produce points that plot analogously to the experimentally determined points. Conversely, by inspection of the experimental points it is possible to deduce the orientation of the major axis of the ellipse. Since the ellipse in reality represents the projection of an irregularity elongated along the magnetic lines of force which at this location have a dip angle of approximately 50 degrees, then for points that belong to a measurement taken before upper culmination the major axis will show a tilt to the west from the true north and south direction, and a tilt of the major axis to the east for a measurement taken after upper culmination.

These results are in agreement with those of *Spencer* [1955] who showed that ionospheric irregularities are elongated along the geomagnetic field lines. Recently *Jones* [1960] has verified Spencer's findings.

The distribution of velocities in hundreds of feet per second for each month is shown in Figure 6*a* and 6*b*. The first horizontal space represents the interval in velocities between 50 and 100 feet/sec, etc. All these distributions are, in a way, suggestive of a Rayleigh distribution curve. On the other hand, velocities higher than 500 ft/sec do not seem to have a tendency toward a statistical fit.

The inserts represent the distribution of drift velocities per quadrant during each month. Ho it is again seen that the drift is mainly to t southeast during November, December, a January, and to the northwest during the su mer months.

To obtain a measure of the size of the patte at the ground along the direction of the min axis, plots have been made, after *Wild a Roberts* [1956], of the average fluctuation du tion in seconds vs. the inverse drift velocity seconds per foot for each of the 12 months which data are available. The slope of a line termined by joining a point with the yields size of the irregularity. Figure 7 shows the p obtained for the month of July 1959. This p shows that the majority of sizes ranged in va between 56,000 and 6,000 ft with a median va of 17,500 ft.

The average size for all other 11 months shown in Table 1. This table also shows

TABLE 1

Month	Size, ft	Velocity, ft/sec	Time hr
1959			
November	12,100	141	20
December	9,200	152	18
1960			
January	3,320	126	16
March	13,100	203	12
April	16,100	232	10
May	10,800	226	08
June	12,100	141	06
July	15,400	230	04
August	15,700	232	02
September	13,400	272	00
October	15,000	272	22
November	10,100	200	20

corresponding values of the average velocity meters per second. The smallest sizes occu during the winter months. If a plot is mad size vs. velocity using Table 1, the resul points will show some scatter but will cle suggest that high values of velocity are ass ated with the bigger sizes and vice versa.

Acknowledgment. The advice and encour ment received from Dr. W. Pfister is hereby g fully acknowledged. This research has been s sored by the GRD of the U. S. Air Force under contract AF 19(604)1918.

References

i, R. B., Method of measuring ionospheric
s by fading at spaced receivers, *J. Atmos-
ic and Terrest. Phys., 12,* 252, 1958.
, H. G., Turbulence in the ionosphere, *J.
hys. Research, 61,* 673–705, 1956.
B. H., A study of ionospheric irregularities
h cause spread F echoes and scintillations
dio stars, *J. Atmospheric and Terrest. Phys.,*
958*a*.
B. H., The diurnal and seasonal variations
read F ionospheric echoes and the scintilla-
of a radio-star, *J. Atmospheric and Terrest.
., 12,* 1958*b*.
M., Diurnal variations of radio-star scintil-
ns, spread F and geomagnetic activity, *J.
ospheric and Terrest. Phys., 10,* 1957*a*.
M., Radio-star ridges, *J. Atmospheric and
est Phys., 11,* 118, 1957*b*.
h, A., The diffraction of galactic radio waves
method of investigating the irregular struc-
of the ionosphere, *Proc. Roy. Soc. (A), 214,*
514, 1952.
I. L., Further observations of radio star
illations, *J. Atmospheric and Terrest. Phys.,*
6, 1960.

Little, C. G., and A. Maxwell, Scintillations of radio star during aurora and magnetic storms, *J. Atmospheric Terrest. Phys., 2,* 1952.

Maxwell, A., in *Physics of the Ionosphere,* P. 166, 167, 1955.

Putter, Von P. St., in *Physics of the Ionosphere,* p. 191, 1955.

Ryle, M., A new radio interferometer and its application to observation of weak radio stars, *Proc. Roy. Soc. (A), 211,* 351–375, 1952.

Singleton, D. G., The geomorphology of spread *F, J. Geophys. Research, 65,* 3615–3624, 1960.

Smith, F. G., Ionos refract of 81.5 mcs radio waves from radio stars, *J. Atmospheric and Terrest. Phys., 2,* 350, 1952.

Spencer, M., The shape of the irregularities in the upper ionosphere, *Proc. Phys. Soc., 68,* 1955.

Wild, J. P., and J. A. Roberts, The spectrum of radio star scintillation and the nature of irregularities in the ionosphere, *J. Atmospheric and Terrest. Phys., 8,* 71, 1956.

(Manuscript received February 6, 1961; revised May 31, 1961).

Preliminary Data on Solar Extreme Ultraviolet Radiation in the Upper Atmosphere

H. E. HINTEREGGER

Air Force Cambridge Research Laboratories
Bedford, Massachusetts

Abstract. Recent measurements of solar extreme ultraviolet photon fluxes in the upper atmosphere have been evaluated. Intensities at the top of the atmosphere are estimated, and experimental values of photon absorption rate densities for August 23, 1960 ($\cos Z \approx 0.8$ over New Mexico) for various important line emissions below 1027 A and the hydrogen Lyman continuum are described. The reference tables include published data to the end of 1960.

ıtroduction. In keeping with the title of the er, it should be emphasized that data for elengths longer than 1300 A (Table 1) have ı included only for the purpose of a quick parison of these nearer ultraviolet radiation es in the same notation and in the same units have been chosen for the presentation of extreme ultraviolet (EUV) data in Table 2. summary data of Table 1 show rounded-off es that have been taken and/or averaged ı work published as of the end of 1960.

he present tabular compilation has benefited tly from comments about mimeographed ts of December 1960 which were circulated rmally. Since the individual responding agues should not share any blame for ible errors in the over-all tabulation, most he helpful correspondence is acknowledged only cumulatively. Particular thanks, how-, are due S. Chapman for his most detailed onse including suggestions for a more con-ent tabular arrangement, presenting numbers ıe form $a \times 10^b$ in the space-saving notation dopted for both Tables 1 and 2.

Tables 1 and 2 the radiation spectrum is ribed both in terms of photon flux densities mber flux,' Φ) and in terms of energy flux ity ('intensity,' I). The listed data of $\Phi(\lambda)$ $\Phi(\lambda_1/\lambda_2)$ represent 'integral' fluxes defined as

$$\Phi(\lambda) \equiv \int \Phi_\lambda \, d\lambda$$

(specific line around λ)

$$[\Phi(\lambda)] = \text{cm}^{-2}\,\text{sec}^{-1} \qquad (1)$$

and

$$\Phi(\lambda_1/\lambda_2) \equiv \int_{\lambda_1}^{\lambda_2} \Phi_\lambda \, d\lambda$$

(all lines and/or continua)

$$[\Phi(\lambda_1/\lambda_2)] = \text{cm}^{-2}\,\text{sec}^{-1} \qquad (2)$$

where Φ_λ designates the theoretical 'differential' spectral photon flux density, $[\Phi_\lambda] = \text{cm}^{-2}\,\text{sec}^{-1}\,\text{A}^{-1}$. However, the latter has been omitted from the tabulation to save space and also because (*a*) most of the listed data refer to measurements in which the individual line shapes have not been resolved, and (*b*) the emphasis of this presentation is on Table 2, which covers a region of emission lines superimposed on continuous spectra. The listed data on energy flux density ('intensity') are also given in integral form. They are defined as

$$I(\lambda) \equiv h\nu \cdot \Phi(\lambda) \quad [I(\lambda)] = \text{erg}\,\text{cm}^{-2}\,\text{sec}^{-1} \qquad (3)$$

and

$$I(\lambda_1/\lambda_2) \equiv \int_{\lambda_1}^{\lambda_2} h\nu \cdot \Phi_\lambda \, d\lambda$$

$$[I(\lambda_1/\lambda_2)] = \text{erg}\,\text{cm}^{-2}\,\text{sec}^{-1} \qquad (4)$$

respectively. The redundancy of listing $I(\lambda)$ next to $\Phi(\lambda)$ seemed desirable, since many specific aeronomical applications appear clearer (or merely simpler) in terms of either one of the two quantities, $I(\lambda)$ or $\Phi(\lambda)$, whereas for some applications it is advantageous to think in terms of both.

Both Tables 1 and 2 list more or less empirical

values of a certain altitude $h^*(\lambda)$ in the earth's atmosphere, defined as the level at which a certain monochromatic solar photon flux is reduced to the fraction $1/e$ of the corresponding flux on top of the atmosphere,

$$\Phi(\lambda, h^*) = (1/e) \cdot \Phi_0(\lambda) \qquad (5)$$

The average incident fluxes of solar photons in the nearer ultraviolet region of the spectrum (Table 1) are known to be rather constant throughout a full cycle of varying solar activity. Moreover, the main structure of the lower part of the earth's atmosphere, which is responsible for practically all absorption of the nearer ultraviolet radiation, $\Phi(1300/3000$ A), is nearly free of diurnal, latitudinal, seasonal, or solar-cycle related variations. Neither of these two facts, however, should be claimed for the extreme ultraviolet and soft X-ray region (Table 2).

For the EUV region, say for $\lambda < 1300$ A, both the long-term variations of $\Phi_0(\lambda)$ over the solar cycle and the short-term variations during solar flares appear to be very different for different sections of the spectrum covered by Table 2. Empirical data on these variations are still extremely meager. It seems likely on various grounds that transient variations related to flares are incomparably more pronounced in the X-ray region than for the main fluxes of extreme ultraviolet photons of longer wavelengths, say above 100 A or so. In particular this distinction of solar X rays has been clearly established experimentally at least relative to the strongest single EUV line, i.e. the hydrogen Lyman α, by Friedman's work. Although Friedman has shown that the total solar H Ly-α flux remains rather constant even during major solar flares, our present knowledge of long-term variations over a full solar cycle is poor, even for this very strong H Ly-α line. The situation is, of course, worse for other important emission lines, e.g., the He^+ Ly-α line at 304 A, since photon fluxes in the range from about 100 to 1000 A were not measured at all before the past maximum of the solar cycle. Consequently we have only a few measurements during the early part of the declining phase, and no reliable picture of systematic variations of $\Phi(100/1300$ A) can be given as yet. We have only one set of observations (from the last rocket monochromator experiment on August 23, 1960) that gave significantly lower fluxes for both H Ly-α and He^+ Ly-α as compared with those measu earlier.

Another important distinction between data of Table 1 and Table 2 is related to var tions in the structure of the upper atmosph (thermosphere) that lead to changes of height $h^*(\lambda, Z)$ at which a photon flux fo given wavelength and zenith angle Z is redu to $(1/e)\ \Phi_0(\lambda)$. The atmospheric attenuat characteristics for wavelengths ranging fr about 1000 down to 200 A are particula complex, since these photon fluxes are at same time responsible for nearly all the ioni tion and heating of the part of the atmosph say about 120 or 130 km, where the flu $\Phi(1000/200$ A) undergo their most rapid atten tion. The interplay of the primary absorpt processes, many types of collision reacti (among neutral, exited, and charged particl diffusion, and heat conduction cannot yet formulated with the necessary accuracy quantitative details that would be required a truly reliable computation of the atmosph extinction coefficients

$$\mu(h, \lambda) = \sum_i n_i(h)\sigma_i(\lambda) \qquad [\mu] = \text{cm}^{-1}$$

The present difficulties for theoretical deter nations of $\mu(\lambda, h)$ are mainly due to the lac good data on the relative concentrations of different neutral constituents (i.e., n_i/n). fortunately the composition is still lar unknown, even though the mass density $\rho(h$ now quite well established. Another handica still presented by the limited accuracy of cr section data, at least for certain wavelen particle species, and/or thermal conditions. W is often called a 'small' error of a 'factor of the weighted mean absorption cross sect $\sigma = \Sigma(n_i/n)\ \sigma_i$, may introduce an error o much as a factor of 100 in the correspon calculated transmission, $\Phi(h)/\Phi_0$, whenever true value of Φ/Φ_0 is about 10 per cent or lo Since a fraction of 10 per cent of some f large incident flux $\Phi_0(\lambda_1)$ usually has a stro local effect than a fraction of 50 or more cent of a proportionately weaker solar emiss $\Phi(\lambda_2)$, we conclude that (*a*) improvement absolute cross-section data, as well as the ne composition data, are mandatory for quantit theoretical determinations of the EUV extin characteristics of the real upper atmosphere, (*b*) direct experimental values of photon abs

TABLE 1. 3000–1300 A

Note: h^* data for overhead sun ($Z \sim 0°$). $a \times 10^b \equiv a^b$ in Φ_0, I_0, data.

$h\nu$, ev	Top of Atmosphere: Φ_0, ph/cm² sec	Top of Atmosphere: I_0, erg/cm² sec	h^* $\Phi(h^*) \equiv \Phi_0/e$ (approx.), km	σ(M), Absolute Absorption Cross Section for Species M, cm²	Remarks
4.3	1.5^{15}	1.0^{4}	30–40	$\sigma(N_2, O_2, O, N)$ are negligible	Below 3000 A: Strong absorption by ozone.
4.6	6.8^{14}	5.0^{3}	30–40		
5.0	2.5^{14}	2.0^{3}	35–45	$\sigma(O_3) = 1.2 \times 10^{-17}$	2550 A: Spectral peak of ozone absorption.
5.4	1.3^{14}	1.1^{3}	40	$(O_2) = 5 \times 10^{-24}$ [*Young*, 1960]	Below 2420 A: Weak photodissociation of oxygen (O_2 — Herzberg continuum).
5.9	5.3^{13}	500			
5	2.6^{15}	1.9^{4}	30–45		Mainly absorbed by O_3 above 2300 A; absorbed by both O_3 and O_2 below 2300 A.
6.4	1.3^{13}	130	30–50	$\sigma(O_2) < 6 \times 10^{-21}$	
6.7	5.6^{12}	60	75	$\sigma(O_3) \sim 10^{-18}$ $\sigma(O_2) \sim 3 \times 10^{-20}$ $\sigma(O_2) \sim 1.5 \times 10^{-22}$	 O_2 bands. O_2 Herzberg continuum [*Young*, 1960].
7.1	3.5^{12}	40	85–100	$\sigma(O_2) = 10^{-19}$ -8×10^{-19}	Below 1750 A: Strong photodissociation of O_2 (Schumann continuum).
7.5	1.6^{12}	20	~105	8×10^{-19} $- 4 \times 10^{-18}(O_2)$	
8.0	7^{11}	9	~115	4×10^{-18} $- 1.1 \times 10^{-17}(O_2)$	
8.5	2.6^{11}	3.5	~125	$1.5 \times 10^{-17}(O_2)$ [*Watanabe*, 1958] $1.8 \times 10^{-17}(O_2)$ [*Ditchburn and Heddle*, 1953]	Spectral peak of O_2 dissociation.
9.2	8^{10} (continuum)	1.2	95–125	1.4×10^{-17} $- 4 \times 10^{-19}(O_2)$	
8.8	5^{9} (Si IV)	0.07	~125	$1.4 \times 10^{-17}(O_2)$	
9.3	1^{10} (C II, Si II)	0.15	~110	$2.2 \times 10^{-18}(O_2)$	
9.5	1^{10} (Si II, O I)	0.15	~95	$5 \times 10^{-19}(O_2)$	
9.5	1.1^{11} (total)	1.5	95–125	4×10^{-19} $- 1.4 \times 10^{-17}(O_2)$	
6.2/ 9.5	2.5^{13} (total)	260	50–125		Mainly absorbed by molecular oxygen; no ionization.
4.2/ 9.5	2.6^{15} (total)	1×10^{4}	25–125		Mainly absorbed by ozone and molecular oxygen; no ionization.

TABLE 2. $\lambda < 1300$ A

Note: h^* data estimated for summer day 1960, near noon, temperate latitudes.

λ or λ_1/λ_2, A	$h\nu$, ev	Φ 235 km, cos $Z \approx 0.8$, 8/23/60, New Mexico, ph/cm² sec	Estimated for Top of Atmosphere August 1960		h^* Estimated, $\Phi^* \equiv \Phi_0/e$, cos $Z \approx 1$, km	σ_0(M) or σ_i(M) Absolute Cross Sections Total Absorption −, or Ionization; Species M, 10^{-18} cm²	Remarks
			Φ_0, ph/cm² sec	I_0, erg/cm² sec			
1300–1200 A							
1300/1200	10.0	~5^9	5^9 (continuum)	0.08	70–135	0.01–$40_0(O_2)$ Rapidly variable with λ	Notation for Φ: a^b means $a \times 10^b$ throughout tables.
1265/1259	9.9	2.5^9	2.5^9 (lines, Si II)	0.04	~100	$0.5_0(O_2)$	
1248/1239	10.0	~1^9	~1^9 (lines, N V)	~0.01	~105	$0.5_0(O_2)$	
1216	10.2	2^{11}	2^{11} (H Ly α)	3.3	~75	$0.01_0(O_2)$, $0.000_0(N_2)$, 2.4_0(NO), 2.0_i(NO)	H Ly α: Considered as main source of normal *D*-region ionization (quiet sun).
		(3.7^{11}) 210 km	(3.7^{11})	(6.0)	(GRD 1/19/60 estimated max. error 20%)		
			3.7^{11}	6.0	Preferred value from many ion-chamber measurements by Friedman and collaborators, NRL, up to spring 1960 (estimated experimental error 10–20%).		
For spectral shape of H Ly-α line see *Tousey* [1961]				~0.1	Lowest values from earlier NRL experiments found closer to minimum of solar cycle; low value, however, possibly attributed to instrumental error.		
				0.1–10	Extreme excursion believed to be possible; actual variation probably within a factor of 10 and quite possibly less, even under conditions of major flares [*Friedman*, 1961]; H Ly-α first detected photographically at University of Colorado [*Rense*, 1953].		
1206	10.2	4^9	4^9 (line, Si III)	0.07	~115	$15_0(O_2)$	
1300/1200	10.0	2.1^{11}	2.1^{11} (all lines + continuum)	3.5	70–135 see Ly-α	0.01_0–$40_0(O_2)$ rapid variation with λ 2_i(NO) for H Ly-α	Mostly absorbed by O_2; the dominant line, H Ly-α, is believed to be partly absorbed by NO, causing the normal *D*-region ionization.

1200/1100	~10.8	~3^9	~3^9 (continuum estimated)	~0.05	70–120	0.01_0–$6_0(O_2)$	
1176	10.6	~2^9	~2^9 (C III)	~0.03	~100	$1.3_0(O_2)$	
1200/1100	~10.8	~2^9	~2^9 (other lines)	~0.03	70–120		
1200/1100	~10.8	~7^9	~7^9 (all lines + continuum)	~0.10	70–120	$\sigma_0(O_2)$ rapidly variable with λ	Absorbed by O_2; contribution of $\leq 5\%$ to Friedman's Ly-α detectors (NO chamber with LiF window).
1100/1000	~11.8	~2^9	~2^9 (continuum estimated)	0.03	80–120	0.05–$6_0(O_2)$	
1038/1031	11.9	3^9	3^9 (lines, O VI)	0.06	~100	$1.0_0(O_2)$; $\sigma_i = 0$	Contribution $\leq 2\%$ NO ion chamber signals.
1026	12.0	2.2^9	2.2^9 (H Ly-β)	0.03	~105	$1.7(O_2)$, $0.9_i(O_2)$	Below 1030 A: photoionization of molecular oxygen H Ly-β causes much of the ionization in lower E region.
1006	12.2	7^8	7^8 (N III)	0.01	~105	$2.0_0(O_2)$, $1.5_i(O_2)$	
1100/1000	11.8	8^9	8^9 (all lines + continuum)	0.13	80–120	0.05_0–$6.0_0(O_2)$; 0_i–$1.5_i(O_2)$	See note above; absorbed mostly by O_2.
1000/900	~13.0	2^9	$\leq 2^9$ (continuum estimated excluding Ly continuum)	≤ 0.03	110–250?	1.5_0–$54_0(O_2)$; 1.3_i–$3.8_i(O_2)$; 0.01–$300_0(N_2)$	Sharp N_2-absorption bands (see $\sigma_0(N_2)$).
993/990	12.5	3^8	3^8 (Si II, N III, O I)	0.006	115	1.6_0–$20_0(O_2)$; 1.4_i–$10_i(O_2)$; $\sim 0.5_0(N_2)$	Mostly absorbed by O_2.

TABLE 2. Continued

λ or λ_1/λ_2, A	$h\nu$, ev	Φ 235 km, cos $Z \approx 0.8$, 8/23/60, New Mexico, ph/cm² sec	Estimated for Top of Atmosphere August 1960		h^* Estimated, $\Phi^* \equiv \Phi_0/e$, cos $Z \approx 1$, km	σ_0(M) or σ_i(M) Absolute Cross Sections Total Absorption −, or Ionization; Species M, 10^{-18} cm²	Remarks
			Φ_0, ph/cm² sec	I_0, erg/cm² sec			
			976–800 A				
976	12.7	4^9	4^9 (C III line)	0.08	∼115	8.5_0, $8.0_i(O_2)$; $3_0(N_2)$	Significant contribution to E-region ionization.
972	12.7	3^8(?)	1^9(?) (H Ly-γ)	0.02(?)	250–300 (?)	$\leq 300_0(N_2)$, 'effective' cross section very uncertain	H Ly-γ may contribute to upper atmosphere heating (Nicolet, private communication). This line, 'missing' in all photographic spectra until recently discovered in exposure at 220 km [*Purcell, Packer, and Tousey*, 1960]. N_2 absorption spectrum is extremely complex. $\sigma(\lambda)$ varies over many orders of magnitude and is not accurately known.
949	13.0	3.5^8	3.5^8 (H Ly-δ)	0.006	∼130	$4_0(O_2)$, $3_i(O_2)$; 0.2_0–$2.0_0(N_2)$	
937/912	∼13.7	$\sim 1^9$	$\sim 1^9$ (rest of Ly series)	∼0.02	115–160	4_0–$20_0(O_2)$; 3_i–$15_i(O_2)$; 0.2_0–$10_0(N_2)$(?)	
1000/911	∼12.8	8^9	8^9 (all lines + continuum)	0.16	110–160 (300?)	1.5_0–$50_0(O_2)$; 1.3_i–$38_i(O_2)$; 0.01_0–$300_0(N_2)$	Significant contribution to ionization and heating in E region (some also in F_1); also see note for H Ly-γ.
912/900	13.7	3^9	3^9 (H Ly continuum)	0.07	∼135	4_0–$14_0(O_2)$; 3.5_i–$9.7_i(O_2)$; $<0.1_0$–$150_0(N_2)$; 7_i(H) 2.6_i–3.0_i(O)(theoretical values adopted close to Dalgarno, private communication)	Below 911 A: photoionization of atomic oxygen (also H) H Ly continuum: dominating cause of ionization and heating of E region, contributing source of F_1 region and highest F_2.
900/840	∼14.1	5^9	5^9 (H Ly continuum)	0.11	∼140		

835/833	14.9	7^8	7^8 (lines, O II, III)	.017	~140	$14.5_0(O_2)$; $4.7_i(O_2)$; $10_i(N)$; $3.0_i(O)$; $\sigma_0(N_2)$ = ?	Below 850 A: photoionization of atomic nitrogen.
911/800	13.6/ 15.6	9^9	9^9 (all lines and continua)	0.20	~135	4.5_0–$30_0(O_2)$; 3.8_i–$9_i(O_2)$; $\sigma_0(N_2)$ = ?	Ionization and heating in E and F_1 regions; see notes above.
			800–500 A				
790/888	15.7	5^8	7^8 (lines, O II, III)	0.018	~185	$30_0(O_2)$; $13_i(O_2)$; $8_i(N_2)$; $3_i(O)$; $10_i(N)$	Below 797 A: photoionization of molecular nitrogen; $\sigma_0(N)$ = σ_i (N) and $\sigma_0(O)$ = σ_i (O) (values taken close to those calculated by Dalgarno, private communication).
780/770	16.0	4.5^8	6^8 (lines, Ne VIII)	0.015	~175	$10_i(N_2)$; 22_0, $11_i(O_2)$; $10_i(N)$; $3.4_i(O)$	
704, 702	17.6	2.8^8	6^8 (lines, O II)	0.016	~220	$20_i(N_2)$; $25_i(O_2)$; $10_i(N)$; $7_i(N)$	
800/700	17.6/ 20.7	1.2^9	1.4^9–3^9 (all lines + continuum)	0.04–0.10	~180 mostly	See above.	Apparently modest contribution to ionization and heating of F_1 and F_2 region.
630/625	20.0	9^8	2^9 (lines, O V, Mg X)	0.064	~250	$20_i(N_2)$; $23_i(O_2)$; $11_i(N)$; $12_i(O)$	
610	20.3	6^8	1.5^9 (line, Mg X)	0.05	~250	$22_i(N_2)$; $25_i(O_2)$; $10_i(N)$; $12_i(O)$	
584	21.2	8^8	3^9 (He I res. line)	0.10	~250	$22_i(N_2)$; $25_i(O_2)$; $12_i(N)$; $13_i(O)$	Probably strongest monochromatic flux dissipated in F_2 region.
555/521/ 500	22.5/ 23.7/ 24.7	5^8	1.3^9 (lines, O II, IV: Si XII, C III)	0.05	~250	·	
700/500	17.6/ 24.7	2.8^9	7.8^9 (all lines + continuum)	0.26	~250	$12_i(O)$, $22_i(N_2)$, $11_i(N)$, $12_i(O_2)$	Dominant cause of ionization and heating in F_2 region.

TABLE 2. Continued

λ or λ_1/λ_2, A	$h\nu$, ev	Φ 235 km, cos $Z \approx 0.8$, 8/23/60, New Mexico, ph/cm² sec	Estimated for Top of Atmosphere August 1960		h^* Estimated, $\Phi^* \equiv \Phi_0/e$, cos $Z \approx 1$, km	σ_0(M) or σ_i(M) Absolute Cross Sections Total Absorption −, or Ionization; Species M, 10^{-18} cm²	Remarks
			Φ_0, ph/cm² sec	I_0, erg/cm² sec			
			500–260 A				
500/400	24.8/ 29.5	7^8	1.5^9 (all lines + continuum)	0.07	220	12_i(O), 15_i(N_2), 5_i(N); 20_i(O_2)	Apparently modest contribution to *F*-region ionization and heating. Φ_0(500/300 A) data uncertain by a factor of about 2.
370	33.5	3^8	4.5^8 (line, C III)	0.024	190	10_i(O), 13_i(N_2), 20_i(O_2), 2.6_i(N)	(Identification of specific solar emission lines as shown is tentative except for He^+ Ly-α.)
360	34.5	3^8	4.5^8 (C III, N III, Ne II)	0.025	190	10_i(O), 12_i(N_2), 20_i(O_2), 5.7_i(N)	
335	37.0	4.3^8	8^8 (line, N IV?)	0.047	190	8.5_i(O), 10_i(N_2), 17_i(O_2), 4.3_i(N)	
323/310	39.5	2^8	4^8	0.026	180	7.8_i(O), 6_i(N_2), 15_i(O_2), 3.5_i(N)	
304	41.0	2.1^9	4^9 (He^+ Ly-α)	0.25	180	10_i(O), 4_i(N_2), 20_i(O_2), 2.9_i(N)	First detected photographically in 1958 [*Violett and Rense*, 1959] and photoelectrically in 1959 [*Hinteregger*, 1960*a*, *b*].
285/282	43.5	5^8	8^8 (lines, N IV, Ne III?)	0.05	160	8.5_i(O), 5_i(N_2), 17_i(O_2), 2.3_i(N)	
280/260	45.0/ 47.5	5^8	7.5^8 (lines, O II, III, IV: N V; C IV)	0.045	155	7.5_i–8.0_i(O); 6_i–7_i(N_2); 15_i–16_i(O_2); 1.9_i–2.2_i(N)	
400/260		4.3^9	7.7^9 (all lines + continuum estimated)	0.467			Major source of heating and ionization in F_1 region.

260–60 A						
259/228	47.5/ 54.5	1.5^9 (lines, including He II Ly-β + continuum)	0.12	~150	$5_i(N_2)$; $15_i(O_2)$; $7.5_i(O)$	Estimated error of a factor of 3.
228/166	54.5/ 74.0	5^9 (lines + continuum)	0.5	~140	1_i–$5_i(N_2)$; 5_i–$10_i(O_2)$	Same source of data; estimated error of a factor of 4.
260/166	47.5/ 74.0	~6.5^9 (lines + continuum)	0.65	140–150	(Probably more than one ion-electron pair per absorbed photon)	Important source of E- and F_1-region ionization; may be in error by as much as a factor of 4 (listed values are more likely to be too high than too low).
166/105	74/ 120	~5^8?	~0.07?	~135	0.3_i–$1_i(N_2)$; 2_i–$5_i(O_2)$	Least accurate estimate from 1/29/60 GRD experiment (factor of 10).
105/60	120/ 205	~1.5^9	~0.35	~110	Probably up to about 6 ion pairs per absorbed photon	Important source of E-region ionization; error in Φ_0 (from GRD data) estimated as high as factor of 5.

Note: All flux data in the section of the table between double rules are based on extrapolated *assumed* calibration factors ($\lambda < 300$ A) for GRD rocket monochromator flown on January 29, 1960, near noon from White Sands, New Mexico. Therefore the experimental accuracy of these data remains undetermined. The experiment was performed under normal solar conditions (compare with summary that follows).

Summary Reference for $\lambda < 200$ A

λ or λ_1/λ_2, A	$h\nu$, ev	Estimated for Top of Atmosphere August 1960		h^* Estimated, $\Phi^* = \Phi_0/e$, cos $Z \approx 1$, km	Number of Ion Pairs per Absorbed Photon	Solar Activity	Remarks
		Φ_0, ph/cm^2 sec	I_0, erg/cm^2 sec				
200/44	61/280	5^8–5^9 --- up to 5^{10}	0.1–1 --- up to 9	<140	~2 to 10	Normal --- Flares (class 2+)	From NRL photoionization measurements with different fillers and assuming gray body radiation of $T \sim 5$–7×10^5 deg K [*Kreplin*].
60/44	205/280	5^7–5^8 --- up to 5^9	0.02–0.17 --- up to 1.7	<100	~6 to 10	Normal --- Flares	Same source of data; $T \sim 5 \times 10^5$ deg K.
105/60	120/205	$\sim 1.5^9$	~0.35	~110	~4 to 6	Normal	GRD 1/29/60 experiment (see above).
20–8	620/520	4^5–2^7 --- up to 1^9	4^{-4}–2^{-2} --- up to >0.9	85–105	~20 to 50	Normal --- Flares	NRL data with $T \sim 2 \times 10^6$ deg K [*Kreplin*].
<8	>1500	$<1^5$ --- up to $>2^6$	$\sim 1^{-3}$ --- up to >0.2	<90	>50	Normal --- Flares	NRL data 1949/60 (enhances *D*-region ionization during flares).

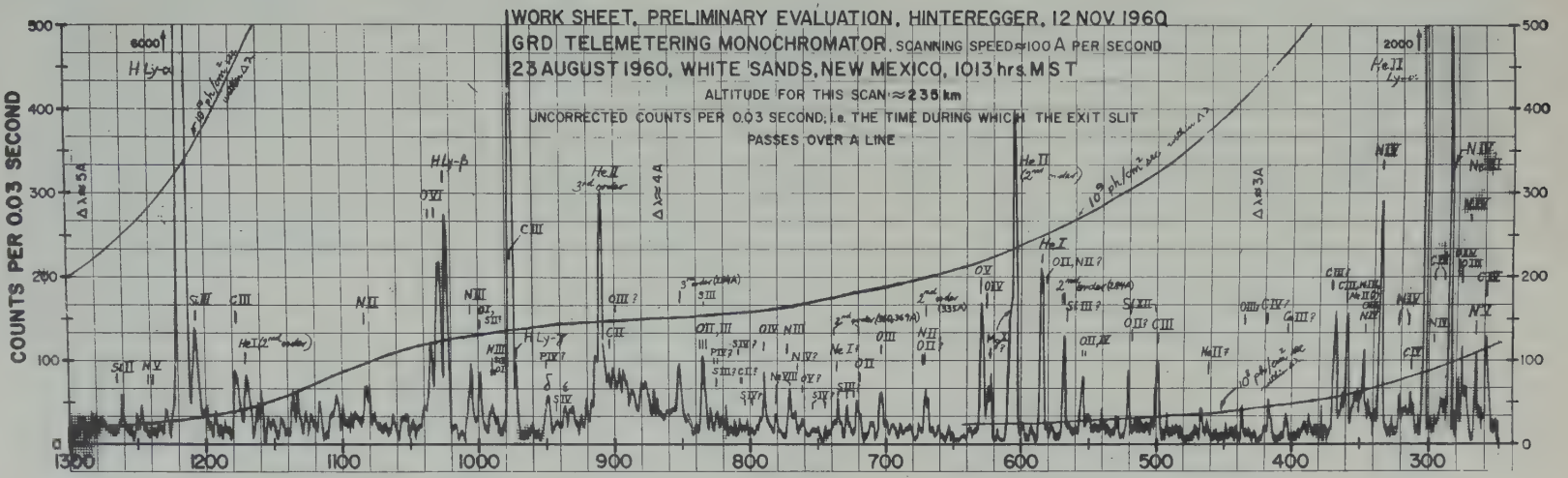


Fig. 1. Uncorrected counting rates from a complete wavelength scan (duration 10 seconds) at an altitude of about 235 km for a solar zenith angle of about 37° (cos $Z \approx 0.8$). The curves marked 10^8, 10^9, and 10^{10} ph/cm² sec identify the specific ordinate value on an absolute scale of photon flux density within the range $\Delta\lambda$ of wavelengths accepted by the instrument, when it is set to wavelength λ. The wavelength (λ) is indicated as abscissa (marked in angstrom units) giving the wavelength position as it was telemetered, i.e., without corrections. Because of improper performance of the pointing control, the raw data of photon fluxes had to be corrected (by adopting the H Ly-α signal as a reference) to obtain more reliable curves of the flux attenuation in the atmosphere, $\Phi(\lambda, \Delta\lambda)$ versus altitude, as shown in Figure 2.

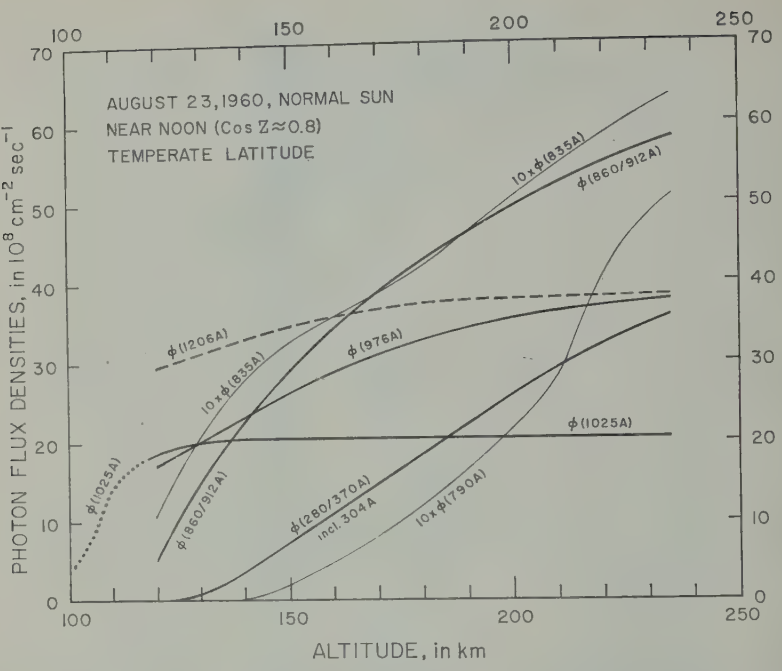


Fig. 2. Vertical attenuation of various solar extreme ultraviolet photon fluxes in the upper atmosphere. The data shown stem from the August 23, 1960, rocket monochromator experiment, during which the solar pointing control operated outside its normal accuracy limits. Therefore the curves shown are not the raw data but normalized data relative to the H Ly-α flux which was known to have been constant (within about 10 per cent) from the simultaneously telemetered measurements with an NO ion chamber (with LiF window).

Important conclusions about the composition of the atmosphere may be drawn from atmospheric attenuation characteristics such as shown.

Examples. (*a*) *1206 A*: Combination of the data $\Delta\Phi(235\text{–}140\text{ km})/\Phi(235\text{ km}) \approx 0.12\ (\pm 0.08)$, $\sigma_0(N_2) \ll \sigma_0(O_2)$, and $\sigma_0(O_2) \approx 1.5 \times 10^{-17}$ cm² implies $N(O_2, 140\text{–}235\text{ km}) \approx (8 \pm 6) \times 10^{15}$ cm^{-2}, i.e., probably: $N(O_2, 140\text{ km up}) \leq 10^{16}$ cm^{-2}.

(*b*) *976 A*: Combination of the data $\Delta\Phi(235\text{–}140\text{ km})/\Phi(235\text{ km}) \approx (0.36 \pm 0.12)$, $\sigma_0(O_2) \approx 8.5 \times 10^{-18}$ cm², and $\sigma_0(N_2) \sim 3 \times 10^{-18}$ cm² implies the relation $N(N_2, 140\text{–}235\text{ km}) = (1.2 \pm 0.4) \times 10^{17}\text{ cm}^{-2} - 2.8 \times N(O_2, 140\text{–}235\text{ km})$, i.e., $N(N_2, 140\text{–}235\text{ km}) = (1.2 \pm 0.4) \times 10^{17}$ cm², if $N_{O_2} \ll N_{N_2}$, and if $(N_2) = 3 \times 10^{-18}$ cm² is correct (which is really *quite uncertain*).

(*c*) *835 A and 860/912 A*: A comparison implies that $N(N, 140\text{–}235\text{ km})/N(N_2, 140\text{–}235\text{ km}) \leq 0.13 \pm 0.1$ if $|\sigma_0(N_2, 835\text{ A}) - \bar{\sigma}_0(N_2, \text{Ly continuum})| \leq 10^{-18}$ cm².

The extremely tentative character of the above conclusions must be emphasized, since they are based on a single experiment (of rather poor pointing accuracy). It should be noted, too, that the foregoing estimates refer to the specific atmospheric conditions of the August 23, 1960, experiment.

tion rate densities, determined from the relation

$$a(\lambda, h) = (\partial\Phi/\partial h)_{exp} \cos Z \qquad (7)$$

seem to be more reliable than values calculated from the relation

$$a(\lambda, h, Z) = \mu_{theor}(\lambda, h) \times T_{theor}(\lambda, h, Z) \times (\Phi_0)_{exp} \qquad (8)$$

even if we were to assume that the absolute incident flux, $\Phi_0(\lambda)$ in equation 8, were known much more accurately than the absolute local flux gradient, $\partial\Phi/\partial h$, could be measured. calculate $\mu(\lambda, h)$ theoretically, only the lo values n_i, besides σ_i, are needed.[1] A calculat

[1] Because of systematic *diurnal variations* total density (serious above about 200 km) in composition (serious above about 100 k even the local extinction coefficient $\mu = \Sigma\, n_j\, \sigma$ also a function of the zenith angle. Thus one ne theoretical models of $n_j = n_j(h, Z)$ rather t merely models of $n_j = n_j(h)$ for accurate oretical determination of μ from assumed accu data on cross sections.

the transmission $\Phi(h)/\Phi_0$, i.e. T_{theor} in equation 8, however, requires the values of $n_i(h)$ for whole atmosphere above the point for which wants to determine the photon absorption density.

Extreme ultraviolet photon absorption rate sities calculated by relation 7 from the gust 23, 1960, experimental data of fairly nochromatic attenuation measurements between 120 and 235 km are presented in the explanatory Figure 3. It should be emsized, however, that the accuracy of solar nting of the monochromator axis throughout vertical probing flight was very poor, so t we had to resort to a somewhat arbitrary malization relative to the interpolated signals ained for H Ly-α for the two adjoining wavegth scans. The assumption that Φ(H Ly-α) fact was practically constant was borne out the results from an ionization chamber with windows and NO gas filling on the same icle (NO chamber quite similar to Friedman's l-known Lyman-α detectors).

Figures 1, 2, and 3 are more conveniently cribed in the legends than in the text. It uld be emphasized here, however, that the terial presented is considerably less accurate n the data that can logically be expected to obtained from several experiments scheduled the near future. We hope to evaluate any experimental results with less delay than present ones. It should be admitted that a ter account of cross-section data could have n incorporated in the present Table 2. A more ful revision, however, would have caused rther delay not warranted by the otherwise ted accuracy of much of the experimental ton flux data in the preliminary tables and grams.

Discussion. The experimental data on the ton fluxes Φ(1300/260 A) at 235 km of gust 23, 1960, given here are lower than those orted for an altitude of 210 km on January 1960 [e.g., *Hinteregger*, 1960*a*, *b*]. This is resting since the August experiment was ducted somewhat earlier in the day and for lue of cos Z closer to unity (i.e., both reasons ld suggest a generally higher flux). Only the erved decrease in the H Ly-α flux from about $\times 10^{11}$ to 2×10^{11} ph/cm^2 sec can be med with certainty to be mostly a true ease. The decrease in the observed value of

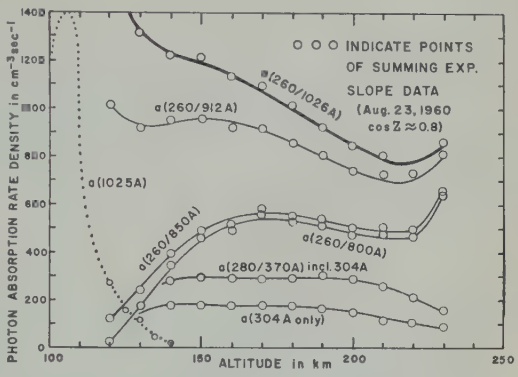


Fig. 3. Absorption rate densities of solar extreme ultraviolet radiation in the upper atmosphere. The ordinates represent the number of photons (of the identified wavelength or wavelength range) absorbed per unit volume per unit time. Since for all cases shown the average number of ion electron pairs produced by one absorbed photon is close to unity, the ordinates represent at the same time the corresponding contributions to the ion production rates for the E region and lower part of the F region.

Φ(304 A) from 3×10^9 (January 1960) to 2×10^9 ph/cm^2 sec (August 1960) is *likely* to be true, too; however, it is still *possible*, in this instance, that the entire difference is merely the accidental result of two experimental errors, say of +15 and −20 per cent, respectively. A similar reservation, of course, applies to many other important photon fluxes, e.g., that in the hydrogen Lyman continuum.

The changes in the 'observed' fluxes (i.e., from our January 1960 data to our August 1960 data) are not very large, and some of them can be explained at least partly by the better resolution and lower background of the later experiment. The differences between the estimated EUV photon fluxes 'on top of the atmosphere' shown in earlier publications and those given in Table 2 are considerably larger, but they are actually less significant physically, since they reflect mainly the quality of uncertain assumptions about density, composition, and absolute cross sections. The values of extrapolated incident fluxes given here[2] (Φ_0 and I_0 in Table 2) imply a model of EUV transmission of the upper

[2] These estimates are based primarily on simple extrapolations of the observed vertical attenuation profiles (assuming more or less constant scale heights above 235 km) rather than on any published or privately assumed 'atmospheric models.'

atmosphere that seems to be more realistic than the one used for our preliminary estimates earlier [e.g., *Hinteregger*, 1960*a*, *b*]. The final decision about the actual atmospheric opacities above the altitudes of the present observation, however, must be postponed until reference measurements from satellite-borne EUV monochromators have been achieved.

References

Ditchburn, R. W., and D. W. D. Heddle, *Proc. Roy. Soc. (London), A, 220,* 61, 1953.

Friedman, H., *Space Astrophysics,* edited by W. Liller, McGraw-Hill, p. 107, 1961.

Hinteregger, H. E., *Astrophys. J., 132,* 801, 1960*a*.

Hinteregger, H. E., *Tenth International Astrophysical Symposium Liège,* 1960*b*.

Hinteregger, H. E., *Space Astrophysics,* edited by W. Liller, McGraw-Hill, pp. 34, 74, 1961.

Jacchia, L. G., *Smithsonian Observatory Rept.* 1959.

Jacchia, L. G., *Smithsonian Observatory Rept.* 1960.

Kreplin, R. W., *International Aeronomy Symposium,* Copenhagen, to be published.

Priester, W., and others, *Mitt. Univ. Sternwarte Bonn,* no. 34a.

Purcell, J. D., D. M. Packer, and R. Tousey, *Proc. First Intern. Space Sci. Symposium,* North Holland Publishing Co., Amsterdam, p. 581, 1960.

Rense, W. A., *Phys. Rev., 91,* 229, 1953.

Tousey, R., *Space Astrophysics,* edited by W. Liller, McGraw-Hill, p. 1, 1961.

Violett, T., and W. A. Rense, *Astrophys. J., 1* 954, 1959.

Watanabe, K., *Advances in Geophys., 5,* 153, 19

Young, P. A., Thesis, Reading University, 1960.

(Manuscript received April 14, 1961.)

Frictional Effects and the Meridional Circulation in the Mesosphere

BERNHARD HAURWITZ[1]

Planetary Sciences Department, The Rand Corporation
Santa Monica, California

Abstract. The observed warm winter temperatures in the upper mesophere at high latitudes, where no direct heating by solar radiation takes place, require vertical descent of air from the lower ionosphere into the upper mesosphere. Such descent leads to adiabatic heating and to stronger heating because of the recombination of oxygen atoms into oxygen molecules. It is shown that the curvature of the vertical profile of the mean zonal wind component results in frictional meridional components of motion of the right direction and of a reasonable order of magnitude to produce the divergence required for such a descent of the air into the high mesosphere over the subpolar regions during the winter season. A more detailed computation of the frictional meridional wind components gives meridional-circulation systems similar also to those required for an explanation of the maximum of the total ozone content at high latitudes in late winter or early spring.

1. Introduction. Recent rocket ascents at rt Churchill, Canada [*Stroud, Nordberg, and ndeen,* 1960], have apparently confirmed lier conjectures [*Kellogg and Schilling,* 1951] it the upper part of the arctic mesosphere is rmer during the winter than during the sum- r. From the relatively few observations it not yet be concluded with certainty that the h winter temperatures in the upper meso- here over Fort Churchill are representative of whole arctic region. But because of the ab- ce of any observational evidence and of any usible physical reasons to the contrary, it is erally assumed that this phenomenon is char- eristic of the whole arctic mesosphere in win- , and this view is adopted here.

These high winter temperatures of the upper sophere cannot be explained as an effect of ar heating [*Murgatroyd and Goody,* 1958]. ey must therefore be due to dynamic proces- specifically to vertical motions, because with arctic mesosphere being warmer than layers the same height at other latitudes, horizontal rection cannot explain these high tempera- es. Vertical motions cannot be measured di- ly, but can only be deduced indirectly, for ance, from the divergence of the horizontal city. Further, the explanation of large-scale tical motion is also most readily given in terms of the horizontal divergence. In polar regions, with which we are here mainly concerned, meridional motions are of particular interest as causes of vertical motion because poleward motion implies convergence and equatorward motion implies divergence.

The increasing, but still sparse, wind observations from the upper atmosphere show, as expected for dynamic processes, that there is a well-developed zonal circulation with characteristic differences between summer and winter on which less persistent and smaller meridional motions are superimposed. However, despite its greater variability and smaller intensity, the meridional component of the circulation is in many respects more important than the stronger zonal circulation. It is hardly necessary to belabor this point, but attention is called to the fact that a suitable meridional circulation is invoked not only to explain the high temperatures of the upper mesosphere in winter, but also to account for the high ozone content in the polar atmosphere at the end of the winter, which cannot be attributed to photochemical ozone production *in situ.* Thus, it becomes desirable to deduce the meridional circulation itself quantitatively from dynamic principles.

In the present paper an attempt is made in this direction. It is not claimed that the effect to be discussed necessarily gives the whole story. But it may at least contribute toward a better

[1] On leave from the High Altitude Observatory, versity of Colorado, Boulder, Colorado.

understanding of some of the puzzling aspects of the mesosphere. Since, to all appearances (just as in the lower atmosphere), the zonal circulation in the mesosphere is well developed, it seems logical to begin with this component in the consideration of mesospheric dynamics.

2. The meridonal component of motion due to friction. The prevalence of zonal motion in the terrestrial atmosphere is due to the earth's rotation. Because in the absence of any forces absolute angular momentum will be conserved, a mass displaced from one latitude to another along a path parallel to the earth's surface will rapidly acquire a strong zonal component of motion. Meridional components of motion are therefore completely overshadowed by the zonal components, except in the trade wind zones, if the average picture of the large-scale atmospheric circulation is considered. Since analyses of the radiative balance and of the momentum balance, on the other hand, show clearly that a meridional transfer of heat and momentum must take place, it was pointed out quite some time ago, by *Exner* [1925] for the heat transfer and by *Jeffreys* [1926] for the momentum transfer, that such a transport can occur when pressure gradients with zonal components exist. Then angular momentum is no longer conserved, and air can move in meridional direction along the isobars. The zonal pressure gradient cannot, of course, be in the same direction all around the earth; therefore, closed cells of low and high pressure or sinusoidal wave patterns should exist, such as are actually observed in the lower atmosphere. There can be no doubt that similar pressure configurations do play a similar role in the mesosphere, and *Teweles* [1961], in a discussion of the Churchill rocket data, has demonstrated their existence convincingly. But these sinusoidal flow patterns would not give a net meridional mass transport.

Such a net meridional mass transport would result from frictionally caused meridional motion. Since the atmospheric motions are largely geostrophic, the effect of friction is generally small, except in the boundary layer at the earth's surface. But the effect of friction is a factor that is present all the time, and it may therefore be quite effective despite its smallness.

In the lower atmosphere the frictional effect is for all practical purposes not due to the molecular but to the eddy viscosity. The same is assumed to be true for the mesosphere. The eddy stresses with which we shall be concerned are $-\rho\,\overline{u'w'}$ and $-\rho\,\overline{v'w'}$, where u', v', and w' are the three turbulent velocity components. Since there is no direct information available about the turbulent velocities in the upper atmosphere, the two eddy stress terms will be expressed, as usual, by the horizontal mean velocity components u, v, with the aid of Prandtl's mixing length theory,

$$-\rho\,\overline{u'w'} = \mu\frac{\partial u}{\partial z} \qquad -\rho\,\overline{v'w'} = \mu\frac{\partial v}{\partial z}$$

The parameter μ is the coefficient of eddy viscosity. Although it is in general not a constant, its possible variability will be neglected in the following discussion for lack of information.

To obtain a quantitative estimate of the frictional effect, we consider a coordinate system with the x axis pointing south in the direction of increasing colatitude θ and with the y axis pointing east in the direction of increasing longitude λ. The z axis is pointing vertically upward. The wind components are u, positive towards south (a north wind in meteorological terminology), and v, positive towards east (a west wind in meteorological terminology). Further we let ρ be the air density, p the pressure, f the Coriolis parameter ($f = 2\,\omega\cos\theta$), ω the angular velocity of the earth's rotation ($\omega = 7.29 \times 10^{-5}\ \mathrm{sec}^{-1}$), θ the colatitude, and r the earth's radius. We assume equilibrium between the Coriolis force, the pressure gradient force, and the frictional force, so that[2]

$$-fv = -\frac{1}{\rho\,r}\frac{\partial p}{\partial\theta} + \frac{\mu}{\rho}\frac{\partial^2 u}{\partial z^2} \tag{1}$$

$$fu = -\frac{1}{\rho\,r\sin\theta}\frac{\partial p}{\partial\lambda} + \frac{\mu}{\rho}\frac{\partial^2 v}{\partial z^2} \tag{2}$$

Since we wish to derive the frictionally induced meridional circulation due to the zonal motion, we assume that the pressure field is independent of the longitude λ, so that the pressure term in the second equation is zero. In the layer next to the ground, the physical postulates expressed by

[2] Because of the spheroidal shape of the earth the left-hand sides of (1) and (2) should contain the factor $(1+v/2\omega r\sin\theta)$. But unless v is comparable to the linear velocity of the earth's rotation $\omega r\sin\theta$ which may be true very near the poles, this factor may be regarded as unity.

above equations lead to the wind distribution own as the Ekman spiral. At higher levels the viations from the geostrophic winds are small, least for such values of μ as apply in the lower nosphere.

Under these conditions the zonal component the wind may be, as pointed out long ago by *llwo* [1934], approximated by the geostrophic nd v_g due to the meridional pressure gradient. en, approximately,

$$v = v_g = \frac{1}{f}\frac{1}{\rho r}\frac{\partial p}{\partial \theta} \tag{3}$$

d

$$u = \frac{1}{f}\frac{\mu}{\rho}\frac{\partial^2 v_g}{\partial z^2} \tag{4}$$

more complete derivation of these approxitions will be found in the Appendix. Similar uations have been used by *Prandtl* [1932] for a cussion of the general circulation.

Equation 4 shows that a frictional meridional nd component must exist whose intensity and ection depend on the curvature of the vertical file of the zonal wind. Some typical zonal nd profiles and the resulting frictional meridal wind components are shown in Figure 1. Physically, this effect is easily understood. nsider, for instance, the case illustrated in ure 1*a*. From the level 1 to 2, the wind rease is less strong than from 2 to 3. Hence shear, directed along the positive y axis, reases with elevation, and the shearing force, portional to the vertical rate of shear change, elerates the fluid at 2 above the geostrophic ed. The air motion of level 2 thus becomes fast for the existing pressure gradient, and a nponent to the south results. (We confine selves here, as always in this paper, to the thern hemisphere.)

To estimate the value of the meridional coment resulting from friction we may assume t

$$= \frac{1 \text{ m/sec}}{(5 \text{ km})^2} = 4 \times 10^{-10} \text{ cm}^{-1} \text{ sec}^{-1} \tag{5}$$

ch corresponds to values taken from the n zonal wind profiles. In individual cases, curvature of the wind profile may of course considerably larger, as is indicated by the ng turbulence observed in the high mesoere. A representative value for the Coriolis

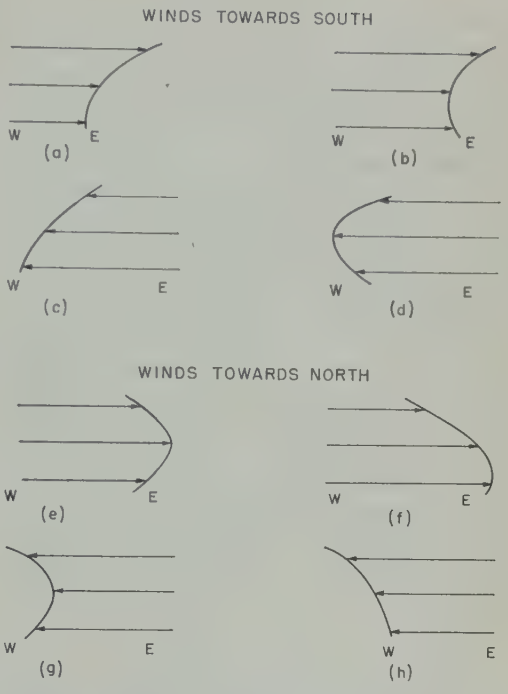


Fig. 1. Curvature of vertical zonal-wind profile and meridional frictional wind component.

parameter is $f = 10^{-4}$ sec^{-1}, which corresponds to about 45° latitude. More difficult is the choice of a representative value for the kinematic viscosity $\nu = \mu/\rho$. *Lettau* [1951] suggested as a maximum value for the coefficient of eddy diffusivity 10^7 cm^2/sec, which is about 10^4 times larger than the coefficient of molecular viscosity around 70 km. Since, in the surface layers, the coefficient of eddy viscosity is about 10^5 times larger than that of molecular viscosity, the value 10^7 cm^2/sec may not be too unreasonable, although it may well be too large by an order of magnitude. With these numerical values, $u = 40$ cm/sec. Since u depends linearly on the various quantities, it is easy to see how it will change for different numerical values.

We are interested not only in the meridional motions but also in the resulting vertical motions, which depend on the latitudinal variation of u. A representative value of the meridional changes of $\partial^2 v/\partial z^2$ is 1 m/sec/(5 km)^2 per 5° latitude, and therefore over this distance u may change by 40 cm/sec. Suppose that the southward flow across 62.5° latitude is 40 cm/sec, that across 57.5° latitude it is 80 cm/sec, and that this flow extends from 80- to 90-km elevation. The

vertical velocity required to compensate for this meridional divergence would be about 0.7 cm/sec or 600 m/day, neglecting the vertical variation of density. This value is of the magnitude required to account for the high temperature of the upper mesosphere over Fort Churchill. A more accurate computation based on the equation of continuity for spherical coordinates and allowing for the vertical density change does not yet seem justified in view of our lack of accurate knowledge of the zonal wind distribution.

3. Estimates of the frictional wind component from the temperature field. Equation 4 will be used later (section 4) to make quantitative estimates of u. But it is of some interest to consider how the curvature of the zonal wind profile and the resulting meridional motion are related to the vertical and meridional temperature distribution. Since the zonal wind can be assumed to be geostrophic, the thermal wind relation,

$$f\frac{\partial}{\partial z}\left(\frac{v_g}{T}\right) = \frac{g}{T^2}\frac{\partial T}{r\,\partial\theta} \tag{6}$$

may be used, where g is the accceleration of gravity and T is the temperature in °K. It follows by differentiation of the thermal wind relation that

$$\frac{\partial^2 v_g}{\partial z^2} = \frac{v_g}{T}\frac{\partial^2 T}{\partial z^2} + \frac{g}{fT}\frac{\partial^2 T}{r\,\partial\theta\,\partial z} \tag{7}$$

To obtain an estimate of the magnitude of the terms in this equation, we consider winter conditions over White Sands, New Mexico, and Fort Churchill, Manitoba, as illustrated in Figure 13 of the paper by *Stroud, Nordberg, and Bandeen* [1960], from which the approximate values of the temperature and vertical temperate gradients shown in Table 1 are obtained. For White Sands the temperature gradient between 40 and 45 km is 2°/km; between 45 km and 50 km it is 0°/km. Assigning these values to the middle of each layer we find for White Sands

$$\frac{\partial^2 T}{\partial z^2} = \frac{0°/\text{km} - 2°/\text{km}}{5\text{ km}} = -4° \times 10^{-11}\text{ cm}^{-2}$$

and the same value holds for Fort Churchill. The zonal winds v_g, which may be assumed to be geostrophic, at these altitudes and latitudes

TABLE 1. Approximate Values of the Temperature and Vertical Temperature Gradients

Height, km	White Sands T, °K	White Sands dT/dz, deg/km	Fort Churchill T, °K	Fort Churchill dT/dz, deg/km
40	250		230	
		2		4
45	260		250	
		0		2
50	260		260	
		0		0
55	260		260	
		−2		−2
60	250		250	
		−2.5		0 approximately
80	200		250	

are about 60 and 30 m/sec, respectively, so that

$$\frac{v_g}{T}\frac{\partial^2 T}{\partial z^2} = -0.9 \times 10^{-9},$$

$$-0.5 \times 10^{-9}\text{ cm}^{-1}\text{ sec}^{-1}$$

for White Sands and Fort Churchill. To estimate the second term on the right-hand side of (7) we choose the layer from 40 to 45 km. For White Sands $dT/dz = 2°$/km, for Fort Churchill 4°/km. Since the latitude difference between Churchill and White Sands is 27°, corresponding to 3000 km,

$$\frac{\partial}{r\,\partial\theta}(\partial T/\partial z) = \frac{2°/\text{km} - 4°/\text{km}}{3000\text{ km}} = -0.67° \times 10^{-13}\text{ cm}^{-2}$$

and

$$\frac{g}{fT}\frac{\partial^2 T}{r\,\partial\theta\,\partial z} = -2.6 \times 10^{-9}\text{ cm}^{-1}\text{ sec}^{-1}$$

In the example considered here, the two terms on the right-hand side of (7) have the same sign but this obviously need not always be the case. The second derivative of the zonal wind would thus be 7 times larger than that used in equation (5), resulting in a frictional meridional wind component of 3 m/sec. This value may be somewhat high for a mean meridional wind component, but it must be remembered that in this computation a coefficient of eddy viscosity was used which according to *Lettau* [1951] is a maximum estimate. The point of the present calculation is to demonstrate that significant value

r the frictional meridional wind may also be btained if the curvature of the vertical wind rofile is estimated from the temperature field. It would thus be possible to compute the ictional meridional wind component from the ertical temperature distribution in a meridional oss section rather than from the zonal wind eld. Since the zonal wind field and the meridional mperature cross sections are made consistent y means of the thermal-wind relation, both ethods would give substantially the same sults. On the other hand, the computation by eans of the zonal wind is somewhat more irect. Therefore, it has been used for the mputation of the meridional wind components the following section.

4. Determination of the frictional meridional ind component from the mean wind field. The mputation of the meridional frictional wind mponent was based on the values obtained by *atten* [1961] and used by him in the construction cross sections of the average zonal wind comnent. The zonal wind velocities were available tables for each fifth degree of latitude from 0° to 65°N and from 20- to 100-km altitude in eps of 5 km. If h_{n-1}, h_n, h_{n+1} are three consecuve heights 5 km apart at a given latitude, $v/\partial z^2$ for the elevation h_n is expressed by the nite second difference

$$\left(\frac{\Delta^2 v}{\Delta z^2}\right)_n = v_{n+1} - v_n - (v_n - v_{n-1})$$

$$= v_{n+1} + v_{n-1} - 2v_n$$

he unit of these expressions is m/sec/5 km/5 n $= 4 \times 10^{-10}$ cm^{-1} sec^{-1}, which has been used the later diagrams of $\partial^2 v/\partial z^2$. These values for $^2/\partial z^2$ at a given latitude have been smoothed y the simple formula

$$\overline{\left(\frac{\Delta^2 v}{\Delta z^2}\right)_n} = \frac{1}{3}\left[\left(\frac{\Delta^2 v}{\Delta z^2}\right)_{n-1} + \left(\frac{\Delta^2 v}{\Delta z^2}\right)_n + \left(\frac{\Delta^2 v}{\Delta z^2}\right)_{n+1}\right]$$

$$= \frac{v_{n+2} + v_{n-2} - v_{n+1} - v_{n-1}}{3}$$

hese smoothed values for given heights have een further smoothed with respect to the titude by an analogous procedure, so that

$$\left(\frac{\Delta^2 v}{\Delta z^2}\right)_{n,\phi_k} = \frac{1}{3}\left[\left(\frac{\Delta^2 v}{\Delta z^2}\right)_{n,\phi_{k-1}} + \left(\frac{\Delta^2 v}{\Delta z^2}\right)_{n,\phi_k} + \left(\frac{\Delta^2 v}{\Delta z^2}\right)_{n,\phi_{k+1}}\right]$$

where ϕ_{k-1}, ϕ_k, ϕ_{k+1} denote three latitudes, such that $\phi_{k+1} - \phi_k = \phi_k - \phi_{k-1} = 5°$. With this smoothing process, mean values for $\partial^2 v/\partial z^2$ for heights from 30 to 90 km and latitudes from 35° to 60°N were obtained for summer and winter. Since the zonal wind distribution during the earlier part of the winter differs considerably from that in the later part, Batten constructed two different meridional cross sections of the zonal winds, one for November-December, the other for January-February, and, accordingly, $\partial^2 v/\partial z^2$ was also computed separately for these two winter periods.

According to (4), the meridional wind component is inversely proportional to the Coriolis parameter f, and hence to the sine of the latitude which varies between 35° and 60° from 0.57 to 0.87. But in view of our lack of knowledge concerning the coefficient of viscosity μ and its variations it does not yet seem worth while to apply a correction for latitude. The density ρ varies through the level considered here through three orders of magnitude, so u would increase considerably with elevation unless μ undergoes similar changes or, in other words, unless the kinematic coefficient of viscosity remains unchanged. Furthermore, we are mainly interested in the convergence and divergence of mass and the resulting vertical motions, so we are really more concerned with ρu than with u itself. It is not desirable, therefore, to correct for density changes with elevation.

For these same reasons it seemed best simply to plot the quantity $\partial^2 v/\partial z^2$, and this has been done in Figures 2 to 6. The unit is, as explained before, m/sec/(5 km)^2 $= 4 \times 10^{-10}$ cm^{-1} sec^{-1}, and, as discussed following (4), if $\mu/\rho = 10^7$ cm^2 sec^{-1}, $f = 10^{-4}$ sec^{-1}, this unit would correspond to $u = 40$ cm/sec.

Summer conditions are shown in Figure 2. A strong southward component should exist between 60 and 70 km at higher latitudes, and this component broadens toward the south. Above this southward motion the frictionally caused motion would be directed northward, but it would be of less intensity than the southward flow below. The northward flow appears to extend to the highest levels for which data are available, except at 55° and 50° latitude at 90 km where a weak, and therefore doubtful, southward component is indicated. It seems unlikely, therefore, that air is on the average

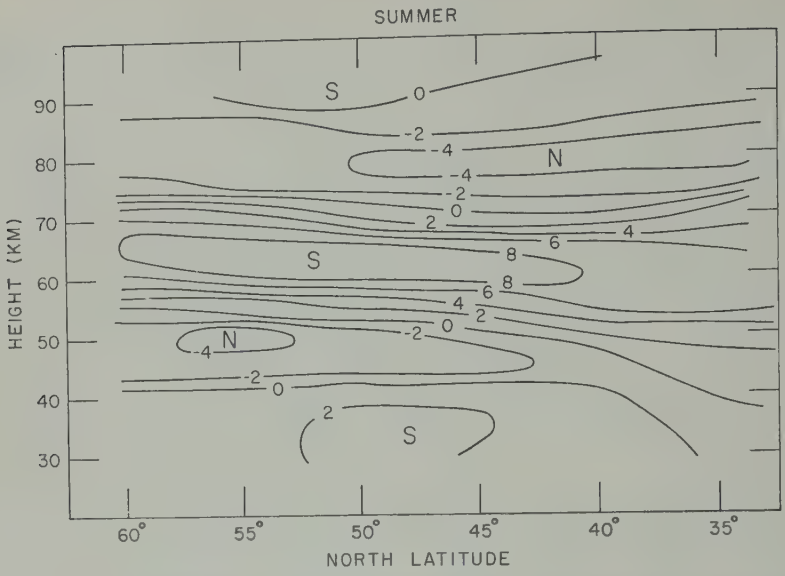


Fig. 2. Meridional distribution of the curvature of the vertical zonal-wind profile; unit 4 $\times 10^{-10}$ cm^{-1} sec^{-1}. With $\nu = 10^7$ cm^2/sec, $f = 10^{-4}$ sec^{-1} corresponding to a meridional velocity of 40 cm sec^{-1}. Positive (negative) values imply a frictional wind component to the south (north). Summer conditions.

descending towards the mesopause over the arctic regions during the summer and being heated.

Dr. Diran Deirmendjian has suggested to me that this summerly northward flow in the upper mesosphere and above, which is replaced by a southward flow during the winter (Fig. 3), may transport and concentrate cosmic dust at high latitudes and thus explain why noctilucent clouds are observed in summer but not in winter.

Another, but weaker and less extensive, northward flow is indicated between 55 and 45 km at higher latitudes, but it becomes very narrow and lower south of 45° latitude. In the upper stratosphere the frictional current is to the south, but it is much weaker than that in the mesosphere.

During the winter (Fig. 3) conditions are simpler than in summer, and the directions of the meridional motions are largely reversed. In the upper stratosphere the flow is to the south, most of the mesosphere is taken up by a strong northward flow, and at the top of the mesosphere and above, the flow is again southward. A schematic diagram of the winter circulation is shown in Figure 4. There is, of course, some uncertainty about these circulations north of 60°N and south of 30°N because data are lacking, and for this reason the circulations in Figure 4 have in part been shown by broken lines.

The southward flow at and above the mesopause requires descending motion at high latitudes, which would explain the high temperatures in these regions as being caused by adiabatic warming and to heating by recombination of oxygen atoms, as suggested by *Kellogg* [1961]. The northward flow in the lower mesosphere and the upper stratosphere may be responsible for the northward transport of ozone and the high-latitude maximum of total ozone content at the end of the winter, although this northward flow does not reach quite as low as the lower limit of the region where ozone would be in photochemical equilibrium.

A meridional circulation in the same direction as the lowest one in Figure 4 has been derived by *Libby and Palmer* [1960] from radioactive-fallout data. But the southward branch of this circulation is much lower, and consequently the northward flow also begins at a lower altitude than that shown here (Fig. 4). This discrepancy may at least partly be due to the fact that the circulation scheme derived by Libby and Palmer applies to the whole year.

If the periods November-December and

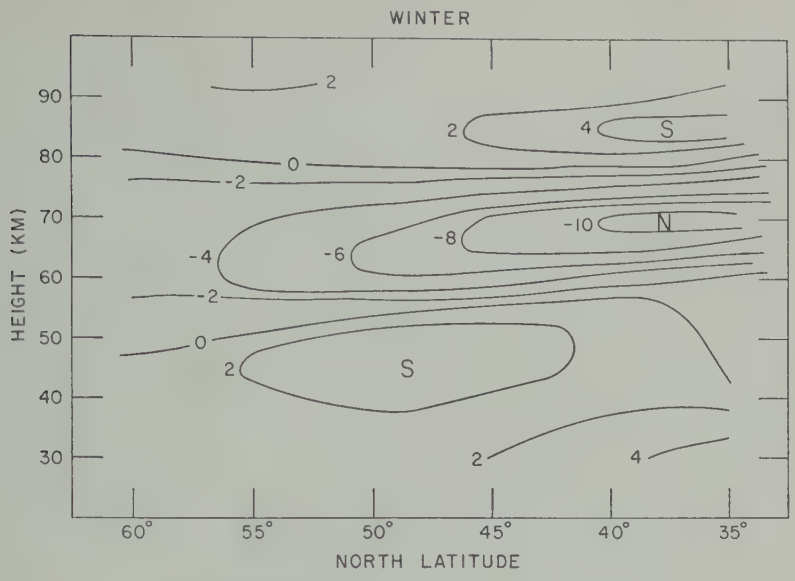


Fig. 3. Meridional distribution; winter conditions.

nuary-February are considered separately, the her simple picture presented in Figure 3 for e whole winter becomes somewhat more mplicated. During the first part of the winter ig. 5), a northward frictional component is tained throughout most of the mesosphere d the stratosphere except, in the case of the atosphere, for latitudes south of 50°N and ghts below 35 km and, in the case of the sosphere, only at the top at higher latitudes. uring the second part of the winter (Fig. 6) e southward flow in the upper stratosphere ends farther to the north. (The distribution $\partial^2 v/\partial z^2$ in the lower part of Figure 6 is rather nfused, perhaps because fewer data are avail- e than for the whole winter and hence irregu- ities may not be smoothed out as much as in . 3). At the top of and above the mesosphere southward flow is also found during the ond part of the winter, although it is now ter developed at low than at high latitudes. vertheless, conditions are favorable for descent air from higher levels to the mesosphere oughout the whole winter. It is suggestive t, according to *Stroud, Nordberg, and Bandeen* 60], the high temperatures at Fort Churchill found in early as well as in late winter.

. Consideration of energy relationships. Since tion is assumed to be active in the model sidered here, the zonal circulation has to be maintained against the effects of frictional dissipation. Without considering in any detail questions of energy supply or loss, we may make some rough estimates of the magnitude of the dissipation. If **F** denotes the frictional force, and **V** the velocity vector, then the dissipation D in a vertical column of unit area between two levels z_1 and z_2 is

$$D = \int_{z_1}^{z_2} \mathbf{V}\cdot\mathbf{F}\rho\, dz$$

where the minus sign has been omitted. Since we assumed that $F = \nu\, \partial^2 v_g/\partial z^2$ it follows, with (4), that

$$D = \int_{z_1}^{z_2} v_g \nu \frac{\partial^2 v_g}{\partial z^2}\, \rho\, dz$$

$$= f \int_{z_1}^{z_2} w v_g \rho\, dz = \frac{f}{g} \int_{p_2}^{p_1} w v_g\, dp \qquad (8)$$

The kinetic energy for the same column is

$$K = \frac{1}{2} \int_{z_1}^{z_2} v_g^2 \rho\, dz = \frac{1}{2g} \int_{p_2}^{p_1} v_g^2\, dp \qquad (9)$$

With the value of ν that was assumed before, $u \sim v_g/100$; therefore, $D \sim 0.02\, fK$. Since $f \sim 10^{-4}$ sec^{-1}, the dissipation would destroy the original kinetic energy in about 6 days if it maintained its rate (or the kinetic energy would

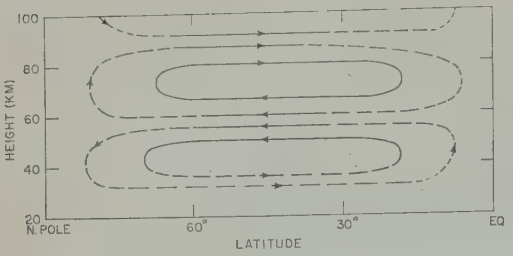


Fig. 4. Schematic presentation of meridional circulation in winter.

decrease to $1/e$ of its original value if the ratio D/K remained constant).

To obtain an order-of-magnitude estimate of the kinetic energy, we let $v_g \sim 50$ m/sec, $p_1 \sim 10{,}000$ microbars, the pressure at about 30-km altitude, $p_2 \sim 4$ microbars, the pressure at 85- km altitude. Then $K \sim 12.5 \times 10^7$ erg cm^{-2} = 3 cal cm^{-2}, and $D \sim 6 \times 10^{-6}$ cal/cm^2/sec. The mass of air between 30 and 85 km is approximately 10 g/cm^2. If the heat generated by D were used to raise the temperature of the air column uniformly, a temperature rise of about 0.2°K per day would result. This amount appears not unreasonable. It should also be noted that the sign of D will in general not be the same everywhere in the air column, since it depends on the signs of v_g and $\partial^2 v_g/\partial z^2$. For a more detailed study of this question, it would be best to compute D directly from the numerical data. But it appears from these estimates that no particular difficulty arises when the energy of these motions is taken into consideration.

6. General comments. For a few days during the winter and summer, direct wind observations to great heights at Fort Churchill were obtained by *Stroud, Nordberg, and Bandeen* [1960]. In some cases, these winds show the components in the directions deduced here; in other they do not. This is to be expected because, in the first place, the mean meridional components are so small in general (less than 1 m/sec) that they cannot be measured directly. Second, they are by the nature of their derivation mean motions, and at specific times and specific longitudes they may not be present.

In the model discussed here for the meridional motions it is assumed that a steady state exists and it is demonstrated that, in this steady state, meridional motions due to friction are to be expected. How this steady state develops is not considered here, but it appears that the motions appropriate for an increase of the total ozone at high latitudes toward the end of the winter and for warming of the high polar atmosphere can be maintained by friction if the observed zonal-wind distribution is established.

It is tempting to use the obtained meridional velocity components for a computation of the vertical motions by means of the equation of continuity. The continuity equation would also show any obvious inconsistencies in the meridional velocities derived here and would thus permit a further smoothing of the meridional circulation scheme. But before such a refinement is undertaken, the zonal-wind sections should be extended to lower and especially to higher latitudes where the spherical shape of the earth becomes particularly important in continuity considerations.

It is finally suggested that considerations of the zonal frictional flow analogous to those presented here could be extended to other planetary atmospheres, especially an atmosphere like Jupiter's which shows evidence of strong zonal circulations, and to the sun with its latitudinal variation of the angular velocity of rotation.

Appendix

Derivation of the frictional wind component in a vertically changing pressure field. Equations 1 and 2 may be written with (3):

$$-fv = -fv_g + \nu \frac{d^2u}{dz^2} \tag{10}$$

$$fu = \nu \frac{d^2v}{dz^2} \tag{11}$$

where it is again assumed that the kinematic coefficient of viscosity $\nu = \mu/\rho$ is constant. The zonal geostrophic wind is assumed to be a function of the elevation. If (9) is multiplied by the imaginary unit i, and if $u + iv = w$ denotes the complex horizontal wind vector,

$$\frac{d^2w}{dz^2} - \frac{if}{\nu} w = \frac{f}{\nu} v_g \tag{12}$$

If we let

$$\lambda = (f/2\nu)^{1/2} \tag{13}$$

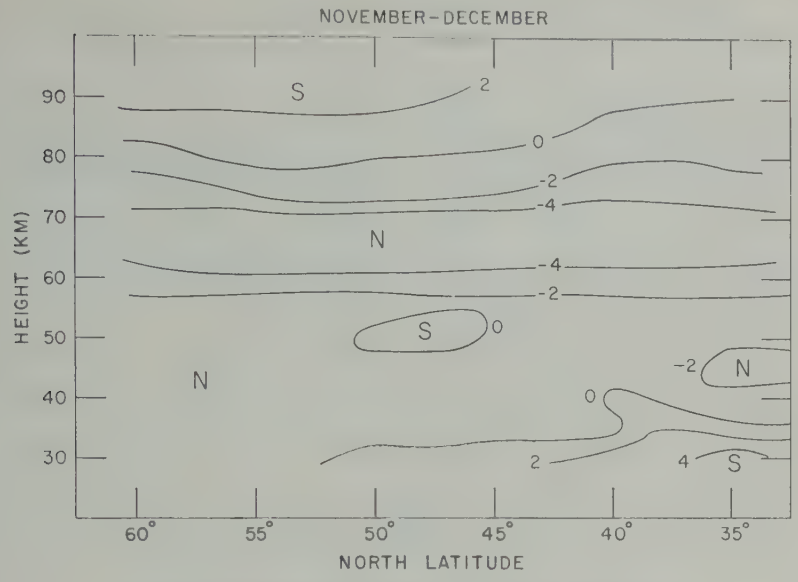


Fig. 5. Meridional distribution; November-December.

e solution of this equation can, by well-known ethods, be expressed in the form

$$w = A_1(z)e^{(1+i)\lambda z} + A_2(z)e^{-(1+i)\lambda z}$$

ere

$$\frac{dA_1}{dz} = \frac{f}{2\mu(1+i)\lambda}\, e^{-(1+i)\lambda z} v_g$$

$$\frac{dA_2}{dz} = -\frac{f}{2\mu(1+i)\lambda}\, e^{(1+i)\lambda z} v_g$$

e two coefficients, A_1 and A_2, can be expressed terms of v_g and its derivatives. To find this pression, we consider the integral

$$I = \int f(z)e^{mz}\, dz$$

ere $f(z)$ is an arbitrary function whose deriv- ves exist, and where m is an arbitrary con- nt. Repeated integration by parts yields

$$= \frac{e^{pz}}{p}\left[f - \frac{f'}{p} + \frac{f''}{p^2} - \frac{f^{(3)}}{p^3} \pm \cdots + (-1)^n \frac{f^{(n)}}{p^n}\right] + \frac{(-1)^{n+1}}{p^{n+1}} \int e^{pz} f^{(n+1)}\, dz$$

his expression is applied to determine A_1 and , and if the values for A_1 and A_2 are sub- uted into the expression for w, the terms with odd derivatives of v_g cancel each other and

$$w = C_1 e^{(1+i)\lambda z} + C_2 e^{-(1+i)\lambda z} + i\frac{f}{2\nu}\frac{1}{\lambda^2}\left[v_g - \frac{i}{2}\frac{1}{\lambda^2} v_g'' - \frac{1}{4}\frac{1}{\lambda^4} v_g^{(4)} + \frac{i}{8}\frac{1}{\lambda^6} v_g^{(6)} + \frac{1}{16}\frac{1}{\lambda^8} v_g^{(8)} \pm \cdots\right] \qquad (14)$$

The first two terms on the right-hand side of this equation with the arbitrary integration constants C_1 and C_2 represent the solution of the homogeneous equation (12). This solution may be equated to zero in the free atmosphere away from boundary surfaces. If C_1 and C_2 are not put equal to zero, w will increase exponentially with the distance from an arbitrarily chosen level—a physically unrealistic situation. Equating real and imaginary parts of the remaining solution, we find that

$$u = \frac{\nu}{f} v_g'' - \frac{\nu^3}{f^3} v_g^{(6)} \pm \cdots \qquad (15)$$

$$v = v_g - \frac{\nu^2}{f^2} v_g^{(4)} + \frac{\nu^4}{f^4} v_g^{(8)} \pm \cdots \qquad (16)$$

If only the first terms on the right-hand sides are retained, we obtain the approximate expressions (3) and (4).

From practical considerations, one would be

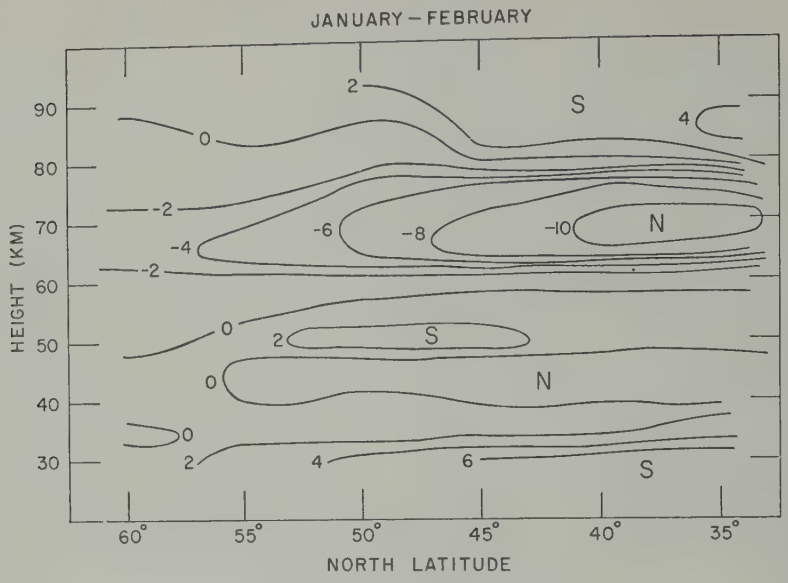


Fig. 6. Meridional distribution; January-February

inclined to neglect the higher derivatives in the expressions for u and v because they are difficult to determine. It is, however, not obvious a priori that this may be done. Consider, for instance, a vertical profile of the form

$$v_g = \bar{v}_g \cos(\pi/D)z$$

which has curvatures of opposite sign at the height intervals D. Then, at $z = 0$,

$$v_g'' = -(\pi^2/D^2)\bar{v}_g \quad v_g^{(6)} = -(\pi^6/D^6)\bar{v}_g$$

Hence

$$u = -\frac{\nu}{f}\frac{\pi^2}{D^2}\left(1 - \frac{\nu^2}{f^2}\frac{\pi^4}{D^4} \pm \cdots\right)$$

Inspection of some of the zonal wind cross sections prepared by Batten suggests from the position of the zones of maximum easterlies and westerlies that $D \sim 40$ km. If we assume, for $\nu = 10^8$ cm^2/sec, 10 times the maximum value suggested by Lettau,

$$\frac{\nu^2}{f^2}\frac{\pi^4}{D^4} = \frac{10^{16}}{10^{-8}}\frac{0.38}{10^{24}} = 0.38$$

a value which is not small compared with 1. But the value assumed for ν is probably too large, and its reduction by at least one order of magnitude would reduce the ratio to 0.0038. The approximation expressed by (3) and (4 therefore seems justified on theoretical ground also and not merely because the higher deriva tives of v_g cannot be accurately determined.

Acknowledgement. I should like to thank m colleagues in the Planetary Sciences Departmer of the Rand Corporation for many helpful discu sions of the problems considered here. In particul I should like to express my appreciation to M E. S. Batten who made available in an easil usable form the data on which the numerica computations were based.

References

Batten, E. S., Wind systems in the mesosphere an lower ionosphere, to be published in *J. Meteoro* 1961.

Exner, F. M., *Dynamische Meteorologie*, 2nd ed J. Springer, Vienna, pp. 215–218, 1925.

Jeffreys, H., On the dynamics of geostrophic wind *Quart. J. Roy. Meteorol. Soc., 52,* 85–101, 1926

Kellogg, W. W., Warming of the polar mesospher and lower ionosphere in winter, to be publishe in *J. Meteorol.*, 1961.

Kellogg, W. W., and G. F. Schilling, A propose model of the circulation in the upper strat sphere, *J. Meteorol., 8,* 222–230, 1951.

Lettau, H., Diffusion in the upper atmosphere, *Compendium of Meteorology,* edited by T. Malone, American Meteorological Society, Bo ton, Mass., 1951, p. 325.

Libby, W. F., and C. E. Palmer, Stratospheric mi

ng from radioactive fallout, *J. Geophys. Research, 65,* 3307–3317, 1960.
ollwo, H., Zur Wirkungsweise der Reibung in der freien Atmosphäre, *Beitr Phys. Atmosph., 22,* 25–45, 1934.
urgatroyd, R. J., and R. M. Goody, Sources and sinks of radiative energy from 30 to 90 km, *Quart. J. Roy. Meteorol. Soc., 84,* 225–234, 1958.
andtl, L. Meteorologische Anwendungen der Strömungslehre, *Beitr. Phys. Atmosph., 19,* 188–202, 1932.
roud, W. G., W. Nordberg, and W. R. Bandeen, Rocket grenade measurements of temperature and winds in the mesosphere over Churchill, Canada, *J. Geophys. Research, 65,* 2307–2323, 1960.
Teweles, S., Advance copy, Time section and hodograph analysis of Churchill rocket and radiosonde winds and temperatures, Paper presented at the New York meeting of the American Meteorological Society, January 1961.

(Manuscript received April 28, 1961.)

Adjustable Potential-Gradient-Measuring Apparatus for Airplane Use

B. VONNEGUT, C. B. MOORE, AND F. J. MALLAHAN

Arthur D. Little, Inc.
Cambridge, Massachusetts

Abstract. An apparatus for measuring the electrical potential gradient from aircraft by the use of radioactive, ionizing probes is described. An adjustable rotating capacitor system has been devised that permits compensation for asymmetry in the exposure of the probes. While this arrangement compensates for the effects of charge on the airplane, it does not compensate for the effects of space charge produced by the airplane.

It is concluded that all airplane gradient measurements in clouds or intense fields, whether made with this or any previous apparatus, are not to be trusted because of errors caused by this space charge. As the result of these errors the gradients measured in weakly electrified clouds are probably too large and the large gradients measured near thunderstorms are probably too small. Examples of gradient records obtained with this apparatus near a source of artificially produced space charge are presented.

INTRODUCTION

n previous papers [*Vonnegut, Moore, and ıme,* 1957; *Vonnegut and McCaig,* 1960; *nnegut and Moore,* 1961] we have de- ibed instrumentation in which radioactive bes were used to measure the atmospheric tric potential gradient from an airplane. To id errors from autogenous and induced charge the airplane with these instruments, we used probes symmetrically exposed. If the two bes are placed in such a position that they equally affected by charge on the airplane, difference in their potential is a measure of external potential gradient alone.

ince most airplanes are nearly symmetrical h respect to a vertical plane fore and aft ng the center of the fuselage, it is a simple tter to install symmetrically two identical bes on either side. It is much more difficult, vever, to install two probes above and be- th the airplane or fore and aft so that effects harge on the airplane will be nullified.

)ur procedure heretofore has been to make best guess as to an electrically symmetrical allation and then to adjust by trial and error lengths or positions of the masts to minimize effect of airplane charge. In general, it is not sible to adjust the masts in flight, so proper ancing of the apparatus is a long and tedious

Vith the new apparatus to be described, it is not necessary to balance the apparatus by adjusting the probes. Instead, this apparatus can be readily balanced in flight by a simple adjustment of the electromechanical device coupling the probes to the electronic amplifier.

APPARATUS

Radioactive probes. Since the effective impedance of the ventilated 1000-microcurie polonium probes that we use is very high, of the order of 10^{10} ohms, it is necessary to exercise considerable care to be sure that they are well insulated. The insulators supporting the probes are critical points in the installation, for they are exposed to the free atmosphere and their surfaces are likely to become contaminated. In previous installations we used a simple Teflon bushing to support the rod holding the probe; we experienced some trouble in maintaining the high resistance of the insulation, because dust, dirt, moisture, insects, and spiderwebs sometimes bridged across and caused leakage.

In this apparatus we have used somewhat larger and more elaborate insulators, illustrated in Figure 1, that provide much longer leakage paths and do not bridge over easily. We feel that the effort involved in their design and fabrication was well worth while, for they gave no trouble during the several months of operation.

Coupling device. As we have pointed out in

previous publications, the two polonium probes used to measure the gradient cannot be connected directly to conventional electrometers, for one side of these must be electrically grounded. Instead it is necessary to use an electromechanical device that isolates both probes from ground while transmitting a signal that is proportional to the voltage difference between them.

The coupling device used in this apparatus is the rotating capacitor shown in Figure 2. It consists of two fixed plates (A and B) side by side, and an asymmetric rotor (R) mounted on a shaft and turned by a small motor so that as it rotates it moves over first one and then the other of the fixed plates. A small pin fastened to the rotor serves as a commutator so that as it passes over one plate it is grounded and as it passes over the other it is connected to an electrometer. One of the exposed electrodes used to measure the gradient is connected to plate A and the other to plate B.

To understand the operation of the coupler let us first assume that the two radioactive probes are mounted symmetrically with respect to the airplane, so that when charge is present on the airplane the probes are at the same potential. The two fixed plates, A and B, are so arranged that when the nuts holding them are turned they move back and forth with respect to the rotor. If they are so adjusted as to be at the same distance from the rotor, then as the rotor moves from one to the other it experiences

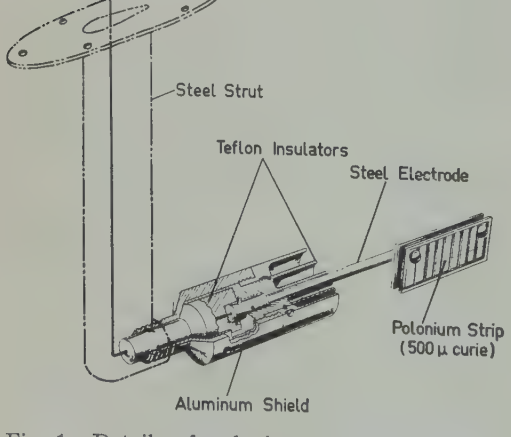


Fig. 1. Details of polonium probe mounted on Teflon insulator.

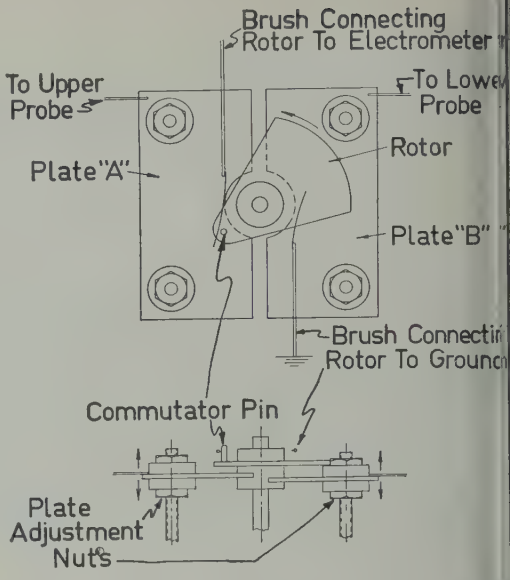


Fig. 2. Drawing of adjustable electromechanic coupling device used in measurement of atmo pheric potential gradient from a charged aircra

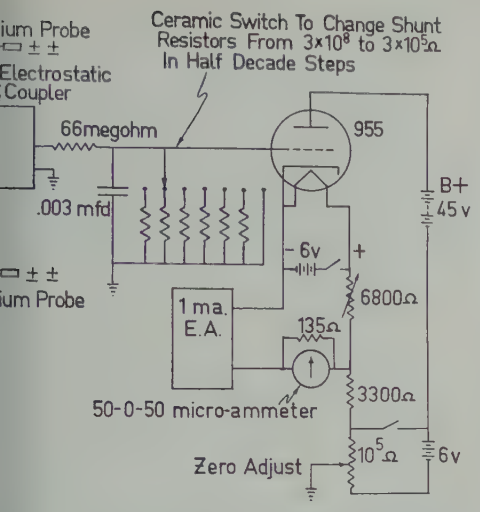
no change in potential, and the signal to t electrometer caused by charge on the airpla is zero.

Now if, as will generally be the case, t probes are not electrically symmetrical with r spect to the airplane, then the charge on t airplane will cause one of the probes and i plate to have a higher potential than the oth with respect to the airplane. With this apparat the higher potential of the one plate simply c be compensated for by reducing its capacitan coupling to the rotor—by moving it back wi the adjusting nuts until the charge on the ai plane produces no signal.

In practice the apparatus is balanced b charging the airplane in flight with a hig voltage d-c power supply and by adjusting t plates until the charge produces no effect.

Electrometer and recorder. For the pote tial-gradient measurements we made from P-38, we had a recorder sensitive enough to operated by the few microamperes supplied b an electrometer tube.

The apparatus described here was used in light, single-engine airplane having no suitab power for a sensitive recorder, and we therefo had to use a spring-driven recorder that requir 1 milliampere to drive it full scale. According we used an electronic amplifier capable of su



g. 3. Schematic of battery powered electrom-used for measurement of potential gradient. circuit operated a 1-ma recorder directly.

g this much larger output. We succeeded vising the simple, single-tube, battery-pow-amplifier shown in Figure 3, which worked except for the minor inconvenience of a near response near full scale. Since the r for this amplifier, as well as the power he small motor driving the coupler, was lied by internal dry batteries, our instru-ation was completely independent of the ane for power.

Calibration

e installation of our probes on the wing of ght plane shown in Figure 4 had such geo-ical symmetry that initially we did not ad-the coupler in flight but rather balanced it e laboratory. Near the end of our opera-when we were able to obtain a high-voltage y to charge the airplane, we tested the ical symmetry of our installation. We l that the system was fairly well balanced hat the effect of charge on the airplane was ensated to within about 10 per cent. On asis of our previous experience we believe our fair-weather measurements outside s were not affected significantly by charge e aircraft.

determined the calibration of our appara-y comparing our measurements from the ne with potential-gradient measurements ned from our polonium-probe installations on the ground. We made these calibrations during the afternoon, when, because of convective mixing in the lower atmosphere, the potential gradient showed little or no variation with altitude. From repeated low-level passes, some only about 5 meters above the ground, we determined that a gradient of 1 volt cm^{-1} measured on the ground corresponded to a potential of 70 volts measured between the probes. (Simultaneous airplane measurements of space charge concentration, with apparatus to be described in a future publication, showed densities less than 1 elementary charge cm^{-3}, so we believe that this represents a valid calibration of the instrument.) Since the vertical separation between the probes was 88 cm, we see that the presence of the airplane and the supporting masts reduced the gradient to about 80 per cent of the undisturbed value.

Limitations of Potential-Gradient Measurements from Airplanes

The charge released into the air by the airplane places a serious limitation on measurements of the potential gradient. An airplane can produce space charge in several ways: (1) by electrification of the exhaust, (2) by contact electrification resulting from collision with cloud, aerosol, and precipitation particles, and (3) by point discharge. The configuration of the space-charge plume released into the atmosphere around the airplane is undoubtedly quite variable, depending on air speed, altitude, engine throttle setting, magnitude and orientation of the external potential gradient, etc. Because of the complicated and variable geometry of the



Fig. 4. Installation of potential gradient probes on wing of Tripacer aircraft.

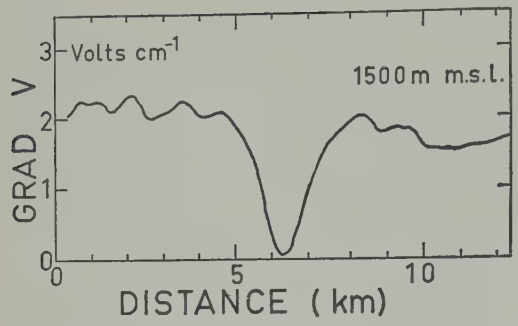


Fig. 5. Typical recording of atmospheric potential gradient observed over a clear-air convection column above positive charge source, July 15, 1960.

charge produced by the airplane, its effects cannot be compensated for as can the charge carried on the airplane surface.

Fortunately, in fine weather outside clouds in low potential gradients, the space charge produced by the airplane is so small that it has a negligible effect on measurements. In clouds and precipitation the space charge produced by the airplane is undoubtedly a source of considerable error. Because of its effects, potential-gradient determinations made from an airplane in weakly electrified clouds or precipitation usually give values that are somewhat too high.

Even when corrections are made for effects of charge residing on the airplane, we question the accuracy of potential-gradient measurements made from airplanes in or near thunderstorms, such as those reported by *Gunn* [1948], *Byers and Braham* [1949] *Gish and Wait* [1950], and *Fitzgerald and Byers* [1959], because of the disturbing effects of the large quantities of space charge released from the airplane. The gradients of 100 or 1000 volts cm^{-1} reported in these observations produce fields at the propeller tips, wing tips, nose and tail that far exceed breakdown. Observations of intense St. Elmo's fire from airplanes and *Gunn, Hall, and Kinzer's* [1946] measurement of currents of several milliamperes flowing to the airplane can leave no doubt that the space charge being emitted is so intense that accurate estimates of the undisturbed gradient are impossible. Since one might expect that the charge produced by corona from the airplane would in general reduce rather than increase the gradient about the airplane, it appears that airplane measurements of intense gradients probably give results that are qui bit smaller than the true values.

Accordingly, we are inclined to believe the gradients around and in thunderstorms be larger than the gradients presently belie to exist. If this is true, the conduction curr above storms calculated from gradient m urements are probably somewhat smaller tha actually the case.

Experimental Results

During the summer months of 1960 abou flights were made with this equipment as of a joint study of fair weather atmosph electricity carried out by groups from New Y University, the Illinois State Water Survey, Arthur D. Little, Inc. Throughout this prog the gradient measuring apparatus proved q troublefree. While we doubt the accuracy of measurements made near thunderstorms, w gradients in excess of 40 v cm^{-1} were obser we believe the apparatus gave reliable and teresting data outside of clouds during weather when the gradients were only a volts cm^{-1}.

Typical records showing gradients that sulted from artificially produced space ch are shown in Figure 5, which illustrates perturbation in the gradient over a clear convection column carrying positive charge, in Figure 6, which shows the perturbation

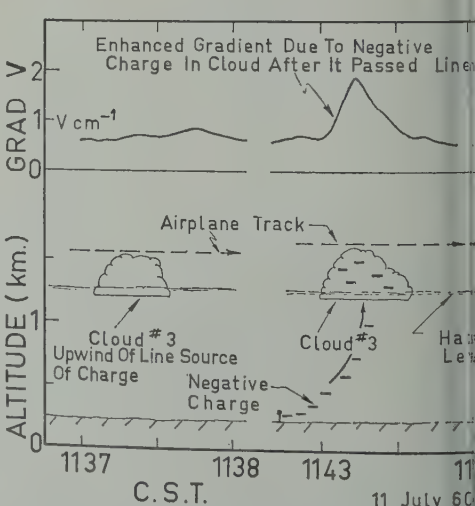


Fig. 6. Enhanced fair weather gradient small cumulus cloud growing from negatively trified air.

gatively charged small cumulus. A detailed nt of our results with this apparatus will esented in forthcoming publications.

knowledgments. We wish to thank Glenn out, Director of the Meteorological Group of llinois State Water Survey, for providing the ersity of Illinois airplane used in this work. are indebted to F. L. Lancaster and D. D. y for the installation of the equipment on lane. We thank J. William Bullock for his lent job as pilot and for his many helpful stions.

References

s, H. R., and R. R. Braham, Jr., *The Thunderrm,* U. S. Dept. of Commerce, Washington, C., p. 85, 1949.

erald, D. R., and H. R. Byers, Aircraft obvations of convective cloud electrification, *Atmospheric and Terrest. Phys., 15,* 254–261, 9.

O. H., and G. R. Wait, Thunderstorms and the earth's general electrification, *J. Geophys. Research, 55*(4), 473–484, 1950.

Gunn, R., W. C. Hall, and G. D. Kinzer, Precipitation static, *Proc. IRE (Waves and Electrons), 34*(4), 156–161, 1946.

Gunn, R., Electric field intensity inside of natural clouds, *J. Appl. Phys., 19,* 481–484, 1948.

Vonnegut B., and D. A. McCaig, Airplane instrument for measurement and vectorial presentation of electrical potential gradient, *J. Geophys. Research, 65*(7), 1959–1963, 1960.

Vonnegut, B., C. B. Moore, and M. Blume, Preliminary investigation of the distribution of space charge in the lower atmosphere, *Artificial Stimulation of Rain, Proc. First Conference on the Physics of Cloud and Precipitation Particles,* Pergamon Press, New York, 1957.

Vonnegut, B., and C. B. Moore, Jr., Apparatus using radioactive probes for measuring the vertical component of atmospheric potential gradient from an airplane, *Bull. Am. Meteorol. Soc. 42,* 1961.

(Manuscript received April 18, 1961; revised May 10, 1961)

The Diurnal Variation of K Indices of Geomagnetic Activity on Disturbed Days in 1940–1948

SETH B. NICHOLSON

Mount Wilson and Palomar Observatories, Carnegie Institution of Washington
California Institute of Technology
Pasadena, California

OLIVER R. WULF

United States Weather Bureau, California Institute of Technology
Pasadena, California

Abstract. From the eight daily K numbers for the 5 disturbed days of each month in the 9 years 1940-1948 from six observatories in moderately low latitudes, local- and universal-time components of the diurnal variation of these K indices have been computed. The local-time component shows no pronounced seasonal change. It has a maximum near 21 hours. The separate yearly average for each of the 9 years shows a fairly regular change in amplitude over these years. The change is particularly marked from 1943 to 1947, and is of such character as might be occasioned by an increase over this interval in a separate local-time component having a daytime maximum. Its occurrence over these years suggests that it may be related to the solar cycle. The universal-time component shows a pronounced seasonal change. When it is examined as the yearly average for each of the 9 years separately, although large differences from year to year are found, apparently in considerable measure at random, nevertheless there appears to be a significant yearly average.

eomagnetic activity as measured by the K ces exhibits a diurnal variation that appears ontain both a local-time and a universal- component. In studying the K numbers n six observatories in moderately low lati- s, we have found that the local-time com- ent is more pronounced than the universal- component at low values of activity, but in the average the amplitudes of the two ponents are comparable at higher values of vity. We have recently discussed the diurnal ation of the K indices on quiet days [*Nichol- and Wulf,* 1961], and have called attention rather conspicuous change, possibly related he solar cycle, over the years 1940 through in the character of the local-time com- nt. The present paper contains results for rbed days.

he eight daily K numbers for the 5 disturbed of each month were used for the 9 years through 1948 [*Johnston, Scott, and Bal-* 1948; *Howe and Weisman,* 1949] from the bservatories—Alibag, Watheroo, Honolulu, on, San Juan, and San Fernando—which airly evenly distributed in longitude. These he same observatories that we have earlier used in obtaining results for all days [*Nicholson and Wulf,* 1955, 1958] and for the 10 quiet days [*Nicholson and Wulf,* 1961]. The 9-year-average departures of the K numbers for each of the eight 3-hour intervals were computed for each observatory for each month of the year. The 12-month-average departures for each of the eight intervals were also computed for each observatory for each of the 9 years.

These six-station sets of departures were combined to give a local- and a universal-time component for each 9-year monthly average, and for each individual yearly average in the manner described in *Nicholson and Wulf* [1961, p. 1139].

The 9-year average local-time component of the diurnal variation of K for the 5 disturbed days is shown in Figure 1. The unit used throughout is 0.01 K. Figure 1 indicates a local-time variation of considerable amplitude and of much the same form from month to month. The amplitude is somewhat greater near the equinoxes than near the solstices.

The average of the 12 monthly variations for these 9 years is shown at the foot of Figure 1. The 12 months contribute to this average with

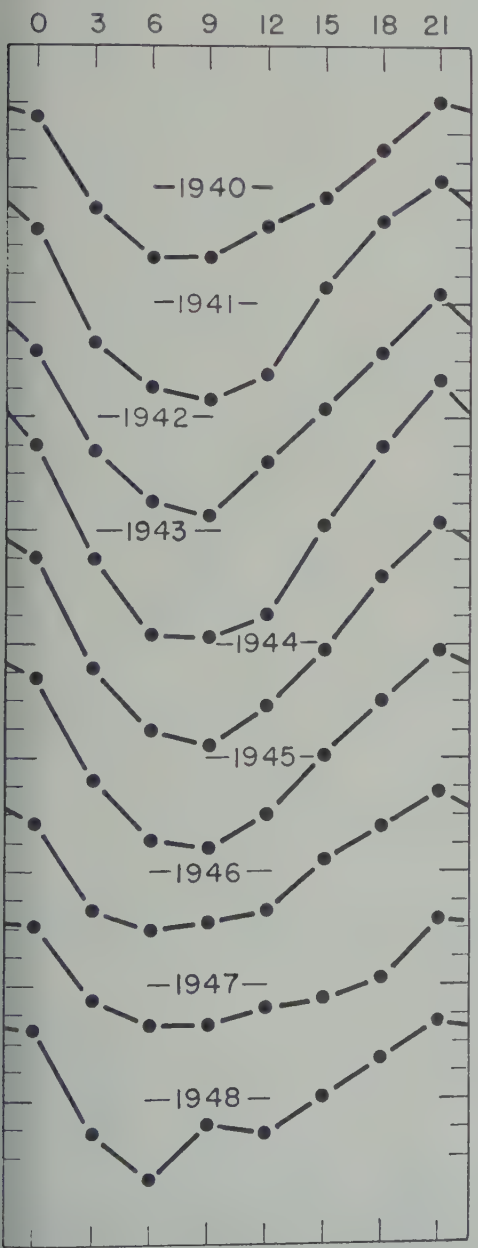
a considerable degree of consistency. The standard deviations of these eight average values were computed from the twelve values of which each is the average. These standard deviations contain, of course, the small seasonal change mentioned above, as well as the random fluctuations of the results. The largest proves to be 2.4 units (0.024 K) in the 21st hour. The dots used in the figure have a radius of approximately 2.5 units. Figure 1 shows that, in the 9-year average, these data for the 5 disturbed days yield a local-time component that has a maximum near 21 hours and a minimum between 6 and 9 hours.

The local-time component is also illustrat in Figure 2, but here as the nine separate yea averages. These indicate a pronounced chan in amplitude over these 9 years. The amplitu is large in 1943 near sunspot minimum a small in 1947, the year of sunspot maximu Thus, as in the data for the 10 quiet da [*Nicholson and Wulf*, 1961], a fairly regu change of the local-time component over th years seems to be present.

This change, moreover, is of approximat the same kind as that in the 10 quiet da (though there is a considerable difference in

Fig. 1. Local-time component of the diurnal variation of K, 1940–1948, for the 5 disturbed days of each month from the six observatories. Unit, 0.01 K.

earance of the two sets of curves [*Nicholson Wulf*, 1961, compare Fig. 3]), namely, one could be described approximately as an in-se, from 1943 to 1947, in the amount of a l-time component with a daytime maximum *yaud*, 1956] relative to that of a local-time



. 2. Yearly average local-time component of diurnal variation of K, 1940–1948, for the 5 rbed days of each month from the six ob-tories for each of the 9 years. Unit, 0.01 K.

component with a nighttime maximum. It is interesting that the disturbed days show a pronounced change over these years similar to that which occurs in the quiet days. Occurring over these years, it seems possible, as suggested for the 10 quiet days, that it may represent a change with the solar cycle. Moreover, occurring in the 5 disturbed days, it is unlikely that it has its origin in the inclusion as K material of some of the variability of the form and amplitude of the quiet-day daily variation of the field.

The universal-time component has an amplitude of the same order as that of the local-time component in this 5-disturbed-day data. The universal-time component is, however, subject to a statistical curvature effect because these days were selected on the basis of the Greenwich (UT) day. In the disturbed days, however, the curvature should be concave downward, opposite that for the quiet days. An estimate of this curvature in the 5-disturbed-day data was obtained for the months of June and September as samples. This was done in the same manner as for the 10 quiet days (q.v.). The six station samples of curvature were similar to one another for each of the 2 months. Averaged for each month, they gave the results shown in the lower left-hand portion of Figure 3. The standard deviations of these average values were computed from the six values of which each of the sixteen is the average. The largest standard deviation was 2.1 units in the interval from 0 to 3 hours for September. The dots used in the figure have a radius of approximately 2.5 units.

The monthly-average universal-time component, as derived from the original departures, minus the average curvature for June and September (that is, corrected approximately for curvature), is given in the main portion of Figure 3. A pronounced seasonal change of form is evident, roughly similar (though of greater amplitude) to that shown by all days [*Nicholson and Wulf*, 1955, 1958], in which no correction for curvature is necessary. The form near one solstice does not appear to be the negative of that near the other, although it might be approximately so described, and the form and amplitude of the average of the two sets of 4 solstitial months resemble those of the 4 equinoctial months, and thus also of the yearly average [see *McIntosh*, 1959]. This yearly average universal-time component—that is, the average of

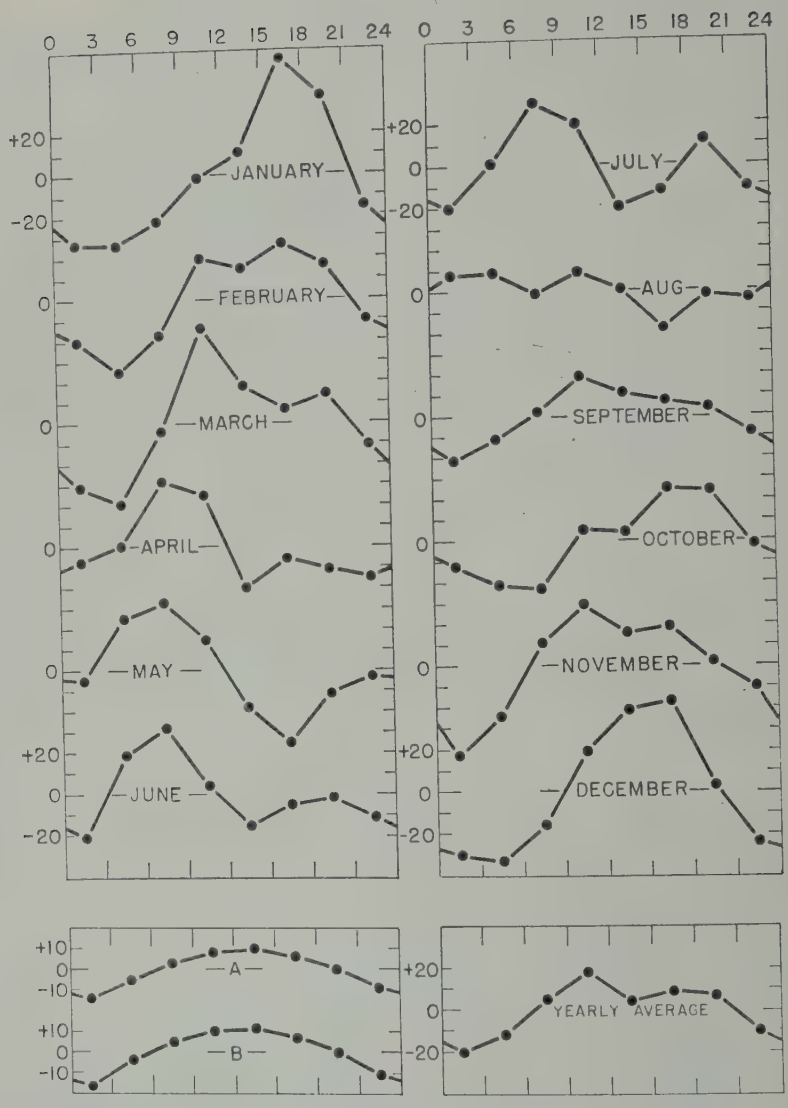


Fig. 3. Universal-time component of the diurnal variation of K, 1940–1948, for the 5 disturbed days of each month, corrected approximately for statistical curvature. A and B illustrate statistical curvature for June and September, respectively.

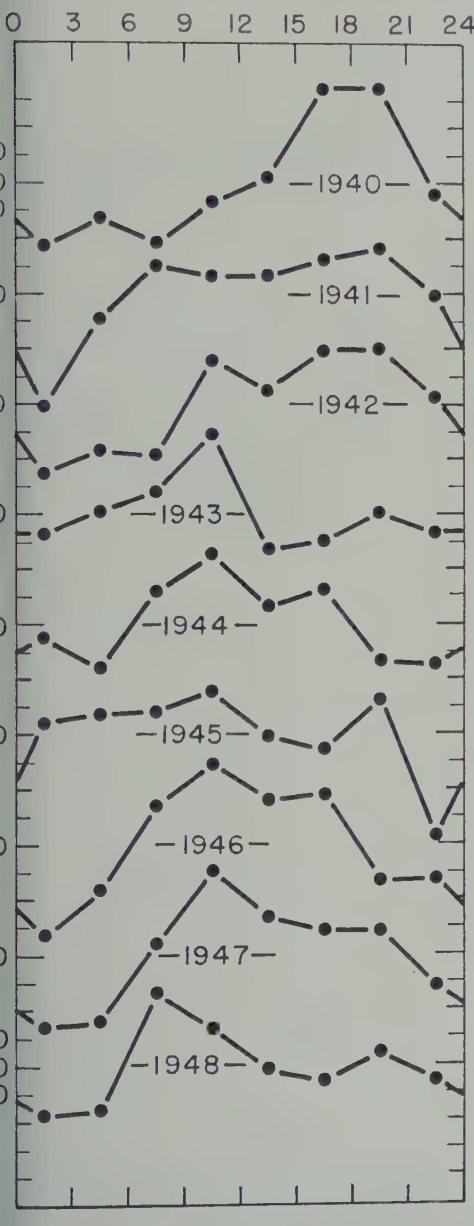
the twelve monthly curves of Figure 3—is shown in the lower right-hand portion of that figure.

When the yearly average universal-time component is computed for each year separately (and corrected approximately for curvature as above) the results shown in Figure 4 are obtained. A large variability of form from year to year is apparent. The variability seems to be, in considerable measure, random. This is striking when comparison is made with the corresponding curves for the local-time component in Figure 2, where a fairly regular change over th years is shown.

The average of the nine curves of Figur must, however, be the same as the averag the twelve monthly curves of Figure 3, g in the lower right-hand portion of that fig When the standard deviations of these e 9-year-average values are computed from nine values (Figure 4) of which each is average, the largest of these proves to be units (0.052 K) in both the intervals from

ours and from 18 to 21 hours. The mean of eight standard deviations is 4.3 units. The s used in the figure have a radius of approxtely 2.5 units.

he material of Figures 3 and 4 suggests that, the variability of the form of the yearly



g. 4. Yearly average universal-time compo- of the diurnal variation of K, 1940–1948, for 5 disturbed days of each month for each of 9 years, corrected approximately for statistical ature.

average universal-time component from year to year over these 9 years, apparently in large measure at random, there was nevertheless a persistent tendency for disturbance to be somewhat less at certain universal-time hours, such as in the interval from 0 to 3 hours than at other times, such as in the interval from 9 to 12 hours.

In the universal-time component for the 12 individual months shown in Figure 3, there is indication, in the average, of a somewhat smaller amplitude in the months of the June half of the year than in those of the December half, and possibly also a suggestion of some semidiurnal character in the June half of the year to a greater extent than in the December half. This brings to mind a circumstance concerning the distribution in longitude of the earth's magnetic field in the two hemispheres that seems of some interest here, although it may have no relation to the features of Figure 3 just mentioned. Owing to the large regional anomalies in the two hemispheres, the intensity of the field at the subsolar point (and at higher latitudes), as this point moves around a parallel of latitude, passes through two maxima during the course of a day near the June solstice, and the change of intensity is of smaller amplitude than near the December solstice, when the intensity of the field passes through but one maximum. In view of the possibility that winds in the ionosphere cutting the earth's magnetic field may contribute to geomagnetic disturbance, the above circumstance seemed worth mentioning.

Acknowledgment. The assistance of Miss Myrtle Richmond who helped with the computational work is gratefully acknowledged.

References

Howe, H. H., and E. K. Weisman, Geomagnetic indices K and C, 1948, *Bull. 12b,* Association of Terrestrial Magnetion and Electricity, International Union Geodesy and Geophysics, Washington, D. C., 1949.

Johnston, H. F., W. E. Scott, and E. Balsam, Geomagnetic indices C and K, 1940–1946, *Bull. 12;* 1947, *Bull. 12a;* Association of Terrestrial Magnetism and Electricity, International Union Geodesy and Geophysics, Washington, D. C., 1948.

Mayaud, P. M., Rapports scientifiques des Expeditions Polaires Francaises S IV 2, *Ann. geophys., 12,* 84–101, 1956.

McIntosh, D. H., On the annual variation of magnetic disturbance, *Phil. Trans. Roy. Soc. London, A, 251,* 525–552, 1959.

Nicholson, S. B., and O. R. Wulf, The diurnal variation of irregular geomagnetic fluctuations, *J. Geophys. Research, 60,* 389–394, 1955.

Nicholson, S. B., and O. R. Wulf, The diurnal variation of irregular geomagnetic fluctuations, II, *J. Geophys. Research, 63,* 803–806, 1958.

Nicholson, S. B., and O. R. Wulf, The diurnal variation of K indices of geomagnetic activity on quiet days in 1940–1948, *J. Geophys. Research, 66,* 1139–1144, 1961.

(Manuscript received May 12, 1961.)

On the Relation between the Spectrum of Turbulence and the Diabatic Wind Profile[1]

J. A. BUSINGER

Department of Meteorology and Climatology
University of Washington, Seattle

Abstract. A simple model of the spectrum of atmospheric turbulence using Kovasznay's transfer mechanism in wave-number space leads to a diabatic wind profile which fits the observations well and gives some insight into the origin of the rather large empirical coefficient in the interpolation formulas as given by Ellison, Yamamoto, and Panofsky and by Blackadar and McVehil.

Introduction. In recent studies on the diatic wind profile [*Ellison,* 1957; *Businger,* 59; *Yamamoto,* 1959; *Panofsky, Blackadar, d McVehil,* 1960] definite progress has been ade in the description of the unstable case. particularly good fit with the data was obned by *Panofsky, Blackadar, and McVehil* 960] using the expression

$$S^4 - \alpha\zeta S^3 - 1 = 0 \qquad (1)$$

ere

$$S = \frac{\kappa z}{u_*}\frac{\partial v}{\partial z},$$

limensionless wind gradient.

$$\zeta = \frac{g}{T}\frac{\partial T/\partial z + \Gamma}{\partial v/\partial z}\frac{\kappa z}{u_*},$$

limensionless height.

α = an empirical constant.
κ = Von Karman's constant.
z = height.
v = mean wind speed.
u_* = friction velocity.
g = acceleration due to gravity.
T = absolute temperature.
Γ^a = adiabatic lapse rate.

uation 1 is a consequence of *Ellison*'s [1957] eory and has been independently derived by *mamoto* [1959].

The theory is still incomplete because it does not predict the value of α. In fact the empirical value for this coefficient is surprisingly large, Panofsky, Blackadar, and McVehil found 18 and Yamamoto found 55 with a rather wide scatter around this figure. It was suggested [*Businger,* 1959; *Panofsky, Blackadar, and McVehil,* 1960] that α is the relative efficiency of the convective and mechanical energy sources. The reason why the convective energy source is much more efficient can possibly be found by analyzing the variance spectrum of the vertical wind component.

In this paper it will be shown that, with a simple model of the spectrum of turbulence based on Kolmogoroff's similarity hypothesis and *Kovasznay*'s [1948] transfer hypothesis of the decay of isotropic turbulence, an equation similar to (1) can be derived which will describe the diabatic profile equally well and will help to explain why the coefficient α is rather large.

The spectrum of turbulence and the diabatic wind profile. Under steady-state conditions, if the divergence of energy is neglected the equation of energy balance can be written as

$$u_*^2\frac{\partial v}{\partial z} + \frac{gH}{c_p\rho T} - D = 0 \qquad (2)$$

where H is the convective heat flux density and D is the dissipation rate of turbulent energy. The first term is the rate at which mechanical energy enters and the second term is the rate at which convective energy enters the reservoir of turbulent energy. (Note that the last term may be both positive and negative.)

The shape of the spectrum will depend on the distribution of the input over the wave num-

[1] Contribution 59, Department of Meteorology d Climatology, University of Washington, Seat-

bers, on the mechanism of the input, and on the mechanism of decay.

Our interest will be focused on the spectrum of the vertical velocity component, because the turbulent transfer processes in the surface layer are associated with this component. We assume that the mechanical energy enters the vertical component at one wave number k_m and that the convective energy enters at another, lower wave number k_c, whereby the ratio k_m/k_c is independent of height. The wave numbers k_m and k_c are different because the mechanical energy enters the turbulence in the horizontal velocity component. It requires some time before part of this energy is distributed over the vertical velocity component. The convective energy, however, enters the vertical velocity component directly; therefore we expect the convective energy to enter at a lower wave number than the mechanical energy.

To make our problem tractable we assume that as soon as the vertical velocity component is established the turbulence may be considered isotropic and that the transfer of energy $W(k)$ across a wave number depends only on the three-dimensional spectrum estimate $E(k)$ at the same wave number, which is Kovasznay's hypothesis. Although this hypothesis must be an oversimplification of the mechanism of decay as was shown by *Stewart and Townsend* [1951] results obtained with it by *Reid and Harr* [1959] are encouraging.

According to Kolmogoroff's similarity hypothesis we must have in the inertial subrang

$$W = Ak^{5/2}E^{3/2} \qquad (3$$

where A is a numerical constant.

For wave numbers in the inertial range large than k_m we have $W = D$, and for wave number in the range $k_c < k < k_m$ we have $W = gH/c_p\rho T$. Equations 2 and 3 determine the total turbulen energy, which can be expressed as

$$\int_0^\infty E\,dk = \frac{3}{2A^{2/3}}\left\{\left(\frac{gH}{c_p\rho T}\right)^{2/3}(k_c^{-2/3} - k_m^{-2/3}) + \left(\frac{gH}{c_p\rho T} + u_*^2\frac{\partial v}{\partial z}\right)^{2/3}k_m^{-2/3}\right\} \qquad (4$$

We assume that the eddies contribute to th turbulent transfer in proportion to their ow scale or inversely in proportion to their wav number. This suggests that we have for th coefficient of turbulent transfer, K, the followin proportionality

$$K^2 \propto \int_0^\infty \frac{E}{k^2}\,dk \qquad (5$$

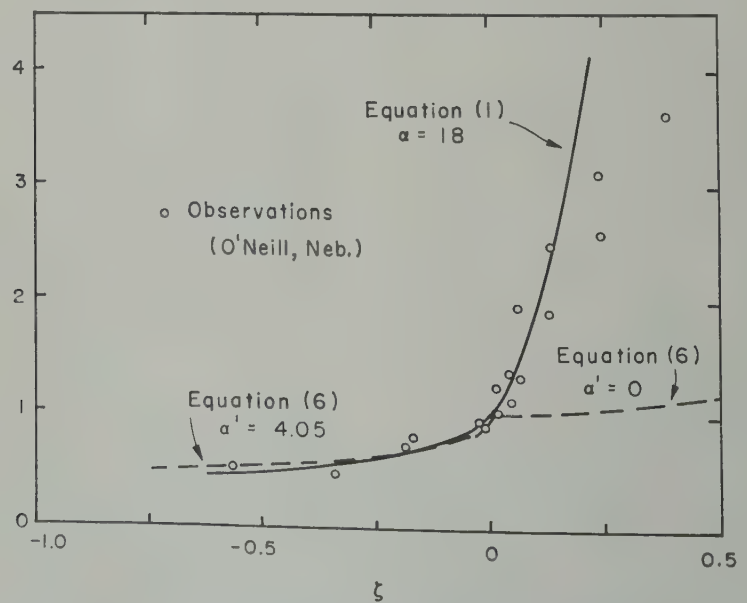
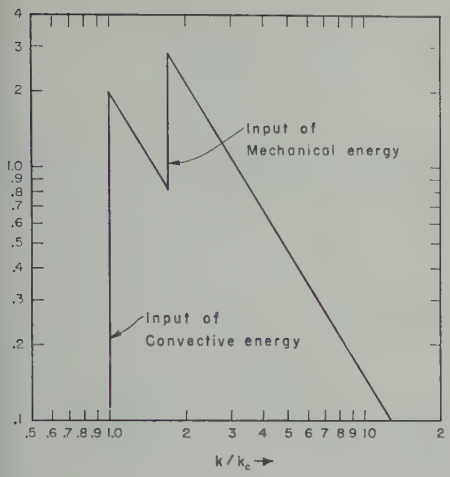


Fig. 1. Comparison between equations 1 and 6 and observations from O'Neill [see *Panofsky, Blackadar, and McVehil*, 1960].



g. 2. The three-dimensional isotropic model rum for equal rates of energy input from the ective and mechanical sources (i.e., K_H/K_M = —1).

use the variance of the vertical velocity ponent is proportional to the turbulent gy when the turbulence is isotropic. Eval- g the right-hand side of (5) and then sting the proportionality to come out cor- y in the neutral case, we find for the diabatic profile

$$-R_f^{2/3}[(km/k_c)^{8/3} - 1] + (-R_f + 1)^{2/3}\} = 1 \qquad (6)$$

e $R_f \equiv (K_H/K_M)$ Ri $= (K_H/K_M)\ \zeta/S$. tion 6 is the main result of this paper. ough the form of this equation differs from a comparison between the two equations is ble. The factor $K_H/K_M\ \{(k_m/k_c)^{8/3} - 1\} \equiv$ (6) plays a similar role as α in (1). With = 1.7 and $K_H/K_M = 1.3$ (i.e. $\alpha' = 4.05$), tion 6 gives as good a description of the as equation 1 (see Fig. 1). So far, not much imental evidence has been collected con- ng the ratio k_m/k_c. The value of 1.7, however, s quite reasonable with respect to the vational material presented by *Panofsky McCormick* [1960]. At the same time, this t indicates why in the interpolation formula large value of α is required.

the stable range the model of the spectrum no longer applies, because in this case ective energy leaves the reservoir of turbu- energy and only mechanical energy is ied. The convective energy loss can take place only from eddies that contain energy, i.e. from wave numbers equal to or larger than k_m. Therefore we might expect that the ratio of k_m/k_c decreases. Also the value of the turbulent Prandtl number seems to decrease with increasing stability. These two effects lead to a reduction of the coefficient α'. The observations in the stable range show considerable scatter and make it difficult to decide what the actual value of α' should be. The difficulty is probably caused by the fact that it takes a long time to establish steady conditions with a stable stratification because the turbulent transfer is greatly reduced. It may even be that the steady state of u_* and H constant with height is never reached in the surface layer. Observations from the polar regions may be valuable in this respect.

Equation 6 leads to the following expressions for momentum and heat transfer:

$$u_*^2 = \left(\kappa z \frac{\partial v}{\partial z}\right)^2 \left\{-R_f^{2/3}\left[\left(\frac{k_m}{k_c}\right)^{8/3} - 1\right] + (1 - R_f)^{2/3}\right\}^{3/4} \qquad (7)$$

and

$$H = -(\kappa z)^2 \frac{\partial v}{\partial z}\left(\frac{\partial T}{\partial z} + \Gamma\right)\frac{K_H}{K_M} \left\{-R_f^{2/3}\left[\left(\frac{k_m}{k_c}\right)^{8/3} - 1\right] + (1 - R_f)^{2/3}\right\}^{3/4} \qquad (8)$$

These equations may be tested against observations.

Discussion. The model of the spectrum presented here is an oversimplification. The energy does not enter at one particular wave number but probably enters in a random fashion around that wave number. Furthermore, the turbulence is definitely not isotropic in the range where the energy enters. It is because of our lack of ability to handle a more realistic turbulent model that we resorted to the very simple model sketched above. We believe, however, that the macroscopic results indicate promise for this line of research.

It is tempting to speculate a little further on the implications of the model with respect to the spectrum of the vertical velocity, because many observations of this spectrum have been made. *Panofsky and McCormick* [1960] give a

valuable summary of the observations and a semiempirical formula of the vertical velocity spectrum.

Our model spectrum is strictly a three-dimensional isotropic spectrum; its shape is illustrated in Figure 2. The vertical velocity spectrum $\Phi_w(k)$ is strictly a transversal spectrum and is related to the isotropic three-dimensional spectrum by the relation [see *Batchelor*, 1953, p. 50].

$$\Phi_w(k) = \tfrac{1}{4}\int_k^\infty \left(1 + \frac{k^2}{k'^2}\right)\frac{E(k')}{k'}\,dk' \qquad (9)$$

Working this out for our model spectrum in Figure 2 we obtain

$$\Phi_w(k) = 0.218\left(\frac{D}{A}\right)^{2/3} k^{-5/3} \quad \text{for} \quad k > k_m$$

$$\Phi_w(k) = 0.218\left(\frac{gH}{c_p\rho T A}\right)^{2/3} k^{-5/3} + \frac{3}{44}\left[\frac{u_*^{\,2}\dfrac{\partial u}{\partial z}}{A}\right]^{2/3} k^2 k_m^{-11/3} + \frac{3}{20}\left[\frac{u_*^{\,2}\dfrac{\partial u}{\partial z}}{A}\right]^{2/3} k^{-5/3} \quad \text{for} \quad k_c < k < k_m$$

$$\Phi_w(k) = \frac{3}{20}\left(\frac{gH}{c_p\rho T A}\right)^{2/3} k_c^{-5/3} + \frac{3}{20}\left[\frac{u_*^{\,2}\dfrac{\partial v}{\partial z}}{A}\right]^{2/3} k_m^{-5/3} + \frac{3}{44}k^2\left\{\left[\frac{u_*^{\,2}\dfrac{\partial u}{\partial z}}{A}\right]^{2/3} k_m^{-11/3} + \left(\frac{gH}{c_p\rho T A}\right)^{2/3} k_c^{-11/3}\right\} \quad \text{for} \quad k <$$

This spectrum, when multiplied by k, is co parable to the spectra plotted by Panofsky a McCormick (see Fig. 3).

The discontinuities in the spectra are a c sequence of the assumption that all the r chanical energy enters at k_m and all the c vective energy at k_c. This will not be the ca and when we assume that the energies en in a random fashion around the respective w numbers, k_m and k_c, the model spectrum will show any discontinuities and may be of the fo indicated by the broken lines in Figure 3. similarity between these curves and the served curves by Panofsky and McCormick

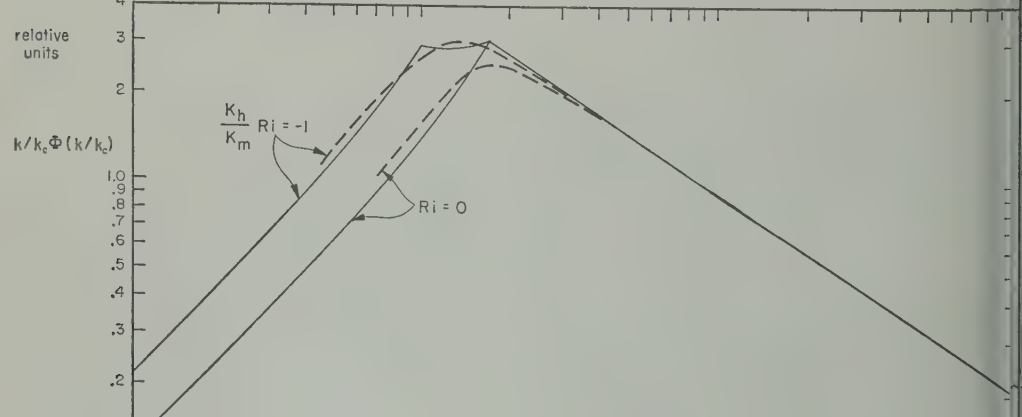


Fig. 3. Solid lines: The spectrum of the vertical velocity derived from the model spectrum in Figure 2 for Ri = 0 and (K_H/K_M) Ri = −1. The total energy input in both cases is the same. Broken lines: Possible shape of the spectra when a random energy input distribution exists around wave numbers k_m and k_c. Although the energy input in the neutral and unstable case is the same, the maximum will be higher and at lower wave number for the unstable case.

stive. It was thought, however, that trying roduce a specific random model generating mooth curves in Figure 3 would be too lative.

cnowledgment. This research was supported t by the Office of Naval Research under proj- 7 252, contract Nonr 477(24).

References

elor, G. K., *The Theory of Homogeneous rbulence,* Cambridge University Press, 197 , 1953.

ger, J. A., A generalization of the mixing- gth concept, *J. Meteorol., 16,* 516–523, 1959.

n, T. H., Turbulent transport of heat and mentum from an infinite rough plane, *J. Fluid ch., 2,* 456, 1957.

sznay, L. S. G., The spectrum of locally isotropic turbulence, *J. Aeronaut. Sci., 15,* 745–753, 1948.

Panofsky, H. A., A. K. Blackadar, and G. E. McVehil, The diabatic wind profile, *Quart. J. Roy. Meteorol. Soc., 86,* 390–398, 1960.

Panofsky, H. A., and R. A. McCormick, The spectrum of vertical velocity near the surface, *Quart. J. Roy. Meteorol. Soc., 86.,* 495–503, 1960.

Reid, W. H., and D. L. Harris, Similarity spectra in isotropic turbulence, *Phys. Fluids, 2,* 139–146, 1959.

Stewart, R. W., and A. A. Townsend, Similarity and self-preservation in isotropic turbulence, *Phil. Trans. Roy. Soc. London A., 243,* 359–386, 1951.

Yamamoto, G., Theory of turbulent transfer in non-neutral conditions, *J. Meteorol. Soc. Japan, 37,* 60–70, 1959.

(Manuscript received February 4, 1961; revised May 10, 1961.)

Some Evidence on the Effect of Nonlinearity on the Position of the Equilibrium Range in Wind-Wave Spectra[1]

BLAIR KINSMAN

Chesapeake Bay Institute, Johns Hopkins University
Baltimore, Maryland

Abstract. Measurements of spectra at short fetches and low wind speeds suggest that nonlinear effects with preferred frequencies may be present. If this be true, the range of frequencies immediately above the energy peak can not be an equilibrium range describable by a single unique power law.

n the study of turbulence the concept of an ilibrium range in the spectrum has been veloped from a consideration of the effects of nonlinear terms in the equation of motion g. 1). For any part of the spectrum to be in tistical equilibrium, the interactions transring energy from wave number to wave mber must have a time scale very much less n the decay time of the turbulence. This dition rules out an equilibrium range in the inity of the wave number of maximum energy, and requires that k_0, k, and k_η be separated several decades. Dimensional argument then ws $E(k) \sim k^{-5/3}$ in the inertial subrange *nze*, 1959]. Measurements by *Grant, Stewart, l Moilliet* [1960] in the Seymour Narrows, C., show good agreement with this expected avior.

n the study of surface waves, a similar cept had its genesis in an effort to explain a ularity found in wave spectra measured by *rling* [1959]. Figure 2 shows measured spectra ich, while divergent at low frequencies, all lie hin a narrow power band above 0.8 cps. e trend of the band is well described by a ver law of the form $P \sim f^{-5}$. This behavior of wave spectra led to the suspicion that, like bulence spectra, wave spectra might also have equilibrium range. *Phillips* [1958], from a sideration of the limiting configuration of face waves, showed that an equilibrium range y well exist, and by dimensional argument he ived a -5 power law for it. The range of

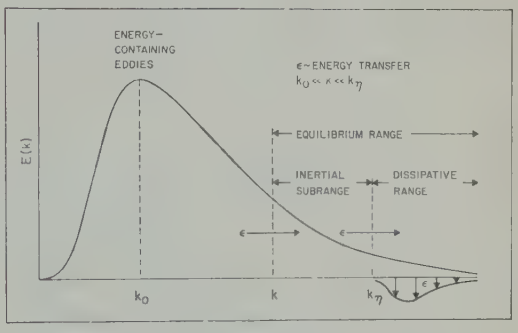


Fig. 1. Schematic turbulence spectrum.

wave numbers or frequencies in which an equilibrium range could be expected was not established, but *Pierson* [1959] offered evidence that in sharply peaked spectra it could not begin at less then twice the frequency of the major power peak. This warning seems to have been generally overlooked, and in attempts to find a universal unique power law averages of spectra have been used as soon after the power peak as the dispersions become small.

In July and November 1958, field measurements of wind waves at short fetches and low wind speeds were made [*Kinsman*, 1960]. Figure 3 shows the average of 8 spectra computed from the July records, and Figure 4 shows the average of 16 spectra computed from the November records. The mean winds during the recording periods ranged from 3.88 to 8.20 m/sec; the fetches ranged from 1700 to 3000 meters. The frequencies at which maximum power occurs range from 0.55 to 0.8 cps. Both figures show the same characteristic compression of scatter at

[1] Contribution 55 of the Chesapeake Bay Institute.

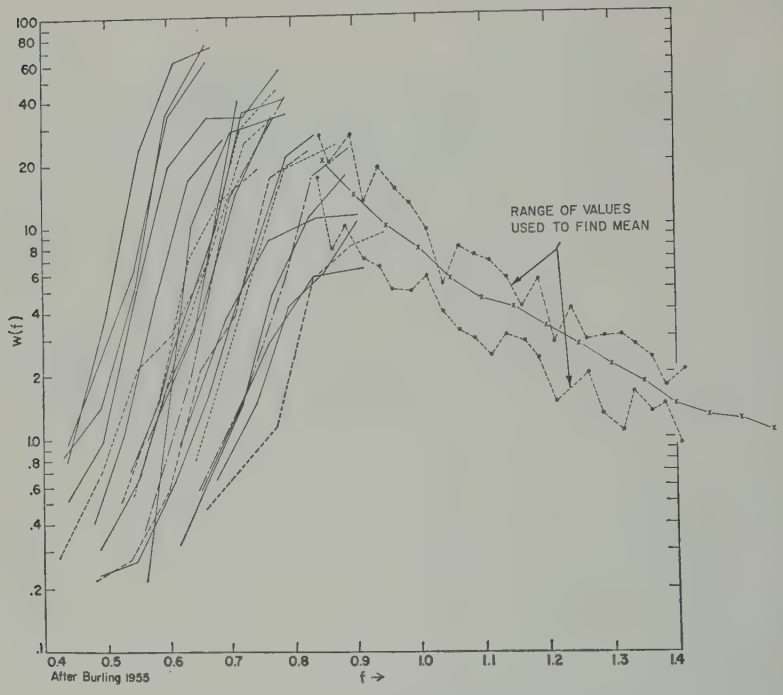


Fig. 2. Wave spectra measured by Burling.

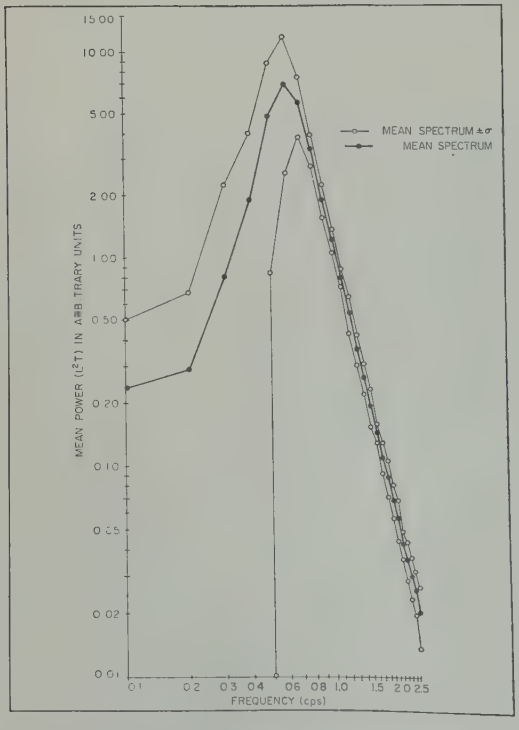


Fig. 3. Mean of 8 measured wave spectra.

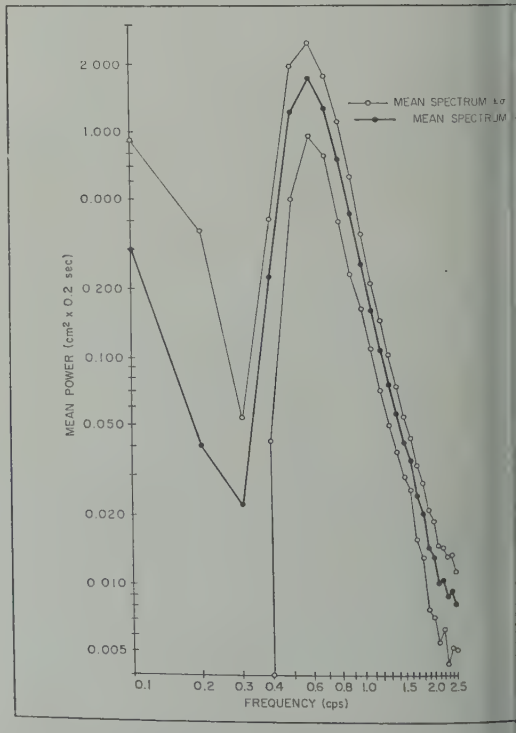
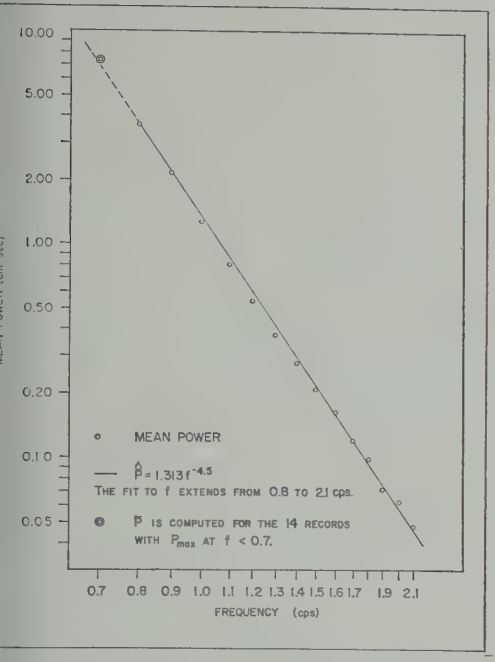


Fig. 4. Mean of 16 measured wave spectra.



. 5. Best-fit line 0.8 to 2.1 cps to the mean of the 24 wave spectra of Figures 3 and 4.

her frequencies as do Burling's results. How-r, for these records the best-fit straight line h a simple power dependence is $P \sim f^{-4.5}$ g. 5).

Similar computations by *Hicks* [1960] on his n data and on data by Cox gives $P \sim f^{-4.7 \pm 0.5}$ l $P \sim f^{-5.5}$. An extrapolation of the Neumann ctrum gives $P \sim f^{-6}$.

Consideration of the details of the spectra at quencies immediately above the peak power gests that argument about the agreement or agreement of the power laws is not an argu-nt about physical reality. Figure 6 shows a ical spectrum from the sets used to form the rages shown in Figures 3, 4, and 5. It appears be quite narrow and Pierson's warning may l apply. If a smooth curve were faired through points above 0.6 cps, there would seem to be light excess of power in the vicinity of the ble frequency, i.e., at 1.2 cps. These features characteristic of all the spectra.

f we make a log-log plot of the individual ctrum for frequencies greater than 0.7 cps g. 7), the smooth appearance of the mean ctrum is replaced by a series of energy excesses ced along a line whose trend might be a .5, −5.0, or −5.5 power law depending upon one's feeling about it. Again, this is characteristic of all the spectra.

TABLE 1. Positions of Energy Excesses Relative to the Position of the Maximum Energy for 14 Spectra

Record	f_1/f_{max}	f_2/f_{max}	f_3/f_{max}	f_4/f_{max}	f_5/f_{max}
067	1.48		2.08	2.54	3.08
068		1.84	2.38	2.69	3.23
069	1.45	1.73	2.18	2.73	3.64
070		1.82	2.09	2.82	3.18
075		1.91	2.36	2.82	3.45
076	1.45	1.91	2.36	2.73	3.00
081		1.67	2.25	2.58	3.50
082	1.23	1.53	2.08	2.77	3.00
083	1.25	1.83	2.33	2.67	3.00
084		1.92	2.46	2.69	3.00
085	1.45	1.82	2.36	2.64	3.27
086	1.36	1.73	2.27	2.64	3.00
093	1.42	1.67	2.00	2.58	2.92
094	1.25	1.92	2.42	2.75	3.08
Mean	1.37	1.79	2.26	2.69	3.17
σ	0.11	0.15	0.12	0.06	0.18

Nonlinear effects have been incorporated in two recent studies: *Tick* [1959] and *Phillips* [1960]. Although they are widely divergent in approach, they have one common result. Both indicate that energy will be transferred from the region of maximum energy to a preferred higher frequency or frequencies. Tick locates it at a frequency somewhat greater than double the frequency of the principal power peak. Phillips suggests a series of frequencies which includes the double frequency. It seems likely that preferred frequencies for energy relocation will be a feature of any study which includes nonlinear effects.

Sixteen of the November records were analyzed at a high resolution so that an estimate could be made of the frequencies at which excess energy occurred. Two of these records were rejected because they contained evidence of motorboat wakes. The results for the remaining 14 records are shown in Table 1. The values have been scaled in each case by the frequency at which the maximum power occurred. They show very little dispersion, and the means agree within about 5 per cent with the sequence of frequencies derived by Phillips, only excepting the value 2.26 for the double frequency which disagrees by 13 per cent. The double frequency is thus more nearly where it would be expected according to Tick.

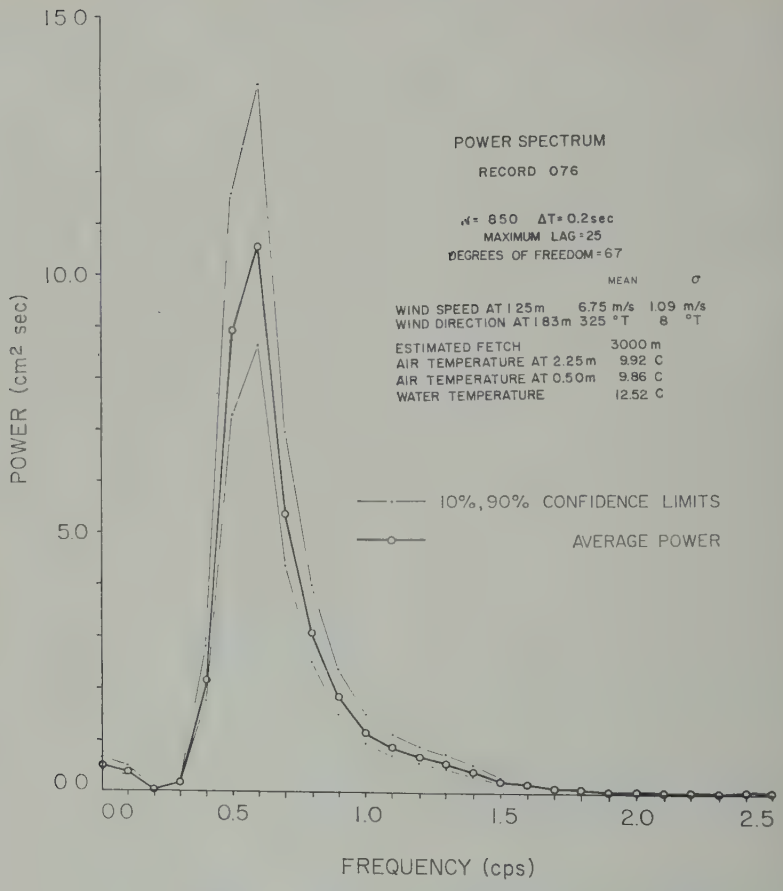
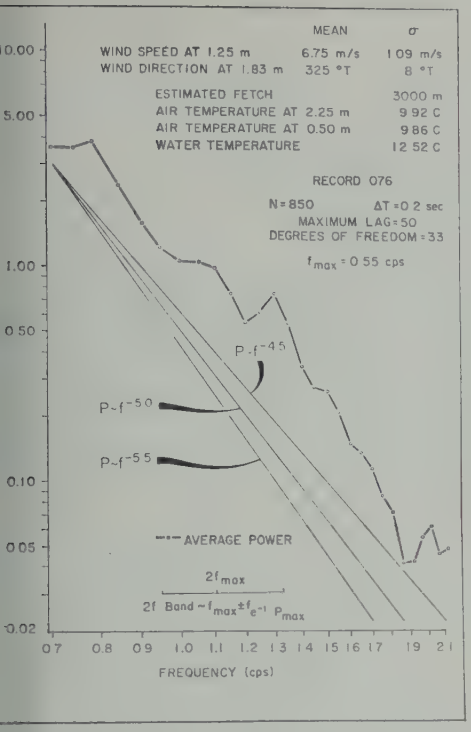


Fig. 6. A typical wave spectrum.

The values in Table 1 prove nothing, since the survey was not designed specifically to establish them. They are statistically submarginal; they are suggestive because they are persistent.

If the effect of nonlinearity is to accumulate energy selectively, then an equilibrium range in any reasonable meaning of the term is not to be expected at less than the double frequency. It might almost be anticipated that we should look much farther out by analogy with turbulence, in which a separation of decades is required. Whatever their source, each individual spectrum is marked by a regular sequence of energy excesses. It is trivially obvious that only a little injudicious averaging of spectra like these, wi their peak powers at different frequencies, ma produce the observed variations in the power la

Since the emperor wears no clothes, it useless to discuss their cut and quality. It appea that no measured wave spectra have be carried over a large enough frequency band wi enough precision to exhibit the equilibriu range. The frequency range presently availab for study is one in which small selective effec may be expected to appear. Instead of smotheri these selective effects in indiscriminate average it would be well to determine them with so precision.



7. Log-log plot 0.7 to 2.1 cps of the wave spectrum of Figure 6.

References

Burling, R. W., The spectrum of waves at short fetches, *Deut. Hydrograph Z., 12,* 2, 1959.

Grant, H. L., R. W. Stewart, and A. Moilliet, Turbulence measurements in inshore waters, *Pacific Naval Laboratory, Esquimalt, B. C. Report 60—8,* 1960.

Hicks, B. L., The generation of small water waves by the wind, 1, Comparison of data from different sources, *Coordinated Science Laboratory, Rept. M86,* University of Illinois, Urbana, Ill., January, 1960.

Hinze, J. O., *Turbulence,* McGraw-Hill Book Co., N .Y., 1959.

Kinsman, B., Surface waves at short fetches and low wind speeds—a field study, *Chesapeake Bay Inst. Tech Rept. 19 Reference 60–1,* 1960.

Phillips, O. M., The equilibrium range in the spectrum of wind-generated waves, *J. Fluid Mech., 4,* 426–434, 1958.

Phillips, O. M., On the dynamics of finite amplitude unsteady gravity waves, 1, The elementary interactions, *J. Fluid Mech., 9,* 193–217, 1960.

Pierson, W. J., Jr., A note on the growth of the spectrum of wind-generated gravity waves as determined by non-linear considerations, *J. Geophys. Research, 64,* 1007–1011, 1959.

Tick, J. L., A non-linear random model of gravity waves, 1, *J. Math. and Mech., 8,* 5, 1959.

(Manuscript received April 12, 1961.)

Net Precipitation in a Northern Hardwood Forest

RAYMOND E. LEONARD

Laconia Research Center
Northeastern Forest Experiment Station
Laconia, New Hampshire

Abstract. The two components of net precipitation, throughfall and stemflow, were measured during two summer leaf periods in the White Mountains of New Hampshire. Throughfall was caught in roving gages located at predetermined, randomly selected points. Stemflow was measured on two randomly located groups of trees. Regression equations were developed for a comparison of throughfall with gross rainfall. Throughfall accounted for 82 per cent of the gross rainfall. Strong differences in amounts of stemflow were found between various hardwood species. Stemflow values ranged from 1 per cent of gross rainfall for a storm of 0.07 inch to 6 per cent for a storm of 1.00 inch; the mean value was 5 per cent.

INTRODUCTION

1955, the Hubbard Brook Experimental st was established in the White Mountains lew Hampshire as the center for a forest rshed management research project of the heastern Forest Experiment Station, U. S. st Service. Shortly thereafter, a search of literature on interception was made for ination applicable to this area. No useful data found. Accordingly, the study described in paper was made as a basis for estimating ception losses from an uneven-aged northhardwood forest. It was conducted during wo summers of 1958 and 1959.

Interception is commonly defined as that portion of rain that is caught by the tree and returned to the atmosphere by evaporation. The rain that is not caught by the tree is called *net rainfall.* Most of the net rainfall reaches the ground by filtering through the canopy as *throughfall;* a smaller part runs down the tree stems as *stemflow.*

Interception by a forest canopy cannot be measured directly but may be arrived at by subtracting net rainfall from gross rainfall. In this study, net rainfall was determined by measuring its components: throughfall and stemflow.

Net rainfall reaching the ground under a for-



Fig. 1. A representative forest stand with storage drums used for stemflow studies.



Fig. 2. Representative forest canopy above throughfall gage. (Note multilayered structure and few openings.)

est canopy has been studied by a number of investigators. Results from early research were summarized by *Horton* [1919] and *Kittredge* [1948]. A more recent review of the literature was presented by *Delfs* [1955].

Study Area

The study at Hubbard Brook Forest was conducted on a southeastern aspect with a slope of about 15 per cent and an elevation of 1500 feet. Here the average annual precipitation is about 50 inches, of which about 30 inches falls during the growing season or leaf period. Mean summer temperatures are 75°F; winds are predominantly from the west.

The forest stands, harvested about 50 years ago, are classified as uneven-aged northern hardwoods. About one-half of the trees are American beech and one-third are sugar maple. The crown canopy was between 85 and 98 per cent close Figures 1 and 2 illustrate the forest stand a canopy conditions.

Methods of Study

Three ½-acre plots were located in a fore having generally similar stand conditions; sp cies and stand characteristics are given in Tab 1. The three plots, 500 feet apart, were su divided into 10-foot grid squares.

Throughfall was caught in five rain gages the standard Weather Bureau type. The gag were placed on the ground in the center of fi grid squares randomly selected in each of t plots. These gages were moved to a new set randomly selected points after a rainfall of 0 inch or more (measured in the open).

Stemflow was measured in two randomly lected groups of trees located between t throughfall plots. In all there were 37 trees: c group on 1/20 acre contained 15 trees and t other on 1/10 acre had 22 trees. These tre with diameters ranging from 1.0 to 14.7 inch included all major species common to the area

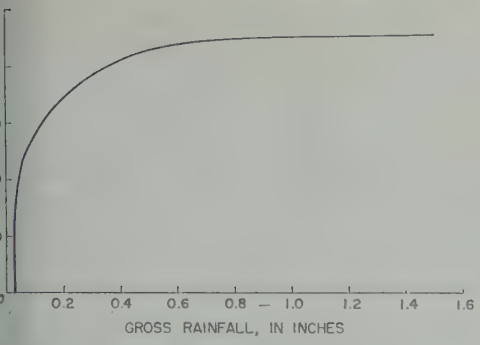
All 37 trees were equipped with zinc coll projecting 0.75 inch from the tree trunk. watertight junction of the collar with the t was made with roofing cement. Water flowi from the collars on the larger trees was caug in 55-gallon drums and measured volumetrica Stemflow from the smaller trees was caught 5-gallon cans and weighed on a spring scale.

Rainfall in the open—gross rainfall—was termined by averaging measurements obtain in four openings located within 1000 feet of t plots. Three of the openings contained one sta

TABLE 1. Tree Cover on Plots Projected to an Acre Basis

Plot	Number of Trees	Basal Area			Species Composition,* per cent			
		Total, ft²	By Diameter Classes, per cent		Beech	Sugar Maple	Yellow Birch	Miscell neous
			1–10 in.	11+ in.				
1	668	143	53	47	51	25	16	8
2	590	132	49	51	56	18	12	14
3	724	129	77	23	40	41	12	7
Average	660	135	60	40	49	29	13	9

* Based on the number of trees per acre.



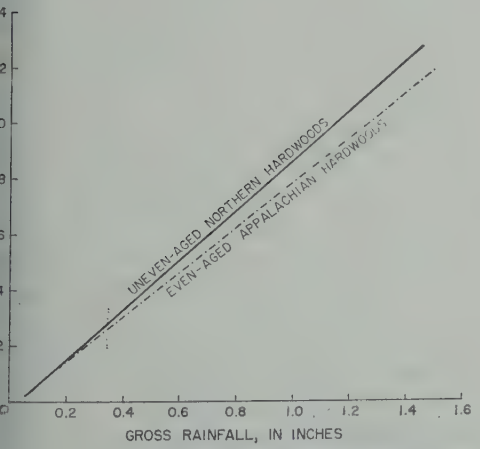
g. 3. The relationship between throughfall gross rainfall; throughfall is expressed as a entage of gross rainfall.

rain gage each; a recording rain gage was ed in the fourth clearing. Measurements of s rainfall, throughfall, and stemflow were le after each storm. (For this study, a storm defined as any period of rainfall followed 6 hours of clear weather.)

Results

hroughfall. Throughfall measurements from three plots for 34 storms were tested by ariance analysis to determine whether dif- nces in the plots influenced throughfall. No ificant difference was found in throughfall veen the three plots. Because of this, through- data for the three plots were grouped, and a mon regression equation was developed for ughfall on gross rainfall:

$$\hat{Y} = 0.8984X - 0.030 \qquad (1)$$



4. The relationship between throughfall and gross rainfall for two types of forest.

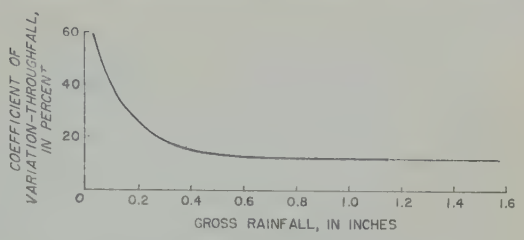


Fig. 5. The relationship between coefficients of variation of throughfall and gross rainfall.

where $\hat{Y}$ is throughfall, X is gross rainfall and the standard error of estimate is ± 0.03.

Throughfall plotted as a percentage of gross rainfall is presented in Figure 3. From this curve it may be observed that percentage of throughfall is fairly constant for storms greater than 0.80-inch depth.

Throughfall–gross rainfall regressions obtained from this study were similar to a regression developed for a 50-year-old, fully stocked, even-aged Appalachian hardwood forest in West Virginia [*Trimble and Weitzman,* 1954] (Fig. 4).

During the course of this study, considerable variation in catch among the five gages in each of the plots was noticed. For example, throughfall ranging from 1.05 to 1.73 inches was recorded for a storm totaling 1.47 inches of gross rainfall. Relatively larger variations were noted in lighter storms. Throughfall measurements varying from 0.06 to 0.18 inch were found under the canopy for a storm of 0.16-inch gross rainfall.

To investigate this, 216 one-quart cans were placed at random throughout the three plots. Measurements of canopy closure over each point were taken with a spherical densiometer [*Lemon,* 1957] and a Weston illumination meter, model

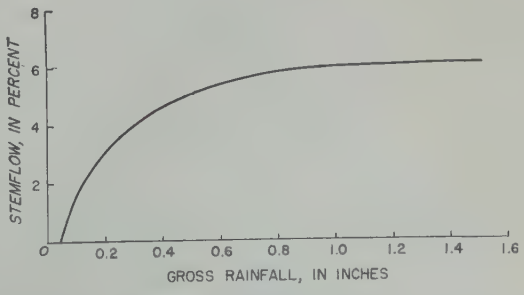


Fig. 6. The relationship between stemflow and gross rainfall; stemflow is expressed as a percentage of gross rainfall.

756. Little correlation was found between canopy-density measurements and throughfall.

The conventional methods of measuring tree canopy density—for example, spherical densiometer, photographs, and light meters—are based on resolving the total space occupied by the leaves into one plane. However, in passing through the canopy, rain can be influenced by any number of obstructions in its fall to the ground: throughfall passes through a canopy of three dimensions.

A further reason for the lack of correlation between canopy-density measurements and amounts of throughfall is that the photographs, densiometer, and light-meter readings taken above the gage resolve the canopy density from a cone-shaped space. However, rainfall caught in the gage may or may not come from a cone-shaped space. Even a few small leaves just above the gage may greatly influence the amount of rain caught; such a diverse leaf arrangement is shown in Figure 2.

Throughfall not only varied greatly from point to point but also it was seldom consistently higher or lower at a given point than averages for all gages.

Coefficients of variation of throughfall were calculated for a selected range of storms. Data from 216 measurements per storm for 8 storms are presented in Figure 5. This curve illustrates that throughfall variation is essentially uniform throughout the forest for storms of 0.50 inch or greater.

Stemflow. Stemflow from 20 storms ranging in size from 0.07 to 1.47 inches of gross rain was measured on the two groups totalling trees.

Area-inches of stemflow were computed adding all stemflow in cubic inches collec from the two groups of trees for each storm a dividing this total by the area bounded by vertical projection of the canopy edge of two groups.

The results of stemflow expressed as a p centage of gross rainfall are given in Figure It appears that, once rainfall in the open reach 0.80 inch, stemflow expressed as a percentage gross rainfall tapers off and does not incre much beyond 6 per cent.

Stemflow was found to be a linear funct of the amount of gross rainfall per storm. regression equation was developed for ar inches of stemflow on gross rainfall:

$$\hat{Y} = 0.0563X - 0.0024$$

where $\hat{Y}$ is area inches of stemflow, X is gr rainfall, and the standard error of estimate ± 0.007.

Net rainfall, throughfall, and stemflow in lation to gross rainfall are given in Figure 7

Although amounts of stemflow are small re tive to net rainfall (Fig. 7), they are not ins nificant. Stemflow from a 10-inch (d.b.h.) bee tree during a 1.00-inch storm amounted to gallons of water. According to *Voigt* [1960] v ter accumulated from stemflow was found to concentrated at the base of tree trunks wit approximately 1 foot of the tree. If we assu this to be our area, 30 gallons of water from 10-inch beech will equal 7.4 inches depth of ra 7.4 times the depth of gross rainfall.

This concept of stemflow is of hydrologic a biologic importance. Water running down bole of the tree may follow roots into the [*Voigt,* 1960] and thus expedite soil moist recharge. *Stout* [1956] found that tree roots f quently terminate in a mass of fine rootlets s rounding and lying at the base of neighbor trees. This suggests that after storms the c centrations of stemflow at tree bases may se as sources of water for roots of adjoining tr

Striking differences in amounts of stemf were found among various species. In all ca the American beech had the greatest amount water running down its smooth-barked st

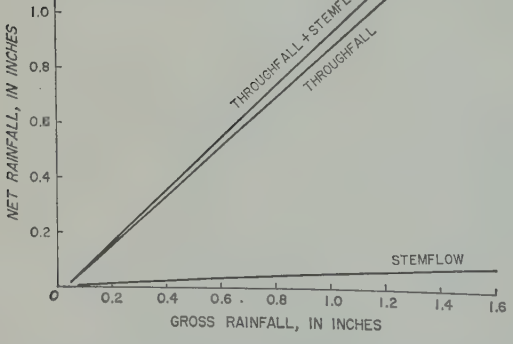


Fig. 7. The relationship between net rainfall (throughfall plus stemflow), throughfall, and stemflow to gross rainfall.

n average, only two-thirds as much water d down the rough-barked sugar maple as down beech trees. Stemflow on curly-barked w birch trees averaged about one-half the unt measured on beech of comparable size. sitions of the individual tree canopies above below the surrounding forest canopy had a ed effect on the amount of stemflow col-d. It was not uncommon for a tree with a n protruding above the surrounding forest ave 30 to 50 per cent more water running its stem than a tree of the same species similar diameter but in the same plane as surrounding forest canopy. Leaning trees had a greater amount of stemflow than ght trees of the same species with similar eter and height because their stems pre-a greater horizontal surface area to falling pitation.

t precipitation. The equation for estimat-he net precipitation under an uneven-aged nern hardwood forest as studied is:

$$\hat{Y} = 0.9547X - 0.0324 \qquad (3)$$

e $\hat{Y}$ is net precipitation and X is gross all.

easurable rainfall did not filter through the by for storms of less than 0.03 inch. Stem-was not measurable for storms of less than inch. Therefore, for rainfalls between 0.03 0.05 inch, only the throughfall equation (1) d be used. The combined stemflow-through-(net precipitation) equation (3) is applic-to storms greater than 0.05 inch.

nen computing net precipitation under the canopy, it must be considered that the data in this study are based on individual storms as measured in the open. As an example, four rains of 0.25-inch depth in the open would each deposit 0.21 inch or a total of 0.84 inch of water on the forest floor; whereas a single rain of 1.00 inch measured in the open would deposit 0.92 inch of water on the forest floor.

In summarizing the data from two summers' observations it was found that net precipitation —throughfall plus stemflow—averaged 87 per cent of the gross rainfall measured in the open, of which 82 per cent was throughfall and 5 per cent was stemflow.

References

Delfs, J., Die Niederschlagszurückhaltung im Walde (Interception of precipitation in the forest), *Mitt. Arb Kreis Wald u. Wasser, Koblenz,* no. 2, 1955.

Horton, R. E., Rainfall interception, *Monthly Weather Rev., 47,* 603–623, 1919.

Kittredge, J., *Forest Influences,* McGraw-Hill Book Co., New York, 394 pp., 1948.

Lemon, P. E., A new instrument for measuring forest overstory density, *J. Forestry, 55,* 667–669, 1957.

Stout, B. B., Studies of the root system of deciduous trees, *Black Rock Forest Bull. 15,* 1–45, 1956.

Trimble, G. R., Jr., and S. Weitzman, Effect of a hardwood forest canopy on rainfall intensities, *Trans. Am. Geophys. Union, 35,* 226–234, 1954.

Voigt, G. K., Distribution of rainfall under forest stands, *Forest Sci., 6,* 2–9, 1960.

(Manuscript received December 16, 1960; revised April 14, 1961; presented at the Forty-first Annual Meeting of the American Geophysical Union, Washington, D. C., April 1960.)

Projecting the Effect of Changed Stream Stages on the Water Table

J. E. REED AND M. S. BEDINGER

U. S. Geological Survey, Little Rock, Arkansas

Abstract. The position and shape of the water table under certain conditions may be considered to be the sum of two components of head, namely, the boundary component and the accretion component. In an aquifer of given hydraulic characteristics, the boundary component of head is determined by the stream stage and areal shape of the aquifer; the accretion component of head is determined by vertical gain or loss of water to the aquifer and by the areal shape of the aquifer. The boundary component may be obtained by electric-analog methods. By subtracting the boundary component from the observed position of the water table, the accretion component can be obtained. A change in river stage imposes a new boundary component on the system. The effect of changed stream stages on the water table may be obtained by adding the accretion component to a new boundary component caused by changed stream stages.

ntroduction. The construction of dams for droelectric power, flood control, and naviga- n inevitably produces certain changes in the draulic regimen of streams. Many of these nges are predictable, and subsequently can seen and measured. Less apparent, although as inevitable, are changes that occur in und-water reservoirs with which the streams hydraulically connected. An analogy may drawn between the relationship of the streams sea level or the reservoir level behind a dam ch are the effective base levels of the streams, that of an aquifer and a stream, which may be considered to act as a base level for the water table. Changes in the water table reflect changes in stream stage in a manner similar to that in which changes in stream stage are brought about by changes in the base level of a stream. A method is proposed by which the effect of changes in the stage of a stream on a hydraulically connected acquifer may be projected within the limits of certain assumptions.

Boundary and accretion components of head. The head distribution in an aquifer under equilibrium or steady-state conditions is the result of the rate and distribution of recharge to and dis-

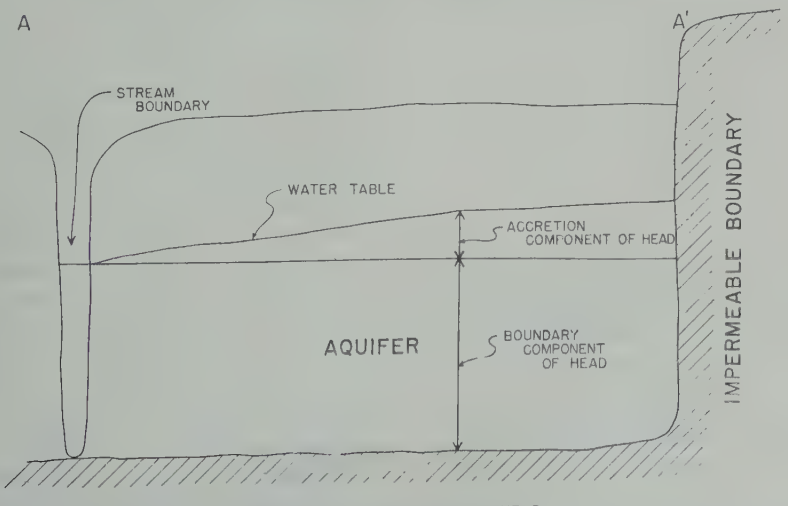


Fig. 1. Section through hypothetical aquifer showing boundary and accretion components of head.

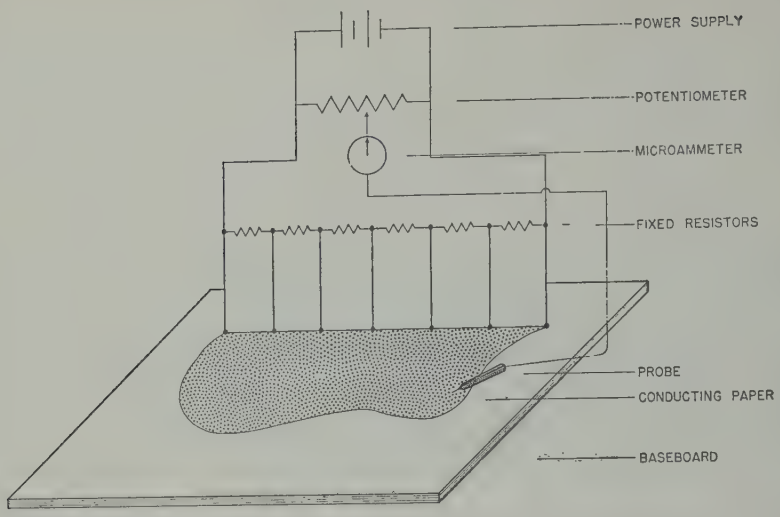


Fig. 2. Semischematic wiring diagram of conducting-paper analog field plotter.

charge from the aquifer, the transmissibility of the aquifer, and the nature and configuration of the hydrologic boundaries of the aquifer.

Assume a homogenous aquifer enclosed by boundaries which are either impermeable or have fixed values of head. Also, if the differences in head are assumed to be small in relation to the thickness of the aquifer, the head distribution may be separated into two components of head.[1]

One, the boundary component of head, is determined by the type and configuration of the hydrologic boundaries and the head distribution on the boundaries. This component would represent the actual water table were there no accretion to the aquifer.

The second, the accretion component of head, is determined by the ratio of the rate of accr tion to the transmissibility and by the areal ge metric shape of the aquifer and the nature of t hydrologic boundaries. Accretion is used here represent the net rate at which water is gain or lost vertically through the aquifer surface response to external forces. Infiltration of pr cipitation, evapotranspiration, and vertical inte formational leakage are examples of accretio The accretion and boundary components a shown in Figure 1. The aquifer and water tab shown in the figure and referred to under t section 'Field application,' are modifed from actual set of field conditions.

Determination of boundary component. T boundary component can be determined by ther numerical or electrical methods. Numeri methods are described by *Southwell* [1948] a have been used by *Stallman* [1956] in the anal sis of ground-water flow.

The analogy between the flow of ground wat and electricity was first recognized by *Slicht* [1898]. The analogy may be employed to dete mine the boundary component.

The conducting-paper analog field plotter h been used by many investigators. It is limited steady-state flow in two dimensions in a hom geneous field with known boundary conditio In using the analog plotter the flow field is d termined while an electric current passes throu a conducting paper. A semischematic diagram a field plotter is shown in Figure 2.

[1] The linearity of the equation of two-dimensional flow,

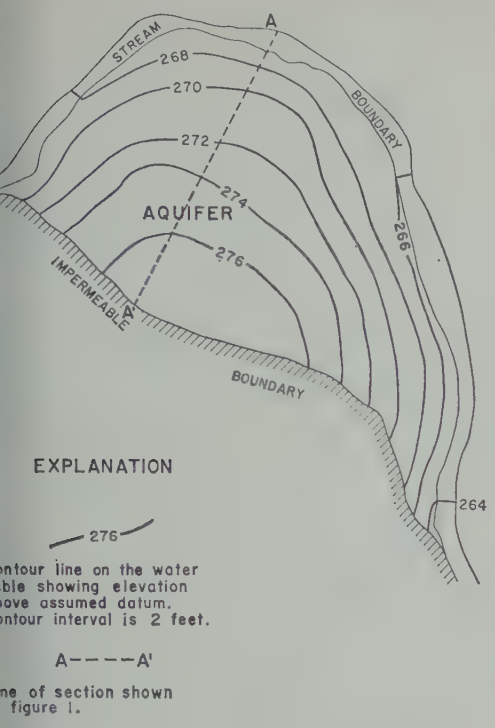
$$\partial^2 h/\partial x^2 + \partial^2 h/\partial y^2 = -W/T$$

can be used, where h is the head, x and y are the space coordinates, W is the rate of accretion, and T is the coefficient of transmissibility of the aquifer. The boundary conditions are $\partial h/\partial n = 0$ along the impermeable boundary and $h = f(x, y)$ along the stream boundary. The solution can be the sum of two components, $h = u + v$, where

$$\partial^2 u/\partial x^2 + \partial^2 u/\partial y^2 = 0$$

$$\partial^2 v/\partial x^2 + \partial^2 v/\partial y^2 = -W/T$$

The boundary conditions are $\partial u/\partial n = 0$ and $\partial v/\partial n = 0$ along the impermeable boundary and $u = f(x, y)$ and $v = 0$ along the stream boundary.



ig. 3. Map of hypothetical aquifer showing contour lines on the water table.

The series of resistors provides a number of al potential drops between the positive and ative terminals of the power source. Leads n the series can be placed in contact with or more boundaries of the paper in order to resent sloping streams. The resistance through analog plotter is much less than the resist- e through the conducting paper, and the del has a negligible effect on the uniformity of intervals between the constant potential nts. Also, the probe circuit is of sufficiently n resistance so as not to load the model ap- ciably. Because there is no flow across the tact between the aquifer and permeable ma- als the paper is trimmed at this boundary. potentiometer, microammeter, and probe used in determining the positions of the lines qual potential in the conducting paper. With probe in contact with a point of known age, or known head, along the stream bound- , the potentiometer is adjusted so that no cur- flow is indicated by the microammeter. With setting on the potentiometer the probe is ed across the paper connecting points of no current flow; the line is a contour of constant head.

Determination of accretion component. The rate of accretion usually differs areally with the various types of surface materials, and the effects of accretion may be determined by observation. If the present head distribution or position of the water table is known, the accretion component may be found by subtracting the head distribution in the aquifer due to the boundary component from the actual head distribution in the aquifer.

Field application. For an assumed change in head distribution along the stream boundary of an aquifer we assume that, after equilibrium is established in the aquifer, there is (1) no appreciable change in transmissibility of the aquifer, (2) no change in accretion to the aquifer, and (3) flow is in two dimensions. The changed head distribution in the aquifer will be due solely to the change in the boundary component. If the boundary components before and after the change in stream stage are known, the head distribution may be determined graphically by the

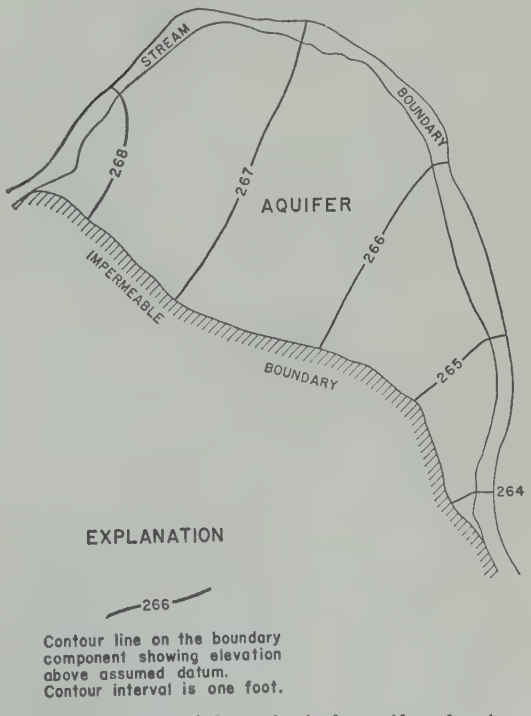


Fig. 4. Map of hypothetical aquifer showing contour lines on the boundary component of head.

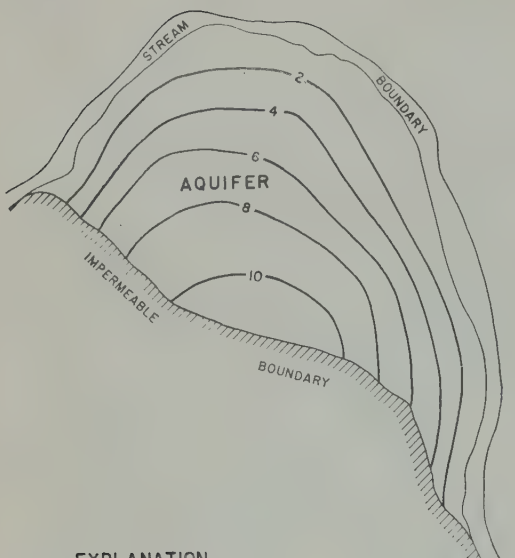


Fig. 5. Map of hypothetical aquifer showing thickness of the accretion component of head.

following procedure. (1) A water-table map of the aquifer is superposed on a map of the existing boundary component. The accretion component is then found by determining the difference in elevation of the water table and boundary component. (2) The map showing the thickness of the accretion component is superposed on the map showing the boundary component due to the change in stream stage. The water table that is due to changed stream stages is then found by adding the accretion component to the boundary component resulting from the change in stream stage.

Consider the aquifer shown in Figure 3, which is bounded on one side by an impermeable geologic unit and on the other side by a stream in free hydraulic communication with the aquifer. The boundary component of this aquifer, determined with the aid of the conducting-paper analog field plotter, is shown in Figure 4. The accretion component, shown in Figure 5, is determined by obtaining the difference in the water table and the boundary component. The effects of three hypothetical changes in strea stages are as follows.

1. Assume that the stream in Figure 3 is in pounded, resulting in a flat pool with an elev tion of 270 feet in the stream segment borderi the aquifer. Because of the changed stream stag the boundary component would be a flat surfa having an elevation coincident with that of t pool elevation. After equilibrium conditions a established in the aquifer, the water table wou have a configuration shown by the lines depic ing the accretion component (Fig. 5). The elev tion of the water table is determined by addi 270 to the accretion component.

2. Assume that part of the water in the strea shown in Figure 3 is diverted, resulting in a lov ering of the stream surface by 2 feet, but th the stream retains the same slope. The bounda component due to the changed stream sta would be 2 feet lower but would have the sam configuration as the boundary component show in Figure 4. After equilibrium conditions we established in the aquifer the water table wou be 2 feet lower but would have the same co

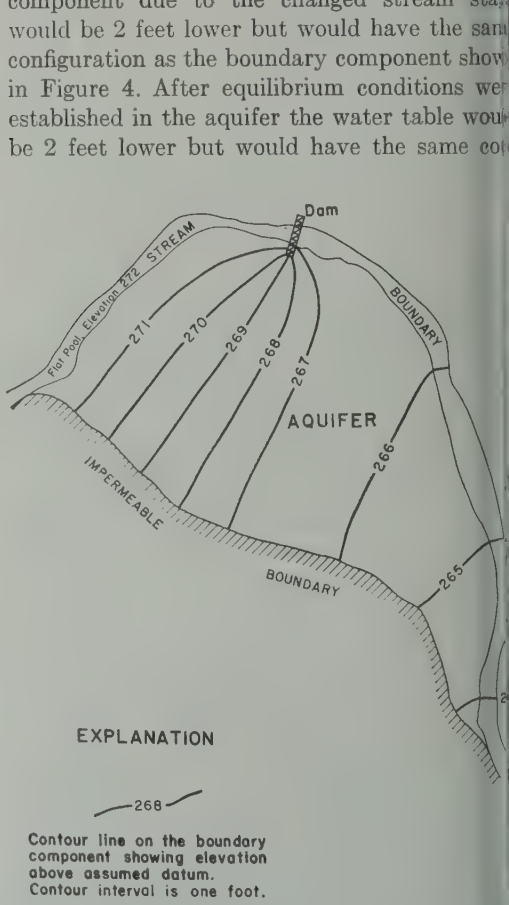
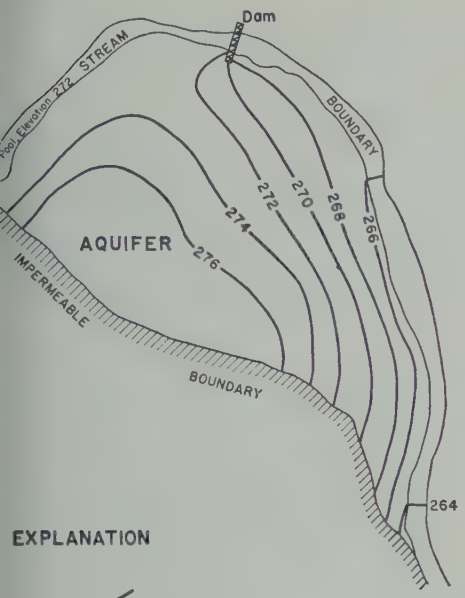


Fig. 6. Map of hypothetical aquifer showi contour lines on the boundary component of he after impoundment of stream.

tion as the water table shown in Figure 3. Assume that a dam is constructed in the n adjacent to the aquifer, resulting in the lary component shown in Figure 6. The



our line showing
ation of water table
e assumed datum (obtained
dding the accretion component,
e 5, to the boundary component,
e 6.)
our interval is 2 feet.

7. Map of hypothetical acquifer showing r lines on the water table after impound- of stream.

configuration of the water table after equilibrium conditions are established (Fig. 7) is determined by adding the accretion component in Figure 5 to the new boundary component.

Conclusions. The method described above affords a means of projecting the effect of changed stream stages on an aquifer if the field conditions meet the following assumptions before and after the change in stream stage: (1) Ground water is in steady-state flow in two dimensions. (2) Rate of accretion to the water table is not a function of time. (3) Coefficient of transmissibility is constant. (4) There are well-defined hydrologic boundaries; the aquifer is in free hydraulic communication with stream boundaries and there is no flow across impermeable boundaries.

Acknowledgments. This paper was prepared by the U. S. Geological Survey in cooperation with the U. S. Army Corps of Engineers.

Publication authorized by the Director, U. S. Geological Survey.

References

Slichter, C. S., Theoretical investigations of the motion of ground waters, *U. S. Geol. Survey 19th Ann. Rept.*, pt. 2, 295–384, 1898.

Southwell, R. V., *Relaxation Methods in Theoretical Physics*, Oxford University Press, 248 pp., 1948.

Stallman, R. W., Numerical analysis of regional water levels to define aquifer hydrology, *Trans. Am. Geophys. Union, 37*, 451–460, 1956.

(Manuscript received May 5, 1961; presented at the Forty-second Annual Meeting of the American Geophysical Union, Washington, D. C., April 9, 1961.)

Fluctuations of Ground-Water Levels Caused by Dispersion of Salts[1]

F. A. KOHOUT

U. S. Geological Survey, Miami, Florida

Abstract. Certain wells tapping the zone of diffusion between fresh and salt water in the Miami, Florida, area showed anomalous residual water-level drawdowns after being pumped. Graphs comparing fluctuations of water levels and chloride contents show that the anomalies are caused by dispersion-motivated changes in the density of the water in the casing. Dispersion produces fluctuations of water level under natural conditions as well as after pumping. In an area where true fluctuation of the water table due to normal recharge and discharge amounted to about 3 feet, dispersion produced an observed water-level fluctuation of 0.7 foot. The fluctuations occur so subtly that erroneous conclusions concerning changes in ground-water storage are possible unless interpreted carefully.

roduction. Generally recognized causes of uations of ground-water level are natural re- e and discharge, pumping, tidal action, quakes, evapotranspiration, and changes in spheric pressure. In areas of salt-water con- nation, fluctuations of water level may be d, also, by diffusion-dispersion phenomena ring in the casings of wells that tap the of diffusion between fresh and salt water 1). Frequently, water-level fluctuations of kind are obscure, and, as they are not re- to changes in ground-water storage, careful pretation is required to insure that water- measurements are meaningful. The purpose s paper is to illustrate how dispersion may o cause a change of water level in a well.

ctuations induced by pumping. In the e of routine water sampling, certain wells e Miami, Florida, area that were equipped automatic water-level recorders appeared ve residual water-level drawdowns of sev- enths of a foot after being pumped. Owing e high permeability of the Biscayne aquifer e Miami area (50,000 to 70,000 gpd/sq ft) ual drawdowns of this magnitude were not ted as a result of pumping for short periods w rates. The unusual aspect was that a ery curve (from the pumping) did not ap- on any of the recorder charts (Fig. 2). After rous pumpings (each one producing a simi- rawdown), no persistent decline of water relative to other wells was detected.

The reason for the drawdown and lack of recovery is apparent in Figure 3 where the water levels of wells F 198 and F 192 are plotted comparatively with the chloride concentration of water in the casing of well F 198. Well F 192 is located a short distance from well F 198 and is used to show the regional (and normal) fluctuation of water level. Before well F 198 was pumped on March 12, the chloride content of water in the casing was 685 ppm and its water level was 0.21 foot higher than that of well F 192. After pumping stopped, the chloride content of water in the casing of well F 198 had increased to 7950 ppm, and consequently the density had increased. The water level was then 0.16 foot lower than that of well F 192. During the afternoon of March 12 and on March 13 and 14, the water in the casing of well F 198 freshened so rapidly that the daily-average water level rose in opposition to the areal decline shown by the hydrograph of well F 192. Subsequently, the hydrographs of the two wells gradually diverged as the chloride content of the water in well F 198 decreased to its prepumping concentration.

This test shows that the water level of a well fluctuates as a result of dispersion-motivated changes in the density of the casing water. In the majority of wells, the recovery of water level resulting from dispersion is quite imperceptible and can be detected only by comparison with a companion well.

Water-level fluctuations under natural conditions. The dispersion rate shown in the test on

ublication authorized by the Director, U. S. gical Survey.

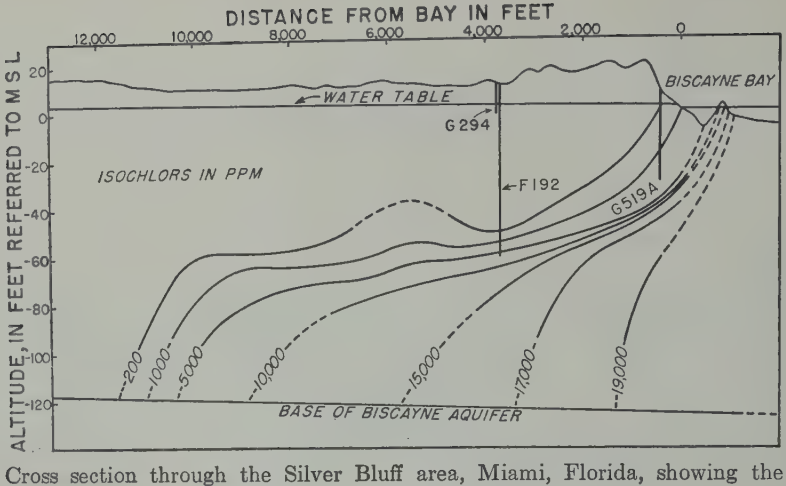


Fig. 1. Cross section through the Silver Bluff area, Miami, Florida, showing the zone of diffusion, November 2, 1953.

well F 198 directed attention to whether the upward rate was as great as the downward rate. A test was devised to observe the relative rates of dispersion with and against the pull of gravity. It was expected that a rapid freshening of the water in the casing of well F 192 would occur when the salt-water front (Fig. 1) was pushed seaward by high water-table conditions dur the rainy season. The dispersion in this would be downward, aided by gravity. As water table declined below a certain critical tude, the salt-front movement would reverse an inland direction, and the chloride concent tion of the water in the aquifer just below

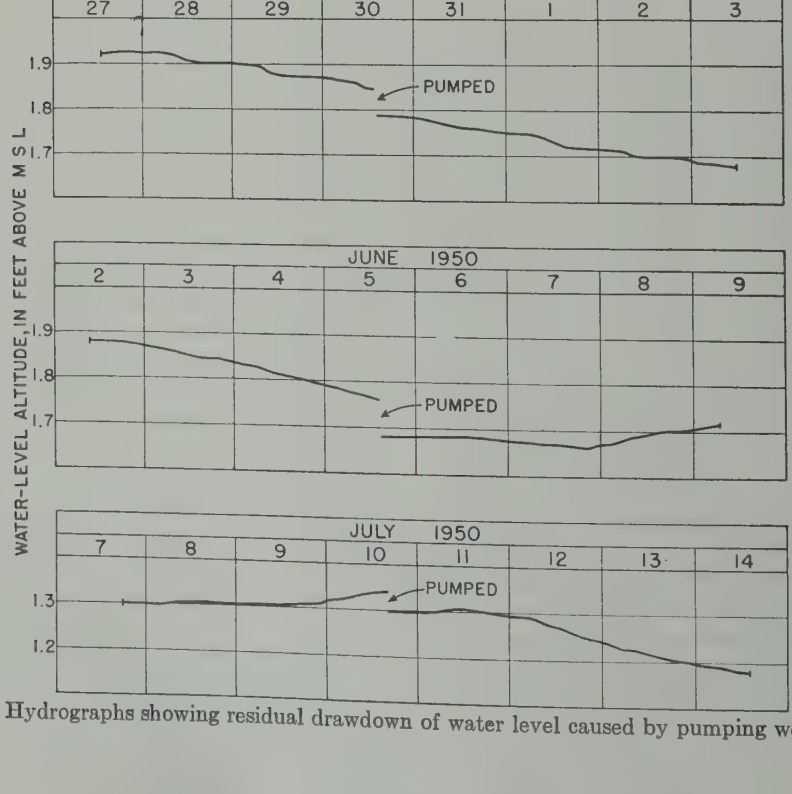
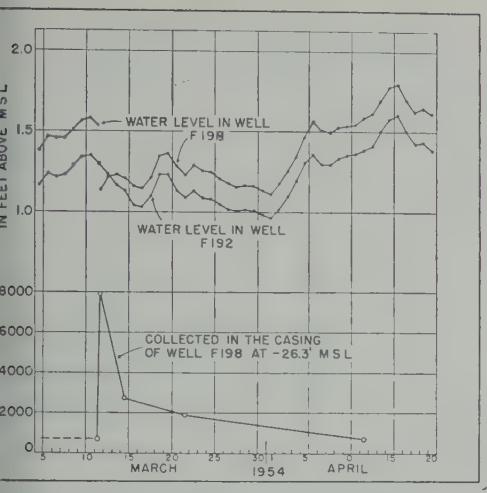


Fig. 2. Hydrographs showing residual drawdown of water level caused by pumping well G 580.



. 3. Graph showing density drawdown and recovery of water level in well F 198.

tom of the casing would increase to a higher ue than that of the water in the casing. The persion in this case would oppose gravity.

n Figure 4 fluctuations of chloride content l water level in wells F 192 and G 294 are npared. Because well G 294 is a shallow fresh-water well at the same location as F 192 (Fig. 1), its water level represents true changes in ground-water storage and may be used as a standard. The difference in water level between the two wells, then, shows the fluctuation of water level caused by dispersion of salt occurring in the water in the casing of well F 192.

The high water levels of late September and October 1953 produced a sharp decrease in chloride content at the −60.7-foot depth in well F 192. The decrease of chloride content at −46.7 feet (in the casing) lagged only slightly behind. In comparison, the difference in water level between wells F 192 and G 294 decreased in direct relation to the freshening of the water in the casing of well F 192.

Between December 1953 and May 1954, the chloride concentration of water just below the casing gradually increased about 4000 ppm; during the same period, the chloride content of the water in the casing increased less than 300 ppm. The upward rate of dispersion in the casing of well F 192 was much slower than the downward rate. However, the water-level difference, as shown by the upward trend of the difference curve, increased in relation to the in-

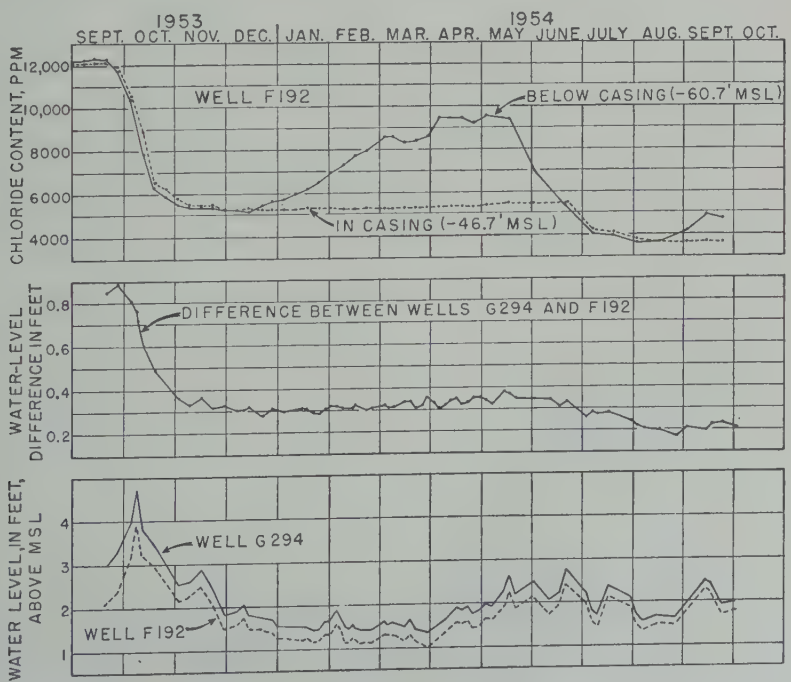


Fig. 4. Graphs showing dispersion-motivated fluctuations of water level in well F 192 for natural conditions.

crease of chloride content of the water in the casing. Thus, under completely natural conditions, the water level of a salty well may fluctuate by a diffusion mechanism that is independent of changes in ground-water storage.

The true fluctuation of the water table amounted to about 3 feet for the whole year, but in well F 192 the dispersion produced an observed fluctuation of seven-tenths of a foot or about 25 per cent of the total. In spite of this significant percentage, the fluctuations of water level resulting from the dispersion would not be recognized without careful analysis.

Molecular diffusion or dispersion? The great difference in the downward and upward rates of chloride change shown in the preceding test leads to consideration of the mechanisms that produce the differing rates. Molecular diffusion, the spontaneous process by which molecules or ions of a solute move in a solvent from points of high concentration to points of low concentration, is a slow process compared with dispersion which includes both molecular diffusion and convection, the mechanical transfer of one fluid into the region of another by hydraulic movement.

Figure 5*a* shows the chloride distribution (by titration) in well F 192 during downward movement of ions, and Figure 5*b* shows the distribution (by electrical conductivity) in well G 519A during upward movement of ions. Other experience has shown that these distributions are characteristic of the respective directions of ion flow. Although no data are available, it may be assumed that the distribution of chloride content in the casing water of well F 192 from January to May 1954 (Fig. 4) was similar to that shown in Figure 5*b*.

A comparison of Figure 4 with Figure 5 shows that the chloride content of water in the casing of well F 192 (−46.7 ft) decreases rapidly under the low downward concentration gradient (Figure 5*a*) and increases very slowly under the high upward concentration gradient that undoubtedly was present from January to May (Fig. 5*b*). In both cases, the ion flow is properly oriented with respect to the concentration gradient. but the rates of ion flow have an inverted relationship with respect to concentration gradient.

Were ion movement to occur only by molecular diffusion, the latter circumstance would contradict potential-gradient theory. Therefore, it

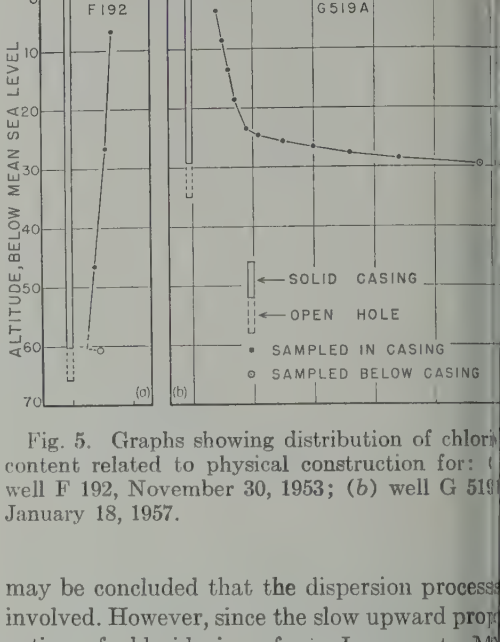


Fig. 5. Graphs showing distribution of chlori content related to physical construction for: (well F 192, November 30, 1953; (*b*) well G 519 January 18, 1957.

may be concluded that the dispersion process involved. However, since the slow upward prop gation of chloride ions from January to M 1954 is not greatly inconsistent with the sl rate of ion flow that might be expected fr molecular diffusion alone, the upward moveme may be considered to be more closely related pure molecular diffusion than the downwa movement.

Clearly, the rapid downward movement chloride ions (Fig. 4) is caused by the dispers process. Gravity, the convective agent, acts up the unstable density condition that exists wh the chloride content of water in the casing greater than that at the casing terminus. I crete volumes of high-density water in the cas settle downward and are replaced by volu of low-density water rising upward from casing terminus. Upon coming into close c tact, the concentrations of the individual umes are rapidly unified by molecular diffus Thus, the hydraulic transfer and molecular fusion combine to produce a high rate of fre ening under the low downward concentra gradient shown in Figure 5*a*.

From the foregoing, water-level fluctuat caused by the dispersion phenomena may be pected to follow the general pattern of r change when ion movement is downward slow change when ion movement is upward. upward movement is especially subtle becau

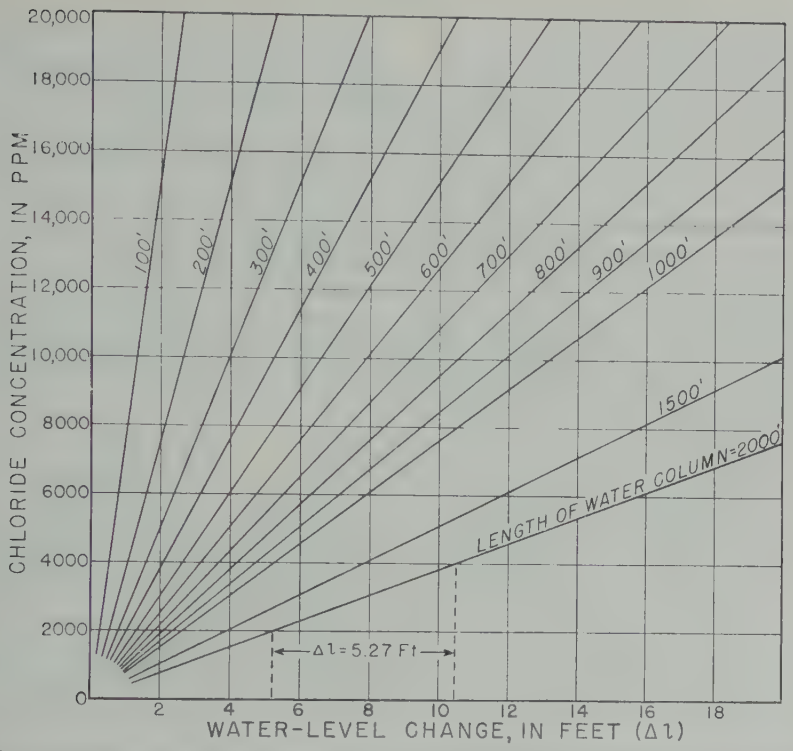


Fig. 6. Graph relating water-level change (Δl) to chloride concentration for various lengths of water column.

l zone of diffusion develops in the lower part
ıe casing (Fig. 5*b*). As the ions move above
terminus of the casing, their mass increases
lensity of water in the casing and the water
drops as though the density increase were
ibuted throughout the total length of the
g.

agnitude of water-level fluctuation. The re-
n between the rise of fluid in the casing of
ll and the pressure p at the casing terminus
ven by the equation

$$p = \rho g l$$

e ρ is the density of water in the casing, g
e acceleration due to gravity, and l is the
ured length of water column above the cas-
erminus. As the change in salt concentration
e casing water by dispersion does not change
ressure in the aquifer at the casing termi-
the right term of the above equation may
uated for two concentrations of salt water
g densities ρ_1 and ρ_2:

$$\rho_1 g l_1 = \rho_2 g l_2$$

$$l_2 = \frac{\rho_1 l_1}{\rho_2}$$

If we let $l_2 = l_1 + \Delta l$, the equation may be rewritten

$$l_1 + \Delta l = \frac{\rho_1 l_1}{\rho_2}$$

$$\Delta l = \frac{(\rho_1 - \rho_2) l_1}{\rho_2} \qquad (1)$$

where Δl is the change in length of the salt-water column relative to the initial length l_1. The value Δl may be considered, also, as the change in water level caused by the change in density of the casing water.

Figure 6 relates (1) to chloride content for various lengths of water column. Consider a well with a water-column length (l_1) of 2000 feet in which the chloride content increases by dispersion or pumping from 2000 ppm (ρ_1 = 1.00290) to 4000 ppm (ρ_2 = 1.00555) [*Parker, Ferguson, and Love,* 1955, Fig. 171, p. 599]. Substituting these data into (1) yields

$$\Delta l = \frac{(1.00290 - 1.00555)\ 2000}{1.00555} = -5.27 \text{ ft}$$

The negative value indicates that the water level in the well would decline 5.27 feet during the density change. In Figure 6 the intercepts of the lines representing 2000- and 4000-ppm chloride with the water-column trace of 2000 feet may be projected to the Δl axis to yield the same value. Polarity of the Δl value relative to the initial length l_1 is negative (subtracts from the l_1 value) if the chloride content of the casing water increases and is positive (adds to the l_1 value) if the chloride content of the casing water decreases.

Summary. Calculations show that fluctuations of water level due to dispersion of salts may have large magnitude. The dispersion occurs more rapidly when ion flow is aided by gravity than when opposed by gravity. Thus, water-level fluctuations caused by the dispersion phenomena may be expected to follow the general pattern of rapid change when ion movement is downward and slow change when ion movement is upward. As the ions move above the terminus of the casing during upward mov ment, their mass increases the density of wat in the casing and the water level drops though the density increase were distribut throughout the total length of the casing.

In an area where true fluctuations of the wat table amounted to 3 feet, dispersion produced observed fluctuation of seven-tenths of a foot about 25 per cent of the total. In spite of t significant percentage, fluctuations of water lev resulting from dispersion are so obscure th they will not be recognized without care analysis.

Reference

Parker, G. G., G. E. Ferguson, and S. K. Lo Water resources of southeastern Florida, w special reference to the geology and ground w ter of the Miami area, *U. S. Geol. Survey Wa Supply Paper 1255*, Superintendent of Do ments, Washington, D. C., 965 pp., 1955.

(Manuscript received May 1, 1961; presented the Forty-second Annual Meeting of the Americ Geophysical Union, Washington, D. C., April 1961.)

Ground-Water Investigations in a Saline Area of the Red River Valley, North Dakota[1]

LEO C. BENZ, ROME H. MICKELSON, FRED M. SANDOVAL, AND CARL W. CARLSON

Agricultural Research Service
U. S. Department of Agriculture
Grand Forks and Mandan, North Dakota

Abstract. Investigations in a saline area of the Red River Valley in North Dakota indicate that salt-affected soils are caused by high water tables, poor drainage conditions, and saline artesian waters. A 3-year study conducted in a 200-square-mile area shows that rainfall was a major contributor to the high and fluctuating water table. Chemical composition of the ground waters indicate that the Dakota sandstone artesian waters are the most likely source of salt.

INTRODUCTION

Estimates indicate that there are approxitely 400,000 acres of land in the Red River ley of North Dakota affected by excessive centrations of salts. About one-half of this eage, located on the lake plain near the Red er, is in Grand Forks County. The problem a has a high water table, poor drainage, and artesian conditions. Those areas in Grand Forks County affected by high concentrations of soluble salts are shown in Figure 1. Moderately affected areas are utilized in the production of salt-tolerant crops; the more salty areas are either idle or are used for grazing or haying.

The study area, also shown in Figure 1, consists of about 200 square miles in east central Grand Forks County. Ground-water data have been obtained since 1957 from 60 observation wells and 15 piezometer batteries located within the study area. Ground-water and soil data indi-

[1] Contribution from Soil and Water Conservaon Research Division, Agricultural Research Service, U. S. Department of Agriculture.

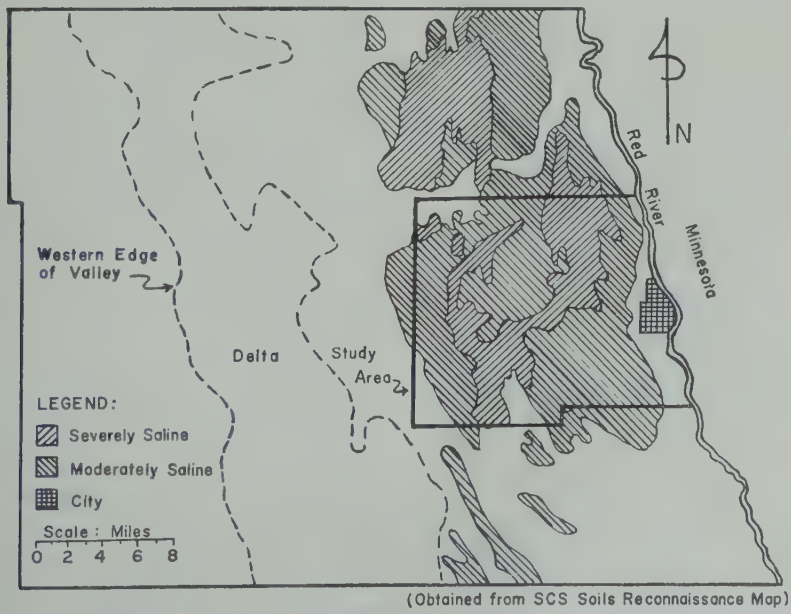


Fig. 1. Map of Grand Forks County, North Dakota, showing salt-affected areas and study site.

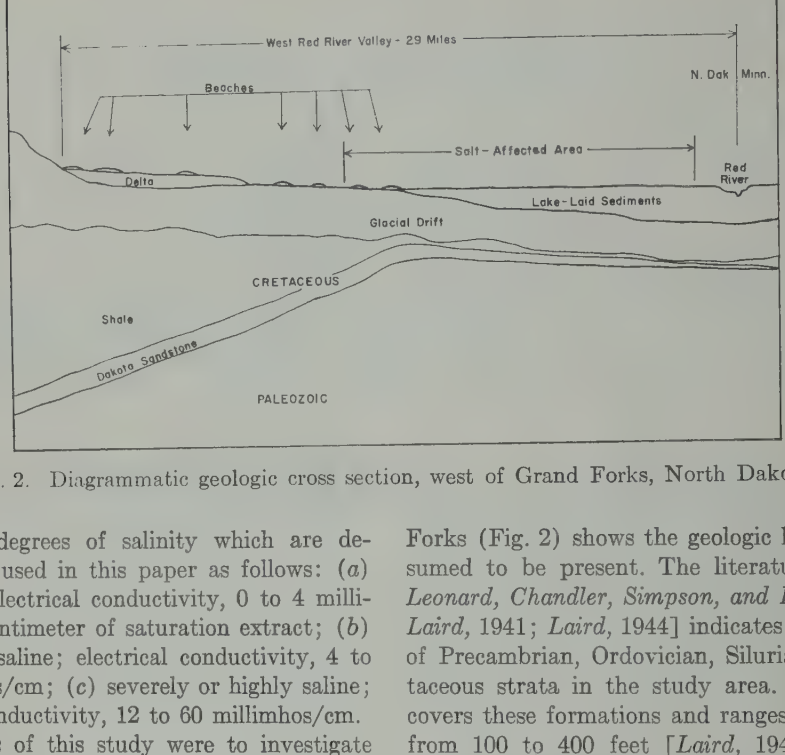


Fig. 2. Diagrammatic geologic cross section, west of Grand Forks, North Dakota.

cate three degrees of salinity which are described and used in this paper as follows: (*a*) nonsaline; electrical conductivity, 0 to 4 millimhos per centimeter of saturation extract; (*b*) moderately saline; electrical conductivity, 4 to 12 millimhos/cm; (*c*) severely or highly saline; electrical conductivity, 12 to 60 millimhos/cm.

Objectives of this study were to investigate and evaluate (*a*) water-table levels, (*b*) sources of ground water, (*c*) ground-water flow gradients, (*d*) artesian and downward flow conditions, and (*e*) ground-water quality and chemistry.

General Features

Climate. The climate of the Grand Forks area is classed as dry-subhumid [*U. S. Dept. of Agriculture,* 1941] Annual precipitation averages 20 inches which includes 30 inches of snow. About 67 per cent of the precipitation falls during the frost-free period of 126 days. Extremes in monthly mean temperatures range from 70.7°F in July to 4.4°F in January.

Geology and soils. The Red River Valley has a geological history of several glaciations in which several lakes were formed during advances and recessions of the glaciers [*Johnston,* 1916; *Lemke and Colton,* 1958; *Upham,* 1895]. The most recent glacier, as it melted and receded northeastward, formed the large ancient glacial Lake Agassiz [*Hainer,* 1946]. Numerous beaches were formed as the water level of the lake dropped.

A diagrammatic cross section west of Grand Forks (Fig. 2) shows the geologic horizons pr sumed to be present. The literature [*Gaug Leonard, Chandler, Simpson, and Budge,* 193 *Laird,* 1941; *Laird,* 1944] indicates the presen of Precambrian, Ordovician, Silurian, and Cr taceous strata in the study area. Glacial dr covers these formations and ranges in thickne from 100 to 400 feet [*Laird,* 1941; *Simps* 1929]. The glacial drift is overlain by lacustri sediments near the Red River and by delta sediments near the western edge of the valle Between these two areas the glacial drift is e posed [*Upham,* 1895].

The Cretaceous shale formations decrease thickness toward the east and were very pro ably eroded by the glaciers. Where this occurr the glacial drift lies directly on the lower Cr taceous members which include the Dako sandstone formation. The Dakota formation is part of the Dakota artesian system and consis of a micaceous white sandstone which carr highly mineralized water under pressure [*Lai* 1944].

Figures 2 and 3 illustrate principal phys graphic areas based on soil parent materi [*Sandoval and Shoesmith,* 1961]. The sout western portion of the study area is glacial ti the northeastern portion is lacustrine sedimen Most of the area under investigation has so derived from deep lacustrine or lake-laid se ments. Logs from domestic wells indicate th sediments to be over 100 feet thick near Gra Forks, decreasing in thickness towards the we

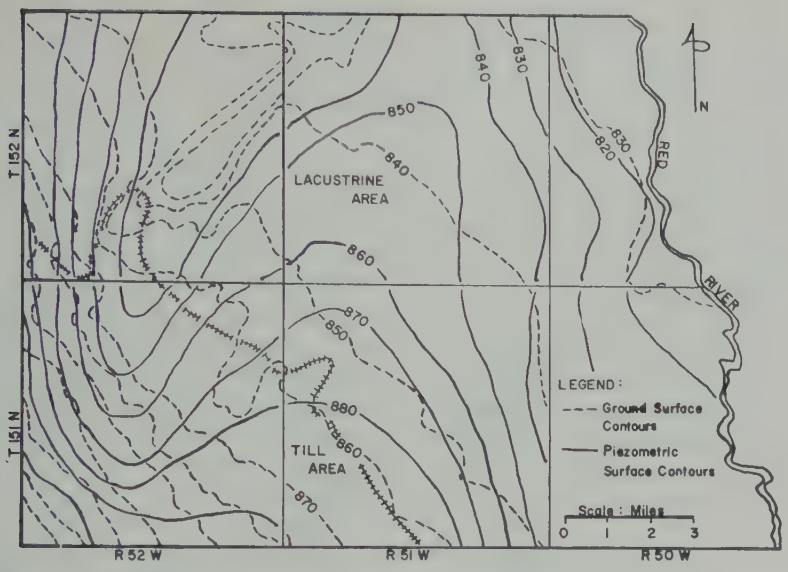


Fig. 3. Ground surface and piezometric surface contours. The hatched line separates the glacial till and lacustrine areas.

se lacustrine soils have a silt loam or silty loam surface texture of high organic matcontent. Subsoils vary from silt to silty clay n, and at substratum depths, below 3 or 4 , the materials range in texture from silt to clay. Lacustrine varving is clearly evident. n many acres of the problem area the glacial is near or at the surface. Soils developed n glacial drift lie at a higher elevation than deep lacustrine materials. Variable textures the surface, consisting of shallow lakeed and/or reworked materials over a com-, slightly gravelly clay loam glacial drift, are acteristic of these soils.

he area farther west is a delta. The delta erial, consisting of silts and sands, is 30 to feet thick and was deposited by glacial ams flowing into the valley [*Upham,* 1895]. alinity problem does not exist in this gen- well-drained area, so it was not included ne study.

tesian pressure. Free-flowing artesian wells prevalent in the area studied. The wells e in depth from 35 to 350 feet. Sources of r are the Dakota sandstone aquifer and also and gravel lenses located in the glacial . These lenses probably receive their water, igh interconnections, from the Dakota sand-. Owing to the highly impermeable shale ying the sandstone the artesian waters would normally be held in their place. *Laird* [1944] stated that these waters probably reach the surface by entering the sand and gravel lenses in the glacial drift in areas where the shale is thin or completely removed. *Simpson* [1929] explained artesian head in shallower aquifers as being due to their northeastward dip. He also stated that the waters may have been stored in the sand and gravel lenses at the time of deposition by glaciers.

The artesian waters are highly mineralized and are not generally used for domestic purposes. Good water is obtained from shallow nonartesian wells, 10 to 20 feet deep, on the beaches and in the delta area [*Simpson,* 1929].

Topography. The ground surface slopes in a northeasterly direction. Ground surface contours are shown in Figure 3. Gradients near the Red River average 2 to 3 ft/mile and increase to 15 to 20 ft/mile at the western edge of the valley. Surface drainage is generally poor because the fluvial cycle is at an early stage of development [*Augustadt,* 1955].

Much of the problem area, particularly the deep lacustrine soils, is characterized by a system of low intersecting minor ridges and depressions. In the area studied, the relief difference is from several inches to several feet with a range in width from 75 to 500 feet. Geologists [*Colton,* 1958; *Horberg,* 1951] believe the ridges were

formed by fractured lake ice which lay on the soft lake sediments. During this formative period the lake level apparently fluctuated.

Salt-affected soils occur but are not confined to the ridge-depression topography. It would appear that this type of microrelief accentuates the problem. Investigations have shown that although the ridges are highly saline the depressions are comparatively nonsaline [*Sandoval, Carlson, Mickelson, and Benz*, 1961].

Study Procedures

Climatic data were obtained from the Weather Bureau at Grand Forks. Additional measurements of rainfall were taken with recording rain gages located to obtain a good representation of the study area.

Observation wells and 20-foot piezometers were installed in an area of approximately 200 square miles (see Fig. 1). A 2-mile grid pattern was used. The wells were 12 feet deep and have both 4-inch and ⅜-inch diameter casings perforated in the bottom 10 feet.

Piezometer batteries were installed in areas of varying degrees of salinity and at different elevations. Each battery consisted of a 20-, 40-, and 60-foot ⅜-inch-diameter pipe. These pipes and the small-diameter observation wells were installed by a jetting technique [*Richards*, 1954]. Water levels in the observation wells and piezometers were measured monthly and usually 1 to 2 days after any rainfall of more than ½ inch.

Measurements of pressure from artesian wells were obtained by attaching a Bourdon-type pressure gage or, where pressures were low, a simple water manometer to the outlet of the flowing well. A high percentage of the wells were old and had corroded casings; therefore, measurements were obtained only from domestic wells that were less than 5 years old.

Samples of ground water were obtained from many locations to evaluate chemical properties. Laboratory methods used are described in USDA Handbook 60 [*Richards*, 1954]. Shallow ground waters were collected from wells cased with inert materials (coal-tar-impregnated fiber pipe) to eliminate interference on colorimetric determination of divalent cations. Artesian water samples were obtained from domestic wells in the area.

Hydraulic conductivities were taken both in the laboratory and in the field. The piezometer and auger-hole methods [*Richards*, 1954] were used in the field, and Uhland soil cores were used in the laboratory [*Uhland and O'Neal*, 1951].

Results and Discussion

Climate. Precipitation during the period 1959 to 1960 was near the annual mean of 20.0 inches: in 1957, 22.04 inches, in 1958, 17.8 inches, and in 1959, 17.37 inches.

Water table. A 3-year record has shown that the water table follows a definite seasonal pattern. During the winter the water table recedes but a sharp rise occurs in the spring as the frost leaves the soil and the snow melts. Fluctuations occur during the summer and are probably due primarily to percolating rain water and evapotranspiration.

Rainfall has a pronounced effect on the water table. This is shown in Figure 4, where the monthly water tables at two sites and monthly precipitation for a 2-year period, 1958 and 1959, are plotted. The two sites shown, SW¼ 14 T152N-R51W (Rye township) and SW¼ 16 T151N-R50W (Grand Forks township) are, respectively, a highly or severely saline and slightly to moderately saline area. Both areas are cultivated. The moderately saline area is cropped continuously; the highly saline area is alternately cropped and fallowed. Surface drainage is much better at the slightly saline than at the highly saline site. The soil at both locations is derived from lacustrine sediments that are more than 60 feet deep.

The observation well at the severe site shows greater fluctuations and a higher average water table than the well at the slightly saline site. The average water table during the period was 5.16 feet below the ground surface at the highly saline location compared with 9.5 feet at the slightly saline site. During the growing season the water-table depth was 3.8 feet at the severely affected site, compared with 9.0 feet at the slightly affected site.

The curves indicate that the highest water table occurred during the growing season and that fluctuations were caused by rainfall. In February and March 1959 the water table at both locations was more than 9 feet below the ground surface which was the low for the two seasons. The water table lowering during the winter could have been caused mainly by one of two factors: (*a*) moisture movement upward to

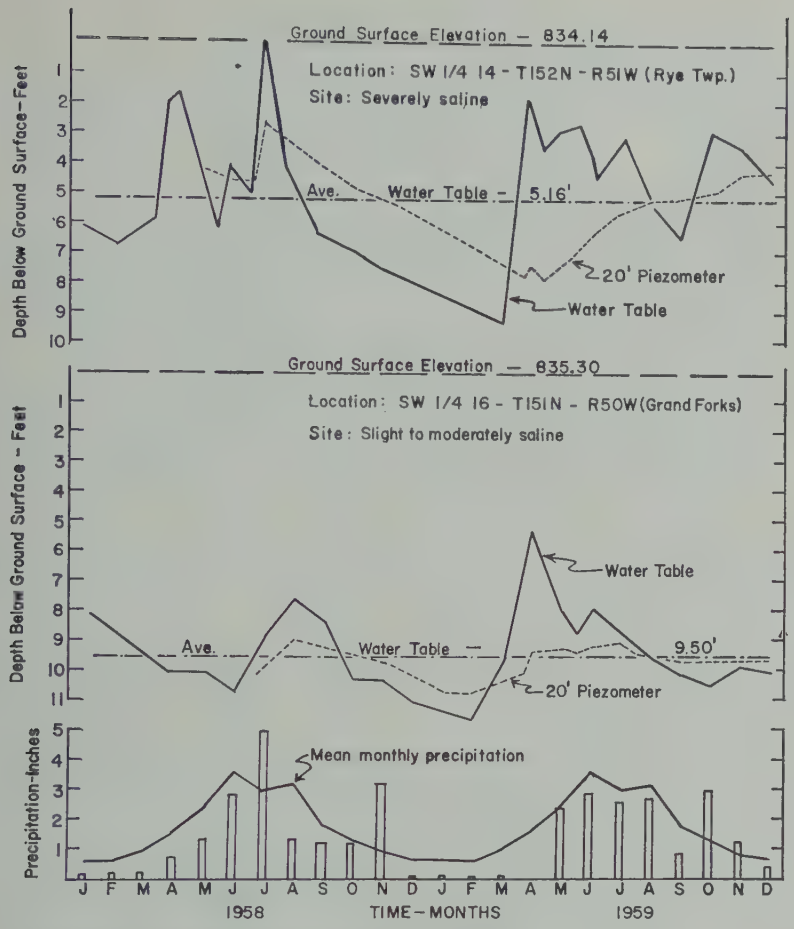


Fig. 4. Water-table fluctuations at two sites plus monthly rainfall during a 2-year period.

the freezing front [*Crabb and Smith, Garstka,* 1944]; (*b*) horizontal movement ter due to hydraulic gradients.

ter levels in the 20-foot piezometers which ljacent to the observation wells of 14 Rye 6 Grand Forks are also plotted in Figure 4. uctuations followed the same general pat- s the observation well waters. Water-level ations in the piezometers were very sub- compared with the observation-well water

isobath map of the water table (Fig. 5) ates the average for the year 1958; depth water table was obtained from monthly gs. Total annual rainfall in 1958 was 2.20 below normal. The areas are delineated 2-foot increments. Sloughs or low-lying had very shallow water tables. A large saline area in township 152N-R51W also indicates a high, possibly perched, water table. The average for the year 1958 water table in the entire study area was 6.1 feet. It was highest in July with an average depth of 3.3 feet and lowest in February 1959, when the average depth was 9.0 feet.

The size of the areas of high water table varied during the year, becoming larger during the spring and high rainfall season and decreasing in size with periods of low rainfall. The data indicate a relationship between the high water table and the highly saline areas.

Hydraulic gradients, obtained from observation-well readings, indicate that ground-water movement was toward the northeast with slopes similar to those of the ground surface. Hydraulic conductivities obtained on lacustrine soils indi-

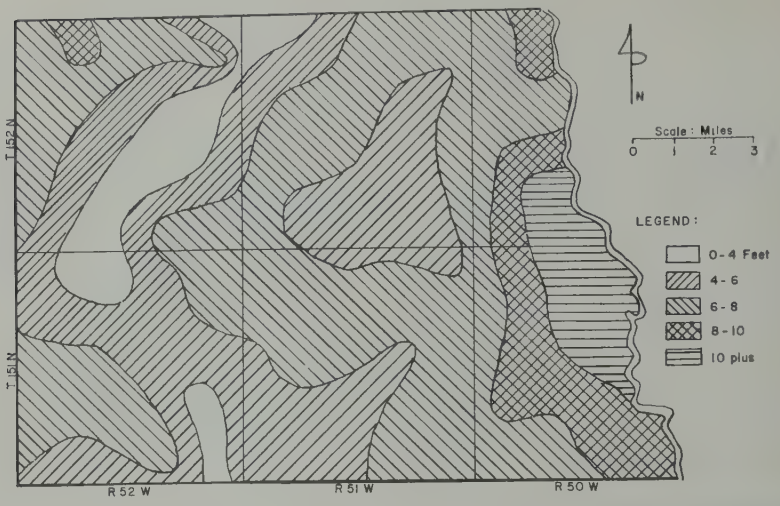


Fig. 5. Water-table isobath map based on yearly average of monthly readings, 1958.

cated horizontal rates of ⅛ to 8 cm/hour at depths above 6 feet. These rates usually decreased with depth. Glacial-drift soils had variable permeabilities, but generally they were very low owing to their compactness.

Piezometer gradients. Piezometer batteries in the study area indicated upward gradients. Typical gradients for three locations are shown in Figure 6. The actual water level in each piezometer is given with respect to the ground surface. The three locations are representative of three degrees of soil salinity—severe at SW¼ 14-T152N-R51W (Rye Twp.), moderate at N½ 8-T151N-R51W (Brenna Twp.), and slight to nonsaline at SW¼ 16-T152N-R50W (Falconer Twp.).

Surface drainage is good at the slightly saline location but poor at the other two. At the moderately saline location, glacial drift was 15 feet below the ground surface. The piezometers here were terminated in clay loam till. Piezometers at the other two locations were terminated in fine-textured lacustrine sediments. The pressure head is not great at locations which are representative of the area.

At the first or highly saline location the pressure head at 60 feet below the ground surface was such that it brought the water level 2 feet above the ground surface. Soils are fine-textured, compact, and varved, a condition that greatly affects upward and horizontal movement of water. Head losses upward through the soil profile ranged from 0.40 ft/ft at the second or moderate location to 0.05 ft/ft at the third or nonsali location.

Deep piezometer water levels were relativ constant throughout the record period w slight fluctuations occurring due to precipitati If large fluctuations had occurred during seasons it would have indicated that sour other than the artesian aquifer were contribut water. Irrigation is not practiced in the vall however, the delta and beach areas lying higher elevations could possibly contribute the high-water-table conditions. The relativ steady-state water levels of deep wells piezometers, however, preclude this theory.

Artesian head. The hydraulic head was termined from domestic artesian wells loca in the study area. Wells ranged in depth fr 35 to 350 feet. A contour map of the piezomet surface is given in Figure 3.

The data indicate no flowing wells above 890-foot ground elevation contour line. In eastern portion of the study area, near the I River, static water levels of wells were about feet elevation. Most of these wells were be pumped. Within the study area, the piezome surface lies above the ground surface betw the eastern and western borders. In this a nearly all of the domestic wells were flowing.

There appears to be some relationship betw the high-piezometric-surface area and the verely saline areas. Where the piezometric p sure head is high, soil salinity is also high. T may be where the confining impervious sh

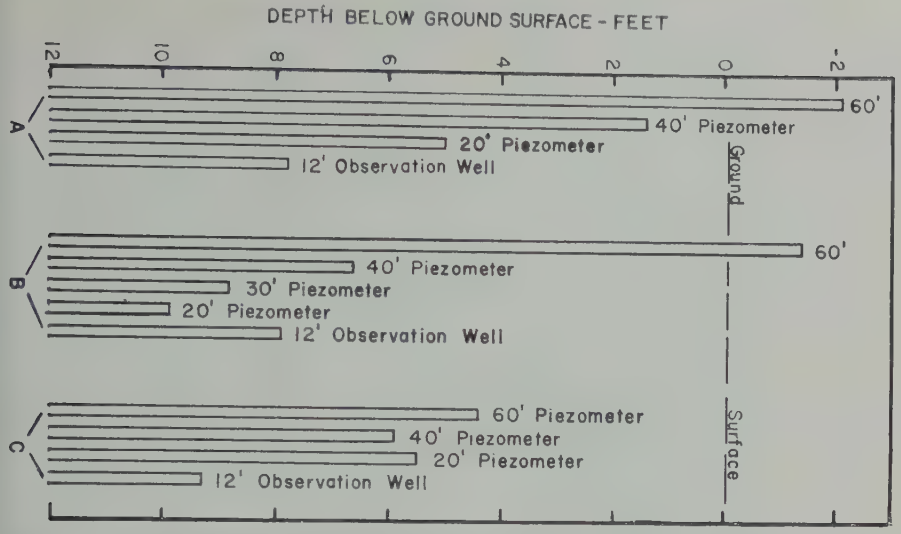


Fig. 6. Upward gradients shown by piezometer batteries at three locations on March 22, 1960. *A*. Severely saline location (SW¼ 14-T152N-R51W). *B*. Moderately saline location (N½ 8-T151N-R51W). *C*. Negligible salinity location (SW¼ 16-T152N-R51W).

the Dakota sandstone are very thin or ed, allowing considerable seepage into the ying glacial drift. It may also be an area e the glacial drift contains sand and gravel s that lie near the ground surface and have ection with the Dakota.

ie amount of water fed into the area by ar- n sources does not appear to be of major equence, although it is sufficient to con- te salts and keep the substratum depths rated. This is pointed up by the water table sion during the fall and winter months. It is evidenced by the small pressure head shown iezometer batteries and flowing artesian .

ound-water chemistry. Chemical analyses aters from the shallow water table, which obtained from 12-foot observation wells, vaters from deep artesian wells are given in e 1. Samples 1 through 9 are representative ow waters from both lacustrine and glacial reas.

e most saline shallow ground waters were e lacustrine area. Samples 1 and 2 are repre- tive waters of the lacustrine area, on flat ndulating relief, respectively. Salt concen- ns in these waters were variable, but elec- conductivity values of nearly 60 milli- /cm (approximately 40,000 ppm) were d. Magnesium was the dominant cation, fol- lowed closely by sodium. Calcium and boron were low. Although chlorides were the dominant anions in the most saline waters, sulfates were frequently present in greater quantities than chlorides in the moderately saline areas.

Samples 3 and 4 were taken from observation wells located 300 feet apart on a ridge and the adjacent depression in a lacustrine area. The difference in ground surface elevation was 0.9 foot. Salt content of the water in the ridge well was considerably higher than that in the depression well. A short distance from this site, with approximately the same type of ground surface relief, the ridge ground water analyzed 45 millimhos/cm (36,692 ppm) while the water from the adjacent depression had an electrical conductivity of only 1.2 millimhos/cm, or 714 ppm concentration [*Sandoval, Carlson, Mickelson, and Benz,* 1961].

Sample 5 was obtained from a well-drained lacustrine site on the eastern edge of the problem area. Salinity and artesian head at this location were low.

Samples 6 through 9 are representative shallow ground waters from areas where glacial till was near the ground surface. The most saline water, sample 6, was obtained from a semislough area which had a consistently high water table. Shallow ground-water samples 7 through 9 had lesser concentrations of salts. These glacial till

TABLE 1. Chemistry of Ground Waters, Grand Forks, North Dakota*

Sample No.	Depth, ft	Electrical Conduct., mmho/cm	Solids, ppm	Boron, ppm	Ca, me/l	Mg, me/l	Na, me/l	SO_4, me/l	Cl, me/l	Soluble Na, %
				(NW¼ 35-T152N-R51W; Highly saline, lacustrine, flat relief)						
1	12	43.7	30,688	0.1	71	228	253	81	472	46
				(NW¼ 8-T151N-R51W; Strongly saline, lacustrine, ridge on relief)						
2	12	29.9	28,206	0.1	28	305	144	275	202	30
				(SE¼ 25-T152N-R51W; Moderately saline, lacustrine, ridge on relief)						
3	12	6.6	5,515	tr	30	29	17	22	48	22
				(300 feet distant and 0.9 feet lower than sample 3, nonsaline depression)						
4	12	3.0	2,231	0.1	17	10	6	13	16	20
				(SW¼ 16-T152N-R50W; Nonsaline, lacustrine)						
5	12	4.3	4,233	tr	24	34	6	57	3	9
				(NE¼ 9-T151N-R52W; Highly saline, semislough over till)						
6	12	16.8	11,860	2.3	36	33	114	37	146	62
				(NW¼ 36-T151N-R52W; Moderate to strongly saline, till, flat relief)						
7	12	10.5	7,380	2.1	21	19	75	41	69	65
				(NE¼ 8-T150N-R51W; Moderate salinity, till, gentle ridge)						
8	12	7.7	7,986	0.4	24	75	17	87	25	14
				(SW¼ 28-T151N-R52W; Nonsaline, interbeach area over till)						
9	12	3.1	2,943	0.2	23	16	3	32	5	8
				(SE¼ 33-T152N-R51W)						
10	248	10.8	7,440	3.0	19	13	83	30	80	71
				(SW¼ 34-T152N-R51W)						
11	103	6.4	4,530	2.8	14	5	50	32	33	72
				(NW¼ 9-T152N-R51W)						
12	?	8.0	5,338	3.0	13	7	64	30	51	75
				(NW¼ 33-T153N-R51W)						
13	120	7.6	5,204	2.9	13	7	60	30	47	73
				(SE¼ 17-T153N-R51W)						
14	175	17.3	11,740	3.8	28	19	143	37	148	75
				(SE¼ 23-T151N-R52W)						
15	90	10.5	7,929	3.6	9	28	85	36	86	70

* Samples numbered 1 through 9 were taken from 12-foot observation wells; samples 10 through were taken from deep artesian wells.

waters indicated that sodium was the dominant cation and also that boron was high.

Chemical data from six flowing artesian wells are given in samples 10 through 15. These waters —which presumably originate from the Dakota sandstone—were quite similar in chemistry, varying principally in concentration. Sodium was the dominant cation (from 70 to 75 per cent) and chlorides were higher than sulfates. The boron content was higher than in the shallow ground waters.

There was a similarity in composition of the deep artesian waters and shallow ground waters from the glacial till areas. This indicates that artesian sources are principal contributors of salts to the ground surface in the till. The till areas lie at a higher elevation, and drainage is toward the lacustrine area. High magnesium and low boron content in shallow waters of the lacustrine area show either that there is a diffe source of salt or that the fine-textured lacust sediments probably fix or filter out the boron contribute magnesium. Most likely the la is true.

Summary and Conclusions

1. The salt-affected area studied has a water table, poor drainage conditions, and sa artesian waters.

2. Rainfall was a major contributor to water tables. Water tables rose 3 to 7 feet ing the growing season, when 65 to 70 per of the yearly precipitation normally oc Maximum rises and near-ground-surface fluc tions usually occurred during the first ha the growing season.

3. The water-table depth followed a seas pattern. During the winter it dropped; in

ng a sharp rise occurred, probably due pri-ily to frost leaving the soil and downward olation of snow-melt. Summer fluctuations urred and were due chiefly to percolating rain er. If autumn precipitation was normal the er table slowly receded.

Flat topography and poor surface and in-al drainage contribute to the high water ta-. Runoff occurs principally in the spring, n soils are frozen, and during high-intensity s. Highly saline areas were usually areas ng high water tables. Salt concentrations of shallow waters in excess of that found in the sian waters are probably due to evapotran-ation forces.

The similar chemical composition of shallow er in glacial drift and deeper artesian waters cates that waters from the Dakota sandstone primary sources of salts. Shallow ground ers from lacustrine sediments had a different nical composition than the artesian waters, bably owing to the tendency of the lacustrine ments to fix or filter out boron and con-ute magnesium.

Upward flow gradients indicated upward er movement in the soil profile. Amounts of er fed into the area by artesian sources are cient to contribute salts and keep the soil stratum well saturated with water.

Concentrations of salt occur in both glacial t and lacustrine sediment ground waters. The est acreage is in the latter. Glacial drift lies higher elevation, and salinity in the drift be due to nearness of the sand and gravel es in the drift to the ground surface. In the strine areas, salts are probably due to wa-being fed into these areas by the higher-ation sand and gravel lenses in the drift /or by seepage upward through the fine sedi-ts.

knowledgments. Ground-water samples were yzed by M. G. Keyes and J. T. Hatcher and rted by L. V. Wilcox of the U. S. Salinity oratory, Riverside, California.

References

istadt, Walter W., Drainage in the Red River lley of the north, *Yearbook Agr., U. S. Dept. r.*, 569–575, 1955.

Colton, Roger B., Note on the intersecting minor ridges in the Lake Agassiz Basin, N. Dakota, *N. Dakota Geol. Survey Misc. Publ., 10,* 74–77, edited by W. M. Laird, R. W. Lemke, and Miller Hansen, May 1958.

Crabb, G. A., and J. L. Smith, Soil temperature comparisons under varying covers, *Highway Research Abstr., 22*(11), 67–68, 1952.

Garstka, W. V., Hydrology of small watersheds under winter conditions of snow cover and frozen soil, *Trans. Am. Geophys. Union,* 838–1060, 1944.

Gauger, A. W., A. G. Leonard, E. F. Chandler, H. E. Simpson, and W. D. Budge, Geology and natural resources of North Dakota, *Univ. N. Dakota Bull. 11,* Jan. 1930.

Hainer, John L., The geology of North Dakota, *N. Dakota Geol. Survey Bull. 31,* 46 pp. 1946.

Horberg, Leland. Intersecting minor ridges and periglacial features in the Lake Agassiz Basin, North Dakota, *J. Geol., 59,* 1–18, 1951.

Johnston, W. A., The genesis of Lake Agassiz, *J. Geol., 24,* 625–638, 1916.

Laird, Wilson M., Guide for geologic field trip in northeastern North Dakota, *N. Dakota Geol. Survey Bull. 12,* 1941.

Laird, Wilson M., Selected deep well records, *N. Dakota Geol. Survey Bull. 12,* 1941.

Laird, Wilson M., The geology and ground water resources of the Emerado Quadrangle, *N. Dakota Geol. Survey Bull. 17,* 1944.

Lemke, Richard W., and Roger B. Colton, Summary of the Pleistocene geology of North Dakota, *N. Dakota Geol. Survey Misc. Ser. 10,* May 1958.

Richards, L. A., Ed., Diagnosis and improvement of saline and alkali soils, *U. S. Dept. Agr., Agr. Handbook 60,* 160 pp., 1954.

Sandoval, F. M., C. W. Carlson, R. H. Mickelson, and L. C. Benz, Effects of runoff prevention and leaching water on a saline soil, *Can. J. Soil Sci.,* 1961.

Sandoval, F. M., and Lloyd Shoesmith, Genetic soil relationships in a saline glacio-lacustrine area, *Soil Sci. Soc. Am. Proc.,* 1961.

Simpson, H. E., Geology and ground water resources of North Dakota. *U. S. Geol. Water Supply Paper 598,* 1929.

Upham, Warren, The glacial Lake Agassiz, *U. S. Geol. Survey Monograph 25,* 1895.

Uhland, R. E., and A. M. O'Neal, Soil permeability determinations for use in soil and water conservation, SCS-TP-101, Washington, D. C., Jan. 1951.

U. S. Department of Agriculture, *Yearbook Agri., Climate and Man,* 17–19, 1053–1054, 1941.

(Manuscript received February 6, 1961; revised May 16, 1961.)

Some Implications of the Highly Saline Water off the Southwest Coast of Florida

FRANK CHEW

Gulf Coast Research Laboratory
Ocean Springs, Mississippi

Abstract. An extensive body of highly saline water (37.5 per mil and more) was observed off the southwest coast of Florida in the summer of 1956 when drought conditions existed in central and southern Florida. The existence of this water mass is evidence against upwelling and against the adjacent Florida west coast runoff being the source of the less saline water farther offshore, two postulated conditions that have sometimes formed the basis of some supposed Red Tide mechanisms in this region. Evaporation and precipitation computations indicate that this highly saline mass was formed mainly in the region northwest of Key West. This understanding, together with the known northward advection, enabled us to estimate the magnitude of the lateral eddy diffusion. In turn, this determination is used in discussing the efficacy of a supposed Red Tide convergence mechanism. Estimate of errors is also included.

ntroduction. The southwest coast of Flor- is one of recurrent Red Tide outbreaks [e.g., *Gunter, Williams, Davis, and Smith,* 1948]. the absence of adequate data, there are many flicting theories and much speculation on the ses and development of the Red Tide. The l of adequate data is still far from being lized, but some recent data do permit a pre- inary and partial assessment of a few of the ories.

he salinity data independently collected by Marine Laboratory, University of Miami, by the U. S. Fish and Wildlife Service are e in showing a period when an extensive y of coastal water is highly saline. We shall delineate the pertinent factors in the for- ion and development of this mass. Then we ll estimate the magnitude of the lateral y diffusion and discuss its implication for a tulated convergence mechanism. Finally, we ll call attention to the evidence presented this highly saline mass against upwelling and inst the Florida west coast rivers being the nary sources of the offshore low-salinity gues.

he pattern of high salinity. The salinity a are taken from the reports by *Marvin* 55], *Finucane and Dragovich* [1959], and *w, Bein, and Stimson* [1959]; the last re- is also the source of data for an evapora- computation.

he tongue of high-salinity water is most evi- in Figure 1 for August 25 to September 1, 6. Defined as being in excess of 36.6 per mil, the tongue is more than 450 km in length and has an average width of about 45 km. The core of the tongue, defined as salinity in excess of 37.6 per mil, is nearly homogeneous with depth in both salinity and temperature (with negligible exception caused by diurnal heating in calm weather).

Figure 2 presents the surface salinity pattern observed along approximately east-west sections whose locations are identified in Figure 3 by station numbers. Salinity in excess of 36.6 per mil is evident in all sections, except for the most northerly one identified by station number 106–119, occupied in July 1955.

Figure 4 presents a salinity-time graph for two Florida Bay stations identified as D-10 and D-11 in Figure 3. Except for brief periods, all salinities were in excess of 36.6 per mil, with that at D-11 reaching a maximum of 49 per mil in July 1956. At D-11, in 9 feet of water, both surface and bottom salinity and temperature were taken in 1955. These show negligible vertical variation (greatest difference in salinity at top and bottom of water column was 0.04 per mil). Subsequently, all samplings were taken only from the surface. Farther west, at D-10, in 13 feet of water, the vertical variation in both temperature and salinity is slightly larger but is still negligible in most instances.

For contrast, Table 1 presents the surface salinity at an east-west section off the mouth of Boca Grande as indicated in Figure 3 by the line marked 4 through 8. All salinities, except one, are less than 36.6 per mil.

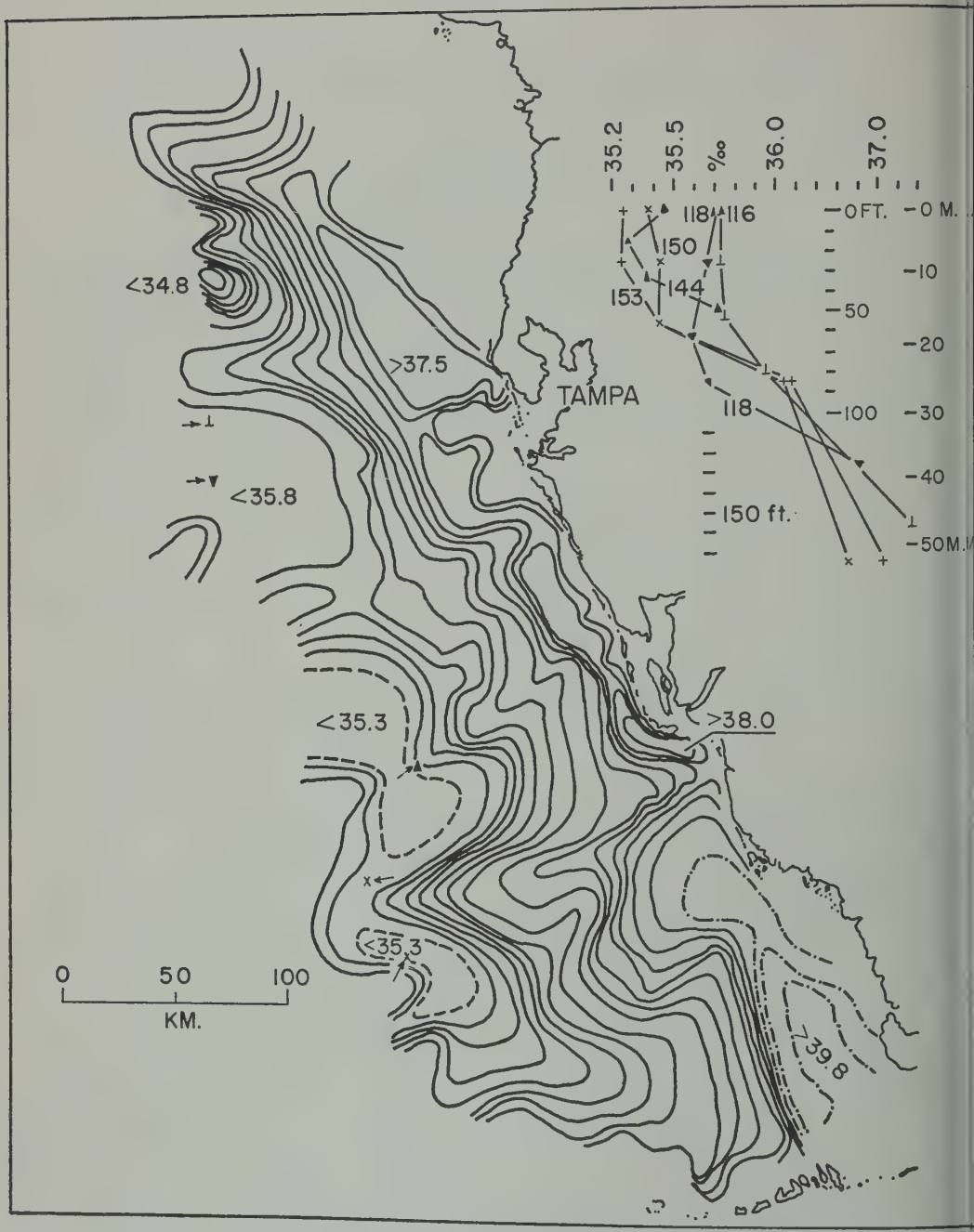


Fig. 1. Surface salinity for the period August 25 to September 1, 1956. Inset shows vertical salinity profiles of selected stations (reproduced from *Chew, Bein, and Stimson,* [1959]),

Formation of high-salinity water. In the open sea, when evaporation exceeds precipitation, highly saline water will form if advective and vertical mixing processes are small. Along a coast, the additional factor of river discharge must be considered.

In central and southern Florida, 1956 was year of drought. Rainfall deficit for represent

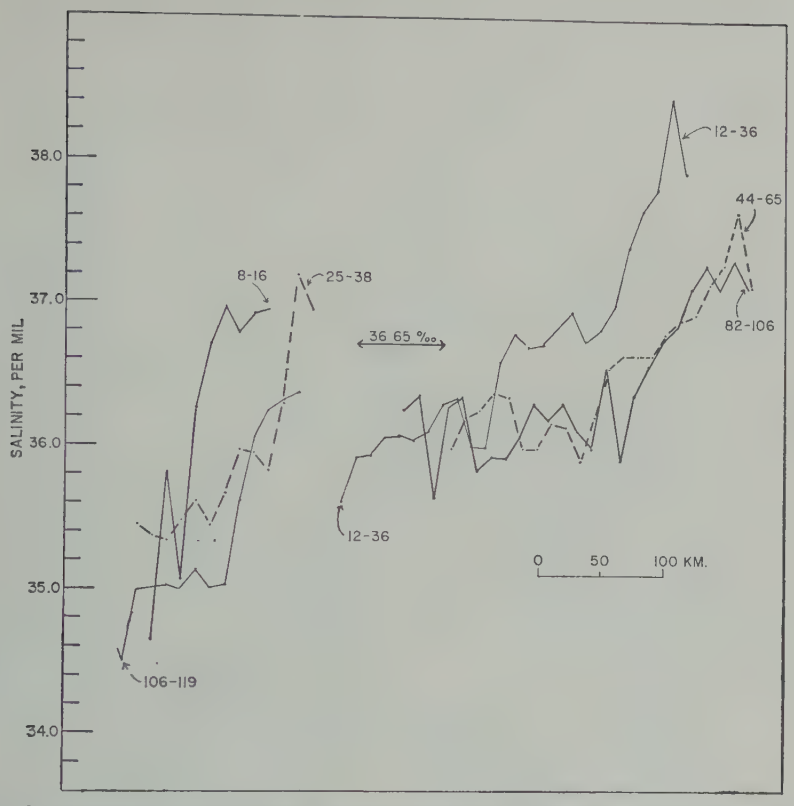


Fig. 2. Surface salinity along nearly east-west section. Locations are identified in Figure 3 y station number. Large double-headed arrow marks the 36.7 per mil salinity. (The ordinate salinity in parts per thousand, and the abscissa refers to horizontal distance.)

coastal stations along the western and ern coast is given in Table 2.

nfall deficit was also reflected in stream- leficiency. The larger rivers—Withlacoo- Peace, Caloosahatchee, and Kissimmee— he diffuse water flow through the Ever- all showed a marked decrease in discharge e. Typical of this decrease is that of the mee River, shown in Figure 5 (adapted Figure 3 of the Geological Survey *Water y Paper 1434*).

ears of normal rainfall, even the so-called rivers along the southwest Florida coast relatively small discharge. Primarily, this ause of their relatively small drainage . For example, the Apalachicola River in vest Florida has a discharge that is usu- me 5 times the combined total of all river rges from Tampa Bay south to Key West. ms of runoff per unit length of straight line, the runoff from Clearwater, just of Tampa Bay, to Cape Sable averages to 0.6 m^3/sec km. *Bumpus* [1955], in studying the circulation south of Cape Hatteras, considered a runoff of 1.9 m^3/sec km as being 'very small.' During the 1956 drought, runoff was reduced to 1/5 to 1/3 normal, and therefore the factor of river discharge in the formation of high-salinity water may be neglected. This is indicated additionally by direct salinity observations at passes and river mouths showing salt water invasion of estuarine regimes.

The relation between mean surface salinity on the one hand, and the difference between mean evaporation and mean precipitation ($E - P$) on the other has been studied by *Wüst* [1936] and *Jacobs* [1951], among others. In this paper, we shall relate the quantity ($E - P$) to the mean salinity in yet another way. We shall approximate the mean of E by computation based on the sea surface temperature and meteorological data collected on University of Miami cruises, and we shall approximate the precipitation over water by that observed at

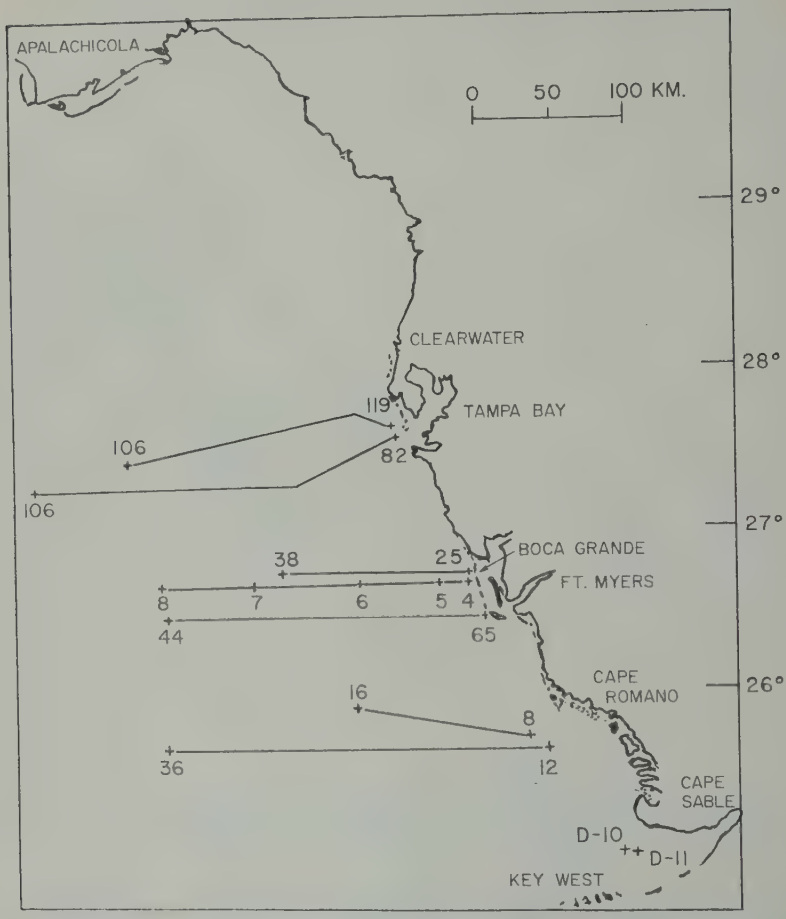


Fig. 3. Geographic locations of cross sections and stations. Stations D-10 and D-11 are northeast of Key West.

coastal land stations. It is realized that the precipitation pattern, especially short-term precipitation, is irregular and that its extrapolation even to contiguous areas is not strictly valid. However, it is probably a good first approximation when longer-term means like monthly or seasonal averages are used.

The evaporation data. On all University of Miami cruises off the Florida coast (cited above), sea surface temperatures were taken with bucket thermometers,[1] wet and dry bulb air temperatures with a sling psychrometer, wind observations with a cup anemometer a Ventimeter (a simple, hand gage giving w speed only). All observations taken over wa of depths less than about 10 fathoms were vided into three groups, according to whet the location of observation is south of 26°0 (zone A), north of 26°00′ to 27°6.5′N (z B), or north of 27°6.5′N (zone C). For fu reference, the hydrographic stations whose o are so utilized are listed in Table 3 accor to University of Miami cruise number and graphical zone. It is seen that the numbe observations for each set ranges from 6 to with an average of 21.

The difference in vapor pressure between sea surface and the air ($e_w - e_a$) as der from sea surface temperature and wet- minus dry-bulb air temperature is plotte

[1] Although *Ewing and McAlister* [1960] found a cool, thin surface layer capping the layer in which the so-called sea surface temperature is determined, so that the vapor pressure over water should be based on the cool thin layer, it is felt that this refinement is unnecessary in this paper since the constant in the evaporation equation used here is empirically determined.

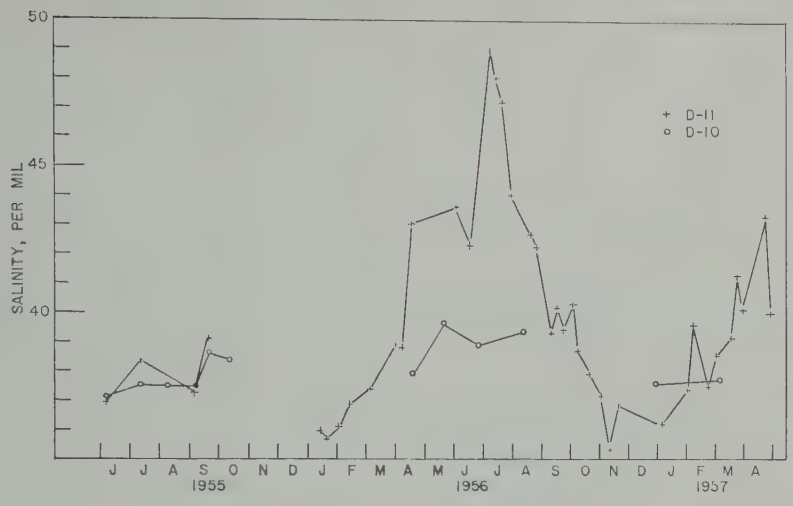


Fig. 4. Salinity-time plot of Florida Bay stations D-10 and D-11.

re 6*a* in millibars. Even though the num- of observations is small in some cases, th curves can be drawn through all points. seasonal regularity is marked; the mini- is in January and February and the maxi- in late August. From minimum to maxi- the magnitudes differ by a factor of 10.

LE 1. Surface Salinity at East-West Transects off Boca Grande as Observed by the U. S. Fish and Wildlife Service

	Salinity (‰) for Various Stations				
Date	4	5	6	7	8
1949					
9–12	35.12	35.41	35.97	36.69	36.20
9–10	35.97	35.77	36.02	36.27	
20–27	35.88	35.26	35.53	35.23	
11–14	35.64	35.59	35.61	33.30	
1–4	34.96	35.64			
25–					
ot. 1	25.68	35.01	35.25	34.88	33.31
5–12	30.70	31.69	35.21	35.39	35.88
3–9	34.42	34.76	35.26	35.82	36.22
1–8	32.77	34.74	35.75	36.11	36.17
950					
1–11	33.93	35.12	35.86	36.67	
9–15	34.22	35.35	35.64		
2–8	35.21	35.61	36.20	36.17	
30					
r. 5	35.39	35.52	36.26	36.06	
27–					
y 4	35.30	35.59	36.09	35.64	35.19
8–14	36.17	35.91	36.27	35.53	36.38
11–13	35.88	36.13	35.59	34.00	
21–24	35.95	36.38	34.78	32.88	33.71

TABLE 2. Rainfall Deficit for 1956 (Source: U. S. Weather Bureau)

City	Deficit, inches	Percentage of Mean
Key West	17.9	46
Tampa	21.2	43
Miami	19.4	32
Ft. Myers	13.4	25
Apalachicola	9.1	16

This means that the mean evaporation is largely determined by mean $(e_w - e_a)$ since the mean winds seldom vary by that much.

To increase the stability of the short-term winds, we use the simple arithmetical average of winds from three sources. One is from shipboard observation coincident with the temperature data. Two are from coastal stations, of which one is the average wind for the month in which the cruises occur (or occur for the most part), and the other is the average of the period coincident with the cruise period. The three coastal stations selected are Key West, Ft. Myers, and Tampa, taken to represent zones A, B, and C, respectively.

The evaporation formula used is that of *Jacobs* [1951]:

$$E = M(e_w - e_a)W_a \qquad (1)$$

where E is amount of evaporation in 0.1 cm/day, M is the evaporation coefficient, $(e_w - e_a)$ is vapor pressure difference of water and air in millibars, and W_a is the mean wind speed in

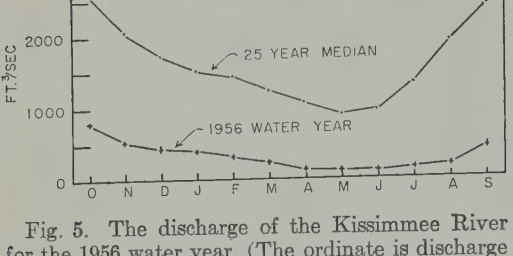


Fig. 5. The discharge of the Kissimmee River for the 1956 water year. (The ordinate is discharge in cubic feet per second. Adapted from *U. S. Geological Survey Water Supply Paper 1434.*)

m/sec. M changes slightly with wind and altitude [*Roden*, 1959]; we use M equals 0.14, which corresponds to a mean wind of 4 m/sec and an altitude of 3 m. The computed evaporation is given in Figure 6*b*. For the indicated period, the evaporation curves for all three zones are similar. The period of maximum evaporation is the warmer half of the year, much as in the Gulf of California [*Roden and Groves*, 1959] but in contrast to other regions with opposite phase. This is reasonable, since the dry, continental, winter air masses responsible for winter evaporation maximum in some other regions do not generally materialize here, and the strong subtropical, summer insolation raises the water temperature and hence the vapor pressure of water to a summer peak. For the year 1956, the total amounts of evaporation for zones A, B, and C are respectively, 93, 102, and 68 cm/year, obtained by summing the area under the appropriate evaporation curve in Figure 6*b*. This compares with a mean 115 cm/year for the whole North Atlantic [*Jacobs*, 1951]. The difference between zones A and B is probably not real, but the much lower value for zone C is in line with the general trend of northward decrease in evaporation from latitude 20° to 25°.

(E — P) for 1956. We shall now inquire into the difference between evaporation and precipitation for 1956, when the salinity of the coastal water was most pronounced. We consider the period February 3 to May 29 between University of Miami cruises 5604 and 5613 and the period May 30 to August 29 between University of Miami cruises 5613 and 5616. We approximate the precipitation for these periods in zones A, B, and C by the amount measured by the U. S. Weather Bureau at Key West, Ft. Myers, and Tampa, respectively. The t evaporation and precipitation and their sta ard errors for the periods for the three zo are given in Table 4, columns 3 and 4.

Roden [1959] discussed the errors in computation of evaporation from equatio He accepted the theory as correct and con ered the effect of data reliability and the m nitude of random and systematic errors. For computed rate of exchange of sensible heat almost entirely to evaporation, he arrived total error of about 40 per cent, which we h accepted as the standard error of our com tation as shown in Table 4.

Error in precipitation is due mostly to e in extrapolation beyond the immediate vici of measurement. Since there are no orogra effects and there is no strong current origi ing from a distant source in the area of inte extrapolation of seasonal rainfall from coa stations to the immediately adjacent w areas appears reasonable and may involv standard error of no more than 20 per c This error is shown in Table 4.

We define the standard error of (E — P) the square root of the sum of the error v ances of E and P. On this basis, the magni of (E — P) for the indicated periods is g in Table 4, column 5.

(E — P) and observed salinity. Even in absence of evaporation data, a qualitative tion can be established between salinity and cipitation (hence runoff).

1955 was a year of minor drought at Myers and Key West, but of normal rai at Tampa. According to Figure 2 for C 5502, the salinity was normal off Tampa, v off Boca Grande and Cape Romano it wa excess of 36.6 per mil.

1949 was a year of near normal rainfa Ft. Myers. The Fish and Wildlife Service t sects off Boca Grande in that year show Table 1) nearshore salinity (stations 4 an lower than those for the corresponding se in 1950 when minor drought conditions vailed at Ft. Myers.

1956 was a year of severe drought which on the heels of the minor 1955 drought, as we have seen, coastal water with salini excess of 36.6 per mil was very extensive.

However, a qualitative relation between cipitation and salinity cannot answer the

TABLE 3. Tabulation of Stations Whose Data are Used in Evaporation Computation

es	5502 July 20–29, 1955	5513 Oct. 22–Nov. 1, 1955	5604 Jan. 25–Feb. 3, 1956	5613 May 29–June 6, 1956	5616 Aug. 25–Sept. 1, 1956	5624 Dec. 11–17, 1956	5703 Mar. 19–28, 1957	5710 May 17–29, 1957
				Station Numbers				
	1–9	1–13	1–2	1–14	1–21	1–28		1–5, 192–194
		130–138	155–165			179–180	1–13	161–172
	22–28	14–29	138–146	63–73	33–61	38–74	14–35	154–160
		122–129				140–159		38–47
	51–61	30–49	120–129	79–84	62–67	75–95*	36–49	129–145
	117–121	116–121	51–72		80–92	109–134		86–94

ncluding 22 observations at an anchor station.

ant question of whether the observed exten- body of highly saline water was generated ely locally, was obtained entirely by advec- or was formed in part locally and in part dvection. The $(E - P)$ data in Table 4 ate that most of the highly saline water n of Cape Romano was advected into the n from the south, where evaporation ex- d precipitation by a considerable amount. area of formation of high-salinity water ars to be triangular in shape, delineated by e southward from Cape Romano to Key , the chain of Florida Keys, and the south- shore of the Florida mainland. This area includes the relatively stagnant Florida There are no published salinity data for ay proper, but the Fish and Wildlife Serv- ata given in Figure 4 for two stations at estern edge of the bay indicate that it was ervoir of high-salinity water in the sum- of 1956.

teral eddy diffusion. We are now in a on to estimate the magnitude of the lateral diffusion and to assess one aspect of a Red theory.

the mass of highly saline water moves ward from its primary region of formation e south, its salinity change may be de- d by the equation

$$Dt) = K(d^2s/dx^2) + (s_0/H)(E - P) \quad (2)$$

left-hand term is the salinity change fol- g the individual mass. The first right-hand is the lateral diffusion with constant lateral diffusivity K. The last term is the salinity e caused by $(E - P)$ in water of original y s_0 and of depth H to which the effect of $P)$ extends.

did not follow the high-salinity water. However, current measurements reported by Chew (in preparation) indicate a northward coastal movement of about 5 cm/sec. If we assume this speed to hold throughout the region of interest, it is possible to evaluate the magnitudes of the different factors in (2) and incidentally to determine K.

We evaluate (Ds/Dt) from observations on successive cruises. On May 29, 1956, during cruise 5613, the salinity in a large region northwest of Key West was found to be 37.5 per mil. If this water mass moved northward at 4.5 km/day, then 92 days later, on August 29, 1956, it would have reached a position 414 km downstream. At that position and on that day, during cruise 5616, the salinity was also found to be 37.5 per mil. Hence (Ds/Dt) is zero; this is so even if the mean speed of the water mass differs from that assumed by 20 per cent because of the large extent of the 37.5 per mil masses at both termini.

We evaluate the $(E - P)$ term in (2) with the help of the computed values in Table 4, column 5. The average depth of the total water column in the highly saline region is about 1000 cm. However, the average depth to which the effect of $(E - P)$ penetrates is probably less and may lie between 500 and 1000 cm. For the period May 30 to August 29, 1956, the magnitudes of the $(E - P)$ term in (2), for s_0 equals 37.5 per mil and H equals 500 cm, are given in Table 4, column 6.

Since the highly saline mass passed through the three zones, we may assume the mean of column 6 in Table 4 to apply. That is, the mass of 37.5 per mil salinity water, located just northwest of Key West on May 29, 1956, on passing through the three zones to reach a position 414 km downstream was subjected to a desiccating

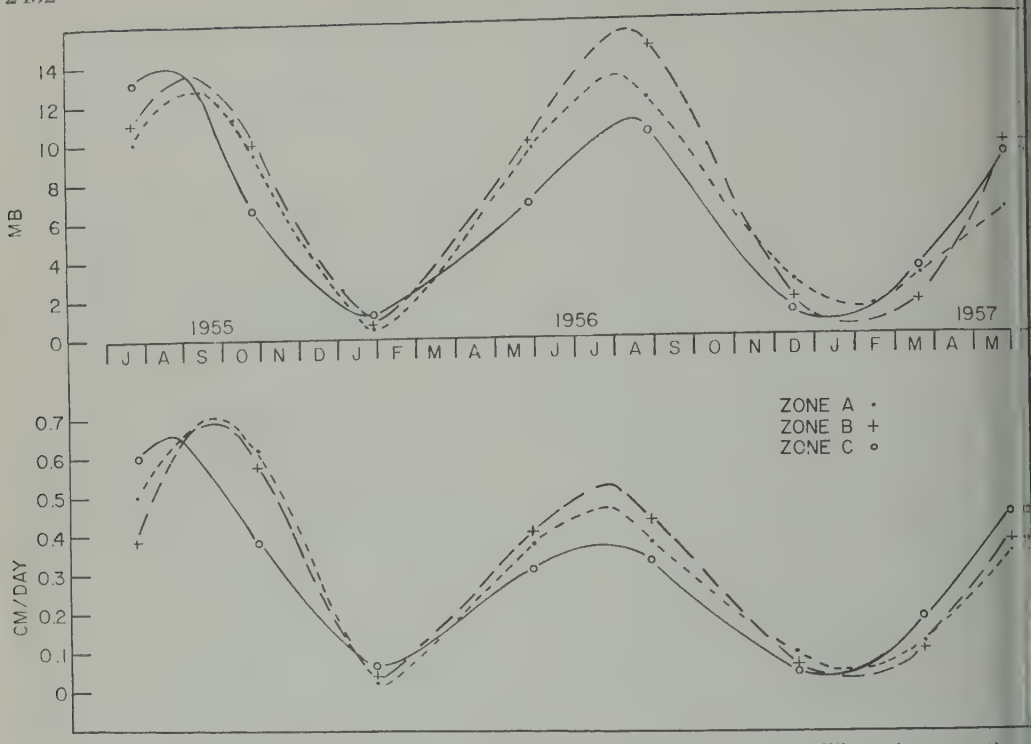


Fig. 6. *a*. (Upper part) Computed vapor pressure difference ($e_w - e_a$), in millibars, between the sea surface and the air. *b*. (Lower part) Computed evaporation in 0.1 cm/day.

process of net evaporation which increased the salinity by an amount (1.5 ± 0.8) per mil in 92 days, if H is 500 cm.

We evaluate the surface salinity profiles along three ship tracks and obtain the factors in the diffusion term in (2). The values are listed in Table 5. If H is much closer to 10 m, the magnitude of K is halved. Thus K is of the order of 1.5 to 4 × 10^5, or about ¼ to ½ of that for the California current [*Mao*, 1951], perhaps an equally sluggish but a much wider coastal current under the action of greater wind stress.

Chew [1955], in an earlier study of the circulation in this Red Tide region, suggested a convergence mechanism whose efficacy was premised on an eddy diffusion of small magnitude. The diffusion result of the present study furnishes a mean to assess the effect on the postulated convergence. Let us follow a unit surface cube embedded in the 37.5 per mil water mass located in the northwest vicinity of Key West, considered in the first portion of this section. Moving northward slowly, the cube gained in salinity from an excess of evaporation over precipitation. The total gain en rc amounted to 1.5 per mil. However, this gai not retained but is dissipated by turbulent n ing with the less saline water to the west. the end of the 92-day journey, therefore, net salinity change of the cube is zero. The saline water to the west is taken at 35.5 mil; hence, en route, the original cube n have mixed with a quantity of 35.5 per mil ter amounting to 0.75 of its initial value.

The net effect of the above turbulent di sion may be considered from another poin view. Let the thickness of the unit surface c be held constant. The diffusion effect on salinity of the cube is equivalent to sprea uniformly the extra salts (1.5 per mil) ca by evaporation over an additional horizo area of 0.75 of its initial value. In other wo the diffusion effect may be considered as equ lent to a horizontal divergence of area of 75 cent in 92 days.

The intensity of the horizontal converg postulated by Chew amounts to a reductio 1/5 of its initial horizontal area in 40 d

TABLE 4. The Magnitudes of E, P, $(E - P)$, and $(E - P)(s_0/H)$

ne	Date	E, cm	P, cm	$(E - P)$, cm	$(E - P)(s_0/H)$, salinity
A	1	23 ± 8.6	10 ± 2.0	13 ± 8.8	
	2	39 ± 15.6	8 ± 1.6	31 ± 15.7	2.3 ± 1.2
B	1	29 ± 11.6	24 ± 4.8	5 ± 12.6	
	2	41 ± 16.2	44 ± 8.8	3 ± 18.4	1.2 ± 0.6
C	1	19 ± 7.6	13 ± 2.6	6 ± 8.8	
	2	30 ± 12.0	33 ± 6.6	3 ± 13.7	0.9 ± 0.5

eb. 3 to May 29, 1956.
Iay 30 to Aug. 29, 1956.

the divergence equivalent of diffusion and ılated convergence can be considered to be ive, we may first allow the divergence to ıte. A unit surface area at the end of 40 is expanded by diffusion by (40/92) (0.75) per cent, or expanded to a total horizontal of 1.33. On the other hand, convergence ces the area of 1.33 to (1.33/5) or 0.27 at nd of 40 days. If diffusion is increased by ıer cent, the final area after convergence is 5) or 0.34 of the initial area. It thus ap- that lateral eddy diffusion does not sig- ntly reduce the efficacy of the postulated rgence mechanism. A related conclusion of egligibility of lateral mixing is reached by *ing* [1958] in his study of halocline forma- in the North Pacific subarctic transition, e the current strength appears to be of the order as that of the north-going current

e less saline water offshore. We have seen the drought simplified the diffusion com- ion. We shall now see how this fortuitous ion permits another conclusion. *Parr* 5] and *Chew* [1955, 1959] have drawn tion to the offshore tongues of surface, less water some 90 to 180 km west of the la west coast. Indications of these tongues lso be seen in the Fish and Wildlife Serv- ata in Table 1; e.g., the surface salinity at ns 7 and 8, some 140 to 180 km offshore, ss than 34 per mil in August 1950. If these e tongues were derived primarily from ischarge of Florida west coast rivers south arwater, there ought to have been no sig- ntly large amount of them offshore during rought of 1956. Figure 1, however, shows ive regions of less saline water, and Table ws that stations 7 and 8 have a range of surface salinity greater than, and a minimum surface salinity less than, those observed at station 6, which is located farther inshore. The possibility of the low-salinity water at stations 7 and 8 having come directly from the east is thus very unlikely. We can conclude, therefore, that the offshore low-salinity tongues were not derived from the adjacent Florida west coast rivers.

Upwelling. Another conclusion can be drawn. In an attempt to explain the presence of a relatively saline 36.3 per mil water off Tampa Bay, *Parr* [1935] suggested both the possibilities of excess evaporation and of upwelling of a subsurface intrusion. But he favored the latter. He supposed that the prevalent summer easterlies, blowing from land to sea in this area, provided the energy to move the surface layer of coastal water seaward to be replaced by high-salinity subsurface water. This suggestion was accepted by several writers; among them, *Graham, Amison, and Marvin* [1954] attributed the sharp increases in total phosphorus toward the bottom of some water columns to this possible cause.

The easterly wind regime for May through August, 1956, was near normal. According to Parr, upwelling should then occur, bringing up water of salinity of about 36.3 per mil. But, as we have seen, observation indicated an exten-

TABLE 5. Values of Spatial Change in Salinity and Lateral Eddy Diffusivity

Cruise	Stations	(d^2s/dx^2), salinity/cm^2	K, cm^2/s
5613	57-65	-5.1×10^{-13}	$(3.7 \pm 2.0) \times 10^5$
5616	76-81	−6.3	(3.0 ± 1.6)
5616	64-71	−4.3	(3.9 ± 2.4)

sive body of water of salinity greater than 37.5 per mil. Since this highly saline tongue is also one of higher temperature, it cannot be argued that upwelling did occur but that the salinity of the upwelled water was increased by evaporation. In fact, relatively cold, upwelled water would have retarded evaporation, as is found off California [*Roden,* 1959]. Upwelling, therefore, is very improbable, as *Chew* [1955] concluded earlier on the basis of north-south advection in this area.

Conclusion. The high-salinity water in 1956 was an unusual phenomenon, at least in the sense that the drought associated with it was unusual. At Key West and Tampa the rainfall in 1956 was the lowest in their respective 50-year records. At Ft. Myers it was one of the three lowest for the same period. Immediate recurrence of the extensive body of high-salinity water is therefore not likely. It was a fortunate coincidence that the field work occurred at a time when nature was showing one of her vagaries. This permitted a simplification of an otherwise much more complex situation. It is pertinent to ask, however, how much one may safely extrapolate from a study of a simplified situation.

The extent of the high-salinity water, some 450 km long, 45 km wide, and 5 to 10 fathoms deep, is small in oceanographic scale. The climatic factors resulting in the high-salinity phenomenon appear to be largely local and therefore are very unlikely to have any significant effect on the Loop Current which supplies the primary motional energy to the northward coastal current (Chew, in preparation). The conclusions regarding the magnitude of the horizontal eddy diffusivity, the source of the less saline tongues offshore, the implausibility of upwelling, and the average width of the current, however, can be applied to most situations in this area.

References

Bumpus, D. F., The circulation over the continental shelf south of Cape Hatteras, *Trans. Am. Geophys. Union, 36*(4), 501–611, 1955.

Chew, Frank, On the offshore circulation and a convergence mechanism in Red Tide region off the Florida west coast, *Trans. Am. Geophys. Union, 36*(6), 963–974, 1955.

Chew, F., S. J. Bein, and J. H. G. Stimson, A report of Florida gulf coast cruises, Marine University of Miami, Miami, Florida, Refer 59–1, mimeographed, Submitted to the offi Naval Research, 109 pp., 1959.

Ewing, G., and E. D. McAlister, On the the boundary layer of the ocean, *Science, 131*(3 1374–1376, 1960.

Finucane, J. H., and A. Dragovich, Counts of Tide organisms *Gymondinium breve* and as ated oceanographic data from Florida west c 1954–57, *U. S. Fish and Wildlife Serv., Spec Rept. 289,* 1959.

Fleming, R. H., Notes concerning the haloclin the northeastern Pacific Ocean, *J. Marine search, Sears Foundation, 17,* 158–173, 1958.

Graham, H. W., J. M. Amison, and K. T. Ma Phosphorus content of waters along the coast of Florida, *U. S. Fish Wildlife Serv., Sci. Rept. 289,* 1954.

Gunter, G., R. H. Williams, C. C. Davis, F. G. W. Smith, Catastrophic mass mortali marine animals and coincident phytoplan bloom on the west coast of Florida, Nove 1946–August 1947, *Ecol. Monograph 18,* 309 1948.

Jacobs, W. C., The energy exchange betwee and atmosphere and some of its consequer *Bull. Scripps Inst. Oceanog., Univ. Calif.,* 27–122, 1951.

Mao, H. L., Eddy diffusivity coefficient of P water off the California coast, determine statistical parameters of hydrodynamic e tions, Doctoral thesis, Scripps Institutio Oceanography, (unpublished), 1951.

Marvin, K. T., Oceanographic observations in coast Florida waters, 1949–52, *U. S. Fish Wil Serv., Spec. Sci. Rept. 149,* 1955.

Parr, A. E., Report on hydrographic observa in the Gulf of Mexico and the adjacent st made during the Yale Oceanographic Exped on the *Mabel Taylor* in 1932, *Bull. Bing Oceanog. Collection, Yale Univ., 5*(1), 1–93,

Roden, G. I., On the heat and salt balance o California current region, *J. Marine Rese Sears Foundation, 18*(1), 36–61, 1959.

Roden, G. I., and G. W. Groves, Recent oce graphic investigation in the Gulf of Califo *J. Marine Research, Sears Foundation,* 10–35, 1959.

U. S. Geological Survey, Surface water supp the U. S., 1956, *U. S. Geol. Survey Water Su Paper 1434, part 2-B,* U. S. Govt. Printing O Washington, D. C., 1958.

Wüst, G., Oberflächensalzehalt, Verdunstung Niederschlag auf dem Weltmeere, *Länderk liche Forschung,* Festschrift Norbert Krebs, 359, 1936.

(Manuscript received February 25, 1961 revised May 3, 1961.)

Some Experiments in Dispersion

JACOB BEAR

Technion–Israel Institute of Technology
Haifa, Israel

Abstract. The aim of the experiments was to study the tracer distribution caused by dispersion in one- and two-dimensional fields of flow and to compare the experimental results with the theoretical formulas developed previously by the author [*Bear*, 1961; also *Bear and Todd*, 1960]. Two models were employed: a one-dimensional sand column and a two-dimensional Christiansen filter. It has been experimentally verified that the growth of the transition zone which develops when an initially abrupt interface is displaced from its original position depends upon the path of the mean point and is independent of the flow velocity. The variance which was used to define the tracer concentration distribution was shown to be directly proportional to the total distance traveled by the mean point of the distribution. The constant of dispersion of the porous medium was determined experimentally. The effect of the lateral constant of dispersion for cases where the interface makes an angle with the direction of the uniform flow was demonstrated. Experimental results agree with theory.

INTRODUCTION

he general approach to the problem of dis-ion in porous media has been previously dis-ed by the author [*Bear*, 1961] and need not epeated here. It is the purpose of the present er to describe experimental work carried out erify some of the ideas expressed in the first er.

xperiments were performed on two models: ne-dimensional sand column and a two-ensional Christiansen filter. In the two fol-ng sections the apparatus for each model, measuring techniques, and the results of the ous tests are described.

he one-dimensional sand column was used nly to show that the tracer-concentration ribution resulting from the movement of an ally abrupt interface depends only upon the l distance traveled. Special attention was n to the case of a fluctuating velocity field. Christiansen filter was used to study the ersion of a point injection in a uniform uni-ctional as well as in a fluctuating field of . It was also used to study the transition which develops at an interface making an e with the direction of the flow.

COLUMN DISPERSION

pparatus. The experiments were conducted 4-inch Lucite column packed with clean wa sand. Figures 1 and 2 show the general appearance of the column and accessories. The Ottawa sand consisted of spherical quartz grains having a Hazen uniformity coefficient of 1.30 and an effective grain size of 0.45 mm. The intrinsic permeability of the sand in the column was experimentally determined to be 229 darcys (hydraulic conductivity of 0.22 cm/sec).

Fluids used in the dispersion tests were tap water with approximately 18 ppm total dissolved solids and a solution of sodium chloride in tap water at a concentration of 200 to 500 ppm. By subtracting the background concentration from readings of both displaced and displacing fluids, the relative concentration, C/C_0 (with C being the instantaneous concentration of the tracer and C_0 the constant concentration of the liquid in the voids), at a given point was obtained. Special techniques were used to avoid entrapment of air while filling the column.

The column consisted of three parts: a lower reservoir (to insure uniform outflow from the column), the sand column with a net length of 110.6 cm between the two screens, and an upper reservoir. The upper reservoir provided a uniform abrupt front over the column's cross section when the displacing fluid was introduced from above into the saturated sand column. A unidirectional or fluctuating flow could be maintained at any desired rate by means of two constant-head reservoirs.

Electric probes were used to measure concentrations in the sand column. The advantage of

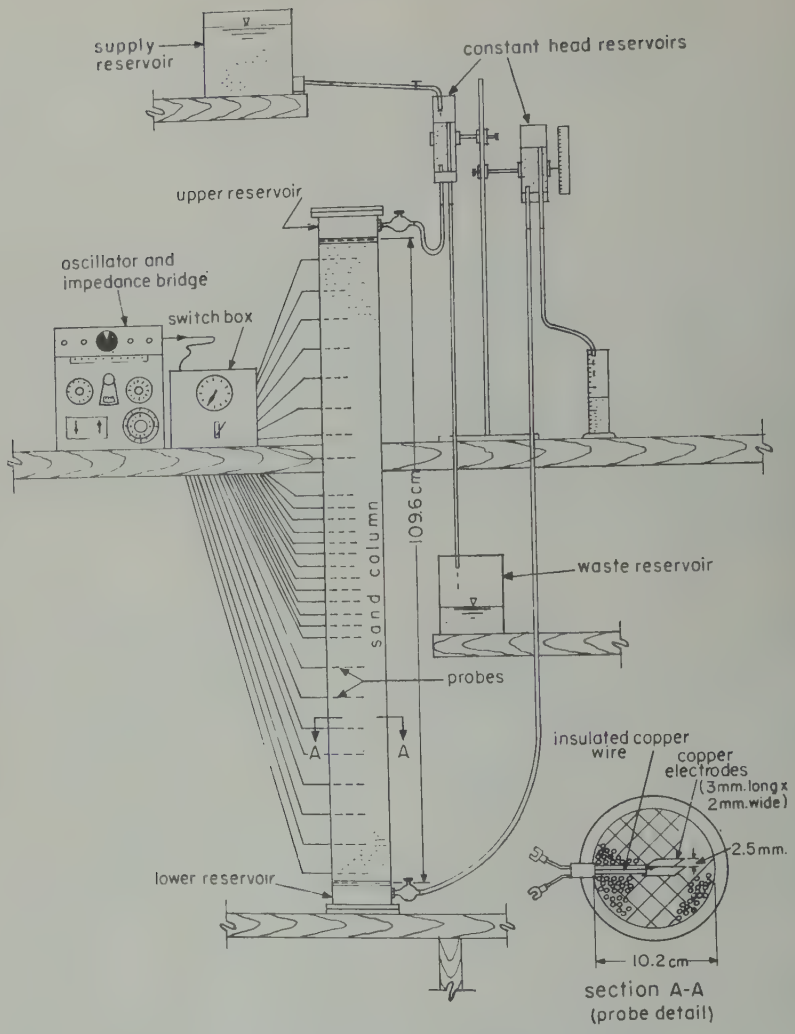


Fig. 1. Schematic diagram of sand column and accessories.

using electric measurements *in situ* is that there is no need to extract volumetric samples, thus disturbing the flow pattern, and that results are obtained faster than by chemical determinations.

The probes were made of two insulated copper wires 1.5 mm in diameter, flattened at the ends to form a plane approximately 2 mm wide and 3.5 mm long. The two planes were fixed parallel to each other at a distance of 2.5 mm apart. The two outside surfaces were insulated by coating. The probes were inserted into the column with the planes in the direction of the flow (Fig. 1) and with sand grains filling the space between the electrodes. Twenty-nine such probes were inserted into the sand column along longitudinal axis. Spacings were 1.7 cm in central part of the column, increasing to 5.0 near the ends of the column.

The probes were connected to the electric cuit by a multiple switch. An oscillator ampli was used as a 12-volt 1000-cps current sup High frequency was used to avoid polarizat Resistance readings (from 1 to 100,000 oh were made on an impedance bridge with an curacy of ± 0.5 per cent.

The resistance to the flow of electric cur between the two electrodes of each probe pends upon the electric conductivity of



g. 2. Photograph of sand column assembly.

ium between them. The latter, in turn, de-
ls upon the concentration of the solution in
pores. The size and geometry of the probes
of the (nonconductive) sand grains sur-
nding them determine the relationship be-
en the resistance at the probe and the re-
vity of the fluid, the total resistance being
portional to the resistivity. Because of varia-
s in size of electrodes and in the geometry
he solid matrix between the electrodes, the
o of resistivity to resistance, ρ/R, had to be
rmined separately for each probe as part of
calibration procedure. The resistivity was
related to the NaCl concentration by
dard curves available in the literature (e.g.,
ternational Critical Tables, vol. 6).
ne probes, owing to their shape, measure the
resistivity of the fluid in the sand pores
een the electrodes and are almost unaffected
oncentrations in the neighborhood. There-
the concentration distribution along the
nn can be determined at any instant by
ltaneous readings. Actually, this was done
topping the flow and quickly taking resist-
readings at the various probes. Most pre-
investigators have measured the time
tion of concentration at the end of a sand

column. It should be noted that the two curves, C/C_0 against distance traveled along the column and C/C_0 against length of flow as obtained by converting time (at one point) to distance, are not the same. However, because the slopes of the curves at $C/C_0 = 0.5$ happen to be the same, both can be used for the determination of the constant of dispersion. Only spatial variations of concentration are considered in the present work.

Procedure. Two types of tests were conducted in the sand column. In the first, the sand column was initially saturated with a salt solution and then a front of tap water was translated through the column causing a transition zone to be developed. In the second, the front, after passing the center of the column, was allowed to fluctuate several times at various amplitudes. Test a-1, shown in Table 1, serves as an example for both types of tests. Its first part describes the development of a transition zone in a unidirectional flow, while its later stages show the transition zone developed by a fluctuating flow. These stages are described in Table 2. Figure 3 is a graphical representation of the relative tracer distributions along the column for the given travel times.

Results. Results of the various tests were summarized in two graphs: total volume of flow against the total path traveled by the point at which $C/C_0 = 0.5$, and the variance, σ^2, of the resulting tracer distribution against the total path. Both were found to be linear relationships. This linear relationship is also true for the fluctuating case and thus confirms the statement [*Bear*, 1961] that the dispersion for the one-dimensional case depends only on the total path and the variance of the normal distribution (gaussian distribution) which approximately describes the tracer concentration distribution is directly proportional to this total path. Figure 4 shows these results for test a-1. The computed porosity is

$$P = \frac{\text{total displaced volume}}{\text{total path} \times \text{cross-sectional area}}$$

$$= \frac{4760}{176 \times 81} = 33.4 \text{ per cent}$$

as compared with 34.3 per cent obtained by weight and volume measurements. The values of the standard deviation σ were obtained from the curves of Figure 3 by taking half the distance

TABLE 1. Relative Concentrations for Test a-1

Probe No.	Distance, cm	ρ/R, cm	C/C_0, %				
			a	*b*	*c*	*d*	*e*
4	17.0	0.488	0.3	0.3	0.0	0.0	0.0
5	22.5	0.449	0.0	0.0	0.0	0.0	0.0
6	27.5	0.532	0.3	0.8	0.5	0.5	0.3
7	33.0	0.511	0.3	0.8	0.3	0.5	0.3
8	37.7	0.388	0.3	1.3	0.3	0.3	0.3
9	43.0	0.565	0.5	17.5	0.5	1.0	0.5
10	45.5	0.426	0.3	42.3	0.5	1.3	0.8
11	48.2	0.507	0.8	68.6	1.0	3.7	2.0
12	49.7	0.387	2.2	85.3	4.2	9.4	4.7
13	51.5	0.611	3.5	96.3	10.6	21.5	10.9
14	53.6	0.415	9.5	98.8	20.2	38.5	19.8
15	55.4	0.517	21.7	98.8	37.8	53.2	34.8
16	57.2	0.513	50.3	98.8	58.8	72.2	53.1
17	59.3	0.451	78.0	100.0	77.8	85.0	69.2
18	61.3	0.417	94.5		92.4	91.5	84.5
19	63.2	0.369	94.5		98.7	98.0	92.6
20	65.4	0.541	98.7		99.0	99.0	97.4
21	68.2	0.446	98.7		96.8	98.5	96.4
22	73.4	0.456	100.0				97.0
23	78.2	0.404	97.5				98.5
24	83.3	0.401	98.7				
25	88.6	0.390	100.0				

Average velocity of flow: 1.6 cm/min.
a, *b*, *c*, *d*, *e* are travel times shown in Figure 3.

between the points of relative tracer concentration 15.9 and 84.1 per cent. This was done because the slope of the curves at the 50 per cent point was not well defined. These two values, 15.9 and 84.1 per cent, are the values of the normal distribution at $\pm\sigma$. The constant of dispersion was found to be

$$D_l = \frac{\text{increase of variance}}{2 \times \text{total path}} = \frac{19.4 - 1.5 = 0.051}{2 \times 176}$$

where 1.5 is the value of the variance at $L =$ caused by the fact that the initial interface w

TABLE 2. Summary of Results of Test a-1

Direction	ΔV, cm³	V, cm³	ΔL_{50}, cm	L_{50}, cm		L, cm	σ, cm	σ^2, cm²	No. Curve
				Computed	Test				
Down	1545	1545	57.2	57.2	57.2	57.2	2.7	7.3	*a*
Down	350	1895	13.0	70.2		70.2			
Up	653	2548	24.2	46.0	46.2	94.4	3.4	11.6	*b*
Up	297	2845	10.5	35.3		104.9			
Down	575	3420	21.3	56.8	56.4	126.2	3.8	14.5	*c*
Down	310	3730	11.5	68.3		137.7			
Up	355	4085	13.2	55.1	55.1	150.9	4.1	16.8	*d*
Up	325	4410	12.1	43.0		163.0			
Down	350	4760	13.0	56.0	56.9	176.0	4.4	19.4	*e*

ΔV = incremental flow volume.
V = total flow volume.
ΔL_{50} = increment in position of point at which $C/C_0 = 50\%$.
L_{50} = position of 50% point.
L = total path (computed).

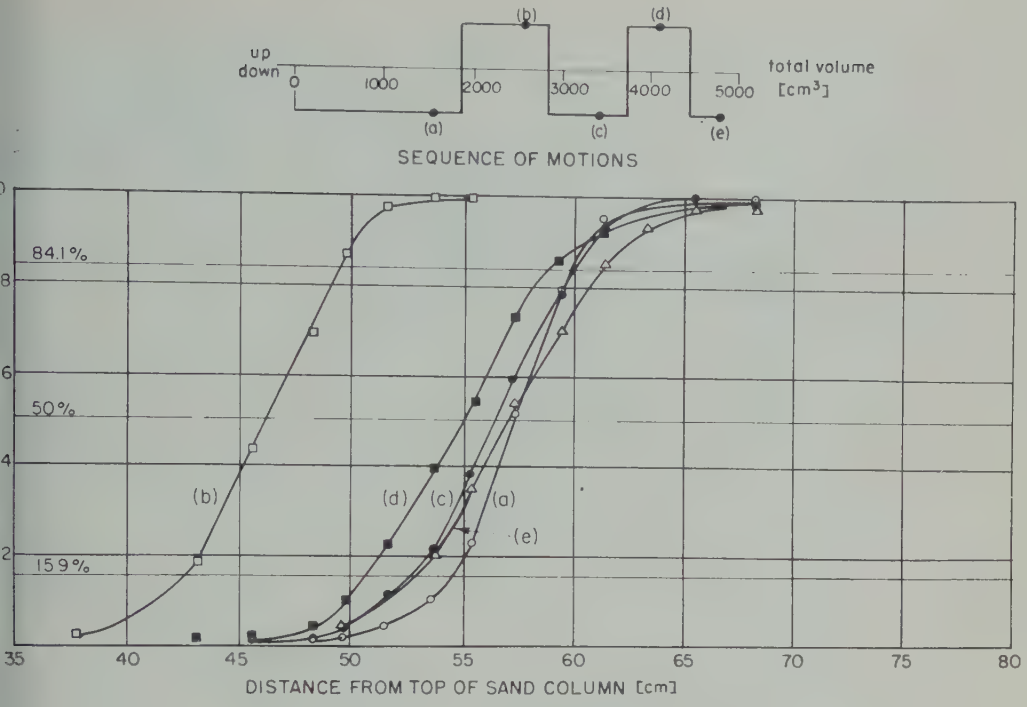


Fig. 3. Relative tracer concentrations for test a-1.

abrupt. Similar results were obtained in other s with the same sand packing.

Two-Dimensional Model

pparatus. The experiments were conducted a two-dimensional Christiansen filter. The istiansen filter is a tank with glass or Lucite walls packed with ground glass of a known grain size distribution representing the porous structure of the prototype. When the porous medium is completely saturated with a fluid which has the same refractive index as the medium, the latter becomes transparent at the laboratory temperature. Light transmission is restricted,

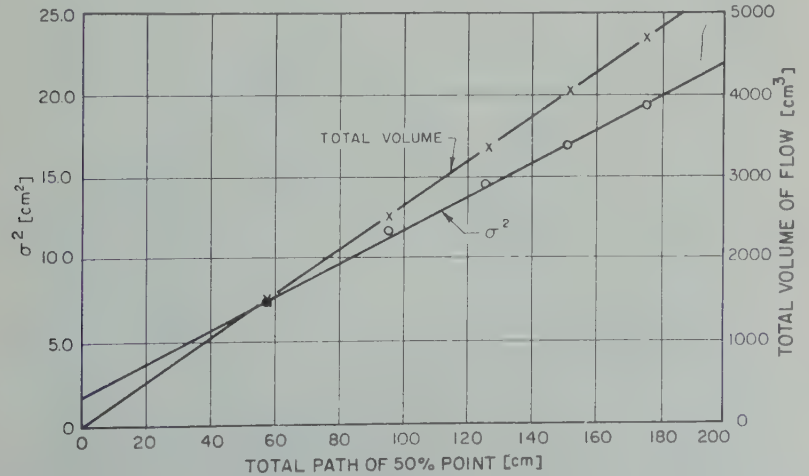


Fig. 4. Relations of total volume flow and variance to total path of 50 per cent concentration point for test a-1.

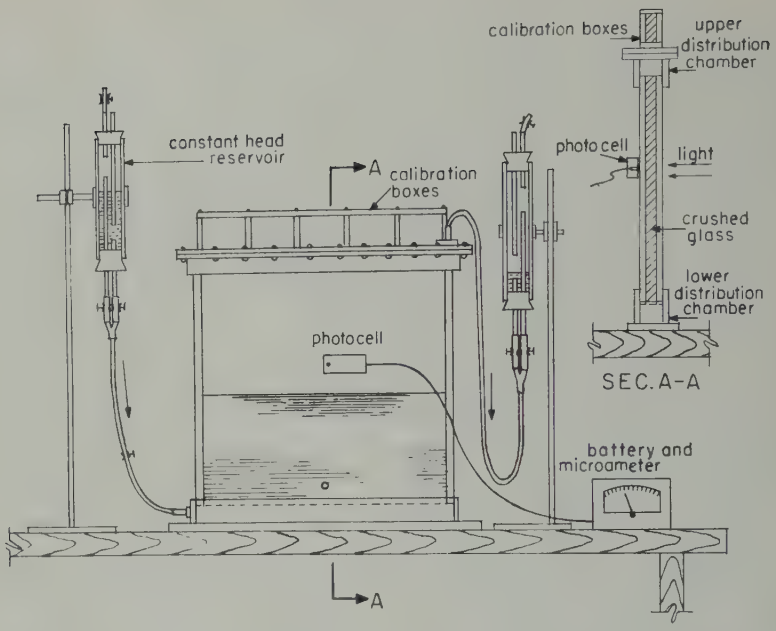


Fig. 5. Schematic diagram of two-dimensional Christiansen filter.

however, to a narrow range of wavelengths. This range shifts if the temperature of the liquid is changed. Satisfactory, though less accurate, results are also obtained in ordinary white light instead of monochromatic light.

When the flow of two miscible fluids is studi one of the components is marked with a d thus allowing concentration profiles in the mi ing zone to be mapped. In a similar way, three-dimensional field of flow can be stud

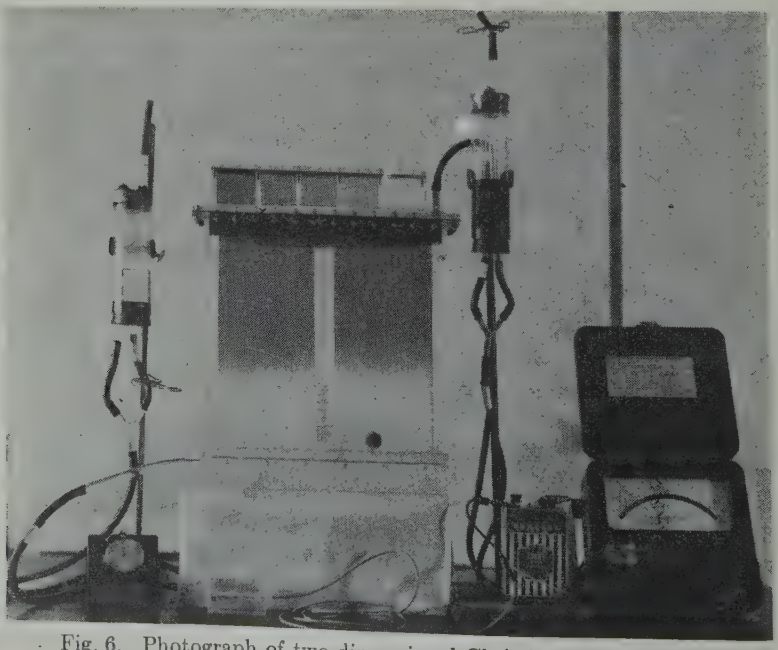


Fig. 6. Photograph of two-dimensional Christiansen filter setup.

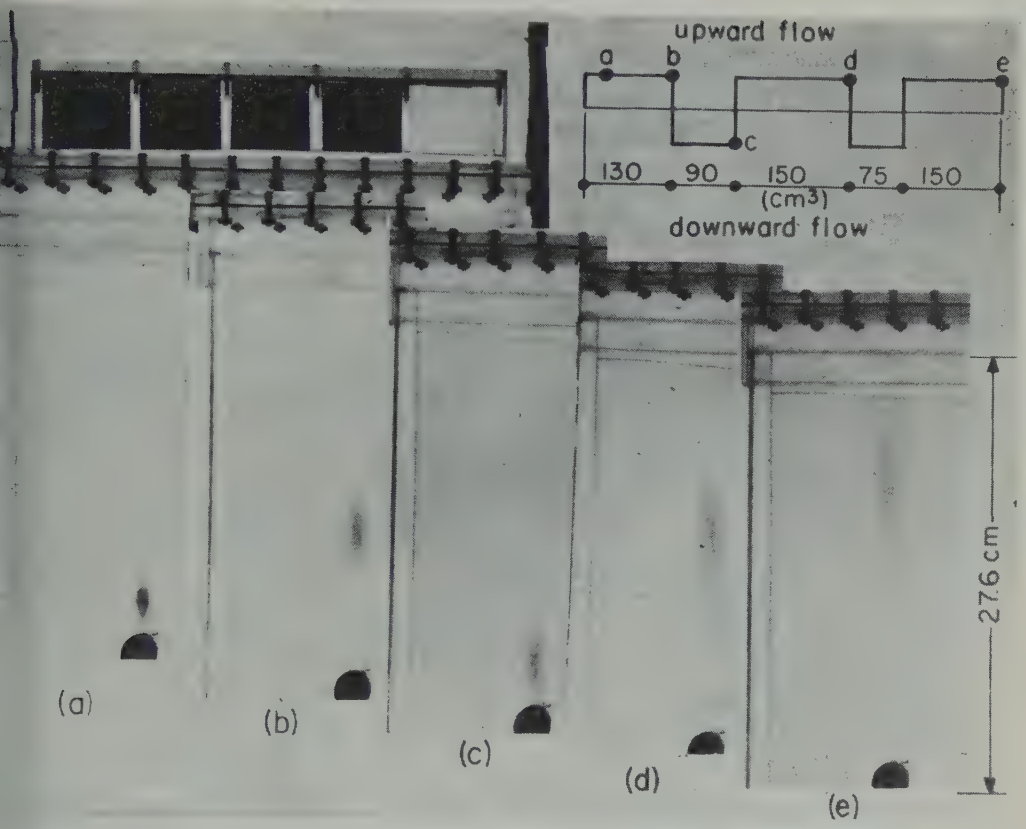


Fig. 7. Dispersion of a point tracer injection subjected to a fluctuating velocity (test b-1).

ally. Various devices can be used for detect-hanges in tracer (dye) concentration in one- two-dimensional models. In a common iod use is made of a photoelectric cell, the tance of which changes according to the in-ty of light which reaches it. When a beam onstant parallel light passes through the el, its intensity is reduced by the dyed fluid. e changes are recorded as changes in the sity of electric current when the photo-ric cell is operating under a constant volt-Measurements are made with a microam-r. A constant temperature is very important ise the refractive index is very sensitive to ges in temperature. Information on the tiansen filter has been published by, among s, *Van Meurs* [1957] and *Deutsch* [1960]. ilar model was also used by *de Josselin de* [1958] for dispersion studies.

e two-dimensional field of flow for the pres-nvestigations was simulated by a Lucite 27.6 cm high, 27.6 cm long, and 1.1 cm thick (inside dimensions), filled with crushed Pyrex glass. By means of two chambers at the top and bottom of the model and two constant-head reservoirs, a uniform field of flow in either direction can be maintained in the model at any desired velocity. Views of the model are given in Figures 5 and 6.

The refractive index of the glass was 1.4720. The liquids used in the experiments were aqueous solutions of $ZnCl_2$. The refractive index of the solution was adjusted to 1.4710 to 1.4720 with a density of 1.748 to 1.755. About 61 per cent $ZnCl_2$ by weight was needed to obtain the required refractive index at the prevailing laboratory temperature. The tracer solution was identified by adding 0.3 per cent by volume of green food coloring to the $ZnCl_2$ solution. This addition did not change the refractive index appreciably, but slightly reduced the tracer's density. The density was readjusted by adding $ZnCl_2$.

A Clairex cadmium sulfide photoconductive

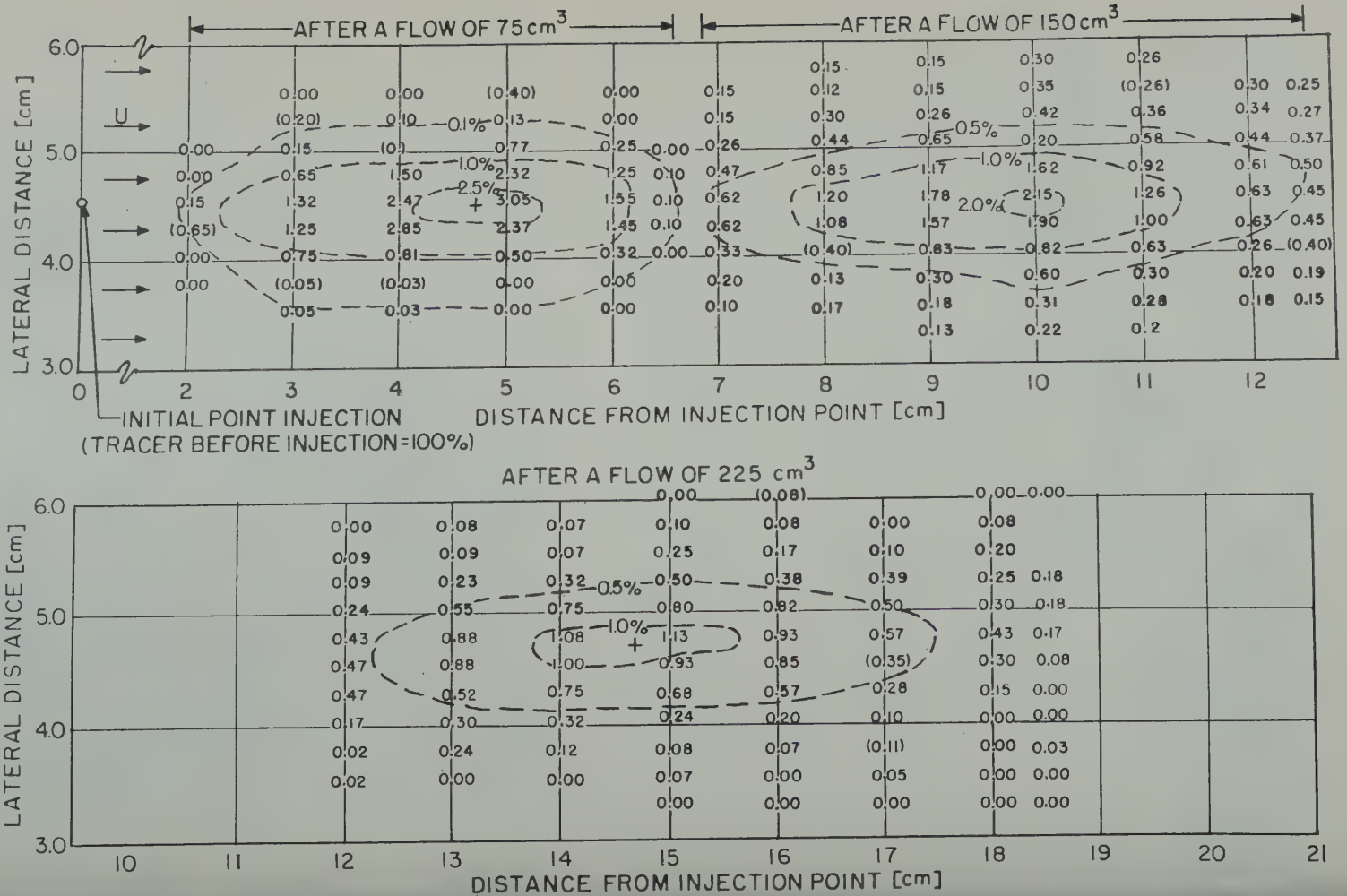


Fig. 8. Tracer distribution resulting from a point injection (test b-2).

ype CL-2P, with a 4-mm light inlet was or detecting changes in the tracer concen-n. A No. 2 photoflood light at a distance m was used as a light source. The photo-ic cell was connected to a 22.5-volt battery sensitive microammeter. The photoelectric as moved on a fixed coordinate system at ack of the model and current readings were on the microammeter.

tead of a general relationship between cur-nd tracer concentration, which would take nt of light-intensity and temperature vari-, a separate calibration curve was deter- experimentally for each set of readings. was done by using five boxes of the same ial as the model, with the same thickness acked with the same crushed glass. These were filled with known tracer concentra- and their microammeter readings were at the beginning and at the end of each readings (see Fig. 5). The calibration thus obtained was then used for that par- set of readings. The boxes were placed same plane as the model itself and were ted to the same light conditions.

cedure. Three types of experiments were cted in the two-dimensional model: dis-n from a point injection, dispersion at an ace in a unidirectional and/or a fluc-g field of flow, and dispersion at an ace which is not perpendicular to the direc-f the flow in a unidirectional and/or a fluc-g field of flow. In all cases, the field of as uniform, i.e., a constant velocity along the flow cross section. Some representative tests are described below.

Test b-1. Dispersion from a point injection subjected to a fluctuating velocity. The field of flow was subjected to a sequence of upward and downward movements at a velocity of 0.32 cm/min. Figure 7 shows a set of photographs taken during these tests.

Test b-2. Dispersion from a point injection in a unidirectional field of flow with an average velocity of 0.33 cm/min. Figure 8 shows relative tracer concentration and a few lines of equal concentration.

Test b-4. Dispersion at an interface which is perpendicular to the fluctuating field of flow. The lower half of the model was filled with a colorless fluid while the upper half, with an almost abrupt interface between them, was saturated with dyed fluid. Readings were taken along vertical lines at $\frac{1}{3}$ and $\frac{2}{3}$ of the model's width and were averaged to yield the position of the interface and the tracer concentration distribution across the transition zone at the various stages of the flow as shown in Figure 9. Average velocity during the fluctuations was 0.47 cm/min. (absolute value). The first part of the test can serve as an example of a test with unidirectional flow. The sequence of curves shown in Figure 9 corresponds to (*A*) the initial position of the interface, (*B*) after a flow of 25 cm³ downward, (*C*) after additional flow of 25 cm³, (*D*) after additional flow of 25 cm³ downward, (*E*) after addition flow of 75 cm³ upward, (*F*) after additional flow of 50 cm³ upward, (*G*)

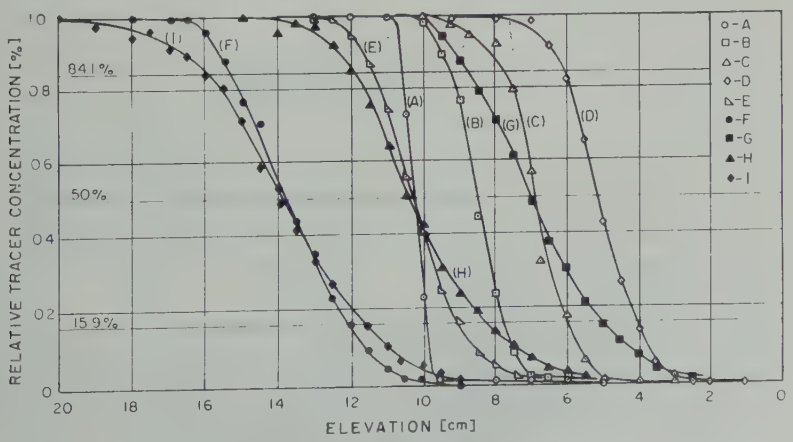


Fig. 9. Tracer concentration distribution for fluctuating flow (test b-4).



Fig. 10. Interface at an angle to the direction of flow (test b-6).

after additional flow of 100 cm³ downward, (*H*) after additional flow of 50 cm³ upward and (*I*) after an additional flow of 50 cm³ upward.

Test b-6. Dispersion at an interface which is not perpendicular to the direction of the flow in a uniform fluctuating velocity field. An abrupt interface which makes an angle of 53° with the direction of the flow (see Fig. 10) was introduced into the model. The transition zone which developed by the fluctuating velocity field was measured along lines perpendicular to the initial interface and average values were computed for relative tracer concentrations. These are shown in Figure 11. To avoid the turning of the interface owing to a slight density difference, the interface was kept horizontal with the poten gradient making an angle of 53° with it.

Results. Tests b-1 and b-2 yielded infor tion about the manner in which a tracer p injection is dispersed in a uniform field of f According to *de Josselin de Jong* [1958], concentration distribution of a tracer point jection at concentration C_0 around a point (g which is displaced a distance $L = ut$ in the rection of the uniform two-dimensional fiel flow from its original position (x_0, y_0) is given

$$C(x, y; x_0, y_0) = \frac{C_0 N}{2\pi\sigma_x\sigma_y} \cdot \exp\left\{-\frac{m^2}{2\sigma_x^2} - \frac{n^2}{2\sigma_y^2}\right\}$$

where

u = uniform velocity of flow.
t = time of flow.
σ_x, σ_y = standard deviation of the distribu in the x and y directions, respecti
m, n = the coordinates of the point $(x,$ a coordinate system centered at (These are given by $m = x - (x_0 +$ $n = y - y_0$.
N = a unit area (e.g. 1 cm²).

The standard deviations are defined by

$$\sigma_x = (2D_I L)^{1/2}; \quad \sigma_y = (2\,D_{II} L)^{1/2}$$

where D_I and D_{II} (cm) are the longitudinal transverse constants of dispersion of the po media, respectively. D_I and D_{II} are prope of the porous medium only, and as such should be correlated to the medium prope

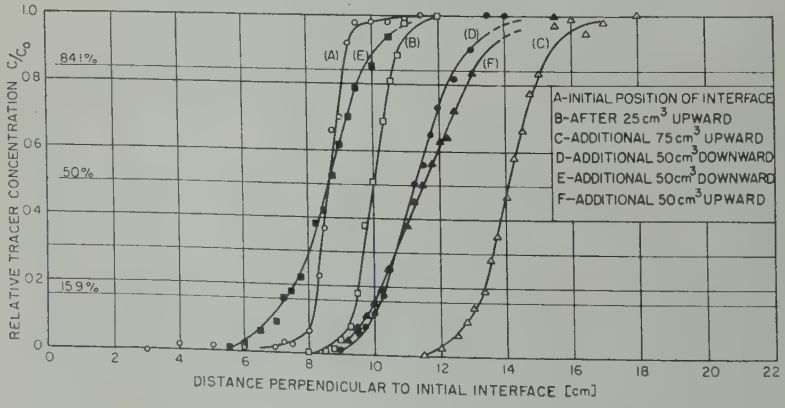


Fig. 11. Tracer concentration distribution for test b-6.

size and pore-size distributions, packing, Several attempts have been made to ine these correlations, but no final results t available.

n (1) it follows that lines of equal con- tion take the form of ellipses centered at splaced mean point and oriented with their axes in the direction of the flow. The on of an ellipse corresponding to a certain concentration is obtained by letting the sion under the exponential sign be equal ertain constant. If the major and minor re σ_x and σ_y, parallel to the x and y axes, tively, then the equation of this ellipse is

$$\frac{x^2}{\sigma_x^2} + \frac{y^2}{\sigma_y^2} = 1 \qquad (2)$$

ellipses are seen in Figure 8. The actual tracer concentration (theoretically 100 nt) is unknown because of the mixing that place during the injection process. The successive mean positions have the relative ntrations of 3.10 per cent (at 4.7 cm, ^{3}), 2.15 per cent (10.0 cm, 150 cm^3), and per cent (14.7 cm, 225 cm^3). Average ty obtained from the mean position is

$$\frac{\text{displaced volume}}{\text{path} \times \text{cross section}} = \frac{225}{14.7 \times 33.4}$$

$$= 45.8 \text{ per cent}$$

mpared with 46.3 per cent obtained by ring weights and volumes.

n (1) it follows that

$$L_1\left(\frac{C}{C_0}\right)_1 = L_2\left(\frac{C}{C_0}\right)_2 = \cdots \qquad (3)$$

get a rough estimate of the longitudinal dispersion constant. For this position $2\sigma_x = 2.7$ cm and $D_{\text{I}} = \sigma_x^2/2L = 0.062$ cm.

Finally, the ratio $D_{\text{I}}/D_{\text{II}}$ can be estimated from the ellipses of equal concentrations which have the common formula

$$\frac{m^2}{\sigma_x^2} + \frac{n^2}{\sigma_y^2} = E\frac{C}{C_0} \qquad (4)$$

where E is a constant which depends upon the particular value of tracer concentration under consideration. The ratio $D_{\text{I}}/D_{\text{II}}$ is given by the ratio of the major and minor axes of the various ellipses. From the ellipses of Figure 8 one obtains the values for $D_{\text{I}}/D_{\text{II}}$: 18.7, 20.5, 7.0, 18.5, 14.5, 22.7, and 22.0, with an average of 17.7. *Blackwell* [1959] mentions ratios of $D_{\text{I}}/D_{\text{II}}$ of up to 24. One should recall that molecular diffusion was neglected in the present work. This is justified in the present experiments by the fact that when an abrupt transition zone was left for a full week no change of concentration was observed. Nevertheless, molecular diffusion is the only mechanism which will cause mixing in a fluctuating flow.

The results of tests b–4 and b–6 are represented graphically in Figures 12 and 13. Two curves are used to summarize graphically the results of each test. One curve gives the relationship between the total volume of flow and the total distance traveled by the point of 50 per cent relative tracer concentration. It can be seen that this is a linear relationship. Similar results were obtained for all fluctuating flow tests.

The slope of this line, when the cross-sectional area is given, indicates the porosity of the porous medium. For example, for test b–6:

$$\text{ty} = \frac{\text{volume of flow}}{(\text{cross-sectional area}/\cos 37°) \times \text{path of 50\% point}} = \frac{200}{(31.5/\cos 37°) \times 10.9} = 46.5\%$$

rresponding values of $L_i(C/C_0)_i$ computed Figure 8 are 14.6 cm, 21.5 cm, and 16.6 th an average of 17.4 cm. At every mean n the values which are 84.1 per cent of aximum relative tracer concentration can nputed, and the corresponding ellipse of concentration at the standard deviation plotted. Because the tracer distribution ches the bivariate normal distribution t some distance from the original point on, the last mean position will be used to

as compared with 43.7 per cent obtained by weight and volume measurements.

The S-shaped curves of relative tracer concentration across the transition zone are apparent in Figures 9 and 11. These curves are based on a relatively large number of points, and they approximate the error function distribution which is uniquely defined by its mean and its standard deviation. A straight line was also obtained in all tests (including the fluctuating ones) when the variance σ^2 was plotted against

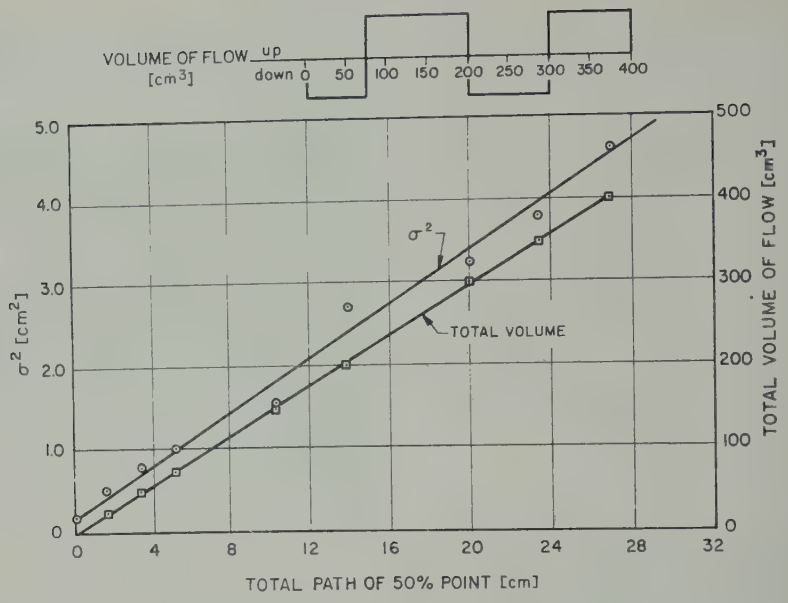


Fig. 12. Relations of total volume of flow and variance to total path of 50 per cent concentration point for test b-4.

total length of travel. This agrees with the theory [*Bear*, 1961]. The slope of this straight line gives the longitudinal constant of dispersion of the porous medium:

For test b-4,

$$D_1 = \frac{\sigma^2}{2L} = \frac{4.47}{2 \times 26.9} = 0.083 \text{ cm}$$

For test b-6,

$$D_1 = \frac{\sigma^2}{2L} = \frac{1.77}{2 \times 13.6} = 0.065 \text{ cm}$$

Test b–5 (not described here) was perfor with the same packing as test b–6 and it yiel $D_I = 0.093$ cm, but this test had the inter perpendicular to the direction of the flow, whe in test b–6 the angle between the interface the direction of the flow was 53°. *Bear* [1 developed for this case the relationship

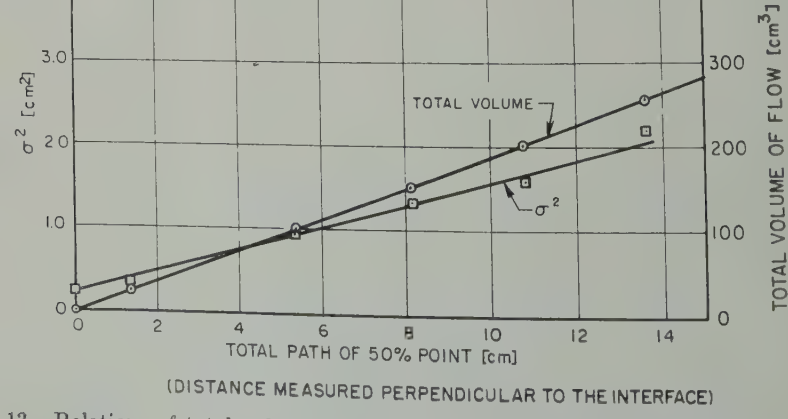


Fig. 13. Relations of total volume of flow and variance to total path of 50 per cent concentration point for test b-6.

$$D_\alpha = D_I \sin^2 \alpha + D_{II} \cos^2 \alpha \qquad (5)$$

e

= the angle between the interface and the direction of the flow.

, D_{II} = longitudinal and lateral constants of dispersion of the porous medium.

= directional constant of dispersion associated with the direction α.

e, if $D_{II} = D_I/10$, then $D_\alpha = 0.093 \times$ 53 + 0.0093 $\cos^2$ 53 = 0.063 cm, or if = $D_I/20$, then $D_\alpha = 0.061$ cm. Both results with the experimental result of $D_\alpha = 0.065$ btained in test b–6.

Conclusions

e development of a transition zone when itially abrupt interface between two miscible is displaced from its original position has experimentally demonstrated. The growth e transition zone depends upon the path of ean point and is independent, when the of diffusion is neglected, of the velocity e flow field. For the one-dimensional field ow the thickness of the transition zone nds upon the total distance that the front raveled. The variance of the concentration bution is directly proportional to the total nce traveled by the point of 50 per cent ve tracer concentration. This is also true fluctuating flow field. All experiments were ucted in the range of velocities in which rsion is governed by convection. In general, v flow rates, dispersion both in the direction nd perpendicular to the direction of the flow is dominated by molecular diffusion. gher flow rates the dispersion depends upon rocess of mixing by the porous media, with ular diffusion still prevailing at the interface between the two miscible fluids within each elementary flow channel.

The constants of dispersion of the porous medium were determined experimentally. Both lateral and longitudinal constants of dispersion have to be considered when the interface makes an angle with the direction of the flow.

Acknowledgment. The experimental work described was carried out in the Hydraulics Laboratory of the University of California, Berkeley, as part of a project in ground-water hydrology, sponsored by the Water Resources Center of the University of California.

I wish to express my thanks to Professor David K. Todd for his guidance and helpful suggestions and to Professor S. Irmay for reviewing the manuscript. I am indebted to Dr. G. de Josselin de Jong for his invaluable advice and to Messrs. G. E. Wilson and R. L. Ferral for assistance in performing the experiments.

References

Bear, J., On the tensor form of dispersion in porous media, *J. Geophys. Research, 66,* 1185–1197, 1961.

Bear, J., and David K. Todd, The transition zone between fresh and salt waters in coastal aquifers, Hydraulics Laboratory, University of California, Berkeley, *Water Resources Center Contrib. 29,* 156 pp. Sept. 1960.

Blackwell, R. J., Laboratory studies of microscopic dispersion phenomena in porous media, A.I.Ch. E.-S.P.E. Joint symposium on fundamental concepts of miscible fluid displacement, San Francisco, 18 pp., Dec. 1959.

de Josselin de Jong, G., Longitudinal and transverse diffusion in granular deposits, *Trans. Am. Geophys. Union, 39* (1), 67–74, 1958.

Deutsch, E. R., Optical scanning of liquid concentration in flow studies with porous models, *Nature, 185* (4714), 675–676, 1960.

Van Meurs, Pr., The use of transparent three-dimensional models for studying the mechanism of flow processes in oil reservoirs. *Trans. AIME, 210,* 295, 1957.

(Manuscript received April 4, 1961.)

In-Place Measurement of Permeability in Heterogeneous Media
2. Experimental and Computational Considerations

R. WILLIAM NELSON

Hanford Laboratories Operation, General Electric Company
Richland, Washington

Abstract. The computational problem pointed out in part 1 of this sequence of papers is evaluated in some detail. The problem arises from the need for compromise between the accuracy of calculated permeability and the ease of performing the calculation. Finite difference methods were expected to provide such a compromise. However, imprecision in numerical differentiation prevented use of the difference method. A study of the accuracy required for measuring permeability indicates that 7.5 times as much variation is allowable in the permeability as in the potential pattern. Since potential patterns are the tools needed to treat practical problems, errors in permeability measurements as great as 37 to 75 per cent may be tolerated and still provide answers within the common engineering accuracy range of 5 to 10 per cent. Linear flow approximations are found to give rather reliable permeability results for lateral flow systems. The geometrical shape of net elements in a *properly constructed flow net* for heterogeneous soils is utilized in the method. An expression for the approximation error is presented for application to any problem being analyzed.

troduction. In a preceding paper [*Nelson,*], theoretical consideration was given to a od for measuring in-place permeability of ogeneous media. In brief, it was shown that alysis of the piezometric head distribution e existing flow regime, combined with a few ace permeability measurements used as a dary condition, makes it possible to deter- the permeability distribution over the n of interest.

e desirable practical features of the method than the capability of considering hetero- y are that the piezometric head is rather measured and that a very large soil sam- r in a sense the entire soil mass, is utilized e method. These facts are encouraging and contribute toward filling a long-recognized for obtaining reliable values of permeabil- *Isherwood and Pillsbury,* 1958; *Brooks,* . However, an examination of the compu- al problem pointed out in the previous is required. This paper is concerned with perimental evaluation of methods for over- g the computational difficulties.

e computational problems arise from the red potential being in tabular form rather being an algebraic function. Yet first and l spatial derivatives of the potential are l in solving for the permeability distribution. Three possibilities for overcoming this problem are:

1. Fit algebraic expressions to the tabular potentials.
2. Get tabular values of the derivatives through numerical differentiation for use in appropriate finite difference equations to give the permeability distribution numerically.
3. Use simpler linearized flow expressions to calculate the permeability in tabular form over the region being analyzed.

The complexity in getting surface fittings makes method 1 impracticable for common engineering use. Other considerations covered during analysis of method 2 further indicate the undesirability of method 1; accordingly it will not be considered further.

The finite difference approach (method 2) has been rather exhaustively examined and is reported elsewhere [*Nelson,* 1959]. Accordingly, only the major results will be presented here. In any case the inherent inaccuracy found in common methods of numerical differentiation makes this method unacceptable for our purposes. Aside from the résumé of method 2, the remainder of the present discussion is on linearized flow approximations. Before these items are considered further the experimental obser-

vations which allow analysis of methods 2 and 3 will be described.

Experimental procedure. The long-recognized analogy between a saturated soil-water system and an electrical conducting material [*Muskat,* 1946] made possible the use of electrical analogs to obtain the experimental data. Better data are obtained from the analogs than from the actual system because the electrical measurements can be carried out with greater precision. The electrical analogs are also cheaper and simpler to make. The experimental difficulty in using three-dimensional models led to studying only two-dimensional flow systems. Accordingly, only lateral flow systems have been studied through analogy [see *Nelson,* 1959, p. 48].

Five electrical analogs simulating two-dimensional saturated soil-water systems of variable conductance were made from Teldeltose[1] conducting paper. Various patterns of resistance variability were imposed on the square analogs by cutting many 5/16-inch-diameter holes in the conducting paper. Silver paint backed by metallic conductors was placed along two opposite edges of the square analog to form equipotential boundaries. A potential difference was placed between these boundaries, causing current to flow across the analog. A square grid was then laid out on each of the models and the voltage was measured at the grid points.

The voltages were determined by using a null indicator and a calibrated potentiometer in parallel with the conductance model [*General Electric Company,* 1950]. With this equipment, fluctuations in line voltage do not affect the measured potential since the *percentage* of applied potential difference is always measured. Three readings were taken at each grid point and were averaged to give a representative value of potential. The pooled standard deviation for these measurements based upon 3510 observations was 0.00088 in a measurement range between 0 and 1.

The first four of the five analogs were made up of 81 grid points arranged in a 9 by 9 array. Upon completion of the measurements on the first four analogs it was apparent that more observations of potential between the regular grid points would be helpful in analyzing t numerical differentiation problem. A fifth an log containing a 12 by 12 array was construct Three intermediate observation points we established between each pair of regular gr points. The experiments with this fifth anal will be utilized in describing the remainder the procedure, typifying the observations ma with all the analogs.

After the voltage observations were comple the conductance analog was cut into 2-in squares and the resistance of each square w measured. Preliminary work indicated th measurement errors became large for un smaller than 2 inches, and the advantages more detailed information on the variation resistance were thus offset. It was necessary measure the resistance under controlled tempe ture and humidity conditions since changes atmospheric conditions caused variations of much as 2 per cent.

Under controlled conditions of temperat and humidity the average of three measu ments was considered to be the representat value of resistance for a square. The best e mate of the combined variation (pooled sta ard deviation) due to instrument error specimen preparation was 56.6 ohms in a me urement range of 1500 to 4900 ohms. The pected measurement variations are ±1.0 ±5.6 per cent for the potential and resista observations, respectively.

A further check on the reliability of the perimental data was obtained by comple the measurement cycle (measurement closu This consisted in using the measured value resistance to redetermine the potential dis bution when the boundary conditions used the original analogs were imposed. The rede mined potential values could then be compa with the originally measured values.

Analog 5 (12 by 12 array) was specifi examined for measurement closure with a tal computer using the Gause-Sidel method overrelaxation. An overrelaxation factor of to 1.4 was found optimum to reduce the nu ber of iterations required. The redeterm voltages calculated in this manner had a st ard deviation from the original values of 0.00 the median of the measurement range b 0.500. The measurement closure analysis indicated the accuracy of the data to be

[1] Developed and produced by Western Union Telegraph Company, Development and Research Department, 60 Hudson Street, New York 13, N. Y.

, thereby insuring a valid basis for further ysis.

ne measured voltage from the analog was to compute the distribution of resistance comparison with the measured values. Such ocedure provides an evaluation of the finite rence method and a linearized approach for ng resistance distributions.

rmeability determined from finite difference tions. To determine the permeability dis- ution with a finite difference technique, we the appropriate difference equation and dary conditions for two-dimensional flow. re these difference equations can be solved, erical values of the first and second partial vatives of the potential are needed as varia- coefficients. Having the variable coefficients, can form a system of sequential algebraic tions in the unknown permeabilities and e them to give the permeability at a finite ber of points over the region being analyzed. fore the finite difference form is obtained, ill be desirable to reduce the three-dimen- al expressions [*Nelson,* 1960, equations 13 14] to two dimensions by considering only e systems having essentially lateral flow, i.e.

$$\partial\phi/\partial z \doteq 0 \tag{1}$$

$$K = T/b_0 \quad \text{or} \quad T = Kb_0 \tag{2}$$

e b_0 is a constant aquifer thickness, T is the transmissibility, ϕ is the potential, k is the aulic conductivity, and z is the vertical linate as defined in the previous paper. two-dimensional equation then becomes

$$\frac{T}{x} + \frac{\partial\phi}{\partial y}\frac{\partial T}{\partial y} + \left(\frac{\partial^2\phi}{\partial x^2} + \frac{\partial^2\phi}{\partial y^2}\right)T = 0 \tag{3}$$

h is the relationship used in the experimental . For lateral flow systems the boundary ition when T is dependent is

$$\Gamma[T(x, y)]_{\phi(x,y)\doteq c_0} = 0 \tag{4}$$

e $\Gamma(T)$, the boundary function in T, is fied along some equipotential line $\phi(x, y) \doteq$ hich crosses the whole flow region.

e finite difference equivalent of (3) is ned upon substituting the definition of the al derivatives of T with respect to x and y then approximating the limit through use e finite distance h. In this case, if h is ned equal in both the x and y directions, (3) becomes

$$\left(\frac{\partial\phi}{\partial x}\right)_{ij}\left(\frac{T_{ij} - T_{i-1,j}}{h}\right) + \left(\frac{\partial\phi}{\partial y}\right)_{ij}\left(\frac{T_{ij} - T_{i,j-1}}{h}\right) + \left(\frac{\partial^2\phi}{\partial x^2} + \frac{\partial^2\phi}{\partial y^2}\right)_{ij} T_{ij} = 0 \tag{5}$$

and the boundary condition from (4) is

$$\Gamma_{ioj} = T_{ioj} \tag{6}$$

where i is the x-coordinate index (general direction of flow being in x direction) and j is the y-coordinate index in unit multiples of h.

The point pattern is a three-point group with the system of algebraic equations being sequential, and the fundamental domain is defined by (6). Care must be exercised to assure use of the correct variable coefficients in the first pair of equations in the sequential system of the ith column; otherwise the solution proceeds in the usual orderly manner. The difference formulation is discussed in general by *Fort* [1957] and presented in detail for this problem elsewhere [*Nelson,* 1959].

A technique is now available for calculating the values of transmissibility, provided the first and second spatial derivatives of ϕ are known numerically with sufficient accuracy. Numerical differentiation as used here requires rather precise results since the partial derivatives are utilized as coefficients in (5). Three differentiation methods were used. They were Gregory-Newton differences [*Kopal,* 1955; *Wylie,* 1951], Bickley's differentiated Lagrangian interpolation formula [*Bickley,* 1941; *Bickley and Miller,* 1940; *Southwell,* 1946] and differentiated Chebyshev polynomial fittings of the first kind [*Jones,* 1946; *Miller,* 1946; *Szego,* 1939].

Of the three methods for numerical differentiation, the Chebyshev polynomials provided the most consistent numerical values for the derivatives. This is consistent with general Fourier theory, since Chebyshev expansions have the orthogonality property over the range -1 to $+1$. The Chebyshev expansions are more strongly convergent in the least-squares sense than are the ordinary power series expansions [*Kopal,* 1955; *U. S. Natl. Bur. Standards,* 1952]. The reason for also examining the difference and

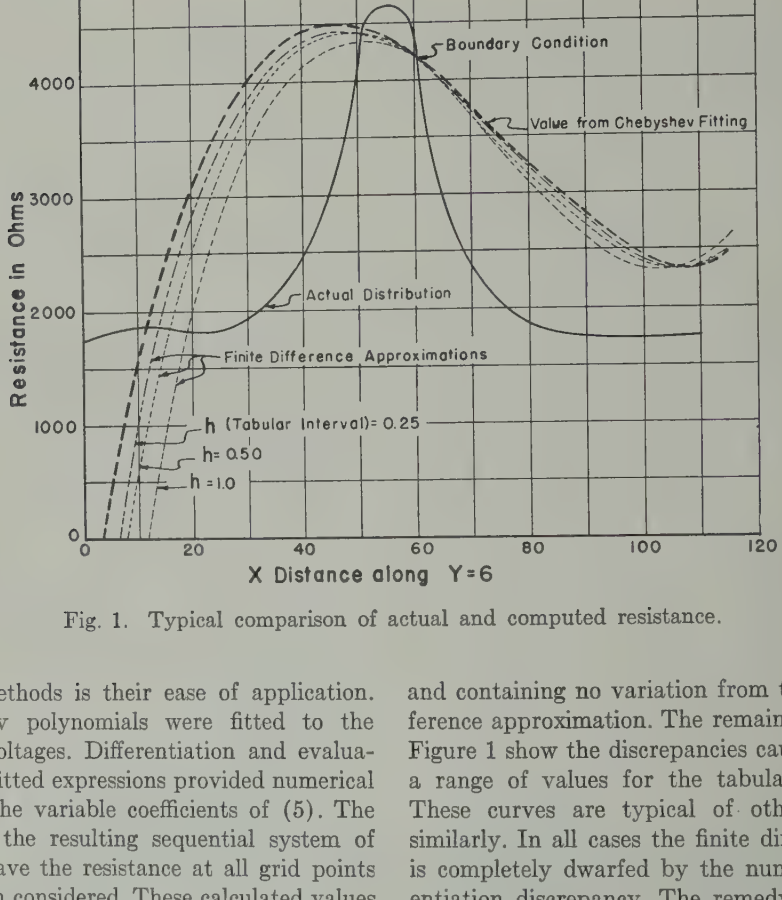


Fig. 1. Typical comparison of actual and computed resistance.

Bickley's methods is their ease of application.

Chebyshev polynomials were fitted to the measured voltages. Differentiation and evaluation of the fitted expressions provided numerical values for the variable coefficients of (5). The solution of the resulting sequential system of equations gave the resistance at all grid points in the region considered. These calculated values of resistance were compared with the measured values from the electrical analogs. The mean of the absolute differences between measured and calculated values was 818 ohms, or 34.9 per cent of the mean measured resistance.

The two possible causes for such large differences are (1) discrepancies arising in the numerical differentiation of ϕ, which is used in the sensitive role of variable coefficients in the difference equation, and (2) undue error, proportional to the magnitude of h, introduced by the finite difference approximation (see discussion preceding equation 5). These two possibilities can be separated by considering a typical example (Fig. 1) taken from analog 5. In Figure 1 the solid curve is the true measured resistance along the general flow direction x. But the heavy dashed curve is the calculated resistance based upon the fitted Chebyshev polynomials and containing no variation from the finite ference approximation. The remaining curv Figure 1 show the discrepancies caused by u a range of values for the tabular interva These curves are typical of others anal similarly. In all cases the finite difference is completely dwarfed by the numerical di entiation discrepancy. The remedy is eith get more precise methods of numerical di entiation or to discard the finite differ approach as impracticable. When consid possibilities for finding better differenti methods, two questions arise: How prec must the derivatives be known? What p bilities are there for attaining this preci Work on the first question has been comp and will be reported here. The second que is currently being investigated and will b subject of a third paper in this sequence.

This precision required for the derivativ dependent on the accuracy required in th sistance or reciprocal transmissibility valu turn, the required accuracy of the transmis ity depends upon the precision desired in th sults derivable from such determinations. primary concern of the ground-water hydro is usually the prediction of the expected p

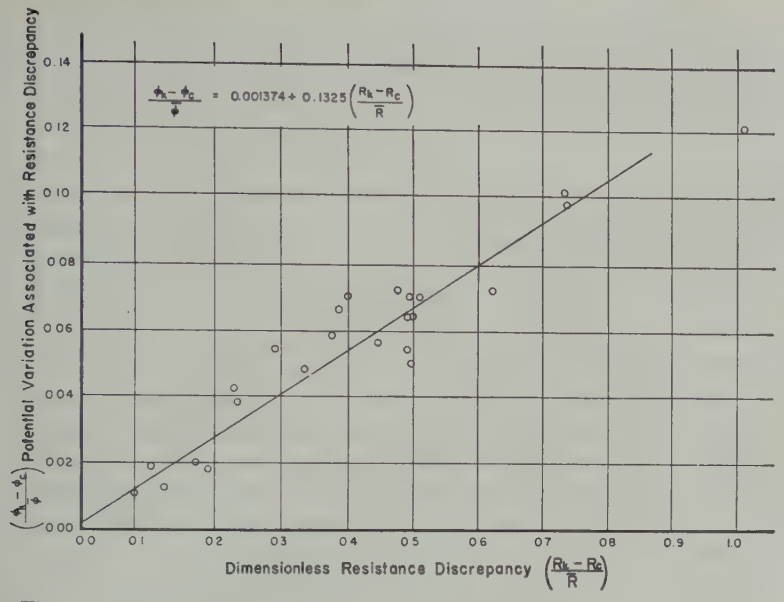


Fig. 2. Effect of resistance discrepancy on maximum potential variation.

distribution after structures such as wells ains are installed. In practice the required of accuracy is specified in terms of potendistributions. Accordingly, information is d to change a desired accuracy level in tial to an equivalent statement for the missibility or resistance.

ta to indicate the relationship between reice and potential variation were obtained the computed resistances which were n to deviate by a given amount from the ired values. The computed resistances were in the computer to redetermine the potenistribution. The method has already been bed in connection with measurement clounder Experimental Procedure.

e redetermined potentials show much closer ment with the original measured voltages he calculated resistances show with measresistances. For example, associated with .9 per cent resistance error was a potential pancy of only 9.3 per cent. As will be seen, tter value is unexplainably high.

relationship between potential and resistariation is shown in Figure 2. The dimens resistance discrepancies, i.e., measured nce $R_k/\bar{R}$ minus the calculated resistance n Figure 2, are the maximum discrepancies along a line approximating a streamline. otential differences associated with the resistance discrepancies were obtained from the measured potential $\phi_k/\bar{\phi}$ minus the calculated potential $\phi_c/\bar{\phi}$. The variables $\bar{R}$ and $\bar{\phi}$ are the mean resistance and potential, respectively, for the analog on which the discrepancy was observed.

The data shown in Figure 2 provide the needed relationship between resistance and potential error. They are useful for finding the allowable variation in resistance from the known or estimated tolerable limits of error in potential. Interpretation of the data in Figure 2 shows that in general only about 2/15 as much precision is required in the resistance determination as for the potential. In other words, 7.5 times as much error can be tolerated in the calculated resistance (reciprocal transmissibility values) as in the final potential distribution being predicted. Evaluation now changes to the linearized approximate flow relationships from which the permeability in essentially lateral flow systems is determined.

In the linearized flow approach an approximate semigraphical method is simple and may be beneficial in lateral flow systems, since it circumvents the differentiation difficulty. Two variations of this method will be considered; in both a properly constructed flow net is used.

The use of a *proper flow net* will expedite application of the linearized flow analysis. The

commonly accepted practice for drawing flow nets in a uniform medium will provide the basis for constructing a proper flow net for heterogeneous conducting material. These requirements are:

1. The incremental difference in potential between successive equipotentials is a constant.
2. Streamlines are everywhere orthogonal to equipotentials for an isotropic heterogeneous medium.
3. The spacing between streamlines is such that the same quantity of fluid passes between each pair of streamlines making up the flow system.

All these requirements are essentially the same as common flow net convention for a homogeneous medium. As a result of requirement 3, however, the streamlines may have a rather erratic spacing at some places in the flow net for a heterogeneous medium. Occasionally it is convenient to insert dashed streamlines intermediate to regular streamlines in regions of very low permeability. If this is done, the flow net can no longer be classified as proper but forms a utilitarian flow net which must be used with care. In such a case the discharge in every stream tube is not a constant value, and corrections must be applied when analyzing the geometrical aspects of the resulting flow net elements. The *proper flow net* provides the basis for the linearized flow approximations which will now be examined.

In the first variation of the linear method the width, and consequently the area, of any stream tube making up the flow net is assumed to be constant. This is equivalent to assuming strictly one-dimensional flow. Since the rate of flow and the cross-sectional area of the stream tube are assumed to be constant, Darcy's law combined with linear continuity reduces to the relationship that the resistance to flow (reciprocal of the transmissibility) is directly proportional to the potential gradient. This may be written as

$$\frac{T_2}{T_1} = \frac{R_1}{R_2} = \frac{\partial\phi_1/\partial s_1}{\partial\phi_2/\partial s_2} \doteq \frac{\Delta\phi_1/\Delta s_1}{\Delta\phi_2/\Delta s_2} \qquad (7)$$

Since $\Delta\phi_1$ is equal to $\Delta\phi_2$ by requirement 1 for a proper flow net, (7) reduces to

$$R_1/R_2 = \Delta s_2/\Delta s_1 \qquad (8)$$

where R_1 and R_2 are the resistances at two points along the stream tube, ϕ_1 and ϕ_2 are potentials at these points, s is the distance al a stream tube, and Δs is the incremental tance between equipotentials at the points de nated by the subscripts 1 and 2.

The experimental data described previo were used in examining the first approxim procedure. The measured potentials were u in drawing proper flow nets for analogs 4 an and the incremental distances between equ tentials (Δs_n) were measured along the len of each streamline. The boundary condition was used as the starting value for R_1. The v of R_n ($n = 2, 3, 4$, etc.) at any point along streamline could then be calculated from measured ratio $\Delta s_1/\Delta s_n$ using (8). Values o along the streamline were assumed to repre the values of resistance midway between equipotentials and were plotted on a map of analog. Lines of equal resistance were drawn interpolation to form isoresistance maps for of the analogs. Figure 3 shows such a map analog 5.

The isoresistance maps were used to deter the effective resistance for the 2-inch squ for which the resistance had been measured perimentally. The effective resistances found by multiplying the areas lying betw isoresistance lines by the mean resistanc these areas, adding the products for all a within the 2-inch square, and dividing the by 4.

Comparison of the resistances calculate the above manner with those measured in experimental procedure showed the mean a lute differences to be 359 ohms (17.3 per c and 261 ohms (11.5 per cent) for analogs 4 5, respectively. The potential discrepancies sociated with these resistance differences 2.36 per cent and 1.70 per cent in the s order. These potential discrepancies are avc values for all the discrepancies in analogs 4 5 which were found from calculations with computer. The validity of Figure 2 is stre ened by the plotted positions of these dis ancies, i.e., 0.173 and 0.0236, 0.115 and 0.01 that figure.

Closer scrutiny of the data for the first proximation showed that the differences largely for high values of resistance, the puted values being smaller than those m ured. The predominant cause for the

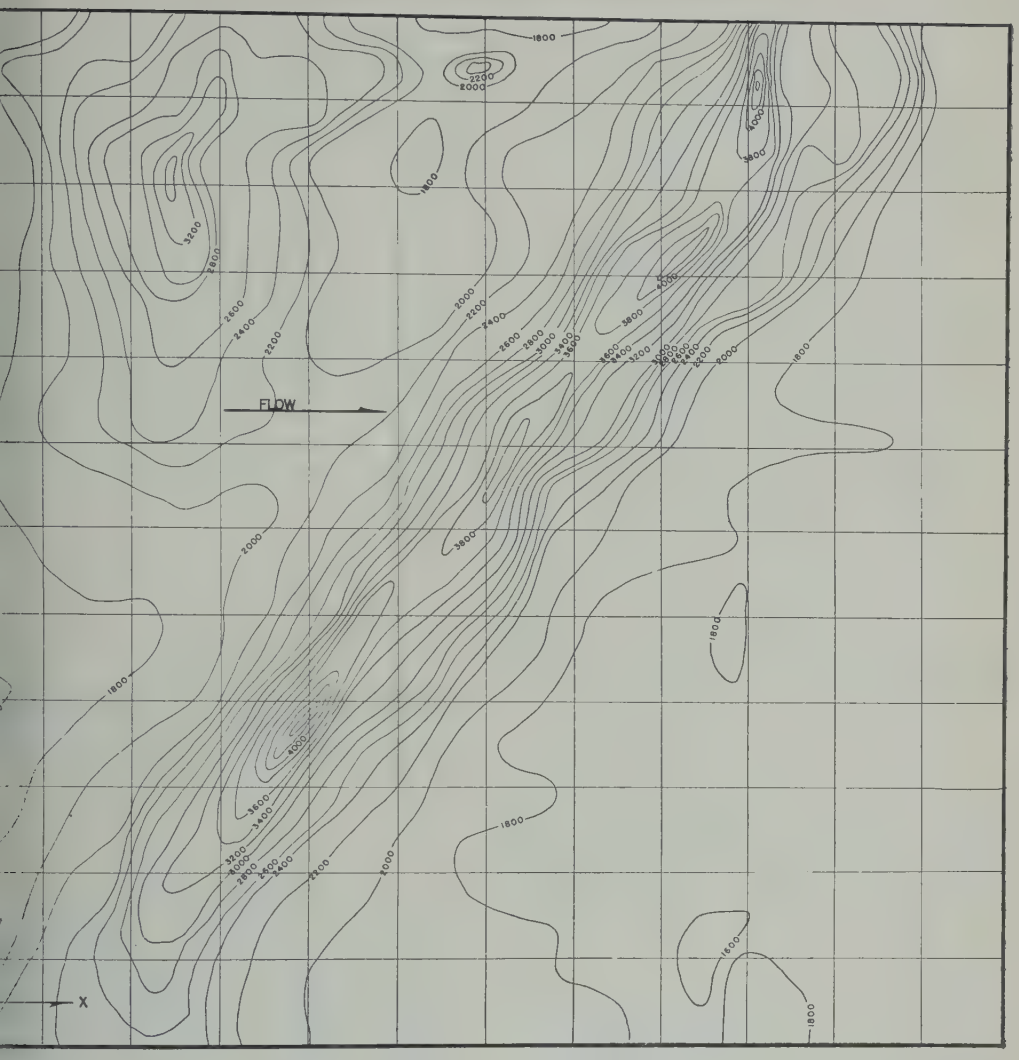


Fig. 3. Isoresistance map of analog 5.

ıtly lower values was found to be the as-
ɔtion that the area of flow is constant.
second modification of the linearized flow
oximation can further reduce the error by
g into account the change in area along
m tubes. Again assuming only one-dimen-
l flow and letting Δs be the average in-
ental distance along the stream tube be-
ı equipotentials and b be the average width
e stream tube, we can equate the flow at
points along the stream tube and thus
fy (8) by the stream tube width. Equation
n becomes

$$\frac{T_1}{T_n} = \frac{R_n}{R_1} = \frac{(b_n)}{b_1}\frac{(\Delta s_1)}{\Delta s_n} \tag{9}$$

The procedure used with (8) was used again with (9) to get the effective resistance of the 2-inch square. A comparison of resistance values computed with (9) with those experimentally measured gave mean absolute differences of 244.8 ohms (11.83 per cent) and 198 ohms (8.43 per cent) for analogs 4 and 5, respectively. The potential discrepancies associated with these resistance differences as obtained from Figure 2 are 1.57 per cent and 1.12 per cent for analogs

4 and 5, respectively. We believe that some 5 or 6 per cent of the resistance difference is the result of human error in drawing streamlines to complete the flow net. Unfortunately, the electromechanical equipment required to prove or disprove this belief is not available at the present time.

Discussion of linearized approximations. A thorough understanding of what is implied by assuming linear flow will make it possible to evaluate the error introduced by the approximation. Saying that flow is essentially linear implies that the velocity v_n in the direction normal to the general stream tube direction is so small in comparison with the velocity v_s along the flow that it can be ignored, i.e.,

$$v_n \ll v_s \tag{10}$$

Then by Darcy's law

$$\partial\phi/\partial n \ll \partial\phi/\partial s \tag{11}$$

where n is the direction normal to the general flow and s is the direction tangential to the flow. If this is the case, then, approximately,

$$\partial\phi/\partial n \doteq 0 \tag{12}$$

i.e., no energy will be expended in expansion or contraction of flow. If this were strictly true, all stream tubes would of necessity have straight parallel boundaries with the area available for flow being constant. This is the real physical system described by (8). The limitations it contains are:

1. Any energy utilized in the divergence, convergence, or curvature of flow along the stream tube is negligible when compared with that expended in flow along the stream tube.

2. The cross-sectional area available for flow along the length of the stream tube is constant.

The first of these limitations is inherent in the application of (9), but not the second. Accordingly, (9) gives a better estimate of experimental results than does (8).

Let us now determine an expected error function for item 1 for use with (9). This would provide an expression from which the importance of the energy utilized in convergence or divergence of flow can be determined.

We consider a stream tube in heterogeneous porous media through which fluid is flowing at a steady rate Q. We let the difference in potential between two equipotential surfaces ϕ_1 and bounding a flow net element be $\Delta\phi$. If both and the diameter of the stream tube are cho rather small, then R_v, the total resistance flow of the stream tube element between ϕ_1 ϕ_2, is

$$R_v = \rho_v/F \tag{}$$

where ρ_v is the specific resistance and F i parameter having dimensional units of len which completely describes the geometrical c figuration of the conducting element.

To evaluate F we suppose that an identica geometrical model of the above stream t segment is made of a conducting material known specific resistivity ρ_u. Then the total sistance R_u is

$$R_u = \rho_u/F \tag{}$$

and F is given by

$$F = \rho_u/R_u \tag{}$$

Substituting (15) into (13), rearranging, expressing R_v in terms of Q and $\Delta\phi$ through of Ohm's law, which is analogous to Dar law, we get an expression for ρ_v,

$$\rho_v = R_v F = \frac{\Delta\phi/Q}{R_u/\rho_u} \tag{}$$

In two-dimensional cases, as are here sidered, R_u is easily found experimentally tracing the geometrical shape of a flow net ment and cutting this shape from electrical ductance paper of known specific resistance

Figure 4*a* may help in visualizing the str tube element. R_u can be measured with a st ard bridge to give the resistance between ϕ_1 ϕ_2. Hence, all the variables in the right-h side of (16) are known and ρ_v is obtained. cordingly, the true mean effective resistanc the stream tube element is known. Let us examine what is implicitly assumed for this element by the linearized flow approximati

In the linear approximation the implicit sumption is that F_a is of the form

$$F_a = b/d$$

where F is the geometry factor defined a with the a subscript denoting the assume approximate factor, d is the average dist between ϕ_1 and ϕ_2, and b, when combined

it thickness out of the page, is the cross-onal area of flow. If we use the symbols n in Figure 4, (17) becomes

$$F_a = \frac{b_1 + b_2}{d_1 + d_2} \tag{18}$$

approximate specific resistance ρ_a has the form as ρ_v in (16), and substitution of for F_a gives

$$\rho_a = R_a F = \frac{\Delta\phi/Q}{(d_1 + d_2)/(b_1 + b_2)} \tag{19}$$

ming the ratio of the true value ρ_v to the roximate value ρ_a we get

$$\frac{\rho_v}{\rho_a} = \frac{d_1 + d_2}{b_1 + b_2} F \tag{20}$$

$$\rho_v = \frac{d_1 + d_2}{b_1 + b_2} F \rho_a \tag{21}$$

n $\rho_v/\rho_a = 1$ there is no approximation er-or no correction term required for ρ_a; there-the resistance error function for the linear roximation is

entage error (resistance)

$$= \left|1 - \frac{d_1 + d_2}{b_1 + b_2} F\right| \times 100 \tag{22}$$

expression can be used to determine the r due to approximation of any flow net ent by obtaining F through the experi-tal technique described previously.
ie associated error in potential is found by tituting (22) into the expression of Figure 2.

entage error (potential)

$$0.14 \pm 13.25 \times \left|1 - \frac{d_1 + d_2}{b_1 + b_2} F\right| \tag{23}$$

ation 23 is probably the more important re-nship to the engineer because prediction of ential distribution is the usual goal. It may f interest to note the respective resistance potential discrepancies of the flow net ele-shown in Figure 4. The percentage resis-error is 6.8 per cent and the potential dis-ancy was 1.04. The resistance correction in this case is 0.932; that is, ρ_a as calcu-from (19) must be multiplied by 0.932 to the correct value of ρ_v.

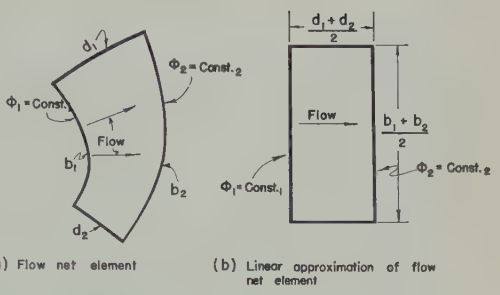


Fig. 4. Schema of a flow net element and its equivalent linear element.

It now appears that the linear assumptions provide a way to determine the permeability in essentially lateral flow systems to within 5 per cent maximum potential error at critical areas, with an average linearization error over the whole region of about 1 per cent. Further, such an approach is computationally rather simple because only ratios are involved in getting the permeability distributions along stream tubes. Accordingly, it may have rather general utility in ground-water studies.

Acknowledgment. Portions of this work were sponsored by the author's earlier employer, the Agricultural Research Service, U.S.D.A. The encouragement and help of Dr. W. D. Kemper of the Department of Agriculture is gratefully acknowledged.

References

Bickley, W. G., Numerical differentiation formulae for numerical differentiation, *Math. Gaz., 25* (263), 19–27, 1941.

Bickley, W. G., and J. C. P. Miller, Numerical differentiation near the limits of a difference table, *Phil. Mag., 7th ser., 33,* 1–18, 1940.

Brooks, R. H., An approximate solution for transient flow toward equally spaced drains above an impermeable boundary, *J. Irrig. and Drain. Div., Proc. Am. Soc. Civil Engrs, 87*(2), 1961.

Forsythe, G. E., What Are Relaxation Methods? in *Modern Mathematics for the Engineer,* edited by E. F. Bechenbach, McGraw-Hill Book Co., New York, 428–447, 1956.

Fort, Tomlinson, Partial linear difference equations, *Am. Math. Monthly, 64*(3), 161–167, 1957.

General Electric Company, *Instructions Analog Field Plotter,* Catalog no. 112L152G-1 and G-2, Schenectady, N. Y., 50 pp., 1950.

Isherwood, J. D., and A. F. Pillsbury, Shallow ground water and tile drainage in the Oxnard Plain, *Trans. Am. Geophys. Union, 39,* 1101–1110, 1958.

Jones, C. W., and others, Tables of Chebyshev

polynomials, *Proc. Roy. Soc. Edinburgh, 62,* 187–203, 1946.

Kopal, Zdenek, *Numerical Analysis,* John Wiley & Sons, New York, 556 pp., 1955.

Miller, J. C. P., Two numerical applications of Chebyshev polynomials, *Proc. Roy. Soc. Edinburgh, 62,* 204–210, 1946.

Muskat, M., *The Flow of Homogeneous Fluids through Porous Media,* J. W. Edwards, Ann Arbor, Mich., 763 pp., 1946.

Nelson, R. William, In-place measurement of permeability in non-homogeneous media through an analysis of the steady potential distribution, Unpublished thesis on file, Library, Colorado State University, Fort Collins, Colorado, 1959.

Nelson, R. William, In-place measurement of permeability in heterogeneous media, 1, Theory a proposed method, *J. Geophys. Research,* 1753–1758, 1960.

Southwell, R. V., *Relaxation Methods in Theoret cal Physics,* Oxford University Press, Londo 229–238, 1946.

Szego, G., *Orthogonal Polynomials,* Americ Mathematical Society, Colloquium Publicatio New York, 401 pp., 1939.

U. S. National Bureau of Standards, Tables Chebyshev polynomials, $S_n(x)$ and $C_n(x)$, *Ap Math. Ser. 9,* pp. v–xxv, 1952.

Wylie, C. R., Jr., *Advanced Engineering Mathe matics,* McGraw-Hill Book Co., 359–403, 1951

(Manuscript received February 27, 1961.)

Estimation of Electrical Conductivity from Chemical Analyses of Natural Waters

JOHN LOGAN

International Cooperation Administration
Operations Mission to Haiti

Abstract. Several methods of estimating the electrical conductivity of natural waters from their chemical analyses are tested statistically with a previously undescribed empirical method. Standard errors of estimate resulting from the latter are less than 7 per cent for each of two tests; this value is in the range of sampling and analytical error in many cases.

INTRODUCTION

wing to the simplicity of its determination to its great significance in many investiga-s, electrical conductivity has become a fre-ıtly measured parameter of natural waters. usefulness extends into such specialties as nage and irrigation engineering, oceanogra- and limnology, soil fertility, petroleum tech-gy, and ground-water hydrology. Indeed, it n becomes valuable or even necessary to esti-e conductivity from the results of a labora- analysis when that property was not meas- or reported.

ecause of the nature of the variables in-ed, no simple method of estimation can be rely satisfactory. Electrical conductivity is cipally a function of the specific conductivi- of the several ions in solution, their concen-ions, and the temperature. Variations due to perature are either eliminated by measuring luctivity at the standard reference of 25°C minimized by a mathematical adjustment the temperature of measurement to 25° he use of accepted corrections appropriate 'average' mixed-salt solutions [*Richards,* , Table 15]. The more important variations to ionic synergism and antagonism in mixed ions are most complex, however. Perhaps e could be analyzed by multiple correlation about six independent variables, but it is ible that the results would not justify the ustive investigation that would be required. veral rather simple methods of estimation available, but experience has demonstrated large errors may result from their use. In ttempt to improve the reliability of the estimate, an empirical method has been developed over a period of several years. In the present study, this empirical method is tested statistically against the others. Additional methods were derived during this test and were also tested.

THE SAMPLES

For the statistical test, samples of chemical analyses were taken from the literature. The first sample is from a recent publication of the U. S. Geological Survey [*Hem,* 1959] which presents many data concerning natural waters of diverse origins. From that source, all 'complete' analyses (i.e., those with determinations of the usual ions found in waters and of conductivity) were taken (1) in which significant amounts of uncommon ions such as borates and phosphates were not present and (2) whose ionic sums did not exceed 1000 equivalents per million (epm). The latter exclusion is justified because of the great rarity of waters with such concentrations which are not largely sodium chloride, and for such solutions the single-salt relation of conductivity to concentration may be used with rather high accuracy.

The second sample is from a publication of the U. S. Department of Agriculture [*Richards,* 1954, Table 12] and is itself a sample of the chemical characters of river waters that are used for irrigation in the western United States.

Samples 1 and 2 consist of 49 and 25 analyses, respectively. Note that the samples were not selected with mathematical rigor, but for expediency. The first merely consisted of the largest collection of analyses of diverse chemical

types within the author's references; the second represents a more restricted group. The values of conductivity and concentration of the individual analyses of both samples are presented graphically in Figure 1.

Definitions

EC = electrical conductivity, micromho/centimeters at 25°C; the common unit of the ground-water and irrigation specialist.

T = ionic sum; half of the sum of anions and cations, equivalents per million (epm).

s = standard error of estimate, micromho/cm.

$s_{\%}$ = standard error of estimate based on percentage deviations of calculated values of EC from measured ones.

The Method of Estimate

The several methods of estimate that w tested are described as follows:

1. *EC = 100T.* This is the best kn estimating formula and is commonly used ground-water and irrigation specialists.

2. *The method of Dunlap and Hawthorne* [19 The following equation is widely used by pe leum engineers, particularly in the field electric log interpretation:

$$C_e = 0.95\ Ca + 2.00\ Mg + 1.00\ Na + 1.26$$
$$+ 0.27\ HCO_3 + 1.00\ Cl + 0.50\ SO_4$$

(The factor for SO_4 is raised to 0.55 w total salinity exceeds 10,000 parts million.)

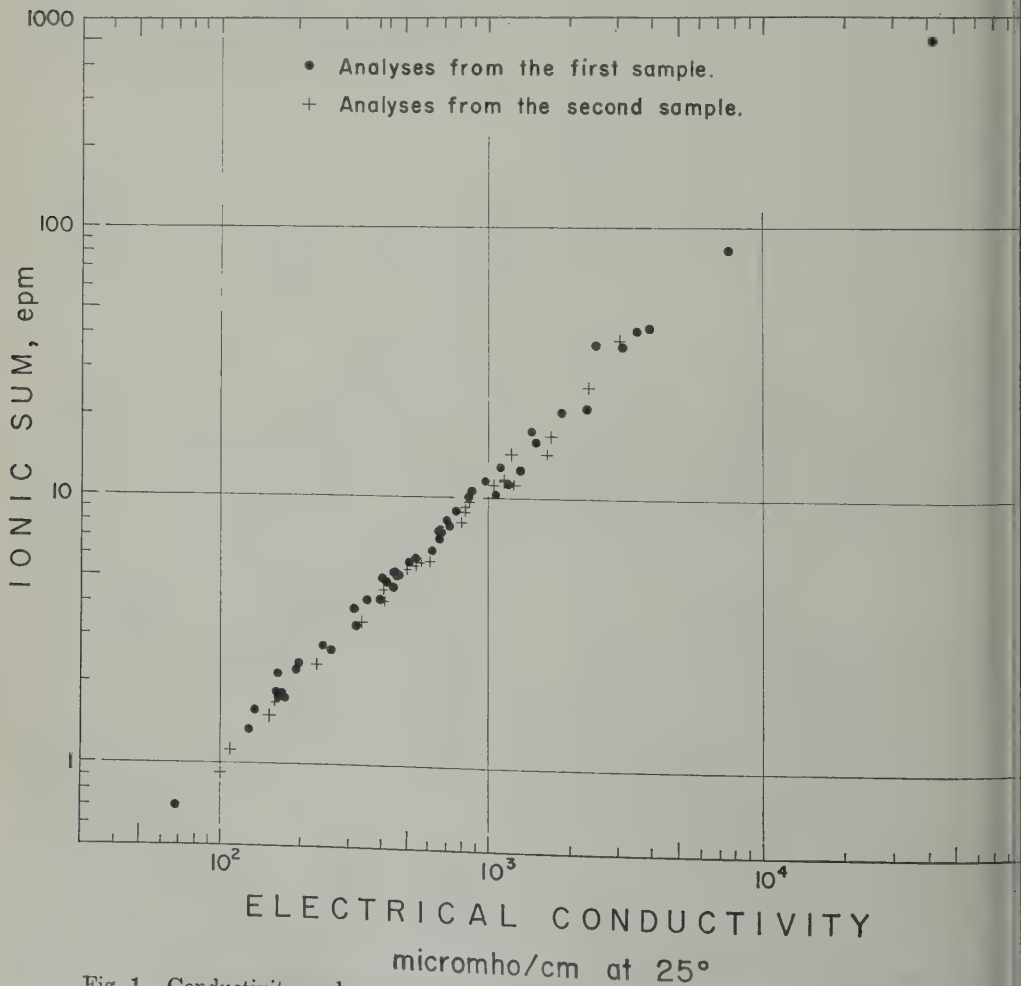


Fig. 1. Conductivity and concentration of the individual analyses of the two samples.

hich the values of the several ions are ssed in terms of ppm and C_e is the 'equiva- concentration' in ppm of a solution of m chloride whose conductivity is the same at of the sample in question. It is convenient onvert this concentration either to con- vity or to its reciprocal, resistivity, by use blished graphs [for example, *Richards*, 1954, 4; *Schlumberger Corp.*, 1957, p. A-6]. When ssed in terms of ohm-meters (the unit of etroleum engineer), resistivity r, and EC are ed by the equation $r = 10^4/EC$.

Linear correlation. The linear least-squares lation of the 49 analyses of the first statistical sample is

$$EC = (84.4T) + 58.9$$

4. *Logarithmic correlation.* A least-squares correlation of the logarithms of the parameters of the first statistical sample provides the estimating equation:

$$EC = 69.0T^{1.143}$$

5. *The 'Handbook 60' graph.* Figure 4 of U. S. Department of Agriculture Handbook 60 [*Richards*, 1954] is a graph of the relation between EC (in millimho/cm) and T for rather concentrated soil solutions for which values of T

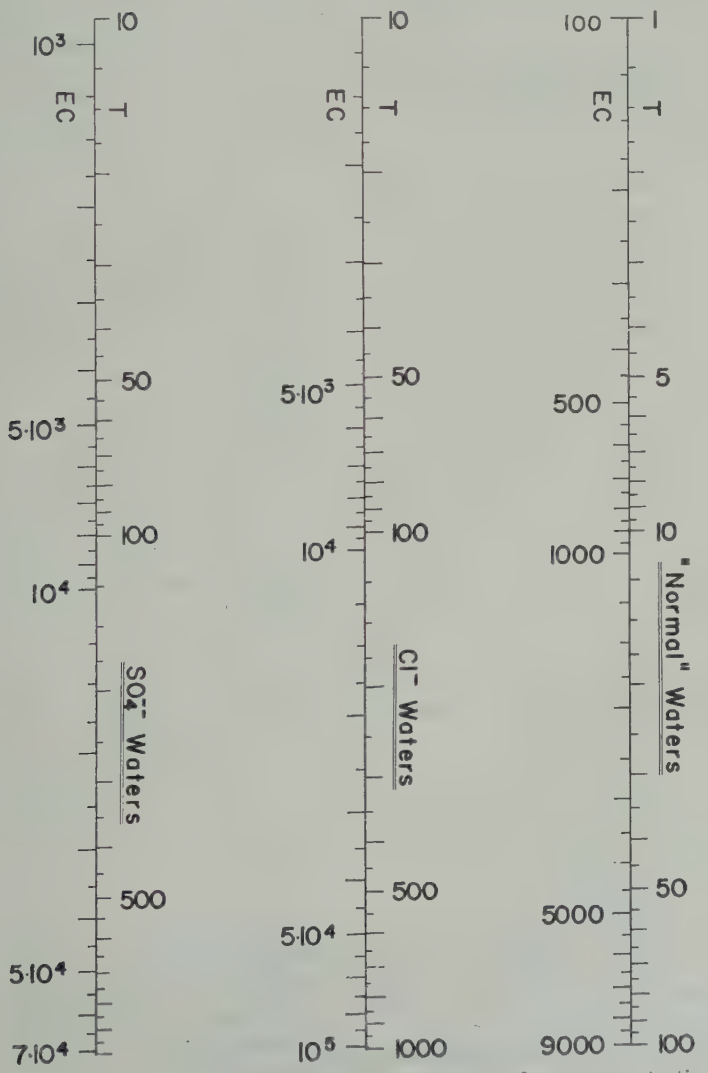


Fig. 2. Nomographs for estimating conductivity from concentration.

exceed 10 epm. Certain irrigation engineers and other specialists have used this graphic relation for the estimate in question. Writing EC in micromho/cm yields the equation of the curve:

$$EC = 121T^{0.916}$$

When T is less than 10 epm, the estimating equation $EC = 100T$ is used.

6. *A modification of the Rossum method.* The Rossum method of diluted conductance [*Rossum*, 1949] provides a check on the accuracy of a chemical analysis. It was not intended as a means of estimating conductivity, but it may be used for that purpose through a modification. A first estimate of conductivity (EC') is obtained by the relation

$$EC' = (52.0\ Ca + 46.6\ Mg + 48.9\ Na + 72.0\ K + 84.6\ CO_3 + 43.6\ HCO_3 + 75.9\ Cl + 71.0\ NO_3 + 73.9\ SO_4)$$

in which the concentrations of the several ions are expressed in milliequivalents per liter. The first estimate is then corrected according to the following schedule:

(*a*) When T is less than 10 epm, or when T exceeds 10 epm with bicarbonate being the predominant anion, $EC = EC' - (EC'^{1.447}/157)$.

(*b*) When T exceeds 10 epm and if chloride is the dominant anion, $EC = EC' - (EC'^{1.380}/178)$.

(*c*) When T exceeds 10 epm and if sulfate is the dominant anion, $EC = EC' - (EC'^{1.436}/116)$.

These corrections were derived from the two samples under consideration by least-squares correlations.

7. *The empirical method.* The empirical method has been developed over a long period and has been fitted and refitted to a great number of analyses. It takes the following forms, depending on the concentration of the water and on the nature of the principal anion:

(*a*) When T is less than 1 epm, $EC = 100T$.

(*b*) When T falls between 1 and 3 epm, $EC = 12.27 + 86.38T + 0.835T^2$.

(*c*) When T falls between 3 and 10 epm, $EC = T\,[95.5 - 5.54\ (\log T)]$.

(*d*) When T exceeds 10 epm and if bicarbonate is the dominant anion, $EC = 90.0T$.

(*e*) When T exceeds 10 epm and if chloride is the dominant anion, $EC = 123T^{0.9388}$.

(*f*) When T exceeds 10 epm and if sulfate is the dominant anion, $EC = 101T^{0.9489}$.

(*g*) If T is greater than 1000 epm, this meth is not to be used.

It is convenient to solve the preceding relati and to plot EC as a function of T either nomographs or as curves on log-log graph pa Nomographic solutions are presented as Figur on which the 'chloride' and 'sulfate' segme are used only for conditions (*e*) and (*f*) abo and the 'normal' segment is used for all ot cases.

Note that two of the several methods (3 an were derived from the data of the first largest statistical sample; they were include the test to provide more complete control. method of Dunlap and Hawthorne and modified Rossum method are the only one which the actual concentration of all of common ions is considered. In the empir method the nature of the principal anion for rather concentrated waters is considered.

Results

Electrical conductivity was computed for analyses of both samples by each of the meth described above, and the standard errors estimate were calculated. Additionally, the centage of error between estimated and m ured values and the standard errors of estim of the percentages were computed. This la value ($s_{\%}$) is more significant than the for (s) in the present case because the largest m nitude of EC (41,500) is some 600 times la than the smallest (69). A standard error of units has little importance at $EC = 41{,}500$, a method that includes such an error at EC 69 is not useful. The 'percent standard erro

TABLE 1. Comparison of the Several Metho Estimating Electrical Conductivity

Method	First Sample (49 analyses)		Second Sam (25 analy	
	s	$s_{\%}$	s	
1. $EC = 100T$	1130	14.2	148	
2. Dunlap-Hawthorne	273	12.0	105	2
3. Linear correlation	155	18.5	114	1
4. Logarithmic correlation	5890	38.4	271	1
5. Handbook 60 graph	872	12.6	87	
6. Modified Rossum	374	6.9	91	
7. Empirical	91	6.6	72	

ate, $s_{\%}$' can be used with equal significance ghout the range of values, and it provides er comparison among the several methods does s.

e results of the comparisons are listed in 1. Standard errors of estimate range from nan 7 to more than 38 per cent. Errors for garithmic correlation are so large that this od has little practical value.

a rare coincidence, $s_{\%}$ of the empirical od is identical for both samples and is ally the same as is $s_{\%}$ of the modified am method. The slight differences between wo were not tested for significance. A sub- e analysis suggests that the empirical od provides more accurate estimates for ntrated waters while the modified Rossum od furnishes better results in the more nor- anges (i.e., T less than 10 epm).

en though $s_{\%}$ of the two methods is almost cal, estimates may be made much more rap- by use of the empirical method. About two- s of the time, it will include errors of less 7 per cent, which is comparable to the ling and analytical errors of many waters. empirical method is therefore recommended to those wishing to make rapid estimates of electrical conductivity from the results of chemical analyses of water samples.

The nomographs of Figure 2 are also useful for the more common reverse procedure—the estimate of the ionic sum from electric conductivity. The empirical method will provide more accurate results than will the estimating equation $T = EC/100$.

References

Dunlap, H. F., and R. R. Hawthorne, The calculation of water resistivities from chemical analyses, *J. Petrol. Technol., Tech. Note 67, 3,* 1951.

Hem, J. D., Study and interpretation of the chemical characteristics of natural waters, *U. S. Geological Survey, Water Supply Paper 1473,* 1959.

Richards, L. A., Ed., Diagnosis and improvement of saline and alkaline soils, *U. S. Dept. Agr., Handbook 60,* 160 pp., 1954.

Rossum, J. H., Conductance method for checking accuracy of chemical analyses, *Anal. Chem., 21,* 631, 1949.

Schlumberger Well Surveying Corp., *Log Interpretation Charts,* privately printed, Houston, 1957.

(Manuscript received July 16, 1960; revised April 28, 1961.)

Elastic Wave Interferometry—A New Tool[1]

I. TOLSTOY

Columbia University, Hudson Laboratories
Dobbs Ferry, New York

Abstract. A harmonic source in a vertically stratified waveguide excites a number of propagating modes, each having its own characteristic wavelength in the horizontal direction. These modes interfere, giving characteristic oscillations of the wave field amplitude as a function of range from the source. It is pointed out that in the case of a three-layered half-space the interference wavelength Λ of the first two modes is very sensitive to layer properties. In particular, if one examines the effect of the second (intermediate) layer, it is seen that this wavelength is most sensitive in that range of parameters for which the usual seismic techniques are mostly inadequate. In principle the method can be used in any properly chosen frequency range for both elastic and liquid media. It also appears that transient wave recordings (explosions, earthquakes, microseisms, etc.,) obtained by a sufficient number of receivers could be filtered to determine Λ and thus to utilize this technique. Tables providing sufficient coverage for a large variety of model types would not be difficult to calculate by means of currently available computing machinery.

roduction. The purpose of this note is to e a new geophysical technique for deter- g the acoustic and elastic parameters of a ed geologic section. It is based upon meas- ents of the *interference wavelength* of at two modes of propagation (preferably the owest ones) excited by a harmonic source. nly previous application of this idea was d to acoustic waves in a three-layered fluid *toy,* 1958], but it can clearly be general- o cover a much broader class of problems includes not only the obvious extension to waves in elastic media but also most prob- of seismological interest. This technique is ially interferometric and is similar in con- to the determination of the thickness of ilms by light interference. The important displayed in this paper is the great sensi- of this approach when applied specifically tions for which seismic techniques are inadequate or difficult to apply.

ciples. Consider as an example the prop- n of acoustic waves in a three-layered vaveguide (Fig. 1) or the similar case of vaves in a three-layered elastic half-space. a single frequency source in the top layer ell known that at sufficiently long ranges e order of 10 times the waveguide thick- the wave field is almost exclusively due lly reflected, i.e. guided, waves. At such the up- and down-going wave fronts are essentially plane and can be visualized in terms of parallel systems of rays. It is further known that, for a given frequency, only a discrete, finite set of angles of incidence allow for the unattenuated propagation of totally reflected energy. These correspond to the permissible modes of propagation at that frequency, i.e., to modes whose low-frequency cutoff is less than the source frequency. If this frequency and/or the source and receiver depths are properly chosen the first two modes can, for all practical purposes, be excited to the exclusion of all others. These two modes, corresponding to two trains of internally reflected plane simple harmonic waves traveling at different angles, interfere with each other in approximately periodic fashion. It is then easily shown [*Tolstoy,* 1958] that the wave field amplitude at some constant depth has the following dependence upon range:

$$A = R^{-1/2}[A_1^2 + A_2^2 + 2A_1A_2 \cos (k_1 - k_2)R]^{1/2} \quad (1)$$

where A_1 and A_2 are constants determined by the source power and source-receiver depths, R is the horizontal distance from the source, and k_1 and k_2 are the wave number eigenvalues corresponding to the source frequency. In other words the wave field amplitude has, as a function of R, the form sketched in Figure 2. The distance between successive maxima or minima (constructive or destructive interference of the two modes) is, to a good approximation,

$$\Lambda = \frac{2\pi}{k_1 - k_2} \quad (2)$$

umbia University, Hudson Laboratories
ution 102.

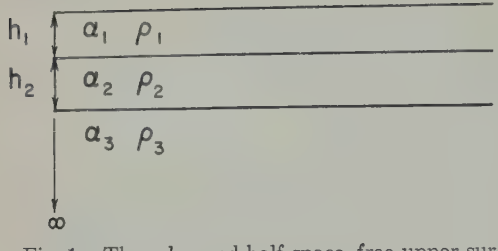


Fig. 1. Three-layered half-space, free upper surface. α_1, α_2, α_3 are sound velocities for the fluid case or shear wave velocities for Love waves; ρ_1, ρ_2, ρ_3 are densities.

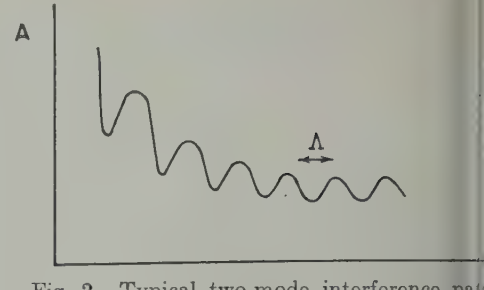


Fig. 2. Typical two-mode interference pa displayed by a record of wave amplitudes v range.

We call this the 1-2 *mode interference wavelength.* Equation 2 is not exact, in view of the slight warping produced by the $R^{-1/2}$ factor in (1), but is quite sufficiently accurate for large R.

Sensitivity. Some numerical results are available for the special case of the three-layered fluid waveguide of Figure 1, and are displayed in Figures 3, 4, and 5. These results are applicable to the study of sub-bottom layering in shallow seas. However, they are incomplete, in the sense that they are limited to a certain range of bottom parameters. The writer's purpose in displaying them is merely to illustrate the behavior of Λ under typical conditions.

Figure 3 shows curves of constant Λ/h_1, for selected frequencies, as a function of α_2/α_1, h_2/h_1, for given α_3/α_1 and $\rho_1 = 1$, $\rho_2 = \rho_3$. These curves were calculated for

$$\alpha_1 = 1509 \text{ m/sec}$$

$$h_1 = 19.81 \text{ m}$$

We may apply these results to other values α_1', h_1', by keeping Λ/h_1 invariant and sc the frequency to

$$f' = f \frac{h_1}{\alpha_1} \frac{\alpha_1'}{h_1'}$$

The important feature is the sensitivity of curves throughout the exhibited range beyond, and especially their sensitivity to α For example, if $h_2 = 1.5h_1$ and if $\Lambda = 1$

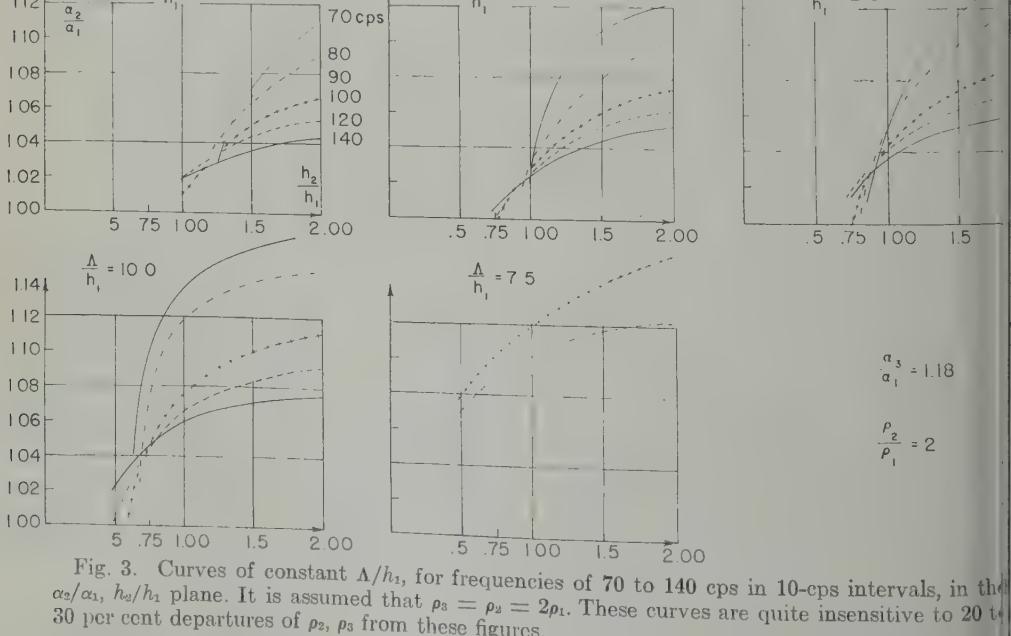
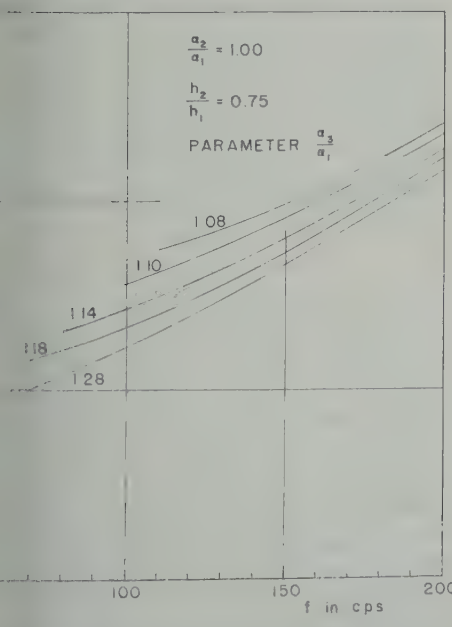


Fig. 3. Curves of constant Λ/h_1, for frequencies of 70 to 140 cps in 10-cps intervals, in th α_2/α_1, h_2/h_1 plane. It is assumed that $\rho_3 = \rho_2 = 2\rho_1$. These curves are quite insensitive to 20 t 30 per cent departures of ρ_2, ρ_3 from these figures.

= 120 cps, then $\alpha_2 = 1.045\alpha_1$ whereas if
$10.00h_1$, $\alpha_2 = 1.085\alpha_1$.
e manner in which such curves can be used
actice is as follows. Suppose that refraction
ner methods have been used to show that
~ 1.18 and $h_3 \gg (h_1 + h_2)$. [In which
the parameters of layer 3 can indeed be
ately determined by seismic methods].
measure Λ/h_1 for at least two frequencies.
ing α_1 and h_1, we can then uniquely
mine α_2 and h_2. For example, if for con-
s (3), we were to measure at 70 cps
$17.5h_1$ and at 140 cps $\Lambda = 10h_1$ we would
$\alpha_2 = 1.07\alpha_1$, $h_2 = 1.5h_1$, from Figure 3.
would be of interest to see these curves
ued into the region $\alpha_2/\alpha_1 < 1$. But it is
ly clear from the trends in Figure 3 that
g as α_2 is of the order of α_1 the method
ns very sensitive.
ures 4 and 5 show some typical results for
vs f under various assumptions for α_3/α_1.
seen that sensitivity to this parameter is
moderate and is greatest for small α_2/α_1.
shows that only a few more sets of curves
e type shown in Figure 3 are needed to
lete the picture.
ally, Figure 6 shows that Λ/h_1 is quite
tive to variations of ρ_2 in the vicinity of



Illustrating Λ/h_1 versus f, for $\alpha_2/\alpha_1 = 1.00$
$h_2/h_1 = 0.75$ for various values of α_3/α_1.

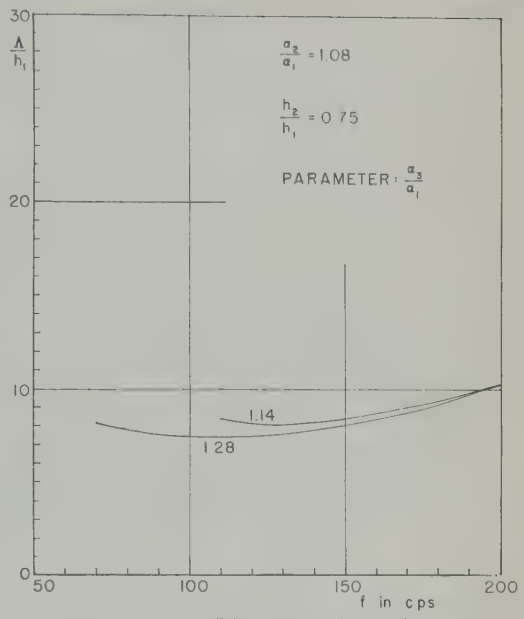


Fig. 5. Same as Figure 4, with $\alpha_2/\alpha_1 = 1.08$. Note that Λ/h_1 is rather insensitive to α_3/α_1 in this case.

$\rho_2 \sim \rho_3 \sim 2\rho_1$, so that the densities can fortunately be discarded as significant parameters.

Discussion. Looking at these results first in terms of the model of Figure 1, we see that this is a sensitive method for determining α_2 and h_2, at least in the range of parameters involved in Figure 3. These correspond to moderate and small values of h_2/h_1 and α_2/α_1, i.e., to cases in which the usual seismic methods are either quite unreliable (refraction shooting) or require extreme care (reflection shooting).

An example of the application of these ideas is to be found in an earlier paper [*Tolstoy*, 1958]. In that work, preliminary refraction profiles gave

$$h_2 = h_1$$
$$\alpha_2 = 1.04\alpha_1 \qquad (5)$$
$$\alpha_3 = 1.18\alpha_1$$

whereas the method of mode interferences gave

$$h_2 = 0.9h_1$$
$$\alpha_2 = 1.12\alpha_1 \qquad (6)$$
$$\alpha_3 = 1.24\alpha_1$$

as a more probable model.

This model turned out to be entirely consistent with (*a*) a comparison of calculated and

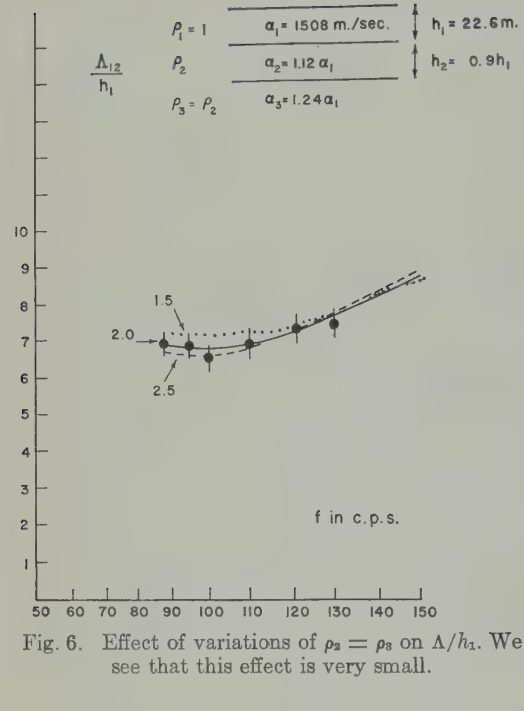


Fig. 6. Effect of variations of $\rho_2 = \rho_3$ on Λ/h_1. We see that this effect is very small.

experimental first-mode group velocity curves [*Tolstoy*, 1958] and (*b*) the detailed juxtaposition of calculated and experimental two-, three-, and four-mode excitations. In this connection the reader is also referred to a later paper by *Clay* [1959], who, using the same model and better data, achieved truly superior agreement between theory and experiment.

On the other hand, the preliminary model (5) obtained by refraction shooting techniques failed to provide agreement under both (*a*) and (*b*) [*Tolstoy*, 1958].

To conclude, we must emphasize that:

1. If the method is to be used systematically in connection with the simpler three-layer waveguides, such as those governing the propagation of sound in shallow seas or of Love waves in the earth's crust, a certain number of tables such as those shown in Figure 3 remain to be calculated, and these should include a realistic range of cases for which $\alpha_2 < \alpha_1$. The amount of calculation involved in these computations is not particularly large, especially if the procedure is well planned, e.g., by a calculation of curves for constant Λ and f directly from the characteristic equation.

2. The principle can be extended to more complex problems such as the use of Rayleigh waves in stratified elastic media. For exam the methods and calculations of *Dorman, Eu and Oliver* [1960] can be applied in this cont The degrees of model complexity to whic would be fruitful to extend the method rer to be determined.

The principle of the method depends upon fact that each mode is characterized by a g wave number, irrespective of the mechanis propagation. Thus one may be dealing acoustic waves, elastic waves, etc., as lon one is concerned with the far field for w the effects of the head wave are unimpor and the mode pattern is firmly established.

3. Although the principle involves the ca simple harmonic wave trains and is at its when used in conjunction with a cw so narrowband filtering of receiver outputs sh enable one to extract the same type of info tion from records of shots, earthquakes, m seisms, etc. Thus the method is seen to considerable generality.

4. It may be that higher-mode interfer wavelengths could also be used in this ma However, it is a fact that the most stra forward procedure from both theoretical experimental points of view is to use the lo two or three modes.

5. Finally it must be noted that instrum tion for the use of this method exists. A prof of cw sound sources for work at sea has developed in the last twenty years or so. On we might point out the recent work of *Cra Doty, and Lee* [1960] which could easil adapted to the needs of the present method

Acknowledgment. This work was supporte the Office of Naval Research.

References

Tolstoy, I., Shallow water test of the the layered wave guides, *J. Acoust. Soc. A* 348, 1958.

Clay, C. S., Propagation of band-limited n layered wave guide, *J. Acoust. Soc. Am.*, *31* 1959.

Dorman, J., M. Ewing, and J. Oliver, Stu shear-wave velocity distribution in the mantle by mantle Rayleigh waves, *Bull.* *Soc. Am.*, *50*, 87, 1960.

Crawford, J. M., W. E. N. Doty, and M. R Continuous signal seismograph, *Geophysi* 95, 1960.

(Manuscript received March 22, 1961.)

Surface Heat Flow from a Differentiated Earth

GORDON J. F. MACDONALD

Theoretical Division, Goddard Space Flight Center
National Aeronautics and Space Administration
Washington 25, D. C.

Abstracts. Numerical calculations have been carried out on the development of surface heat flow in model earths. The bulk radioactivity of the earth is taken equal to that of chondritic meteorites. The initial temperature reaches 2600° at 1200 km. The heat flow for a model in which the radioactivity is uniformly distributed in the outer 600 km is 90 ergs/cm²/sec. If the radioactivity is concentrated in the outer 100 km, the present-day surface heat flow is 68 ergs/cm²/sec. The initial heat contributes about one-fifth the surface heat flow. The examination of the relations between initial heat, radioactive distribution, and heat flow suggests that if the earth has the radioactive composition of chondritic meteorites, then a near-surface concentration of heat sources must have proceeded at temperatures well below the melting point of silicates. Radioactivity lower by a factor of 2 would remove the indicated discrepancies.

roduction. *MacDonald* [1959] calculated development of the temperature distribution the mantle assuming heat transport by tive conductivity damped by electrical conity at high temperatures. The radioactivity he earth as a whole was assumed equal to of chondritic meteorites. Different distrins of radioactivity and initial temperatures considered in the calculations. Two princiesults were: (1) Models of the earth reced the present heat flow of 50 ergs/cm²/ within a factor of 2. (2) If the initial erature reaches 2600° at 1200 km, then ombined contributions of the initial heat f chondritic radioactivity lead to a heat f about twice that observed, provided the ources are uniformly distributed over the 600 km of the earth.

rk [1961] determined the effect of upward ntiation on the heat flow for models in- at a low temperature, and showed that esulting heat flow approximates the obvalue. It might be suggested that a ntration of heat sources toward the surwould allow an initially high temperature together with a chondritic composition, explain the present heat flow. A number culations have been carried out to test this hesis. A near-surface concentration of ources over all geologic time reduces the t surface heat flow. Unless the heat s are concentrated within the upper 100 km, the reduction in heat flow is not sufficient to allow an initial temperature of 2600° at 1200 km. If the earth has a radioactive composition comparable to that of chondritic meteorites, then the earth must have differentiated in some fashion at temperatures well below the melting temperature of silicates.

Calculations. The assumed average concentration of uranium, thorium, and potassium is 1.1×10^{-8} g/g, 4.4×10^{-8} g/g and 8.0×10^{-4} g/g, respectively. Models are considered in which this radioactivity is concentrated in outer shells of 100 to 600 km thicknesses. The temperature at a time 4.5×10^{9} years is shown in Table 1. Radiation is assumed to contribute to the thermal conductivity and the opacity is $\epsilon = 10$ cm^{-1}. The parameters common to all models are listed

TABLE 1. Initial Temperature Distribution

Depth, km	T, °C
100	1880
200	1970
300	2050
400	2120
500	2180
600	2250
800	2370
1000	2490
1200	2600
1500	2640
2000	2930

TABLE 2. Parameters Common to All Models

Parameter		Value
Surface temperature		0 °C
Index of refraction		1.7
Heat capacity		1.3 joules/g °C
Lattice conductivity		0.025 joules/cm sec °C
Decay constants	U^{238}	1.54×10^{-10} years^{-1}
	U^{235}	9.71×10^{-10} years^{-1}
	Th^{232}	0.499×10^{-10} years^{-1}
	K^{40}	5.5×10^{-10} years^{-1}
Heat generation	U	3.07 joules/g year
	Th	0.82 joules/g year
	K	1.12 joules/g year

in Table 2. The details of the calculations are given in *MacDonald* [1959].

The surface heat flow resulting from varying distribution of heat sources is shown in Figure 1. If the radioactivity is chondritic and confined to within the upper 600 km, then the surface heat flow is 90 ergs/cm^2/sec. If the radioactivity is concentrated toward the surface, the surface heat flow decreases. This results from the greater escape of heat produced in the past by the decaying radioactive elements. If the radioactivity is concentrated within the upper 100 km, then the present-day surface heat flow should be on the order of 68 ergs/cm^2/sec. The variation of heat flow with depth of burial of heat sources suggests that if the earth were initially hot (temperature of 2600° at 1200 km), and if the radioactive composition is that of chondritic meteorites, then the present-day surface heat flow can be explained if the concentration of radioactivity is within the upper few tens of kilometers of the earth. Such concentration might

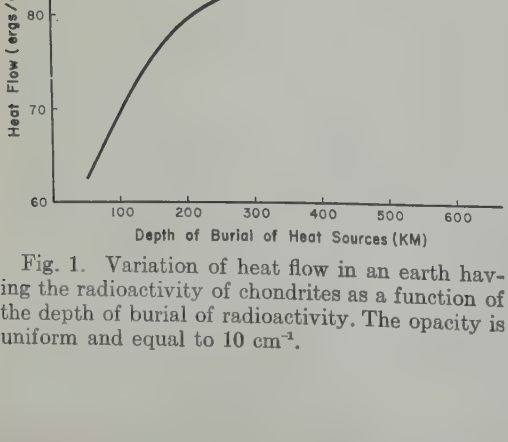


Fig. 1. Variation of heat flow in an earth having the radioactivity of chondrites as a function of the depth of burial of radioactivity. The opacity is uniform and equal to 10 cm^{-1}.

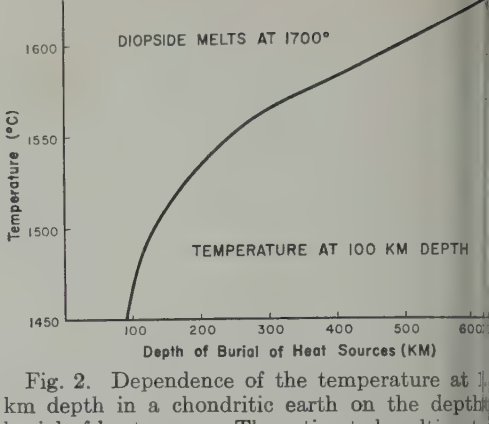


Fig. 2. Dependence of the temperature at 1 km depth in a chondritic earth on the depth burial of heat sources. The estimated melting t perature of diopside at 100 km is indicated comparison.

be acceptable in continental regions. Howe the oceanic heat flow approximately equals heat flow in continental regions, and the parent degree of differentiation in oce regions is far less than in continental regi Based solely on consideration of the sur heat flow, the calculations suggest that a l initial temperature can be ruled out if hypothesis of a chondritic composition is m tained and if heat is transferred prima through conduction coupled with radiation. ternatively, a radioactivity lower than tha chondrites by something less than a factor would permit models of an earth with init high temperatures. Such a radioactivity w result if it were assumed that the mantle a was of chondritic composition and that matter composing the core contained no ra activity.

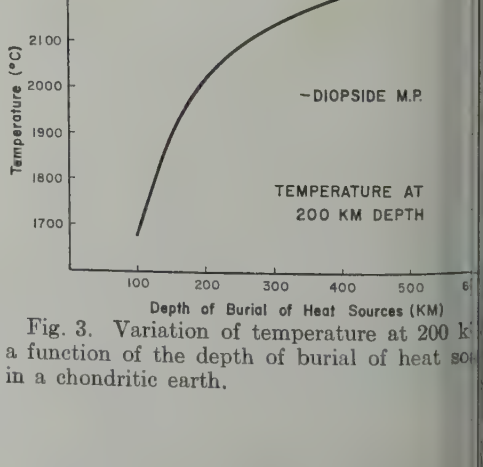
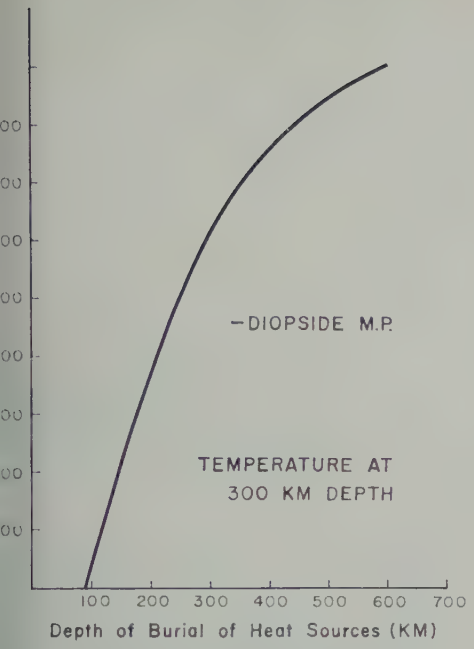
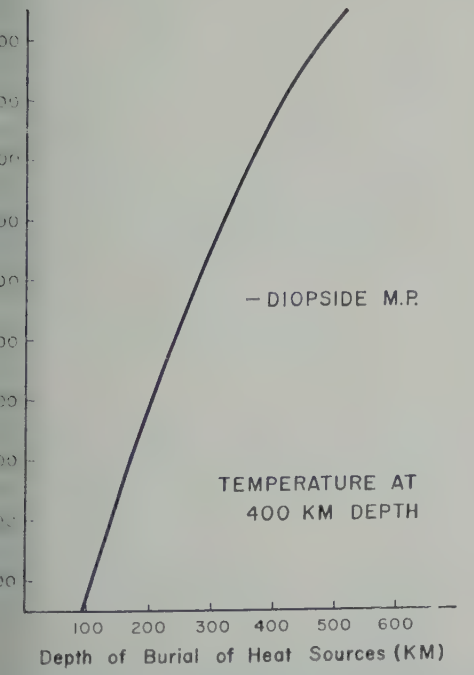


Fig. 3. Variation of temperature at 200 k a function of the depth of burial of heat so in a chondritic earth.



. 4. Variation of temperature at 300 km as
ction of the depth of burial of heat sources
hondritic earth.



5. Variation of temperature at 400 km as
tion of the depth of burial of heat sources
hondritic earth.

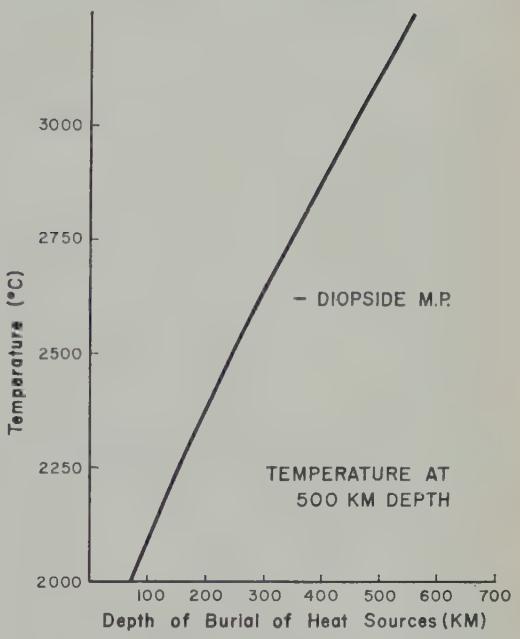


Fig. 6. Variation of temperature at 500 km as a function of the depth of burial of heat sources in a chondritic earth.

Figures 2–6 show the present temperature at various depths as a function of burial of heat sources. The estimated melting temperature of diopside, [*Boyd and England,* 1958] is also indicated. This estimate is based on direct experiments for pressure up to about 30,000 bars, and is most uncertain for depth greater that 100 km [*MacDonald,* 1959]. The present temperature at 200 km is far exceeded if the heat

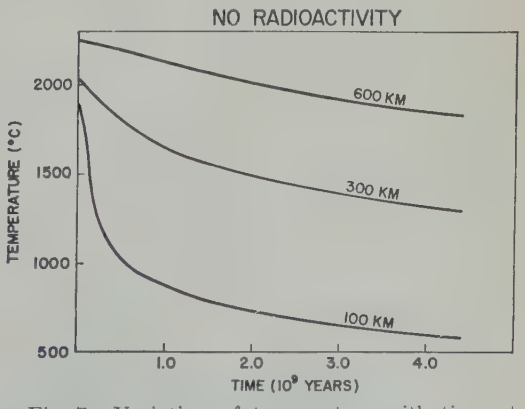


Fig. 7. Variation of temperature with time at depths of 100, 300, and 600 km in a nonradioactive earth with an initial temperature as given in Table 1. Opacity is 10 cm^{-1}.

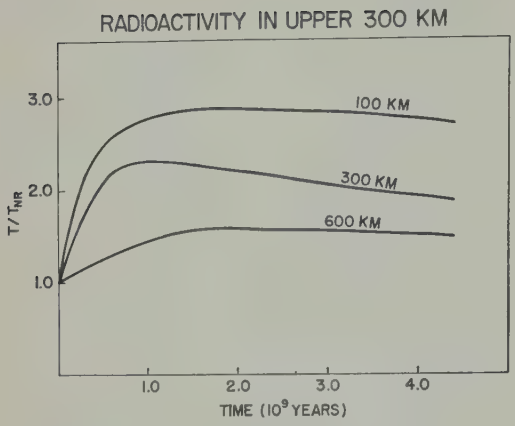


Fig. 8. Ratio of temperature in an earth with chondritic radioactivity concentrated in the upper 300 km to the temperature in a nonradioactive earth. The initial temperature is given in Table 1.

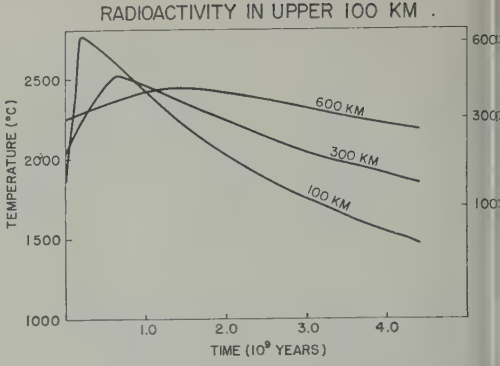


Fig. 10. Development of temperature at 1 300, and 600 km in time, assuming chondritic radi activity is uniformly distributed in the upper 1 km of the mantle. The estimated temperature a depth of melting of diopside is shown for co parison.

sources are buried as deep as 500 km. If the heat sources are concentrated in the upper 200 km, then the material at 300 km in depth and greater does not undergo melting, provided that the fusion curve is approximated by the melting point of diopside. Figures 4–6 show that melting will not take place at depths greater than 300 km, provided the heat sources are concentrated in the upper 200 km. Melting will take place at 500 km if the heat sources are buried within the upper 300 km. Seismic observations [e.g., *MacDonald and Ness*, 1961] strongly suggest the presence of a low velocity layer extending from the base of the crust to a depth on the order of 150 km. If the low velocity layer is due to a close approach of the actual temperature to the melting temperature, t calculations suggest that the heat sources shou be distributed in the upper 200 km. If a great depth of burial of heat source is assumed, th the melting takes place at greater depths whe the seismic results indicate a more normal var tion of velocity with depth. An alternative terpretation of low velocity layer is due *Lyubimova* [1959]. She assumes that the me ing curve is reached owing to a T^{-1} decrease thermal conductivity. Laboratory data are n sufficiently extensive to rule out the requir variation in conductivity.

Effect of initial heat. An indication of t role that initial heat plays in the developme of near-surface temperature and heat flows c be obtained by considering the development temperatures in an earth in which radioactivi

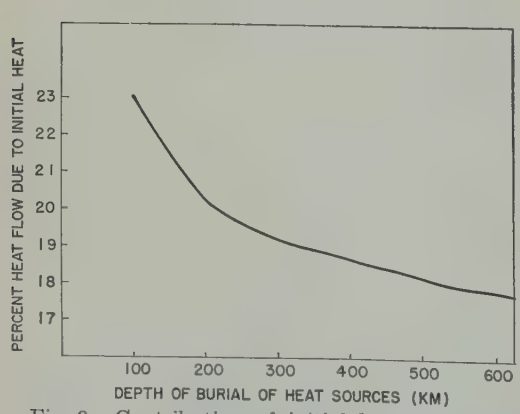


Fig. 9. Contribution of initial heat to surface heat flow to the total heat flow in an earth having the initial temperature listed in Table 1.

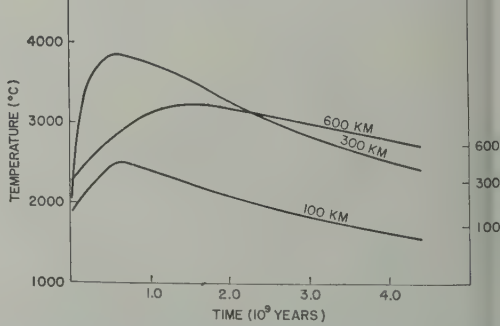


Fig. 11. Development of temperature with ti in an earth having chondritic radioactivity u formly distributed in upper 300 km.

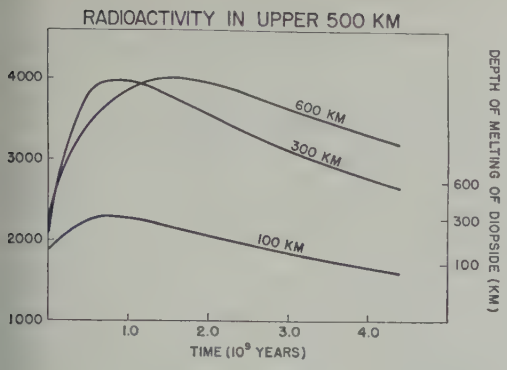


Fig. 12. Development of temperature with time a chondritic earth having radioactivity uniformly distributed in upper 500 km.

absent. Figure 7 shows the development of emperature in time for an earth whose initial emperature is that given in Table 1. Temperatures in the outer 100 km undergo significant ooling. The ratio of the temperature of a model ith radioactivity in the upper 300 km to the emperature for an earth without radioactivity given in Figure 8. The radioactivity increases he temperature near the surface, whereas the emperature at greater depths remains more or ss constant. Figure 9 summarizes the effect f the initial heat on the present-day surface eat flow. If the radioactivity is buried near the rface, then initial heat contributes one-ourth of the total radioactivity. If the radioctivity is buried over greater depths, then the ercentage contribution of the initial heat to he surface heat flow is less. This results from he fact that initial heat plays a role similar to eeply buried radioactivity. If the radioactivity concentrated near the surface, then much of he heat due to a high rate of heat production the past is lost, and the heat flowing from he deep interior makes a proportionately reater contribution to the surface heat flow. If he radioactive heat sources are deeply buried, hen the heat produced by the high initial rate radioactive heat remains trapped within the rth, and the percentage contribution to the itial heat flow is less.

Initial heat contributes about one-fifth the resent heat flux. If a lower initial temperature assumed, the proportional contribution of itial heat decreases, though not linearly beuse of the T^3 dependence of the radioactive nductivity. The high rate of heat production in the past provides an additional source of heat. The coincidence of the present surface heat flow with the present rate of heat production of a chondritic earth therefore implies either a combination of a low initial heat with a near-surface concentration of radioactive materials or a lower radioactivity for the earth.

Figures 10, 11, and 12 summarize the development in time of the temperature distribution in the upper mantle. If the radioactivity is initially concentrated in the upper 100 km, then the melting point of diopside is exceeded in the upper 300 km during the first 10^9 years. The temperature drops below the postulated melting temperature at 100 km only at 3×10^9 years. If the radioactivity is more deeply buried (Figs. 11, 12), then the temperature exceeds the melting temperature in the upper mantle over most of the 4.5×10^9 years. The combination of chondritic radioactivity and a high initial temperature leads to melting of the mantle over a large part of geologic time. This in turn implies that heat may be transported by convection as well as by radiation plus conduction.

Clark [1961] has carried out similar computations on surface heat flow in a differentiated earth. He finds that the discrepancy between the calculated and observed heat flow can be removed or kept small, provided the earth is differentiated and the initial temperature is low. Clark's results and those of the present paper imply that a chondritic model of the earth requires a near-surface concentration of heat sources at temperature well below the melting temperatures.

References

Boyd, F. R., and J. England, Melting of diopside under high pressure, *Carnegie Institution Washington Year Book, 57*, 173, 1958.

Clark, S. P., *Heat Flow From a Differentiated Earth, J. Geophys. Research, 66*, 1231–1234, 1961.

Lyubimova, H. A., On the temperature gradient in the upper layers of the earth and on the possibility of an explanation of low velocity layer, *Bul. Acad. Sci., USSR, Geophys. Ser.*, 1861–1863, 1959.

MacDonald, G. J. F., Calculations on the thermal history of the earth, *J. Geophys. Research, 64*, 1967–2000, 1959.

MacDonald, G. J. F., and N. F. Ness, Study of the earth's free oscillations, *J. Geophys. Research, 66*, 1865–1911, 1961.

(Manuscript received June 5, 1961.)

Gravity Measurements over the Southern Rocky Mountain Trench Area of British Columbia

G. D. GARLAND AND E. R. KANASEWICH

Department of Physics, University of Alberta
Edmonton, Alberta, Canada

THOMAS L. THOMPSON

School of Mineral Sciences, Stanford University
Stanford, California

Abstract. A series of negative gravity anomalies found along the southern part of the Rocky Mountain Trench in Canada is interpreted to be the effect of relatively deep basins in the trench floor. These are apparently filled with light material and are separated from each other by regions of only thin cover over bedrock of normal density. The pattern obtained is very suggestive of a system of longitudinal and transverse faults, and the gravity field is therefore consistent with the theory that the trench, in this vicinity, was produced chiefly by downfaulting.

Introduction. Gravity measurements in itheastern British Columbia, Canada, have lded anomalies which show interesting rela-nships to some of the major structural fea-es of the area. In particular, the gravity field ovides new information on the form of the cky Mountain Trench in the region. The nch, 'a long, narrow, intermontane depres-n' [*Daly,* 1912, p. 596], extends for over 1000 les in a northwest direction from Montana to Yukon territory. Numerous theories of its gin have been suggested, some of which are ntioned below, but further study of the form d structural relations is required. In south-tern British Columbia, where the trench is o 12 miles wide, its floor is largely covered h drift or loosely consolidated sedimentary k, and geophysical measurements can be used advantage to indicate the depth of this cover. pattern of gravity anomalies is found over trench which is not unlike that observed r other rift valleys. The gravity map also ws certain effects related to major faults ich are transverse to the direction of the nch.

The measurements to be described were made ween 1958 and 1960, in part by one of the hors (T.L.T.) during a geological study of area and in part on special trips from Ed-nton. Support was received from the Na-nal Research Council of Canada, and through a loan from the Erickson Fund for students of geology at Stanford.

Geological description of the area. The areal geology west of the trench is dominated by a broad north-trending Purcell geanticline which exposes a thick sequence of Precambrian sedimentary rock (Fig. 1). The sequence is repeated in the form of three giant north to northwest plunging folds. These are bounded by four major faults which are transverse to the trend of the geanticline. From north to south, the faults are called MacDonald, Hall, St. Mary, and Moyie-Lenia. The trend of the two northern faults merges with the trend of the trench. The St. Mary and Moyie-Lenia faults trend across the trench [*Rice,* 1937].

Similar faults east of the trench, approximately opposite the St. Mary and Moyie-Lenia faults, are the Wild Horse and Dibble faults, respectively. These faults are an integral part of the Rocky Mountain structural pattern which at this latitude is characterized by low angle thrust faulting [*Henderson and Dahlstrom,* 1959].

A Mesozoic age for the development of these faults is implied from regional considerations. First, the St. Mary fault developed concurrently with the emplacement of granitic rocks [*Rice,* 1941] which are 106 million years old [*Beveridge and Folinsbee,* 1956]. Second, the Dibble fault, in the Rocky Mountains, is part of the Lara-

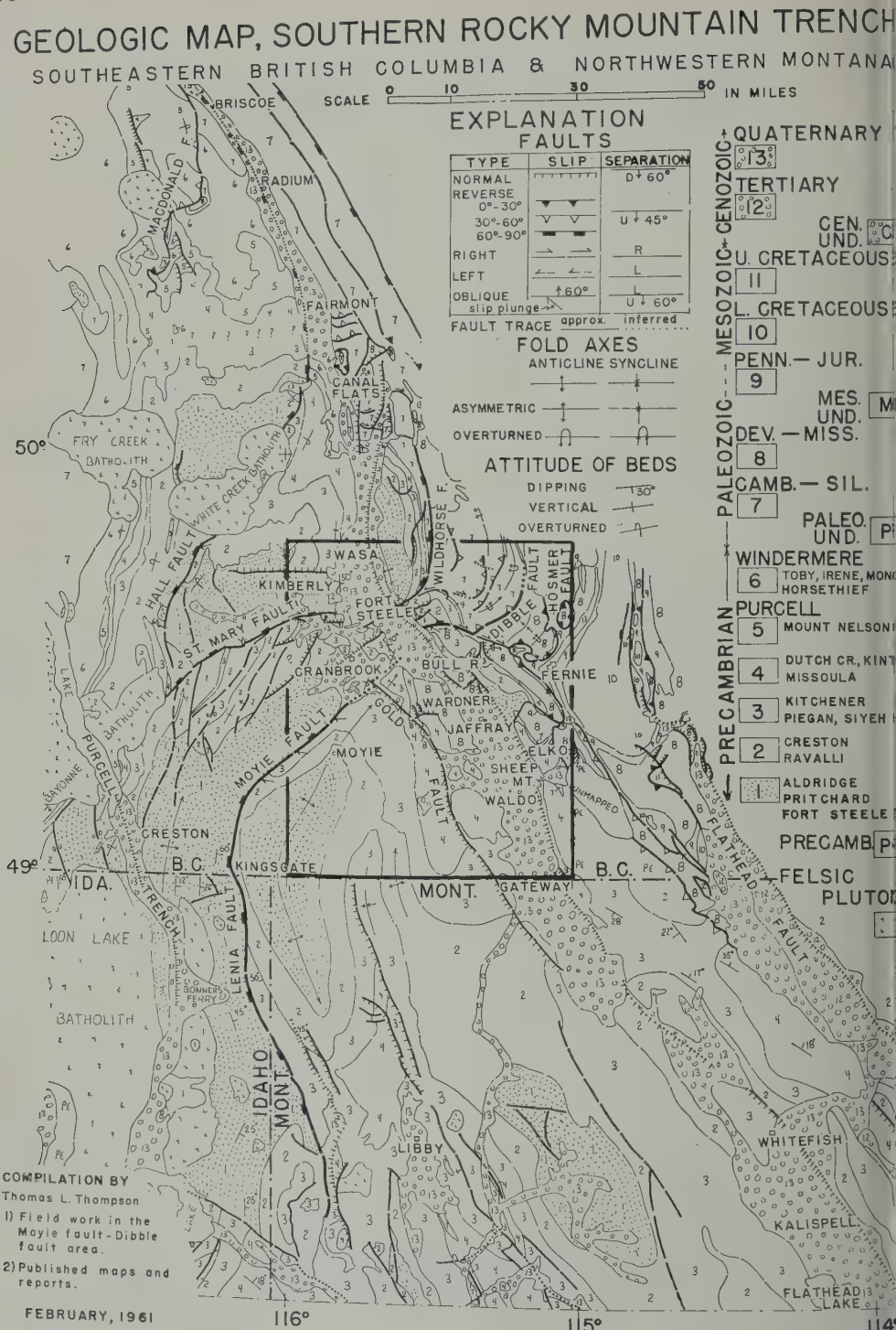


Fig. 1. Geologic map of southeastern British Columbia and adjacent areas. The formation shown in pattern are those with which the principal density differences are associated. The area covered by the gravity map, Figure 2, is outlined.

) system of thrust faulting. Structure of ozoic age is also transverse to the trend of trench near Cranbrook. Rocks of early ozoic age rest on Precambrian rocks north- of the Moyie-Lenia and Dibble faults, eas rocks of late Paleozoic age rest on the ambrian rocks southeast of those faults.

ne numerous theories of origin for the trench been reviewed by *Eardley* [1951, pp. 303– and *North and Henderson* [1954, pp. 82– . Some writers believe it is the result of ero- without fault control; others conclude that s resulted from erosion along a zone of fault- Suggested fault origins encompass devel- ent as a graben, by thrust faulting, by e-slip faulting, or by a combination of e. Certain theories seem to explain the sur- geology in one portion of the trench but contrary to the evidence in other portions. area of controversy is in southeastern Brit- Columbia.

ensity of rock materials. The lightest ma- ls of importance, sand, silt, and gravel of ozoic age, are presumed to have an average ity of 2.2 g/cm³. This figure is derived from es which are shown in the *Handbook of ical Constants* [1942] for water-saturated nentary materials of Tertiary and Quater- age. The average density of such materials t logically be as low as 2.1 or as high as g/cm³ depending on the relative amounts degree of compaction and cementation of lifferent types of sedimentary deposit.

ne density of water-saturated rock speci- s from areas adjacent to the trench were rmined by means of a fulcrum beam bal- with a direct reading scale. An estimate of ive percentages of the various rocks in the nentary rock column is made in the deriva- of average densities for the different rock ences (Table 1).

erage density for the Precambrian sequence be significantly greater than 2.7 g/cm³ be- e of concentration of mafic sills in the lower and the presence of mafic flows and/or nite in the upper part. The average den- of the Kitchener formation varies from to 2.78 g/cm³ depending on the amount of nite. Specimens from basalt flows in the n formation show a density contrast relative erage bedrock of about 0.1 g/cm³.

afic sills in the Precambrian sequence reach significant proportions only in the Aldridge formation west of the trench. These sills make up at least 70 per cent of a 5000-foot-thick section near Kimberly and a 4000-foot-thick section near the International Boundary at Kingsgate [*Schofield*, 1915, pp. 73–74]. The average specific gravity of these sections (about 2.9 g/cm³) indicates a density contrast of 0.2 g/cm³ relative to the rock column without sills.

Method of gravity measurements. The first gravimeter measurements in the area were made during a regional survey of a large portion of southern British Columbia by the Dominion Observatory in 1954 [*Garland and Tanner*, 1957]. During the course of this work, a network of base stations was established with a North American gravimeter, and this network was simultaneously adjusted to pendulum observations to provide the gravimeter scale constant. A number of the base stations are within the area of the present study, and these, notably Cranbrook, Wardner, and Elko, have been used as starting points for the more detailed work.

All the observations made between 1958 and 1960 were made with the Worden gravimeter of the University of Alberta. Virtually all circuits of measurements were connected directly to one of the above bases, and there was therefore no problem of adjustment. For stations lying in the main river valleys, adequate control for both position and elevation was obtained from the excellent maps of the Columbia River Basin series of the Department of Mines and Technical Surveys. For stations in areas not covered by these maps, elevations in general were obtained by aneroid barometer readings. It is realized that in a mountainous region a single determination by this method is uncertain by 10 feet or possibly more, but most stations were visited more than once, specifically to repeat the barometer reading. It is very unlikely that elevation errors could materially affect the form of either the gravity contours or the profiles to be discussed.

The gravity anomaly map (Fig. 2) shows simple Bouguer anomalies, computed for a density of 2.67 g/cm³. Terrain corrections were in fact computed for many of the stations, and the corrections for a few stations, in deep valleys or on peaks, were as large as 20 mgal. However, because corrections are not available for all stations, largely due to the incomplete coverage

TABLE 1. Densities of Rocks

Rock Unit and Type	Thickness, feet	Number of Samples	Density of Water-Saturated Rocks, g/cm³	
			Range	Averages
Late Paleozoic	(7,000)			
Rundle formation	2,800			
Limestone		6	2.64–2.69	2.67
Banff-Exshaw formation	700			
Shale		1		2.41
Chert		1		2.58
Palliser formation	1,800			
Limestone		6	2.61–2.68	2.65
Fairholm group	1,600			
Gypsum		1		2.20
Shale		1		2.41
Limestone		4	2.64–2.69	2.67
Dolomite		10	2.76–2.81	2.79
Quartzite		2	2.63–2.68	2.66
Conglomerate		1		2.71
Quartzite and dolomite		4	2.63–2.72	2.70
Early Paleozoic	(17,000)			
Beaverfoot-Briscoe formation	1,800			
McKay group	8,000			
Limestone		1		2.67
Tanglefoot formation	4,000			
Limestone		2	2.65–2.70	2.68
Dolomite		2	2.78–2.80	2.79
Eager formation	3,000			
Lutite		5	2.4 –2.7	2.62
Cranbrook formation	500			
Dolomite		1		2.78
Quartzite		2	2.60–2.64	2.62
Precambrian (Purcell Series)	(30,000)			
Kintla group	2,000			
Dolomite		2	2.83–2.84	2.84
Quartzite		4	2.68–2.72	2.69
Kitchener and Siyeh formations				
At Moyie Lake	8,500	8	2.66–2.74	2.69
Near Fisher Peak, east of Fort Steele	7,500	6	2.70–2.78	2.72
S.E. of Fort Steele	2,500	8	2.74–2.81	2.78
Creston formation	5,000			
Ft. Steele and Aldridge formations	15,000			
Argillite		7	2.60–2.78	2.65
Quartzite		2	2.56–2.61	2.58
Igneous rocks				
Mafic sills (Purcell intrusive rocks or Moyie sills)				
Schofield [1915]	3,900	?		2.99
East of trench		4	2.79–2.84	2.82
Mafic flows (Purcell extrusive rocks)	1,500?	3		2.82
Monzonite stock				
Bull River		4	2.51–2.58	2.56

by large-scale contour maps, and because the main pattern of anomalies over the trench is not altered by the terrain effect, only the simple Bouguer anomalies are shown.

Tables of observed gravity, station position and elevation, and terrain effect where avail are not being published, but are availab required.

Gravity minima along the trench. An e ination of the Bouguer map reveals the pre

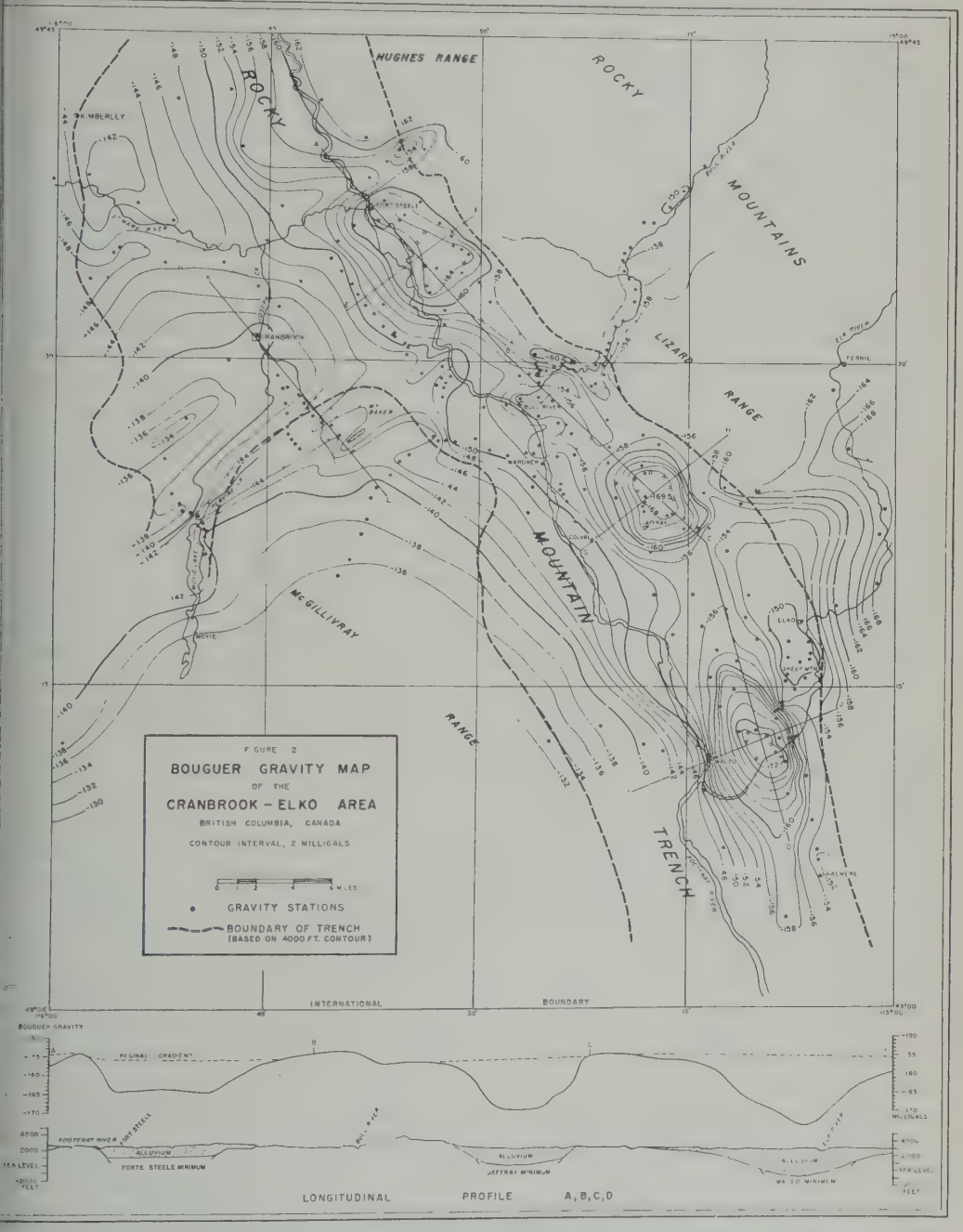


Fig. 2. Bouguer gravity map of the Cranbrook-Elko area.

three large negative anomalies. The amplitude of the anomalies decreases to the northwest. The origin of those lows can be elucidated from a study of the densities of the rocks in the area and from an examination of the shape of the anomalies. Samples taken from the small monzonite stock at Bull River have an average density of 2.56 g/cm^3. However, a gravity low is not measured in the vicinity of Bull River or on Sheep Mountain, which also has intrusive

outcrops. Therefore it does not seem that buried granitic rocks have caused the observed lows, and the density of the stocks must be close to the sedimentary sequence at depth.

Silts, sands, and gravels of Quaternary age blanket the floor of the trench. Coarse clastics of Miocene age are exposed along the St. Mary River [*Rice*, 1937]. Similar sedimentary deposits of Tertiary age have been mapped in the 'trench-like' Flathead valley of northwestern Montana (Fig. 1). There is, therefore, a good chance that other Tertiary deposits are buried within the trench. The possibility of Cenozoic volcanic material within the trench is considered unlikely, since such rocks have not been reported in the southern part of the trench in British Columbia or north of Flathead Lake in Montana [*Pardee*, 1950, p. 365]. The gravity lows are attributed to poorly consolidated clastic sediments of Cenozoic age.

Gravity methods are very effective in determining the thickness of light material filling a basin around which bedrock crops out. Provided the density contrast is sufficient, estimates of the form and depth of the basin may be made with rather more certainty than is the case in other problems of gravity interpretation. Investigations of anomalies similar to the present ones have recently been published [*Thompson and Sandberg* 1958; *Stewart*, 1958; *Thompson*, 1959; *Pakiser, Press, and Kane*, 1960].

If the horizontal dimensions of the structure are several times the vertical dimensions, a satisfactory estimate of the depth of fill h beneath a station is given by the solution to the Bouguer expression:

$$h = \frac{\Delta g}{2\pi k\sigma} \qquad (1)$$

where

k = the gravitational constant
σ = density contrast.
Δg = the observed Bouguer anomaly.

In other situations, the basin may be approximated by one or more vertical cylinders [*Heiland*, 1940, p. 147] or by surface distributions of mass. *Nettleton* [1942] has tabulated the solid angles subtended by circular laminar disks. The mass of the cylinder is considered to be condensed upon the median plane and the gravity anomaly obtained from the tabulated solid angles. It is then possible to calculate the ap proximate anomaly at stations off the axis.

The largest and southernmost anomaly is th Waldo minimum (Fig. 3). Northeast of th Waldo minimum is a small positive anoma centered at Elko. It is underlain, in part, by th Dutch Creek formation (also known as th Kintla group) around Elko and in part by intru sive outcropping at Sheep Mountain. This gra ity high represents the higher density of th Purcell series (2.7 g/cm^3) as compared with th density used in making the Bouguer correctio (2.67 g/cm^3). From longitudinal and transver cross sections of the Bouguer anomalies, th regional gradient can be estimated. This region gradient is due, in part, to terrain effects and part to deep-seated density variations (relate to isostatic compensation) which are not of in terest here. The residual anomaly, relative outcrops of bedrock, amounts to −19 mgal o this southernmost minimum. If the density di ference between fill and bedrock is −0.5 g/cm then the thickness of fill is about 3500 feet. Th density difference is thought to have a precisio of ±0.1 g/cm^3. The calculated depth may be great as 4400 feet or as small as 2900 feet.

The 14-mgal gravity minimum at Jaffra (Fig. 4) is in the shape of a square, 3 miles a side. The depth of fill is calculated to be 230 feet. From scattered outcrops to the north an east of this anomaly *Leech* [1958] mapped west-dipping fault on the east wall of the trench There is a large gravity gradient which confirm the presence of this fault. The area northwest o the Jaffrey minimum is particularly interestin as it consists of a late Paleozoic sequence tha rises 1600 feet above the level of the trenc floor. It is broken up by faulting and is evident a small horst adjacent to the graben whic makes up the Jaffray gravity minimum.

The Fort Steele gravity minimum (Fig. 4) h 8 mgal of closure. It is rectangular in shape wi dimensions 3 by 4 miles. The calculated dep of fill is 1400 feet. The Dibble fault, which h gypsum in the footwall, may extend into th trench and widen the southern end of the Fo Steele minimum. North of Fort Steele the be rock must be beneath a thin cover of till. The is a suggestion of a fourth minimum 4 mil north of Fort Steele.

Faults and transverse structures. A line gravity minimum trends along the Moyie-Le

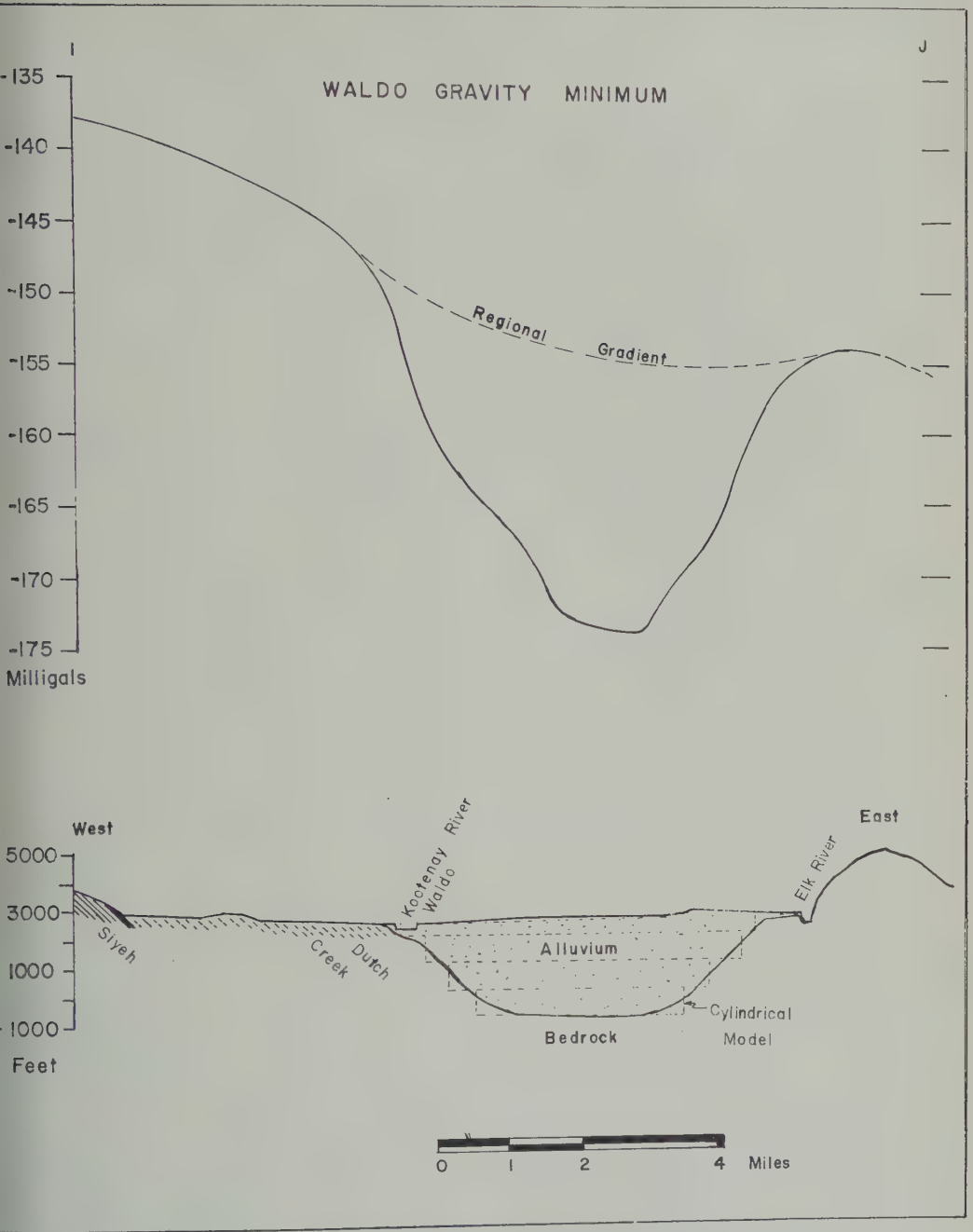


Fig. 3. Gravity profile and geologic section across the Rocky Mountain Trench at Waldo. The location of the profile is shown in Figure 2. Vertical exaggeration is 2:1.

ault south of Cranbrook to Moyie Lake. This inimum does not appear to be related to low-ensity fill because several low anomaly values re near bedrock. The Purcell sediments on both sides of the fault have nearly the same density, so they could not materially affect the gravitational field. It is proposed that the Moyie sills are responsible for the minimum trend. The sills

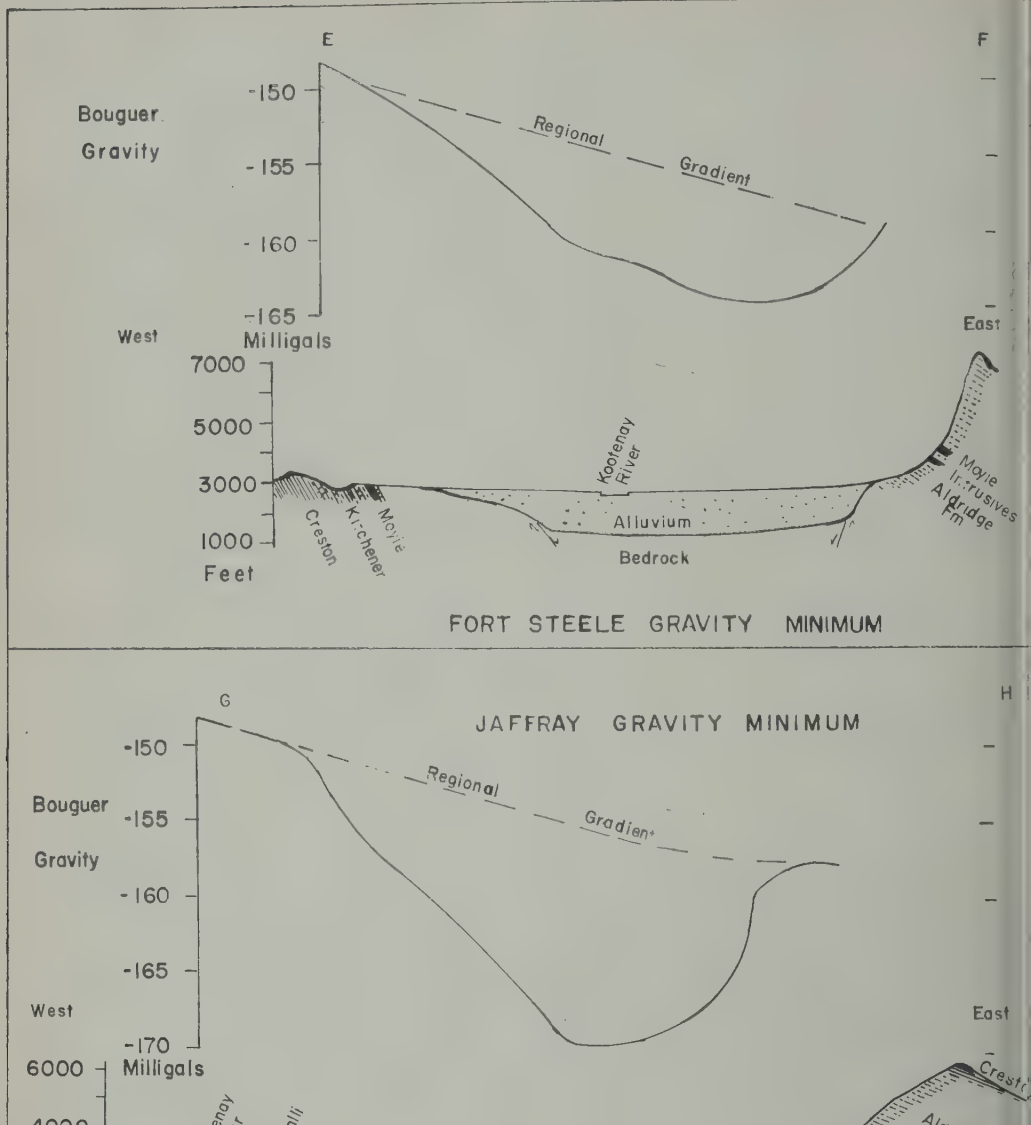


Fig. 4. Gravity profile and geologic section across the Rocky Mountain Trench at Fort Steele and Jaffray. The locations of the profiles are shown in Figure 2. Vertical exaggeration is 2:1.

of predominantly mafic material have intruded the Aldridge formation. The density relations have been reviewed, and a density excess of about 0.20 g/cm^3 between a purely sedimentary sequence and one intruded with Moyie sills apparent.

Figure 5 illustrates the gravity anomaly acr the Moyie-Lenia fault. Below it is a cross s

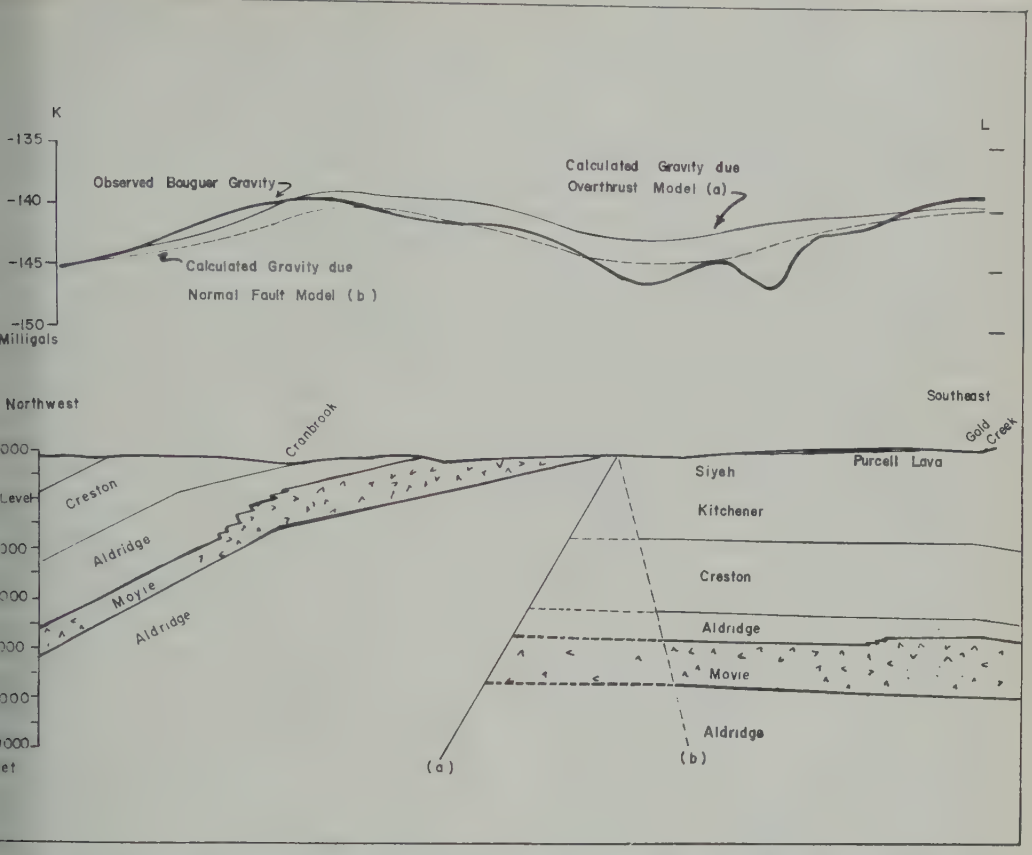


Fig. 5. Gravity profile and geologic section across the Moyie-Lenia fault in the Purcell Mountains. The location of the profile is shown in Figure 2. The calculated anomaly profiles for cases (*a*) and (*b*) are for an excess density of the Moyie sill of 0.2 g/cm^3. No vertical exaggeration.

showing two solutions which produce a simi- gravitational field. The theoretical gravity duced by the Moyie sills and the Purcell ex- ions has been calculated with the aid of a -dimensional graticule [*Nettleton,* 1942]. re elaborate computations are not warranted l more complete geologic and geophysical are available. The Moyie-Lenia fault pre- s one of those unusual situations in which ensity excess produces a negative gravity naly. A closer fit between the observed and retical gravity could be made by adding a ll amount of fill. Intense shearing of the along the fault plane may have decreased lensity. On Peavine Creek the Aldridge sedi- ts and sills are converted from massive rocks loscly cleaved, fissile phyllitic rocks in many es. (G. B. Leech, written communication). Much of the area is blanketed with a heavy cover of timber, and outcrops are obscured by recent deposits so that the thickness of the section containing the sills is not known. In the theoretical cross section it is shown to increase in thickness from 2000 to 5000 feet toward the southeast. The interpretation is not changed significantly if the single sill shown in the diagram is actually composed of numerous sills separated by sediment. The Purcell extrusives on top of the Siyeh formation contribute a small positive anomaly on the southeast block.

The normal fault solution produces a better fit, but this solution is not unique and a slight redistribution of the mass in the overthrust case would also produce good agreement. *Kirkham* [1930] reviewed the data on this fault and concluded that it was an overthrust with a steep

fault plane that dips westward. The fault plane forms an arc, concave to the east, that runs for 118 miles through British Columbia, Idaho, and Montana (Fig. 1). *Leech* [1960] believes this fault 'to be chiefly an oblique thrust whose hanging-wall moved relatively upward and northeastward.' Most geologists seem to agree that this fault has a very steep dip, and our gravity investigation supports this view. A detailed gravitational and magnetic survey along the entire length of the break would be useful in determining the shape of this fault at depth.

The relative low along the Moyie-Lenia fault diminishes as the trench is approached. This is readily understandable since the upper part of the Purcell sequence dips eastward under the trench. The Moyie intrusives in the northwest fault block have been buried too deeply to cause a detectable gravity anomaly. It is doubtful that a direct connection can be shown between the Moyie-Lenia and the Dibble faults by gravity methods.

Summary. The most apparent gravity effects of the area lie along the Rocky Mountain Trench. These indicate the presence of three deep basins, now filled with unconsolidated material, along the trench between Fort Steele and the International Boundary. The basins are thought to represent down-faulted blocks along longitudinal and transverse faults within the trench. *Leech* [1959] observed that 'South of latitude 49°30′, the Trench seems due fundamentally to block faulting and lacks important strike-slip displacements.' The gravity data confirm this observation and provide evidence that the amplitude of block faulting decreases as one proceeds northward from the International Boundary toward Fort Steele.

While the gravity anomalies by themselves give information chiefly on the present form of the trench, and it would be unwise to attempt to draw conclusions on the origin from them alone, there is in fact other evidence that the trench, at least in this area, is due to Cenozoic block faulting. This evidence may be briefly summarized as follows (Fig. 1):

(*a*) Paleozoic and Mesozoic structures trend across the trench without significant lateral offset. Therefore, the trench cannot have been the site of significant strike-slip faulting at this latitude.

(*b*) The Moyie-Lenia fault of late Meso age is broken by the Gold normal fault, numerous normal faults cut the rocks wit and adjacent to the trench. A major fault al the east side of the trench near 49°30′N was r ognized by *Dawson* [1885, p. 150]. *Schof* [1915, p. 93] called this a normal fault, *Schofield* [1921] in accordance with *Daly* [19 believed the trench was caused by normal fa ing along the eastern side. *Leech* [1960] n a series of faults, many of which are nor along the west boundary of the trench. block of late Paleozoic rocks in the bottom the trench northeast of Wardner is broken by normal faulting. Normal faults, which transverse to the trench in the Fort Ste Kimberly area, die out in relatively short tances in the rocks adjacent to the trench.

(*c*) The rocks east of the trench stand str turally and topographically higher than rocks west of the trench [*Leech,* 1959, p. 3 This fact is readily explained in terms of a w dipping normal fault system within the tre

(*d*) The trench can logically be associa with Cenozoic block faulting in northwest Montana and the northern Flathead Val *Pardee* [1950] described Cenozoic block fa ing in northwestern Montana, *Eardley* [1 pp. 499–500] suggested that the Rocky Mo tain Trench and other trenches to the w (Purcell, Selkirk, Okanagan) are part of a Cenozoic system of trenches' which is, in t related to the Basin and Range Province of w central United States. *Price* [1959] conclu that sediments of Tertiary age rapidly accu lated in the 'trenchlike' Flathead Valley du an interval in the active life of the Flath fault.

(*e*) Miocene lake beds in the floor of trench, along the St. Mary River, have folded and faulted [*Rice,* 1937, p. 25]. It se likely that other Tertiary sediments are bu beneath the thick blanket of Quaternary ments which cover the floor of the trench.

(*f*) The trench is along a line of reco seismic activity [*Woollard,* 1958, p. 1136].

It is of interest to note that the patter negative anomalies found along the trenc rather similar to that observed in the most cent surveys of the East African rift va [*Sutton,* 1960]. Although the gravity ma

lard [1936], based on relatively few stations, cated continuous negative anomaly strips g the rifts, the recent work indicates that most intensive negative effects tend to occur separated, closed features. There is thus a gestion that the African anomalies also are , at least in part, to low-density fill over a series of downfaulted blocks, rather than to rmation of the crust as a whole. It is im- tant to note that over such a structure the sence of outcrops in some places is no guar- ee that negative anomalies elsewhere are not to light fill.

References

eridge, A. J., and R. E. Folinsbee, Dating ordilleran orogenies, *Trans. Roy. Soc. Can.*, , sect. 4, 19–43, 1956.

lard, E. C., Gravity measurements in East frica, *Phil. Trans. Roy. Soc. London A, 235*, 5–531, 1936.

y, R. A., Geology of the North American ordillera at the forty-ninth parallel, *Geol. urvey Can. Mem., 38*, 1912.

vson, G. M., Physical and geological features the Rocky Mountains, *Geol. Survey Can. nn. Rept., 1*, 1885.

dley, A. J., *Structural Geology of North Amer- a*, Harper, New York, 1951.

land, G. D., and J. G. Tanner, Investigations gravity and isostasy in the southern Canadian ordillera, *Publs. Dominion Observatory, Ot- wa, 16*, 169–222, 1957.

dbook of Physical Constants, Geol. Soc. Am. pec. Paper 36, 1942.

land, C. A., *Geophysical Exploration*, Prentice- all, New York, 1940.

derson, G. G. L., and C. D. A. Dahlstrom, irst order nappe in the Canadian Rockies, *Bull. m. Assoc. Petrol. Geologists, 43*, 641–653, 1959.

cham, V. R. D., The Moyie-Lenia overthrust ult, *J. Geol., 38*(4), 364–374, 1930.

ch, G. B., *Fernie Map-Area, West Half, British olumbia*, Geological Survey of Canada, 1958.

ch, G. B., The southern part of the Rocky Mountain Trench, *Can. Mining Met. Bull., 62*, 10–16, 1959.

Leech, G. B., *Map 11–1960, Fernie (West Half) British Columbia*, Geological Survey of Canada, 1960.

Nettleton, L. L., Gravity and magnetic calculation, *Geophysics, 7*, 293–310, 1942.

North, F. K., and G. G. L. Henderson, The Rocky Mountain Trench, *Alberta Soc. of Petrol. Geol. Guidebook*, 1954.

Pakiser, L. C., F. Press, and M. F. Kane, Geophysical investigation of Mono Basin, California, *Bull. Geol. Soc. Am., 71*, 415–448, 1960.

Pardee, J. T., Late Cenozoic block faulting in western Montana, *Bull. Geol. Soc. Am., 61*(4), 359–406, 1950.

Price, R. A., and D. U. Wise, *Map 1–1959 Flathead, British Columbia and Alberta;* Geological Survey of Canada, 1959.

Rice, H. M. A., Cranbrook Map-Area, British Columbia, *Geol. Survey Can. Mem. 243*, 1937.

Rice, H. M. A., Nelson Map-Area, east half, British Columbia, *Geol. Survey Can., Mem. 228*, 1941.

Schofield, S. J. Geology of Cranbrook Map-Area, British Columbia, *Geol. Survey Can. Mem. 76*, 1915.

Schofield, S. J., The origin of the Rocky Mountain Trench, *Trans. Roy. Soc. Can., ser. 3, 14*, 61–97, 1921.

Stewart, S. W., Gravity survey of Ogden valley in the Wasatch Mountains, north central Utah, *Trans. Am. Geophys. Union, 39*, 1151–1157, 1958.

Sutton, G. H., Gravity observations along the western rift valley of Africa (Abstr.), Intern. Assoc. of Seism. and Phys. of the Earth's Interior, Helsinki Assembly, 1960.

Thompson, G. A., Gravity measurements between Hazen and Austin, Nevada: A study of basin-range structure, *J. Geophys. Research, 64*, (2), 217–230, 1959.

Thompson, G. A., and C. H. Sandberg, Structural significance of gravity surveys in the Virginia City–Mount Rose area, Nevada and California, *Bull. Geol. Soc. Am., 69*, 1269–1282, 1958.

Woollard, G. P., Areas of tectonic activity in the United States as indicated by earthquake epicenters, *Trans. Am. Geophys. Union, 39* (6), 1135–1150, 1958.

(Manuscript received March 27, 1961; revised May 10, 1961.)

Size and Mass Distribution of Cosmic Dust

TAIVO LAEVASTU

Fisheries Division, FAO, Rome

OTTO MELLIS

Mineralogical Institute
University of Stockholm

Abstract. The size distribution of the cosmic spherules found in sediments shows that the total mass of particles in equal size (diameter) intervals remains constant. The size distribution of cosmic dust in space, as computed from the data obtained by impact measurements by artificial satellites, shows the same distribution in the interval of particle diameters approximately 5 μ and 15 μ, and as determined by indirect extrapolation the distribution is probably valid for larger particles.

In various investigations it is necessary to imate the total mass of cosmic dust reaching t area of the earth per unit time, or to esti- te the density of this dust outside the earth's nosphere. These estimates must usually be de from fractional counts of cosmic spherules, lected from sediments, glaciers, or the air, or m the impact counts by artificial satellites, knowing the lightest particle that can be nted at an assumed impact velocity. The imates can be accurate if the size and mass tribution of the cosmic dust is in some way ular, uniform, and known. In the following rt paper, an attempt is made to establish s size and mass distribution on the basis of estigations of cosmic spherules found in sedi- nts and the result compared with the data impact counts of satellites 1958α and 1959η. The present authors measured and counted cosmic spherules with diameters > 20 μ *evastu and Mellis,* partly published, 1955] g. 1). Their count of smaller spherules is btful because of difficulties and imperfections separation of the very small spherules from clay. *Crozier* [1960] perfected the separa- methods and measured and counted mainly ller spherules. The number of spherules $>$ μ counted by him was about 30 times less n our counts. To make these two counts com- able on the same basis, Crozier's counts (2213 ticles < 20 μ) have been multiplied by 30 plotting Figure 1.

From the plotted data on this figure it can be concluded that the mass of particles in every equal diameter interval is very nearly constant ('theoretical' curve of the figure):

$$V_1 N_1 = V_2 N_2$$

where V is volume (or mass) of a single spherule in a given size group (diameter interval) and N is the number of spherules in this size group. The size distribution curve of spherules from the Antarctic [*Thiel and Schmidt,* 1961] substantiates the above conclusion.

The size and mass distribution of dust outside the earth's atmosphere can be checked against the curve in Figure 1 with the impact counts of the satellites 1958α (Explorer I) and 1959η (Vanguard III). The lowest diameters of spherules counted by these satellites can be derived from the data on the lightest particle that can be counted at an assumed impact velocity and by assuming a specific gravity of 5. These computed diameters are: 1958α, 6.75 μ; 1959η, 10.8 μ. The ratio of influx in impacts m^{-2} sec^{-1} (0.007 and 0.0017 impacts m^{-2} sec^{-1}, respectively) [*La-Gow and Alexander,* 1960, Fig. 12] agrees almost exactly with the theoretical curve (Fig. 1). This also indicates that the size distribution of cosmic dust in space in the interval of particle diameters approximately 5 μ and 15 μ is the same as the size distribution of cosmic spherules on the earth's surface. The satellite data do not give us the size distribution of larger particles in space, except by indirect, somewhat doubtful extrapolation using the impact counts of all

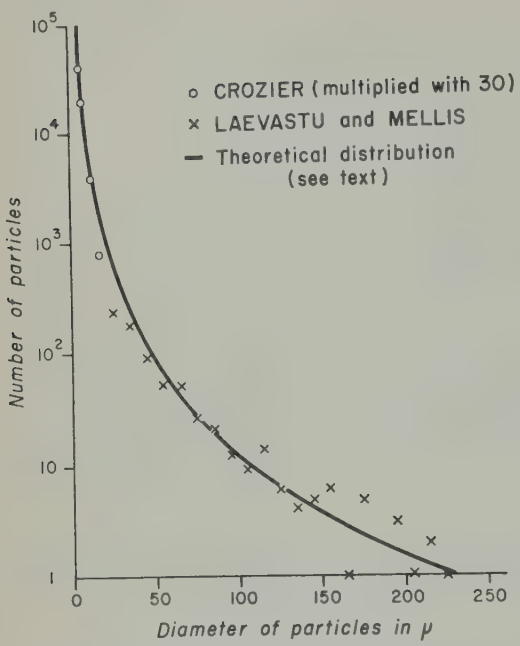


Fig. 1. Distribution of the number of 'cosmic black spherules' in different size groups.

particles per unit area and time and the ratio of impacts between the two satellites mentioned earlier. In making this extrapolation, account is taken of the fact that essentially all cosmic particles > 250 μ in diameter are intercepted by the planet Jupiter and therefore do not reach the earth [*Öpik*, 1951]. The extrapolation indicates, however, that the distribution of the larger particles might also very well follow the curve on Figure 1.

It is not within the scope of the present short paper to compute the amount of cosmic spherules reaching the surface of the earth annually. However, from Figure 1, the data given by *Crozier* [1960] (19 spherules > 5 μ per m^2 and hour), and the data from 1959η [*LaGow and Alexander*, 1960], the calculations with the above-mentioned data give approximately and 0.4 g cosmic spherules km^{-2} of the ea per hour. The estimates of the rate of fall cosmic spherules to the earth, based upon counts from sediments, depend, among ot things, on the exact determination of the rat sedimentation. As the value calculated fr satellite data is considerably higher, it gives ditional support to the conclusions of *Hi* [1961], who found that a fraction of parti measured by satellites are in closed orb around the earth. This conclusion is also logi because the speed of the majority of cos particles (which is calculated on the basis size distribution) is only slightly above the ea escape speed. The speed distribution of the c mic particles has been computed by *Öpik* [Discussion at the end of *Laevastu and Me* 1955] based on a size distribution very sim to that shown in Figure 1, so there seems be no need for revision of this calculation present.

References

Crozier, W. D., Black, magnetic spherules in s ments, *J. Geophys. Research, 65*(9), 2971–2 1960.

Hibbs, A. R., The distribution of micrometeor near the earth, *J. Geophys. Research, 66*(2), 3 377, 1961.

Laevastu, T., and O. Mellis, Extraterrestrial m rial in deep-sea deposits, *Trans. Am. Geop Union, 36*(3), 385–389, 1955.

LaGow, H. E., and W. M. Alexander, Satel measurements of cosmic dust, *IGY Bull. Trans. Am. Geophys. Union, 41*(3), 516– 1960.

Öpik, E. J., Astronomy and the bottom of the *Irish. Astron. J., 1*(5), 145–158, 1951.

Thiel, E., and R. A. Schmidt, Spherules from antarctic ice cap, *J. Geophys. Research, 66* 307–310, 1961.

(Manuscript received April 12, 1961; revised May 11, 1961.)

Abstracts of the Papers Presented at the Forty-Second Annual Meeting, American Geophysical Union Washington, D. C., April 18–21, 1961

OHN A. S. ADAMS and PAUL C. RAGLAND (Detment of Geology, Rice University, Houston, .), *Autoradiographic and Radiometric Screen- of Samples for Absolute Age Determinations.* ndestructive α autoradiographs and radiometric erminations, together with routine petrographic X-ray diffraction analyses, have been very ful in predicting the success of obtaining meanful absolute ages from subsequent isotopic lyses of zircons. In this and other laboratories, utoradiographs have shown (1) minor concenions of highly radioactive monazite in concenes originally considered to be 'pure' zircon; radiocolloids in samples which also had unally high amounts of readily soluble lead; (3) presence of high concentrations of α emitters rack fillings in zircon; (4) wide variations of missions per unit volume within zircon suites arated from sediments or metasediments; little o variation in zircon suites from bentonites; general, there appears to be a systematic dease in α activity per unit volume of zircon as grain size and silica content of the igneous ce rock decrease; (5) heterogeneous distribu- of α emitters within individual zircon grains. n with the limited amount of data available, ust be considered distinctly possible that autoiographic screening of samples would be helpin experimentally determining which samples meet the criteria of homogeneous population ircons, pure zircon, uniform distribution of α vity, and closed system. Samples that do not t these criteria give rise to serious errors in olute age determinations based upon isotopic lyses, radiation damage, or lead-α data. With ons separated from bentonites it has been pose to estimate the radiogenic lead to about 10 cent by an α-activity measurement-stratihic age calculation. This estimate, together the autoradiographic screening, can be done an impure zircon concentrate that contains few as 300 to 400 grains. Gamma-ray specetry has been confirmed by isotope dilution e accurate to within 10 per cent in determinas little as 250 μg of uranium in a zircon conrate. These nondestructive radiometric deterations are very helpful in deciding if adequate ple is in hand to attempt an isotopic analysis.

M. MANSFIELD ADAMS (Lawrence Radiation oratory, University of California, Livermore, f.), *A Direct Method for Investigating the rior of the Earth.* Direct access to the crust the upper portion of the mantle may be achieved by letting a high-temperature (>1100°C) reactor core melt the rock in which it is placed and fall through the resulting magma. Data gathering and retrieval seem feasible. A schematic design is given of the proposed instrument.

H. W. ALBERS and J. F. MILLER (U. S. Naval Weather Facility, Norfolk, Va.), *The Navy's Ship Routing Program.* In 1956 the U. S. Navy Hydrographic Office began testing a method of weather routing ships that had been developed by R. W. James. The success of this test led the Commander of the Military Sea Transportation Service to request that the program be expanded and provided to all ships under his command making transoceanic voyages. Combatant ships also began to request the service. Since the mission of the Hydrographic Office is research and development, the responsibility for providing this service was transferred to the Naval Weather Service. This transition began in the fall of 1958 and was completed in July 1959. Since that time the program has continued to grow until now most naval ships, when making voyages which are compatible with ship routing, use the service. Efforts to improve the service within the current forecast capability are continuing, though ultimate perfection of ship routing is dependent on improvements in long-range forecasting.

R. ERNEST ANDERSON, WALTER HAYS, and WILFORD F. WEEKS (Department of Geology, Washington University, St. Louis, Mo.), *Some Structural Aspects of the Missouri Precambrian.* Detailed field studies of scattered exposed areas of felsites in the Precambrian of southeastern Missouri have revealed both lineaments and subsidence structures associated with extrusion and high-level intrusion of acid rocks. Two steeply dipping Precambrian fault systems have strikes of N65W and N10 to N20E and form the boundaries of subsided and deformed blocks of layered pyroclastics. The fault zones are healed by intrusive rhyolitic breccias. Fold and fracture attitudes within the displaced blocks are approximately parallel to the boundary faults. Porphyritic rhyolites characterized by steeply dipping, subplanar features and the rhyolitic breccias which bound them along nearly vertical contacts are interpreted as intrusive rocks. The boundaries as well as the primary structures of these intrusives tend to have attitudes which are coincident with the fault systems mentioned above. They represent Precambrian structural elements which gave rise

to fissure-type intrusion and volcanic effusion. A single fissure vent may contain evidence of multiple activity. Brecciation ranging in degree from simple net veining to intense comminution and entrainment together with large volumes of pyroclastics attest to the explosive character of the volcanic activity. Structural and textural relations together with variations in the ferrous/ferric ratio, as evidenced by the iron oxides, suggest that some of the intrusive units were degassed and rapidly cooled and that the movement of gases produced fragmental phases. Rock textures range serially from slightly devitrified glasses to granophyric and micrographic. The principal textural variations as well as the large- and small-scale structural elements were developed during the period of volcanism. The results of paleomagnetic, mineralogic, structural, and textural investigations suggest a very high degree of stability for the entire area.

J. E. André and H. W. Anderson (Pacific Southwest Forest and Range Experiment Station, Berkeley, Calif.), *Variation of Soil Erodibility with Geology, Geographic Zone, Elevation, and Type of Vegetation in Northern California Wildlands.* Samples of the top 6 inches of mineral soil were taken at 168 places in northern California. Analyses were made to determine physical characteristics of these soil samples, yielding various erodibility indexes. The samples were selected in the major soil-geologic types of the state, under standard conditions of slope (west, 20 per cent), at ranges in elevation (1000 to 4000 feet), by vegetation types (trees, brush, and grass), and in three separate zones (north coast, south coast, and Sierra). A multiple regression analysis related the 'surface-aggregation' and 'dispersion' ratios (used as indices of erodibility) to geologic type, vegetation type, zone, and elevation, and their interactions. The 'surface-aggregation ratio' was significantly related to each of these. Soil developed from igneous rock was about 2½ times as erodible as soil developed on basalt. Erodibility was greatest under brush, less under trees, and least under grass. No clear-cut relation of erodibility to elevation was found. The interaction of zone and geologic rock type showed significant variation in erodibility. The prediction equation explains 52 per cent of the variability in erodibility in soils. The results have application in studies of sedimentation from watersheds.

Milo J. Andre (Climatic Center, U. S. Air Force, Washington, D. C.), *Use of Climatic Transition Probabilities in Problems of Applied Climatology and Extended Forecasting.* The application of two mathematical techniques to a class of applied climatological and extended-range forecasting problems is outlined. One technique, a formal method in which stochastic matrices are used, leads to a probabilistic 'extended forecast' of a parameter, or a refinement of climatic probabilities for the near future which incorporates effect of a prescribed initial condition. In other technique linear programming is used calculate the most probable sequence of par eters associated with an initial condition, a l range forecast, and the climatology of the l tion. Both techniques are formally capable giving quantitative data about weather in the r future, which is frequently needed for plann and is not normally obtainable by usual t niques. Simple applications of each technique be illustrated, and the wide scope of further ap cations will be suggested.

J. K. Angell and D. H. Pack (U. S. Weat Bureau, Washington, D. C.), *A Study of Vert Oscillations of Tetroons Released from Wall Island.* During January 1960, eight tetroons (c stant-volume, superpressured balloons) were leased from Wallops Island for flight at appr mately 3000 feet. The tetroons were tracked the very accurate FPS-16 radar, thus permitt the delineation of relatively high-frequency roon oscillations. Flights within an air mass hibited small-scale vertical oscillations of m period near 10 minutes, approximately the 'n ural' period of oscillation of air parcels in atmosphere with the given stability. Two fli released 20 minutes apart and within, or v near to, a cold frontal zone, exhibited ne identical large-scale vertical oscillations of m period near 30 minutes. These pronounced hei variations apparently were associated with a m ing vertical-motion system which in turn probably associated with frontal corrugati moving almost parallel to the frontal intersect with the ground. The speed of movements these corrugations indicated that they might atmospheric equivalents of oceanographic e waves.

J. R. Apel and S. F. Singer (University Maryland, College Park, Md.), *Magnetic Eff of Trapped Particles.* We have calculated magnetic effects produced by a trapped-part distribution in a dipole field seen by a dete traveling outward in the plane of the equa We find that a decrease of about 70 gam occurs up to 25,000 km, followed by a transi region, then by an increase starting at 50,000 which cannot exceed 3 gammas. We have two model distributions which appear to be sistent with experimental results. With these sults we can now reproduce the 'magnetic nature' of any reasonable distribution of trap particles. For example, the Explorer VI re may be represented by a distribution startin 25,000 km and ending fairly abruptly at 40,000 Sample magnetic signatures of other particle tributions are given. The Lunik I data canno completely explained in terms of trapped p cles, and another mechanism must be postul to account for their detailed features.

USTAV ARRHENIUS (Scripps Institution of nography, University of California, La Jolla, f.), *Petrological Studies of the Surface of the n: Some Plans and Developments for Tele- ered Experiments.* During the next few years mpts will be made to place transmitting in- ments into orbit around the moon and to land r instruments on the moon. Some of these de- s are planned to furnish information on the ental and mineral composition of the moon's ace. A discussion is given of the pertinent ciples and of some technical aspects of hods now being developed.

EORGE B. AUSTIN (U. S. Navy Mine Defense oratory, Panama City, Fla.), *Navigation Ref- ce Markers with Applications to Near-Shore nographic Investigations.* The techniques and for three basically different navigation refer- markers under development at the Mine ense Laboratory, Panama City, Florida, are ribed. Although developed for use in mine ntermeasures, these markers should be of value he oceanographer interested in accurate loca- above, on, or in the near-shore marine en- nment. The master reference buoy accurately tions a radar target and other visual markers eet above the sea surface. Plotting charts for with the buoy have been developed by the oratory and will be available from the Navy drographic Office at an early date. Styrofoam er reflectors have been developed to provide ffective underwater Sonar target. The triplane er reflector with a short pendant and a bag and for an anchor is economical to produce in ntity. The target is compatible with commer- y available fish-finder types of Sonar. The l reference marker is a small expendable, weight, explosive anchor buoy which was de- ped for use from helicopters or small craft. A ly moored float is automatically positioned he sea surface to mark very accurately a nel or position of interest to the oceanog- er.

EORGE BACKUS (University of California, La , Calif.) and FREEMAN GILBERT (Geophysical ice, Inc., Dallas, Tex.), *Rotational Splitting of ree Oscillations of the Earth.* The rotation of the is shown to be the major cause of splitting of ree oscillations of the earth. Also, power spectra fficiently high resolution ought to show more two components in a split line, permitting ification of the angular dependence of the ation producing the line. The rotation is treated small perturbation, the small parameter being atio of the frequency of rotation to the lowest frequency of the nonrotating system. Degener- odes of the latter are split to first order by the ion, while nondegenerate modes are affected to second order. In the nonrotating system, $2l + 1$ modes with the angular behavior of lth-order spherical harmonics $Y_{ml}(\theta, \varphi) = P_l^m(\cos\theta)e^{im\varphi}$ all have the same frequency. If the axis is chosen to be the axis of rotation, then these modes, slightly corrected, remain normal modes of the rotating system but their frequencies are shifted by amounts proportional to m and the rotation rate. The constant of proportionality depends on the radial distribution of displacement in the nonrotating mode for spheroidal modes.

H. L. BARNES (Department of Geophysics and Geochemistry, Pennsylvania State University, University Park, Pa.), and W. G. ERNST (Institute of Geophysics, University of California, Los Angeles, Calif.), *Alkalinity in Hydrothermal Solutions.* Primary igneous and metamorphic minerals contain ionic groups which, in aqueous solutions at low temperatures, are generally either weak acids or strong bases. However, hydrolysis of these groups at low temperatures is not sufficient evidence to demonstrate the alkalinity of hydrothermal solutions without data on the ionization constant K in aqueous fluids of each group as functions of P and T. K is known at some (P, T) condition for H_2O, HCl, KCl, NaCl, and KOH in supercritical aqueous solutions and to near the critical point of H_2O for about fifteen other compounds. K for all compounds studied increases with pressure and, except for water, decreases with temperature. The decrease in K between 25° and the critical point is considerably greater for acids than for bases, the difference becoming more pronounced with increasing valence of the acid. Therefore, near the critical point HCl becomes essentially a molecular compound causing salts such as NaCl and KCl to have the same effect on the alkalinity of aqueous fluids as NaOH and KOH. Above the critical temperature, isothermally increasing pressure increases K_{HCl} at a greater rate than K_{KOH}. KCl at 450° and roughly 2000 bars is neutral in reaction, being acidic at higher and alkaline at lower pressures; NaCl behaves similarly. The close approach to ideality of mixing by NaOH solutions (determined experimentally by equilibrium with brucite and periclase) correlates closely with the extent of ionization. The extent of ionization in the fluid phase also fixes the alkalinity and the ionic solubility and consequent mobility of silica and other constituents in metamorphic and igneous environments.

CHARLES A. BARTH (Jet Propulsion Laboratory, California Institute of Technology, Pasadena, Calif.), *Molecular Oxygen Airglow of the Earth and Venus.* An analysis of rocket measurements of the ultraviolet and infrared molecular oxygen airglow of the earth gives the reaction rate of the emission mechanism and the deactivation coefficient of the excited molecules. Astronomical observations have established the presence of 1 km-atm of carbon dioxide in the upper atmosphere of Venus, but the abundance of other atmospheric gases is unknown. The photodissociation of carbon dioxide produces atomic oxygen in the upper

atmosphere above the region where carbon dioxide is present. The maximum density of atomic oxygen will occur at approximately the same molecular oxygen partial pressure as on the earth. The oxygen dissociation rate will be greater because of the greater intensity of solar radiation at the top of the atmosphere. It is to be expected that the recombination of oxygen atoms in the upper atmosphere of Venus will radiate the molecular bands of the oxygen airglow as they do in the earth's upper atmosphere. If the proportion of inert gas, such as nitrogen, in the atmosphere of Venus is greater than the proportion in the earth's atmosphere, then, compared with the earth, the level at which collisional deactivation is effective will be higher. Also, the airglow intensity above this level will increase, but the airglow intensity lower will remain the same. Thus, the intensity of the oxygen airglow of Venus should be only slightly greater than it is on the earth.

William A. Bassett (Brookhaven National Laboratory, Upton, N. Y.) and Paul F. Kerr (Columbia University, New York, N. Y.), *Potassium-Argon Ages of Volcanics near Grants, New Mexico*. Age determinations of seven potassium-bearing specimens from the youthful volcanic area just north of Grants, New Mexico, date one of the several recognized periods of volcanic activity. Obsidian masses along the north edge of the mesa are dated at 3 ± 1 m.y. Perlite which is being mined in an open pit on the north edge of the mesa corresponds in age to the obsidian. Plagioclase from an andesitic plug which pierces the mesa contains only 0.43 per cent K. Two age determinations made on the plagioclase give 4 m.y. and 9 m.y. but are considered unreliable because of the paucity of potassium. The perlite, which is a porous glass, contains only an expectable amount of air argon for a volcanic glass and seems to have lost no appreciable amount of radiogenic argon. Thus, preliminary observations suggest that meteoric water, which would probably introduce air argon, is not responsible for the hydration of this material. In the absence of air argon it seems possible that the water in the perlite is magmatic. Metamorphosed Todilto limestone (Jurassic) found in the Section 33 mine beneath the lava cap contains uraninite which has been dated on a single unconfirmed specimen at 78 ± 5 m.y. (Kulp and Miller, 1960). Investigation of the nearby sequence of volcanic rocks has been undertaken in an attempt to obtain definitive age data on the environment of the uranium occurrence.

Harold A. Bedient (U. S. Weather Bureau, Washington, D. C.), *The Increased Data-Processing Capacity of the National Meteorological Center*. In the past year the new computing equipment of the Joint Numerical Weather Prediction Unit has more than doubled the computer output on the national facsimile circuits and on the teletype circuits. The over-all problems of chan over are discussed together with prospects for future of reliable and timely products.

John C. Behrendt (Geophysical & Polar search Center, University of Wisconsin, Madis Wis.), *The Filchner Ice Shelf, Antarctica.* ophysical and glaciological results of the 1957-1 and 1958-1959 traverse parties operating from E worth Station have been reported previou These data have been integrated in an atter to give a unified picture of the Filchner ice sh and its environs. The following conclusions presented and discussed. A large trough under the eastern section of the ice shelf and exte back into the unexplored head of the shelf. Be ner Island is a grounded ice feature on Berk Bank, a vast morainal area extending far out i the Weddell Sea. The eastern section of the shelf is flowing forward at a high velocity and vast amount of ice lost at the ice front is not anced by accumulation over the shelf area. A la amount of the high ice of east Antarctica is pr ably drained by the eastern portion of the sh entering via the Recovery and Slessor glaciers the wide ice stream apparently flowing down tween the Dufek massif of the Pensacola Mo tains and the Horlick Mountain Range. A passing the constriction caused by Berkner Isl and Coats Land the ice shelf thins rapidly spreading as it approaches Weddell Sea. freezing or melting at the bottom of the shel insignificant. It is suggested that Berkner B and the trough were formed by glacial action some past time of lower sea level. The a beneath the Filchner ice shelf is essentially isostatic equilibrium and the thickness of earth's crust is consistent with that to be expec for a continental margin.

J. C. Behrendt, R. J. Wold, and T. S. Laud (Geophysical & Polar Research Center, Univer of Wisconsin, Madison, Wis.), *Preliminary Re on the USARP 1960–1961 Geophysical Air T verse*. Seismic ice thickness determinations w made at selected landings between the Kohler Hudson Mountains in northern Marie Byrd La Reconnaissance geology observations were m at these two previously unvisited ranges. Gra base stations were established at various locati with high-accuracy, high-range gravimeters to p vide control for the oversnow traverse part Magnetic profiles were obtained during flights o various areas of east and west Antarctica. A clear magnetic resonance magnetometer was u to measure the field.

Ari Ben-Menahem (Seismological Laborat California Institute of Technology, Pasad Calif.), *Radiation of Surface Waves from Fi Moving Sources*. A theory is given for the p agation of Rayleigh and Love waves from fi moving faults in an elastic half-space. The met

sists in obtaining basic solutions for surface ve displacements from directional impulsive rces and then integrating these solutions over finite body in question. In the case of moving lts the fault is realized by moving the source ng a segment with finite speed and integrating pole's contribution across a finite rectangle h arbitrary dip and strike. In general it is nd that the finiteness of the source plays a ninant role in the wave pattern whenever the velength of the radiation is of the order of the lt's length. It is demonstrated how this theory y be used to evaluate the velocity of rupture, fault length, and the strike angle if one knows phase difference and amplitude ratio of G or waves recorded at a single station from opite directions.

LEO C. BENZ and ROME H. MICKELSON (Agricultural Research Service, U. S. Department of riculture, Grand Forks. N. Dak.), and FRED M. NDOVAL and CARL W. CARLSON (Agricultural Rerch Service, U. S. Department of Agriculture, ndan, N. Dak.), *Ground-Water Investigations a Saline Area of the Red River Valley, North kota.* Studies show that precipitation is a major tribution to high and fluctuating water tables in aline area of the Red River Valley in North kota. Salt-affected soils are caused by high ter tables, poor drainage conditions, and saline sian waters. Water tables rose 3 to 7 feet dur the growing season when 65 to 70 per cent of yearly precipitation normally occurs. The ter table receded during the fall and winter nths, if precipitation was near normal, and a rp rise occurred in the spring. Strongly saline as were usually poorly drained areas having sistently high water tables and the greatest ward flow gradients. Chemical compositions of ground waters indicate that the Dakota Sandne artesian waters are the most likely source salts. Amounts of water fed into the area by sian sources are probably small; however, the sian aquifer keeps the substratum well satued with water and salts. The 3-year study was ducted on a 200-square-mile area in east cen Grand Forks County. Data were obtained n observation wells 12 feet deep, 20-foot piezeters located on a 2-mile grid, 15 piezometer teries, and numerous domestic wells.

OSEPH W. BERG, JR. (Institute for Defense alyses, Washington, D. C.), KENNETH L. COOK eophysics Department, University of Utah, Salt e City, Utah), HARRY D. NARANS, JR. (Shell Co., Edmonton, Alta., Canada), and RICHARD LEAMER (Mobil Oil Co., New Orleans, La.), *mic Profiles in Northwestern Utah: Pilot nge and Grouse Creek Range Area.* From Au t 10 to September 5, 1959, seismic refraction reflection studies were conducted in northtern Utah. Two seismic refraction profiles e established. The first, which was in the area lying east of the Pilot Range, was about 55 km in total length and extended south from about 10 km southeast of Lucin, Utah, to about 13 km north of Wendover, Utah. The second, which was in the area lying west of the Grouse Creek Range, was about 95 km in total length and extended north from a point about 15 km north of Wendover to the vicinity of the town of Grouse Creek, Utah. The two profiles were reversed for about 47 km of the distance. Commercial seismic prospecting equipment, modified to pass frequencies between about 3 and 50 cps, was used. Results of this study show that materials having velocities of about 2.0, 5.5, 6.2, and 7.4(?) km/sec exist at depths of about 0, 0.8, 4, and 24 km, respectively. The apparent dips of the horizons for 5.5 and 6.2 km/sec were about ¼°N and 2½°N, respectively. Reflections from the horizon at an approximate depth of 24 km were picked on seismograms taken at five of the recording locations. A second reflection was picked on four of the above five seismograms that could result from a reflecting horizon at a depth of about 27 km.

LOUIS BERKOFSKY (Atmospheric Circulations Laboratory, Air Force Cambridge Research Laboratories, Bedford, Mass.), *A Generalized Form for Vertically Integrated Numerical Forecasting Models.* It is assumed that the temperature at any level in the model atmosphere is expressible in the form

$$T(x, y, p, t) = T^*(p) + \sum_{i=1}^{n-1} \alpha_i(p) T_i(x, y, t)$$

where $T^*(p)$ is a standard temperature distribution and n is the number of layers. It is then possible to derive the corresponding forms for the static stability, the stream function, and the rotational part of the wind. The model equations consist of n prognostic equations—a vorticity equation for the mean flow and a system of $(n - 1)$ equations for the T_i (x, y, t)—; and two diagnostic equations—a vertical motion for the mean flow and the continuity equation for the divergent part of the wind. The barotropic, thermotropic, and three-parameter models are deducible from the general system. A table is presented, showing the increase in the number of terms in each equation as the number of parameters is increased.

P. D. BHAVSAR (School of Physics, University of Minnesota, Minneapolis, Minn.), *Gamma Rays from the Solar Cosmic-Ray-Produced Nuclear Reactions in the Earth's Atmosphere.* An attempt has been made to understand the processes which lead to atmospheric γ-ray production in nuclear reactions due to solar cosmic rays. The total cross section for γ-ray production in air by protons of 30 to 300 Mev may be calculated. It is found to be $\sigma_\gamma \approx 940 \times 10^{-27}$ cm^2. Measurements of γ rays by balloon-borne detectors are very useful in the absence of very high altitude observations at a

middle latitude station like Minneapolis because they allow the determination of the flux of protons stopping well above the balloon altitudes. This information enables one to estimate the effective geomagnetic cutoff during the magnetic storms accompanying the solar cosmic-ray event. Such estimations during the May 12, 1959, event show that solar protons of energy as low as $\sim$ 40 Mev were allowed at the latitude of Minneapolis.

Maurice Blaik (Columbia University, Hudson Laboratories, Dobbs Ferry, N. Y.), *Deep-Hole Seismic Noise Correlation and Spectra.* Seismic noise in the earth is propagated the same way as low-frequency acoustic and seismic signals. That is, noise can be considered as being caused by many incoherent sources. In horizontally layered media, seismic noise may be expected to vary with depth. This variation depends upon all the seismic parameters for all the layers involved in the seismic disturbances. In this connection, data are presented showing qualitative verification of the predicted relationships between vertical geophone motion due to seismic noise and the variation of seismic velocity with depth. The geologic environment consists of about 600 meters of unconsolidated sediments overlying rock at a particular location on Fire Island, New York.

Duncan C. Blanchard (Woods Hole Oceanographic Institution, Woods Hole, Mass.), *The Cyclic Exchange of Sea-Salt and Organic Material between the World Ocean and the Atmosphere.* With the assumption of a steady state between the production rate and the rate of removal, the author has computed the flux of salt nuclei from sea to atmosphere. The rate of removal calculations take into account the salt that returns to earth by sedimentation, washout by rain, and fallout over the continents. The result, given as a function of latitude and season, indicates that the sea-salt flux from December to February reaches a maximum in each hemisphere at latitudes of about 50°. This flux amounts to 9×10^{-11} and 8×10^{-11} g cm^{-2} sec^{-1} in the northern and southern hemisphere, respectively. The corresponding fluxes from June to August are about 1.5×10^{-11} and 11×10^{-11} g cm^{-2} sec^{-1}. The total production of sea-salt by the world ocean remains relatively constant over the seasons and is about 3×10^{9} metric tons per year. The same sea water drops that carry the salt into the atmosphere may also carry organic films away from the sea surface. The mechanism by which these films are removed, and its dependence on drop size, are discussed.

J. Bogárdi (Hydraulics Laboratory, Research Institute for Water Resources Development, Budapest, Hungary), *Some Aspects of the Engineering Application of Theory in the Field of Sediment Transportation.* The effect of hydrological conditions on the sediment transport capacity of a watercourse can be observed by investigat the relationship between the sediment concen tion C and the mean velocity in the cross sec v, along the entire length of a river from c section to cross section. The relationship C $f(v)$, as established by the author's investigat in the Danube River, shows that for six c sections a given sediment concentration requ an appreciably higher mean velocity in the stream cross sections than in those farther do stream. No hydrodynamic explanation can be gi for this phenomenon, yet obviously the m velocity corresponding to a given set of hydrol conditions is related to the sediment load, w in turn is also in agreement with the hydrol conditions of the river. For stations on the s river, similar exponents are found in the rela $C \alpha Q^{l}$, but among different rivers the expon vary. Hence, a relationship was developed for exponent l in terms of (1) the average widt the catchment area, (2) the mean discharge, the ratio of peak to minimum discharge, and the discharge per unit of catchment area. T are other circumstances to be taken into consid tion when applying theoretical results to engin ing problems. In numerous instances the fa (e.g. bottom velocity, energy gradient) that w be necessary are inaccessible to measurement natural watercourses. The shortcomings of t retical relationships can be traced back to circumstance that the relationships are determ under largely identical experimental condit and thus the possibility of allowing for diffe conditions is precluded from the very beginn Relations have also been developed for the p of sediment movement in terms of particle and shear velocity.

Bruce A. Bolt and James Dorman (Lam Geological Observatory, Columbia Univer Palisades, N. Y.), *Phase and Group Velocitie Rayleigh Waves in a Spherical, Gravitating E* Periods of spheroidal eigenvibrations, of harm order $n > 20$, have been computed for self-grav ing inhomogeneous spheres representing a va of earth models. The periods are used to de phase and group velocities for the fundam and first higher mode of Rayleigh waves ha periods $T < 320$ sec. Comparisons are made tween velocities for different spherical m and with corresponding velocities calculated the same physical parameters using the Thom Haskell matrix method for a nongravitating earth. The comparisons show (*a*) that the i sion of gravity reduces the phase velocity by km/sec ($\sim$ 0.6 per cent) near $T = 300$ sec by only 0.01 km/sec ($\sim$ 0.2 per cent) near 150 sec; and (*b*) that the sphericity increase phase velocity by 0.3 km/sec ($\sim$ 6 per cent) $T = 300$ sec and by 0.06 km/sec ($\sim$ 1½ per near $T = 150$ sec. In striking contrast, for 1 $T < 250$ sec, the group velocities for the sph case remain within 1 per cent of the correspo

cities for the horizontally layered case. A p velocity minimum occurs close to $T = 220$ The variation with depth of the relative lacement amplitudes and the perturbed grav- onal potential is illustrated for one earth el in the cases $n = 30, 80, 110$. By comparison these theoretical results, recent observations hase and group velocities of Rayleigh waves measured periods of some spheroidal oscilla- s are consistent with an earth's mantle having nsity distribution similar to that of model A tructed by Bullen, and having P and S velocity ibutions similar to those calculated by Guten- . A group velocity dispersion curve which esponds to the first higher mode (or first shear e) of Rayleigh waves has also been computed $20 < T < 150$ sec ($500 > n > 40$) for a crust ontinental type. The curve has a minimum at elocity of 4.30 km/sec ($T = 60$ sec) and a imum at a velocity of 4.55 km/sec ($T = 25$. These extrema may be associated with the e S_a.

X. Bostick, Jr., and H. W. Smith (Electrical ineering Research Laboratory, University of as, Austin, Tex.), *A Discussion of the Analysis niques Involved in the Magnetotelluric hod of Subsurface Resistivity Analysis.* The uations of the earth's natural electric and netic fields (magnetotelluric field) contain ificant information concerning the electrical erties of the earth's subsurface structures. At- pts to analyze recordings of these fluctuations rms of the properties of these structures have, ever, met with only partial success. The ntial advantages of the magnetotelluric hod are sufficiently numerous to warrant a iled study of the procedures involved in the isition, analysis, and interpretation of the rimental data. A fundamental analog of the dimensional, homogeneous, isotropic, layered el is introduced for the purpose of discussing tral methods of determining the apparent e impedance. Departure of the actual system the simple models, including the effects of dimensional inhomogeneities and anisotropies ting in the nonorthogonality of the **E** and **H** ors are discussed. It is shown that it is often ise to employ statistical methods in obtaining unique apparent resistivity estimates required he simple models. This fact results from the ral nonstationarity of magnetotelluric data. ific techniques of a deterministic analysis are ussed.

allace Broecker (Lamont Geological Observa- , Columbia University, Palisades, N. Y.), *on Dioxide Exchange between Ocean and osphere.*

. Brook, N. Kitagawa, and E. J. Workman w Mexico Institute of Mining and Technology, rro, N. Mex.), *The Effectiveness of Continuous Currents versus Return Strokes in Lowering Charge to Earth.* The return stroke has long been regarded as the major agent by which negative charge is lowered to earth in lightning flashes to open terrain. We have found that the continuous mode of discharge which occurs in the intervals between or directly following the return strokes in a multiple flash lowers, on the average, 5 times more charge than does the average return stroke. Measurements of the simultaneous photographic and electric field records of 200 flashes from three storms show that 50 per cent of all flashes to ground contain at least one continuous current interval with an average current of 132 amp and a mean duration of 150 msec. Thus, 20 coulombs of charge is lowered in the continuous current interval as compared with an average value of 4.2 coulombs for the individual return strokes. With an average value in these storms of 7 strokes per flash (determined from high-speed photographs), the average flash containing one continuous current interval lowers 57 coulombs to ground, or twice as much charge as the purely intermittent flash. The assumed value of approximately 20 coulombs per flash, which is based upon the return stroke alone, must therefore be revised upwards.

John A. Brown, Jr. (U. S. Weather Bureau, Washington, D. C.), *The Operational Analysis Program at the JNWP Unit.* On December 15, 1960, the Joint Numerical Weather Prediction Unit undertook the analysis and distribution of additional meteorological parameters for the northern hemisphere on an operational, routine basis. Analyses of heights, temperatures, and winds are performed twice daily for the pressure surfaces at 850, 700, 500, and 300 mb. The technique and several examples are presented.

R. M. Brown (Defence Research Chemical Laboratories, Ottawa, Ont., Canada), *Dispersal of Bomb Tritium in the Waters of the Ottawa Valley.* Tritium deposited over the Ottawa drainage basin in the years 1954-1960 has appeared in the Ottawa River in a manner analogous to drainage from a mixed reservoir. A fractional turnover rate of 0.27 per annum and a volume of 2.6 times the annual rainfall is indicated for the system when allowance is made for evaporative recycle. The fraction of evaporated water derived directly from fresh precipitation has been estimated as 0.55 ± 0.1. This indicates that 30 per cent of the precipitation in the district evaporates without mixing into the main water complement of the system, and 10 per cent of the storage water evaporates per annum. At the end of 1960, the tritium concentration in the Ottawa River was 240 t.u., that of tributary streams about 200 t.u. The rain-water tritium level was 80 t.u. Evaporative feedback from surface waters to the atmosphere accounts for rain-water tritium being a factor of 6 above the natural level. A peak in rain-water tritium con-

centration, rising to 4 times the preceding and subsequent levels, was observed in the early summer of 1960, probably as a result of increased stratosphere-troposphere transfer in the spring months.

R. R. Brown (University of California, Berkeley, Calif.) and R. G. D'Arcy (Enrico Fermi Institute for Nuclear Studies, University of Chicago, Chicago, Ill.), *Nuclear Reactions of Solar Protons in the Atmosphere, July 1959.* In the course of balloon observations of solar protons at College, Alaska, during July 1959, a large flux of γ radiation was observed extending to atmospheric depths as great as 250 g/cm^2. This radiation varied with the observed proton intensity and exhibited no fast intensity fluctuations during quiet geomagnetic periods. From a detailed analysis of the intensity, absorption length, and time variations of this γ radiation, it is concluded that it consisted largely of 0.3- to 7-Mev γ rays from the inelastic scattering of solar protons and accompanying knock-on neutrons in the atmosphere. The mechanisms involved in this process are discussed. From the observed γ radiation and a calculation of the efficiency of production of γ rays by 50- to 300-Mev protons in air, a maximum flux of 3000 protons cm^{-2} sec^{-1} was estimated over College, Alaska, after the class 3+ flare of July 10, 1959, and a flux of 20,000 protons cm^{-2} sec^{-1} after the class 3+ flare of July 14. These results are in agreement with calculations of the proton fluxes from cosmic noise absorption, using the same proton spectra. Some implications of such intense solar proton bombardment of the polar caps are discussed.

R. R. Brown, (University of California, Berkeley, Calif.), T. R. Hartz (Defence Research Telecommunications Establishment, Shirley Bay, Ottawa, Ont., Canada), B. Landmark (Norwegian Defence Research Establishment, Kjeller, Lillestrøm, Norway), H. Leinbach (Geophysical Institute, University of Alaska, College, Alaska), and J. Ortner (Kiruna Geophysical Observatory, Kiruna, Sweden), *Large-Scale Electron Bombardment of the Atmosphere at the Sudden Commencement of a Geomagnetic Storm.* A large-scale electron bombardment of the upper atmosph was observed with the sudden commencem of a geomagnetic storm at 0146 UT on Ju 27, 1960. The electrons, by their ionizing effe in the upper atmosphere, produced an increase ionospheric absorption of cosmic radio noise wh was observed by riometers in Alaska, Sweden, Norway, as well as X-ray effects, by bremsstr lung, which were observed by a balloon-bo radiation instrument over central Alaska. Hi latitude riometers located at Thule, Greenla and Resolute Bay, Canada, did not show increas absorption at the time of the sudden commen ment, indicating that electron bombardment confined to lower latitudes in the vicinity of auroral zone. Balloon observations of the ev indicate that the principal electron bombardm lasted about 5 minutes, a total of 3 to 9 $\times$ electrons with energy greater than 50 kev hitt 1 cm^2 of the atmosphere in this time. Possi mechanisms responsible for the electron precipi tion are discussed.

James Brune, Maurice Ewing, and John K (Lamont Geological Observatory, Columbia U versity, Palisades, N. Y.), *Group Velocities Rayleigh Waves of Period Greater than 380 S onds.* Recent theoretical and experimental inve gations of the free periods of spheroidal oscillat of the earth have shown good agreement (Als Sutton, and Ewing; Benioff, Press, and Smi Bogert; Ness, Harrison, and Slichter; *J. Geoph Research,* 1961). The group velocities obtai from the measured periods of free oscillation the earth do not show a flattening of the gr velocity curve beyond 380 seconds, such as t which has been reported from studies of prog sive mantle Rayleigh waves of orders $R8$ to R (Ewing and Press, 1954; Benioff and Press, 195 Agreement between results obtained from the t methods of determining group velocity has b attained by (1) correcting mantle Rayleigh w data for the polar phase shift (Brune, Nafe, Alsop, 1961) and (2) revision of the order num of the wave train to which the longest-period servations have been assigned. The revised terpretation of the group velocity data for lo period Rayleigh waves is presented in the tab

Investigator	Earthquake	Period, sec	Wave Train	Group Vel., km/sec	Group Ve from Fre Periods, km
Ewing & Press (1954)	Kamchatka (1952)	480	$R12(R10^*)$	4.97	5.00
Benioff & Press (1958)	Mongolia (1957)	630	$R26(R18^*)$	6.02	6.10
Present authors	Chile (1960)	530	$R18$	5.24	5.30

* The previous identification of wave train is shown in parentheses.

UCIEN M. BRUSH, JR. (Department of Mechanics and Hydraulics, State University of Iowa, a City, Iowa), *Exploratory Study of Sediment fusion.* A study was made of the diffusion of s beads in a submerged axisymmetric jet in er to compare the characteristics of the diffon of sediment with those of the diffusion of nentum in free-turbulence shear flow. A verti- ¼-inch jet of sediment-laden water was di- ed downward into a relatively large cylindrical k of still water. Small concentrations of nearly erical glass beads, both within and above the kes range in size, were introduced into the rculating system. The efflux velocity of the was maintained at 30 ft/sec or more to lessen relative importance of the fall velocity of the ividual particles. Concentration profiles of the iment were measured at various downstream ions in the zone of established flow and were pared with the velocity profiles at the same ions. The diffusion characteristics of the sedint-laden water were analyzed by use of the apximate theories derived for clear water jets. results are applied to the suspended-load ation presently used for two-dimensional flow open channels. Certain conclusions are drawn to the propriety of the assumptions pertaining the fall velocity and sediment diffusion used deriving this equation.

L. BUCHANAN (Sonar Systems Branch, Sound ision, U. S. Naval Research Laboratory, Washton, D. C.), *Reaction of Electronic Components High-Pressure Environment.* The rising tempo oceanographic research portends a large inse in the use of electronic instrumentation in ious forms of deep ocean probes. For reasons of nomy in weight and cost, great advantages ld accrue if electronic equipment could be rated in the natural environment of the sea. To end, a series of commonly used electronic ponents have been tested in an oil bath under rostatic pressures up to 10,000 lb/in^2. Coments of each type tested have been found which operate satisfactorily at all pressures up to 00 lb/in^2. Diodes, transistors, and even vacuum es have been found which operate at this high ssure. Entire circuits capable of operation at 00 lb/in^2 have been built from readily available ponents. One interesting component is a comtion carbon resistor which exhibits a reduction resistance which is proportional to pressure. s pressure dependance is higher for resistors a higher nominal value of resistance. A 200,-ohm resistor, for example, exhibits a resistance uction of 25 per cent at 10,000 lb/in^2 and is an xpensive and convenient pressure transducer. h resistors are in use in the investigation of racteristics of plastic materials under hydroic pressure.

J. K. BUETTNER (Department of Meteorology Climatology, University of Washington, Seattle, Wash.), *The Lunar Surface.* The top layer of the moon will be important for landing, living, and movement of astronauts. Optical data indicate a coarse structure for the surface material. Radio and radar results partly confirm and partly disagree with optical and thermal observations. Calculations by Lettau and by Buettner from surface temperatures during eclipses yield low values of the surface thermal contact coefficient and of the heat conductivity of the first decimeters. However, their assumption of a conductivity independent of temperature is probably incorrect since radiation is responsible for a substantial part of the heat exchange in the porous matter. Another thermal problem arises from the vacuum-cementing of the granules. Any explanations of the surface porosity will have to account for the fact that eclipse temperatures, and therefore thermal data, are about equal for lunar center maria and for the mountainous south pole. Also, the observed extreme temperature variations are a consequence and not the cause of the porosity. If ionizing radiations cause the lunar erosion they should also erode meteors, comets, etc. This would give us a cosmogonic mechanism for reconverting solidified stellar matter to primordial dust.

A. G. W. CAMERON (Chalk River Laboratories, Chalk River, Ont., Canada), *Anomalous Isotopic Composition of Xenon in the Earth's Atmosphere.* It has been found by J. H. Reynolds that the composition of atmospheric xenon differs in all isotopes from that of cosmogenic xenon extracted from stone meteorites. Some of the differences can probably be attributed to the presence of xenon decay products from two extinct radioactivities, I^{129} and Pu^{244}. However, anomalous abundances of Xe^{124}, Xe^{126}, Xe^{128}, and Xe^{130} require the operation of some additional mechanism. The variations of the isotopic composition of silver extracted from various meteorites, discovered by V. R. Murthy, probably cannot be attributed to the extinct radioactivity Pd^{107}, but must probably also be attributed to the additional mechanism. One possibility is that atmospheric xenon and some meteoritic silver were once in the sun and were subjected to neutron irradiation during the deuterium-burning phase of solar evolution. The Xe and Ag anomalies are consistent with this hypothesis, but new data of Reynolds on Kr anomalies do not support it. A more attractive hypothesis is that the original solar nebula, derived from a condensation of the interstellar medium, was chemically and isotopically inhomogeneous. There could be different ratios of the products of neutron capture on slow and fast time scales and of bypassed nuclei not made by neutron capture, as well as modifications produced by neutron capture during deuterium burning in stars that store parts of the interstellar medium for a time and eject it in their red giant phases. In this case the meteorites may have general isotopic anomalies in most of their heavy elements.

F. A. Campbell and H. Baadsgaard (University of Alberta, Edmonton, Canada), *The Bruderheim Meteorite, Chemistry and Mineralogy*. Bruderheim is a gray chondrite belonging to Urey's low iron group and Prior's group 2—the bronzite-olivine chondrites. A chemical analysis is as follows:

SiO_2	40.18	Na_2O	1.22	
TiO_2	0.12	K_2O	0.14	
Al_2O_3	2.16	P_2O_5	0.29	
Fe°	11.54	H_2O^-	0.01	
FeO	11.37	H_2O^+	0.10	
FeS	3.66	Ni^0	1.29	
MnO	0.33	Co^0	0.06	
MgO	25.03	Cr_2O_3	0.60	
CaO	1.74	C	0.035	
			Total	99.87

The silicate minerals in order of abundance are olivine (Fo 75), pyroxene (En 80), plagioclase (An 6), and glass. The metallic minerals are kamacite (6% Ni), taenite (28% Ni), troilite, and chromite. The K-Ar dates obtained are: whole meteorite, 1900 m.y.; feldspar fraction, 1600 m.y.; pyroxene fraction, 1800 m.y.

W. H. Campbell (National Bureau of Standards, Boulder, Colo.), *Auroral Zone Short-Period Micropulsations*. Magnetic field oscillations with periods of 5 to 30 seconds were investigated in Alaska from September 1959 through August 1960. Daily and seasonal variations in activity showed a correlation of micropulsations with typical disturbances of solar-terrestrial type. The close correspondence of micropulsations with *E*-region ionospheric phenomena as measured with the auroral photometer, riometer, and C-3 ionosonde lead to an empirical relationship of magnetic field micropulsations with ionospheric electron density. The geographical extent of micropulsations and possible physical models are discussed.

C. W. Carlston (U. S. Geological Survey, Washington, D. C.), *Bomb Tritium in the Hydrologic Cycle*. During a period of thermonuclear bomb testing from March to November 1958, samples of precipitation, runoff, and shallow ground water in the New Jersey coastal plain and at a small watershed near Madison, Wisconsin, were collected for tritium analysis. At Wharton tract, near Batsto, New Jersey, bomb tritium was found in ground water to a depth of at least 15 meters below the water table, and there was a progressive increase in tritium content upward from that depth to just below the water table. Tritium analyses indicated that the base flow of the Mullica River is obtained almost entirely from groundwater inflow from just below the water table. Tritium water budget studies at Lebanon State Forest in the New Jersey coastal Plain and at upper Black Earth Creek basin near Madison, Wisconsin, indicate that more than half of the tritium from fallout during the period March 1 to July 30, 1958, was exported from the watershed[s] evapotranspiration and runoff.

H. Carmichael and J. F. Steljes (Atomic [E]ergy of Canada, Ltd., Chalk River, Ont., Cana[da]. *Evidence for Storage of Solar Cosmic Rays w[ith] the Magnetic Configuration Responsible f[or] Forbush Decrease*. Three major solar-flare [r]adio-noise outbursts, associated with a large [s]pot, occurred in rapid succession on Nover[n]10, 11, and 12, 1960, starting at 1000, 0304, [a]1320 UT, respectively. Solar cosmic radiation [g]erated in the third of these outbursts produc[ed] conspicuous increase in sea level neutron inten[sity]. At Deep River, Ontario, the intensity had rea[ched] a maximum and was declining when a sudden [en]hancement occurred followed by some r[apid] fluctuations. There was no significant solar acti[vity] at this time, some 5 hours after the start of [the] flare. About half an hour later a sharp (Forbu[sh] decrease of the intensity of galactic cosmic ra[y] tion occurred. Sudden-commencement magn[etic] storms had also occurred during this time. [It] reasoned that these storms and the Forb[ush] decrease were produced by an expanding pla[sma] cloud from the flares of November 10 and 11 [and] that the sunspot field entrained in the c[loud] formed a magnetic bottle (T. Gold, *J. Geop[hys.] Research*, 1959) attached to the sun in which h[igh] energy particles injected by the flare of Noven[ber] 12 were trapped and were being stored. As [the] plasma front passed the earth, the neutron m[oni]tor suddenly sampled the higher flux of the trap[ped] solar cosmic-ray particles.

James H. Carpenter and E. Dixon Sta[ffor]d (Chesapeake Bay Institute, Johns Hopkins U[ni]versity, Baltimore, Md.), *Circulation Pattern [in] Tributary Estuarine Embayment*. Evidence is [pre]sented for three-layered circulation in the Pata[psco] River estuary. There is negligible fresh wate[r] flow to the head of this embayment, which h[as] vertical salinity gradient maintained at the m[outh] by two-layered circulation in the Chesapeake [and] Water flows in at the mouth on the surface [and] on the bottom in the ship channel, while m[ixing] produces water of intermediate density w[hich] flows out at mid-depths. Industrial wastes [can] be used to trace this outflow.

N. L. Carter, J. M. Christie, and D. T. G[riggs] (Department of Geology and Institute of [Geo]physics University of California, Los An[geles] Calif.), *Experimentally Produced Deform[ation] Lamellas and Other Structures in Quartz*. [The] St. Peter sand was deformed by compression [in a] simple squeezer at pressures ranging from [50] 100 kilobars and temperatures varying from [room] 700°C. Abundant undulatory extinction, defo[rma]tion lamellas, and deformation bands were [pro]duced in many of the quartz grains in the s[pec]imens. Of these structures, the undulatory ex[tinc]tion and most of the deformation lamella[s]

distinguishable from those found in naturally formed quartz. Pronounced undulatory extinction, generally in zones parallel to the *c* axis, is mmon. Deformation bands, resembling sharply fined zones of undulatory extinction, were rded in about 10 per cent of the grains. Most nds are subparallel to the *c* axis of the grains d hence differ from natural deformation bands, ich are steeply inclined to the *c* axis. The de-rmation bands in the samples develop in planes high shear stress. Deformation lamellas were oduced in over half of the grains, and more than e set was observed in many grains. The lamellas e inclined at low angles to the base and are mmonly associated with zones of undulatory tinction, to which they are almost normal. The nellas develop in planes of high shear stress. is orientation of artificial deformation lamellas planes of high shear stress supports the hypothe- of Turner (1948) and others and may be of nificance for the interpretation of natural nellas. Quartz has also been recrystallized on a e scale in the squeezer at high temperatures. ore extensive recrystallization has been pro-ced by us in flint, quartzite, and single crystals der differential stress in other types of appara-. The recrystallized products show marked pre-red orientations.

W. B. Chadwick (National Bureau of Stand-ds, Boulder, Colo.), *Variation of Sporadic E th Sunspot Number, 1949–1959.* The question of e dependence of sporadic *E* on the sunspot cycle s largely been unresolved; many investigators ve obtained conflicting answers. Results are esented which cover daily-hourly values for 11 ars at three ionosphere sounding stations, Col-e, Washington, and Huancayo, chosen as repre-tative of the three main sporadic-*E* zones. All ee stations were under the same quality-con-l measures during this period, which included highest yearly average sunspot number for er 200 years. Correlation coefficients for yearly nt of $fEs > 5$ Mc/s vs. yearly average sunspot mber were found to be: College, −0.68 (day-ne only, −0.63); Washington, −0.52 (night y, −0.52); Huancayo, −0.42 (night only, 0.66). Hourly and monthly correlations are also cussed. Certain correlations of *fEs* with mag-ic index *Ap* will be presented. The remarkably sistent results obtained by use of the Phillips mula $\log_{10} P = a + bf$, will be given. (P = bability of occurrence of $fEs > f$, f = frequency c/s), a and b are adjustable constants). An in-ental outcome is the confirming of diurnal and sonal trends at stations in the auroral, north perate, and equatorial zones through use of ny more data than have hitherto been avail-e.

ydney Chapman (University of Alaska, Col-e, Alaska), *Lunar Effects and Winds.* The on produces a tide in the atmosphere. This tide manifests itself in many ways. The barometer acts as a tide gage, and the lunar tidal variations of atmospheric pressure have been well determined at many points widely distributed over the earth. These variations of air pressure occur adiabatically, at least at Batavia where the very small associated lunar semidiurnal variation of air temperature has been determined. In the ionosphere the lunar atmospheric tide has a much greater amplitude, and the tidal rise and fall of the ionized layers has been found at many places. The ionospheric tides induce electric currents which reveal themselves in the lunar geomagnetic tides. The atmospheric tide also affects the impact of cosmic-ray mesons at ground level. But the lunar tidal air currents, although among the simplest features of the tide, have been too little studied. Proposals are made for new work on the lunar tidal winds.

J. E. Chappelear (Shell Development Company, Houston, Tex.), *Shallow-Water Waves.* The physical problem is to calculate the profile and velocity components of a wave, subject to the conditions that the effects of viscosity and surface tension can be neglected. The flow is required to be steady, irrotational, and two-dimensional, and the depth of the water is assumed to be small and constant. The shallow-water approximation, first proposed by Friedrichs, is employed, and two additional orders of approximation, beyond the three calculated by Keller, are obtained. The formulas describing the solitary wave are obtained as a special case, and the velocity of the solitary wave so obtained is found to agree almost exactly with the Boussinesq-Rayleigh formula, $c = [gd(1 + H/d)]^{1/2}$, where c is the wave velocity, d is the depth, and H is the wave height. This velocity differs by no more than 2 per cent from the experimental values of Stephan and Dailey.

Edwin J. Chernosky (Ionospheric Physics Laboratory, Geophysics Directorate, A. F. Cambridge Research Laboratories, Bedford, Mass.), *The Variable-Area Technique for Obtaining Magnetic Data.* A magnetograph that produces variable-area film records has been designed, and units have been placed in operation from arctic to equatorial latitudes. A flying-spot photoelectric scanner and a digital analyzer which processes the scanner output have been designed and are being built. This system will provide the normal hourly value data plus more detailed data on magnetic activity that is not readily obtainable by the usual manual-reading methods. The present magnetograph design was developed in cooperation with Ruska and resulted in part from the intentions of Vestine, Tuve and Gebhardt to make multiple-station geomagnetic recordings that could be adapted to mechanized analysis procedures. A standard suspended-magnet variometer is used with a simple optical system to provide the variable-area recording on 70-mm film at speeds up to

300 mm per hour. The output from the digital analyzer can yield rates of change or other desired parameters for further research. The digital output will also be suitable for making spectral analysis. The scanner and analyzer were designed in cooperation with Travis, Bailey and Morris, and Tormollan.

Frank Chew (Gulf Coast Research Laboratory, Ocean Springs, Miss.), *Transverse Component of the Florida Current off Miami.* A selected group of over 1200 surface current measurements made by Pillsbury in 1885–1886 in the Florida current off Miami is analyzed for transverse component. The selection is based on the objective criterion that the average wind force measured from an anchored station be less than a certain number on the Beaufort scale. It is shown that there exists a time-independent transverse surface component whose pattern and magnitude across the Florida current match those obtained in a group of 576 Geomagnetic Electrokinetograph observations and are in further agreement with Stommel's analysis of an independent Pillsbury series of 633 measurements. The pattern shows a westward transverse surface current component along the western edge of the Florida current off Miami and an eastward transverse surface component across the remainder of the current.

Frank Chew and K. L. Drennan (Gulf Coast Research Laboratory, Ocean Springs, Miss.), *Eastward Flow of the Mississippi River Discharge.* Over 10,000 ballasted drift bottles have been set adrift off the eastern side of the Mississippi delta. In addition, five monthly salinity and temperature samplings of the surface water layer in the same vicinity have been made. Drift bottle returns have been obtained from Havana, Cuba, the Florida east coast, Louisiana, Texas, and Mexico. An attempt is made to relate the eastward bottle movement to the patterns of winds and water salinity and temperature.

John F. Clark (National Aeronautics and Space Administration, Washington, D. C.), *The NASA Geophysics Satellite Program.* The fundamental question to be answered by geophysical satellite research is, what is the nature of the control exerted by the sun over events on the earth? Significant progress is being made toward answering this question, particularly in Explorer satellite studies of atmospheric and ionospheric structure, the radiation belts, the magnetosphere, and the near interplanetary plasma. Over the next two years, NASA geophysical satellites will be launched at an average rate of one every two months, using the Juno II, Delta, Scout, Thor-Agena, and Atlas-Agena vehicle systems. Investigations which will be conducted include atmospheric structure and composition; micrometeoroid density; ionospheric structure, composition, and propagation characteristics; cosmic radiation, solar particles and trapped particles; the geom netic field; and the cislunar interplanetary plasr Of particular importance will be the simultane measurements conducted from the 900-lb orbit geophysical observatories, in polar or highly centric orbits, commencing in 1963.

Roy S. Clarke, Jr. (Smithsonian Instituti Washington, D. C.), and Maxwell K. Carr (U. S. Geological Survey, Washington, D. *Comparison of Tektite Specimens from Mart Vineyard, Massachusetts, and Empire, Geor* Experimental studies have been made on tek specimens from Martha's Vineyard, Massac setts, and Empire, Georgia. Chemical and physi properties of these specimens are remarka similar, although their gross morphologies are ferent. The results of the determination of selec physical properties and of chemical analyses the specimens are given in the table.

Property	Source of Specime	
	Martha's Vineyard	Georg
Index of refraction	1.485	1.4
Density, g/cm³	2.332	2.3
Magnetic susceptibility, emu/gram × 10^{-6}	3.90	3.6
Chemical analysis, %		
SiO_2	80.6	80.5
Al_2O_3	11.3	11.2
Fe_2O_3	0.4	0.3
FeO	2.2	2.4
CaO	0.7	0.6
MgO	0.7	0.6
MnO	0.05	0.0
Na_2O	1.1	1.1
K_2O	2.4	2.3
TiO_2	0.5	0.4
H_2O^-	<0.1	<0.0
H_2O^+	<0.1	<0.0

Absorption spectra were determined for the ra 350 to 2500 mμ and were found to be identical similar to those previously reported for tekti Microscopic study showed inclusions typical tektites, flow structure generally conforming the surface of the specimens and the strain. Se quantitative spectrographic analyses were sistent with chemical analyses for 11 compou and 14 elements. Thirty-five elements to wh the method was sensitive to 0.01 per cent or were not detected. The chemical data are sistent with the pattern of tektite analyses general but do not fit into the pattern of recognized tektite group. These data do not tradict the claim that these specimens are gen tektites. However, it has not been possible

ve categorically that they are of natural origin. ir remarkable similarity requires explanation suggests that an artificial origin is a possibil- Geologic field evidence is needed to remove ambiguity.

AMES C. COBB (Chemistry Department, Brook- en National Laboratory, Upton, N. Y.), *De- nination of Lead Isotopes by Alpha Activation alysis.* An activation analysis technique has n developed for the investigation of the iso- ic composition of lead in materials where the tomary wet chemistry–mass spectrometric pro- ure is inapplicable because of lead contamina- . The method involves α bombardment of the ple which induces $(\alpha, 2n)$ reactions on the l isotopes to produce polonium isotopes. Po- ially, all four lead isotopes can be determined his way, but the long half-life of Po^{209} ($\sim$ 200 rs) precludes its determination with any great ision. Three feldspars of known lead isotopic position have been run as standards. These polonium activities which correspond to the l isotopic composition within 2 per cent. A run the carbonaceous chondrite Murray yielded a $^{08}/Pb^{206}$ ratio of 3.07, in good agreement with terson's primordial Pb^{208}/Pb^{206} ratio of 3.11. ainable sensitivity is limited by the amount ime available on the cyclotron, but it is hoped ; Pb^{204}, Pb^{206}, and Pb^{208} may be measured on ples with a total lead concentration of 0.1 n.

OHN D. COCHRANE (Department of Oceanogra- , A and M College of Texas, College Station, .), *Some Observations of Mass Field and Sur- Flow in the Yucatan Current.* Although rly important to the circulation in the Gulf Mexico, westward intensification in the Yucatan ent has not received much attention. During cruises of the Texas A & M Research Ship algo this feature was rather closely studied in region north of Yucatan strait. It is most rly shown in the vertical temperature profiles. herm slopes were found which are comparable hose occurring in the Gulf Stream proper. The hward extent of these extreme slopes is not wn. A band of strongly sloping isotherms ex- ds through Yucatan strait, where slopes are test, at least to the northeast corner of Cam- e bank. A few current measurements suggest speeds in the band are subgeostrophic and there is a component of current across the d.

LVIN J. COHEN (Mellon Institute, Pittsburgh, , *A Semi-quantitative Hypothesis of Tektite in by Asteroid Impact.* Geochemical evidence esented to indicate that the moldavite-strewn in southern Bohemia and Moravia is con- d with the impact which produced the Ries Nordlingen. The further experimental work ssary to prove or disprove this hypothesis is discussed, and possible locations for new moldavite fields are suggested. This hypothesis, applied to the more meager geochemical and geological data of the North American tektite discoveries, predicts a strewn field of tektite deposits of circa 29.4×10^6 years of age extending from Maine to northern Florida and through Texas. The only *obvious* terrestrial feature having the necessary size and geographical position for the impact crater is the Gulf of St. Lawrence. Geological field work necessary to prove or disprove this is discussed. Evidence obtained from these two tektite fields is applied to the southeast Asia–Australia tektite fall. This complex field resulted from impact of at least two large bodies entering together. The first hit south of the Australian continent and the second in southeast Asia (possibly in Laos). These impinging bodies must have been large enough to cause atmospheric blowout in order for tektite fields to exist. The probability of still other tektite fields is discussed along with the stability of tektite glass and its stress etching. It is shown that this hypothesis unifies all tenable experimental evidence available.

ALVIN J. COHEN (Mellon Institute, Pittsburgh, Pa.), *Impact Crater Glasses, A Systemization.* All known terrestrial impact glasses produced by nickel-iron meteorites contain coesite. Impact glasses low in nickel and iron usually do not contain coesite but can contain cristobalite. Other impact glasses containing no crystalline phases usually cannot be easily associated with a crater for two reasons. All these facts as well as data on all known and probable impact glasses are discussed. Based on this evidence, some predictions are made concerning properties of lunar surface materials. Reasons are given why certain terrestrial impact craters might be of secondary origin related to lunar maria and why others must be excluded. The relationships between chondrites and tektites are discussed.

P. J. COLEMAN, JR., and C. P. SONETT (National Aeronautics and Space Administration, Washington, D. C.), and LEVERETT DAVIS, JR., (California Institute of Technology, Pasadena, Calif.), *On the Interplanetary Magnetic Storm: Pioneer V.* During a period of intense solar activity between March 26 and April 6, 1960, measurements of the magnetic fields in interplanetary space were obtained with the space probe Pioneer V. The component of the fields associated with the solar plasma ejected during this period attained strengths of 40 gammas or more (compared with an average value of 2.7 gammas during normal periods). It is argued that these comparatively high fields existed in interplanetary space for many hours. From estimates of the plasma velocity, the radical extent of these regions of high field is calculated to be 0.7 A.U. The fields associated with these regions were observed to be quite regular. Similar results accompanied most of the

more intense solar activity during the flight of Pioneer V. Possible implications of these results are discussed.

R. Convit (Instituto Nacional de Obras Sanitarias, Caracas, Venezuela), *Experience with Artificial Rainfall Stimulation in Venezuela.* Artificial rainfall stimulation has been practiced in Venezuela since 1954. Little information, however, is available for the period 1954–1957. Although the results of the 1958–1960 period are not fully evaluated, a direct correlation is apparent between cloud seeding and rainfall yield. 1959 was generally very dry, particularly in the areas where no silver iodine generators were installed. Rainfall for the year amounted to about 20 per cent of the 10-year average. Silver iodine appeared efficient on the stratiform clouds in the lowlands as well as in the mountains, particularly at night. Rain was observed with little cloud cover, but the seeding cannot be definitely credited with causing it until final evaluation has been made of all data. Normal freezing levels at 14,000 to 15,000 ft and cumulus tops at 20,000 to 30,000 ft presented ideal conditions for cloud seeding from aircraft. However, cost and operational difficulties limited these apparently satisfactory experiments.

Kenneth L. Cook (University of Utah, Salt Lake City, Utah), *The Problem of the Mantle-Crust Mix: Lateral Inhomogeneity in the Uppermost Part of the Earth's Mantle.* The material which has compressional wave velocities of 7.4 to 7.7 km/sec, and which exists beneath many active tectonic belts, is postulated to be a mixture of rocks of mantle and crustal types. The belts include mid-ocean ridges, island arcs, and rift valleys (both oceanic and continental). The total area of these belts, though still incompletely charted, is estimated to be at least 10 per cent of earth's surface. The uplift and lateral extension, as well as the high heat flow and volcanism generally characteristic of the active belts, indicate expansion and an upwelling of convection currents in the mantle, thus giving lateral inhomogeneities in the uppermost mantle. It is postulated that the mantle-crust mix is composed of a mixture of eclogite and basalt (or gabbro) in the phase transformation zone, which may be of considerable thickness. In such active belts, the existence of the Morohovicic discontinuity as an abrupt boundary between rocks of contrasting density and velocity is questioned, and the depth of isostatic compensation probably extends deeper into the uppermost mantle than is generally recognized. The extension of the East Pacific rise into the western part of North America (in part after Heezen, 1960, and Menard, 1960) is given as an example of one of these active tectonic belts and is postulated to include three 'median' rifts, the Mexico and Colorado plateaus, the Basin and Range province, and the great basalt, lava, and volcanic plateaus of the western United States. The 'median' rifts, which follow belts of seism and probable high heat flow, include (1) the system passing through the Gulf of Califo Sulton trough, Great Valley of California, and to sea along the San Andreas fault zone, and entering the continent in Alaska; (2) the bel grabens immediately east of the Sierra Neva and (3) the major rift system which extends, branch of (1), from the Gulf of California thro western Arizona, central Utah (including newly discovered rift valleys reported by C and Berg, 1956, 1958, 1961), southeastern Id western Wyoming, western Montana, and Br Columbia. These rifts are comparable structura though perhaps on a smaller scale, to the valleys of Africa and the median rifts of mid-Atlantic and mid-Indian Ocean ridges. fault-block mountains of the Basin and Ra province are strikingly similar to the 'rift-mo tain' systems of the mid-Atlantic ridge. A mo based on the hypothesis of a convection cur cell in the mantle as developed by Vening Mei and applied to the East Pacific rise by Mer (1960), is applied to a generalized crustal sec across the western part of the United States. model can be used to explain some features gives difficulty in explaining others, and there needs modification. On the tentative assump that the horizontal limb of the convection cur cell lies at a depth of about 150 to 200 km, model can be used to explain the Gutenberg l velocity layer in the upper mantle; but the l velocity channel would probably be restricted horizontal extent.

H. H. Cooper, Jr. (U. S. Geological Sur Tallahassee, Fla.), *Type Curves for Nonste Radial Flow in an Infinite Leaky Aquifer.* coefficients of transmissibility and storage o leaky artesian aquifer and the leakage of its fining bed may be determined by superposin plot of nonsteady-state drawdowns on a famil type curves. The type curves may be used to predict drawdowns when the aquifer and fining-bed coefficients are known.

Donald E. Cotten (New York University, York, N. Y.), *Implications of Diurnal Varia in Counting Rates of Neutron Monitors.* The istence of a solar daily variation in cosmic neutron count is confirmed by regular varia of its amplitude and peak time with geomagn latitude (G. Schwachheim, *J. Geophys. Resea* 1960), longitude, and month (orientation of a These dependences indicate that it is not du diurnal pressure variations. The diurnal varia in local time is much larger than that in univ time or in sidereal time, which implies that due chiefly to cosmic rays from the sun ra than to an anisotropy in the galactic cosmic ra tion. This is supported by agreement betw observed dependences, especially regarding im zones and monthly variation of amplitude,

ll's predictions based on a reasonable spec- of solar protons impinging on an assumed red dipole field of the earth.
parture from such predictions, and from et symmetry in geomagnetic dipole coordi- indicate that the higher multipoles are icant in influencing solar cosmic rays. Here al attention is paid to peak times, which are comparable from station to station than are tudes. A very small variation in universal may exist and can be explained by the ro- of the earth.

H. Cram, Jr. (Department of Geology, Rice ersity, Houston, Tex.), *A Crustal-Structure ction Survey in South Texas.* On August 11, sixty oil exploration and research seismo- crews attempted to record two shots det- d in the Texas Gulf coastal plain. The shot s were located in San Jacinto and De Witt ties, Texas. The shot point line was approx- ly parallel to the strike of the Tertiary ents, and the distance between the shot s was 260 km. More than 3000 lb of explosives placed in five holes at each shot point. The f the charge was at a depth of 100 ft and bottom at 250 ft. The average Bouguer aly in the region is −25 mgal. The shot it was keyed to a 140-cps reference signal nitted by radio station KTRH, Houston. and later refracted arrivals were used to ate the velocity structure. This delineation upported by events identified as reflections the refractors. The results indicate thickness- ity relationships as follows: 2.0 km of 2.3 ec, 5.3 km of 3.94 km/sec, 12.5 km of 5.38 ec, 13.2 km of 6.92 km/sec. The Mohorovicic tinuity is represented by a velocity of 8.18 ec, and the total crustal thickness is 33 km. ration for the project took 2 months al- h the actual recording took only 1 hour.

ES H. Crocket and John W. Winchester artment of Geology and Geophysics, Massa- tts Institute of Technology, Cambridge,), *Study of the Dilute Solid Solution of in $CaCO_3$ and Its Relevance to the Marine emistry of Zn.* The dilute solid solution of in $CaCO_3$ (where $Zn/Ca << 0.01$) has investigated by measuring the distribution radiotracers Zn^{65} (γ, 245 days) and Ca^{45} 60 days) between a precipitate and its ated aqueous solution (ionic strength 1) at 25°, 35°, and 50°C. The precipitate, d by outgassing a solution of $CaCO_3$ in saturated with CO_2 and containing the racers, was digested for 2 weeks and sepa- by filtration and rinsing with a dilute solu- f nonradioactive Zn^{++}. At 50°C the distribu- f Zn between crystals (calcite) and aqueous omogeneous (independent of fraction of Ca itated), and the ratio $(Zn^{65}/Ca^{45})_{solid}/(Zn^{65}/$ queous was 3.2± 0.2. Assuming a ratio of solubility product constants of $CaCO_3$ and $ZnCO_3$ of 34, the Raoult's law activity coefficient of $ZnCO_3$ in the solid solution is about 10.6 at 50°C. At 25° and 35°C the distribution was very close to logarithmic, even on prolonged digestion, indicating an extremely slow recrystallization rate. The logarithmic distribution ratio was $\lambda = 4$ to 6, probably owing to a combination of solid solution and some occlusion of very strongly adsorbed Zn^{++} during crystal growth. These measurements may be used to interpret some aspects of the marine geochemistry of Zn.

A. R. Croft (U. S. Forest Service, Ogden, Utah), *Some Sedimentation and Erosion Phenomena along the Wasatch Mountain Front.* The paper describes the kind and amount of sediment produced by a small 2100-acre drainage basin on the Wasatch Mountain Front, Utah, since settlement and during the recent geologic past. The sedimentation record is as follows: (1) for a very long period in the remote past only fine silts and clays, (2) a sudden change, lasting for several thousand years, to bouldery alluvium with 15-ton rocks, (3) silts and clays for several thousand years, and (4) bouldery alluvium since about 1912, much like the early bouldery deposits. The recent change in sediment production, from silts and clays to bouldery alluvium, was caused by damage to the watershed mantle of vegetation and soil as a result of excessive use. Although the cause of the earliest change of the same character is not known, the author's hypothesis suggests that it was also brought about by a change in watershed conditions related to the wide climatic fluctuations that caused the most recent recession of ancient Lake Bonneville to the present Great Salt Lake. Probable watershed cover (and sediment) during this period are thought to be perpetual snow (silts and clays), followed by a combination of snow and/or bare mineral bouldery alluvium), and finally the development of a complete cover of soil and vegetation (silts and clays).

Z. F. Danes (Boeing Airplane Company, Seattle, Wash.), *Numerical Solutions of Radiation Belt Parameters.* Integrals appearing in expressions for various parameters of particles trapped in the earth's magnetic field are formidable. Therefore, numerical solutions were obtained. At points where second-order approximations are permissible analytic integrations of the approximate solution were also performed and used to check or supplement the numerical data. Results are shown graphically.

Z. F. Danes (Boeing Airplane Company, Seattle, Wash.), *The Sudden Impulse of August 25, 1958.* The sudden impulse which occurred at about 1300 UT, August 25, 1958, was analyzed on records from about fifty IGY observatories. Data were reduced so as to define the impulse vector in components of the geomagnetic (dipole) field.

The northern geomagnetic component is almost everywhere positive, evenly symmetrical with respect to the geomagnetic equator, and increasing from about $+5\ \gamma$ at the equator to about $+50\ \gamma$ near $\pm 60°$ latitude; the eastern geomagnetic component is erratic; the vertical component has odd symmetry with respect to the equator, reaching, in the northern hemisphere, a minimum of about $-5\ \gamma$ near 20°, and a maximum of about $+10\ \gamma$ near the 45° latitude. Results are compatible with a sudden decrease in number of particles trapped along a field line crossing the earth's surface at a latitude of about 50°.

A. C. Daughtry, Douglas Perry, and Milton Williams (Production Research Division, Humble Oil and Refining Company, Houston, Tex.), *Isotopic Composition of Magnesium in Sediments.* In our research on the distribution of magnesium isotopes in sedimentary materials, we have made determinations of the isotopic composition of magnesium in sea water, in recent carbonate sediments in which magnesium is co-precipitated with calcium carbonate, in dolomitized limestones, and in dolomite synthesized in the laboratory. In the laboratory synthesis of dolomite, in which calcium carbonate is allowed to react with a solution of magnesium chloride at elevated temperature and pressure, it appears that the lighter magnesium isotopes are utilized preferentially in the formation of dolomite. That a similar situation exists in nature is indicated by comparison of the average magnesium isotopic composition of dolomitized limestone with the isotopic composition of magnesium in sea water and in recent carbonate sediments.

G. L. Davis, G. R. Tilton, and G. W. Wetherill (Geophysical Laboratory and Department of Terrestrial Magnetism, Carnegie Institution of Washington, Washington, D. C.), *Ages of Minerals from the Basement Rocks of the Southern Appalachian Region.* The ages of samples of zircon and biotite from crystalline basement rocks in North Carolina and Tennessee have been measured by isotope dilution methods. The results can be interpreted as showing evidence of periods of metamorphism 1000 to 1100 m.y. ago, 850 to 950 m.y. ago, and 350 to 500 m.y. ago, confirming or substantiating earlier reports from the Carnegie and Lamont laboratories. Still older ages of 1300 m.y. were found for zircons from gneisses exposed on the northwest flank of the Appalachian belt, indicating the presence there in Precambrian times of igneous rocks comparable in age with the 1350-m.y.-old rocks that underlie central and southwestern United States. Periods of crystallization of igneous granites are indicated at 700 to 850 m.y. and around 500 m.y. Rocks formerly grouped under the term 'Cranberry' do not appear to have a single age.

Leverett Davis, Jr., and David B. J. Chang (California Institute of Technology, Pasad Calif.) *Synchrotron Radiation as the Source Jupiter's Polarized Decimeter Radiation.* The servation by Radhakrishnan and Roberts (*P Rev. Letters,* 1960) that the 31-cm radiation f Jupiter is polarized and that it seems to be r intense and most intensely polarized at dista of the order of 3 radii from the axis of rota provides grounds for distinguishing between various sources proposed by G. B. Field *Geophys. Research,* 1959, 1960.) Only the cy tron and synchrotron mechanisms will give po zation. The former requires polar fields of order of 10^4 gauss and has other implausible tures. Models based on synchrotron radiation have undesirable features but seem more rea able. They require fields of the order of 0.1 gauss in the emitting region and about 60 t as much at the pole. They also require that electrons have energies in the 5- to 75-Mev r and densities of the order of 10^{-3} to 10^{-2} The electrons must be mainly in flat helices the equatorial plane and suitably distribute radius. It appears necessary that they be acc ated in the field; the possibility of a suit mechanism should be investigated. The large strength of Jupiter suggests that its dynamo operate in a larger fraction of the volume does the earth's.

J. Cl. De Bremaecker, Paul Donoho, Martin Graham (Rice University, Houston, T and G. P. McCouch (General Radio Comp Concord, Mass.), *Electronic Digital Seismogr* Operational principles of and experimental re from two different types of digital seismogr are presented. The two instruments differ in method by which seismic signals are use modulate the signal from a local oscillator the AM approach the signal from the oscillat modulated by a three-terminal displacemen capacitance transducer attached to the mass long-period seismometer. The modulated s is amplified and passed through a phase sens demodulator. It is then filtered to eliminate microseisms and is recorded in analog form monitoring purposes. The very long periods filtered, amplified, and applied to a coil-and- net transducer to keep the boom centered tenuation of the long periods is 3 db at 31 and 40 db for infinitely long periods. Drift is eliminated. The output from the demodu can also be applied to an analog-to-digital verter and recorded on magnetic tape in a fo acceptable by a computer. A static magnific of 10^6 can easily be obtained. In the FM app a resistor is used in parallel with one of capacitors of the bridge. The output of the b is applied to a tuned circuit, amplified, and to drive the bridge. Capacitance variations in frequency changes which are easily dig and recorded. A dynamic range greater tha db and a gain of 10^6 can easily be obtained.

. J. Dessler (Lockheed Aircraft Corporation, ssiles and Space Division, Palo Alto, Calif.) Robert Karplus (University of Vienna, Aus-), *Neutron Decay and the Changes in the Van en Radiation Belt.* It has been observed that electron flux in the outer zone of the radiation undergoes changes that are associated with magnetic storms. These observations appear to inconsistent with either direct solar injection local acceleration. We have suggested that the nic-ray albedo represents a satisfactory source the entire radiation belt (*Phys. Rev. Letters,* 71, 1960). Hess (*J. Geophys. Research, 65,* 3107, 0) has argued that the strength of such a neu- decay source is adequate to account for the trons with energies greater than 100 kev. A del will be presented which can contribute, in t, to the major fluctuations in the observed nsities of the radiation belt. In this model a stant number of electrons is assumed to be sent in the radiation belt (as must be the case neutron decay is the source of the outer zone, e the weakness of this source implies very long ticle lifetimes). The model involves a system two diamagnetic ring currents (for which there bservational evidence) that can temporarily nsfer part of the magnetic energy involved in eomagnetic storm to the Van Allen belt elec-ns.

V. G. Deuser and L. F. Herzog (Department Geophysics and Geochemistry, Pennsylvania te University, University Park, Pa.), *Rb-Sr Determinations of Muscovites and Biotites n Pegmatites of the Blue Ridge and Piedmont.* -Sr ages of 18 mica specimens from pegmatite urrences of the Blue Ridge and Piedmont vinces were found to lie in the range of 250 to m.y. Samples from the Piedmont generally eared to be younger than those from the Blue ge. It seems, however, that the metamorphic-tonic events that produced the large number granites and pegmatites in this region did not ct the area in as uniform a manner as was uced by some previous workers. Discordantly ages of muscovite rich in Sr but poor in Rb, xisting with biotite in two localities, are tenta-ly attributed to the preferred incorporation of ntium by the muscovite; in these cases, ntium abnormally rich in Sr^{87} apparently was en up from digested country rock.

. W. Dickson (Geology Department and In-ute of Geophysics, University of California, erside, Calif.), *The Pressure Coefficient of the ubility of Cinnabar in Solutions of the System S-Na_2S-H_2O at 50°C.* The effects of pressure Na_2S concentration on cinnabar solubility in eous solution was determined at 50°C by the of a specially designed solubility apparatus, 'hydrothermal solution equipment.' At 2.04 cent Na_2S and 1 bar, the percentage of HgS .05; at 1500 bars, the percentage of HgS is 0.60. At constant pressure, increasing the Na_2S concentration increases cinnabar solubility at an increasing rate. At 750 bars and 1.37 per cent Na_2S, the percentage of HgS is 0.35; at 2.04 per cent Na_2S, the percentage of HgS is 0.80; and at 3.80 per cent Na_2S, the percentage of HgS is 2.63. The solubility of cinnabar is known to increase with decreasing temperature. Therefore, an Na_2S solution initially saturated with cinnabar, migrating toward the earth's surface, would become undersaturated because of the pressure and temperature decrease. Processes other than temperature or pressure drop are required for HgS to precipitate. Diluting a saturated solution causes supersaturation. Dilution or reactions tending to diminish sulfide ion concentration, such as reaction with wall rock, are possible natural processes involved in the precipitation of HgS from Na_2S solutions.

Bruce R. Doe (California Institute of Technology, Pasadena, Calif., and Geophysical Laboratory, Carnegie Institution of Washington, Washington, D. C.), *Lead Isotopes in Ore and Nearby Rocks Near Balmat, N. Y.* Near Balmat, New York, tabular replacement bodies of sulfides parallel the layering in marbles of a metamorphic complex which is correlated with the Precambrian Grenville series. Textural relations between sulfides and silicates suggest the ores were formed during the retrograde stage of a regional metamorphism that occurred about a billion years ago. The isotopic composition of lead from galena is uniform in an individual mine. The model lead ages of these galenas are in good agreement with the time of mineralization determined from the age of the metamorphism. The isotopic composition of cryptic lead from marble is not uniform today and apparently was not uniform a billion years ago. The bulk isotopic composition of lead in marble could have been similar to that of the ores at the time of mineralization. However, the marbles could have been the source of the ores only if the ores are the well-mixed product of a poorly mixed source. The ore lead is clearly not a representative sample of lead from feldspars of nearby synkinematic granites and pegmatites.

Robert F. Doolittle and Carl D. Graves (Space Technology Laboratories, Inc., Los Angeles, Calif.), *The Scintillation Chamber: A New Tool for Space Physics.* The particle-detecting element of the scintillation chamber is a crystal. However, unlike the scintillation counter, in which a photo multiplier pulse indicates the passage of an ionizing particle through the crystal, the scintillation chamber allows the actual path or track of the particle through the crystal to be photographed. It offers a number of advantages, unique for space research, over conventional counters or track-forming detectors. Track pictures televised and telemetered to ground stations will be much like those from bubble or cloud chambers and will allow both the identification of the radiation en-

vironment and the determination of its time changes and energy spectrum. Further, the scintillation chamber does not have to be sampled at random, but can be triggered by desired classes of events. The STL scintillation chamber has been operated at the California Institute of Technology synchrotron during the past months in order to determine the most suitable applications of this instrument to space physics. A report on this work is given.

George B. Dowling (U. S. Navy Mine Defense Laboratory, Panama City, Fla.), *The Bathyconductograph, a New Oceanographic Tool.* The MDL bathyconductograph (BC), developed for rapid field surveys of the depth variation of electrical conductivity, shows promise of being a useful oceanographic tool. Derived from the bathythermograph (BT), which it resembles both in appearance and operation, it uses standard BT slides to record electrical conductivity vs. depth. Used in conjunction with the BT, it provides a convenient method for measurement of the gross structure of temperature and salinity from a moving ship. Some results of such measurements in the Bering and Chukchi seas are presented. The accuracy attained by developmental models to date is about 2 per cent of the reading; however, a calibration with a surface sample before each lowering permits the accuracy to approach the resolution, which at present is about ¾ of 1 per cent. Improved servomechanism characteristics in models under development will lead to an accuracy of ¼ to ½ of 1 per cent, which will allow determination of salinity (assuming a BT error of ¼ of 1 per cent) to about 0.3 parts per thousand. The BC should prove particularly useful in nearshore and estuarine studies, where salinity gradients are often large.

Frank J. Dragoun (Agricultural Research Service, U. S. Department of Agriculture, Hastings, Nebr.), *Rainfall Energy as Related to Sediment Yield.* An evaluation of the relationship of the kinetic energy of a rainstorm with suspended sediment yields for two complex watersheds is presented. The relation is developed on the hypothesis that cultivated acres are the predominant source of soil erosion. This statistical analysis is extended to include the interaction effects of rainfall energy as functions of several factors, such as rainfall intensity and antecedent moisture. The results are examined and compared with the relationships of other rainstorm factors and watershed characteristics as a means of estimating sediment yields.

A. J. Dragt (Lockheed Missiles and Space Division, Palo Alto, Calif.), *Effect of Hydromagnetic Waves on Van Allen Protons.* It is generally accepted that the proton component of the Van Allen belt (the inner zone) arises from cosmic ray albedo neutron decay. On the basis of this theory, almost as many protons should be deposited b yond 2 earth radii from the earth's center as a deposited near the earth's surface. However, mea urements indicate that the proton flux decreas very rapidly beyond 2 earth radii. A model proposed in which this rapid decrease is caus by hydromagnetic waves. These waves affect t magnetic moments of protons whose veloci along a field line is sufficient to cause a Doppl shift in the hydromagnetic wave frequency up the proton cyclotron frequency. As a result, t mirror points of these particles undergo a rando walk into the atmosphere. This resonance conc tion, in conjunction with certain theoretical pro erties of hydromagnetic waves, accounts for t location of the outer boundary of the proto zone. In addition, the model affords two predi tions: (1) At the outer edge of the proton zon the maximum energy of the trapped proto should decrease as r^{-11} with geocentric distanc (2) The proton flux in the outer zone may rise measurable values during magnetically quiet tim (e.g., sunspot minimum).

Earl G. Droessler (National Science Found tion, Washington, D. C.), *Atmospheric Sciences the National Science Foundation.* For almo three years the National Science Foundation h had a major-program effort in support of t atmospheric sciences. The record of the Found tion to date is presented and is found to cover broad research program on upper-air physics well as most phases of meteorological researc including major research programs on antarct meteorology and on weather modification search and evaluation. Support has also been pr vided for a range of educational activities and f certain scientific publications. A few data a offered.

H. A. Einstein and R. B. Krone (Universi of California, Berkeley, Calif.), *Experiments Determine Modes of Cohesive Transport in S Water.*

J. I. Ewing (Lamont Geological Observato Columbia University, Palisades, N. Y.), *Rece Developments in Marine Geophysics.* The mari geophysics program at Lamont Geological O servatory has been concentrated recently alo two principal lines of investigation. The first these is the development of equipment and tec niques to measure earthquake and other seism signals with detectors located on the deep s floor. This allows us to study the propagation seismic waves which have not crossed a contine ocean boundary and thus offers great possibiliti of extending our knowledge of the differences b tween oceanic and continental structure. Resu to date have included three successful measu ments with short-period (0.5 to 1 sec) instrume in water depths between 4.7 and 5.7 km. Analy is incomplete, but at least one earthquake *P* wa

several long-range seismic refraction profiles recorded. The second program has been one eflection measurements made from a moving utilizing a drum or chart recorder to provide matic correlation, integration, and profiling vents. The record produced is analogous to a dard echo-sounder record, allowing immediate ection and interpretation of results. In shal- water, good results have been obtained with igh-voltage spark source. In deep water, a ane-oxygen gas exploder has been used to bottom penetration of up to 1 km, and small osive charges have achieved penetrations of 5 km.

HODES W. FAIRBRIDGE and OSWALD A. KREBS, (Department of Geology, Columbia Univer- New York, N. Y.), *Sea Level and the South- Oscillation.* An average curve for the world ual mean sea level for the century 1860–1960 been obtained from a carefully selected series orld tide-gage records. Data have been elim- ed from tectonically unstable areas and other ously anomalous records. Five-year running ages provide us with a residual curve that approach a eustatic standard (probably o-eustatic). The lowest point of sea level was it 1890; the mean rise from 1900 to 1950 was mm/yr, but the decade of fastest rise was –1956 with 5.5 mm/yr. The pattern varies ewhat if plotted ocean by ocean. The non- othed, annual curve shows a 2- to 3-year city of 10- to 30-mm amplitude. The world e closely matches the peaks of the 2- to 3- atmospheric pressure cycle known as the thern Oscillation,' being in phase with the heast Pacific node. The reciprocal, Indian an node is well reflected in the Indian Ocean, periodically dominates over the Pacific pat- in the Atlantic Ocean. When the effect of a sure anomaly of 1 mb is taken as equivalent 10-mm change in sea level, it is found that is still a large residual, generally in the same e. It would seem that associated wind systems mainly responsible.

Y. FAN, P. MEYER, and J. A. SIMPSON (En- Fermi Institute for Nuclear Studies, Uni- ty of Chicago, Chicago, Ill.), *Dynamics of the r Radiation Belts.* The spatial and temporal ges of the density and spectrum of the elec- in the outer radiation belts were systemati- studied with a proportional counter telescope oard Explorer VI. It is shown that (*a*) the agnetic field undergoes a world-wide distor- in space during magnetic storms, (*b*) the rtion of the magnetic field produces large- changes in the pitch angle distribution of the ed electrons, resulting in the changes of the tion intensity along the lines of force, and n addition to the large-scale changes of in- ty, there is a slow radial motion of the peak sity distributions in the geomagnetic field.

R. M. FARQUHAR (Geophysics Laboratory, University of Toronto, Toronto, Ont., Canada), *Lead Isotope Abundance Variations among Galenas from the Keewatin Geological Province.* Variations in the abundance of lead isotopes in samples from the Sudbury and Thunder Bay regions of the Keewatin geological province have already been reported. Isotopic analyses of three other suites of lead minerals from the Keewatin are presented, and, for two of these, graphs of Pp^{207}/Pb^{204} against Pb^{206}/Pb^{204} are linear. The slopes of these lines have been determined, and possible interpretations of the results in terms of known geological events are discussed.

G. FAURE and P. M. HURLEY (Massachusetts Institute of Technology, Cambridge, Mass.), *The Ratio Sr^{87}/Sr^{86} in Oceanic and Continental Basalts.* The isotopic composition of strontium in a number of oceanic and continental basalts of subcrustal origin has been determined by means of solid-source mass spectrometry. The abundance of Sr^{87}, which is a daughter product of Rb^{87}, increases in time as a function of the Rb/Sr ratio of the material. The ratio Sr^{87}/Sr^{86} in basalts from numerous geographic localities all over the world was found to vary within narrow limits from 0.705 to 0.711, with a standard deviation for a single analysis of about ± 0.001. The average ratio for 13 oceanic basalts is 0.7074 ± 0.0003. Since Rb has been concentrated in the crust by differentiation of the upper mantle, the Sr^{87}/Sr^{86} ratio of average crustal material is expected to be measurably higher than that found in rocks of subcrustal origin. Analyses of two Paleozoic shale composites from the east and west coasts of North America average $Sr^{87}/Sr^{86} = 0.722 \pm 0.001$. Mantle strontium should therefore have a characteristic Sr^{87} abundance which is low and constant within narrow limits and which distinguishes it from average crustal strontium. Consequently the initial Sr^{87}/Sr^{86} ratio of igneous rocks of unknown origin can be used as a criterion for a crustal or subcrustal origin.

C. E. FICHTEL and D. E. GUSS (National Aeronautics and Space Administration, Goddard Space Flight Center, Greenbelt, Md.), *Nuclear Emulsion Studies of Solar Proton Beams.* The characteristics of three solar particle beams have been studied above the earth's atmosphere with nuclear emulsions flown in Nike Cajun research rockets. The particle characteristics of the moderate solar particle beam of September 3, 1960, are presented. At the time of exposure the flux of protons with energies greater than 13 Mev was approximately two orders of magnitude greater than the cosmic-ray background. If the differential energy spectrum for protons is expressed in the form $dJ/dE = CE^{-\gamma}$, γ is found to vary from approximately 2 at 200 Mev down to appreciably less than 1 at 20 Mev. Nuclei with a charge greater than 3 were detected in the solar beam. The ratio of particles with charge

greater than 3 to singly charged particles above the same rigidity cutoff was found to be consistent with the ratio in the sun's atmosphere, approximately 0.0016, and not with the cosmic-ray ratio, which is an order of magnitude larger. In the November 12, 1960, and November 15, 1960, cosmic-ray events, the proton differential energy spectrum had a much larger value of γ in the low-energy region. The flux of protons with energies greater than 13 Mev was found to be approximately 10^4 times the cosmic-ray background 5 hours after the visible flare.

E. L. Fireman and J. DeFelice (Smithsonian Astrophysical Observatory, Cambridge, Mass.), *Argon 39, Argon 37, and Tritium in the Recently Fallen Bruderheim Meteorite.* The amounts of the radioactive isotopes Ar^{39}, Ar^{37}, and tritium were measured in specimens of the Bruderheim meteorite, which fell on March 4, 1960. (R. E. Folinsbee kindly gave the sample to the authors.) The results are shown in the table.

Element	Half-Life	Decays/g/day
Ar^{39}	325 years	14.5 ± 0.7
Ar^{37}	34 days	29 ± 4
H^3	12.4 years	290 ± 20

Ar^{39} and tritium measurements are being done on the metallic fraction to test whether all the Ar^{39} is produced by the spallation of iron and nickel nuclei and to permit a better comparison of these results with the Ar^{39} measurements that have been done on iron meteorites. Comparison with previous results for the Hamlet meteorite shows that the Ar^{37}/Ar^{39} and H^3/Ar^{39} ratios are identical within experimental errors, even though the amount of Ar^{39} is higher in the Bruderheim than in the Hamlet meteorite. Ar^{39} in other chondrites ranges in value from 6 to 17 decays per gram per day.

Irene Fischer (Army Map Service, Washington, D. C.), *The Geometric Parallax of the Moon.* The recent geodetic connection between Europe and South Africa along the 30th meridian makes it possible to reinterpret the Greenwich and Cape observations of the lunar crater Mösting A made by Christie and Gill in the years 1905 to 1910. Crommelin's result for correction to Hansen's value of mean parallax of the moon and for the flattening of the earth are discussed in terms of a geodetic world datum. A series of observational facts in the form of distances in kilometers can be extracted from the old records.

Joel E. Fisher (New York, N. Y.), *Glacier Ogives of the Forbes Type.* Forbes-type ogives on glaciers occur only below substantial ice falls. Ice-fall areas are too dangerous to investigate afoot; when studied by long-period time-lapse photography, such areas are seen to be intens broken up, kneaded, and thoroughly aerated. T process facilitates seasonal temperature chan *throughout* their depth, in contrast with seasc temperature changes only at shallow depth smooth flowing glaciers. Ogives are spaced 1 ye glacier flow apart. Their white bands are found consist of bubbly-type ice, density 0.89; their d bands are of more solid ice, density 0.92. By c parison, where glaciers exhibit lengthwise la some of bubbly ice and some of solid ice, bubbly ice lanes are traceable to high-altit sources of accumulation, where snow changes firm without appreciable melting; the dark la are traceable to lower accumulation areas wh melt water exists. The following conclusion reached. White bands in ogives represent for comminuted ice-fall material with entrapped which, debouching into the outrunning gla during winter, is consolidated into bubbly-t ice. Dark bands represent ice-fall material wh debouched and reconsolidated into solid ice outflowing glaciers in summer, when the prese of melt water largely eliminated entrapped ai

J. E. Fletcher (Agricultural Research Serv Boise, Idaho), *Characteristics of Precipitation the Southwest.*

E. A. Flinn (United Electrodynamics, I Pasadena, Calif.), C. F. Romney (Headquarte U. S. Air Force, Washington, D. C.), A. M. R and J. R. Woolson (United Electrodynamics, I Pasadena, Calif.), *Analytical Results from L Frequency Seismic Measurements in a Deep W* A set of specially developed, highly sensi seismometers were operated at various depth a 3600-ft well drilled in granite, and another of identical instruments were operated simul eously at the surface. Spectral analysis of sei noise between 5 and 0.2 cps showed that: Noise amplitude at a given frequency falls approximately exponentially with depth. (2) N amplitude at a given depth falls off approxima exponentially with increasing frequency, abo cutoff frequency which depends on depth. The behavior of noise for varying frequency depth agrees with the hypothesis that most of seismic noise in the frequency range consid consists of Rayleigh waves. Rayleigh-wave tenuation with depth was calculated for one m layered structure approximating the structur the region of the well. (4) Increasing wind velo in the well-head area drastically decreased ratio of noise amplitude in the well to noise plitude at the surface, for frequencies abo cps. First-motion amplitudes from about 100 recorded teleseisms ($\Delta > 16°$) were studied. frequencies of the first *P*-phase arrivals were tween 1 and 2 cps; the amplitude of first mo fell off within a depth of 600 meters to rou half the amplitude recorded at the surface, as pected for a homogeneous medium.

R. E. Folinsbee (University of Alberta, Alta., anada) and L. A. Bayrock (Alberta Research ouncil, Edmonton, Alta., Canada), *The Brudereim Meteorite, Fall and Recovery.* Bruderheim, detonating bolide, entered the earth's atmosphere at 1:06 A. M., MST, March 4, 1960, with a ash visible for 200 miles. It was followed by etonations resembling sonic booms audible over n area of 2000 square miles. Ten reliable sightings nd many flash-sound intervals assisted in pinointing the fall area. The fireball, traveling in ne direction of the earth's rotation, had a net tmospheric velocity of only 8 miles/sec, facilitatng entry. Many individual pieces with a total ass greater than 300 kg fell within a well-defined llipse of fall, 3.3 miles long, 2 miles wide (5.5 × 3 km), with its major axis N70W. The larger ieces fell near the southeast apex of the ellipse. alling vertically onto frozen ground at terminal elocity, most of the pieces rebounded onto the ow surface, facilitating recovery. Mapping and ecovery were continued during the spring breakup eriod, yielding a total of 188 sizable pieces eighing 303 kg. The largest piece weighed 31 kg; 00 recovered pieces, each smaller than 100 grams, re uncataloged.

S. E. Forbush (Department of Terrestrial Magetism, Carnegie Institution of Washington, Washgton, D. C.), D. Venkatesan and C. E. McLwain (Department of Physics, State University f Iowa, Iowa City, Iowa), *Intensity Variations in he Outer Van Allen Radiation Belt.* Data on the tensity of the outer Van Allen radiation belt btained on Explorer VII from October 26 to ecember 9, 1959, were analyzed in detail. To late the intensities to location in the belt, the arameter L proposed by McIlwain has been used. alues of L corresponding to 2.9, 3.5, 4.1, and 4.7 arth radii were considered. The variations of tensity at selected values of L were negatively orrelated with geomagnetic activity during this eriod. The results are discussed in terms of posble contributions to auroral zone currents and quatorial ring current.

Guy A. Franceschini (Department of Oceangraphy, A and M College of Texas, College Staon, Tex.), *Water Balance of the Gulf of Mexico.* knowledge of the water cycle affecting the Gulf Mexico is basic to an understanding of gross teractions between the atmosphere and Gulf iters. Both branches of the cycle, atmospheric nd surface, are considered on a monthly and asonal basis for the 1958–1959 water year. Values the separate components are based on conuity considerations for each branch. Results e combined to give a consistent description of e water balance for the basin. During the period udied the Gulf acted as an atmospheric waterurce except during February and March. Effece evaporation losses were greater over the stern half of the basin than over the western half, and average river discharges were not sufficient to overcome these losses. Results are presented, and suggestions are made of the consequences with regard to surface salinity and salt balance of the basin.

Joseph B. Franzini (Stanford University, Stanford, Calif.), *Progress Report—Evaporation Suppression Research.* Various aspects of evaporation suppression by monomolecular films on water surfaces are presented. An attempt to determine the optimum dosage of chemical has been made through evaporation-pan tests. Full-scale field testing at a 40-acre lake on the Stanford campus indicated that to maintain good film coverage the chemical must be applied continuously during windy periods to replace film blown away by the wind. A reduction in reservoir evaporation of approximately 18 per cent was achieved during the periods of film application. There are indications that the best technique of applying the chemical is to spray it under pressure from a boat. On the basis of experience to date it appears that under optimum conditions reservoir water can be saved through use of chemical films at a cost ranging from perhaps $20 to $35 per acre foot. These optimum conditions imply a reservoir of proper size and shape in a region of moderate winds and high evaporation potential.

George D. Freier (University of Minnesota, Minneapolis, Minn.), *Auroral Effects on the Earth's Electric Field.* On October 7, November 13, and December 1, 1960, auroras occurred on quiet, fair-weather evenings and produced electric-field changes measured at the ground. Continuous monitoring of the earth's electric field and the time constant of the air at ground level allowed us to calculate the increased conduction current at the ground level due to space charge generated by charged particles of the aurora stopping in the upper atmosphere. By assuming one-dimensional current flow, we calculated the flux at the surface of the earth to be as high as 10^4 particles cm^{-2} sec. This flux was due to an excess of negative charge brought into the atmosphere by the aurora. On November 7 a coronal-type aurora produced sharp dips in the field, and on November 13 the aurora was sufficiently intense to make the fair-weather field negative for several hours.

Phyllis Freier, S. Biswas, and W. Stein (School of Physics, University of Minnesota, Minneapolis), *Solar Protons and Alpha Particles from the September 3, 1960, Flare.* A class 3+ solar flare started at 0040 UT on September 3, 1960, and reached maximum intensity at 0110 UT. The average proton differential energy spectrum from 0930 to 1700 UT on September 3 has been measured in the energy interval 250 to 800 Mev. In the expression $dN/dE = kE^{-\gamma}$, γ is approximately one from 250 to 400 Mev and increases to approximately 3 at higher energies. The proton cutoff

energy has been measured and is 250 ± 15 Mev. This corresponds to a magnetic rigidity of 0.72 by at Minneapolis. The sudden commencement of the magnetic storm following this flare occurred at 0230 UT on September 4. After this time, protons of energy <250 Mev were also observed. We measured the proton spectrum in the energy interval 80 to 800 Mev from 1700 to 2400 UT on September 4. The solar α-particle differential energy spectra at these two times have also been measured. For α particle $\gamma = 3$ in the energy interval 100 to 200 Mev/nucleon. Before the magnetic storm the ratio of the flux of protons to the flux of α particles in the rigidity region 0.88 to 1.3 by was

$$\frac{J_p}{J_\alpha} = \frac{3500 \text{ part/m}^2 \text{ sec ster}}{120 \text{ part/m}^2 \text{ sec ster}} = 29 \pm 6.$$

Irving Friedman (U. S. Geological Survey, Washington, D. C.) and Alfred C. Redfield (Woods Hole Oceanographic Institution, Woods Hole, Mass.), *Applications to Hydrology of Deuterium Variation in Natural Waters.* The variations in the ratio of the two stable isotopes of hydrogen, protium, and deuterium in natural waters can be measured with sufficient ease and accuracy to make this ratio a valuable hydrological tool. Because the physical and chemical processes that cause a separation of these isotopes are fairly well understood, we can use the isotopes as natural tracers. A few examples are given to illustrate possible uses. (1) Deuterium is concentrated in the residue during evaporation. This fractionation has been studied as a function of temperature and can be applied to evaporation studies. Measurements of the deuterium content of the water in a closed lake and in the inflow water permit the calculation of the percentage of evaporation. (2) Because the deuterium content of precipitation varies with the altitude of precipitation, the source of springs can often be ascertained by the deuterium content of the spring water. It is possible to differentiate connate waters from brines formed by the solution of salt by ground water of meteoric origin. (3) The origin of samples of sea ice can easily be traced. Ice formed by the freezing of sea water will contain much more deuterium than glacial ice.

Irving Friedman (U. S. Geological Survey, Washington, D. C.), *Deuterium in the Atmosphere.*

Melvin Friedman (Shell Development Company, Houston, Tex.), *Petrofabric Analysis of Experimentally Deformed Calcite-Cemented Sandstones.*

Sigmund Fritz (U. S. Weather Bureau, Washington, D. C.), *Geophysical Implication of Tiros Photographs.* The satellite Tiros I photographed many different aspects of the earth's surface a of its atmosphere. For example, geographers m be interested in pictures of sand dunes and d rock formations in North Africa, and other surf features. Oceanographers may study specular flection of sunlight from both calm and ro water surfaces; shoal waters can also be seen the photographs. Ice in the Gulf of St. Lawre has been televised in spring and in autumn. In field of hydrology, photographs of snow in Alps, Himalayas, and the Sierra Nevada prov estimates of the areas covered by snow. Meteo ogists are studying cloud formations both in large-scale cyclonic systems and in the smal scale systems associated with cellular patte cloud streets, and severe local storms.

Sigmund Fritz and Jay S. Winston (U. Weather Bureau, Washington, D. C.), *Some Rad ation Results from Tiros II.* The radiation me urements from Tiros II are influenced mainly the variation in the amount and temperature clouds and water vapor. Some radiation measu ments from the satellite are discussed in relat to the meteorological variables.

Naoshi Fukushima (Geophysical Institute, kyo University, Japan), *Local Increase of G magnetic Activity during the Decaying Stage Magnetic Storms.* During the recovery stage magnetic storms the geomagnetic activity does decrease uniformly all over the world. From servations during the IGY it is found that th are two special regions in high latitudes wh the activity increases with time in contrast to general world-wide tendency of decreasing ac ity. One of these special regions is located in early-morning side of 70° to 80° in geomagn latitude; the other is in the evening side of to 70° in latitude. This fact seems to suggest t trapping of extraterrestrial charged particles the earth's magnetic field has the highest pro bility of occurring at these special regions in h latitudes.

Naoshi Fukushima (Geophysical Institute, kyo University, Japan), *Persistent Disturbanc the Polar Regions on Geomagnetically Q Days.* Even when the geomagnetic *Kp* in shows an extremely low value, there is alw some geomagnetic disturbance. This disturba which shows a peculiar configuration and is fined to the region near the geomagnetic pole considered to be caused by the persistent s wind, which comes to the earth even when solar corpuscular stream responsible for magn storms is practically absent. The amplitude of polar-cap disturbance is of the order of sev tens of gammas, and it varies with season— is, with the incident angle of the solar wind to geomagnetic dipole. In the summer season polar-cap disturbance on quiet days amount

much as a few hundred gammas, especially on daylight side around geomagnetic latitude 80°.

TOY D. GAUL (Department of Oceanography Meteorology, A and M College of Texas, llege Station, Tex.), *The Travel of Internal mperature Fluctuations at Texas Tower 4.* Re- s are summarized for multiple-level water perature measurements at three fixed stations Texas Tower 4, which is east of New York in er 185 feet deep. Analyses of both fall and ng records revealed discrete internal tempera- e anomalies moving onshore at speeds of about not. These anomalies have 'equivalent periods' several minutes, and travel is confined to very row limits of speed and direction.

REEMAN GILBERT and STANLEY J. LASTER (Geo- sical Service, Inc., Dallas, Tex.), *Excitation Propagation of Pulses on an Interface.* It has ntly been found that exact solutions to Lamb's blem exhibit a pulse that is related to a com- root of the Rayleigh function. For normal ues of σ (Poisson's ratio) the pulse arrives at rly the same time as the compressional pulse, when σ is near 0.5 the pulse is more distinct arrives between *P* and *S*. The idea that a se can be associated with a complex root of Rayleigh function has been extended to Cag- d's problem—two solid half-spaces firmly ed at a common plane interface. In this prob- it has long been thought that interface pulses oneley waves) could exist only for certain ues of the elastic parameters. The exact solu- s to this problem show that Stoneley-like es occur for almost all values of the elastic ameters. The Stoneley function has real and plex roots that lie on Riemann sheets other n the sheet of integration. An interface pulse be associated with each root. Theoretical seis- grams for several half-space pairs are presented show the existence of interface pulses and r relation to roots of the Stoneley function. ditions for the existence, radiation, and at- uation of these pulses are discussed. The impli- ons of the role of interface pulses in the ray cture of normal modes (Rayleigh and shear) also discussed.

REEMAN GILBERT and STANLEY J. LASTER (Geo- sical Service, Inc., Dallas, Tex.), *Experimental estigation of PL Modes in a Single Layer.* A nic model has been set up to simulate the blem of two-dimensional elastic wave propa- on in a layer over a half-space. Both the source the receiver are mounted on the free surface he layer. Seismograms are presented as a func- of range. Three distinct modes are present. y are the *PL*, *S*, and Rayleigh modes. Experi- tally determined curves for phase and group city are shown for each mode. By using a dif- nt receiving transducer it was possible to re- two interacting *PL* modes. The two *PL* modes do not overlap in frequency and have been separated. The lower-frequency *PL* mode exhibits many of the features seen on recordings of earthquake *PL* modes. In both modes the period decreases as a function of time. Some of the longer-range *PL* recordings have been phase equalized in order to recover the shape of the refracted pulse. The use of the refracted pulse shape in the quantitative ray theory of Knopoff, Gilbert, and Pilant enables one to realize the correspondence of ray theory and mode theory for the *PL* phase.

THOMAS GOLD (Cornell University, Ithaca, N. Y.), *Permafrost on the Moon.* The possibility is discussed that water is bottled up beneath the moon's surface. A layer of permafrost must be expected in the ground if appreciable amounts of hydrated silicate were present in the material that formed the moon. At quite a shallow depth below the surface, the rate of evaporation of ice would be negligible on the time scale of the moon. Surface features are discussed in relation to such permafrost. The question is raised whether large amounts of water could be contained in the moon, thus accounting for its low mean density.

THOMAS GOLD (Cornell University, Ithaca, N. Y.), *Present Evidence of Particle Fluxes and Fields in the Solar System.* Evidence from solar and general cosmic rays is used together with space probe information to augment the picture of plasma and magnetic fields in the solar system. Events like that of November 12, 1960, prove particularly valuable for this purpose. A dissipation process is discussed which appears to be responsible for allowing magnetized clouds to become disconnected from the sun.

PHILIP A. GOLDBERG (Rand Corporation, Santa Monica, Calif.), *Cosmic-Ray-Induced Atmospheric Refractivity at Extra Low Frequencies.* The effect of electrons produced by cosmic-ray ionization on the refractive index of the atmosphere is treated for the 40- to 90-km altitude range for frequencies of 1 to 10,000 cps. Allowance is made for extremes in value of electron density due to effects of minimum and maximum nighttime electron detachment conditions. Over this frequency range the refractive index undergoes transitions to large values at altitudes which increase with excitation frequency. Transition altitudes are 43 km for 10 cps, 55 km for 100 cps, and 68 km for 1000 cps for maximum nighttime conditions.

JULIAN R. GOLDSMITH (Department of Geology, University of Chicago, Chicago, Ill.), DONALD L. GRAF and JUANITA WITTERS (Illinois State Geological Survey, Urbana, Ill.), and DAVID A. NORTHROP (Department of Geology, University of Chicago, Chicago, Ill.), *Studies in the System $CaCO_3$-$MgCO_3$-$FeCO_3$.* Isothermal sections at 700°, 750°, and 800°C under 15-kbar total pressure were obtained through use of a squeezer-type apparatus. At these temperatures the system contains two

two-phase and two single-phase areas. One single-phase region extends a short distance into the ternary system along the full length of the $MgCO_3$-$FeCO_3$ binary join. The other extends as a thin sliver from dolomite along the $CaMg(CO_3)_2$-$CaFe(CO_3)_2$ ternary join, curving upward and enlarging into the $CaCO_3$ apex after traversing approximately two-thirds of the join. The hypothetical compound $CaFe(CO_3)_2$, not known in nature lies in a two-phase field even at 800°C. Solid solubility, particularly in the vicinity of the ternary join, is little affected by temperature. A quantitative emission-spectrographic procedure for analysis of Ca, Mg, Mn, and Fe in 1-mg dolomite samples is described, and cell sizes are correlated with composition for 20 samples. The $CaCO_3$ content, which can be determined to ± 1 mole per cent at a 67 per cent confidence level, varies from 49 to 56 mole per cent.

A. Rudolf Hanel and W. G. Stroud (U. S. Army Signal Research and Development Laboratory, Fort Monmouth, N. J.), *The Tiros II Radiation Experiments.* The Tiros II meteor satellite, containing two television cameras and a family of electromagnetic radiation experiments, was placed into orbit on November 23, 1960. The medium resolution radiometer on board is a cluster of five sensors. Their optical axis is inclined at 45° to the spin axis of the satellite. The spin of Tiros provides sustaining motion. Channels are sensitive to the following spectral bands: 626.5 μ, 8 to 12 μ, 0.2 to 6 μ, 8 to 30 μ, 0.55 to 0.75 μ. Results give an insight into the energy budget of our planet and its atmosphere. Radiation data are compared with weather maps.

Mahdi S. Hantush (New Mexico Institute of Mining and Technology, Socorro, N. Mex.), *Flow of Ground Water in Sand of Nonuniform Thickness.* Ground-water flow formulas are based on several well-known assumptions, one of which is that the water-bearing stratum is of uniform thickness and, except in a few instances, horizontal. Frequently, however, the aquifer is neither horizontal nor of uniform thickness. The formulas of flow in such an aquifer are, therefore, necessarily different from those based on the above-mentioned assumption. The latter formulas have been used to approximate the flow in aquifers of nonuniform thickness or of sloping beds. In some cases, such an approximation may give fair results under certain limitations. But in many cases, the effect of a sloping bottom or of a nonuniform thickness may not be negligible. In these cases the use of such formulas will lead to the vexations that arise when attempts are made to force the application of formulas to cases to which they do not apply. Approximate differential equations are set up to describe the flow in a sand of nonuniform thickness and/or of sloping beds and to integrate them for several flow systems, such as the flow toward wells, streams, and springs. The results are presented in terms of functions that are already available in tabular form.

B. Harris (University of Nebraska, Lin Nebr.), A. L. Sharp (Agricultural Research ice, U. S. Department of Agriculture, Lin Nebr.), A. E. Gibbs (Bureau of Reclamation, Department of Interior, Lincoln, Nebr.), an J. Owen (Soil Conservation Service, U. S. De ment of Agriculture, Lincoln, Nebr.), *An proved Statistical Model for Evaluating Pa eters Affecting Water Yields of River Basins.* inference drawn from the ordinary multipl gression approach may be questionable when method is used to analyze hydrologic data. A tistical model that avoids some of these u tainties is developed. A Taylor series expa is suggested to obtain exponential and intera terms. Orthogonal transformations are use extract some of the variables for use as predi A rule is exhibited for selecting the single important (based on ability to explain var in the dependent variable) independent var testing its significance, and removing its effec all remaining variables. A second rule is exhi for selecting, in turn, the succeeding most im tant independent variables, testing their sig cance, and removing their effects from other ables. Finally, a rule is exhibited for stopping selection of independent variables when thos maining will not contribute significantly to further reduction of unexplained variance in dependent variable. The net result is the sele of a few from many independent variables t in a 'near best' prediction equation. A meth presented for obtaining the multiple regre equation using only the selected variables. application of the model is illustrated by its in analyzing data from 763 storms on water 3H at the Central Great Plains Experimental tershed, Hastings, Nebraska.

Miles F. Harris, Sidney Teweles, and F erick G. Finger (U. S. Weather Bureau, W ington, D. C.), *Diurnal Variation of Wind, sure, and Temperature in the Troposphere Stratosphere over the Azores.* The diurnal semidiurnal variations of wind, pressure, temperature at Lajes Field, Terceira, Az were computed for each month of the year levels between the surface and the 10-mb Upper-air observations made 4 times daily different scheduled times in each of 2 years, combined to yield an effective record of 3-hourly observations per day, making it pos to compute the 12-hour waves. An analys variance was performed on the 12 monthly v at each level to determine the significance o annual means. This analysis showed that pressure and temperature variation were d mined more accurately than the wind, but possibility of systematic errors in the obs pressure and temperature oscillations should

overlooked. The semidiurnal variations were ınd to agree fairly closely with those at Wash-gton, D. C., where similar computations are ailable for the troposphere during the summer nths. However, the diurnal variations of wind d pressure at the two stations are quite dissimi-, possibly reflecting the 180° phase difference the surface pressure waves. To check the con-tency between the wind and pressure variations Lajes Field, the diurnal and semidiurnal height riations were computed from the wind varia-n at each isobaric surface by the use of a model sed on a linearized form of the equations of otion, frictionless flow, and the assumption that e oscillations are simple progressive waves. Re-lts of this analysis suggest that the radiosonde servations may contain diurnal temperature rors, and smaller semidiurnal errors, which su-rimpose fictitious pressure variations on the true cillations, causing the phase to be moved toward on. This conclusion must be regarded as tenta-ve, since it is not known that the restrictions of e model actually apply.

Stanley R. Hart (Department of Terrestrial Magnetism, Carnegie Institution of Washington, Washington, D. C.), *A Study of Mineral Ages in a Contact Metamorphic Zone.* Rb-Sr ages have been determined on biotites and K-Ar ages on biotites, feldspars, and hornblendes from a contact metamorphic zone between a Laramide intrusive and Precambrian country rock in the Front Range of Colorado. The country rocks are amphibolites and quartzo-feldspathic schists which exhibit mineralogical contact effects over distances of tens of feet. The age of the intrusive is 66 ± 2 m.y. The general age level of the unaffected Precambrian is about 1150 m.y. Sixteen samples were collected over a distance of 2400 ft from the contact. The relationships between the mineral ages are illustrated in the table for two of these locations. The mineral ages at the other locations exhibit a similar pattern of discordance.

Distance, ft	Age, m.y.			
	Biotite K-Ar	Feldspar K-Ar	Biotite Rb-Sr	Hornblende K-Ar
250	80		410	1150
400	450	480	850	

Bernhard Haurwitz (High Altitude Observatory, University of Colorado, Boulder, Colo.), *Periodic Winds in the Upper Mesophere.* The air motions in the layer above 70 km show pronounced 24-hour and 12-hour periods superimposed on the mean motion. The amplitudes of these oscillations are often larger than the mean wind. It is therefore important, for the dynamic interpretation of the observed wind field, to know which part of an actually observed wind value is to be attributed to the mean wind and which part to the periodic components. The theory of these periodic variations is not yet sufficiently established to predict these oscillations, but some reasonably reliable determinations of the diurnal and semidiurnal wind period are available for Jodrell Bank, England, and Adelaide, Australia. These data show that at Jodrell Bank the semidiurnal variation is larger than the diurnal, while at Adelaide the diurnal variation is larger. There is also a pronounced seasonal fluctuation. The diurnal variation has its largest amplitudes in summer and is smallest in winter; for the semidiurnal variations the conditions are reversed. The implications of these results for the dynamics of the mesosphere and especially for the theory of the atmospheric tides is discussed.

Jesse B. Havard (U. S. Air Weather Service, Andrews Air Force Base, Washington, D. C.), *Radiational Characteristics of Water Clouds at Infrared Wavelengths.* The general solution to the problem of electromagnetic radiation extinction by small water spheres is described. This solution allows the computation of factors which lead to quantitative values for the albedo, transmissivity, and, thus absorption of infrared radiation in some wavelength regions by selected water clouds.

Walter Hays, R. Ernest Anderson, and LeRoy Scharon (Department of Geology, Washington University, St. Louis, Mo.), *An Example of the Influence of Remanent Magnetism on Magnetic Intensity Measurements.* Near Ironton, Missouri, oriented samples of an intrusive rhyolitic body were collected along a line 300 feet in length for paleomagnetic measurements. This rhyolitic body is characterized by structural and petrologic homogeneity. Magnetite is the principal iron oxide mineral and consistently forms 2 per cent by volume of the rock. Paleomagnetic measurements, however, reveal great inhomogeneities in the magnetic properties: the magnetic susceptibility varies between 0.78×10^{-3} and 2.03×10^{-3} cgs units; the ratio of the intensity of remanent magnetization to the intensity of induced magnetization varies from 0.21 to 26.91; the direction of remanent magnetization, although significantly different from the direction of the earth's field, is different for each sample; and the polarity of the samples is both normal and reversed. Sharp variations of the order of 2700 gammas in the relative magnitude of the vertical component of the earth's magnetic field, measured at stations located along the sample line, reflect the inhomogeneity of the remanent magnetization in the rhyolite body. A theoretical magnetic profile, calculated on the basis of the direction of the total magnetization in the individual samples along the sample line, has the same gross features as the measured profile. The close correlation of the

variations of the two curves emphasizes the necessity for considering the remanent magnetization of a rock unit when interpreting magnetic intensity measurements made over the unit.

E. F. Heald (Chemistry Department, University of Hawaii, Honolulu, Hawaii), and J. J. Naughton (Chemistry Department, Brookhaven National Laboratory, Upton, N. Y.), *Homogeneous Equilibria in Volcanic Gases.* Volcanic and fumarolic gases have been collected during the 1959–1960 eruption of the volcano Kilauea on the island of Hawaii. Collections were made on chromatographic columns of silica gel contained in portable evacuated glass tubes. Previous laboratory experiments had shown that it was possible to freeze in the high-temperature equilibria of sensitive gaseous mixtures by collecting in such a manner. Analysis of the collected gases was made by modified gas chromatographic procedures. Collections made under the most favorable conditions were used to establish an atomic mass balance for the gas. This, together with available thermodynamic data, made it possible to calculate the homogeneous equilibrium composition for the system by means of an IBM 650 computer. Fair agreement was obtained with the molecular composition of actual samples, and excellent agreement was obtained when a correction was applied for approximately 50 per cent of the measured water being meteoric and not in equilibrium with the volcanic gas system. Homogeneous equilibrium in the primary magnetic gas system was indicated. The potentialities of the computer for calculating the composition and concentration of minor molecular species present in volcanic gases, and for extrapolating to underground conditions with a variety of variables, has also been investigated.

Hugh C. Heard (Institute of Geophysics, University of California, Los Angeles, Calif.), *The Effect of Time on the Experimental Deformation of Rocks.* An adaptable new deformation apparatus has been used for constant strain-rate tests in compression and extension up to 5 kb and 500°C at strain rates from 0.4 to 3×10^{-8} sec^{-1}. Cylinders of Yule marble were extended 10 per cent at 25° to 500°C, both parallel and normal to the foliation. Results at 25°C show slight decrease in strength with decreasing strain rate; at 500°C strengths are decreased 80 per cent from the fastest (0.25-sec duration) to the slowest (35 days). Stress-strain curve characteristics change gradually from strong work hardening to steady-state flow as strain rate is decreased. By applying Eyring's theory for steady-state flow, the strength (σ, kb) at 10 per cent strain is related to strain rate ($\dot{\epsilon}$, sec^{-1}) and temperature (T, °K) thus:

$$\dot{\epsilon} = 2.9 \times 10^{8} \exp(-62{,}400/RT) \sinh(\sigma/0.100)$$

for extension normal to the foliation. For extension parallel to the foliation

$$\dot{\epsilon} = 1.6 \times 10^{7} \exp(-56{,}000/RT) \sinh(\sigma/0.145)$$

The data fit the Eyring equation well; extra- lation on the basis of this equation to a reasona geologic strain rate of 10^{-14} sec^{-1} gives strengths the Yule marble ranging from 500 bars at 300°C 10^{-3} bars at 500°C. Thin sections show that crystallization and other effects previously fo at 600° to 800°C and at strain rates of 10^{-4} s occur at 400° to 500°C and at 10^{-7} sec^{-1}. T suggests that recrystallization in nature may oc at even lower temperatures.

The brittle-ductile transition in Solenhofen li stone has been explored at strain rates of 2×1 and 2×10^{-7} sec^{-1}. The limestone becomes duc at a substantially lower pressure and/or temp ature at the lower strain rate, contrary to res of other experimenters.

Carl E. Hedge (Geochronology Laborator Geochemistry Section, University of Arizona, T son, Ariz.), *Sodium-Potassium Ratios in Muscov as a Geothermometer.* A suite of 30 muscovite sa ples has been analyzed for sodium and potassi with a flame photometer using lithium as an ternal standard. The majority of the samples from gneisses and pegmatites from the Santa Ca lina Mountains in Pima County, Arizona. The mainder are from geologic environments wh allow reasonable estimates to be made of temperature of formation of the muscovite. N of the muscovites studied is associated w paragonite. However, most of them are associa with albite and orthoclase. There is no indicat that the amount of sodium in the muscovites sensitive to the presence or absence of sodi minerals in the immediate area. Yoder Eugster (1954) have studied the temperatu composition relationships for the muscovite-par onite join under 30,000-psi hydrostatic pressu If it is assumed that the increase in sodium c tent with temperature for muscovite found these workers holds also for the equilibrium alb + muscovite → orthoclase + paragonite, t the temperature of the samples analyzed dur this study can be estimated. The temperatu thus evaluated are reasonable. The highest te peratures found in the study were at apparen intrusive contacts. In one case a quartz mon nite had intruded into shales and siltstones fo ing a micaceous contact metamorphic zone. M covite near the contact indicates a temperat of formation of 660°C. At 40 and 80 feet fr the contact, 620°C and 570°C are indicated. gneisses studied indicate temperatures rang from 390° to 550°C. Muscovite from pegmat pods and lenses within the gneissic body indi the same range of temperatures and the s absolute temperatures at any given location. attempt was made to determine whether sodium-potassium ratios had adjusted to the lo temperatures during the cooling process. The sults suggest that these effects were not of m importance. Several analyses were made in ho of finding an authigenic muscovite which wo

a very low sodium-potassium ratio; how-
all the results thus far have indicated that
amples are either detrital or that they are
ctually muscovite.

A. Heiskanen (Ohio State University, Co-
us, Ohio), *The Ellipticity of the Earth's
tor.* The ellipticity of the earth's equator, or
riaxiality of the earth, has been studied for
ntury. Gravity anomalies and, on a smaller
, the astrogeodetic method have been used.
the artificial satellite method also exists, and
interesting to compare the results obtained
he different methods. The efforts of the
atic Institute of the IAG and of the Institute
eodesy, Photogrammetry and Cartography of
are described. We get quite different values
he triaxiality $a_1 - a_2$, where a_1 is the long
a_2 is the short semiaxis of the equator, and
he longitude λ_0 of the long equatorial axis,
nding on what method and what material we
see table).

Source	$a_1 - a_2$, meters	λ_0
stations	300	3°W
n stations	160	48°W
hern hemisphere	168	10°E
hern hemisphere	60	56°W
lite method	205	33°W

e problem of the triaxiality of the earth is
ously not yet definitely solved. If the triaxial-
xists, it is obviously caused by the fact that
mass surplus of the continents and the mass
iency of the oceans are not completely com-
ated. The deeper the disturbing masses are,
easier it is to explain the triaxiality. The in-
t of geodesists in this problem has decreased
g the last decades because the shape of the
itself is most important and can be de-
ined. With the undulation values at hand one
easily realize whether the geoid is closer to
riaxial ellipsoid or to the ellipsoid of revo-
n.

W. Henriksen (U. S. Army Map Service,
ington, D. C.), *Test of an Ultra-Long-Range
nce-Measuring Instrument Using a Satellite
t.* The Army Map Service is engaged in test-
n instrument which should be able to measure
nces up to 6000 km with a precision of 1 part
0,000. This instrument, called Secor, fre-
cy-modulates an emitted UHF signal which
ceived and re-emitted from a down-range
ponder. The phase of the modulation on the
ed signal is then compared with that of the
al modulation. The phase difference is di-
proportional to the total distance traveled
e signal. By measuring the distances from four stations in the Caribbean, with known geodetic coordinates, to an artificial satellite at a height of about 800 km, the performance of the instrument and the validity of the equations are tested.

Harold R. Henry (U. S. Geological Survey and Michigan State University, East Lansing, Mich.), *Sea Water Encroachment with Uniform Vertical Recharge.* The permanent position of the interface separating the fresh water from the sea water is determined when equilibrium is maintained by fresh-water recharge entering the aquifer uniformly by vertical seepage into the water table. This is in contrast to theories which apply to the situation in which the fresh water proceeds almost horizontally over the interface toward the sea and there is no vertical recharge above the interface. The prototype situation considered is the fresh-water lens maintained under an oceanic island or peninsula. The two-dimensional problem is solved by use of the hodograph and its relation to the complex velocity potential. The hodograph is constructed, and is transformed into a rectangle. The complex potential cannot be constructed at first because of the unknown elevation of the water table. This difficulty is circumvented by employing the Hamel variable $\tau + i\theta$, which is the logarithm of the second derivative of the potential. The imaginary part θ is obtained on the boundaries by an inspection of the hodograph. Subsequently, θ is obtained throughout the rectangular hodograph by application of the relaxation technique applied to the finite-difference form of Laplace's equation. The Cauchy-Riemann equations yield τ, and the complex coordinates z of the interface are computed by numerical integration of $Z = \int e^{-(\tau+i\theta)}\, d\bar{q}$, where $\bar{q}$ is the conjugate of the complex velocity. The results for several cases are compared with those obtained by use of the Dupuit assumption.

D. Heymann and O. A. Schaeffer (Chemistry Department, Brookhaven National Laboratory, Upton, N. Y.), *Exposure Ages of Some Iron Meteorites.* The time between the breakup of a planetesimal and the collection by the earth of a fragment of this breakup is called the exposure age of the meteorite. Exposure ages can be obtained by measuring the Cl^{36} and Ar^{39} radioactivity and the Ar^{36} content of these meteorites. Such determinations were made for several iron meteorites.

Meteorite	Activity, dpm/kg Cl^{36}	Activity, dpm/kg Ar^{39}	$Ar^{36} \times 10^8$, cc NTP/g	Cl^{36}–Ar^{36} Age, 10^6 years
Aroos	16.6	16.9	23.5	585
Grant	12.4	...	17.9	595
Norfolk	15.0	14.4	20.6	560
Sikhote Alin	6.3	5.7	4.0	260

Comparison of the Ar^{39} and Cl^{36} activity confirms the previous conclusion (Sprenkel, Davis, and Wiig, *Bull. Am. Phys. Soc.*, 1959) that cosmic-ray intensity has been constant to within 10 per cent during the last 100,000 years. One interpretation of the result that the meteorites Grant, Aroos, and Norfolk all have about the same exposure age is that 580 m.y. ago two or more large objects collided in Space. Sikhote Alin, on the other hand, must have been in an object which suffered a collision 260 m.y. ago.

Walter H. Hoecker, Jr. (U. S. Weather Bureau, Washington, D. C.), *The Pressure Field of the Dallas Tornado.* By making use of a tangential wind field around the tornado derived from scaled moving pictures, and of the cyclostrophic wind equation, we have determined pressure surfaces for the tornado. A total pressure drop of 59 millibars was computed at the center of the tornado at ground level. Typical tornado-cloud profiles are shown to be possible with one pressure field when only the moisture content of the air flowing into the tornado changes. Some simple housing construction-strength figures are used to describe the effect of the moving tornado pressure field on airtight and vented structures, for both on-path and near-miss events.

Thomas E. Hoffer (University of Chicago, Ill.), *A Laboratory Investigation of Droplet Freezing Induced by Insoluble Nuclei.* After a brief description of the experimental equipment, the distribution of freezing temperatures of droplets containing insoluble clay and silver iodide nuclei are presented and discussed. The investigation shows that these droplets do not freeze at temperatures as high as would be anticipated from the observations of other investigators who introduced similar nuclei into the cold chamber. The effect of solute concentration on the freezing temperatures of droplets containing insoluble nuclei and soluble salt is described. The soluble salts were found to decrease the freezing temperature in all cases studied. Extrapolations of the data to cloud processes are discussed with particular emphasis on the problems of the introduction of silver iodide particles into the atmosphere and the effectiveness of these particulates in modifying clouds.

A. C. Holland (Baird-Atomic, Inc., Cambridge, Mass.), *The Effects of Atmospheric Refraction on Angles Measured from a Satellite.* The refraction at a satellite is defined as the angle subtended at a satellite by the actual line of sight and the vacuum line of sight from the satellite to a point on the earth. Assuming that the satellite is above the sensible atmosphere and accepting the well-known expression for the astronomical refraction, we derived the equations for the satellite refraction and the 'first-order error coefficients.' Results of computations show that the refractions at the satellite is always less than 2 per cent of the total or astronomical refraction and that its sen tivity to change in the independent variable small. It is also shown that changes in the as nomical refraction have very little effect on refraction at the satellite.

Heinrich D. Holland (Geology Departm Princeton University, Princeton, N. J.), *On Chemical Evolution of the Earth's Atmosphere.* some time after the formation of the earth, atmosphere was almost certainly strongly reduc The pressure of the main atmospheric constitu was probably small: $p_{CH_4} < 6$ atm, $p_{NH_3} \ll 1$ $p_{H_2} < 0.1$ atm, and the oxidizing effect of los hydrogen from the top of the atmosphere probably balanced by the introduction of hi reduced volcanic gases. As early as 2.0 to 2.5 × years ago, hematite, calcite, and dolomite being formed in sediments. At that time hydr and ammonia must have been absent excep disequilibrium amounts, and methane had prob disappeared. Sediments containing uraninite mineral which normally oxidizes rapidly du weathering today, were formed during the s period. Such occurrences suggest that free ox in more than disequilibrium amounts appe more recently than 1.8×10^9 years ago. The of accumulation of free oxygen since then has controlled by the balance of the rate of buri carbon with sediments, the rate of escape of hy gen, and the oxidation of volcanic gases and ments. The composition of volcanic gases app to have changed only slightly during the 1.8×10^9 years, and the rate of accumulatio oxygen has probably been constant or has decreasing somewhat with time. At the begin of the Paleozoic era, 0.6×10^9 years ago, the ox pressure was probably already more than 0.1

Joshua Z. Holland (U. S. Atomic Energy C mission, Washington, D. C.), *Opportunities Obstacles in Atmospheric Research.* Opportun are derived from the richness of atmosp phenomena and their importance to man from rapidly increasing means of acquiring and cessing information. Obstacles include the plexity and interdependence of these phenom the underdevelopment of scientific manpow this field, and the dispersion of interest, effort support among many agencies. Encouraging t are noted in the broad areas of planning, munication, coordination, budget, and manp and in a number of specific activities, but remains to be done.

R. E. Holzer (Institute of Geophysics, Un sity of California, Los Angeles, Calif.), *Thu storms and the Ionosphere.*

George Hopkins, Jr., F. U. Williams, and McCullough (Electrical Engineering Res Laboratory, University of Texas, Austin, *An Investigation of the Surface Distributi*

urth-Current Activity. During December 1960, e initiated an investigation into the correlation tween earth-current micropulsations at sepa- ted stations. The fixed magnetotelluric station aintained by our laboratory at Austin, Texas, as taken as the base station. This installation d a mobile unit utilizing identical equipment nultaneously recorded 150-minute data samples magnetic tape. Both stations measured geo- aphic north-south and east-west components of e currents. Data were recorded from the 0.01- to 5-cps band. The maximum resolution of the uipment was about 10 μv. The mobile unit has erated at distances ranging from five to several ndred miles from Austin, over the central and astal regions of Texas. Data analysis has been nducted with a view toward establishing the atial variation of the horizontal component of e surface electric field, referred to that at the ed station. The particular items investigated ve been the direction of the resultant horizon- l electric field and the relative time phase of its mponents for several selected frequency bands; e co- and quadrature spectra of power density; d the statistical coherency of the remote and se station field components.

Y. Horibe, M. Kobayakawa, L. I. Gordon, and . Craig (Department of Chemistry, Tokyo Metro- litan University, Tokyo, Japan, and Department Earth Sciences, University of California, San iego, Calif.), *Isotopic Composition of Natural ater.* D/H ratios of surface marine waters between ape Town and Showa Base (the Ongul Islands, e base of the Japanese Antarctic Expedition) owed close correlation with temperature and linity. D/H and O^{18}/O^{16} ratios were measured on ow, ice, and melt water from the Ongul Islands. D for snow and ice ranged from −212 to −150 r mil (SMOW) and δO^{18} ranged from −29.4 to -22.0 per mil (SMOW). For the melt water δD was -133 per mil and δO^{18} was −15.1 per mil, indicating at evaporation and/or sublimation occurred to a rge extent. O^{18}/O^{16} ratios of water vapor samples llected from the atmosphere at the Scripps Insti- tion of Oceanography lay between −12 and −17 $[(O^{18}/O^{16})_{rain}/(O^{18}/O^{16})_{vapor\ during\ rain}]$ usually fell be- ween 1.0100 and 1.0112.

Henry G. Houghton (Department of Meteor- ogy, Massachusetts Institute of Technology, mbridge, Mass.), *Plans and Programs for Geo- ysical Research at M.I.T.* The M.I.T. Center r the Earth Sciences will be housed in a striking story building soon to be erected through the nerous gift of Dr. and Mrs. Cecil A. Green. The nter will include the Departments of Meteor- ogy and of Geology and Geophysics. Education d research will be undertaken in meteorology, eanography, geology, geophysics, and geochem- try. Emphasis is being placed on an integrated proach to the earth sciences. Close cooperation ith, and participation of, the staff of the Woods Hole Oceanographic Institution and of other M.I.T. departments has been established and will be extended. A broad program of research is envisaged in which emphasis will be placed on a quantitative approach to the problems of the earth, the oceans, and the atmosphere.

J. T. Houghton (Clarendon Laboratory, Oxford, England) and Walter Hitschfeld (McGill University, Montreal, Canada), *Radiative Transfer in the Lower Stratosphere Caused by the 9.6-Micron Band of Ozone.* Precise numerical calculations of the flux divergence due to narrow regions of the 9.6-micron band of ozone were made using the relative strengths and positions of the spectral lines calculated by Kaplan, Migeotte, and Neven (1956). The absolute line strength was estimated on the basis of Walshaw's (1957) laboratory measurements. Spectral models or the Curtis-Godson approximation were not used, but Lorentz shapes and uniform widths were assumed for all lines. Calculations up to a height of 33 km were made for two ozone ascents of Brewer and Milford (1960). The atmospheric heating rates for the parts of the band so obtained were then combined to estimate the heating rate by the whole band, with results in qualitative agreement with, though nearly 2 times greater than, those of Plass (1956), who had employed a series of spectral models and numerical information based on earlier laboratory data. The effect of the radiative temperature of the base of the ozone layer (whether of ground or cloud top) appears to be great. The radiative heating by ozone in the 10- to 20-km region is about 0.4° per day for a base temperature of 10°C, but it may disappear altogether if cloud is present just below the tropopause. The procedure adopted can be applied to any absorption band and is flexible enough to permit the use of any desired pressure and temperature dependence of the shape, width, and strength of the spectral lines; results from it might serve as a standard against which conclusions reached by approximate methods can be checked.

James Hurley (New York University, New York, N. Y.), *Interaction between the Solar Wind and the Geomagnetic Field.* There is now considerable evidence of the existence of an interaction between the solar wind and the geomagnetic field. The solar wind is a highly ionized plasma stream and as such may well influence the earth's magnetic field. It is this interaction that we have studied. We have limited ourselves to a two-dimensional model to permit an exact solution to be obtained. (This problem has been partially solved independently by J. W. Dungey, Pennsylvania State University, *Scientific Report 135,* 1960, and V. N. Zhigulev and E. A. Romishevskii, *Soviet Phys.–Doklady, 4,* p. 859, 1960.) The plasma wind is assumed to be incident upon an arbitrarily oriented two-dimensional magnetic dipole. We find that the field is compressed by the plasma and is

confined to form a cavity in the plasma wind. The thickness of the boundary layer within which the plasma and field interact is found to be small. We have determined the equations of this boundary surface and the extent to which the field is changed by such confinement.

P. M. Hurley, H. Hughes, W. H. Pinson, and H. W. Fairbairn (Massachusetts Institute of Technology, Cambridge, Mass.), *Argon Diffusion Coefficients in Micas at Low Temperatures Obtained from Alpine Fault Uplift in New Zealand.* Rapid uplift along the Alpine Fault zone in the South Island of New Zealand has exposed ancient mica schists that were at depths up to 9000 ft prior to the fault displacement. K-Ar age measurements on the micas show losses of argon that vary with the depth of burial up to almost complete loss from biotite at a depth of 9000 ft. The rate of loss of argon from the different samples, correlated with their temperatures before the faulting, yields a consistent set of values for the diffusion parameter D/a^2 at low temperatures. In the relationship $D/a^2 = (D_0/a^2) \exp(-E/RT)$ we derive a value for E, excitation energy, of 25 ± 1 kcal/mole, and for $\log D_0/a^2$ of -2 ± 1 sec^{-1} as alone consistent with these observations, with effectively complete retention of argon at surface temperatures, and with the observed diffusion loss at high temperatures. The assumptions involved are that the biotite lost argon by diffusion and not by alteration or weathering, and that the smooth surface represented by the peak elevations over the Alpine belt of interest is truly representative of the original surface before uplift and glaciation. There are strong arguments for the validity of these assumptions. The diffusion losses observed here at about 100°C are vastly greater than those predicted by extrapolation of laboratory measurements made at 600° to 1000°C.

Louis Hurwitz (U. S. Coast and Geodetic Survey, Washington, D. C.), *Tests of Schuster's Method for the Spherical Harmonic Analysis of the Geomagnetic Field.* Studies are in progress at the Coast and Geodetic Survey to determine the feasibility of producing the 1965.0 world magnetic charts by analytical methods. One of the major steps in the preparation of charts would be the analysis of magnetic values that will have been extrapolated to 1965.0. It is expected that the analysis can be reduced to one dealing with irregularly spaced data on a spherical surface. If equal weighting of data can be used, an iterative trigonometric analysis may overcome the irregular spacing difficulty. The feasibility of such an analysis is now being tested. Other methods under consideration are, first, spherical harmonic analysis; second, analysis by Taylor series; third, analysis by fitting the field of a set of eccentric dipoles to the data. The eccentric dipoles would not necessarily be axial dipoles.

T. N. Irvine (McMaster University, Hamilton, Ont., Canada), *Ultramafic Complex at Duke Island, Southeastern Alaska.* The Duke Island ultramafic complex crops out in two areas totaling square miles. It shows a crude concentric zon having a peripheral rim of hornblende pyroxe enclosing units classified as olivine pyroxe peridotite, and dunite. Pegmatite of hornbl and plagioclase ($\sim An_{95}$) is closely associated, older gabbroic rocks surround and have been tered by the complex. A remarkable gravitati layering occurs intermittently in the olivine-b ing rocks through a possible thickness of 2 m Individual layers are commonly graded accor to grain size, having coarse pyroxene at their and finer pyroxene and olivine in their u parts. The grading is a reliable criterion of where layering is deformed or disturbed. Cou parts of sedimentary structures, such as c bedding, slide conglomerates, and slump st tures in the layering, suggest the action of curr in the magma chamber. A marked struct break, analogous to an angular unconformity a basal conglomerate, occurs within the lay sequence and is attributed to an addition magma to the chamber. The relation of the la ing to the zonal structure within the complex to the gabbroic country rocks suggest that ultramafic rocks have solidified from an ultram magma.

H. M. Iyer (Institute of Geophysics and Pl tary Physics, University of California, La J Calif.), *Computation of Microseismic Noise in Deep Ocean.* Under the assumption that mi seisms are first-mode Rayleigh waves, their ref tion at the continental margin near La Jolla the west coast of the United States was stu The principle of dispersion of Rayleigh wave an isotropic elastic half-space overlain by a li layer was used to compute the velocities of mi seisms for different ocean depths. Refraction grams are presented for Rayleigh waves at sec, 5 sec, 7.5 sec, and 10 sec. It was assu that the waves were radiating out into the o from La Jolla. The ratio of the refracted en to the unrefracted (ideal case) energy was c puted for various directions. For the deep o (1200 ft) this ratio was called the 'transfer f tion of the continental shelf.' It was found tha the case under discussion the continental acted as a low-pass filter with a sharp cutoff proaching about 2 sec. By use of the recipr principle the effect was computed when m seisms approached from deep ocean to land. F available average earth-noise data a rough putation was made of the microseismic noise li to be observed if a seismograph was establi in the deep ocean. The noise was found t many times higher than on land in the s microseism range falling off to the normal background at long periods (about 20 sec).

Imre G. Izsak and Yoshihide Kozai (Smith

Atsrophysical Observatory, Cambridge, Mass.), *ipotential Surfaces of the Earth as Obtained Satellite Motions.* New evidence is presented the existence of the odd harmonics in the 's potential and for the feasibility of deter- ng tesseral harmonics from the motion of lites. The effect of these harmonics, and of even harmonics as well, on satellite orbits is e different from that on gravity measurements. harmonics are easier to separate because the re of their effects is different, and they are r to measure because their effect is amplified. , the geographical distribution of the satellite- ving stations plays a much less important than the distribution of gravity measurements. more extended observational material and oved methods, a fresh determination was e of the coefficients of the third and fifth l harmonics and of the second sectorial har- ic. In connection with the geometrical inter- tion of these terms, it is emphasized again at the present state of the art satellite mo- reveal the gravitational potential of the and not its shape.

MAN K. C. JOHNS (Baird-Atomic, Inc., Cam- ge, Mass.), *Theoretical Study on Probability multaneous Satellite Observations.* In certain cts simultaneous line-of-sight visibility be- n a satellite and a number of stations is neces- for example, for position determination of ellite without orbit determination or for re- g messages between two widely separated autually visible stations by means of com- ations satellites. Since both the refraction absorption of signals increase with the zenith nce and hence cause deteriorations of the ac- y and reliability of information obtained, it essary that the target be observed within a in zenith distance. This study defines the lite visibility condition and derives the prob- y function of simultaneous observations of ellite from a number of stations. Numerical ples are given.

UCE M. JOHNSON, JR. (Washington State Uni- ty, Pullman, Wash.), *An Application of the 650 Computer to the Dimensionless Unit ograph Method of Deriving Unit Hydro- s.* An application of the IBM 650 computer e Dimensionless Unit Hydrograph method iving unit hydrographs from storm hydro- and rainfall data is presented. The emphasis the adaptability of the digital computer to outine repetitive manipulating of data and ating necessary in this trial-and-error ap- h. By using the dimensionless form it is pos- to determine the best fitting unit hydro- for a given basin with the rainfall and hydrograph for a known storm. The For- t program used in this determination is pre- d and explained in general terms. The key on of the program, in which the trial storm hydrograph is calculated and compared with the given storm hydrograph, is explained in detail and serves to point out the adaptability of the computer to this method. Also, this method is compared with the hand solution method.

DAVID S. JOHNSON (U. S. Weather Bureau, Washington, D. C.), *Meteorological Satellite Research and Applications.* The advent of satellites has opened new vistas for meteorology by providing observations on a global basis and measurements not available previously. The use of these data in research and operational experiments is reviewed. Future possibilities for meteorological research and applications using satellite data are also discussed.

FRANCIS S. JOHNSON (Lockheed Aircraft Corporation, Missiles and Space Division, Palo Alto, Calif.), *Particle Energy in the Telluric Hydrogen Corona.* The telluric hydrogen corona is a cloud of neutral hydrogen atoms surrounding the earth. Escape to space of the more energetic particles in this cloud modifies the velocity distribution, which would otherwise be Maxwellian. The average particle energy is lowered by the escape; an effective temperature T_e, such that $\frac{3}{2}kT_e$ equals the average particle energy, can be defined. The effective temperature falls with distance from the earth. Whether the temperature at the base of the exosphere is 1500°K, which is a probable figure near the maximum of the sunspot cycle, or 1000°K, which is a probable figure near the minimum of the sunspot cycle, the effective temperature in the telluric hydrogen corona at a geocentric distance of 5 earth radii is about 500°K.

H. M. JOHNSON (University of Hawaii, Honolulu, Hawaii), *Tropical and Subtropical Atmospheric Systems Observed by Tiros I.* Tiros I pictures of tropical and subtropical systems ranging from very large to mesoscale or smaller are presented. The following are discussed: (1) characteristics of selected types of systems, (2) the significance of these characteristics, (3) relationships among systems and subsystems, (4) uniqueness of systems and recurrence of types, (5) degree of nonrandomness and of apparent randomness, (6) comparison of cloud patterns observed from the satellite with those observed from the ground, and (7) required model refinements. The systems selected for illustration include subtropical cyclones, tropical bands, tropical patches, tropical complex patterns, cloudless systems, and small-scale oriented lines and groups.

H. FREEBORN JOHNSTON (Meteorology Division, National Bureau of Standards, Washington, D. C.), *Thesaurus of Annual Magnetic Values at World Geomagnetic Observatories.* Many very recent annual values have been kindly supplied by the officers in charge of geomagnetic observatories everywhere. Included are values for the period before,

during, and after World War II. Preliminary values are also given for several of the temporary observatories that were occupied during the International Geophysical Year.

Gerald L. Joyner (GeoSciences Division, Texas Instruments, Inc., Dallas, Tex.) and Peter Dehlinger (Department of Geology and Geophysics, Texas A and M College, College Station, Tex.), *Surface-Ship Gravity Measurements in the Gulf of Mexico made Aboard the Hidalgo in June 1958.* Free-air anomalies were calculated from gravity measurements made with a LaCoste-Romberg meter aboard the *Hidalgo* during an IGY cruise in June 1958. The data are presented along two profiles, one in the northeastern Gulf of Mexico and one in the Florida Straits. Time did not permit measurement of the absolute accuracy of the gravity meter; however, comparison of the data with selected classified measurements shows satisfactory agreement. Meter drift is demonstrated to be negligible on the basis of comparison with land base stations. The free-air anomalies appear to follow essentially the subsurface topography. The geologic implications of the data are discussed.

Darrell L. Judge and Paul J. Coleman, Jr. (Space Technology Laboratories, Inc., Los Angeles, Calif.), *Betatron Acceleration of Geomagnetically Trapped Particles.* Detailed analysis of the data from Explorer VI magnetometer and scintillation detector has indicated that these data are correlated in the region of 5 to 8 earth radii. Data have been analyzed which were obtained during the magnetically active periods of August 9 and 18, 1959. It has been observed that fluctuations in the magnitude of the magnetic field are accompanied by in-phase fluctuations of the charged-particle count rate. These correlation data, together with the counter characteristics, make it possible to compute an energy spectrum for charged particles in the outer radiation zone which have energies above the counter threshold. An estimate of the spectrum of electrons with energies greater than 500 kev is presented.

Paul R. Julian (High Altitude Observatory, University of Colorado, Boulder, Colo.), *A Study of Hydrometeorological Time Series.* Recent applications of statistical theory to problems involving a storage reservoir have shown promise of becoming useful and instructive methods. The purpose of this presentation is to examine the assumption made by the afore-mentioned theory of the randomness of the inputs to the storage system, that is, of the stream-runoff amounts. Previous work by various investigators has shown that statistics derived from time series of stream-flow measurements indicate that stream-flow data are not random in time. In this paper, the randomness of point precipitation and stream-flow series are examined by the use of variance spectra. Associated problems of nonstationarity, filtering interval, and confidence levels are briefly cussed. Seasonal precipitation data from a variety of locations are shown, all of which cate that with presently available data such s are indistinguishable from a series of ran numbers. Stream-flow records in the form water-year and annual totals are also exami These show a wide range of departure from domness, apparently depending upon the de of natural regulation and the efficiency of basin runoff process. Variations in the time s with periods longer than the length of record examined by means of special filtering techniq Some conclusions concerning the runoff pr can tentatively be drawn from this analysis the runoff data consistently show more vari associated with these very long oscillations do the precipitation series.

Christian E. Junge, Charles W. Chag and James E. Manson (Geophysics Rese Directorate, Air Force Cambridge Research L ratories, Bedford, Mass.), *A World-Wide St spheric Aerosol Layer.* An aerosol layer has identified in an aerosol collection program which stratospheric balloons and aircraft used. Measurements of horizontal extension vertical distribution indicate that this lay a world-wide phenomenon, displaying little ation with time and latitude. The particles in layer range in size between 0.1 and 2 μ, are v soluble, and contain sulfur as the predom constituent. It is most likely that they are fo within the stratosphere.

S.-K. Kao (Department of Meteorology, versity of Utah, Salt Lake City, Utah), *Tr tories and Diffusion of Particles in a Long At spheric Wave.* Trajectories and diffusion of par in a long atmospheric wave are examined analysis is made of the trajectory of a cons pressure balloon in a long atmospheric wa the 300-mb level, and computations are mad the first and second approximations of the jectory from the solution of the nonlinear tem of the Lagrangian equations for a parti a long wave in a rotating fluid. The factors affect the accuracy of the computed trajec are examined. The computed and the obs trajectories are compared.

M. Kawano and M. H. Wilkening (New ico Institute of Mining and Technology, So N. Mex.), *Some Characteristics of Radon-D ter Ions in the Atmosphere.* The sharp dec in the number of radon-daughter ions obs when a thunderstorm passes overhead can b plained by assuming that these ions are rem by the strong negative field of the storm. In that this phenomenon may be better under the mobility distribution of the radon-dau positive ions has been determined and their tion to the total positive small-ion content

sphere has been studied. The negative-wire ment used to collect the ions was normally sted so that all positive ions having a mobil- reater than 0.3 cm^2 sec^{-1} $volt^{-1}$ were captured. ough some ions with mobility less than this l be collected, their contribution was small. number of ions with mobilities greater than m^2 sec^{-1} $volt^{-1}$ was small, being less than a per cent of the total. A large part of them concentrated in the range from 0.5 to 1.5 sec^{-1} $volt^{-1}$. A good correlation between the n-daughter ion content and the total positive l-ion content as estimated from the con- ivity value of the atmosphere was obtained ir-weather days. The concentration of radon- hter ions can be estimated from the negative- data for those cases in which equilibrium ex- between radon and its daughter products. An oximate value of 10^{-4} ion/cm^3 was obtained.

HN M. KELSO (Space Technology Labora- s, Los Angeles, Calif.), PAUL J. COLEMAN, JR. ional Aeronautics and Space Administration, ington, D. C.), and ROBERT R. MORGAN (Mar- Laboratories, Los Angeles, Calif.), *A Mag- Coil Facility for Space-Vehicle Testing and ration.* A magnetic coil facility has been con- ted at Malibu, California, by Space Technol- Laboratories for use in the Able-5 lunar probe ram carried out for the National Aeronautics Space Administration. The facility will also sed in future space programs and for various rch problems. The central feature of the fa- is a triaxial set of magnetic coils using four per axis in substantially the ratios suggested anselau in 1929 and Braubeck in 1934. The inal radius of the two larger coils on each is 21 ft, and the nominal radius of the two ler coils is 16 ft (the actual sizes of the coils different on the three axes to permit the e coils to be fitted together while preserving roper ratios along each axis). The coil array pported by a structure of aluminum tubing. tolerance in most major dimensions, includ- departure from parallelism and centering on desired axis, was held to ± 0.1 inch. The coil is housed in a nonmagnetic building. A non- netic fixture within the coils supports the e vehicle or test instruments. The control ment is located in a van several hundred rom the coils. A small set of triaxial Helm- coils is used with a proton or rubidium mag- eter to furnish a reference to compensate hanges in the geomagnetic field.

V. KEPPEL (Agricultural Research Service, Department of Agriculture, Tucson, Ariz.), *ecord Storm Event on the Alamogordo Creek rimental Watershed.* A description is given thunderstorm of unusually high intensity h occurred on the Alamogordo Creek experi- al watershed in New Mexico on June 5, 1960. 30 minutes intensities equaled or exceeded any published for first-order weather stations in the United States. At the storm center, 2.03 inches fell in 5 minutes, 2.50 inches in 10 minutes, 3.09 inches in 15 minutes, 3.62 inches in 30 minutes, and 3.93 inches in 60 minutes. These values greatly exceeded the 100-year return-period values for the nearest first-order Weather Bureau stations at Roswell, New Mexico, and Amarillo, Texas. Depth-area relationships for the storm, calculated from the catch of the 55 recording rain gages on the 67-square-mile experimental area, showed that 30 square miles received 2.5 inches or more of precipitation and over 50 square miles received 2.0 inches or more. These values exceed anything else recorded during convective summer thunderstorms on semiarid watersheds in the southwestern United States. Rainfall on the study area varied from a low of 0.15 inch to 4.09 inches at the storm center.

JOHN W. KERN (Planetary Sciences Department, Rand Corporation, Santa Monica, Calif.), *Geomagnetic Field Distortion by Solar Streams as a Mechanism for Production of Polar Auroras and Electrojets.* A new theory is presented for polar auroras and electrojets. The theory is based on adiabatic trapping of particles in the geomagnetic field distorted by a solar stream. The observed locations of auroras and polar electrojets, as well as the observed morphology and drift motion of the aurora, are predicted qualitatively. Interesting features are the predicted charge separation in geomagnetically trapped radiation, mirror-point lowering as a function of time and particle kinetic energy, and the development of fine structure in the trapped radiation such as has been inferred from satellite and probe counting rates.

EDWIN KESSLER, III (Geophysics Research Directorate, Air Force Cambridge Research Laboratories, Bedford, Mass.), *The Condensed Water Precipitated during Convection.* A continuity equation for water substance is solved for time-dependent distributions of vapor and condensate, where the wind fields are representative of banded and radially symmetric convective activity, where initial distributions of water vapor are of several types, and where the ratio of condensate falling speed to maximum updraft varies from 0 to 4. Condensate which by virtue of the air circulation descends into air that is not saturated, is assumed to evaporate immediately. The fraction of condensed water that evaporates during overturning of air within the cell, and that therefore does not reach the ground as precipitation, is sensitive to the initial distribution of water vapor. In an initially saturated model atmosphere, precipitation efficiencies vary from nearly 100 to 35 per cent, decreasing as the updraft/falling speed ratio increases. In an initially subsaturated atmosphere, all the condensed moisture may evaporate before reaching the ground, especially when the lower

levels are comparatively dry. Higher precipitation efficiencies characterize those wind distributions in which updrafts and compensating downdrafts are separated by great distances and in which the downdrafts are spread over a wider area and are therefore comparatively weak.

Blair Kinsman (Chesapeake Bay Institute, Johns Hopkins University, Baltimore, Md.), *Some Evidence on the Effect of Nonlinearity on the Position of the Equilibrium Range in Wind-Wave Spectra.* Measurements of spectra carried out at short fetches and low wind speeds suggest that nonlinear interactions with preferred frequencies may be present. If this is the case, the range of frequencies immediately above the energy peak cannot be an equilibrium range describable by a single unique power law.

C. Kisslinger, E. J. Mateker, Jr., and T. V. McEvilly (Department of Geophysics, Saint Louis University, Saint Louis, Mo.), *SH Motion from Explosions in Soil.* The generation of prominent tangential horizontal (*SH*) motion by an explosive source is not expected on the basis of simple theory. Nevertheless, such motion is observed in almost all cases from both chemical and nuclear explosions. A series of experiments designed to clarify the factors that are significant in producing this motion has been carried out. Useful data have been obtained by surrounding the shot with instruments at equal distances. The results for an unconsolidated medium are presented. The seismograms, recorded at small distances, clearly indicate the asymmetrical pattern of radiation of the *SH* motion in the source region, as contrasted with the symmetrical pattern for the radial and vertical motion. This radiation pattern is the most useful indicator of the nature of the generating mechanism. The combined effect of charge size and depth determine which of two wave forms will appear. The most prominent *SH* motion is in the form of Love waves, but this motion is much more pronounced for shallow shots that produce cratering, or at least surface cracking, than for completely contained shots. An examination of theoretical radiation patterns indicates that crack formation may contribute significantly to the generation of *SH* motion.

N. Kitagawa and M. Brook (New Mexico Institute of Mining and Technology, Socorro, N. Mex.), *Electron Disappearance Processes in the Lightning Channel.* Both Hewitt and Atlas have assumed the electron-ion recombination process in estimating the electron density in the lightning channel. Schonland and Hill, on the other hand, suggested that electron attachment to oxygen is far more effective than electron-ion recombination. From simultaneous photographic and electric-field-change records of cloud-to-ground discharges, it has become possible to estimate the final electron density (i.e., the density of electrons in the channel immediately prior to the succe stroke) as well as the initial electron dens the return stroke channel. The investigati short interstroke intervals reveals that the density of the order of 10^{14} electrons/cm^3 to 10 electrons/cm^3 in 10 msec on the averag in the extreme case, it decays to 10^2 electro in 3 msec. It is shown that the electron-i combination process would take 10^4 secon reach this final density of 10^2 electron whereas the attachment process can redu electron population to 10^2 electrons/cm^3 i seconds. It is therefore concluded that el attachment to oxygen is the dominant p which accounts for the rapid disappearan electrons during the interstroke intervals.

William H. Klein, Billy M. Lewis Curtis W. Crockett (U. S. Weather B Washington, D. C.), *The Interrelation be Daily and Mean Components in Objective perature Forecasts.* Multiple regression equ for predicting 5-day mean temperatures i United States were originally computed fr day mean values of temperature at 700-mb and at the surface, but they gave better operationally when applied to 36-hour fo of height and temperature. Since rederi from daily instead of mean data yielded results, it appears that use of daily valu input in equations computed from mean produces the best mean forecast. In an eff obtain daily temperature forecasts for s days in advance, the accuracy of the 5-day objective temperature predictions was me separately on each of the individual days forecast period. Although perfect mean fo would have been most accurate on the midd of the period, the objective prognoses at maximum accuracy a day or two earlier. parison is made with chance, persistence, tology, and daily predictions prepared at forecast centers. The objective forecasts we perior to these controls on each day of the period, with maximum difference on the thir It is concluded that the objective metho yield operationally useful 48- to 72-hour fo of daily temperature.

D. A. Kniffen and J. E. Naugle (N Aeronautics and Space Administration, G Space Flight Center, Greenbelt, Md.), *Fluxes in the Inner Van Allen Belt.* A cyli stack of G-5 nuclear emulsions has been fl the payload section of a four-stage research into the northern edge of the inner Van belt. The emulsion stack was shielded in tungsten casette and was then exposed ambient radiation by rotation behind a win the wall of the casette covered with a .04 aluminum shield. In this manner, for th time, the flux and energy spectrum was me as a function of position along the trajectory

ket. Eight points along the rocket trajectory e been selected for analysis and preliminary lts are presented for three of these points. rocket was fired on a true heading of 193° n Pt. Arguello, California; therefore, all these nts lie on the same magnetic meridian. The gee point (1884 km, 25.19°N, 123.48°W) and two 1600-km points on the ascending and de- ding portions of the trajectory have been lied. A preliminary analysis indicates that the pe of the differential energy spectrum changes n position in the belt. Also, at comparable en- es and positions in the belt, the flux and the pe of the energy spectrum is in qualitative ement with previous measurements with lsions and counters. The significance and pos- e explanations of the changes in the spectrum discussed.

ENNETH R. KNOERR (U. S. Forest Service, umbus, Ohio), *Exponential Depletion of Soil isture at Forest Sites in the Sierra Nevada.* r general models have been proposed in the ature for the relation between rate of evapo- spiration and amount of available soil mois- Because of gaps in our knowledge of the esses of water movement through the soil plant into the atmosphere, the models have n based on empirical studies. Recent measure- ts of soil moisture at 21 sites in the Sierra ada, California, have been used in the evalu- n of these models under a wide variety of st site conditions. Soil moisture was measured odically at five points at each site during the mers of 1958 and 1959. These measurements red the range of soil moisture from field ca- ty to nearly the wilting point. Soil moisture etion was little affected by recharge from pre- ation during the characteristically dry sum- s. The relation between evapotranspiration soil moisture was determined from the aver- ate of soil moisture change between measure- ts versus the mean soil moisture content for eriod. At all 21 sites the rate of evapotrans- ion was found to have a direct linear relation he amount of available soil moisture. This is model for exponential depletion of soil mois- . In addition, an evaluation was made of the moisture data of other authors, where deple- was not confounded by frequent recharge precipitation. In most cases the data fitted model of exponential depletion, suggesting this model may have fairly wide application il moisture depletion.

A. KOHOUT (U. S. Geological Survey, Miami, *Fluctuations of Ground-Water Levels ed by Dispersion of Salts.* Certain wells tap- the zone of diffusion between fresh and salt r in the Miami, Florida, area showed anoma- residual water-level drawdowns after being ped. Graphs comparing fluctuations of water ls and chloride contents show that the anoma- lies are caused by dispersion-motivated changes in the density of the water in the casing. Dispersion produces fluctuations of water levels under natural conditions as well as after pumping. In an area where true fluctuation of the water table due to normal recharge and discharge amounted to about 3 feet, dispersion produced an observed water-level fluctuation of 0.7 foot. The fluctuations occur so subtly that erroneous conclusions concerning changes in ground-water storage are possible unless careful interpretation is made.

A. F. KRUEGER, JR., and SIGMUND FRITZ (U. S. Weather Bureau, Washington, D. C.), *Cellular Cloud Patterns Revealed by Tiros I.* Some Tiros I photographs of cellular cloud patterns are related to conventional meteorological observations. These cellular patterns occurred at the top of a convective layer that was heated from below and through which there was little vertical variation in wind velocity.

JOHN T. KUO, JAMES N. BRUNE, and MAURICE W. MAJOR (Lamont Geological Observatory, Columbia University, Palisades, N. Y.), *Rayleigh Wave Dispersion in the Pacific Ocean for Periods of 20 to 140 Seconds.* Rayleigh wave trains from the earthquakes of the circum-Pacific belt recorded at Suva, Fiji, in 1958–1960 exhibit the long periods associated with the inverse branch of dispersion. Group velocities have been determined for these earthquakes. Phase velocities have been determined by assuming a constant of integration which is independent of period. This constant was deduced from previous observations of phase velocities for mantle Rayleigh waves. Except across the Melanesia–New Zealand region, dispersion curves for the paths of Rayleigh waves throughout the Pacific ocean are found to be fairly uniform and in agreement with Dorman's theoretical curve 8099, as corrected for the earth's curvature. Both phase and group velocities are comparatively lower for the paths across the Melanesia–New Zealand region. The results indicate a normal oceanic crust and a low-velocity channel of shallow upper boundary in the upper mantle beneath the Pacific ocean and a tectonic complex of thicker crust in the Melanesia–New Zealand region of the southwestern Pacific ocean.

EUGENE C. LAFOND (U. S. Navy Electronics Laboratory, San Diego, Calif.), *Convergences and Divergences in the Near-Surface Layers of the Sea.* Water circulation both at the sea surface and in the thermocline was investigated by dye methods, measurement of thermal changes, and direct observations with underwater television. Zones of both divergence and convergence were commonly found in the surface layers of the sea off San Diego, California. Zones of convergences appeared as lines and patches and were frequently detectable through the concentration of scum on the surface. Divergences were less detectable at the sea

surface, except when the thermocline was near the surface and a rough area formed. The convergences usually resulted from two flows directed nearly toward each other but deflected right or left when the surface water accumulated in the sinking zone. The maximum vertical motion occurred in the thermocline where speeds as great as 15 ft/min were observed. The zones of convergences and divergences were the result of internal wave motion in the thermocline. Other zones of vertical motion were the result of two water masses impinging on each other, one overriding the other, or of the creation of horizontal eddies. These vertical circulations are important for the distribution of the physical, chemical, and biological properties of the sea.

Eugene C. LaFond (U. S. Navy Electronics Laboratory, San Diego, Calif.), *Oceanography in Southeast Asia.* Oceanographic studies are being conducted by the southeast Asian nations of Pakistan, India, Thailand, Indonesia, and South Vietnam. In these countries the emphasis is placed on oceanographic-biological research directed toward the development of marine resources for food. In that part of the world, a northeast monsoon wind system blows during nearly half of the year, and during the remaining time a southwest monsoon blows. Such winds develop horizontal and vertical currents in the sea, and these in turn bring plant-nutrient chemicals up to the euphotic zone. These areas of upwelling together with water mass boundaries are places of high organic production and are favorable for the production of fish food. Summer upwelling zones of high organic production include the western Arabian Sea, western Bay of Bengal, western Gulf of Thailand, and off shore South Vietnam. The winter upwelling areas are off the western coast of India, the eastern side of the Bay of Bengal, and the eastern Gulf of Thailand. These oceanographic studies are a scientific approach directed toward increasing the essential food supply from the sea for overpopulated and undernourished southeast Asia.

Walter B. Langbein (U. S. Geological Survey, Washington, D. C.), *Salinity of Closed Basins.*

L. K. Lau, W. J. Kaufman, and D. K. Todd (University of California, Berkeley, Calif.), *Dispersion in Radial Flow through Porous Media.* A flow pattern was established in a two-dimensional field by a steady radial laminar flow injected through a small finite circular source. Displacing water was introduced instantaneously and continuously. The resulting dispersion can be described mathematically by a boundary-valued, second-order, nonlinear partial differential equation. As no analytic solution could be found for the equation, numerical methods are necessary. However, without resorting to computers the methods are lengthy and tedious. For practical application an approximate solution was devel which is shown to yield excellent results fo conditions studied. Experiments were condu in a 45° circular sand sector having a 36 radius and a 3-inch thickness. The Ottawa used had grain sizes from 0.250 to 0.833 mm. tracer was chloride ion and was detecte chemical titration. Experimental results sh a decrease of the medium dispersion con with radial distance. This is attributed to e inherent in the sampling technique. The con was found to be independent of velocity.

Alan B. Lees (Electronic Specialties Com Los Angeles, Calif.) and Bruce C. Murray vision of Geological Sciences, California Inst of Technology, Pasadena, Calif.), *Special physical Applications of Precise Satellite Vel Observations.* An expression is developed for lite motion in an arbitrarily asymmetric gra tional field and in a near-circular orbit. Thi pression permits precise velocity observatio be used directly in the investigation of terre air drag and tesseral harmonics. The sensi of the method is analyzed in terms of obs tional and other sources of error.

Billy M. Lewis (U. S. Weather Bureau, W ington, D. C.), *Further Technological Advan Automating Extended and Long-Range Fore ing Procedures.* Recent installation of a new, capacity, high-speed data-processing unit a electronic map-drawing machine has result a marked speedup in the production of charts used in operational procedures o Weather Bureau's Extended Forecast Section swifter preparation of these principal tools to earlier distribution of forecasts to field ce Some further improvements will follow on t stallation of a new medium-capacity compu

W. F. Libby (University of California, Lo geles, Calif.), *Tritium Geophysics.* Further of the tritium content of natural waters has the following results: (1) The relative s spheric residence times for molecules and particles are the same. (2) The ratio of triti strontium 90 produced in the Russian O 1958 tests was approximately as expected bomb design considerations. (3) Evidence o upwelling areas in the sea along the Cali coast has been found in samples furnish Professor Emery. (4) A nearly continuous of the tritium contents of the rains and s waters over the world in the past can n pieced together. With this background it i possible to undertake detailed hydrological inations in local areas. Several samples of logical applications are given. The rate of t of ground water into the oceans can be me by using the bomb-produced tritium, which much richer in the ground waters than oceans.

MES P. LODGE (Robert A. Taft Sanitary Engering Center, Cincinnati, Ohio), Chairman, *d Table Discussion on Continental Hazes.* ough observations have been made for cens of apparently natural atmospheric turbidity land, virtually nothing is known about the istry of this material. Went has suggested it results in part from the photochemical ation of terpenes and other plant-derived rs. Goetz has confirmed that at least portions is material are volatile. The present state of nowledge is discussed by a group of workers c field to try to define the experiments necesto understand the chemistry of hazes.

RALD R. MACCARTHY (University of North lina, Chapel Hill, N. C.), *Earthquakes of the rn United States.* No general catalog of the quakes of the eastern United States has been shed since Brigham's paper in 1878, although al state lists have been issued and most of mportant ones are discussed in 'Earthquake ry of the United States' (1956 edition) publ by the U. S. Coast and Geodetic Survey. for such a comprehensive list are now being ted by the writer. As far as possible, only al sources are being consulted—contemporewspapers and other periodicals, diaries, colns of letters, town, county, and state his-, and the like. So far more than 650 separate quakes are listed in our file. These entries, t for those concerning Maine and Virginia, de only those shocks not previously noted y generally accessible listing and those al- listed for which essentially new information ome to hand. All known shocks felt in Maine n Virginia have been included, whether so or not. A preliminary check of the data dy on hand indicates that considerable re- of the published lists is needed. Many important shocks are omitted from the and there are several serious errors in dates. me cases the same shock has been listed under different dates. Further data are being ted.

MES E. MCDONALD (University of Arizona, n, Ariz.), *Role of Natural Silicaceous Dusts Nucleation.* Results are presented of a study e ice-nucleating characteristics of a series of 600 samples of topsoil dusts collected over an mbracing about fifteen western states. A set mparison results for soil samples from several in the humid Southeast are summarized as of a comparison of relative importance of l-region kaolinites and arid-region montlonites as sources of the world-wide backd population of ice nuclei activating near C.

MES E. MCDONALD (University of Arizona, n, Ariz.), *An Analysis of Fallout Hazards ICBM Sites Located Upwind of Cities.* Civil defense hazards being created by emplacement of ICBM launching sites upwind rather than downwind of a number of population centers are examined quantitatively. Three years' fallout-wind (UF) data are summarized for a number of such ICBM-site areas and estimates are made of the probability of lethal-range dosages due to local fallout from enemy surface-burst megaton weapons in event of nuclear attack. Upwind siting of fixed-base ICBM's will be shown to have exceedingly serious civil defense implications.

J. ROGER MCHENRY and LESLIE L. MCDOWELL (Agricultural Research Service, U. S. Department of Agriculture, Oxford, Miss.), *The Use of Radioactive Tracers in Sedimentation Research.* The transport of sediment is being investigated currently with radioisotopes used to 'tag' individual sand particles. Scandium 46, a γ emitter with an 85-day half-life, has been employed. The techniques developed in tagging sand particles and the resistance of the tagged sand grain to abrasion and leaching are discussed. The method of tagging developed has allowed the experimenter to vary the specific activity of the sand particle. Individual sand particles, about 0.4 to 0.5 mm in diameter, have been prepared with an activity of 2 mr/hr with no changes in the physical properties of the sand particles. The attenuation of the scandium 46 γ emissions in air, water, and sand has been evaluated differentially and integrally with a γ-scintillation spectrometer. The use of a γ-scintillation technique has proved satisfactory for laboratory studies, including transport studies in hydraulic flumes. Preliminary field studies indicate that the prepared sand particles perform satisfactorily, and plans for extensive field testing are discussed.

CARL E. MCILWAIN (Department of Physics and Astronomy, State University of Iowa, Iowa City, Iowa), *Application of the Adiabatic Invariants to the Interpretation of Trapped Particle Fluxes in the Earth's Magnetic Field.* It is shown that a parameter L can be defined which has all the desirable properties of the integral invariant I, but which is also nearly constant along lines of force in the earth's magnetic field. It is also shown that the use of a coordinate system consisting of L and the scalar value of the magnetic field B yields a high degree of order in the observed inner zone intensities and substantially aids in the attempts to understand the outer-zone intensities.

D. P. MCINTYRE (Meteorological Service of Canada, Toronto, Ont., Canada), *Meteorological Research in Canada.*

LESTER MACHTA (U. S. Weather Bureau, Washington, D. C.), *Meteorological Interpretations of Tritium Measurements.* The interpretation of ground-level tritium measurements must include

consideration of its three sources. The first is natural cosmic-ray production located mainly in the upper troposphere. The second source is the nuclear test injections, which initially may have been in both the troposphere and stratosphere but are now located only in the stratosphere. The third source is the leaks from atomic energy installations at ground level. The behavior of the atmosphere in transporting and diluting these sources must also be considered. The dilution is primarily controlled by mixing of tritium water with the almost 'dead' ocean water. The importance of continental versus maritime sampling locations is emphasized. A comparison of tritium water concentration with deuterium water concentration is discussed. Examples of the usefulness of tritium in atmospheric studies are illustrated; however, the limitations of tritium observations, because of possible ambiguity in their sources, will also be noted.

J. M. Malville (High Altitude Observatory, University of Colorado, Boulder, Colo.) and G. E. Moreton (Lockheed Solar Observatory, Lockheed Aircraft Corp., Burbank, Calif.), *The Association of the Explosive Phase of Flares with Type III Radio Bursts.* H_α cinematography with high time-resolution reveals some flares with a distinct pre-maximum intensity phase at which time the brightness increases rapidly and the flare borders expand at velocities of several hundred kilometers per second. Such explosive flares are sometimes accompanied by optical disk phenomena indicating ejection of disturbances with velocities up to 2500 km/sec and are closely correlated with intense type III (fast drift) radio bursts. These flares share a characteristic described earlier by Ellison and termed *flash phase:* a time following the initial brightening at which the intensity rises steeply to a maximum. The possibility that a specific phase in the development of a flare could be related to type III emission was tested by a detailed comparison of flares recorded at six frames per minute at Lockheed and bursts detected with a sweep-frequency interferometer at Boulder. During the period August 1959 through January 1961, 37 flares (mostly of subflare importance) were found which had both well-defined flash phases and unambiguous type III bursts occurring between the beginning and end of the flare. 68.4 per cent of the bursts appeared during the interval from 60 sec before onset of the flash phase to 30 sec after. By contrast, the corresponding intervals around the beginning and maximum of the flares included, respectively, 27.8 and 16.7 per cent. Within the interval ± 2 minutes of the flash phase 97.4 per cent of the bursts occurred.

Uri Mané (Meteorological Service, Tel-Aviv, Israel), *Evaporation from a Class A Pan as Indicator of the Yearly Variation in Evaporation from Larger Reservoirs.* Daily comparative observations of evaporation from a 12-ft pan and a class A pan at Lod Airport for a 3-year period summarized. The yearly ratio (evaporation pan/evaporation class A pan) was found similar to that found elsewhere. The yearly tion of the ratio suggests its possible depen upon the continental (or maritime) nature c climate. Simultaneous evaporation measure from class A pans and 12-ft pans at base sta are recommended as a means of determinin monthly values of reservoir evaporation.

Nicholas Manos (Department of Health, cation and Welfare, Washington, D. C.), *We Statistics, and Health–An Index of Air Poll and Its Relation to Health.* The cities in country can be ranked according to an index pollution based on general sources of air poll such as home heating, automobiles, and ind This has been done in many different way shifting the relative emphasis given to the va sources of air pollution. This index, in its va forms, has been correlated with mortality various causes to determine which forms o index correlate with which causes of death findings of the study indicate that four caus death have consistently high positive correla with the various indexes of air pollution malignant neoplasm of esophagus and ston (2) malignant neoplasm of the trachea, bron and lung; (3) arterio-sclerotic heart disease cluding coronary disease; (4) chronic endoca not specified as rheumatic, and other myoca degeneration. The purpose of this paper is to how weather factors can be incorporated int next steps of this study.

Wm. Markowitz and R. G. Hall (U. S. Observatory, Washington, D. C.), *Speed of tion of the Earth and Solar Activity.* The of solar activity on the speed of rotation o earth is discussed. Universal time based o rotation of the earth is obtained from obs tions made with photographic zenith tubes U. S. Naval Observatory at Washington, D and Richmond, Florida. This is compared the system of atomic time, A. 1, derived b Naval Observatory, for the interval 1955 1961.2. The analysis indicates that the rotati the earth is subject to changes in acceleratio not to sudden changes in speed. The leng the day was increasing by about 0.5 msec year up to about 1958. 0 and has been decr by about 0.1 since then. There is no indicati a sudden change in speed during the geoma storms on the sun in July 1959. A comparis ephemeris time, obtained from the orbital m of the moon, with Zurich sunspot numbers 1820 to 1960 does not indicate a relation be speed of rotation of the earth and sunspots.

Henry P. Marx (Travelers Research C Inc., Hartford, Conn.), *Processing Observed for Automatic Entry into Weather Comp*

omatic weather-analysis and forecasting techues are being developed which require edited erved data of many types and from many rces in a minimum amount of time after the e of observation. A systematic approach to the elopment of appropriate input-data-handling niques is discussed. Such an approach should litate the provision of checkout data for techue development but retain its operational tity. The approach involves the development packages' to process both North American and ispheric data. These packages will process rational as well as synoptic data. The initial gram packages have the capability of processall North American operational data including rly airways observations, radar reports, and t reports. The generalized flow diagram of this gram and its subroutines is presented, and design philosophy is discussed. Initial results this and the synoptic program are presented.

. Matsushita (High Altitude Observatory, versity of Colorado, Boulder, Colo.), *Lunar es in the Ionosphere.* All previous work on ar tidal variations in the ionospheric F_2, F_1, E, and D layers is thoroughly reviewed and is pared with recent results of lunar tides obed from the electron density profile data of ionosphere and also with radio observations of ar tidal winds in the ionosphere. A world-wide avior of the lunar tides in different ionospheric rs is obtained. After reviewing lunar tidal ations in the surface atmosphere, geomagnetic ar variations at several places are examined, a new lunar current system at about 100-km ude is suggested. A theoretical discussion is ented of lunar tides in the ionosphere, taking consideration both hydrodynamical and elecdynamical motions.

. A. Melton (University of Arizona, Tucson, .), *Methods for Measuring the Effect of Enmental Factors on Channel Properties.*

. P. Meyer (Department of Geology, Univer of Wisconsin, Madison, Wis.) and W. E. INI (Department of Geological Engineering, ceton University, Princeton, N. J.), *Crustal asurements in the Montana-North Dakota a.* The regional significance of a particular t' solution for explosion seismic profiles in the tana-North Dakota area has been examined. eral agreement is found, in the depth to the horovicic discontinuity, between profiles shot ight angles from a common shot point and ple profiles along the same line. Intermediate rs, however, do not always appear consistent r this broad area, according to data based on reversed and single-ended profiles so far acblished in the area. Because the determination ntermediate layering is based, to a considerable nt, on secondary arrivals, the identification of propagation mode for secondary arrivals has been pursued through the analysis of phase relationships between horizontal and vertical seismometer pairs on explosion crustal-refraction records. The initial event on the record is revealed as compressional in nature, although immediately subsequent events are often found with varying phase relations attributable in part to vertically polarized shear arrivals mixed with compressional arrivals.

David H. Miller (Pacific Southwest Forest and Range Experiment Station, U. S. Forest Service, Berkeley, Calif.), *Folklore about Snowfall Interception.* Analyses of data and findings of 110 investigations of the interception by forest of falling snow suggest that deposition on tree crowns may at times be overestimated and that downward transport of snow, water, and vapor from crowns to forest floor may be underestimated. The difference between these two quantities, upward diffusion of vapor from crowns, or 'loss' of water from a drainage basin, therefore comes into question, especially since direct measurements are lacking. The belief, common enough to be called folklore, that enormous quantities of water are lost by evaporation of crown snow, needs to be re-examined. A relevant fact from climatology is that heat may not be available in quantities necessary to vaporize all the snow believed to be lost. In addition to the systematic biases described, random errors in studies analyzed also remain large. These errors, systematic or random, cannot be reduced much by more measurements of an end-product like throughfall, but have to be isolated in the 12 to 15 individual geophysical phenomena of which snow interception is comprised. Some of these phenomena have been studied in a few environments, but others are victims of common misbeliefs and still others seem almost unknown.

Walter L. Moore (University of Texas, Austin) and Frank D. Masch, Jr. (University of California, Berkeley), *Experiments on the Scour Resistance of Cohesive Sediments.* Previous studies of the scour of cohesive materials as presented in engineering literature and as obtained directly by personal contact are briefly reviewed. Exploratory tests for measuring scour resistance are described, and some correlated results are presented for a test involving scour by a vertical submerged jet impinging on the horizontal surface of a soil sample. The characteristics of the scour surface were observed for a remold and a natural sediment, and the rates of scour were measured by the weight loss of the sample. The results are presented in terms of dimensional parameters. A new apparatus is described, which is designed to permit a direct measurement of a uniform shear stress developed at the surface of a cylindrical sample of a cohesive sediment. Comments are made regarding the direction of future research in this area.

G. W. Morey, R. O. Fournier, J. J. Hemley, and J. J. Rowe (U. S. Geological Survey, Washington, D. C.), *Silica in the Thermal Waters of Yellowstone Park.* Thirty-six thermal springs and geysers in Yellowstone National Park were sampled for chemical analyses. At the time of collection, temperature and *p*H measurements were made in the pools. The range of temperature-corrected *p*H values measured in the pools is 2.0 to 8.75, and values measured a few hours later at room temperature ranged from 2.0 to 9.7. The hottest spring was 95°C and the coolest 40°C. Immediately after each sample was collected, the dissolved silica content was measured in the field by means of the colorimetric molybdenum blue method. Several weeks later both dissolved and total silica determinations were made in the laboratory. Only one sample showed evidence of flocculation and settling of silica to the bottom of the container between the time of field analysis and the laboratory analysis. Dissolved silica *determined in the field* and total silica values were identical for most of the samples. Nine samples had 20 to 40 ppm more total silica than dissolved silica, and one sample contained 134 ppm more total silica than dissolved silica. Both total silica and dissolved silica contents ranged from 50 ppm at Mammoth up to 600 ppm at Norris Basin. In the waters of rapidly discharging springs and geysers, the dissolved silica content is probably controlled by the formation of alteration products and the precipitation of quartz and chalcedony at shallow depths, rather than by the formation of silica gel at the vent. Waters from 21 of the 36 springs sampled had been previously analyzed one or more times by other workers. Waters from eight springs show no change in silica content. Four previous analyses are higher in silica and fifteen are lower in silica. The greatest change in the chemical nature of a spring was found at Porcelain Terrace in Norris Basin, where one spring, known to have been of alkaline chloride type, had changed to acid type with a *p*H of 2.3. The total silica has decreased from about 700 ppm (D. E. White, *Geochim. et Cosmochim. Acta,* 1957) in 1947 to 189 ppm now. This change is attributed to effects of the Hebgen Lake earthquake in 1959. Complete chemical analyses are in progress.

Walter H. Munk, Frank E. Snodgrass, and Gaylord R. Miller (Scripps Institution of Oceanography, University of California, La Jolla, Calif.), *Directional Recording of Swell.* From a triangular array of three bottom-wave records we have obtained daily directional information as a function of frequency over a period of 3 weeks. The major dispersive arrivals are associated with quite definite and reproducible directions, and these show the expected refractional turning at the low-frequency limit (down to 0.03 cps). The arrival of antipodal swell from the Indian Ocean through the Australia-Antarctica window is now defi confirmed.

Wallace B. Murcray (Geophysical Inst College, Alaska), *Infrared Absorption and sion Spectra of the Atmosphere at College, A* Absorption spectra of the atmosphere were at College, Alaska, during moderately cold (—20°F) weather. Path lengths were 7 or masses. The spectra showed an unusual abso feature at about 1 μ. The rotational H_2O between 10 and 15 μ were almost entirely a although the rotation bands beyond 15 μ present. Emission spectra showed radiatio to O_3 and H_2O, but the principle emitter ap to be CO_2. The emission spectra were from a pheres at about —50°F.

V. Rama Murthy (School of Science and neering, University of California, La Jolla, C *The Isotopic Composition of Silver in Iron orites.* Microgram quantities of silver wer tracted from the troilite of Toluca iron met and the metal phases of Sikhote Alin and C Diablo meteorites using anion-exchange niques. Isotopic analyses of silver in iron m ites indicate a ratio of Ag^{107}/Ag^{109} which is per cent higher than for terrestrial silver. I excess Ag^{107} is attributed to the decay o extinct radioactive nuclide Pd^{107}, an unreas short interval of time between the end of n synthesis and the formation of iron meteor indicated. The silver isotopic anomaly i meteorites is too large to be attributed to produced in the galactic synthesis of elemen appears that either some Pd^{107} was produc the solar nebula after its isolation fro galactic medium, or the silver isotope abun in iron meteorites have been changed by nuclear processes in the solar nebula. If the f is the case, other short-lived radioactive nu would also have been produced in the solar n and the theory of extinct radioactivity as th source in the early history of meteorite bodies is put on a firmer footing.

Sanker Narayan and G. P. Woollard (U sity of Wisconsin, Madison, Wis.), *An Eval of the Absolute Reliability of the Proton N Precession Magnetometer.* A proton nuclea cession magnetometer manufactured by Associates was evaluated in terms of ab total field against absolute vertical and hori magnetic variometers over a total field r above 20,000 gammas. The experiment wa ducted between Cut Bank, Montana, an Antonio, Texas, rather than in the laborat order to ascertain whether changes in ma gradient of geologic origin significantly a the readings. The test was conducted as a loop with repeat observations at each site average agreement was 12 gammas with dep of over 100 gammas in areas of strong ma

dients. Another model of the magnetometer nufactured by Littlemore Scientific Company wed only 5-gamma departure in an area of ng magnetic gradient. The repeat reliability this instrument at the same site on different s, after allowing for the diurnal change in d, was found to be 2 gammas. Comparisons of gnetic data obtained with the proton nuclear cession magnetometer in an airplane flying at 0 ft above ground with similar data obtained h a flux-gate total-intensity magnetometer vn at an elevation of 1000 ft over the same k showed no differences exceeding 10 gammas relative values over a 50-mile path after allow- for the difference in elevation. Comparisons of diurnal variations as recorded with a flux-gate al-field instrument and the nuclear precession gnetometer over the same period of time indi- e agreement to 2 gammas between the two truments.

AMES R. NEILON (U. S. Weather Bureau, Wash- ton, D. C.), *Results of Automation in Map duction at the JNWP Unit.* Several aspects of production of meteorological charts by auto- ic curve-drawing equipment are discussed. A rt summary of the problems encountered and methods of solution are given. The increase in ed of dissemination of analyzed and forecast ps of many meteorological parameters is cited. ns for further exploitation of the curve-drawing ipment are presented.

. WILLIAM NELSON (General Electric Com- y, Richland, Wash.), *In-Place Measurement of meability in Heterogeneous Media, 2, Experi- ntal and Computational Considerations.* The putational problem pointed out in part 1 of sequence of papers is evaluated in some de- . The problem arises from the need for com- mise between the accuracy of calculated perme- ity and the ease of performing the calculation. ite difference methods were expected to pro- e such a compromise. However, imprecision in nerical differentiation prevented use of the erence method. The question arising from this ing is: How accurately must the field perme- ity be measured? A study of the accuracy re- ed for measuring permeability indicates that times as much variation is allowable in the meability as in the potential pattern. Since ntial patterns are the tools needed to treat tical problems, errors in permeability measure- ts as great as 37 to 75 per cent may be tol- ed and still provide answers within the com- engineering accuracy range of 5 to 10 per Linear flow approximations are found to rather reliable permeability results for lateral systems. The geometrical shape of net ele- ts is used in a *properly constructed flow net* heterogeneous soils. An expression for the roximation error is presented for application ny problem being analyzed. Some typical field problems indicate that the maximum expected error in the potential is less than 5 per cent at critical points, with an average over-all approxi- mation error of 1 per cent.

N. F. NESS, T. L. SKILLMAN, C. S. SCEARCE, and J. P. HEPPNER (National Aeronautics and Space Administration, Goddard Space Flight Center, Greenbelt, Md.), *Measurements by a Rocket-Borne Rubidium Vapor Magnetometer.* A Javelin rocket carrying a Rb vapor magnetometer was successfully launched in December 1960 from the NASA facility at Wallops Island, Virginia. The flight lasted 20 minutes, and the rocket reached an apogee of 1160 km. During the flight continuous measurements of the total magnetic field were made with extremely high precision and accuracy. Simultaneous ground measurements were made with a similar Rb^{85} magnetometer located near the launching site. The telemetered data were well received with high signal-to-noise ratio. The flight data have been compared with referenced magnetic fields projected upward from coefficient sets deduced from spherical harmonic analyses. The larger-scale deviation of the magnetic field observations are interpreted in terms of spatial errors in the reference fields. Deviations not caused by the reference field are interpreted in terms of sources of magnetic field disturbance. The smaller-scale short-period fluctuations are compared with the ground measurements and interpreted as temporal variations of the magnetic field. Specific aspects related to the instrument as a data collection device and its significance for rapid data reduction and analyses with automatic computers are discussed.

A. CONRAD NEUMANN (Department of Geology, Lehigh University, Bethlehem, Pa.) and DAVID A. MCGILL (Department of Zoology, Yale University, New Haven, Conn.), *Circulation of the Red Sea in Early Summer.* Profiles of temperature, salinity, density, oxygen, and phosphate distribution have been constructed on the basis of 50 hydrographic stations taken in the Red Sea, Gulf of Aden, and Indian Ocean by research vessels *Atlantis* and *Vema* in June 1958. A surface inflow from the Gulf of Aden is found to occur in the Red Sea in opposition to the NNW winds of the summer season. This contradicts the previous description of Red Sea circulation which bases water movements on the seasonal wind pattern. It has been found that evaporation losses in the northern Red Sea are as great as 210 cm/yr and that this effect is greatest in the winter. Evaporation appears to be a stronger influence on the circulation than does the wind at the season of the year represented by the profiles. The inflowing surface water undergoes evaporation and cooling in the course of its northward transport. This produces a northward increase in density at any level above sill depth within the Red Sea basin. A prominent outflow due to the resulting con-

figuration of density surfaces originates in the Red Sea and passes over the sill beneath the surface inflow. Its effects can be traced well into the Indian Ocean. In June, the dense, warm, saline water that fills the Red Sea basin appears to be captive there, exchange being restricted to the shallower levels.

Robert R. Newton (Applied Physics Laboratory, Johns Hopkins University, Baltimore, Md.), *Potential Geodetic Applications of the Transit Satellite.* The transit satellite system will be used for determining the positions of ships at sea. Accurate tracking of the satellites will be accomplished by means of a careful analysis of the Doppler shift in the radio-frequency signals received from the satellites. Among other benefits of this program will be accurate geocentric positions of the tracking stations used in the system and an accurate representation of the earth's gravitational field. Results are presented which show the accuracy of tracking that has been achieved to date, the precision of determining positions of tracking stations, and some preliminary results concerning the gravitational field.

E. P. Ney (University of Minnesota, Minneapolis, Minn.), *Corpuscular Radiation and Meteorology.*

E. P. Ney and W. Stein (School of Physics, University of Minnesota, Minneapolis, Minn.), *Solar Cosmic Rays in November 1960.* Twenty-five balloon flights were made in the period November 12 to November 14. These carried photographic emulsions which were exposed for periods of 2 to 10 hours at pressure altitudes of 4 to 8 mb. Measurements have been made of the angular distribution, energy spectrum, and composition of the solar cosmic rays during this period. Proton fluxes as high as 250 particles/cm^2 sec ster and radiation levels as high as 0.7 r/hour were measured. Because of the great intensity of solar particles, special techniques had to be developed. Among these was a process for microtoming thick emulsions before development. At some times the geomagnetic field at Minneapolis imposed a rigidity cutoff of 0.7 bv (corresponding to a proton energy of 230 Mev). At other times protons were detected down to the energy limit imposed by the air absorption, that is, of about 80 Mev. The ratio of protons to α particles was determined at the time the rigidity cutoff was operative. The sequence of particle events as observed by balloon-borne emulsions is discussed.

John E. Noakes, A. F. Isbell, and Donald W. Hood (Department of Oceanography and Meteorology, Texas A and M College, College Station, Tex.), *Conversion of Carbon Dioxide to Benzene for Liquid Scintillation Counting.* The conversion of carbon dioxide to benzene in over-all yields of better than 30 per cent has been accomplished through the use of acetylene as an intermediate. The critical step in the synthesis is from acet to benzene, since all other steps have been p ously elucidated. The synthesis of benzene acetylene is accomplished at atmospheric tem ture by use of diborane-impregnated alum oxide catalyst. In this synthesis, yields in e of 50 per cent have been obtained, and no compounds than benzene are detectable b chromatography of the product. Fraction studies by Weiss and Shapiro have shown th isotope fractionation occurs during this st the conversion. The benzene synthesized in manner is used directly as a medium for scintillation spectrometry. The productio benzene from carbon dioxide in this manner a powerful tool for low-level counting of C promises to be especially useful in carbon d in which limited amounts of activity are avai

T. J. Nordenson and D. R. Baker (Weather Bureau, Washington, D. C.), *Com tive Evaluation of Evaporation Instrumen* the summer of 1953, the Weather Bureau ini an evaporation project at the Observational and Development Center at Silver Hill, M land. The original installation consisted of s class A evaporation pans, a BPI (sunken) a Colorado (sunken) pan, a Young scr (sunken) pan, and a 15-ft-diameter sunken The 15-ft-diameter pan simulates a lake. Lat insulated BPI pan and a new small experim insulated Fiberglas pan were installed. The cipal objectives of the project are (1) to pr another determination of pan-to-pan ratio the more widely used pans, (2) to provid termination of lake-to-pan ratios for the s pans, (3) to determine effect of non-sta operation of the class A pan, (4) to co evaporation from class A pans constructed o ous metals, (5) to check relations develop the Lake Hefner Report and Weather B Research Paper No. 38 for computing class evaporation and lake evaporation from m ological factors, (6) to study heat transfer th the sides and bottom of class A and BPI pan to determine the effect of cetyl alcohol o evaporation, and (8) to conduct research f development of a new evaporation instru Although the analysis is continuing, the resu far obtained are presented.

John Northrup and Maurice Blaik (Col University, Hudson Laboratories, Dobbs N. Y.), *T Phases from the Dominican Re Earthquake of September 14, 1960. T* phases the Dominican Republic earthquake (mag 4½) of September 14, 1960, were record bottom-mounted, Sofar-depth hydrophon four locations ranging from 800 to 1200 from the epicenter. These *T* phases, displa spectrum analysis equipment, are dispersiv last from 4 to 5 minutes. The leading and t edges of the *T*-phase signatures contain su

quencies, but the main Sofar arrival shows quencies up to 150 cps. An early arrival, corresponding to *P*, contains frequencies as high as cps; later arrivals and aftershocks are in the o 50-cps band. The dispersion shown in these atures is compared with that of two *T* phases n earthquakes of similar magnitude and with t of large underwater Sofar shots recorded at ilar stations. Of these, the Dominican Republhock has the deepest focus, and it excites the st modes. This is believed to account for the g duration of its *T* phase. The predictions of mal mode theory of layered waveguides are l to explain some characteristics of the signas, such as duration, dispersion, first-arrival quency, and maximum frequency of the signals.

Atsuzo Obayashi (Arctic Institute of North erica, Radio Research Laboratory, Tokyo, Ja-), *Propagation of Solar Particles through Interplanetary Space.* A model of the interplanetary gnetic field, which is formed by the outward aming of solar plasma clouds, is presented. s model can account for various characteristics solar particles observed from the earth. The tern excess of the arrival of low-energy solar mic-ray particles as well as the inequality of r travel time with respect to the heliographic tion of the solar flares are explained by a vex magnetic field caused by the rotation of sun. It is shown that the ejected plasma cloud s a magnetic bulge which is linked with the This cloud can trap or sweep out solar cosmic particles depending on the relative position injected particles and of the cloud in space. average speed and the lifetime of such an nding magnetic bulge are estimated from the e delay between solar flares and geomagnetic ms.

M. Okada (Radio Division, U. S. Naval Research Laboratory, Washington, D. C.), *Electric Field Effects on Störmer Q Regions.* The Störmer gions for a magnetic dipole field can be dised by a radial electric field. Of particular in is the time and space variation of *Q* regions n the electric field is time dependent. When e charge is taken into consideration in a simed model of the earth and its gaseous environment, this variation is in the form of a damped tion which allows dumping of charged particinto the auroral region with subsequent eastd and westward drift of the *Q* region at subal latitudes. The frequency of the oscillation ds on space-charge density, among other rs, and the oscillation can be regenerative r certain conditions, the energy being derived the electric field. This particular time-dent electric-field effect is a hydromagnetic omenon not involving magnetic field distor- and it can be considered apart from classical ner particle orbits. Applications to geophysisturbances are discussed.

J. A. O'Keefe and Winifred Sawtelle Cameron (National Aeronautics and Space Administration, Washington, D. C.), *Gravitational Evidence of Differentiation on the Moon.* The displacement of the center of figure of the moon with respect to the center of gravity suggests isostasy and hence differentiation. A statistical study is made to see whether this displacement can be accounted for by a distribution of lumps in the moon's interior, which distribution is consistent with the evidence from the moments of inertia. The study suggests that the displacement is larger than would be expected from this hypothesis; it is thus evidence for the existence of a differentiated lunar crust.

E. J. Öpik (University of Maryland, College Park, Md.), *The Aeolosphere and Atmosphere of Venus.* A self-consistent model of the Venus atmosphere which satisfies the multitude of existing observational data is proposed. Its main properties and the line of reasoning are described as follows. The radiative greenhouse effect cannot account for a surface temperature of 570°K. The blanketing must be due to dust, and the main source of energy must be wind friction at the surface. The term 'aeolosphere' is proposed for the region between the surface and the clouds of Venus, where wind is responsible for grinding and raising the dust, as well as for the heating. Self-consistency requires the opacity to be so high as to impose an adiabatic vertical lapse rate. The potential temperature in the aeolosphere must be nearly constant. Horizontal pressure gradients driving the wind are caused by climatic differences near the top of the dust clouds. The dust may consist of calcium and magnesium carbonates with impurities. Pressure estimates from CO_2 bands and optical scattering point to the presence of two distinct reflecting layers, the visible cloud level at about 0.6 atm and 340°K and an upper haze level at 0.08 atm and 234°K. In the visual and near infrared the upper haze is virtually transparent, owing to forward scattering. In the ultraviolet, and in the infrared beyond 1.4 μ it is opaque. Vertical cross sections of the Venus atmosphere are constructed for 80, 40, and 20 per cent CO_2. For 80 per cent CO_2 the results are somewhat more consistent, yielding a pressure of 4.3 atm at 570°K at the surface, 22 km below the visible cloud level. Despite uncertainties in the H_2O content, its amount is so small as to be nowhere condensable.

H. A. Panofsky (Pennsylvania State University, University Park, Pa.), *Scale Analysis of Atmospheric Turbulence at 2 Meters.* Various scales of the horizontal wind components in stable and unstable air are compared. In stable air, all scales are small, and the scales along the wind are larger than the scales across the wind. In the daytime, all scales are large and about the same in all directions. The speed of translation of turbulent patterns normally does not deviate much from the

wind speed, with one curious exception. The ratio of the Lagrangian scale of lateral components to the Eulerian scale of lateral components averages about 5 in stable air with moderate winds, but is considerably smaller in unstable air.

Bob J. Patton and John L. Fitch (Socony Mobil Field Research Laboratory, Dallas, Tex.), *Anhysteretic Remanent Magnetization in Small Steady Fields.* The phenomenon called anhysteretic remanent magnetization (ARM) has been known for a long time, but it has received relatively little attention. A knowledge of this type of magnetization is necessary for proper application of alternating field demagnetization techniques to rock magnetism problems. Over a considerable range of low values of the steady field, H_{dc}, the ARM intensity is a linear function of H_{ac} when the maximum alternating field intensity, H_{ac}, is constant. The coercive force of the ARM is a function of H_{ac} only, for small values of H_{dc}. Partial anhysteretic remanent magnetization (PARM) is analogous to partial thermoremanent magnetization (PTRM). It is shown that PARM's are additive in the same manner as PTRM's. These properties of ARM are useful in magnetic analyses for determining the magnetic nature of a material and for predicting its behavior on exposure to a magnetic field.

June G. Pattullo (Department of Oceanography, Oregon State College, Corvallis, Ore.), *Seasonal Variations in Heat Storage in the Pacific Ocean during the IGY.* The IGY Island Observatory Program in the Pacific Ocean has made possible a much more complete discussion of the changes in heat content of the ocean with time. Areas sampled for the first time include a number in the southern hemisphere and near the equator. Five samples near the equator at widely differing longitudes exhibit surprisingly large seasonal changes (a difference during the year of 40 to 60 kg cal cm^{-2}). These changes are apparently related to seasonal migrations of the currents and of the water masses associated with them. A comparison is also made between the IGY results and those obtained earlier by the author and others. Some of the areas where direct comparisons were possible show appreciable deviations in heat content between the IGY data and the long-term means, but no clear evidence is found of wide-spread coherence of these deviations.

L. E. Peterson (School of Physics, University of Minnesota, Minneapolis, Minn.), *Gamma-Ray Astronomy Experiment.* Instrumentation is described which is designed to measure the intensity and directional properties of γ rays in space and to monitor the solar intensity continuously from an earth satellite. The detectors cover three broad energy regions, 50 to 150 kev, 0.3 to 1.0 Mev, and 1.0 to 3.0 Mev. Photons in the 50- to 150-kev energy region are detected with a scintill counter using an NaI crystal and a lead pip limator. Preliminary studies from balloons this detector indicate a background equival about 0.1 photon/sec cm^2 at a low latitude. weak solar events should be detectable sin bremsstrahlung burst observed by Winckle others had a flux of 2×10^4 photons/cm^2 sec kev. A Compton coincidence telescope f from two scintillation counters provides a tional detector in the higher-energy regions tons scattered forward in the first counte totally absorbed in the second scintillation c The measured efficiency of the device is abc per cent in the forward direction; it is low a factor of 2 at $\pm 12°$ and a factor of 10 at for Co^{60} γ rays. The counters used in the tele are of the NaI-plastic 'phoswich' combinati reduce particle background effects. These e regions include the γ-ray lines of 0.5 and 2.2 Early balloon results indicate that the equi background intensity should be as low as 0.0 0.03 photon/cm^2 sec in the 0.3- to 1.0-Me the 1.0- to 3.0-Mev regions, respectively, satellite at the equator below the Van Allen

M. N. A. Peterson and Edward D. Go (University of California, San Diego, C *Feldspar Distributions in Deep-Sea Sedi* The abundances, types, and size fractions o spars in South Pacific sediments have been ied in order to ascertain their ultimate and modes of introduction into the marin vironment. Two sizes of particles were ass large (> 32 μ) and small (4 to 8 μ). The f was presumed to contain the locally derive terial whereas the latter should include the fraction along with the local material. provinces of feldspars can be distinguished area that has been studied. On the East rise (in an area bounded by 120°W, 95°W, and 40°S) sanidine is the dominant feldspa abundant quartz is present in the coarse fr Small amounts of orthoclase were also obs These minerals may well reflect a more composition of the crustal rocks of this are the north (in an area bounded by 25°S 155°W, and 90°W) the important feldsp labradorite, which is associated with amounts of augite. Both minerals decre grain size and abundance from west to ea appear to have a volcanic origin in the S Islands and other islands to the west. Be these two provinces is an area, as yet poor fined, in which a more sodic plagioclase, an oligoclase, is important. Along the coast of America the contribution of continental m is evident.

B. B. Phillips and William E. Cobb Weather Bureau, Washington, D. C.), *Ben Measurements of Atmospheric Electric Va at Mauna Loa, Hawaii.* The electrical pro

he lower atmosphere are recognized as factors importance in evaluating atmospheric pollu-. Quantitative measurements of the atmos-ric electric variables, to continue for a 1-year nterrupted period, were begun in August 1960 he Weather Bureau Geophysical Observatory, una Loa, Hawaii (elev. 11,150 ft msl). Contin-s simultaneous measurements are being made he positive and negative conductivities of the the electric field intensity, the rate of ioniza-, the air-earth current, the concentration of itive and negative light ions, and the negative y ion concentration. Nonroutine measure-nts have been made of the Aitken particle sities. Daily observations of solar radiation, ne and carbon dioxide concentrations, specific nidity, and ice nuclei concentration, as well as nosonde measurements and standard recording the meteorological variables—wind, pressure, nidity, and temperature—are available to as-interpretive studies of the electrical measure-nts Together, these measurements will consti-a geological time reference necessary for the ntitative evaluation of pollution trends. It is ned that the collected data will be assembled reproduced on microfilm for distribution to rested scientific groups.

. H. Pinson and C. C. Schnetzler (Massa-setts Institute of Technology, Cambridge, ss.), *Rb-Sr Correlation Studies of Tektites.* nalyses of tektites have revealed that they do ain measurable quantities of radiogenic Sr. ier analyses (Pinson), reporting tektite Sr to of normal isotopic composition, were in error. direct mass spectrometric measurements the 6 ratios of eleven tektites ranged from 0.7168 .7215, averaging 0.7185 ±0.0005. Included are ippinites, indo-chinites, australites, a bediasite, a tektite from Martha's Vineyard. Two davites yielded ratios of 0.7257 and 0.7235. dicate isotope ratio analyses on two indo-ites gave standard deviations of 0.0010 and 07 from a single analysis. K-Ar analyses ynolds) indicate a fusion date of less than 30 . for all tektites and less than 1 m.y. for fic area tektites. Only a negligible increase 7/86 ratio could have occurred in 30 m.y.; efore the measured ratios are essentially the e as at the time of fusion. It appears that es exclusive of moldavites may be cor-ed into a single group on the basis of their 6 ratios. Strikingly low water content (Fried-) is evidence of very high fusion temperatures, h might have disturbed Rb/Sr ratios by ionation. If the measured Rb/Sr ratios are ied and any initial 87/86 value is assumed, calculated age value groups emerge. If the al 87/86 ratio is 0.712, 200 m.y. is obtained Pacific area tektites and 300 m.y. for the site, Martha's Vineyard tektite, and the davites.

Paul W. Pomeroy and Jack Oliver (Lamont Geological Observatory, Columbia University, Palisades, N. Y.), *Seismic Surface Waves from Large, Near-Surface Nuclear Explosions.* Long-period seismic surface waves were recorded at a large number of existing seismic stations from the large near-surface shots detonated by the United States in the Marshall Islands and by the Soviet Union at the Novaya Zemlya test site. Because the source and receiver positions, as well as the origin times, are accurately known for the U. S. shots, it has been possible to deduce oceanic phase velocities for Rayleigh waves with periods from 40 to 15 seconds. This was accomplished by use of the Honolulu seismograms for the Eniwetok-Bikini area. In addition, the long-period horizontal Benioff records from Guam exhibit short-period surface wave trains which have velocities suggestive of the first Love and first shear modes. Normally dispersed Rayleigh wave trains were recorded at Honolulu, Mt. Tsukuba, Suva, and Hong Kong from the larger Marshall Island shots. The Russian nuclear explosions generated several unusual seismic surface waves. Seismographs at Uppsala, Sweden, and Agra, India, clearly recorded waves corresponding to the first shear or *M2* mode. Hong Kong and Agra recorded Love waves from these explosions in addition to normally dispersed continental Rayleigh wave trains. Group velocity data indicate a large sedimentary thickness along the path from New Zealand to Hong Kong. Rayleigh waves from these shots were also recorded at Resolute Bay, Palisades, Ottawa, Waynesburg, Laramie, and Lwiro.

F. Pooler, Jr. (Weather Bureau Research Station, Cincinnati, Ohio), *Stable Air-Flow Patterns at Louisville, Kentucky.* Data from a meteorological network set up to study local air-pollution problems are used to classify and describe surface flow patterns. During periods of stability, appreciable spatial variations of the flow are sometimes found. Although the ground elevation in the vicinity of Louisville varies by less than 500 feet, marked topographic effects on the surface flow are shown. The Louisville urban area causes a surface inflow, which becomes evident when the general flow is weakened, due either to a weak large-scale pressure force or to topographic blocking of flow induced by the large-scale force.

Frank Press, Ari Ben-Menahem, and Nafi Toksoz (Seismological Laboratory, California Institute of Technology, Pasadena, Calif.), *Experimental Determination of Fault Length and Rupture Velocity.* Fault length and rupture velocity may be derived from phase shifts between horizontal and vertical components of free spheroidal oscillations of the earth, and from amplitude ratios of even and odd order mantle Rayleigh waves and *G* waves. The theory is reviewed and examined experimentally with ultrasonic scale modes. Application to the great Chilean and

Kamchatka earthquakes indicates fault lengths of about 1000 km and rupture velocity close to the Rayleigh or shear velocity in silicic rock. The fault lengths are in agreement with Benioff's measurement from the aftershock sequences and Eaton's measurement from duration of T phases. The effect of finiteness of the source on fault plane solutions based on P waves and surface waves is discussed.

P. D. Proctor and G. C. Amstutz (Missouri School of Mines and Metallurgy, Rolla, Mo.) and R. A. Black (U. S. Geological Survey, Washington, D. C.), *Lunar Tectonics and Near-Surface Lunar Composition.* Extra-lunar (exogenous) and intra-lunar (endogenous) origins of the surface features of the moon are discussed. Endogenous forces seem reasonable for numerous observed features. Arcuate faults, peripheral fault patterns, parallel to subparallel ridge-fault-mare boundaries, inward tilted craters, crater topped ridges and faults, grabens, and clefts are all observed in mare areas. Polygonal structures, clefts, fault blocks in large 'craters,' fault trends and spatially related 'craters,' grabens, central peaks and summit craterlets, repeated activity, lava and non-lava covered floors, and possible 'crater' activity up to the present time are observed on the highlands. The features in both types of areas suggest an initial lunar crust which expanded internally and was locally down-faulted, and which was later partly to completely inundated by dark lava flows. Rock compositions and textures are related to the origin of surface features. Basaltic scoria (maria) and pumiceous rhyolite (highlands and rays) with local exhalative mineral deposits are to be expected on the lunar surface.

P. Putnins (U. S. Weather Bureau, Washington, D. C.), *The Correlation between the Pressure Changes at the Surface and Aloft in the Greenland Area.* Nineteen stations in the Greenland area and one station in the central Arctic were investigated with respect to the 24-hourly pressure changes at the surface and aloft (700- and 500-mb levels)—simultaneous changes and with a lag of 24 hours. According to the results obtained there is some justification for the assumption that the 'steering' is initiated in the lower levels of the atmosphere. The complexity of this problem is briefly discussed, as well as the common misconception of V. Ficker's 'primary' and 'secondary' waves.

Mohammed N. Qureshy (Bear Creek Mining Company, Denver, Colo.), *Isostasy in Colorado.* Statistical analysis of different types of gravity anomalies in Colorado, computed from data supplied by Holmer (1954), shows Pratt-Hayford ($D = 113.7$ km) and Airy-Heiskanen ($T = 30$ km) anomalies to be least related to elevations. This indicates validity of these isostatic assumptions in Colorado. The graph of elevations versus free-air and Bouguer anomalies shows a sharp chang slope at an elevation of around 6200 ft. This n sitated fitting two straight lines to these se data. The change in free-air anomaly with in elevation is significantly slower for eleva lower than 6200 ft than for elevations higher this. This change in gradients can be attribute the fact that it is approximately at this level the eastern plains with their thick and exte sediments abut against the Rocky Mount Beyond this level the elevations are higher, the geology encountered is entirely different. disappearance of the sudden change in slope the graphs of isostatic anomalies versus elev lends further support to the conclusion that static equilibrium prevails in Colorado. It is t fore concluded that in areas where terrai rugged, as in Colorado, better knowledge o crust would be obtained by using isostatic a alies.

Rama, M. Koide, and E. D. Goldberg (Un sity of California, San Diego, Calif.), *Pb^{210} i Hydrosphere.* The Pb^{210} produced from the d of radon in the atmosphere has been assayed group of natural waters. Only a small fracti Pb^{210} of atmospheric origin was present in oc waters from the upper mixed layer. Source w for the Colorado River had Pb^{210} abund similar to those of rain. However, downst samples were markedly depleted in this iso indicating a rapid transfer to the sedimen biochemical or inorganic processes.

R. R. Rapp (Rand Corporation, Santa M Calif.), *Wind and Temperature in the Mesosp* Some mean meridional cross sections of win temperature based on recent measurement presented. The accuracy of the measurement the representativeness of the sample are disc Some simple models are set up to test the sistency between the wind and temper patterns. Some hypotheses which have bee vanced to explain the apparent discrepancie tween the observed temperature and the puted radiation temperatures are investigat the light of the observed wind fields.

Ernest C. Ray (Department of Physics Astronomy, State University of Iowa, Iowa Iowa), *On the Inner Zone of Trapped Radi* The preliminary results of a study of data satellite 1958ϵ, made using the integral inv and Alfven 'magnetic moment,' are report comparison of the experimental results wit ories about the spatial distribution of tr protons is made.

J. E. Reed and M. S. Bedinger (U. S. Geol Survey, Little Rock, Ark.), *Projecting the of Changed Stream Stages on the Water* Under certain conditions, the position and of a water table may be considered to be th

two components of head—the boundary com-ent and the accretion component. In an aqui- of given hydraulic characteristics, the boun-y component of head is determined by the am stage and the areal shape of the aquifer; accretion component is determined by vertical n or loss of water to the aquifer and by the al shape of the aquifer. The boundary com-ent may be obtained by electric-analog meth-. By subtracting the boundary component from observed position of the water table, the accre-n component can be obtained. A change in river ge imposes a new boundary component on the tem. The effect of changed stream stages on water table may be obtained by adding the retion component to a new boundary com-ent caused by the change.

K. G. Reinhart and A. R. Eschner (U. S. For-Service, Upper Darby, Pa.), *Effect on Stream-w of Four Different Forest Practices in the palachian Mountains of West Virginia.* After -year calibration, four watersheds on the Fer- experimental forest were logged in 1957–1958. ctices ranged from a commercial clearcut with ger's choice' skid roads to a light selection cut h planned skid roads on moderate grades. For most part, the treatments did not seriously urb the forest floor. Annual flow increased, up 5 area inches on the clearcut watershed the r after treatment. Increases fell into a logical tern with volume cut. Most of the increase ge in the growing season. In the May to Octo-period of 1959, increases were 3.1, 1.8, 1.4, and area inches for per-acre cuts of 8.5, 4.2, 3.7, 1.7 thousand bd ft, respectively. Low flows re augmented, especially for the two heavily watersheds. Effect on high flows was variable; the clearcut watershed some storm period flows he growing season were more than doubled and snow-melt flows were less than expected. e in the logging operation was clearly reflected water quality; maximum turbidities measured 56,000 on the watershed having unplanned roads without provision for drainage and 25 on the watershed with carefully planned roads. Effects of treatment are diminishing passage of time.

Renau, W. Flood, and H. Camnitz (Cornell nautical Laboratory, Inc., Buffalo, N. Y.), *Scattering of Electromagnetic Waves from an ized Gas in the Presence of a Magnetic Field.* spectrum of electromagnetic waves scattered thermal fluctuations of the electron density an ionized gas in the presence of a static, i-uniform, magnetic field has been derived ugh use of the Nyquist noise theorem. Al-ugh the analytical expressions are quite gen-l the results presented are applicable to back-tering only. The spectrum is described for h of the following ranges of wavelength: (1) uch less than the electron radius of gyration, (2) λ less than or equal to the electron radius of gyration and the Debye length, (3) λ much greater than the electron radius of gyration but much less than the ion radius of gyration and (a) greater than the Debye length, (b) less than the Debye length, (4) λ less than or equal to the ion radius of gyration and much greater than the Debye length. The differential scattering cross section per unit volume is unchanged by the presence of the magnetic field.

Charles E. Renn (Department of Sanitary Engineering and Water Resources, Johns Hopkins University, Baltimore, Md.), *Ecology and Fine-Grained Sediments.*

T. D. Reynolds and E. F. Gloyna (The University of Texas, Austin, Tex.), *Permeability Measurements of Rock Salt.* A method is described which has proved to be successful for measuring the permeability of rock salt. Different specimens of salt were studied, and the technique was checked by use of a solid crystal of sodium chloride. Both reactive and nonreactive fluids were used in collecting permeability data. Permeability tests were run on rock salt from both dome and bedded formations. The tests on the dome salt showed it to have a very low permeability whereas most of the tests on the bedded salt showed it to be impermeable. Where there was some measurable permeability under the conditions of the test, it was found that the permeating flow occurred through cracks or fractures in the salt and not through the crystals themselves. These fractures were apparently caused by the relaxation of stress which occurs when underground samples are removed from a compressed formation. The dome salt was found to have more fractures than the bedded salt owing probably to its lower elastic strength. Such surface fractures, found in both types of salt, will be localized in the vicinity of a mine and consequently will not extend throughout a formation.

Donald A. Rice (U. S. Coast and Geodetic Survey, Washington, D. C.), *A Geoidal Section along the 35th Parallel.* Astrogeodetic deflections were observed at 186 stations along the 35th parallel by the Coast and Geodetic Survey in the period 1956–1960. Observing procedures and results are discussed, and an evaluation is given of the various contributions to error in the relative geoid heights. The resulting data are essentially a scaled model of the geoid along a particular section, but without a defined orientation or position on the centered ellipsoid of optimum flattening and scale. An example shows how such a model could be applied to a world gravimetric geoid to derive an optimum equatorial radius.

F. E. Roach (National Bureau of Standards, Washington, D. C.), *Auroral Arcs in Mid-Latitudes.* Subvisible auroral arcs have been frequently

observed with photoelectric photometers at a station located about 18° south of the conventional auroral zone. The arcs are spectroscopically characterized by a strong enhancement of the 6300, 6364 radiation due to atomic oxygen. They occur during times of strong magnetic activity at a height of about 400 km above the earth's surface. They are oriented approximately along latitudes of equal magnetic dip. It has been hypothesized that the occurrence of the arcs is associated with an unusual heating of the upper atmosphere during times of magnetic activity.

W. J. Roberts (Illinois State Water Survey, Urbana, Ill.), *Reducing Transpiration from Plants.* The monomolecular film technique for reducing evaporation from water surfaces has been applied to the problem of transpiration from plants. Hybrid corn grown in soil enriched by various amounts of fatty alcohols, such as hexadecanol, has required up to 40 per cent less water during its growth than control plants. It is theorized that some of the transpiration from corn plants can be safely reduced by the blocking action of molecules of hexadecanol carried through plants and deposited at the stomate water-vapor interface. Although the blocking action could be taking place throughout the plants, testing with C^{14} hexadecanol has produced radio-autographs showing activity not only in the roots and stalks but also throughout the leaves of treated corn plants. Comparative testing has been done in the greenhouse. However, one treated corn crop, grown naturally, yielded over 100 bushels per acre. Chemical tests on this corn show no apparent effect of large doses of hexadecanol added to the roots of the plants. Recent testing of other plants, especially grasses, lends strong encouragement for further research in the area.

Walter Orr Roberts (National Center for Atmospheric Research, Boulder, Colo.), *National Center for Atmospheric Research—A Progress Report.* The National Center for Atmospheric Research (NCAR) came into being in June 1960 in direct response to the expressed need for a national research center devoted to fundamental advances in the science of meteorology. Research plans are now being formulated and a scientific staff is being recruited. NCAR will have three principal functions: (1) It will serve as a center for intellectual activity in meteorology and allied physical sciences, to provide imaginative new attacks from many directions on the problems of the physical processes of the earth's atmosphere. (2) It will conduct small research planning conferences on a national scale to determine the extent to which modifications or enlargements of the scope and conduct of certain forms of research in the atmospheric sciences are needed to serve the public interest. (3) It will, when the planning conferences so recommend, seek to establish national research facilities open to all research groups. Headquarters of NCAR ar Boulder, Colorado, where it will work closely the High Altitude Observatory. NCAR's goal to ensure that the science of meteorology fits fully from the exploitation of new techni of observation and analysis, and to stimulate fullest participation of university research la tories in the resulting advances.

J. Rodier (Hydrological Service of the Offi la Recherche Scientifique et Technique O Mer, Paris, France), *A New Method for H logic Investigations in Arid Countries.* Stan methods for hydrologic investigations are available in arid countries because stream r is an infrequent phenomenon, so it is difficu organize permanent observations of storm floods. A new method of investigation is sented. It has been used for 4 years in the fringe of the Sahara, where rare storms during short seasons in some mountainous reg This method, which has given good results three parts. (1) A sparsely distributed rain network is installed in a certain region. From network we get an insight into the space and distribution of rainfalls. (2) A small natural is selected in a representative area of the r and is equipped for simple measurements. Co uous hydrologic and climatologic observa supply approximate precipitation-runoff rela (3) Extensive surveys are made on many str of the region during several tours throughou rainy seasons. These surveys, together wit formation from nomadic natives, furnish app mate values of peak flows and sometimes of r volumes. In addition, a systematic study o ground-water recharge is made in areas runoff occurs. Some practical details are give the working conditions in arid countries heavy and expensive equipment cannot be

John J. W. Rogers (Department of Ge Rice University, Houston, Tex.), *Variatio Th/U Ratios in Granitic Rocks.* Wide varia are found in thorium/uranium ratios in gr and other plutonic igneous rocks. Attempts been made to relate the variation to the sta petrogenetic evolution or to position in indiv differentiation sequences. In general, no rela ship has been found between the Th/U rati the chemical composition of igneous rocks the ratio does appear to be correlated both a petrographic index of evolution and wit quence of intrusion when the latter is deter ble by field work for individual different series. In comparison with relatively early-cr lizing intrusive igneous rocks, the later-fo and/or more differentiated granites have a range of Th/U ratios and a generally higher age ratio. This relationship has been confirm a high confidence level for a broad sampli igneous rocks by calculation of the linear lation coefficient. A plausible cause of the

n is selective loss of uranium resulting from idation during magmatic evolution. Oxidizing pacity in plutonic systems is, of course, demon- ated by the presence of primary magnetite in rusive rocks, and the variation in Th/U ratio y support current evidence concerning the im- rtance of oxidation in the evolution of granitic agma.

. C. Rose and O. S. Strickholm (Department Geology, University of Wisconsin, Madison, s.), *Reliability of Pendulum Gravity Intervals tween Absolute Sites in Europe and North erica.* Recent absolute gravity determinations dicate that the Potsdam system is too high by proximately 13 mgal. A definitive adjustment quires that the gravity intervals between abso- e sites be known reliably to 0.5 mgal or better. ndulum interconnections made before 1935 have ndard errors of several milligals in contrast to modern results having a reliability of 1 mgal better. Results have been evaluated for the kania invar pendulums, Brown invar and bronze ndulums, Cambridge invar pendulums, CGI lybdenum pendulums, D.O. bronze pendulums, l the Gulf-Wisconsin quartz pendulums, and ghted means have been computed. Combined ults of modern observations made through 1960 dicate the following:

Potsdam (Absolute) — Teddington (NPL 11 floor)	=	−77.94 ± 0.15 mgal
Teddington (NPL 11 floor) — Paris (Sevres A)	=	+255.52 ± 0.21 mgal
Teddington (NPL 11 floor) — Washington, D. C. (CF)	=	+1077.47 ± 0.13 mgal
Teddington (NPL 11 floor) — Madison (12A)	=	+827.55 ± 0.18 mgal
Ottawa (GLF) — Washington, D. C. (CF)	=	+502.71 ± 0.06 mgal

here are uncertainties not revealed in the stand- l errors, as well as major discrepancies between ults of some recent observations with different es of pendulums. A weighted mean of Jeffreys' 48–1949) revised absolute results for Potsdam, shington, and Teddington as well as Paris, ningrad, and Ottawa indicates that the Pots- n system is too high by 12.53 ± 0.38 mgal. The linary mean indicates 13.03 ± 0.80 mgal. Fur- r study is in progress.

Alan Rosen (Space Technology Laboratories, ., Los Angeles, Calif.), *Dynamics of the Outer n Allen Radiation Zones.* The Explorer VI tillation counter traversed the outer radiation ne 130 times between August 7 and September 1959. The instrument was sensitive to electrons ve 200 kev and protons above 2 Mev. Day to variations in intensity and fast fluctuations ng and falling by as much as 3 orders of mag- de in a few seconds have been observed. These tuations were compared with the magnetic d fluctuations observed by the search coil mag- ometer located on the same vehicle and the d fluctuations observed by ground-stationed gnetometers. A few interesting observations were made. For example, a large burst of radiation was observed at a radial distance of 43,000 km from the earth's center and 45° geomagnetic latitude, at 1110 GMT on August 16, 1959. The line of force on which the observation was made intersects the earth's surface at 85° geomagnetic latitude. The magnetometer at Point Barrow, Alaska (68.6°N geomagnetic latitude), recorded a field fluctuation which was correlated with the burst of radiation seen by the scintillation counter. The Byrd Station magnetometer (70.6°S geomagnetic latitude) and the College magnetometer (64.7°N geomagnetic latitude) showed smaller fluctuations which were not clearly correlated with the radiation burst. The experimental data relating to these and similar observations are presented and the significance of the results is discussed. Two source mechanisms for populating the outer zone, neutron albedo and solar injection, are considered, and the experimental evidence relating to them is reviewed.

Henry A. Salmela (Meteorological Development Laboratory, Waltham, Mass.), *Wind Speeds from GMD-1 Ascents Computed Electronically Compared with Plotting Board Results.* For 30 upper wind soundings at Montgomery, Alabama, most of the wind speeds evaluated by plotting board in the field for each minute of ascent up to 7 km and each even minute above that level to 16 km differ only slightly from the corresponding speeds evaluated for each identical interval by an electronic computer. The differences increase with height, but even at 15 km the median absolute difference is only 1.6 m/sec. Some individual differences are large enough, however, to raise questions about the accuracy of winds computed, by present methods, for the upper portions of some flights.

J. E. Sanders (Department of Geology, Yale University, New Haven, Conn.), *Tectonophysics of Late Triassic Deformation, Northeastern United States.* The tectonic history indicated by the Late Triassic rocks of the New York–New Jersey and Connecticut Valley belts is reviewed in light of the broad terrane hypothesis, which states that the now-isolated outcrop belts were formerly continuous. An elongate rift valley, 50 miles wide, is inferred to have been the basin in which these belts accumulated—at least the belts of the Triassic nonmarine sediments and associated extrusive and intrusive igneous rocks. The thickness of Triassic strata now preserved in the two areas is considered to be approximately 30,000 ft. The

strata were essentially horizontal when deposited, but were later tilted toward the northwest in the New York–New Jersey belt and toward the east and southeast in the Connecticut Valley belt. In addition, transverse warped structures of varying sizes have been formed and have been offset by a series of younger, near-vertical faults that are generally diagonal to the axes of the transverse warped structures. Late dikes of porphyritic dolerite have been injected into some faults, and mineral deposits have also formed along some faults. A tectonic history of the area is proposed which is consistent with the field observations. Regional geologic implications of this tectonic history include evidence for dating the widespread uplift and exposure of medial Appalachian Precambrian basement rocks as a Late Triassic event; only local exposures of the basement occurred here previously. Large Triassic faults probably extend into areas beyond the outcrops of the Triassic rocks (for example, along the straight western boundary of the Taconic allochthone in the Hudson Valley). The southward disappearance of the Taconic allochthone may be due to late Triassic transverse crustal warping. Triassic longitudinal crustal arching may have been responsible for the origin of some of the Appalachian drainage. In addition, the igneous rocks of different tectonic episodes might provide radiometric dates that could indicate the time required for the episodes of deformation and yield some idea of how long the various rocks were deeply buried. Effects of deep burial on the rocks have not yet been examined, but a measure of the time during which they were buried should prove valuable in assessing natural reaction rates of silicate mineral assemblages.

Yoshikazu Sasaki (University of Oklahoma, Norman, Okla.), *Effects of Condensation, Evaporation, and Rainfall on Development of Mesoscale Disturbances: A Numerical Experiment.* Solutions for a mesoscale numerical prediction model including the equations of motion and thermodynamics in the (x, z, t) coordinate system were obtained using the IBM 704. At the lower boundary, $z = 0$, considered to be flat surface, and at the upper boundary, $z = 30{,}000$ ft, the kinematic condition $w = 0$ was prescribed. The equations were solved numerically using $\Delta z = 2500$ ft, $\Delta x = 7.5$ n mi, and $\Delta t = 1$ min. An initial condition representing a conditionally unstable stratification of the atmosphere was assumed. The computations were made for the following cases: (1) dry air only, (2) simple condensation process where moisture is assumed to condense when the air becomes saturated, (3) evaporation process considered, in addition to the above condensation process, when air is not saturated but does contain liquid water, and (4) the effect of descending motion of liquid water in order to simulate the effect of falling rain. Computations were carried out for more than 240 4-hour time steps for each of these cases under the same initial condition. It found that the physical instability was influe to a large degree by evaporation as well a condensation, and the degree of instability sensitive to the levels at which condensatio evaporation occurred. The rainfall causes a crease in the instability due to the descendin evaporation levels of liquid water. It was shown that both the thunderstorm high and wake depression formed at low levels under favorable unstable conditions. Further discus of the results is given from the viewpoint of s line formation.

J. F. Schairer and H. S. Yoder, Jr. (Geoph cal Laboratory, Carnegie Institution of Wash ton, Washington, D. C.), *The System Nephe Forsterite-Silica and Its Relation to Crystalliza of Basaltic Magmas.* The phase-equilibrium tions in this system have been determined a phase diagram showing the relations at one atm phere pressure is presented. The portion nephe forsterite-albite is not ternary at liquidus tem atures. A field of spinel is present. The binary albite-forsterite is a thermal barrier between tallization products with enstatitic pyroxene feldspar with or without tridymite as phases one hand and forsterite, feldspar, and nephe on the other hand. The system nepheline-fors ite-silica is one of the limiting systems of system nepheline-diopside-forsterite-silica, w contains the principal normative component simplified iron-free basalt. Compositions in the forsterite-jadeite-albite-enstatite are close in position to some peridotites. Those on the ne line side of the join albite-forsterite yield ne line-bearing products of crystallization while t on the silica side of this join yield only oliv pyroxene, and feldspar with no nepheline.

Marshall Schalk (Department of Geol Smith College, Northampton, Mass.), and Ja D. Hume (Tufts University, Medford, Ma *Sea-Ice Movement of Beach Material in Vicinity of Point Barrow, Alaska.* In years of tive ice movement, sea ice containing rock f ments may push high on the beach above no water level. As the ice melts new materia obviously added to the beach. Most of this m rial appears to be of local origin, but foreign r especially scoriaceous lavas, have been bro into the area southwest of Barrow and, in past, have been used by the natives. In addi ice may push up gravel mounds to heights proaching 3 meters. These mounds, on the narrow, barrier beaches east of Barrow ap from offshore as distinctive landmarks from year to the next. One of the larger mounds surrounded by 'faults' indicating that the stratum had been compressed or displaced u the load. Median diameter at the surface of of the mounds runs over 20 mm and sortin as good as that of gravel in the swash zone d

ummer storms. The excellent sorting is believed be due to a combination of frost action, sim- infiltration of the finer sizes, and washing by e melt water from the original ice and later ow. Extreme storm tides have smoothed out meter ridges in a matter of hours. Nevertheless e ice-shoved material makes an addition to the herwise wasting beaches.

I. I. Schell (Tufts University, Medford, Mass.), *me Causes of the Iceberg Severity off Newundland and Their Implications.* An analysis of e fluctuations in the iceberg severity off Newundland observed mainly during the period pril to June, indicates that approximately 40 r cent of the annual variation is accounted for the winds off Labrador and Newfoundland and e temperatures along the coast, during the preding period December to March. The temperares are a measure of the pack ice off shore that lps keep the bergs from drifting into the bays t shallows along the coast. This implies that less the Labrador current is uniquely correed with the direction and speed of the wind, e wind plays a greater role in the berg regime an is suggested by the relative distribution of submerged and exposed portions of an iceberg. e indicated berg count for this season is in the ighborhood of 500. The long-term average is proximately 400 bergs. There have been as any as 1000 bergs counted in 1904, 1909, 1912, d 1929, and fewer than 10 bergs counted in 1940, 41, 1951, and 1958.

Milton O. Schmidt (Department of Civil Engineering, University of Illinois, Urbana, Ill.), *odetic Engineering Education in West Germany.* Formal programs of higher education in eodetic Engineering have been operating in stern Europe for many years. Some general servations, based on a recent visit abroad, are ade on the scope and quality of such curricula in est Germany. The curriculum at the Institute Theoretical Geodesy at the University of nn is presented, and brief consideration is ven to the teaching staff, students, and physical cilities for instruction and research at the engiering schools in West Germany which offer ofessional four-year programs in geodetic engiering.

Allen H. Schooley (U. S. Naval Research boratory, Washington, D. C.), *Mean Roughss Factor as a Function of Wind Velocity.* The ughness of the facets of a wind-disturbed water face has been expressed in terms of a dimenless 'roughness factor' by the author (IUGG neral Assembly, 1960). Roughness factor was fined as the ratio of flatness tolerance to facet gth. In the same work, the experimentally termined statistical average roughness factor s given as a function of surface slope and local nd velocity. It was shown that the roughness factor increased with wind velocity for small slopes. For surface slopes greater in magnitude than about $+10°$ or $-10°$, the roughness factor became less as the wind velocity increased. It is shown that the mean roughness factor for the whole distribution of surface slopes is an increasing function of wind velocity. The range covered is from about 0.09 roughness factor at 10 knots to about 0.125 at 20 knots.

C. D. Schrader and R. J. Stinner (Lawrence Radiation Laboratory, University of California, Livermore, Calif.), *Remote Analysis of Surfaces by Neutron-Gamma-Ray Inelastic Scattering Technique.* The feasibility of applying nuclear scattering techniques in the remote chemical analysis of unknown materials is discussed. We have measured the spectra of γ rays produced by neutrons in a large sandpile containing various known percentages of the elements O, Mg, and Al, Si, and Fe. A general statement can be made that a 5 per cent abundance of any of these elements can be quantitatively determined to a precision of better than 10 per cent. The method, in which fast gating and timing circuits are used to select only the unambiguously originated γ rays from the neutron inelastic scattering process, appears to be so promising that a miniature pulsed accelerator is now being tested and packaged. Applications to the analysis of the lunar surface, planetary atmospheres, and the earth's mantle are also discussed.

John Schuetz and Sigmund Fritz (U. S. Weather Bureau, Washington, D. C.), *Satellite Pictures of Cloud Streets.* Bands of cumuliform clouds over the Caribbean Sea as observed by Tiros I are described. The possible relationship between the occurrence of these bands and the vertical distribution of the horizontal wind is discussed. The cloud street orientation is compared with the wind direction.

G. P. Serbu (National Aeronautics and Space Administration, Goddard Space Flight Center, Greenbelt, Md.), *Results from a Rocket-Borne Langmuir-Probe Experiment.* Data were obtained from a rocket-borne Langmuir-probe experiment to an altitude of 220 km above Fort Churchill, Canada, in a quiet daytime ionosphere. The electron temperatures deduced from the probe data are in good agreement with the accepted neutral gas temperatures at altitudes above 140 km. Improper corrections for the positive ion component of the diffusion current to the rocket, which component is adversely affected by the high rocket velocity, is thought to have caused the much higher electron temperatures measured below 140 km. The rocket-to-plasma potential was found to be from ½ to 1 volt negative.

A. L. Sharp and W. J. Owen (U. S. Department of Agriculture, Lincoln, Nebr.) and A. E. Gibbs (U. S. Department of Interior, Lincoln,

Nebr.), *A Comparison of Methods of Estimating Precipitation on Watersheds.* Methods of estimating watershed precipitation, and various distribution densities of rain gages for estimating area precipitation, are compared for several watersheds and areas in Nebraska, Kansas, Texas, and Oklahoma. It was found that the use of increasing numbers of rain gages with time may introduce an increasing bias in estimates of watershed precipitation. Sparse networks of rain gages are no better for estimating monthly precipitation than storm precipitation. There are generally significant differences in estimates of storm and monthly precipitation based on sparse and dense networks of rain gages. A comparison of methods of estimating precipitation (Thiessen weights, isohyetal maps) from a given set of rain-gage records showed no significant differences in estimates. A comparison of estimates based on 39, 19, 13, 10, 5, 2, and 1 rain gages in the 100-square-mile Sandstone Creek watershed showed greatly increased error when 5, 2, and 1 gages were used. Arithmetic averages and isohyetal maps produced essentially the same estimates when the same sets of gages were used. Ten gages uniformly distributed over the area produced better estimates than 10 randomly located gages. These data indicate that a density of 1 gage per 10 square miles, uniformly distributed geographically, is required for adequate estimation of storm precipitation on larger creek and river basins.

Edwin B. Shykind (Northern Illinois University, De Kalb, Ill.), *Studies in Quantitative Geomorphology—Geomorphic Implications of the Dendritic Pattern.*

Peter Signer (School of Physics, University of Minnesota, Minneapolis, Minn.), *Cosmogenic and Radiogenic Rare Gases in Chondrites.* The concentration of all the stable isotopes of helium, neon, and argon have been measured for six chondritic meteorites, including Bruderheim and Richardton. The He^4/U, Th, and Ar^{40}/K ages were computed by using averages for the values found for U, Th, and K concentrations in chondrites. For the Bruderheim meteorite the He^4/U, Th, and Ar^{40}/K ages found were 1500 and 1600 m.y., respectively. The variation by a factor of 10 of the ages of the several meteorites as computed from the radiogenic isotopes suggests a serious loss of radiogenic nuclides in some of the cases. Whereas the He^3/Ar^{38} ratios vary by a factor of only about 2, the radiogenic He^4/Ar^{40} ratios vary from 0.12 to 0.84. The fact that the ratios of the cosmogenic nuclides are so nearly the same, even for meteorites having greatly different radiogenic ages, suggests that if there has been a loss of cosmogenic nuclides no large fractionation occurred; shielding effects and variable chemical composition could mask fractionation if it occurred. For the other four meteorites, for which exposure ages were determined earlier (Geiss, Oeschger, and Signer *Z.*, *Naturforsch.*, 1960), the production rates for the cosmog nuclides, He^3, Ne^{21}, Ar^{38}, were calculated t 2.0 ± 0.3, 0.50 ± 0.03, and 0.06 ± 0.02 (in u of 10^{-8} cm^3 STP/g, m.y.), respectively. These duction rates together with the measured He^3, and Ar^{38} concentrations in Bruderheim and R ardton predict exposure ages of 24 and 16 r respectively, for these meteorites.

Leon T. Silver (California Institute of T nology, Pasadena, Calif.), *Major Gabbroic M matic Events and Geochronology.* In the app tion of absolute dating methods to problem correlation in Precambrian terranes, greater u zation of petrologic considerations is suggested guiding the search for significant samples. such concept involves the episodic occurrenc widespread gabbroic intrusions and extrusions served over large segments of continents. You examples of such events, spatially extensive limited in duration, are recorded from st graphic relations since Cambrian time. Altho gabbros are not yet readily dated, demonstr related differentiates containing suitable ra active minerals are well known in many a Further, gabbroic rocks and their differentl are distributed commonly in relatively st crustal regions as well as in orogenic belts. proposed from scattered work by many inves tors as well as from some preliminary new that one such event may have occurred a 1150 to 1200 m.y. ago in North America. Co mation of this event, and of similar older younger events, requires concerted efforts of m workers in geochronology and petrology. Pos rewards are great. Such magmatic events can vide time reference points for correlation bet present isolated exposures of old tectonically tive regions (in this example, Transverse Ra in California and the southeastern Cana Shield) and equally old but relatively stable tal regions (for example, Arizona, Montana, the Lake Superior area). Conversely, once onstrated to be contemporaneous, the charac tics and origins of continent-wide related matic and orogenic phenomena can be evalu Also, widespread sampling of materials de from the lower crust or upper mantle at va known intervals in the earth's history woul feasible.

S. F. Singer (University of Maryland, Co Park, Md.), *Dust Shell around the Earth.* W ple and Öpik have shown that nearby interp tary (zodiacal) dust describes orbits very si to that of the earth. The assumption can ther be made that its geocentric velocity distrib is isotropic. It then follows from Liouville's orem that the hyperbolic orbits of dust par under the influence of the earth's gravitat field will tend to enhance the dust density i vicinity of the earth. A peak density is rea at an altitude of about 1000 km above sea l

s peak is not connected with any effects of the nosphere. The amount of this maximum de- nds on the ratio of geocentric velocity to escape locity from the earth's surface. For a ratio of the enhancement factor (over the interplane- y value) is of the order of 60 and is independ- t of the mass of the dust particle. Smoke parti- s (defined by diameters less than 1 μ) will also gravitationally attracted but, in addition, are ject to electromagnetic and radiation forces. mechanism is suggested which would lead to ir capture and the subsequent increase in the oke particle density around the earth. It is ly that the density of dust plus smoke ex- ds the density of the atmosphere beyond an itude of about 3000 km. In that case, dust pro- les the main limitation to the intensity of the ton radiation belt and explains the existence of naximum at ~2000 km and subsequent decrease the intensity of trapped protons. Accepting this pothesis, we can calculate the dust particle nsity at 6000-km altitude as about 2.6×10^{-20} m^3. A simple experimental test is proposed to t this deduction.

S. F. Singer and E. H. Walker (University of ryland, College Park, Md.), *A Lunar Iono- here.* A peculiar kind of 'ionosphere' is shown exist near the lunar surface. Unlike the usual osphere, the lunar electron layer is not caused photoionization of an existing neutral atmos- eric gas. Instead, bombardment by solar ultra- let photons leads to photoemission from the ar surface and to the formation of a space- rge-limited 'electronosphere' having a density ~10^4 cm^{-3} at the surface. The electric field pro- ced can exert considerable forces on positively rged dust particles which may be liberated m the lunar surface by meteor impact. With appreciable density of dust particles, the space rge is reduced and the ionosphere can expand altitudes of several meters with enhanced elec- n densities. Therefore, the moon has an iono- here made up of positively charged dust parti- s and negative electrons.

Paul A. Siple (U. S. Army Research Office, shington, D. C.), *Correlations of the Earth's lar Motions with Angular Momentum and Seis- city.* Geophysical interrelations between varia- ns in the length of day (L.O.D.), seismicity, d the polar motions from 1900 to 1960 observed the International Latitude Service are an- zed. This analysis employs interpretations of generally accepted fact that the earth's polar tion is an Euler rotation complicated by dy- mic distortions and self-adjustments of a freely ating, plastic-like spheroid. The rate of succes- e formation of polar-motion circles is a meas- of that portion of the earth's total momentum ended by slow turning of the earth's body out the inertial axis. Variations in rate of ro- ion about the spin axis and about the inertial axis are fast and slow simultaneously, but the latter are in the opposite direction to the former and total angular momentum is thereby conserved in a ratio of approximately 6.3×10^{10}. The radii of polar-motion circles, representing the separation of the pole of inertia from the spin pole, may be interpreted as a first-order indication of earth strain which, in turn, requires major earthquakes to reduce the strain and return the poles to closer proximity. Migratory second-order, pulse-like strains occur 8 to 12 times a year (1956–1960) which may or may not trigger earthquakes when the inertial pole responding to mass distribution moves rapidly a few feet away from the spin pole. These pulses are directed along definable meridians in a west to east succession and do not persist for more than a month or so at a time.

William F. Slawson (Geophysics Laboratory, University of Toronto, Toronto, Ont., Canada), and Carl F. Austin (New Mexico Bureau of Mines and Mineral Resources, New Mexico Institute of Mining and Technology, Socorro, N. Mex.), *Definition of a Geological Structure through Lead Isotopes.* The isotopic constituents of lead in galenas from west-central New Mexico appear to be related to the locations of the samples. 'Modern' leads form a belt bounded on either side by 'anomalous' leads. The 'modern' lead belt extends for more than 130 miles and lies essentially along a line defined by the towns of Alamogordo and Socorro, New Mexico. Geologists have postulated a regional lineament to lie under the belt defined by the 'modern' lead samples. This structure is known variously as the Zuni, Zuni-Sacramento, or New Mexico–Utah lineament in the literature. We propose that lead isotopes may show a rational geological control and thus should be among the interpretive tools available to geophysicists and geologists.

Alex. G. Smith, T. D. Carr, N. E. Chatterton, and Heins Bollhagen (Department of Physics, University of Florida, Gainesville, Fla., and Maipú Radioastronomical Observatory, University of Chile) *Spectral Distribution of the Decameter-Wavelength Radiation from Jupiter.* Observations of the decameter-wavelength radiation from Jupiter have been conducted from both hemispheres of the earth during 1960, and have extended from 10 to 27.6 Mc/s in frequency. During the period of these observations, the probability of occurrence of the radiation peaked rather sharply in the vicinity of 18 Mc/s. Data taken in 1958 and 1959 over a more limited range of frequencies show a similar trend. The same quantitative analysis indicates that the activity passed through a minimum in late 1958 or early 1959, showing an inverse correlation with sunspot number. During 1960 dynamic spectra of individual noise pulses were obtained with a swept-frequency receiver utilizing motion-picture recording. These spectra typically showed pulse bandwidths of the order of

a few tenths of a megacycle, although many pulses recorded more recently in 1961 have had broader spectra, ranging up to 1 or 2 Mc/s in width. Some pulses appear to be split, with peaks appearing at two or more closely spaced frequencies. Noise storms frequently were observed to drift up or down the spectrum with the passage of time, with a drift toward lower frequencies being observed more often.

E. J. Smith and D. L. Judge (Space Technology Laboratories, Inc., Los Angeles, Calif.), *Transient Variations in the Extraterrestrial Magnetic Field: Explorer VI.* Data from the Explorer VI magnetometer reveal the existence of transient variations in the distant geomagnetic field with periods exceeding 1 minute. The occurrence of such fluctuations is a characteristic feature of magnetic storms. Correlations have been observed between these variations and ground station magnetometer records, as well as variations in the flux of charged particles as observed by the Explorer VI scintillation detector. Several distinct transients have been analyzed which were observed at geocentric distances beyond 5 earth radii during the magnetic storms of August 16 and September 3, 1959. The experimental data are presented and the physical cause of these transients is discussed.

L. G. Smith (Geophysics Corporation of America, Bedford, Mass.), *Electron Density Measurements by the Asymmetrical Bipolar Probe.* The use of an asymmetrical bipolar probe for measurement of electron density and electron energy distribution in planetary ionospheres is discussed and is illustrated with data from a rocket flight in the terrestrial ionosphere. Consideration of the area ratio of the two probe electrodes shows that the ratio must be greater than the ratio of electron to positive-ion random current densities if the complete energy distribution is to be obtained. If, in addition, the area ratio is made greater than the current density ratio by a factor of 10, the current-voltage characteristic for the smaller electrode may be treated as that of a single probe, studied by Langmuir and Mott-Smith. The compactness and essential simplicity of the instrument make it attractive for inclusion in satellites and space probes.

Stewart W. Smith (Seismological Laboratory, California Institute of Technology, Pasadena, Calif.), *Fine Structure of the Earth's Spectrum.* It has recently been shown that, owing to rotation, the nth mode of oscillation of the earth should be split into a multiplet of $2n + 1$ lines. The digitized recording of the Benioff strain seismometer at Isabella, California, has been extended to include the 26-day interval following the Chilean earthquake, and high-resolution spectral analyses have been carried out on certain narrow frequency bands. Three spheroidal modes and two toroidal modes are found to be split. The measured values of splitting parameter β are:

Spheroidal Mode	β	Toroidal Mode
S_2	0.41	${}_1T_2$
S_3	0.18	${}_1T_3$
S_4	0.14	

The frequency increment between split line given by $\beta/1440$, in cycles per minute. The r mode with a period of 20.46 minutes appears single line. The results for the spheroidal m agree well with theoretical values. Measurem of the toroidal modes are not as reliable, but indicate that the splitting may be significa larger than can be explained by the rotation ef It is noted that the energy level in the line c sponding to $m = 0$ (zonal harmonic) of mod and S_3 appears to increase with time relativ the other modes. Cross spectral analyses have carried out between tide gage recordings of Chilean seismic sea wave in the Los Angeles harbor from May 22 to May 29 and several l period recordings of the earthquake disturb over the same interval. The coherence indic that some of the previously unidentified peak the spectrum of the Chilean earthquake periods greater than that of the fundamental m may be caused by coupling from oscillations in water level along the coast of southern Califo excited by the seismic sea wave. Data from large magnetic storms of July 1959 and Nove 1960 indicate the possibility that magnetoel coupling is sufficient to excite free oscillations.

Mirco P. Snidero (U. S. Weather Bureau, W ington, D. C.), *Data Processing at the JN Unit.* Rapid and reliable data processing, inv ing the reception, reduction, and transmissio meteorological information, is essential if JN is to meet its many commitments. A new puter with 8 to 10 times the capability of previous one used at JNWP is the heart of automatic data-processing system. Other cha in both equipment and technique have been i porated into the system so that it might b handle the increased volume of incoming and going information. This new data-processing tem is described and some comparisons are with the previous system. Mention is also ma additional changes soon to be introduced int system.

Conway W. Snyder (Jet Propulsion Labora Pasadena, Calif.), *Interplanetary Space Ex ments for the Venus Probe Mariner A.* The spacecraft in the NASA planetary program, ner A, will spend three to four months bet Earth and Venus, during which time it is pla to make a variety of measurements on the planetary environment. The principal interp tary scientific questions to be investigated a the intensity, energy spectrum, and charge

n of the galactic cosmic rays, their temporal
l spatial variations, and the mechanism re-
nsible for the variations; (2) the fluxes, ener-
s, and identities of charged particles emitted by
sun, and their correlation with observable
ar and terrestrial events and with the interplan-
ry magnetic field; (3) the intensity, spatial
tribution, and nature of the belt of magnetically
pped charged particles around Venus (if such
ts exist); (4) the intensity and form of the
ar magnetic field; (5) the intensity and general
pe of the magnetic field of Venus; and (6) the
ber, distribution, orbits, energy, and momenta
cosmic dust particles. Electromagnetic radia-
n from Venus and its atmosphere in the ultra-
let and millimeter wavelength regions will be
alyzed for a few hours as the spacecraft passes
planet. The instruments planned for making
measurements are described. Criteria for choos-
experiments for the mission are discussed.

V. M. Snyder (Tennessee Valley Authority, oxville, Tenn.), *Some Possibilities for Multiiate Analysis in Hydrologic Studies.* The techue of multivariate analysis is proposed for ain hydrologic applications where multiple ression produces unsatisfactory results. A multiiate approach circumvents two very restrictive ic premises of the regression technique—conment of statistical error to the dependent iable and assumption of no correlation among independent variables. Elimination of the t premise allows formulation of a single relaship between two variables which is invariant er an interchange of the dependent and indeident variables. Correlation among the indeident variables is overcome by transformation a smaller set of orthogonal components which independent. Transformation back to original iables establishes an equation having terms suring independent contribution of the varies to the prediction of the dependent variable. e disturbing fluctuations of regression coefnts with changing form of the regression equaare suppressed. Comparative calculations of ltiple regression and multivariate analysis are sented for three applications. First, the simple -variable relationship is presented. Second, the rovement in establishing a relationship been the rainfall and runoff is shown. Multivari- analysis produces a logical equation but ltiple regression does not. Third, an applicaof multivariate analysis is shown in improvthe convergence to solution in the iterative nique of nonlinear least squares.

Emanuel M. Sodano (U. S. Army Map Service, shington, D. C.), *Optimum General Solution the Inverse, Direct, and Intersection Problems spheroidal Geodesics.* For many years geodesists e tried to develop an optimum form of solu for computing distances, azimuths, and posis on the spheroid. One such effort was published by this writer (*Bulletin Géodésique,* 1958). Through subsequent discussions with recognized authorities, additional practical and theoretical requisites have been established. For example, the inverse and direct solutions are a perfectly matched pair of rigorous noniterative solutions exhibiting a uniquely natural, simple, and concise pattern. Whereas the inverse and direct solutions are used to compute single geodesics such as base lines, traverses, and guided-missile paths, adjustments of triangulation and trilateration require the simultaneous solution of two intersecting geodesics. This has been undertaken rigorously on the spheroid itself (rather than by application of spheroidal excess to plane triangles) for accurate computation of nets or very large as well as small triangles. The basic spheroidal power series are complemented by closed formulas designed to yield each sought quantity in a single step. A new and better formula for accurately solving short sides of spherical triangles is also presented.

John R. Spreiter and Benjamin R. Briggs (National Aeronautics and Space Administration, Ames Research Center, Moffett Field, Calif.), *Theoretical Determination of the Form of the Boundary of the Solar Corpuscular Stream Produced by Interaction with the Magnetic Dipole Field of the Earth.* The interaction between a neutral stream of ionized solar corpuscles and the field of three-dimensional magnetic dipole, representing the geomagnetic field, is investigated. It is assumed, as is shown to be valid by Ferraro, that the stream is confined to the exterior and the magnetic field to the interior of a hollow, the boundary of which is very thin compared with its dimensions. The shape of the hollow is determined by application of an approximate method of solution. Results are presented for the trace of the boundary of the hollow in the meridian plane containing the sun-earth line and the dipole axis for several relative orientations, and also for the trace in the equatorial plane for the case in which the dipole axis is normal to the sun-earth line. The stability of the boundary is investigated, and it is shown that a portion of the boundary is unstable in the polar regions. A measure of the accuracy of the approximate method of solution is provided by a comparison of the results indicated by exact and approximate solutions of the corresponding two-dimensional problems.

John B. Stall and James C. Neill (State Water Survey Division, Department of Registration and Education, Urbana, Ill.), *A Partial Duration Series for Low-Flow Analyses.* A partial series of low-flow events is described which is particularly useful in the design of an impounding reservoir. The generation of the series is described. An important feature of the series is the introduction of the duration of the low flow as a parameter. For use in Illinois, low-flow series are developed for durations varying from 1 to 60 months. As com-

pared with the more easily interpreted annual series, one of the principal advantages of this partial series is its suitability for use with low-flow periods of duration greater than 12 months. A recurrence interval is assigned to each low flow in the series. Coordinates are presented for the graphical representation of this low-flow series. The runoff is plotted on a logarithmic scale versus the recurrence interval which is plotted on a scale following the extreme value law.

HEINZ STAUFFER (School of Science and Engineering, University of California, La Jolla, Calif.), *Cosmogenic Rare Gases in Stone Meteorites.* The abundances and isotopic compositions of argon, neon, and helium in achondrites have been measured. The rates of production of rare gas isotopes by cosmic-ray-induced spallation depend strongly on the chemical composition of the meteorites. The ratios Ne^{21}/Ar^{38}, He^3/Ne^{21}, and He^3/Ar^{38} are found to be remarkably constant for chrondites, which is to be expected because of their uniform chemical composition. For achondrites, these ratios show large variations. Relative production rates of rare gas isotopes from the different elements can be estimated.

JOHN S. STEINHART (Department of Terrestrial Magnetism, Carnegie Institution of Washington, Washington, D. C.) and George P. Woollard (Department of Geology, University of Wisconsin, Madison, Wis.), *Linear Analysis of the Results of Explosion Seismic Measurements on the Continents.* Relationships between crustal thickness, gravity anomalies, elevation, and observed velocities have been reported or postulated in recent years. To ascertain whether some or all of these relationships were supported by the data from explosion seismology on the continents, results of 73 measurements of crustal thickness were subjected to simple and multiple linear regression analysis. The following equation was fitted to the data: $D = K_1 + K_2V_n + K_3\bar{V} + K_4E + K_5R + K_6B + K_7I$ where D is the crustal thickness, K_i is the ith linear regression coefficient, V_n is the upper mantle velocity, $\bar{V}$ is the mean crustal velocity, E is the elevation, R is the regional isostatic anomaly (5° × 5° areas), B is the Bouguer anomaly, and I is the local isostatic anomaly (1° × 1° areas). The method is far too crude to discover subtle relations between variables, but certain consistent results permit some conclusions: (1) Of the above variables only the Bouguer anomalies and the mean crustal velocities exhibit strong linear relations with crustal thickness. (2) Considered alone in simple regression analysis, isostatic anomalies and elevation also exhibit significant linear relations with crustal thickness. (3) In no case is the constant term significant for gravity anomalies and elevation; thus it is not proper to speak of 'standard crustal thickness' for zero anomaly or elevation. (4) The data from the Soviet Union show consistent disagreement with those obtained elsewhere in the world.

O. S. STRICKHOLM and J. C. ROSE (Departm of Geology, University of Wisconsin, Madi Wis.), *A Discussion of the Pendulum Gra Interval between Washington, D. C., and Ott Ontario.* Pendulum measurements of the gra interval between Washington and Ottawa h been made since 1905. The older measurem before the development of crystal chronome were made with the Mendenhall apparatus. M ern observations with crystal chronometers h been made since 1952 with the Cambridge in pendulums, the D.O. bronze pendulums, and Gulf-Wisconsin pendulums. The older obse tions have a large standard error relative to modern results. Because of the desirability accurate direct comparison of absolute gra results at Washington and Ottawa, the gr from the University of Wisconsin has rece completed multiple pendulum connections in attempt to resolve differences of several mill between the results obtained with the three m ern types of apparatus. It is believed that Gulf-Wisconsin pendulum results for the inte are reliable to 0.1 mgal or better. The tenta result is that the value of gravity at the Ott base station is 502.71 ± 0.6 mgal higher tha is at the Washington base station.

MASAHISA SUGIURA (Geophysical Institute, versity of Alaska, College, Alaska), *Evidenc Hydromagnetic Waves in the Earth's Magn Field.* Elliptically polarized, damped magn waves of period about 6 minutes have been served at College, Alaska. These magnetic w are mostly confined in the auroral zones and found to occur simultaneously at the magneti conjugate regions in the northern and sout auroral zones. The observed magnetic oscilla appear to bear the required features of transv hydromagnetic waves in a gas of anisotropic trical conductivity. These hydromagnetic w are believed to have been generated in the ea outer atmosphere at altitudes of several e radii, and propagated along the lines of magn force. The frequency of occurrence of such netic waves is discussed.

GEORGE H. SUTTON, GARY V. LATHAM, and M RICE EWING (Lamont Geological Observa Columbia University, Palisades, N. Y.), *L Period Feedback Seismographs.* A long-p seismograph with a displacement transducer with feedback to a coil-and-magnet transd combines improved long-period response reduced sensitivity to long-term tilts or ultra-long-period disturbances. The feed greatly reduces the centering problems gene associated with displacement transducers. Va response characteristics can be obtained by ch ing the filtering and the gain in the feed loop. Outputs having different response chara istics can also be obtained from various poin the same system. Automatic or semiauto

oom centering can be accomplished by monitor-
g the level of the feedback signal. Several theo-
tical and actual seismometers employing these
chniques are being evaluated for possible use
lunar or ocean bottom seismograph systems and
improved station instruments.

James S. Sweet (U. S. Weather Bureau, Wash-
gton, D. C.), *Scientific Hydrology and Hydro-
gic Services in the U.S.S.R.* Hydrologic science
d services are prominent in the development of
e national economy of the U.S.S.R. Hydrologic
erature is abundant, but better selectivity could
used in publishing papers. Theoretical analysis
edominates, and a large portion of the litera-
re is devoted to winter hydrologic conditions.
elevant chauvinistic statements and political
opaganda often diminish the reader's confidence
a subject. Instrumentation is adequate and
ere are well-equipped experimental stations.
ganization of the hydrologic services are well
anned for the purposes of national economy.
ie hydrologic network is still inadequate but
swiftly growing. Publication of data is slow, as
is in other countries. Educational and research
ilities for hydrology exceed those of any other
ntry. The general conclusion is that Soviet
drologic activities are modern and progressive.

L. W. Swift, Jr. (Coweeta Hydrologic Labora-
ry, Southeastern Forest Experiment Station,
lard, Ga.) and C. H. M. van Bavel (Southwest
ater Conservation Laboratory, Agricultural Re-
rch Service, Tempe, Ariz.), *Mountain Topogra-
y and Solar Energy Available for Evapotrans-
ation.* The energy balance method of estimating
apotranspiration has been increasingly used by
drologists and agriculturists. Its acceptance by
resters and other workers concerned with steep
untain lands has been impeded by past exam-
es of poor agreement between energy balance
imates and other measurements made on moun-
n sites which have, on flatter lands, produced
se agreement. An adjustment of the solar
ergy quantity, the basic parameter designated
R_A in one energy balance formula, is proposed.
ie computation of this adjustment is briefly
tlined and sample values are presented. Com-
ted seasonal energy distributions for four actual
tersheds illustrate a high winter contrast be-
een slopes but relatively small differences in
mmer.

Manik Talwani, Bruce C. Heezen, and J.
mar Worzel (Lamont Geological Observatory,
lumbia University, Palisades, N. Y.), *Gravity
omalies, Physiography, and Crustal Structure
the Mid-Atlantic Ridge.* In 1958, a Graf sea
vimeter was used aboard the U.S.S. *Compass
and* to obtain continuous gravity measurements
oss the mid-Atlantic ridge. The entire mid-
lantic ridge is characterized by small positive
e-air anomalies, which for the most part range from zero to +50 mgal. The ridge is thus apparently in nearly isostatic compensation, departures being on the side of undercompensation. Bouguer anomalies are systematically smaller over the ridge than over the ocean basins. Minimum values are found over the crest provinces. A median rift valley associated with the mid-Atlantic seismic belt was found in earlier work to show a large positive magnetic anomaly. The free-air anomalies on the U.S.S. *Compass Island* gravity profile show a 50-mgal minimum over the rift valley. The minimum disappears in the Bouguer anomaly, however, showing that it was associated only with the rugged topography. A general structure of the ridge based on seismic refraction studies is assumed, and three possible sections of the ridge structure are presented to show how the structure changes under the crest provinces to provide the necessary isostatic compensation. These structures are discussed in light of the other geophysical anomalies associated with the crest provinces in general and the rift valley in particular.

H. P. Taylor, Jr. (Pennsylvania State University, State College, Pa.), A. L. Albee and Samuel Epstein (California Institute of Technology, Pasadena, Calif.), *O^{18}/O^{16} Ratios of Coexisting Minerals in Three Mineral Assemblages of Kyanite-Zone Pelitic Schist.* O^{18}/O^{16} ratios have been measured for several coexisting minerals in three pelitic schists from the Lincoln Mountain quadrangle, Vermont. The three mineral assemblages are (1) kyanite-chloritoid-chlorite-muscovite-paragonite-quartz-rutile, (2) chloritoid-almandine-chlorite-muscovite-paragonite-quartz-ilmenite, and (3) almandine-biotite-chlorite-muscovite-albite-quartz-ilmenite. Mineralogically and texturally these rocks appear to be equilibrium assemblages, and the three assemblages are possible compatible assemblages in rocks of somewhat different composition at the same metamorphic grade. The rocks were collected within 200 meters of one another from two metasedimentary formations of different gross composition. The area is a simple regional metamorphic terrane uncomplicated by intrusives; thus the field evidence also suggests that these rocks are probably of identical metamorphic grade. In each assemblage quartz has the highest O^{18}/O^{16} ratio and is followed in consistent order by white mica, kyanite, biotite, chlorite, and ilmenite; chloritoid, rutile, garnet, and albite were not analyzed. Within the experimental error, a particular mineral has the same oxygen isotopic composition regardless of which assemblage it occurs in; hence the isotopic fractionations among the minerals are also identical for the three schists. These data strongly suggest that oxygen isotopic equilibrium was established during metamorphism and was attained at the same temperature for all three rocks. In addition, identical O^{18}/O^{16} ratios for a particular mineral in the three rocks indicates that oxygen isotopic exchange occurred between them. The actual O^{18}/O^{16}

ratios of the rocks are in the range that could be expected if the equilibration occurred in communication with a widespread oxygen-bearing fluid of constant O^{18}/O^{16} ratio.

Lee R. Tepley (Lockheed Missiles and Space Division, Palo Alto, Calif.), *Observations of Hydromagnetic Emissions.* Preliminary results of a frequency-time analysis of geomagnetic micropulsations in the frequency range 0.5 to 5 cps are presented. The data from which these results derive were recorded near Palo Alto, California, November 18 to 21, 1960. At times, oscillatory signals of slowly varying frequency were observed continuously for periods of many hours. Signals of more rapidly varying frequency were also observed, but for shorter periods of time, usually 10 to 30 minutes. Oscillations at the same frequencies were found to occur simultaneously on waveform records obtained at California Institute of Technology stations near Ely, Nevada, and near Isabella and Mount Palomar, California. The oscillations are called hydromagnetic emissions, since preliminary evidence implies that they are generated above the ionosphere and are propagated downward by hydromagnetic waves. The period preceding and including the interval during which data were obtained was characterized by magnetic storms and solar-flare activity which produced a number of geophysical effects and undoubtedly influenced the nature of the oscillations.

L. L. Thatcher (U. S. Geological Survey, Washington, D. C.), *Distribution of Tritium Fall Following the 1958 Weapons Tests.* Samples of tritium fallout in 1958 were collected at 12 locations ranging from Puerto Rico to Anchorage, Alaska. Integrated 14-day samples were analyzed in the U.S.G.S. tritium laboratory by electrolytic enrichment of the tritium followed by gas phase counting. Counting was in an anticoincidence array with heavy iron shielding. The sample preparation involved conversion to hydrogen by reaction with hot zinc and admixture of ethyl or methyl ether. The data show wide variations in tritium activity ranging from an average of less than 100 tritium units in coastal areas to several hundred tritium units in the interior of the continent. This observed dilution of tritium fallout in coastal areas by the relatively inactive atmospheric moisture of marine origin has its corollary in the chloride rainout data obtained by Junge's atmospheric chemistry studies which show that the effect of maritime moisture extends approximately 500 miles inland. A relatively poorly defined peak of tritium fallout appeared in late May and June for the continental U. S. stations and in July for northern stations.

Edward Thiel (School of Mines and Metallurgy, University of Minnesota, Minneapolis, Minn.) and Ned Ostenso (Geophysical and Polar Research Center, University of Wisconsin, M son, Wis.), *Seismic Studies on Antarctic Shelves.* Three methods have been employe Little America V to determine seismic velocit a function of depth in the Ross ice shelf: (1) fraction shooting interpreted by means of Herglotz-Bateman-Weichert integral, (2) sei logging of a deep borehole, and (3) Robin's mula relating P-wave velocity to the density temperature measurements made in the bore Results of the three methods are compared, crepancies are discussed, and the preferred P S velocity profiles are presented. From the files and the borehole density measuremen complete determination of the elastic prope of the ice shelf is possible. The effect of cr orientation on seismic velocity is analyzed, a new determination of the variation of velocit ice as a function of temperature is made on basis of recent experimental work.

E. Roy Tinney (Washington State Univer Pullman, Wash.), *The Process of Channel gradation.* Degradation is defined as the lowe of the bed of a channel that occurs whenever sediment discharge into a section of the cha is less than the transporting capacity of the st at that section. The formulation of a degrad theory begins with the equation of continuity sediment. When the tractive force, the depth slope of the energy gradient, and the conventi backwater equation are introduced there resu first order partial differential equation for degradation as a function of time and pos along the stream. Laboratory tests with uni sediment verified this equation for the tran phase as well as the end point. However, b the equation can be applied to natural strea more realistic formula for sediment load mus employed, a quantitative explanation of so which armors the bed and inhibits degrad must be developed, and the seasonal variatio flow rate must be considered.

L. J. Tison (61 Rue des Ronces, Gentbr Belgium), *Local Scour in Rivers.* It has found that the scour in rivers is influenced only by the water velocities but also by the vature of the streamlines. An obstacle wit arbitrary shape placed in a stream produces vatures which are the origin of a scour and an intensity given by the following expressio

$$\frac{1}{g}\left[\int \frac{v^2}{\rho}\,ds - \int \frac{v'^2}{\rho}\,ds\right]$$

where v is the velocity at the surface, v' i velocity in the neighborhood of the bottom, is the radius of curvature of the streamline. integrals are taken along a line tangent at point to the principal normal of the stream Some applications of this relationship betwee scour and the radius of curvature are present

LEMENT J. TODD (Atmospheric Research Group, adena, Calif.), *Presentation to the Forecaster Bottleneck in Meteorology.* The remarkable ed and flexibity of the human mind gives the nan forecaster a distinct advantage over the chine when it comes to solving the extremely ied present weather and short forecast prob- s. At present, however, the forecaster is not e to solve these problems to the full potential the data and communications of the meteor- gical system. The bottleneck is in the fore- er's ability to comprehend and relate the perti- t information which the system presents to . A study of the presentation shows that it oses many unnecessary mental burdens on the ecaster; it taxes low-capacity channels of the nan mind yet ignores channels where greatest ntal abilities lie. Some approaches are suggested lessening the presentational problem. These roaches are compatible with the whole meteor- ical system and simple enough to be used at outlying forecast stations. One of the ap- aches suggested gives the meteorologist the il- on of the terrain rising through the weather aces and make it possible for him to make atitative comparison in three dimensions.

WILLIAM H. TOLBERT and GARRETT G. SALSMAN S. Navy Mine Defense Laboratory, Panama . Fla.), *Nearshore Microtopography of the Sea om Adjacent to Panama City, Florida.* A otopographical study of the sea bottom off ama City, Florida, was conducted. Bottom ons were established to study the size, shape, number of ripples, mounds, and depressions. echanical sieve analysis of bottom sediments made to determine median diameter and sort- coefficient. Seasonal patterns were shown to in the formation decay and areal extent of les, mounds, and depressions. Maximum bot- relief due to sand sediments is of the order inches. Median diameter of local sand sedi- ts range from 0.11 to 0.59 mm. The finer sedi- ts occur close to the shore.

WILLIAM H. TOLBERT and GARRETT G. SALSMAN S. Navy Mine Defense Laboratory, Panama , Fla.), *Marine Life off Panama City, Florida.*

HAROLD B. TOLEFSON and ROBERT M. HENRY tional Aeronautics and Space Administration, ley Research Center, Langley, Va.), *A hod of Obtaining Detailed Wind-Shear Meas- ments for Application to Dynamic Response ems of Missile Systems.* The development of ient missile systems requires more precise surements of the winds and wind shears within atmosphere than are provided by existing ding methods. The gross smoothing inherent lloon soundings effectively filters out the ll-scale wind variations which are of consid- le importance to missile response problems. ethod in which the detailed structure of the vertical wind profile is determined from photogrammetric measurements of the successive positions of a smoke trail left by a vertically rising missile has been developed and applied. The method is described in this paper and its accuracy is discussed. Results in the form of wind profiles for several measurements are presented. Particular attention is given to the continuous and random nature of the wind disturbances as a function of altitude. The implication of these disturbance characteristics to missile response is indicated.

SEAN A. TWOMEY (Commonwealth Scientific and Industrial Research Organization, Sydney, Australia), *Addition of Salt to the Air from Land Surfaces.* Certain results in cloud physics appear to be explainable only by the release from soil surfaces of large numbers of condensation nuclei which are capable of growing into cloud droplets at relative humidities between 100 and 101 per cent. Laboratory experiments have confirmed the fact that dry soil surfaces do release nuclei of this kind when heated by infrared radiation. Evidence is presented that these nuclei are most probably salt particles of submicron size produced from the natural soil salts by processes occurring during the diurnal temperature-humidity cycle. The mass transport of salt produced in this way is probably too small to be measured directly, but the effect, through its influence on the colloidal structure of clouds, may be an important climatic factor.

S. V. VENKATESWARAN (Institute of Geophysics, University of California, Los Angeles, Calif.), and JAMES G. MOORE and ARLIN J. KRUEGER (U. S. Naval Ordnance Test Station, China Lake, Calif.), *Determination of the Vertical Distribution of Ozone by Satellite Photometry.* A method of determining the vertical distribution of ozone and other atmospheric constituents by 2-color photometry of Echo I is described. Vertical distributions of ozone as derived from the photometric observations for two separate satellite passes in December 1960 are given. The material presented is based upon an article by the same title published in the June 1961 *J. Geophys. Research.*

E. H. VESTINE (Rand Corporation, Santa Monica, Calif.), *Some Aspects of the Survey of the Magnetic Field of the Moon and Planets.* The measurement of a lunar or planetary magnetic field by a magnetometer aboard a space vehicle designed for either hard or soft landings is considered. Such a magnetometer would define the magnitude and distribution of the lunar or planetary magnetic field, the magnitude of the noise level in the field, and the possible time variations of the field intensity. Continuous magnetic measurements of field components at points along a terminal landing path reaching the lunar or planetary surface, supported by one or more surface magnetic observatories, should serve most requirements. It is also desirable to note ionization and

energetic particles en route. The time rate of change of these components should also be measured. A large magnetic field would indicate that the body, or a substantial part of it, was probably molten at one time or has a core still in a molten condition. In the case of the moon it may then be inferred that the mantle subsequently cooled in a magnetic field generated within the moon. Any such initial field would decay rapidly with time. The rotation of the planets and their core size in relation to their general magnetic field is discussed.

K. von Bulow (University of Rostock, Germany), J. Green (North American Aviation, Inc., Downey, Calif.), and G. C. Amstutz (School of Mines and Metallurgy, University of Missouri, Rolla, Mo.), *Structural Features of the Moon.* A geometric, purely descriptive nomenclature for the surface features of the moon is not yet available. Most of the terms presently used contain genetic connotations and imply assumptions. In recognition of this fact, an international, purely descriptive terminology is here proposed. It contains subdivisions according to the size, the shape (linear and ring features) and the place of occurrence (terrae, maria). The terminology primarily contains purely geometric terms such as ring, polygon, lime, and wall. In addition, it consists of descriptive and figurative expressions which describe by comparison, such as the terms mare, continent, valleys, fissures, mountains, or rays. Terms are avoided such as volcanic craters, impact craters, meteor scars, which imply a (premature) genetic connotation.

James R. Wallis (U. S. Forest Service, Berkeley, Calif.), *The Relation Between Metal Cations and Soil Erodibility.* The inherent erodibility of 20 soils was indexed using Middleton's dispersion ratio and Anderson's surface-aggregation ratio. These indices were then used as dependent variables for several regression analyses. The milliequivalents per 100 grams of oven-dried soil for the four most plentiful soil cations (Ca, Mg, K, and Na) were determined and then used as independent variables in the regressions. The best fit to the data was found to be a quadratic equation with the milli-equivalents of $Ca^{++} + Mg^{++}$ as the variable. Both the first-power and the second-power terms were significant at the arbitrarily selected 5 per cent level.

L. S. Walter, P. J. Wyllie, and O. F. Tuttle (Department of Geophysics and Geochemistry, Pennsylvania State University, University Park, Pa.), *Phase Relations in the System MgO-CO_2-H_2O.* Investigation of the phase relations in the system MgO-CO_2-H_2O by the sealed capsule technique has demonstrated that melting does not take place in the temperature-pressure region from 600° to 1400°C and from 1000 to 4000 bars. The amount of MgO soluble in the vapor phase at 1000 bars and at temperatures up to 1200°C is less than 1.
per cent. The univariant reaction, $MgCO$
$Mg(OH)_2 \rightleftarrows MgO + V$ proceeds at (*a*) 630°
1000 bars, $V = 6$ wt. per cent of CO_2, and (*b*) 7
at 4000 bars, $V = 4$ wt. per cent of CO_2. The
bon dioxide content of the vapor in equili
with magnesite and brucite decreases with dec
ing temperature and increasing pressure. Br
cannot coexist with a vapor containing more
a small amount of CO_2 in the P-T range studi

William C. Walton and William H. W
(Illinois State Water Survey, Urbana, Ill.),
uating Wells and Aquifers with Analytical M
ods. The application of available analytical r
ods to problems involving the evaluatio
several well systems and aquifers in Illin
described. This evaluation is intended to a
such questions as how much ground wat
available for development and what will b
consequences of exploitation. Actual ground-
conditions are simulated with model aquifers
ing straight-line boundaries, effective w
lengths and thicknesses, hydraulic properties
sometimes confining beds with effective
nesses and vertical permeabilities. Mathem
models are based on model aquifers, the in
well theory, and ground-water formulas.
histories of ground-water development in six
in northeastern, east-central, and central Il
indicate that aquifer behavior actually does
cide rather closely with what would be pred
theoretically with model aquifers and mathe
cal models.

R. K. Wanless, C. H. Smith, W. D. Love
and J. A. Maxwell (Geological Survey of
ada, Ottawa, Ont., Canada), *Magnesium Is*
Variations in Nature. Magnesium isotope st
are being carried out by the Geological Surv
Canada as one phase of a comprehensive
of the ultrabasic rocks of Canada. Since
nesium is a major constituent of these
knowledge of the isotopic distribution in v
geological environments would be invaluab
elucidating processes operative during their f
tion and alteration. The paucity of data i
literature necessitated a reconnaissance surv
magnesium-bearing minerals to establish th
sible existence and range of natural isotopic
tions. A solid-source mass spectrometer equ
with a triple-filament source and an electron
plier detection system has now been asse
and isotopic analyses of a comprehensive
of minerals has been undertaken. Olivine, se
tine, magnesite, brucite, hydrothermal and
mentary dolomite, plant material, and met
magnesium samples have been analysed
spectrometrically. The ratio Mg^{24}/Mg^{26} is sl
but significantly higher in low-temperature
erals (chrysotile asbestos) and plant materia
in high-temperature minerals (olivine) and
oritic magnesium. Analyses are being con

a suite of magnesium-bearing minerals repre-
ting a wide range of geological environments.

D. Q. Wark and R. W. Popham, (U. S. Weather
reau, Washington, D. C.), and W. A. Dotson
K. S. Colaw (U. S. Navy Hydrographic Of-
, Washington, D. C.), *Simultaneous Observa-
ns of Ice from Aircraft and Tiros II.* During
last week of January 1961, reconnaissance air-
ft observations were made of ice conditions
r the Gulf of St. Lawrence and in the Atlantic
Newfoundland. Simultaneous Tiros II narrow-
le pictures were taken. Mosaics of the satellite
tures are shown and compared with visual and
otographic observations from aircraft.

Ferris Webster (Woods Hole Oceanographic
titution, Woods Hole, Mass.), *The Kinetic
rgy Balance of Gulf Stream Meanders.* The
lf Stream, in the region upstream from Cape
teras, executes lateral meanders having periods
about a week. Calculations have been made,
g surface velocity observations, of the trans-
of kinetic energy from these meanders to the
n flow at two separate localities in the Gulf
am. At both locations it was found that the
anders transferred momentum against the
city gradient, which is exactly opposite to
t would be expected if they were frictionally
en. The observations suggest that the mean
of the Gulf Stream is increased by the kinetic
rgy of the meanders and that the meanders
uld therefore derive energy from sources other
n the kinetic energy of the mean flow. The
of meanders in the Gulf Stream appears to
similar, in some respects, to that of large-scale
urbances in the general circulation of the at-
sphere.

. Weertman (U. S. Army Snow, Ice and
rmafrost Research Establishment, Corps of En-
eers, Wilmette, Ill.), *Mechanism for the For-
tion of Inner Moraines Found near the Edge
Cold Ice Caps.* A new mechanism is described
ch explains the formation of inner moraines
he ablation areas of cold ice caps. The mecha-
n involves the freezing of water onto the bot-
surface of an ice cap. This water comes from
er regions of the bottom surface where the
bination of the geothermal heat and the heat
duced by the sliding of ice over the bed is
cient to melt ice. The water freezing onto the
tom surface can trap debris from the bed in
ice. The frozen-in layers of debris will lead to
formation of inner moraines. The older shear
othesis was that the moraine-forming debris
rs were scraped from the bed along active
ar planes in the ice mass. A number of criti-
s are made of the shear hypothesis, which
been advanced to explain moraines occurring
Baffin Island and near Thule, Greenland. It is
cluded that this older hypothesis may be in-
quate to account for these moraines. Although in theory the mechanism proposed in this paper undoubtedly will lead to the formation of moraines, the existing field data are insufficient to prove conclusively that actual moraines have originated by means of this mechanism.

R. C. Wentworth (Lockheed Aircraft Corporation, Missiles and Space Division, Palo Alto, Calif.) and W. M. MacDonald (University of Maryland, College Park, Md.), *The Possible Absence of Equatorial Orbits for Geomagnetically Trapped Electrons.* The Fokker-Planck equation has been used by MacDonald and Walt (*Ann. Phys.*, in press) to derive the general second-order partial differential equation which governs the diffusion of charged particles trapped in a magnetic mirror geometry. If energy loss is ignored, an equation in particle pitch angle and time results. The general solutions to this equation imply that, for equilibrium conditions, equatorial orbits (pitch angle 90° in the equatorial plane) are virtually missing. In this paper the diffusion equation is derived, in pitch angle and time, by examining the results of scattering which occurs at a general point along the line of force. Such an approach enables us to discuss the physical reasons for the absence of equatorial orbits. In the actual radiation belt, energy loss and an unknown source function may modify the situation.

Allen J. West (U. S. Forest Service, Berkeley, Calif.), *Cold Air Drainage in Small Forest Openings.* In analyzing 3 years' snow accumulation data in four small forest openings we found that more water always accumulated in the downhill segment of the openings than in the uphill segment. The small forest openings had dense coniferous borders, were in moderately steep terrain (20 to 40 per cent), and represented north, south, east, and west slopes. For each year and for each aspect, the additional water accumulating in the downhill segment of the snowpack ranged from 3.4 to 13.1 inches and averaged 7.4 inches. This greater accumulation is thought to be associated with cold air draining down the slopes and becoming ponded when it is slowed down by trees at the bottom of the openings. In turn, this ponded cold air reduces snow melt in the winter. A short-term side study showed that less evaporation and lower temperatures occurred in the downslope segment of the openings. Rain on snow and snow creep were not considered to be causes of the greater accumulation. Snow density throughout the openings was about the same.

Harry Wexler (Office of Meteorological Research, U. S. Weather Bureau, Washington, D. C.), *Program and Plans for Meteorological Research in the U. S. Weather Bureau.*

Robert M. White (Travelers Research Center, Inc., Hartford, Conn.), *Meteorological Research at the Travelers Research Center.*

Linwood F. Whitney, Jr., and Sigmund Fritz (U. S. Weather Bureau, Washington, D. C.), *A Tornado-Producing Cloud Pattern Seen from Tiros I.* A small, bright, isolated cloud mass was observed by Tiros I over the Central Plains near an area of known tornado activity. The rectification of the Tiros picture is shown, the meteorological situation is presented, and a comparison of the picture content is made with the synoptic events. Evidence is presented indicating that (1) the first intense convective activity was associated with the isolated cloud mass shown in the picture, (2) the cloud mass was located in an area possessing characteristics found in tornado development situations, and (3) the cloud mass later expanded and spread northeastward spawning hail and tornadoes in central Oklahoma. Several other significant features were seen in the satellite picture, including a prominent boundary separating a very dark area from a somewhat brighter area. This boundary corresponds to a dewpoint 'front' or strong moisture gradient separating very dry air from moister air.

M. H. Wilkening and Minoru Kawano (New Mexico Institute of Mining and Technology, Socorro, N. Mex.), *The Effects of Thunderstorms on the Radon-Daughter Ion Content of the Atmosphere.* Measurements made on Mt. Withington during the summers of 1958 and 1960 show that marked reductions in the concentration of radon-daughter positive ions occur when thunderstorms pass over or near the mountaintop station. The positive ions which result when natural radon and its daughter products decay in the atmosphere are collected on a bare copper wire arranged concentrically inside a sheet-metal tube through which the sample air stream passes. The wire is maintained at a negative potential of 2000 volts with respect to the tube. The presence of a thunderstorm in the vicinity of the station can result in a reduction in the number of radon-daughter ions collected by the apparatus to 1/10 or less of the normal fair-weather value. Correlation with the electric field associated with the thunderstorms indicates that the ions are removed from the air near the ground by strong negative potential gradients. The net upward flux of the ions constitutes a current density of the order of 10^{-16} amp/m^2. Thunderstorms appear to have a relatively minor effect on the actual radon concentration compared with the effect on the radon-daughter positive-ion content.

Dah-Cheng Woo and Ernest F. Brater (University of Michigan, Ann Arbor, Mich.) *Laminar Flow in Routh Rectangular Channels.* An investigation was undertaken to obtain a better understanding of the sheet flow produced by rainfall. Evidence obtained by Wisler and Brater (1959) from runoff plots indicates that such flow may be in the laminar range or in the transition range between laminar and fully developed turbulent flow. To study spatially v
ble flow produced by rain it was first necessa
establish the flow characteristics of steady
form flow for the same range of Reynolds'
bers and roughnesses. Experimental results
presented which should be of value in comp
flow in thin sheets over several types of surf
The range of the critical values of Reyn
number at which flow ceases to be laminar
been more clearly established. Flow in the lam
range deviates from the theoretical to an e
which varies with the surface roughness. For
rough surfaces there is an additional vari
due to slope.

A. H. Woodcock and A. T. Spencer (W
Hole Oceanographic Institution, Woods
Mass.), *Magma-Sea-Air Contact Areas as So
of Sea-Salt Particles.* The numbers and the
of the steam cloud particles arising where m
lava encounters sea water are given. Sampl
these particles were taken from aircraft w
the clouds during the 1960 Kilauea eruptio
Hawaii. Other samples were taken from ex
mental clouds formed in the laboratory. M
scope and flame-photometric methods of ana
showed the particles to be, in major part, sea
Size distribution studies reveal that the flash
ing, resulting from magma-sea-air contact,
duces salt nuclei of a size range in large part
that of nuclei normally arising from the sea
rate of production of these nuclei, per un
surface, is many millions of times greate
steaming magma than on the sea. A few s
kilometers of magma may thus equal in salt
cle production rate the total of all the oceans
possible significance of this finding in we
processes is mentioned.

G. P. Woollard and Ned Ostenso (Depart
of Geology, University of Wisconsin, Ma
Wis.), *Crustal Structure in Antarctica.* On
basis of the relation of gravity anomalies
surface elevation to crustal thickness as
mined in North America, it is possible to d
probable values of crustal thickness in Anta
from the known elevation of the rock surface
ice thickness and Bouguer gravity anomalies
rected for the mass deficiency of the ice. Ea
Antarctica appears to be underlain by a crust
ing a normal continental thickness. We
Antarctica, which consists of an island archip
appears to have a crust which is somewhat th
but which can only be considered to be contin
in character. This conclusion, based on g
and elevation data, is substantiated by long
mic refraction measurements which indic
normal crustal velocity for the area. On
assumption that the crust is regionally disp
downward by the load of superimposed ic
that it is hydrostatically supported by the m
the amount of isostatic rebound to be expec
the ice were removed would be approxim

0 feet. The mean depth of water over the arctic continental shelf, which lies, on the rage, 400 fathoms (2400 feet) below the nor- l level found on other continental shelf areas, ears to substantiate this conclusion.

. P. Woollard and J. C. Rose (University of sconsin Geophysical Research Center, Madison, s.), *An Evaluation of the World's Gravity Con-* . Using both pendulums and gravimeters over past ten years, we have effected ties to most the first-order gravity bases designated by the ernational Gravimetric Bureau as well as to ious national bases. The pendulum data, rked up independently and evaluated along h other pendulum data, have served as a basis calibrating the gravimeter used. Comparisons gravity values on the Potsdam system at the ious bases and the gravity intervals between es, as determined from the pendulum observa- s and gravimeter measurements, show that the ld network now has a general reliability of ut ± 0.4 mgal, although some bases are still arently in error by over 1 mgal. Comparisons gravity values determined by other investi- ors, both at the pendulum bases and at air- ts throughout the world, indicate that most h gravimeter work is good if differences in bration standards are taken into consideration. is applies to work done with gravimeters hav- a high and variable drift rate as well as that e with 'driftless' meters. The largest cause of dom variations that may amount to over 1 al appears to be related to the screw of the ding dial and to dividing-head inaccuracies in bing the reading dial. Comparisons of data en by various international groups doing gravi- ter work are presented. The evaluation of various international gravity standardization ges established with pendulums over the IGY od shows no difference in calibration factor ween the various ranges.

. Wüst (Institut für Meeres Kunde, Kiel, many, and Lamont Geological Observatory, isades, N. Y., 1960–1961), *On the Vertical Cir- ation of the Mediterranean Sea*. In this analy- of about 600 stations (200 winter and 400 sum- stations) the first attempt is made to study, h the help of the 'core method,' the mean dy state of the deep circulation within the le expanse of the Mediterranean Sea, divided sills into eight basins. In spite of the unperi- al fluctuations, we have got some indications he seasonal variations of the Levantine inter- diate current, which has its maximum in the ter. At the surface, six water types are formed ch spread out, either by measurable currents by weak advectional processes, in six core lay- and cause renewal and ventilation all the way the bottom of the basins. On the whole, the diterranean vertical circulation offers, by the sformation of the entering Atlantic water type to the Mediterranean types, an excellent example of interaction between atmosphere and sea. This is demonstrated by a three-dimensional block diagram of the vertical and horizontal distribution of the salinity distribution during winter.

Gilbert Yanow (Douglas Aircraft Co., Santa Monica, Calif.), *Model Calculations of the Upper Atmosphere of Mars*. Mathematical models of the upper atmosphere of Mars were calculated by using chemical compositions which varied from 90 to 98 per cent nitrogen and 2 to 10 per cent carbon dioxide, and by varying environmental conditions. Values are presented in graphical form for density, temperature, mean molecular mass, electron density, and atmospheric gas and ion concentrations as a function of altitude, with two-body and three-body recombination as a parameter. While these data are admittedly speculative, they do appear to indicate the possible existence of a multilayered, fairly dense, high-altitude ionosphere about the planet Mars.

H. S. Yoder, Jr. (Geophysical Laboratory, Carnegie Institution of Washington, Washington, D. C.), and C. E. Tilley (Cambridge University, Cambridge, England), *Derivation of Magma Types from a Primary Magma*. Phase studies at 1 atmosphere have shown that an equilibrium thermal barrier exists between some normative components of the alkali basalt magma series and the tholeiite magma series. The system nepheline (Ne)-diopside (Di)-forsterite (Fo)-SiO_2, which contains the principal normative components of iron-free basalt, is divided by the plane Fo-Ab-Di and appears to constitute such a barrier to the passage, under equilibrium conditions, of liquids between the Ne-bearing and En-bearing portions. Preliminary experiments at 33-kbar pressure indicate that the barrier join Fo-Ab no longer exists because of the instability of Ab and is replaced by jadeite (Jd)-enstatite (En), the point of intersection being represented by a clinopyroxene solid solution. Compositions in the major part of the area Fo-Jd-Ab-En, which are close to some peridotites, may at one pressure yield the Ne-bearing liquids of the alkali basalt magma series and at another pressure yield the En-bearing liquids of the tholeiite magma series. Peridotite or olivine tholeiite compositions, depending on the amount and extent of melting envisaged, appear to be suitable primary magma sources; alkali basalt magma evolving from deeper portions, olivine tholeiite and tholeiite magmas evolving from shallower portions. Other more complex geneses are conceivable. The results also bear on the reported occurrence of pigeonite or pigeonitic augite in Ne-normative rocks, incompatibility of modal nepheline and hypersthene, and occurrence of hypersthene-bearing nodules in alkali basalts.

Isidore Zietz and Kenneth G. Books (U. S. Geological Survey, Washington, D. C.), *Aeromag-*

netic Interpretation and Remanent Magnetization. Quantitative interpretation of aeromagnetic anomalies has been based for the most part on the use of physical models in which the direction of magnetization is parallel to that of the earth's field, although laboratory results show that this assumption is invalid for many rock units. Magnetic fields have been calculated for inclinations of magnetization significantly different from that of the earth's present field. The calculations are for a rectangular flat-topped mass with infinite vertical sides and a 75° inclination of the earth's field. Several significant empirical relationships between the physical model and the computed fields have been obtained. For low dips of magnetization the maximum and minimum points, rather than the points of inflection, mark the edges of the rock masses. The depth calculation techniques described in *Geological Society of America Memoir 47* are based on the assumption of induced polarization, but these same empirical rules can be applied equally well to the total intensity field when remanent magnetization is present. This probably explains the success of the *Memoir* methods when applied to observed aeromagnetic anomalies over sedimentary basins. For rock units having large remanent magnetizations, the dip of the magnetization may be estimated from the ratio between the maximum and minimum anomaly amplitudes, and the declination may be approximated from the horizontal line between the locations of the extreme values. The method has been successfully applied to aeromagnetic data taken over volcanic buttes near the Bearpaw Mountains in Montana.

Alfred J. Zmuda (Applied Physics Laboratory, Johns Hopkins University, Siilver Spring, Md.), *Currents in the Auroral Zone and in the Outer Van Allen Belt.* With first-order orbit theory the current contribution of the primary energetic particles is determined from the presently known particle characteristics of the aurora and the outer Van Allen radiation belt. In auroras the drifts and number density of the primary particles are r too low to account for the current causing th served magnetic variations, although the prim create the auroral ionization and the electric to drive the current which consists mainly o ambient electrons. With regard to the outer Allen belt, the magnetic data obtained with S Cosmic Rocket I indicate the presence of a ward flowing current of density about 10^{-7} am at a geocentric altitude of 21 to 22 $\times$ 10^3 km plication of the known particle character shows that the currents due to the follo sources are much too low, of the order 10^{-12} amp/m^2: curvature of field lines, dipol pulsion, magnetization, and field gradients. suggested that this westward flowing curre driven by a time-dependent electric field ming from either electrostatic or hydromag phenomena occurring at mirror points.

Alfred J. Zmuda (Applied Physics Labora Johns Hopkins University, Silver Spring, *The Variation of Harmonic Coefficients.* The tual dependence of the harmonic coefficients studied in a spherical harmonic analysis of netic data for scattered observatories. In va the number of harmonic terms from on twenty, the following characteristics were fo (1) The first six harmonic coefficients qu reached stable values, in the sense that coefficients varied little in value as the numb harmonic terms was increased from six to tw (2) Some coefficients beyond the sixth were s and some were not. (3) The residual for each ponent series was a monotonic decreasing fun of the number of terms. The series of tw terms represented 97 per cent of the observed and was the best obtainable with the mathe cal routines used in this problem. As the nu of harmonic terms increased beyond twenti coefficients exhibited an irregular behavior; the residual of the series was higher than tha tained with twenty terms.

Geomagnetic and Solar Data

J. VIRGINIA LINCOLN

Central Radio Propagation Laboratory, National Bureau of Standards
Boulder, Colorado

INTERNATIONAL DATA ON MAGNETIC DISTURBANCES

his report continues the series which has eared regularly in this Journal since volume no. 3, 295 (1949). Please refer to that first rt for an explanation of the data given, and olume 59, no. 3, 423 (1954) for the definition I_p.

ote: Additional and final Geomagnetic and r Data appears in due course in the following international publications: "Quarterly Bulletin on Solar Activity" International Astronomical Union, c/o Eidgen. Steinwarte, Zurich, Switzerland; "IAGA Bulletins, Geomagnetic Indices K and C" by J. Bartels, A. Romaña, and J. Veldkamp, International Union of Geodesy and Geophysics, Association of Geomagnetism and Aeronomy, c/o V. Laursen, Meteorologisk Institut, Charlottenlund, Denmark.

PRINCIPAL MAGNETIC STORMS

(Advance knowledge of the character of the records at some observatories as regards disturbances)

servatory Observer-Charge)	Greenwich date	Storm-time		Sudden commencement				C-figure, degree of activity[4]	Maximal activity on K-scale 0 to 9			Ranges		
		GMT of begin.	GMT of ending[1]	Type[2]	Amplitudes[3]				Gr. day	Gr. 3-hr. period	K-index	D	H	Z
					D	H	Z							
(1)	(2)	(3)	(4)	(5)	(6)	(7)	(8)	(9)	(10)	(11)	(12)	(13)	(14)	(15)
	1961	*h m*	*d h*		′	γ	γ					′	γ	γ
	Jan.	None												
G. Keys)	Feb. 4	13 32	7 04	s.c.	0	+9	−3	ms	4	7	6	8	203	52
	Feb. 13	02 53	15 14	s.c.	+0	+5	−3	m	13	4,5	5	10	108	19
	Feb. 16	00 41	17 01	s.c.	+0	+17	−6	m	16	4	5	6	134	26
	Feb. 17	05 12	19 04					m	18	1,4	5	10	115	34
	Mar. 5	17 ..	6 15					ms	5	8	6	6	162	35

Approximate time of ending of storm construed as the time of cessation of reasonably marked disturbance movements in the ; more specifically, when the *K*-index measure diminished to 2 or less for a reasonable period.
s.c. = sudden commencement; s.c.* = small initial impulse followed by main impulse (the amplitude in this case is that of *initial impulse only*, neglecting the initial brief pulse); ... = gradual commencement.
Signs of amplitudes of *D* and *Z* taken algebraically; *D* reckoned positive if towards the east and *Z* reckoned positive if vertidownwards.
Storm described by three degrees of activity: *m* for moderate (when *K*-index as great as 5); *ms* for moderately severe (when 6 or 7); *s* for severe (when *K* = 8 or 9).

SELECTED GEOMAGNETIC AND SOLAR DATA

Kp, Ci, Cp, Ap, K_{Fr}, Rz and Selected Days
April 1961

Day[1]	Three-hour Range Indices *Kp*[2]								Sum	Prel.[3] *Ci*	*Cp*[4]	*Ap*[5]	3-hr. Range Indices K_{Fr}[6] Values	Sum	P
	1	2	3	4	5	6	7	8							
1	5−	4−	4o	3−	2o	2−	2+	3−	24−	1.0	0.9	17	4444 2133	25	
2	2−	3+	4o	2+	3o	2o	3+	3o	23−	0.9	0.8	14	1443 2232	21	
3 D	4o	6o	5−	4o	2+	3−	2+	3−	29−	1.2	1.2	27	5643 2222	26	
4 Q	3o	1+	3−	1−	1−	0+	1o	0+	10o	0.2	0.3	6	3130 1011	10	
5 Q	2+	3o	1o	2−	1−	1o	0+	0o	10o	0.2	0.2	5	2211 0010	7	
6	1+	1−	1o	1o	1+	2−	4−	4−	14+	0.6	0.5	9	1000 1134	10	
7	4−	3+	1−	2o	1o	1−	1o	1o	13+	0.5	0.4	8	4313 1122	17	
8 q	1o	1+	2+	3−	1−	1−	2−	1+	12−	0.2	0.3	6	1132 2122	14	
9 D	2−	2+	3−	6+	5−	3o	3−	2+	26−	1.2	1.2	24	3235 5223	25	
10	4−	4−	3+	4−	3+	3o	3+	3−	27−	1.0	1.0	18	3334 2333	24	
11 D	4o	5o	3o	3+	3+	5+	3+	2−	29o	1.3	1.2	26	4533 3422	26	
12	2o	2−	3+	2o	3+	3−	2+	2−	19o	0.6	0.6	10	2142 3221	17	
13	2−	2+	2−	1+	4−	5+	3−	2o	21−	0.8	0.9	15	2211 3533	20	
14 D	3−	3o	3−	4−	4+	5+	7o	7+	36o	1.5	1.6	54	3333 4356	30	
15 D	8−	7o	6o	3+	3+	4+	3+	3−	38−	1.5	1.7	61	6653 3433	33	
16	3−	3−	2o	2+	3o	3−	3+	4−	22+	0.9	0.8	13	3322 3233	21	
17 Q	1+	2−	1+	1+	2−	1+	1−	0o	9+	0.1	0.2	4	1211 1220	10	
18 Q	1+	2o	2+	2−	1o	1o	0+	1o	11−	0.1	0.2	5	1233 1111	13	
19 q	2−	2+	2o	1o	1+	2o	3−	2+	15+	0.5	0.4	7	2321 0233	16	
20 q	3+	2o	3−	1o	1−	1o	1+	1o	13o	0.3	0.4	7	2231 0111	11	
21 Q	0o	0+	0o	0+	1+	0+	1o	1+	5−	0.0	0.0	2	0100 1012	5	
22	0+	0o	1−	2−	3−	3o	3−	3+	14+	0.6	0.5	8	0011 2234	13	
23	1o	2−	2+	2o	3−	1+	3−	3−	16+	0.5	0.5	8	1233 3133	19	
24	3+	3−	1+	2o	2+	2+	3−	3o	20−	0.7	0.6	11	3212 2233	18	
25	4−	2+	1+	1+	1o	1+	2o	1+	14+	0.4	0.4	8	3211 1021	11	
26	3−	3+	2+	2−	3o	4−	4−	1o	21+	0.6	0.8	14	3422 3332	22	
27	2−	3o	3+	3+	3+	2+	2−	2o	21−	0.8	0.7	12	1334 3222	20	
28 q	3+	2+	2+	1+	1o	1−	2−	1o	14−	0.4	0.4	7	3321 1020	12	
29 q	2+	0o	0o	2o	1−	1o	1+	3o	10+	0.3	0.2	5	2001 1122	9	
30	2+	2−	1+	2o	3−	3−	2−	3+	18−	0.6	0.5	9	2211 2223	15	
									Means:	0.65	0.65	14			
									No. of days:	30	30	30			

Notes:

[1] Five quiet days (Q), ten quiet days (Q or q), five disturbed days (D) selected by Committee on acterization of Magnetic Disturbances, J. Veldkamp, Kon. Nederlandsch Meteorologisch Instituut, D Holland.

[2] Geomagnetic planetary three-hour-range indices *Kp* prepared by Committee on Characterizat Magnetic Disturbances, J. Bartels, Chairman, University, Göttingen, Germany.

[3] Preliminary magnetic character-figures, *Ci*, prepared by J. Veldkamp.

[4] Magnetic character-figures, *Cp*, prepared by J. Bartels.

[5] Average amplitudes *Ap* (unit 2γ), prepared by J. Bartels.

[6] Fredericksburg three-hour-range indices *K* (*K*9 = 500γ); scale-values of variometers in γ/mm: *D* *H* = 2.5, *Z* = 3.3) prepared by Robert E. Gebhardt, Observer-in-Charge, Fredericksburg Magnetic vatory, Corbin, Virginia.

[7] Provisional sunspot-numbers (dependent on observations at Zurich Observatory and its stati Locarno and Arosa) prepared by M. Waldmeier, Swiss Federal Observatory, Zurich, Switzerland.

Letters to the Editor

Ionospheric Reflections below 50 Kilometers during Polar-Cap Absorption Events

J. B. GREGORY

Physics Department, University of Canterbury
Christchurch, New Zealand

n a letter, *Donahue* [1961] has considered transmission properties of the atmosphere for ll angles of solar depression in relation to todetachment of electrons from negative , and has used his findings to show that the k of ionization during polar absorption nts must be close to 50 km. Direct evidence onization at such heights during these events ow available, and it is the purpose of the ent letter to give a preliminary account of e of these data.

bservations have been made at Scott Base, arctica (78°S), for nearly 2 years by means n ionosphere sounder operating at a fixed uency of 2.3 Mc/s. The main purpose of investigation is a study of partial reflections n the lower ionosphere, such as has been ried out at 43°S [*Gregory*, 1961]. Data are ilable once a year when transport of film rds is possible. Analysis so far completed ws that at least twenty polar-cap absorption nts have occurred. Routine observations, en at hourly intervals, usually reveal a com- pattern of partial reflections below *E*-region hts. Under normal conditions, partial reflec- s are almost invariably present between 80 90 km, and sometimes as low as 60 km. ring an absorption event, the presence of ad- onal ionization below 80 km is manifest in ral ways. One of the most sensitive, but not most reliable, indications of this ionization he strengthening of existing partial reflec- . and the appearance of new reflections at r heights than those noted before the event. lack of reliability is due to the requirement a process, such as turbulence, shall exist ltaneously with the increase in ionization ity, in order to produce the variation in re- tive index necessary for reflection. At pres- there is no method, independent of the radio wave observations, available to determine whether such processes were simultaneously present. A second indication of the presence of ionization in regions of high collision frequency is the increase in absorption, which at times is sufficient to prevent detection of reflections at any height, despite the high sensitivity of the apparatus.

Despite some uncertainties of deduction from the observations, it is clear that different events have resulted in different ionization density profiles between 40 and 80 km. In two events, records have been obtained showing the presence of partial reflections, for a period of the order of one day, below 50 km. Figure 1 shows a reproduction of an *h't* record for July 15, 1959, at 12 hours UT, i.e., during darkness. This major event had been in progress for some 5 days before the period illustrated. The photographic record covers an interval of about 8 minutes. At the left of the record, the apparatus was operating at full sensitivity, and reflections were present at two heights, approximately 44 and 49 km. At the right of the record, the system was again at maximum sensitivity, and the two reflections merge with a lower boundary at 43 km. Between the two ends of the record a sequence of steps of gain reduction took place, each 6-db reduction occurring at the white rectangular marker below the record. (Some markers are missing.) The lower reflection disappeared after 6 db of reduction, the upper after 24 db, at a height not exceeding 59 km at the upper boundary. The extension of reflections above 59 km, on the high sensitivity portions of the record, is attributed to oblique path reflections. Under normal conditions, scattered reflections would be expected from about 80 km up to 100 km, with possible sporadic total reflections above this height. The complete absence of reflections above

59 km suggests that absorption, of some 36 db, accompanied the reflections below 59 km. Earlier in the event blank records were obtained, indicating at least 60 db of absorption below any total reflections. A preliminary estimate, involving assumptions concerning the nature of the reflection process, suggests that the electron concentration below 50 km was not less than 100/cm³, and possibly in excess of 500/cm³. This is of the same order of magnitude as deduced by *Bailey* [1959] for the event of February 23, 1956, at the same heights.

The appearance of two partial reflections close to each other is in keeping with many other observations, both at 78°S and 43°S [*Gregory*, 1961]. There is no evidence to show that the reflections at 43 km mark the least height at which ionization was present during this event. It is preferable to admit the possibility that there was no disturbance of the electron density profile sufficient to produce a detectable partial reflection, below 43 km.

In addition to the July 1959 event, another on March 31, 1960, produced weaker but quite definite reflections between 41 and 47 km for 20 hours, and an isolated 47-km reflection occurred at 05 hours on April 2, 1960, following a period of total absorption. The July 1959 event occurred during the polar night. The March 31 event covered both daylight and darkness periods. In general, a characteristic change in reflection heights occurs between day and night, owing to the effect of photodetachment. The reflections between 41 and 47 km on March 31 showed only irregular changes in height, probably due to changes either in the incident ionizing flux or in the atmospheric irregularities involved. Also, little change in strength bet day and night occurred. At these heights col detachment of electrons from negative io appreciable, and the negative-ion/electron sity ratio changes only by a factor of the of 2, as compared with a factor of 10 at 7(between sunlight and darkness conditions reflections on March 31, 1960, below 47 km very weak, and precise measurements of ch in reflection strength were not possible. ever, the two events provide sufficient direc dence to confirm the conclusions of *Hul and Ortner* [1959] and Donahue, that in polar-cap absorption events, ionization is duced below 50 km.

The nature of the ionizing radiation effe at these low heights has been discussed by ous authors, with general agreement that energy protons are the responsible agency present results may be compared with r from equipment in space vehicles. For the 1959 event, *Armstrong, Harrison, Heckman Rosen* [1961] have reported finding trac protons with incident energies down to 42 in a nuclear emulsion stack carried into th ner Van Allen belt on July 21. A peak or pl in the proton spectrum was noted at 80 and this was considered as possibly due to protons.

On the same date reflections between 6 65 km were recorded at Scott Base from 1000 hours, at which time the equipment w advertently put out of action. The sequen lowest reflection heights for the days b this happening was quite continuous, slowly from the 43 km illustrated in Fig for July 15 to 61–65 km on July 21. Sinc

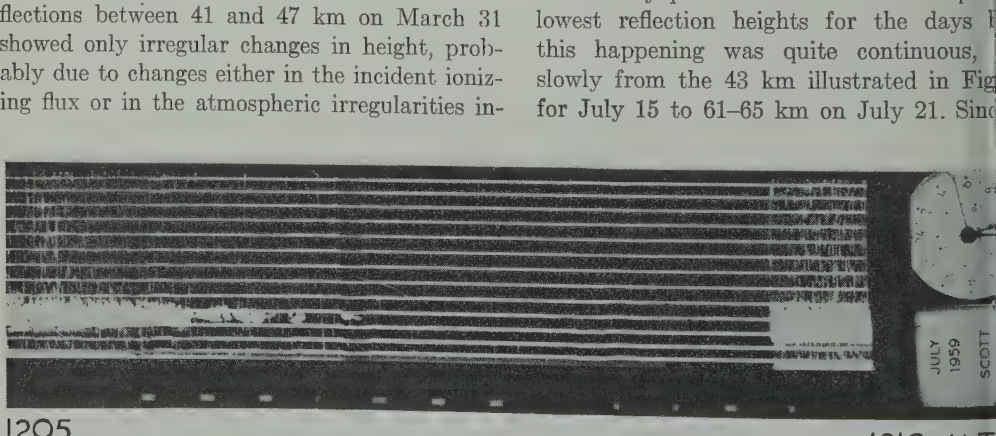


Fig. 1. An *h't* record, at 2.3 Mc/s, for July 15, 1959, at 12 hours UT taken at Scott Base Antarctica. The first height marker appears at 30 km, and the remainder at 10-km interval Reflections down to 43 km are visible. The method of gain reduction is described in the tex The trailing edge of the transmitter pulse, with ground echoes, appears below 30 km.

er ionosphere was not illuminated by sunlight a large fraction of this interval, there is no ubt that the low heights on July 21 were due nusual ionizing radiation consistent with 50– Mev protons. The slow rise in heights can be ributed either to a gradual softening of the iation, or to a reduction in intensity. In the er instance, the reflections noted occurred a region of positive gradient, with height, of tron concentration.

Since the July 1959 event, only the events ering March 31 and April 2, 1960, have pro- ed reflections below 50 km, although nearly other events have caused some changes in ections above 50 km. A comparison of these 1960 events has been made with results of ation measurements made on board satellite plorer VII, and reported by *Van Allen and* [1960]. This shows that the isolated re- tion at 47 km on April 2 at 05 hours occurred ing a period when solar protons were de- ed by the State University of Iowa equip- nt on Explorer VII. The uncertainties in- nt in such comparison are well illustrated by fact that this reflection occurred in the de- ing stages of the proton burst, when count- rates had fallen from above 400/sec at peak, approximately 30/sec, the latter being twice pre-event rate. The series of reflections be- en 41 and 47 km on March 31 occurred dur- a period when the heavily shielded counter the satellite showed no increase in counting s, and while the lightly shielded counter in same vehicle showed a decreasing rate. It is e recalled that Explorer VII observations e to the northern hemisphere below 51° ude, while the 2.3 Mc/s records relate to S latitude. Detailed consideration of this nt, including magnetic conditions, suggests that the reflections of March 31 were possibly due to protons that were not intercepted by Explorer VII. A comparison of detail from this satellite and from Scott Base has been made for other events, and the simultaneous presence of low-height reflections and solar protons noted in several instances. A more detailed survey of these southern polar-cap events is in preparation.

Acknowledgments. The Scott Base lower ionosphere equipment has been provided and maintained by the Ross Dependency Research Committee of the New Zealand Government. Analysis of results was commenced by me in the Department of Physics, State University of Iowa, where Professor James A. Van Allen kindly made available unpublished results of Explorer VII data. Continued support for the analysis is being given by the Office of Naval Research, United States Navy, under contract Nonr 2651(00).

References

Armstrong, A. H., F. B. Harrison, H. H. Heckman, and L. Rosen, Charged particles in the inner Van Allen radiation belt, *J. Geophys. Research, 66,* 351–357, 1961.

Bailey, D. K., Abnormal ionization in the lower ionosphere associated with cosmic-ray flux enhancements, *Proc. IRE, 47,* 255–266, 1959.

Donahue, T. M., A note on polar blackouts, *J. Atmospheric and Terrest. Phys., 20,* 76–79, 1961.

Gregory, J. B., Radio wave reflections from the mesosphere, *J. Geophys. Research, 66,* 429–445, 1961.

Hultqvist, B., and J. Ortner, Strongly absorbing layers below 50 km, *Planetary and Space Sci., 1,* 193–204, 1959.

Van Allen, J. A., and Wei Ching Lin, Outer radiation belt and solar proton observations with Explorer VII during March–April 1960, *J. Geophys. Research, 65,* 2998–3003, 1960.

(Received May 5, 1961.)

Electron Densities in the Outer Ionosphere Deduced from Nose Whistlers

R. L. SMITH

University of Hawaii, Honolulu, Hawaii

An attempt was recently made by *Pope* [1961] to determine the electron density in the exosphere by using nose whistlers. The deduced densities are lower by factors of 5 or more than densities deduced by *Smith* [1960*a*] and by *Smith and Helliwell* [1960], who also used nose whistler data. The discrepancies are even more surprising since Smith had also used, as part of his data, the same data used and previously exhibited in a technical report by *Pope* [1959].

In the following discussion, all figure and equation numbers refer to the paper by *Pope* [1961].

The right-hand side of equation 2 is too large by a factor of 2. Apparently the term 1/2, which appears in the group refractive index formula, was omitted. The same error appears in the unnumbered equation below Figure 2, which presumably makes the time-delay correction factor too large by a factor of 2. In any event, a time-delay correction of

$$t = 4/f^{1/2}$$

is closer to the dispersion one would expect for a double passage through the regular ionospheric layers at night.

The factor of 2 has been reinserted into equation 6. The resulting curves shown in Figures 2, 3, and 4 appear to be correct. Let us compute the electron density from nose whistler spectrograms, assuming a $1/R^3$ distribution. Examination of the nose whistler trains shown in Figure 5 reveals an outstanding nose whistler at 1235 UT, March 19, 1959, with a nose frequency of 5 kc and a time delay to the nose of approximately 2.55 seconds. An additional 0.05 seconds should be added to this figure to account for the propagation time of the causative atmospheric. An additional time of $8/(5000)^{1/2} = 0.11$ seconds (using Pope's correction factor) can be subtracted to account for the propagation through the lower layers, giving $t_n = 2.49$ seconds. The nose frequency can be shifted downward by cycles (again using Pope's numbers) to $f_n = 4{,}800$ cps. Applying the graph in F 3 to the above data, we deduce that the lat of the field line, θ_0, for this nose whistler ponent is 61°, and, furthermore, $t_n/K_2 = 1$ 10^{-2}. The dipole field line passing through earth's surface at 61° magnetic latitude rea a maximum distance of 4.26 earth radii fron center of the earth. The value of K_2 de from the above measurements is

$$K_2 = \frac{t_n}{1.8 \times 10^{-2}} = 1.38 \times 10^2$$

The electron density at 4.26 earth radii is f by using equation 4:

$$N = K_2^2 R^{-3} = \frac{1.91 \times 10^4}{77.4}$$

$$= 246 \text{ electron}$$

This is to be compared with the value of taken from the graph on Figure 7 for the data point, the same distance, and the distribution. It appears that some errors been made in the calculations. Similar e occur in the calculations for other assume tributions. After making suitable correc the electron densities deduced from the shown by Pope are reasonably close to thos duced by *Smith* [1960*a*] and by *Allcock* [1

Smith [1960*a*] has examined 22 nose whi and nose whistler trains received from a nu of different stations at different times. He cludes that the gyro-frequency model (ele density proportional to gyro frequency, o proximately $1/R^3$) fits the data somewhat b than the so-called Johnson model present Pope's paper. The data are not absolutely clusive, however, since each nose whistle give only integrated density along one s field lines. It is clear from the data tha density of the ionization in the outer ionos

not be expressed in terms of a simple oothly varying model, even at one time. In instance a minimum ionization variation oss the field lines of at least 40 per cent was ed. It might also be noted that there are Johnson models of the outer ionosphere. e older model [*Johnson,* 1959], an approxite form of which was used by Pope, has been arded by Johnson on theoretical grounds in or of a model [*Johnson,* 1960] similar to that ussed by *Dungey* [1954].

One of Pope's stated assumptions, that the istler follows the magnetic field lines, and an tated assumption, that the wave normals aligned with the magnetic field, deserve fur- r comment. On the basis of theoretical and erimental evidence, it appears quite likely t whistlers propagate in field-aligned ducts enhanced ionization in the outer ionosphere *ith,* 1960*a,b; Helliwell,* 1959; *Smith, Helli- l, and Yabroff,* 1960]. Furthermore, even ugh the wave normals of whistler energy pped in these ducts may vary considerably, average group velocity is given fairly acculy by assuming that the wave normals are ned with the magnetic field [*Smith,* 1960*a*]. ere is, however, a high frequency cutoff at -half the gyro frequency associated with this de of propagation. A detailed account of se results will appear shortly.

References

cock, G. McK., The electron density distribuion in the outer ionosphere derived from whistler data, *J. Atmospheric and Terrest. Phys., 14,* 185, 1959.

Dungey, J. W., Electrodynamics of the outer atmosphere, *Scientific Report 69,* contract AF 19 (122)–44, Ionospheric Research Laboratory, Pennsylvania State University, September 15, 1954.

Helliwell, R. A., Hybrid whistlers (Abstr.), Program of the joint meeting of URSI and IRE, Washington, D. C., p. 28, May 1959.

Johnson, F. S., The structure of the outer atmosphere including the ion distribution above the F-2 maximum, *Technical Report LMSD–49719,* Lockheed Missiles and Space Division, Sunnyvale, California, April 28, 1959.

Johnson, F. S., The ion distribution above the F_2 maximum, *J. Geophys. Research, 65,* 577–584, 1960.

Pope, J. H., Whistlers and chorus observations, *Arctic Propagation Studies at Tropospheric and Ionospheric Modes of Propagation, Final Report,* contract AF19 (604)–1859, Geophysical Institute, College, Alaska, pp. 51–67, 1959.

Pope, J. H., An estimate of electron densities in the exosphere by means of nose whistlers, *J. Geophys. Research, 66,* 67–75, 1961.

Smith, R. L., The use of nose whistlers in the study of the outer ionosphere, *Technical Report 6,* contract AF18 (603)–126, AFOSR–TN–60–861, July 11, 1960*a*.

Smith, R. L., Guiding of whistlers in a homogeneous medium, *J. Research NBS, 64D,* 505–508, 1960*b*.

Smith R. L., and R. A. Helliwell, Electron densities to 5 earth radii, *J. Geophys. Research, 65,* 2583, 1960.

Smith, R. L., R. A. Helliwell, and I. W. Yabroff, A theory of trapping of whistlers in field-aligned columns of enhanced ionization, *J. Geophys. Research, 65,* 815–823, 1960.

(Received April 6, 1961.)

Some Comments on Obtaining Electron Densities in the Exosphere Using Nose Whistlers

Joseph H. Pope

Geophysical Institute, College, Alaska

In a recent paper [*Pope,* 1961], estimates of the electron density in the exosphere were derived from nose whistler observations. R. L. Smith believes he has found numerical 'errors' in this paper. The differences in the numerical values obtained by Pope and by Smith are due to different assumptions regarding the nature of the whistlers. In the paper criticized by Smith we assume that the observed signals were 'long' whistlers, whereas Smith obviously has based his estimates on a 'short' whistler assumption. 'Long' whistlers have their origin in the observer's (northern) hemisphere to which they return after a reflection from the magnetic conjugate point in the southern hemisphere. 'Short' whistlers originate in the hemisphere opposite that of the observer.

It is usually possible to distinguish between long and short whistlers since the causative spherics for long whistlers are received as relatively strong impulses, whereas those for short whistlers are quite weak, if observed at all, because of the long distance of propagation. One cannot, of course, completely rule out the possibility that the whistlers were short, since under *unusual* propagation conditions, the spheric could propagate via the earth-ionosphere waveguide from regions far south of the equator to these northern areas retaining considerable intensity. However, a spheric that has propagated such large distances will usually show a dispersive 'hook' at its low-frequency end due to the waveguide low-frequency cutoff. The causative spherics of those whistlers shown in Figure 5 [*Pope,* 1961] were unusually strong and failed to show the cutoff hook on the sonagrams. Thus the observed whistlers are more likely long than short.

Equation 6, from which the curves of Figures 2, 3, and 4 were computed, is valid for short whistlers. Therefore, in using these curves to obtain electron densities from long whistlers, the observed times of propagation must be di by 2. If this correction is not made, as in Sm discussion, the error in the constants (K_2, K_3) of equations 3, 4, and 5 will be large factor of 2, and the resulting electron den will be large by a factor of 4. The remaining crepancy in Smith's results is accounted fo scaling uncertainties, the effects of which indicated in Figures 7 and 8 by the horiz and vertical lines on some of the points.

The factors of 2 in equation 2 and the sphere time-delay equation should be delet order to adapt the formulas from the lon the short whistler case, a fact that was im rather than stated explicitly in the text. factor of 8 for the dispersion due to the sphere is correct for the assumed model sphere. A consideration of ionospheric c given by *Johnson* [1960] indicates this may be a little high for the nighttime ionosp during equinoxes at moderately high geo netic latitudes (60°); probably a better would be 4 or 5.

These considerations will not signific affect the conclusions of the paper under sideration. In the remote possibility that whistlers were indeed short rather than different values for the electron density w result. In this case the value for K^2_3 in equ 10 will be about 2570, and the electron den in Figure 8 will vary from 80 to 20 elec per cc in the interval given. The conclusion the Johnson model provides the best fit of distributions will not be affected.

It is not at all clear from Smith's re [*Smith,* 1960, Fig. 24] that the Johnson m (or, as he prefers, the 'Johnson-Smith' m can be discriminated against in favor o gyro-frequency model. His remarks on pag imply his agreement with this statement. of the 22 whistlers considered by Smith entered in his Figure 24 are represented by

or two points while several others have pes which agree with the Johnson model. ncidentally, the equation appearing on page in the quoted report by Smith should read $= .018f_H$ rather than $N = 1200f_H$).

f whistlers propagate according to the *ad hoc* pothesis of field-aligned columns certain diffi- ties in the interpretation of the results arise. e densities obtained would be somewhat her than over-all average electron densities. o, the laws governing the distribution along columns may be significantly different from se governing the distribution as a function of tance from the earth's surface across the field es. In this case it would not be valid to com- re the point-by-point results obtained using law along a field line with the same law as a ction of distance in the equatorial plane. An- er difficulty arises if the field lines are sig- cantly modified by charged particles (i.e., the ar wind'). The field lines can no longer be resented by a magnetic dipole, and the elec- n densities obtained may be modified con- erably.

The differences between electron densities en by *Smith* [1960] and those in the paper der discussion [*Pope*, 1961] can be attributa- to the fact that Smith assumes the gyro- uency model of electron density distribution to temporal variations in the electron den- sity. The difference between the Johnson model and the gyro-frequency model is roughly a factor of 4 [compare Figures 7 and 8 of *Pope*, 1961], whereas temporal variations may be a factor of 3.

It is usually not possible to locate the causative spheric on whistlers obtained at College. Therefore a large number of whistlers observed here are not suitable for analysis. However, two other whistlers that have recently been analyzed show values of electron density about three times higher than those obtained from the March 19, 1959, whistlers. They also indicate a close fit with the Johnson distribution. It appears that the March 19, 1959, whistlers occurred during a period of low electron density in the exosphere.

References

Johnson, F. S. (ed.), *Satellite Environment Handbook*, Technical Report LMSD–895006 Lockheed Aircraft Corporation, Sunnyvale, California, December 1960.

Pope, J. H., An estimate of electron densities in the exosphere by means of nose whistlers, *J. Geophys. Research, 66*, 67–75, 1961.

Smith, R. L., The use of nose whistlers in the study of the outer ionosphere, *Technical Report 6*, contract AF 18(603)–126, AFOSR–TN–60–861, July 11, 1960.

(Received May 11, 1961.)

Extension of Nose Whistler Analysis

R. L. SMITH

Department of Electrical Engineering, University of Hawaii
Honolulu, Hawaii

D. L. CARPENTER

Radioscience Laboratory, Stanford University
Stanford, California

Recent work by *Smith* [1960] on the theory of nose whistlers suggests several methods of obtaining nose frequency and nose time delay information from ordinary whistlers: i.e., whistlers that do not exhibit a 'nose' on the spectrographic records. Since the nose frequency and time delay provide information on whistler path location and on electron density, and since ordinary whistlers occur far more frequently than do nose whistlers, such methods are potentially of great value as tools of research.

The purpose of this letter is to outline one of several possible methods to obtain the nose frequency and the time delay to the nose when the nose is not directly observable. The method is based on the observation that the dispersion characteristics of whistlers are nearly independent of frequency and ionization distribution when normalized with respect to the nose frequency and the low frequency dispersion. This suggests that the dispersion can be written in terms of a universal dispersion function that is a function of f/f_n only:

$$D(f) = tf^{1/2} = D_0 S_1(f/f_n) \qquad (1)$$

where

D_0 is the low frequency dispersion.
f is the frequency.
f_n is the nose frequency.
t is the time delay.
S_1 is a universal dispersion function.

Where f_0 and f_H are the local electron plasma and gyro frequencies, respectively, D_0 may be defined as

$$D_0 = \frac{1}{2C} \int_{\text{path}} \frac{f_0}{f_H^{1/2}}\, ds$$

From a spectrographic analysis one can measure two time delays at two well-separated quencies on one whistler trace. Now, forming t equations in two unknowns, D_0 and f_n, we sc for f_n either graphically or analytically, depe ing on the form of S_1. From f_n and a known va of t at frequency f, t_n is easily obtained thro equation 1.

The basic details of the method follow. C sider an approximation to $D(f)$ suggested Smith:

$$D(f) = tf^{1/2} = D_0 S_0(f/f_{H_1}) = D_0 \frac{2}{\pi} \frac{E(f/f_{H_1})}{1 - f/f_{H_1}}$$

where f_{H_1} is the minimum gyro frequency al the path of propagation (assumed to coinc with a line of force of the earth's magn field), and E is the complete elliptic integra the second kind with modulus f/f_{H_1}. To obt D as a function of f/f_n, we set $\partial t/\partial f = 0$ equation 2 (the nose frequency condition), then solve for $\Lambda_n = f_n/f_{H_1}$. We then have

$$S_1(f/f_n) = \frac{2}{\pi} \frac{E(\Lambda_n f/f_n)}{1 - \Lambda_n f/f_n}, \quad \Lambda_n = 0.386$$

We now consider two time delays t_u and t_L two frequencies f_u and f_L. Figure 1 sh schematically a middle-latitude 'one-hop' whis with upper and lower frequencies of meas ment 8 and 4 kc/s, respectively. (The 30-ms d from $t = 0$ to the atmospheric represents approximate time required for the atmosph to propagate at the speed of light from causative lightning flash to the whistler receiv To eliminate D_0 we form the ratio

$$\frac{D(f_u)}{D(f_L)} = \frac{t_u f_u^{1/2}}{t_L f_L^{1/2}} = \frac{S_1(f_u/f_n)}{S_1(f_L/f_n)} = S_2(f_L/f_u\ ;\ f_u/f_n)$$

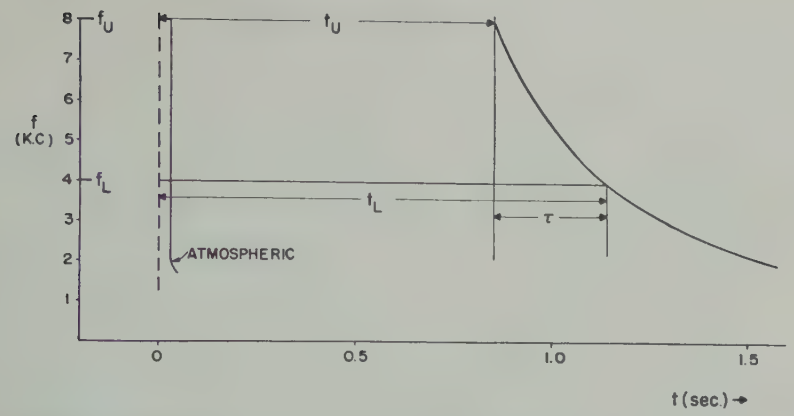


Fig. 1. Schematic illustration of a middle-latitude 'one-hop' whistler, showing measurements for f_n analysis and source identification.

ere the subscripts refer to the upper and ver frequencies of measurement and S_2 is a w function of the ratios f_L/f_u and f_u/f_n. gure 2 shows a plot of S_2 vs. f_u/f_n for several lues of the parameter f_L/f_u.

When the measurements t_u and t_L are actually ade, a value of S_2 may be calculated and a lue of f_u/f_n read from the graph. Since f_u is own, f_n is thus obtained.

To find t_n, we note from (1) and (3) that

$$t_n = \frac{D_0 S_1(1)}{f_n^{1/2}} = \frac{D_0}{f_n^{1/2}}\, 1.456$$

We then have

$$\frac{t}{t_n} = \frac{0.678}{(f/f_n)^{1/2}} \frac{2}{\pi} \frac{1}{1 - \Lambda_n f/f_n} E(\Lambda_n f/f_n) \qquad (5)$$

which is illustrated in Figure 3. With f_u/f_n known, the appropriate value of t/t_n, and thus t_n, is easily obtained from the graph.

Considerations of theoretical and practical error in this method are complex and will be discussed in detail at a later date. That there are limitations to the method is most obvious from Figure 2, where it is clear that a small

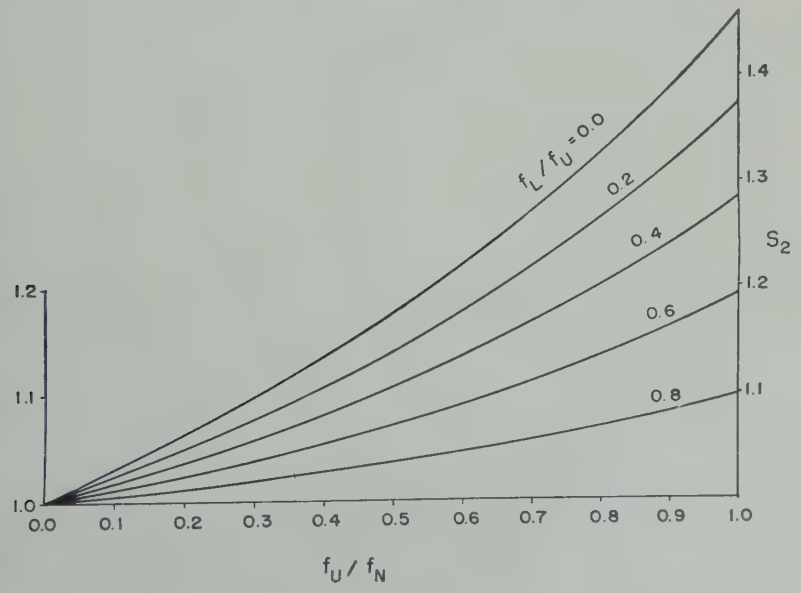


Fig. 2. Graph of S_2 vs. f_u/f_n for various values of the parameter f_L/f_u.

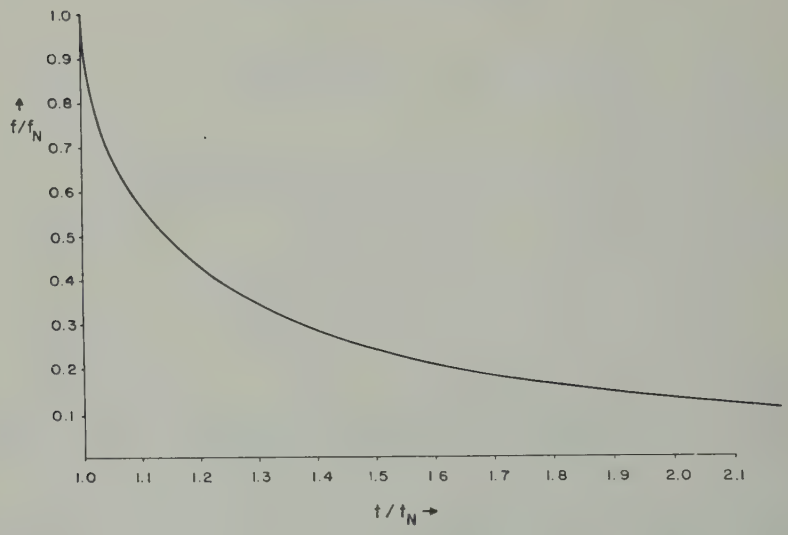


Fig. 3. Graph of f/f_n vs. t/t_n, based on the universal dispersion function S_1.

percentage error in S_2 will cause a very large error in f_u/f_n for low values of f_u/f_n.

Experience shows that it is necessary to have good frequency-time calibration of the spectrographic records, and that the whistler traces should be well defined over the range f_u to f_L. Under such conditions it is possible to obtain statistically reliable values of f_n that range high as 50 kc.

The best way of checking the effectiveness the method is to analyze actual nose whis traces. An example in which three traces measured is shown in Figure 4. The results this whistler and for several others are given

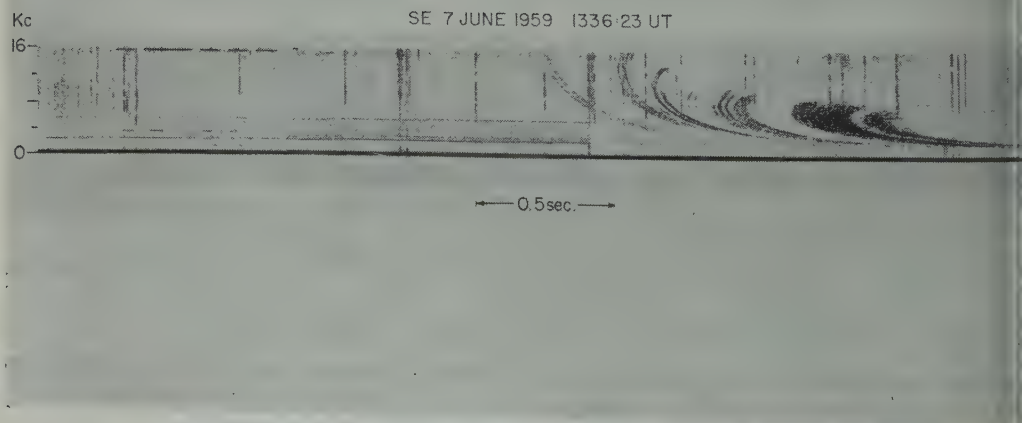


Fig. 4. Two closely spaced nose whistlers recorded at Seattle on June 7, 1959.

TABLE 1. Comparison of Measured and Calculated Values of f_n and t_n of Nose Whistlers

tion	Date	Nose Frequency, kc		Nose time delay, sec,		f_u/f_n	f_L/f_u
		Measured	Calculated	Measured	Calculated		
ttle	June 7, 1959	13.4 ± 0.3	13.3 ± 1.5*	0.823 ± 0.017	0.821 ± 0.041	0.600	0.6
	1335:83 UT	10.7 ± 0.3	10.9 ± 1.1	0.947 ± 0.019	0.938 ± 0.042	0.640	0.5
		7.5 ± 0.2	8.0 ± 0.9	1.182 ± 0.019	1.16 ± 0.055	0.623	0.6
ttle	May 21, 1958	9.9 ± 0.4	10.6 ± 1.1	1.197 ± 0.023	1.189 ± 0.053	0.660	0.5
	1335:57 UT						
ulder	Feb. 5, 1958	12.6 ± 0.5	13.3 ± 1.1	1.204 ± 0.021	1.19 ± 0.042	0.750	0.4
	1235:97 UT						
ttle	Aug. 18, 1959	15.0 ± 0.7	15.0 ± 1.0	0.403 ± 0.019	0.402 ± 0.02	0.801	0.5
	1235:59 UT						
alaska	April 27, 1959	19.3 ± 0.6	19.6 ± 1.4	0.927 ± 0.019	0.927 ± 0.03	0.818	0.5
	0535:15 UT	18.5 ± 1.0	19.1 ± 1.3	0.987 ± 0.021	0.986 ± 0.03	0.787	0.5
		21.0 ± 1.5	20.9 ± 1.2	0.889 ± 0.021	0.889 ± 0.027	0.863	0.722
nford	May 17, 1958	31.0 ± 2.0	28.8 ± 9.5	0.512 ± 0.02	0.528 ± 0.098	0.278	0.5
	1435:87 UT	31.0 ± 2.0	30.7 ± 4.5	0.512 ± 0.02	0.514 ± 0.039	0.522	0.5
		31.0 ± 2.0	31.2 ± 1.6	0.512 ± 0.02	0.510 ± 0.02	0.899	0.5
	1435:88 UT	31.0 ± 2.0	32.9 ± 11.5	0.512 ± 0.02	0.504 ± 0.11	0.260	0.5
		31.0 ± 2.0	30.4 ± 4.6	0.512 ± 0.02	0.515 ± 0.041	0.494	0.6

The errors assigned to the calculated results are not the specific errors associated with the particular istlers in question, but are 'typical' errors associated with the 'typical' whistler for which f_n, f_u, and f_L as indicated. In order to determine the feasibility of calculating f_n and t_n in the manner described above, was necessary to make a preliminary study of measuring error, based on the appearance of typical istlers in the relatively large group of whistlers exhibiting at least a fairly well defined edge over the ge f_u to f_L. The expected errors derived from this preliminary study (and applied to the whistlers listed the table) must be distinguished from the actual measuring errors associated with any particular whistler. several cases listed, the actual measuring errors are smaller than those assigned, owing to extremely d definition of the traces. Only 'typical' errors were recorded, so as to present a cautious picture that uggestive of more general measuring conditions.

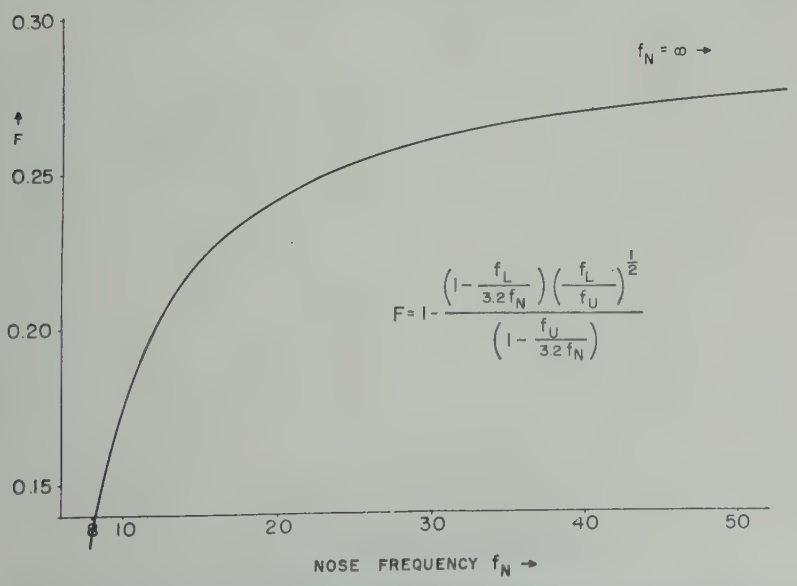


Fig. 5. Graph of F vs. f_n used in whistler source identification (case of $f_L = 4$ kc, $f_u = 8$ kc).

Table 1. In the cases for May 17, 1958, two or more measurements have been made at different frequencies f_u and f_L for a single nose whistler trace.

It is seen that the calculated and measured values agree well, although the former tend to exceed the latter by small percentages in the range near 10 kc/s.

Other methods of analysis may be developed using variations of the scheme outlined above, such as the use of measurements t and $\partial t/\partial f$ at frequency f. Another method depends upon the low frequency behavior of whistlers and requires the measurement of $\partial D/\partial f$ and D at a frequency f such that $f/f_{H_i} \ll 1$.

One serious problem in f_n analysis, and in whistler analysis in general, is the identification of the sources of short (one-hop) whistlers. Whenever possible, the identification should be made by methods that are essentially independent of any particular theory of the frequency-time behavior of whistlers, such as by comparison of whistlers recorded during the same 2-minute period, comparison of events recorded simultaneously in opposite hemispheres, etc. When such 'independent' methods are unsuccessful in a case that is of particular interest, it may be possible to apply the following approach: Instead of the more complicated relation (1), we write, as a reasonable approximation to it,

$$D = tf^{1/2} = D_0 \frac{1}{1 - f/3.2f_n} \tag{6}$$

For two frequencies f_u and f_L, we form

$$\frac{t_u f_u^{1/2}}{t_L f_L^{1/2}} = \frac{1 - f_L/3.2f_n}{1 - f_u/3.2f_n} \tag{7}$$

Then, writing $\tau = t_L - t_u$, we have (Fig. 1)

$$t_L = \tau/F \tag{8}$$

where

$$F = 1 - \frac{(1 - f_L/3.2f_n)(f_L/f_u)^{1/2}}{1 - f_u/3.2f_n}$$

Now, for convenience, we choose f_u = 8 f_L = 4 kc/s, and obtain a graph of F vs. f_n Fig. 5). Then, in a particular case, we guess value of f_n for the trace, measure τ, read F the graph, and thus obtain t_L. If our gue within 25 per cent of the true nose freque this calculated value of t_L will be within rou 6 per cent of true t_L when the true nose quency is near 30 kc/s. For higher values the situation improves, so that the metho particularly useful in the case of middle lati whistlers.

In the case of actual nose whistler traces, is a very simple procedure for obtaining appr mate source identification. Measure $\tau = t_L$ and from the graph of Figure 3 read t/t_n (here t_L/t_n) corresponding to the known f_L/f_n. Then we have

$$t_n = \frac{\tau}{R - 1}$$

If $f_L/f_n > \frac{1}{2}$, the error in τ tends to be the source of error in t_n. For smaller f_L/f_n, the in measuring f_n becomes the important fa In any event, very careful measurements be made, and attention must be restricte traces that are well defined in the range f_L

Reference

Smith, R. L., The use of nose whistlers in study of the outer ionosphere, Ph.D. dis tion, July 11, 1960, *SEL Technical Rep* Stanford University.

(Received May 9, 1961.)

Atmospheric Ion Composition Measured above Wallops Island, Virginia

H. A. TAYLOR, JR., AND H. C. BRINTON

Goddard Space Flight Center
Greenbelt, Maryland

This is a preliminary report of atmospheric composition data obtained over Wallops and, Virginia, from two successful Aerobee Hi rket flights, serial numbers NASA 4.09 and ASA 4.14. These rockets were instrumented marily to determine the composition, pres-re, temperature, and density of the neutral rticle atmosphere above 100 km. An ion mposition experiment, identical for the two nchings, was also included as a part of the yload. Continuous ionosonde monitoring was ovided by CRPL, Fort Belvoir, Virginia, and ATC, Patuxent River, Maryland, during both ng periods.

Aerobee 4.09 was fired at 10:47 AM EST on ril 29, 1960, into a relatively normal, undis-bed ionosphere and reached a peak altitude 248 km. Aerobee 4.14 was fired at 11:41 AM EST on November 15, 1960, into a calming ionosphere, immediately after a period of moderate disturbance, and reached a peak altitude of 230 km.

The ion data were obtained using a Bennett radio frequency mass spectrometer, which was mounted perpendicular to the rocket axis. The positive-ion spectrum was sampled over the range 8 to 46 AMU once every 1.3 seconds. Spectrometer sensitivity was modified by varying the stopping potential in six steps so that spectra at equal sensitivity were recorded at approximately 8-second intervals. The curves shown in Figure 1 represent an average of ascent and descent data, taken at a single sensitivity setting. The primary constituents are plotted according to percentage composition.

As shown, the major constituents detected

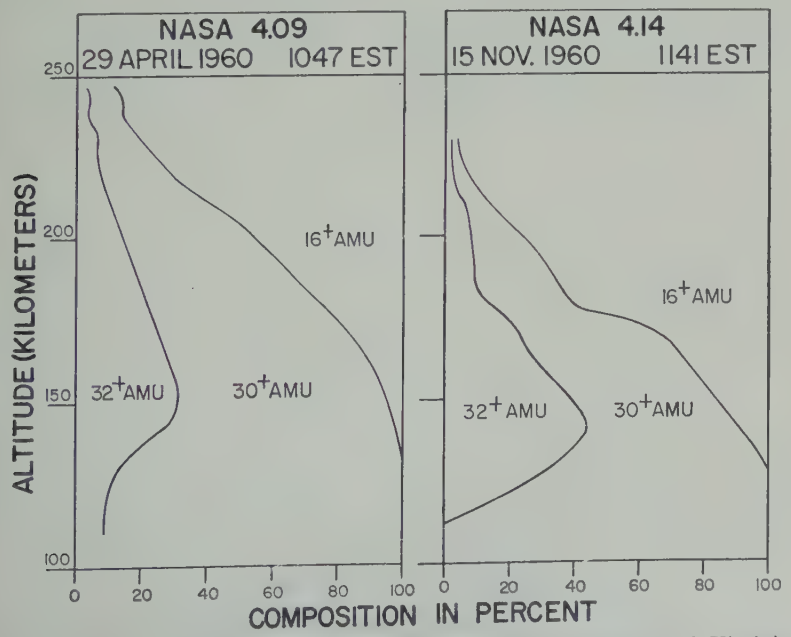


Fig. 1. Distribution of the major positive ions above Wallops Island, Virginia.

on these flights were the ions 32^+, 30^+, and 16^+. The ions 28^+, 18^+, and 14^+ were also detected on both flights, but their sum was at all times less than 5 per cent of the total composition.

A comparison of the composition measured on these flights shows general agreement. A noticeable difference, however, is observed in the abundance of the 30^+ ion. Although it is not apparent in the figure, the higher average level of 30^+ during the 4.09 flight is a result of a significant increase in 30^+ during descent over that observed during ascent, where the 30^+ data from the two flights are in close agreement. Further investigation is being directed toward determining the origin of this apparent anomaly.

These data are also in general agreement with ion composition data obtained with very similar instrumentation above Fort Churchill, Manitoba, Canada [*Johnson, Meadows, and Holmes,* 1958]. In both cases the major and secondary constituents measured were the same. One interesting difference, however, is in the relative amounts of 32^+ and 30^+ observed in the lower altitude region. Above Wallops Island, beginning at 100 km, the 30^+ ion was initially predominant. The 32^+ ion concentration was initially quite low and in each instance reached peak value later in the flight. Above Fort Churchill, however, beginning at 85 km, the 32^+ ion was initially predominant. As discussed previously [*Johnson and Holmes,* 1960], the Churchill data were taken during a polar blackout when the increased 32^+ content could be attributed to increased ionization by hard rays. In comparison, the Wallops Island d were taken under comparatively normal io spheric conditions.

The ion composition measured above 200 is essentially atomic in nature, and predo nantly oxygen (16^+) with diminishing amou of the 30^+ and 32^+ molecular ions. This ag favorably with the generally accepted mode the ion composition in this altitude range, is in direct agreement with ion data obtai both at Fort Churchill and from a simila spectrometer experiment flown aboard Spu III [*Istomin,* 1959*a,b*].

The observations reported in this letter based on a preliminary analysis of the ro data. Corrections for the effects of aspect, ro potential, and other perturbing factors, an more detailed analysis of the data are cont ing and will be reported at an appropriate t

References

Istomin, V. G., *NASA Technical Translation* 1959*a*.

Istomin, V. G., *Doklady Akad. Nauk SSSR,* 81–84, 1959*b*.

Johnson, C. Y., and J. C. Holmes, Ionosph positive ions, *Space Research,* edited by H Kallman-Bijl, North Holland Publishing C pany, Amsterdam, 1960.

Johnson, C. Y., E. B. Meadows, and J. C. Holl *J. Geophys. Research, 63,* 1958.

(Received May 22, 1961.)

Comment on Paper by Henry G. Booker, 'A Local Reduction of *F*-Region Ionization Due to Missile Transit'

CECIL BARNES, JR.

Stanford Research Institute, Menlo Park, California

Booker [1961] suggests that a hole in the ionosphere could be formed in the wake of a missile by the exhaust gases rising because of their high temperature, being replaced by air from below having a lower ion content.

I would like to suggest another possible explanation for the hole formation. The exhaust gases, after emerging from the nozzle into the near vacuum of the *F* layer, will expand immediately by a factor of more than 10^7, until pressure equilibrium is reached. This expansion will actually cool the exhaust, and will also reduce the ion density from roughly 10^{10} electrons/cc to 10^8 electrons/cc. Since the ion density of the *F* layer is typically above 10^4 electrons/cc in the daytime, the expanded exhaust will form a hole through the layer in which the density will be less than 1/10 that of the surrounding atmosphere.

REFERENCE

Booker, H. G., A local reduction of *F*-region ionization due to missile transit, *J. Geophys. Research, 66,* 1073–1079, 1961.

(Received May 8, 1961.)

All-Sky Meteor Rates in the Southern Hemisphere

C. ELLYETT AND C. S. L. KEAY

Physics Department, University of Canterbury
Christchurch, New Zealand

An extensive experiment has just been completed at Christchurch, New Zealand (43°37′S, 172°24′E), to determine meteor rates over the visible sky, using radar equipment with all parameters maintained at constant values throughout the experiment. Results have been obtained for an unbroken year between February 1, 1960, and January 31, 1961.

Two identical transmitters, used alternately as required, maintained a signal of 81 kw peak power and 26 μs pulse width at 69.5 Mc/s, with a pulse recurrence frequency of 150 c/s. Radiated power was monitored hourly, and slight frequency drift was overcome by the installation of 7.5 kva voltage regulators for the whole system.

Two identical well-separated aerials were used for transmitting and receiving. Single crossed folded dipoles above wire-mesh artificial earth screens were used for each aerial.

The echoes were detected by a receiver of noise figure 1.5, followed by an intensity modulated cathode ray tube. Pulse-type interference was greatly reduced by the use of two IF channels in the receiver, one of which, operating with a faster rise time and a frequency just clea the main frequency, acted as a noise pulse tector and suppressed the main channel noise bursts only [*Bennett*, 1958]. In addi a compression amplifier, inserted in the v stage, eliminated slowly varying backgr noise of any significant amplitude, thus o coming changes in echo recognition due to va tions in the background film density [*Lauchlan*, 1960].

Automatic hourly checks of the effect on receiver detector current of a signal from a brated noise generator served to monitor the ceiver performance. A reading of aerial r was recorded every 3 minutes. In addition, c plete systematic checking of all the appar in operation was maintained throughout the periment.

Hourly totals were obtained during 90.5 cent of the whole year.

The histogram of results is given in Figu for 724,681 meteors, from which the follo facts are apparent: (1) A seasonal variatio rate could be expected as a result of the ti the earth's axis, causing a hemispherical

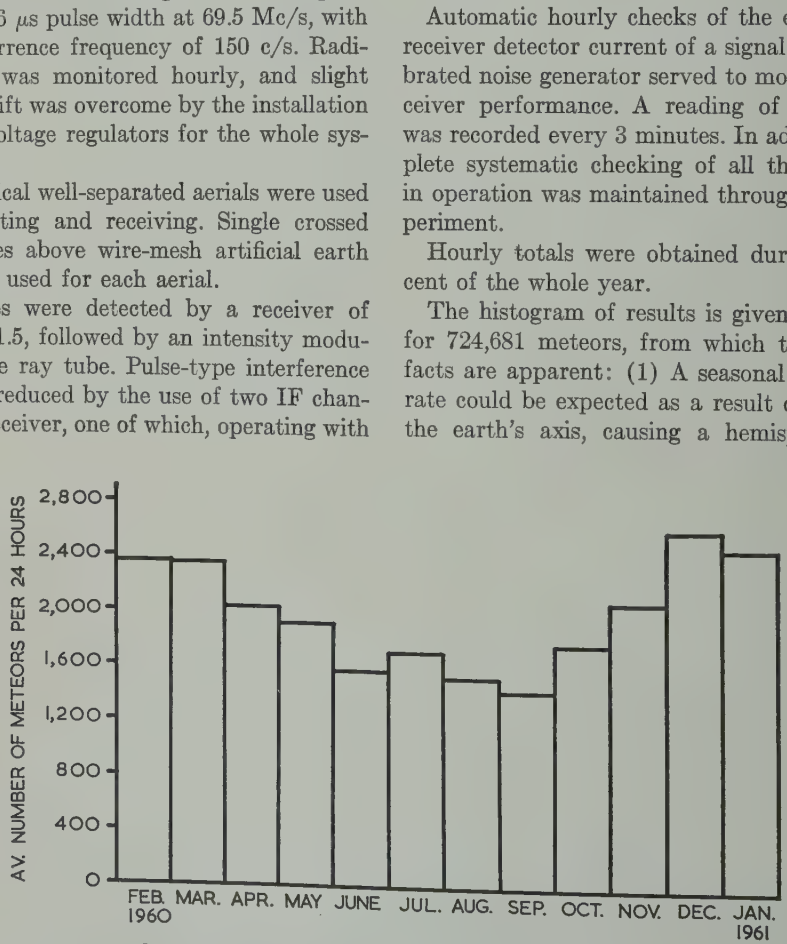


Fig. 1. Average number of meteors per 24 hours.

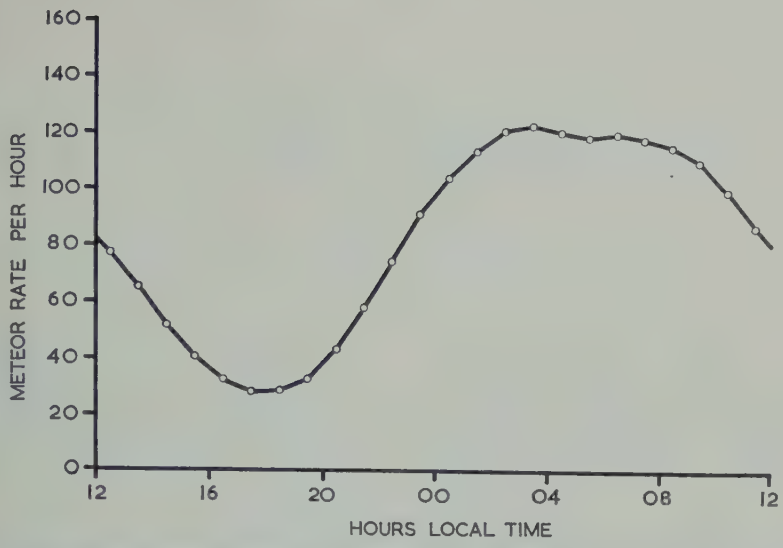


Fig. 2. Hourly meteor rates, centered on the half-hour, averaged over the year February 1960–January 1961. (Minimum at 18h00m NZLT ≡ 18h30m NZST ≡ 06h30m UT.)

unal maximum and vernal minimum. Some idence has been produced in the northern misphere to show that this is so [*Watson,* 41; *Appleton and Naismith,* 1947; *Hawkins,* 56]. The detected rates were generally low, so e influence of larger meteors associated with owers exerted a considerable masking effect. th *Appleton and Naismith* [1947] and awkins [1956] did, however, produce results owing an appreciably higher rate in Septem- r than in March. The converse should hold the southern hemisphere. This is found to true. At the high rates, which have now been asured, the difference between the autumn l spring counts is quite marked. (2) A south- hemisphere shower complex is strong in y-August, and in December another long en- ring group is surprisingly strong. These have significant effect on the annual distribution. Correlations with other results show that the teor rate at 69.5 Mc/s is *not* significantly ered by absorption associated with solar es, magnetic storms, or auroras. This would d to disprove the suggestion by *Appleton l Naismith* [1947] that the annual variation due to an ionospheric cause.

The hourly meteor rate, averaged over the whole year, is shown in Figure 2. The afternoon antapex minimum and the morning peak are very clearly defined. The three maxima reported by *Hawkins* [1956], corresponding to the sun, apex, and antisun positions, are probably merged together by the low time resolution resulting from the aerials used in the present survey. The over-all ratio of maximum to minimum rates is approximately 4:1, but this ratio undergoes substantial variations during the year.

Acknowledgment. The work has been sponsored by the Electronics Research Directorate of the Air Research and Development Command, the United States Air Force, under contract AF64-(500)-6.

References

Appleton, E., and R. Naismith, *Proc. Phys. Soc., 59,* 461, 1947.

Bennett, R. G. T., Ph.D. thesis, University of Canterbury, 1958.

Hawkins, G. S., *Astron. J., 61,* 386, 1956.

McLauchlan, E. C., *Australian J. Phys., 13,* 750, 1960.

Watson, F., *Between the Planets,* Blakiston Company, Philadelphia, 113, 1941.

(Received April 19, 1961.)

Remarks on the Article by A. R. Hibbs, 'The Distribution of Micrometeorites near the Earth'

MAURICE DUBIN

National Aeronautics and Space Administration
Washington 25, D. C.

This letter is addressed to the question whether the data from the Explorer I micrometeorite experiment is indicative of an altitude dependence of the impact rate of micrometeorites, and the attendant implication that perhaps a very large fraction of the particles measured on Explorer I were moving in closed orbits about the earth, as hypothesized in the paper by *Hibbs* [1961].

It has been reported [*Dubin*, 1960*a*, *b*] that the micrometeorite experiment and data from Explorer I have given the following information: (1) the average impact rate over a 12-day period during the month of February for a component of cosmic dust of mass probably greater than 10^{-9} grams; (2) the average daily impact rate over the 12-day period; (3) the possibility of a diurnal variation resulting from the heliocentric velocity of the satellite and the shielding effect of the earth, coupled with (4) an indication that an identifiable higher-than-average impact rate or 'shower' occurred in the 8-hour period during February 2 and 3, 1958, where the impact rate was approximately 50 times greater than the average rate. Further analysis of the data does not lead to an altitude dependence of the rate of impacts, and the conclusions that the particles are mostly in trapped orbits, as given by Hibbs.

The analysis performed by Hibbs is incorrect, based on the following:

(*a*) There were a total of 145 type A impacts recorded without redundancy, with 25 impacts recorded at more than one station.

(*b*) A cosmic dust 'shower' was recorded with a total of 66 impacts, leaving 79 or less sporadic impacts.

(*c*) Hibbs used 127 hits in his analysis in Table 1 and 126 hits in his analysis in Table 2; thus, he probably included some of the imp in the 'shower'; the assumption of the Poi distribution would not be valid for such a sam

(*d*) The assumption of a Poisson distribu is inconsistent with the large variation of daily impact rate.

There was also reported a 'shower' compo first detected on February 2 at 1930 UT, w apparently lasted for nearly 10 hours. The im rate on the satellite during the shower is re sented by a rate nearly three impacts per m ute for a sample of 12 type A impacts reco at Fort Stewart, Georgia, at 01:41 UT on Fe ary 3, 1958, compared with the 12-day ave impact rate of approximately 0.1 impacts minute. Considering the area of the earth ered by the 'shower,' there were a total o impacts [Fig. 2, *Dubin*, 1960*b*] that coul attributed to the 'shower.' In fact, by traci possible radiant for the 'shower,' it appears Woomera, Australia, was able to detect 'shower' on the pass on February 2 at 1833 and later on February 3, at 0043 and 0258 These data may be used to indicate a pos direction of the 'shower,' which evidently nearly in the ecliptic plane with the 'sho particles traveling in a direct orbit about sun. Thus, the total number of impacts might have been in the shower can be enu ated at 66 impacts. Subtracting this numbe impacts from the total sample of 145, there main 79 impacts or less of a sporadic na that could be studied statistically.

(*e*) A diurnal variation is evident after s rating out the 'shower' component.

These statements are explained below.

Let us first review the data from the mi meteorite experiment on Explorer I as rel to the paper by A. R. Hibbs [*Dubin*, 196

ere were recorded during the 12-day period 8 impacts of type A (p. 1049). There were o recorded a total of 17 type B impacts which re not included in the data sample because signal-to-noise ratio made the readout of se impacts somewhat questionable. This rep- ents the total of impacts available on all the ta tapes from Explorer I while the experi- nt was telemetering and received by ground tions, including all the amateur tapes avail- le after the experiment. Of the 178 recorded pe A impacts, 8 were discarded because these curred during the launch and could have re- ted from interference during burning and paration of the rocket stages. By tabulating impacts for each pass, it was possible to minate redundant impacts recorded at two tions simultaneously. There were, therefore, out 25 such impacts which were recorded in region where there was overlap of telemetry, , mostly in the region around the United ates when the satellite was near perigee.

Referring now to the data in Tables 1 and f the article by Hibbs, Table 1 lists a total 127 hits. Thus, particles in the 'shower' must ve been included in this table. In Table 2, bbs lists a total of 126 particles, and again ower' hits probably were included. Hibbs cognized a shower component, for he stated, . . . on four separate occasions stations re- ded sudden bursts of impacts in which the quency was higher than would be expected m a Poisson distribution. . . . These four ups of data were, therefore, rejected from ther consideration in the present statistical alysis.' If shower hits were counted, these uld give added weight at the lower altitudes en the satellite was in the northern hemi- ere, and at altitudes slightly greater than the igee height.

Hibbs further states from Figure 5 that the crometeorite impact rate as a function of ellite local time does not show a diurnal varia- n where Figure 5 represents the complete a. By comparison [Fig. 2, *Dubin,* 1960*b*], er removing the 'shower' component, and with further correction for the 14 impacts that ght be attributable to the same 'shower,' de- ted at Woomera, Australia, there remain ut 58 impacts between the hours of mid- ht and 12:00 noon, and 21 impacts between the hours of local noon and midnight, giving a diurnal ratio of 3 to 1; the ratios of the hit rate before removing the 'shower' component is about 2.1 to 1, which still indicates a diurnal variation. If the ratio is significant, it can be explained on the hypothesis that the large majority of particles detected on Explorer I were traveling in heliocentric orbits.

Finally, were one to agree with the conclusion of Hibbs that the average particle measured by Explorer I was in a closed orbit around the earth rather than on an impact trajectory from a great distance from the earth's surface, these particles would make 'hundreds or thousands of orbits around the earth before descending to the point where they are destroyed by friction with the denser atmosphere.' If the lifetime of such trapped particles were of the order of a month to a year, and if the majority of particles measured on Explorer I were in closed orbits, then the time dependence rate of impacts should be fairly uniform from day to day. However, the data from Explorer I [Fig. 3, *Dubin,* 1960*b*] show an impact rate that varies considerably over the 12-day period. If the data from the first 3 or 4 days in orbit are discounted in Figure 3 (because of the 'shower' component) there are still three days which showed no impacts whatever for a total of only 22 impacts in the 7-day period. It may be noted that the impact rate over this 8-day period is only 2.6×10^{-2} hits per minute, or less than a third of the average rate of 9×10^{-2} hits per minute. The rate over the 12-day period after removing the 'shower' component is 6×10^{-2} hits per minute, which is significantly different from the rate used by Hibbs. In essence, it is doubtful that the Explore I data satisfied one of the necessary and sufficient conditions for applying Poisson statistics, namely, that the chance of registering a micrometeorite impact during a given time interval is the same for all time intervals of equal size, because of the daily variation of the rate.

In summary, the micrometeorite data from Explorer I does not per se support an altitude dependence of the impact rate, and there is insufficient evidence that a component of the cosmic dust detected was in orbit about the earth. Perhaps such dust particles may be discovered soon with satellite detectors capable of measuring velocities and radiants or directions of micrometeoroids in the vicinity of the earth.

References

Dubin, M., Meteoritic dust measured from Explorer I, in *Planetary and Space Science, 2,* 121–129, Pergamon Press Ltd., London, 1960*a*.

Dubin, M., IGY micrometeorite measurements, in *Space Research,* edited by H. K. Kallmann Bijl, North Holland Publishing Co., Amst pp. 1042–1058, 1960*b*.

Hibbs, A. R., The distribution of micromet near the earth, *J. Geophys. Research, 6* 377, 1961.

(Received April 18, 1961.)

Author's Reply to the Preceding Discussion on the Article, 'The Distribution of Micrometeorites near the Earth'

A. R. HIBBS

Jet Propulsion Laboratory, California Institute of Technology
Pasadena, California

a letter written to you, Maurice Dubin several comments on my recent article on meteorite distribution [*Hibbs*, 1961] and elation to his previously published papers *in*, 1960*a* and *b*]. In this letter, I hope to some of the misimpressions which may been generated by Dubin's letter.

ubin states that my analysis was incorrect, g his claim on a number of points. He s that a total of 145 type-A impacts was ded. Although I am indebted to Dr. Dubin uch information on the reduced data which ed in his report, I did not limit my calcula- to those data alone. I reviewed the original tapes from Explorer I and arrived at a number of valid, nonredundant, impact re- ngs of 166. Although this amounts to 21 than the number reported by Dubin, I do el that any differences in our conclusions be ascribed to this difference in number of used in the data.

condly, Dubin refers to a 'shower' group of ts which he feels should be subtracted the data before the application of Poisson tics could be valid. In the 40 hits that I ed from the data, I included 28 from this ver' segment. The number deleted occurred w altitudes, since I did not wish to prejudice conclusions on an altitude effect by arti- ly deleting high-altitude data. This result is by a comparison of Figures 2 and 4 of aper [*Hibbs*, 1961].

evertheless, the flux rate of the remaining ts during February 2 and 3 is still much er than average, as pointed out by Dubin. refore, it is worthwhile to investigate the ts when all of these high-flux data are ex- d from consideration. Dubin suggests that shower' lasted for about 8 to 10 hours. How- I feel that exceptionally high flux rates oc- d at least from 1833 UT on February 2 through 1826 UT on February 3, nearly 24 hours. This includes a total of 95 class-A impacts out of the 166 which I used originally.

If these impacts are all deleted, the resulting histogram is shown in the accompanying figure. A straight line can be fitted to this histogram in the same manner as that described in my paper to determine the nature of the altitude effect and, following the analysis in the paper, to determine the probable speed at infinity of the particles responsible for the flux included in the histogram. The critical number is $(R/N)(\partial N/\partial R)$ as described in the discussion following equation 12 [*Hibbs*, 1961]. In my original paper, this quantity was -2.0. With the complete 'shower' flux deleted from the data, this number becomes -2.1, only slightly more negative and thus apparently slightly more indicative of a trapped-particle population. However, the total number of hits included is now reduced to 71, so that the statistical validity of the conclusion is even less certain than that of the original analysis.

Thus, since in my original paper I pointed out that the conclusion could not be firmly asserted on statistical grounds, and since the difference between the computed velocity and escape velocity was only about one standard deviation of the data, the conclusion with more data deleted is even less certain. Nevertheless, the strong altitude effect is still displayed, and the data even with the 'shower' impact completely deleted still show the closed-orbit phenomenon.

I hope that this clarifies the mistaken impressions which Dubin evidently had and which he indicated in his letter. The flux originally deleted was all at low altitude. By deleting all of the 'shower' components, the conclusions are not changed. If any change does exist, it makes the apparent slope even stronger than that reported in the original analysis. This is, of course,

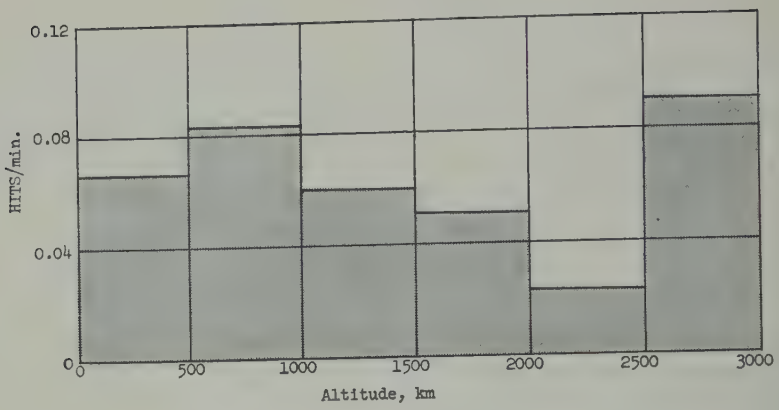


Fig. 1.

exactly contrary to the impression made by Dubin's statement: 'If shower hits were counted, these would give added weight at the lower altitudes when the satellite was in the northern hemisphere and at altitudes slightly greater than the perigee height.'

Dubin in his remarks on the diurnal variations refers to the total number of hits recorded between certain hours of the day. Perhaps a more physically meaningful quantity is the flux recorded during these hours, taking into account the length of time during which good data were obtained during various hours. It was this total flux which was reported in Figure 5 [*Hibbs*, 1961].

If all of the 95 'shower' impacts suggested herein are deleted, one finds that the conclusions which I reached [*Hibbs*, 1961] are not changed. The flux from midnight to noon is 0.057, whereas that from noon to midnight is 0.056. This does not indicate the strong variation which Dubin suggests on the basis of looking at total hits alone. If only the flux during the 10 hours suggested by Dubin for the 'shower' is deleted, then the flux of the remaining counts between night and noon is 0.072, whereas that from to midnight is 0.056. The ratio between two times is 1.3 to 1.0 compared with the reported by Dubin on a count comparison

These apparent percentage variations in rate are more than adequately accounted f the basis of the orientation of the trajec That is, the satellite passed through perigee ing the early morning hours and as a c quence of the altitude effect recorded a h impact rate during these hours than at times.

References

Dubin, M., Meteoritic dust measured from plorer I, *Planetary and Space Science, 2,* 129, 1960*a*.

Dubin, M., IGY micrometeorite measurem *Space Research,* edited by H. K. Kallmann North Holland, Amsterdam, pp. 1042–1058, 1

Hibbs, A. R., The distribution of micromete near the earth, *J. Geophys. Research, 66,* 377, 1961.

Discussion on 'The Origin of Microseisms'

J. N. NANDA

Office of Scientific Research and Development
Naval Headquarters, New Delhi, India

he origin of microseisms has been ascribed he author to the action of oriented winds on gh sea surfaces [*Nanda*, 1960]. Earlier, *guet-Higgins* [1950] had explained that the rference of opposite components in the two-ensional wave spectra of the sea surface t give the pressure on the sea bottom respon-e for the generation of microseisms.

or the following reasons the author was ouraged from putting too much reliance on Longuet-Higgins theory for the incoherent

) The simplifications in his article 3.1 require r be large compared with λ and so in equa-s 190, 193, 194 etc, u and v are to be such $(u^2 + v^2)^{1/2} \gg 1$, which invalidates the ysis since all elements of phase space are no er equally probable. The analysis conflicts the requirements of the ergodic theorem.

) The seismic disturbance is calculated for ean pressure term acting at a point. In case steps are taken logically, the mean energy be given by an expression similar to his 196, it will be incorrect to regard the mean sure thus obtained to be acting on a point the purposes of arriving at the seismic litude at a distant point. For generation of oseisms, the resultant force has to be the t vector sum of contributions from unit s in phase space which approaches zero very lly. It is more likely that the greater portion he energy derivable at the sea bottom from ncoherent sea is dissipated or scattered back the local irregularities of the sea bottom. s when the calculations along the lines of guet-Higgins' theory are carried out in dance with the ergodic theorem, that is out requiring R to be large and including boundary conditions regarding horizontal vertical motions at the boundaries, pre-ably a certain pressure term of random phase ld still be obtainable at sea bottom. The or would suggest that this term might be source of turbulence reflected in the occurrence of ripples and rounded pebbles at sea bottom, rather than the cause of microseisms.

In case large-scale standing waves (more strictly, opposite waves of the same wavelength but not necessarily of the same amplitude) were to exist, one would easily arrive at very large microseismic amplitudes. But it is not plausible to assume the existence of coherent waves.

In the paper by the author, a derivation has been given for the interaction of winds with standing waves under the assumption that the back side of the waves is completely inactive under turbulent conditions except for affecting the value of the factor S. This is seen to be a small interaction, and it has no bearing on the main calculation of the interaction of the oriented winds with the rough sea surface. Since coherent standing waves are not expected, this interaction is not of much significance as far as generation of microseisms is concerned.

The author's theory does not require a coherent sea. A certain individuality of sea roughness over short range is required, and this is plausible because roughness is an extensive property. If there is a prominent undulation of the surface, for purposes of roughness, an area large compared with the wavelength of the undulation will naturally have to be considered. When sea roughness is experimentally observed, by radar reflection, for example, a considerable area is illuminated. For the observed microseisms at Cochin, in the example given in the author's paper, the observed amplitude will be obtained if the cyclic terms in the sea roughness are assumed to be in phase over about 30 wavelengths (the wavelength corresponding to a time period of 3.5 seconds is about 20 meters).

When oriented winds act suddenly on a rough sea surface, a depression/elevation of the surface is caused. This depression has been calculated in the paper only for shallow seas (assumption of homogeneous water and gradient currents acting down to the sea bottom). To extend the theory to the deep ocean, this depression will

have to be calculated under the assumption of a dead level slightly below the surface when there is a sudden passage of the oriented winds. An empirical value for the depth of this dead level can be obtained from experience of storms over shallow seas. The microseismic amplitudes will then depend on depth only in the sense of the c_m's of equation 24 in the author's paper (same as in Figure 2 of Longuet-Higgins' paper).

References

Nanda, J. N., The origin of microseisms, *J.*... *phys. Research, 65,* 1815–1820, 1960.

Longuet-Higgins, M. S., A theory of the orig... microseisms, *Phil. Trans. Roy. Soc. Lond... 243,* 1–35 (1950).

Longuet-Higgins, M. S., Discussion of paper ... N. Nanda, 'The origin of microseisms,' *J.*... *phys. Research, 66,* 994, 1961.

(Received May 9, 1961.)

Discussion of Paper by W. Barclay Kamb, 'The Thermodynamic Theory of Nonhydrostatically Stressed Solids'

G. J. F. MACDONALD

Theoretical Division, Goddard Space Flight Center
National Aeronautics and Space Administration
Washington 25, D. C.

mong the major points of difference be-
en my approach [*MacDonald*, 1960] and
t of *Kamb* [1959, 1961] the following may
noted:

. An anisotropic crystal placed in a stress
i can have at least one orientation in which
re is no further tendency to reorient. The
librium orientation is independent of the
hanism by which the orientation might be
eved. Possible mechanisms include solid or
ace diffusion and nucleation, or diffusion
ough an external medium and nucleation.
external medium may determine the rate
eorientation, but it does not influence the
l equilibrum state, provided that the me-
n does not react chemically with the crystal.
. Kamb contends that in the variational
tment the contributions from rotation
ld be included in the expression for the
ual strain. In the virtual process [*Mac-
ald*, 1960] the components due to rotation
negligibly small. An infinitesimal change in
stress acting on a crystal does not bring
t a finite rotation. This would be true if
problem were one of the deformation of a
elastic rod.

3. As Kamb states, my theory predicts the results of certain idealized experiments. Kamb does not discuss any simple experiment in which his theory correctly predicts orientation that mine does not predict.

It should be noted that a number of inconsistencies appear in Kamb's paper. As an example, on page 266 the reader is asked to believe that the scalar quantity, specific volume, is a function of crystal orientation.

Finally, it should be emphasized that in any theory of orientation the irreversible aspects of deformation must be taken into account. Neither of the theories under discussion does this.

REFERENCES

Kamb, W. B., Theory of preferred cystal orientation developed by crystallization under stress, *J. Geol., 67*, 153–170, 1959.

Kamb, W. B., The thermodynamic theory of nonhydrostatically stressed solids, *J. Geophys. Research, 66*, 259–271, 1961.

MacDonald, G. J. F., Orientation of anisotropic minerals in a stress field, *Geol. Soc. Am. Mem. 79*, 1–8, 1960.

(Received May 19, 1961.)

Discussion of Paper by W. Barclay Kamb, 'The Thermodynamic Theory of Nonhydrostatically Stressed Solids'

ABRAHAM HOFFER

Department of Physics, Pennsylvania State University
University Park, Pennsylvania

The following remarks refer to the writer's concluding statements with regard to the applicability of his theory to the treatment of petrofabric problems.

Kamb [1961] apparently fails to consider that in any valid thermodynamic treatment a given state of free energy should be independent of the manner in which it may be arrived at. The orientation which an anisotropic solid will strive to acquire with respect to the initial stress distribution is independent of the mechanism by means of which the preferred orientation may be acquired. Processes of solution and redeposition, annealing recrystallization, and intragranular—as well as intergranular—movements should all be expected to lead to the same results. In fact, any natural fabric is the product of a continuous succession of combinations of such processes, each diminishing in intensity while others become more effective with the changing conditions of the immediate metamorphic environment.

It may be pointed out that stress deviations in nature are rarely imposed spontaneously on a randomly oriented mineral assemblage, but are more likely to develop gradually both in magnitude and orientation. Under such conditions, and considering the general sluggishness at the temperatures prevailing in the crust of the direct and indirect componental movements and reactions involving the common rock-forming minerals other than carbonates and ice, it is questionable whether the mineral assemblage and its orientation can ever catch up with steady-state requirements. The patterns of preferred orientation which one observes in tectonites reflect at best in a qualitative manner the most severe of the more recent phases of metamorphic conditions imposed by tectonic agencies.

The concept of preferred mineral orientation as a trend is logically incompatible with the notion of stability and a state of thermodyn equilibrium, which would require not mere statistically significant departure from ran ness, such as one observes in rocks, but a st uncompromising, and complete orientatio the fabric, unless the thermodynamic treatm is capable of rigorously specifying the e amount of departure from randomness and exact amount of preference for a specific orie tion that is required to minimize the free en

The structural petrographer finds comfo the premise that, if he knew (1) the compli or stiffnesses of a linearly elastic anistropic as a function of temperature, (2) the size shape of this body, as well as the tempera at a given instant of geologic time at which body was not plastically deformed by flexu torsion, and (3) the absolute magnitude the three principal stress axes at that ins he could conceivably derive at least one of eral possible states of orientation (dimensi as well as crystallographic) of the body respect to the three principal stress axes a given instant, for which the free energy minimum. What chance is there of success treating, with the help of Kamb's theory, lems of preferred mineral orientation in mineralic aggregates with polymodal pa size and particle shape distributions, whi the rule in the commonly segregated (into l and lenses) metamorphic rocks—even on questionable assumption that the specime examines had reached at any one time i geologic history (including the present) a st state? The answer is left to the critical re

REFERENCES

Kamb, W. Barclay, The thermodynamic theo nonhydrostatically stressed solids, *J. Geo Research, 66*, 259–271, 1961.

(Received February 20, 1961;
revised April 21, 1961.)

Factors Influencing Thickness of the Earth's Crust[1]

B. F. HOWELL, JR., AND R. A. WOODTLI

Department of Geophysics and Geochemistry
Pennsylvania State University, University Park, Pennsylvania

Earth scientists have for many years visual-
d the crust of the earth as a layer of rela-
ely light, crystalline material of one average
mposition floating on a more plastic layer of
ater density and different composition. Ac-
rding to the theory of isostasy, the height of
earth's surface at any place is a function
the average density of the underlying rock
umn. The most widely accepted view today
hat relatively light rocks extend to greater
ths beneath continents than elsewhere.
untains are held up by their roots. A world-
e discontinuity in the velocity of transmis-
n of seismic waves is known to exist. It lies at
uch shallower depth under oceans than un-
continents. It is natural to associate this
nic (Mohorovicic) discontinuity with that
uired by isostatic theory.

The nature of the compositional change at the
continuity has not been determined. It has
n suggested that the rocks immediately be-
th this boundary are richer in iron and re-
d elements and hence are denser than those
mediately above it. On the other hand, it is
ible that the change is only one of phase
m a lighter to a denser crystal form. If this
he case, it is necessary to explain why the
se change occurs at a lesser depth beneath
oceans than beneath the continents.
overing [1958] attempted to explain this in
ns of the difference in temperature-pressure
ironment beneath the continents and the
ns. Because the temperature at the bottom
he ocean is lower than the temperature at
depth beneath the continents where the
ssure is the same, the temperature at any
n pressure beneath the oceans must gener-
be lower than under the continents. Since
pressure at which a particular phase trans-
ation occurs increases as temperature in-
creases, it will occur at a greater depth beneath the continents.

One implication of this is that for the continents themselves, assuming that the average temperature gradient with depth is everywhere the same, the depth at which a particular phase change will occur will be a function of surface temperature. If the Mohorovicic discontinuity is due primarily to a phase change, its depth should vary with surface temperature.

The mean annual temperature at the earth's surface in the center of the continents varies roughly from about −20°C to 35°C, being largely a function of latitude and elevation but controlled also by the tempering effect of large bodies of water and by wind patterns. If Lovering's formula is accepted for the relation between the temperature and pressure of the phase transformation,

$$dT/dp = 0.046°\text{C/bar} \qquad (1)$$

then the effect of surface temperature can be calculated from

$$\frac{dH}{dT} = \frac{dp}{dT}\frac{dH}{dp} = \left(\frac{1}{0.046°\text{C/bar}}\right) \cdot \left(\frac{10^6 \text{ dynes/cm}^2\text{/bar}}{980\rho \text{ dynes/cm}^3}\right) = \frac{2.22 \times 10^4}{\rho} \text{ cm/°C} \qquad (2)$$

where T is temperature, p is pressure, H is depth, and ρ is density. Assuming that the average density of the rocks of the crust is 2.8 g/cm^3,

$$\frac{dH}{dT} = 0.8 \times 10^4 \text{ cm/°C} = 0.08 \text{ km/°C} \qquad (3)$$

A 12.5° change in surface temperature would be required to cause a 1-km change in depth to the Mohorovicic discontinuity. Present methods

Contribution 60-62, College of Mineral Indus-
s, The Pennsylvania State University.

TABLE 1. Data Used

No.	Location	References	Crustal Thickness, km	Surface Elevation, m	Distance to Nearest Edge of Continent, km	Aver Surf Temp ture,
1	Maryland-Virginia	*Tatel et al.* [1953, 1955] *Tuve et al.* [1948, 1954]	27.5	30	280	14.
2	Minnesota	id.	37	460	1900	4.
3	Tennessee-Virginia	id.	39	800	780	11.
4	Colorado Plateau	id.	34	2300	800	10.
5	S. Arizona-New Mexico	id.	28	1500	700	15.
6	Seattle (W)	id.	19	230	160	10.
7	Utah	id.	29	2100	1060	7.
8	Southern California	*Shor* [1955]	31.9	1500	200	17.
9	Eastern Pennsylvania	*Katz* [1955]	32.7 ± 3.3	210	290	11.
10	Northern New York	id.	34.8	130	620	5.
11	Eastern New York	id.	36.0 ± 2	200	260	9.
12	Quebec-Ontario	*Hodgson* [1947, 1953]	36.0	300	1480	0.
13	Blaubeuren	*Reich* [1953]	27.6	640	1000	7.
14	Haslach	*Förtsch* [1952] *Reich, Schulze, Förtsch* [1948]	31	750	1070	7.
15	Helgoland (N. Germany)	*Reich* [1950] *Schulze and Förtsch* [1950] *Willmore* [1950]	27.4	114	1290	8.
16	Champagne	*Rothé* [1958]	30	450	510	8.
17	Transvaal (W)	*Gane et al.* [1946, 1956] *Willmore, Hales, Gane* [1952]	35.5 ± 1.4	1300	700	18.
18	Transvaal (S)	id.	34.7 ± 1.0	1250	450	18.
19	Transvaal (E)	id.	34.1 ± 2.0	770	140	20.
20	Transvaal (N)	id.	36.6 ± 2.4	1090	470	17.
21	Wellington	*Eiby and Dibble* [1957]	18.2	360	70	11.

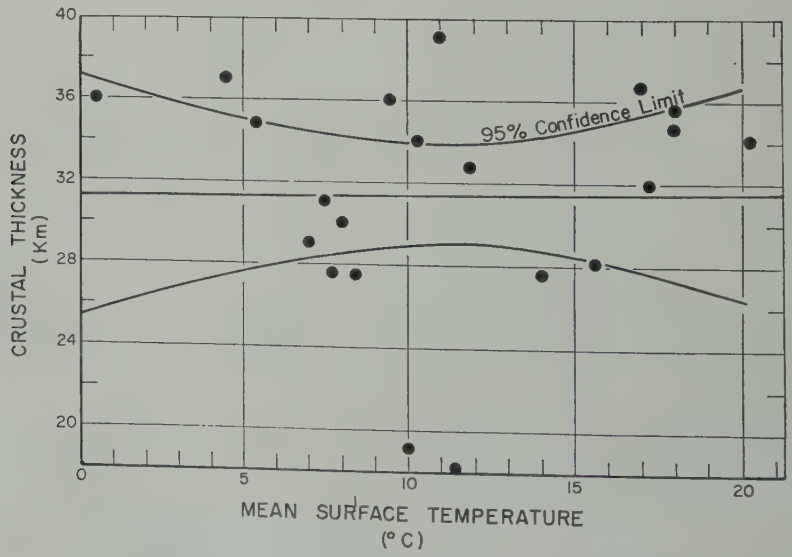


Fig. 1.

crustal-thickness measurement, at their best, barely adequate for measuring thickness to s accuracy. Therefore, considering that the al effect of the temperature range on the tinents is only a little over 4 km, the effect temperature on the thickness of the crust, if xists, might readily have been overlooked in stal-thickness studies.

To test this hypothesis, 21 measurements of tinental crustal thickness were selected from published literature and tested for a cor- tion of thickness with surface temperature. rtinent data are listed in Table 1. The thick- s measurements used were taken from lists blished by *Gutenberg* [1955], *Tatel and Tuve* 55] and *Eiby and Dibble* [1957]. All the veys listed by these authors were used ex- t those for which the original papers were readily available for checking or which did contain enough of the original data to per- precise determination of the location of the vey. The figures used were taken from the st recent publications available at the time test was started. This arbitrary method of ction of profiles (using only surveys listed three review papers) was chosen in an at- pt to avoid insofar as was possible any bias arding the relative accuracy of different asurements. In retrospect, it appears likely t this choice of data was not ideal for dis- ering meaningful correlations. It did, how- r, serve adequately the purposes of the ex- iment. Average surface temperature for the ions of the surveys were obtained from *Hann* 11], *Kendrew* [1937], *Robertson and Sellick* 33], *Visher* [1954], and *Ward and Brooks* 36].

The crustal-thickness data are plotted against face temperature in Figure 1. The least- ares straight line through these points is

$$H = 31.3 \text{ km} + 0.009T \text{ km/°C} \qquad (4)$$

e coefficient of correlation for these data is o. The temperature coefficient is approxi- tely one-tenth that predicted by Lovering. It st be pointed out that small differences in estimated average surface temperatures may nge the value and even the sign of the slope the line. It is concluded that there is no sig- cant evidence of a dependence of crustal ckness on surface temperature.

A correlation of crustal thickness with surface elevation was also made, based on the isostatic concept. Because most of the profiles were several hundred kilometers long, a rough average surface elevation for each was estimated from topographic maps of the continents. Crustal thickness is plotted against surface elevation in Figure 2. The least-squares straight line through these points is

$$H = 30.2 \text{ km} + 0.00155h \text{ km/m} \qquad (5)$$

where h is surface elevation in meters. The coefficient of correlation in this case is 18.5 per cent, which is too low to show a significant correlation between the two variables considered.

As an additional means of seeing whether the correlations are meaningful, a third correlation not based on any theory explaining crustal thickness was made. The distance of the center of each of the seismic profiles from the nearest outer edge of the continental shelf was measured. Figure 3 shows crustal thickness plotted against distance to the edge of the shelf on semilogarithmic paper. The least-squares line through these points is

$$H = (12.5 + 7 \log_{10}\Delta) \text{ km} \qquad (6)$$

where Δ is distance to the edge of the continent in kilometers. A similar plot on linear paper was best fitted by

$$H = (29.2 + 0.0033\Delta) \text{ km} \qquad (7)$$

For the linear plot, the coefficient of correlation was 23.5 per cent; for the semilogarithmic plot it was 43.8 per cent. The coefficient of correlation of the semilogarithmic plot is reliable only at the 95 per cent level of significance; the linear plot is not reliable even at this level.

It must be realized that the three variables tested are not independent of one another. Elevation generally increases with distance from the edge of a continent; and as elevation goes up, temperature goes down. Thus, if there is a significant correlation of any one variable with crustal thickness, some correlation of all three is to be expected. The poorness of all correlations shows that no one of these factors is alone responsible for crustal thickness. The poorness of the correlation with temperature casts doubt on Lovering's phase-change hypothesis. The large degree of scatter of the elevation data challenges the assumption that surface elevation is a good measure of crustal thickness. As far as

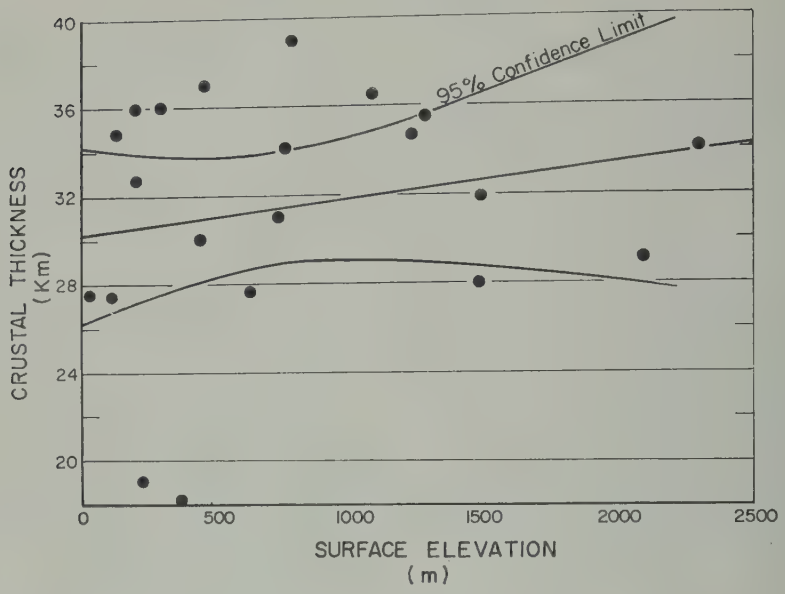


Fig. 2.

the data reviewed here are concerned, it would be more reasonable to suppose that the continental roots are primarily disk-shaped, with their maxima near their centers.

It is realized that the number of data which have been analyzed is insufficient to lead to definite conclusions. Since the work described here was completed a more extensive stud crustal thickness has been made by *Stei* [1960]. He investigated the relationship tween crustal thickness and several vari (but not surface temperature or distanc the edge of the continents). He found tha single variable can be used to predict cr thickness and that a weighted function of r crustal velocity and Bouguer gravity ano together shows the best linear correlation found, as was found in this study, that o poor correlation exists between surface e tion and thickness of the crust.

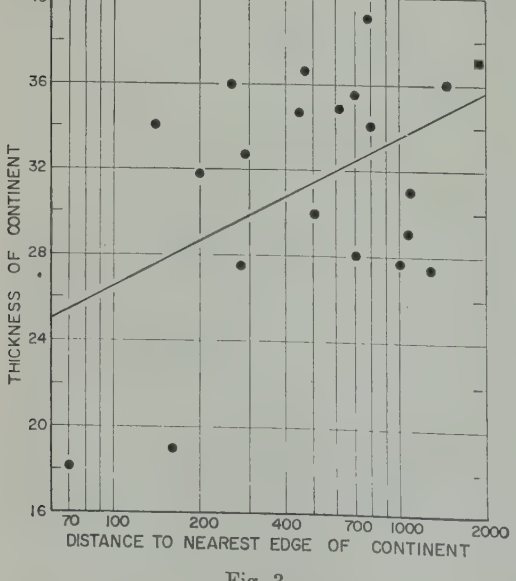


Fig. 3.

One other conclusion which can be d from this simple study is that accurate dete nations of crustal thicknesses are needed. clear determination is to be made of whic the variables tested is the most importan controlling the thickness of the earth's c then greater accuracy than is claimed for measurements is needed. An accuracy of c determination of better than ±1 km is ne if a relation with surface temperature is so Most profiles are hundreds of kilometers Over this distance surface temperature, e tion, and distance from the edge of the cont all vary. Therefore, point-by-point depth desirable rather than a single figure for the v profile.

knowledgments. We wish to thank Mr. Yo- Nakamura for his help in making certain of calculations reported above and the National nce Foundation for funds which made this y possible.

References

y, G. A., and R. R. Dibble, Crustal structure oject, *New Zealand Dept. Sci. Ind. Research, eophys. Mem. 5,* 1957.

n, H., *Witterung und Klima in Mitteleuropa,* irzel Verlag, Zurich, 1954.

sch, O., Analyse der seismische Registrierungen r Grosssprengung bei Haslach im Schwarzwald n 28. April 1948, *Geol. Jahrb., 66,* 65–80, 1952.

e, P. G., A. R. Atkins, J. P. F. Sellschop, and Seligman, Crustal structure in the Transvaal, *ull. Seism. Soc. Am., 46,* 293–316, 1956.

e, P. G., A. L. Hales, and H. O. Oliver, A smic investigation of the Witwatersrand earth mors, *Bull. Seism. Soc. Am., 36,* 49–80, 1946.

enberg, B., Wave velocities in the earth's crust, *ol. Soc. Am. Spec. Paper 62,* 19–34, 1955.

n, J., *Handbuch der Klimatologie,* vols. 2-3, rlag von Engelhorn, Stuttgart, 1911.

gson, J. H., Analysis of travel times from rock- rsts at Kirkland Lake, Ontario, *Bull. Seism. c. Am., 37,* 5–17, 1947.

gson, J. H., A seismic study in the Canadian ield, 1, Refraction studies based on rockbursts Kirkland Lake, Ont., *Publs. Dominion Obs.,* 111–163, 1953.

, S., Seismic study of crustal structure in Penn- lvania and New York, *Bull. Seism. Soc. Am.,* 303–325, 1955.

drew, W. G., *Climatology,* Clarendon Press, xford, 1937.

ering, J. F., The nature of the Mohorovicic scontinuity, *Trans. Am. Geophys. Union, 39,* 7–955, 1958.

h, H., Geologische Ergebnisse der seismischen obachtungen der Sprengung auf Helgoland, *ol. Jahrb., 64,* 243–266, 1950.

h, H., Ueber seismische Beobachtungen der akla von Reflexionen aus grossen Tiefen bei n grossen Steinbruch-Sprengungen in Blau- uren am 4. März und am 10. Mai 1952, *Geol. hrb., 68,* 225–240, 1953.

Reich, H., G. A. Schulze, and O. Förtsch, Das geophysikalische Ergebnis der Sprengung von Haslach im südlichen Schwarzwald, *Geol. Rundschau, 36,* 85–96, 1948.

Robertson, C. L., and N. P. Sellick, *Handbuch der Klimatologie,* vol. 5., part 10, Borntraeger, Berlin, 1933.

Rothé, J. P., Quelques expériences sur la structure de la croûte terrestre en Europe occidentale, in *Contributions in Geophysics in Honor of Beno Gutenberg,* 135–151, Pergamon Press, London, 1958.

Schulze, G. A., and O. Förtsch, Die seismischen Beobachtungen bei der Sprengung auf Helgoland am. 18. April 1947 zur Erforschung des tieferen Untergrundes, *Geol. Jahrb., 64,* 205–242, 1950.

Shor, G. G., Jr., Deep reflections from southern California blasts, *Trans. Am. Geophys. Union, 36,* 133–138, 1955.

Steinhart, J. S., Explosion studies of continental structure, Ph.D. thesis, Dept. of Geology, University of Wisconsin, 1960.

Tatel, H. E., L. H. Adams, and M. A. Tuve, Studies on the earth's crust using waves from explosions, *Proc. Am. Phil. Soc., 97,* 658–669, 1953.

Tatel, H. E., and M. A. Tuve, Seismic exploration of a continental crust, *Geol. Soc. Am. Spec. Paper 62,* 35–50, 1955.

Tuve, M. A., R. W. Goranson, J. W. Greig, W. J. Rooney, J. B. Doak, and J. L. England, Studies of deep crustal layers by explosive shots; *Trans. Am. Geophys. Union, 29,* 772, 1948.

Tuve, M. A., H. E. Tatel, and P. J. Hart, Crustal structure from seismic exploration, *J. Geophys. Research, 59,* 415–422, 1954.

Visher, S. S., *Climatic Atlas of the United States,* Harvard University Press, 1954.

Ward, R., and C. F. Brooks, *Handbuch der Klimatologie, The Climate of North America,* Borntraeger, Berlin, 1936.

Willmore, P. L., Seimic experiments on the north German explosions 1946–1947, *Phil. Trans. Roy. Soc. London A, 242,* 123–151, 1950.

Willmore, P. L., A. L. Hales, and P. G. Gane, A seismic investigation of crustal structure in the western Transvaal, *Bull. Seism. Soc. Am., 42,* 53–80, 1952.

(Received March 9, 1961; revised May 15, 1961.)

Corrigendum

Marshall H. Cohen and Martin L. Dwarkin wish to point out an error in their article, 'Perpendicular Intersections with a Dipole Field,' which appeared in the February 1961 issue of the Journal. The labels on Figures 6 a should read 'Radians per sphere radius,' in of 'Degrees per sphere radius.'

AMERICAN GEOPHYSICAL UNION

UNSELFISH COOPERATION IN RESEARCH

AMERICAN GEOPHYSICAL UNION

1515 Massachusetts Avenue, N.W., Washington 5, D. C.

Established by the National Research Council in 1919 for the development of the science of geophysics through scientific publication and the advancement of professional ideals.

QUALIFICATIONS FOR MEMBERSHIP

Membership of the AGU shall consist of Members, Associate Members, Student Members, oration Members, and Supporting Members.

Those eligible as candidates for election to the grade of MEMBER shall be:

MEMBER (a) Persons who have made an active contribution to geophysical research through observation, publication, teaching, or administration. Definite evidence should be presented to the Membership Committee. "Publication" may include books, articles, unpublished manuscripts, inventions, or development of geophysical instruments.

(b) Persons who have made active practical application of geophysical research. It should be shown that the nominee's work has not been purely routine, but that it has tended to create new knowledge of, or to broaden or strengthen the application of, geophysical research. In general, the minimum qualifications for membership will be not less than three years of professional experience in some phase of geophysics.

(Continued on next page)

Cut along this line

APPLICATION FOR MEMBERSHIP

e refer to qualifications on reverse side and designate below type of membership desired:

Member ($10) ☐ Associate ($10) ☐ Student ($4.50) ☐ (1961)

ication forms for Corporation and Supporting Membership are available upon request.

Surname *First Name* *Middle Name*

Preferred mailing address for publications

Permanent address

Place *Month* *Day* *Year of Birth* 4. *Country of citizenship/naturalization*

Nature of work and title and/or military rank; name and address of organization with which you are associated.

Check section or sections with which affiliation is desired.

- ☐ Geodesy
- ☐ Seismology
- ☐ Meteorology
- ☐ Geomagnetism and Aeronomy
- ☐ Oceanography
- ☐ Volcanology, Geochemistry, and Petrology
- ☐ Hydrology
- ☐ Tectonophysics

EXPERIENCE (List below, use added sheets as necessary)

Dates: From To Name and address of organization Title, duties, nature of work

EDUCATION (List Below, use added sheets as necessary)

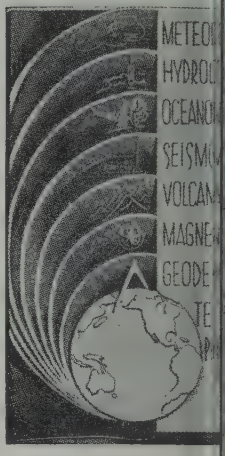
Dates: From To School Address Major Subject Degree, if any; year

(over)

(*Continued from previous page*)

Those eligible as candidates for election to the grade of ASSOCIATE MEMBER be:

ASSOCIATE MEMBER Persons who have an active interest in physical processes of the Earth or tech assistance in the application of geophysics. In general, the minimum qualificatio associate membership will be acceptable training or experience in some field of geophysics or allied science.



CORPORATION AND SUPPORTING MEMBER Corporations and other interested organizations shall be eligible as candidates for election to CORPORATION or SUPPORTING MEMBERSHIP. They shall have the privilege of designating a representative who has the rights and privileges of Members (use special form).

STUDENT MEMBER Those eligible as candidates for election to the grade of STUDENT MEMBER shall be persons who are graduate or undergraduate students in residence at least half-time and who are specializing in the geophysical sciences. Teaching or research assistants enrolled in more than half of a full-time academic program may also be eligible for Student Membership. Student Members shall have all the privileges of Members except that they shall not vote or hold office.

Cut along this line

*9. References: Please list below names and addresses of two or three references; include me of the AGU or others who know you well.

*10. Titles of technical contributions or publications, particularly those in the geophysical science where published.

*11. Brief statement of any special interests or qualifications in the geophysical sciences.

Date_____ _____

Written Signature

12. (STUDENT MEMBERS ONLY) The person whose signature appears above is known t

and is a student majoring in _____ (subject) at _____

(Name of college or university) expected to graduate in_____(year) with the degree of____

☐ He is a full-time student, or ☐ a teaching or research assistant enrolled in more than ha full-time academic program.

_____ ☐ Check here if faculty sponsor is a member o

(*Signature of faculty sponsor*) and willing to act as a regular sponsor for as membership as well.

_____ _____

(*Typed or printed name of sponsor*) (*Title*)

* Applicants for student membership may omit Questions 9, 10, and 11, but must fill in Quest

Please return form with check or money order payable to American Geophysical Union, 1515 chusetts Ave., N.W., Washington 5, D. C.

AMERICAN GEOPHYSICAL UNION

UNSELFISH COOPERATION IN RESEARCH

CORPORATION AND SUPPORTING MEMBERSHIPS

The American Geophysical Union is a non-profit scientific organization established by National Research Council. Its Council is the United States National Committee of International Union of Geodesy and Geophysics; official adherence by the United es is through the National Academy of Sciences-National Research Council.

acts from the Statutes:

Article 3. Membership—The membership of the American Geophysical Union shall s follows:

(e) *Corporation Members*—Corporations and other organizations interested in geophysics elected by the Council of the Union. The designated representative of each such organization shall enjoy the privileges of a Member.

(g) *Supporting Members*—Corporations, other organizations, and individuals interested in geophysics and desirous of supporting the Union may become members under the following classifications upon election by the Council.

(Continued on next page)

Cut along this line

American Geophysical Union

PROPOSAL FOR _____ MEMBERSHIP

he Council, American Geophysical Union
1515 Massachusetts Avenue, N.W., Washington 5, D. C.

lemen:

As an indication of our interest in the aims and activities of the American Geophysi-Jnion, and to assist in maintaining and extending its program of publication and work in the development of the geophysical sciences, the undersigned applies for _____ Membership in the AGU and, until further notice, agrees to pay al dues at the rate established for this classification of membership, in accordance the information set forth above and on the following page.

pany or Organization _____

_____ Title _____

(Signature)

(over)

(*Continued from previous page*)

of the Union . . .: Contributing Members, . . . Sustaining Members, . . . B factors. . . . Each Supporting Member and the designated representative shall enjoy the privileges of a Member.

Corporation Members shall pay dues of not less than $100 for each calendar y Dues for Supporting Members shall be as follows:

Contributing Members	$500
Sustaining Members	$1000
Benefactors	$5000

Lists of Corporation Members and Supporting Members will be published in issue of the *Transactions*, and will be included in the Membership Directory as dis units.

By Laws provide that one copy of each issue of the *Transactions*, *Journal of Geop cal Research*, any published *List of Members and Officers*, and any other publication w may be approved for free distribution to the membership shall be sent to each Corpora and Supporting Member. Each organization in good standing may purchase any avai publication of the Union at the established member discount.

AMERICAN GEOPHYSICAL UNION
1515 Massachusetts Ave., N.W.
Washington 5, D. C.

Cut along this line

Address _____

City _____ State _____

General fields of activity _____

The following person is designated as our representative in this membership _____

_____ Title _____

Number of units of membership desired (this will be taken as one unless otherwi dicated) _____

Place _____

Date _____

Contents

(*Continued from back cover*)

PAGE

me Experiments in Dispersion.....*Jacob Bear* 2455

-Place Measurement of Permeability in Heterogeneous Media. 2. Experimental and Computational Considerations.....*R. William Nelson* 2469

timation of Electrical Conductivity from Chemical Analyses of Natural Waters *John Logan* 2479

astic Wave Interferometry—A New Tool.....*I. Tolstoy* 2485

rface Heat Flow from a Differentiated Earth.....*Gordon J. F. MacDonald* 2489

ravity Measurements over the Southern Rocky Mountain Trench Area of British Columbia.....*G. D. Garland, E. R. Kanasewich, and Thomas L. Thompson* 2495

e and Mass Distribution of Cosmic Dust.....*Taivo Laevastu and Otto Mellis* 2507

stracts of the Papers Presented at the Forty-Second Annual Meeting, American Geophysical Union, Washington, D. C., April 18–21, 1961..... 2509

omagnetic and Solar Data.....*J. Virginia Lincoln* 2573

tters to the Editor:

Ionospheric Reflections below 50 Kilometers during Polar-Cap Absorption Events.....*J. B. Gregory* 2575

Electron Densities in the Outer Ionosphere Deduced from Nose Whistlers *R. L. Smith* 2578

Some Comments on Obtaining Electron Densities in the Exosphere Using Nose Whistlers.....*Joseph H. Pope* 2580

Extension of Nose Whistler Analysis.....*R. L. Smith and D. L. Carpenter* 2582

Atmospheric Ion Composition Measured above Wallops Island, Virginia *H. A. Taylor, Jr., and H. C. Brinton* 2587

Comment on Paper by Henry G. Booker, 'A Local Reduction of *F*-Region Ionization Due to Missile Transit'.....*Cecil Barnes, Jr.* 2589

All-Sky Meteor Rates in the Southern Hemisphere..*C. Ellyett and C. S. L. Keay* 2590

Remarks on the Article by A. R. Hibbs, 'The Distribution of Micrometeorites near the Earth'.....*Maurice Dubin* 2592

Author's Reply to the Preceding Discussion on the Article, 'The Distribution of Micrometeorites near the Earth'.....*A. R. Hibbs* 2595

Discussion on 'The Origin of Microseisms'.....*J. N. Nanda* 2597

Discussion of Paper by W. Barclay Kamb, 'The Thermodynamic Theory of Nonhydrostatically Stressed Solids'.....*G. J. F. MacDonald* 2599

Discussion of Paper by W. Barclay Kamb, 'The Thermodynamic Theory of Nonhydrostatically Stressed Solids'.....*Abraham Hoffer* 2600

Factors Influencing Thickness of the Earth's Crust *B. F. Howell, Jr., and R. A. Woodtli* 2601

rrigendum.....*Marshall H. Cohen and Martin L. Dwarkin* 2606

(Journal of Geophysical Research, Vol. 66, No. 8, August 1961)

Contents

PA

Intensity Variations in Outer Van Allen Radiation Belt
S. E. Forbush, D. Venkatesan, and C. E. McIlwain 2

Some Effects of Diamagnetic Ring Currents on Van Allen Radiation
A. J. Dessler and Robert Karplus 2

Energy Spectrum and Angular Distributions of Electrons Trapped in the Geomagnetic Field.....*J. B. Cladis, L. F. Chase, Jr., W. L. Imhof, and D. J. Knecht* 2

The Observed Outer-Belt Electron Distribution and the Neutron Decay Hypothesis
W. N. Hess, J. Killeen, C. Y. Fan, P. Meyer, and J. A. Simpson 2

Three-Frequency Measurements of Auroral Absorption
Syed Ziauddin and P. A. Forsyth 2

The Analysis of Transient Modes of Propagation across the Auroral Zone
B. J. Fulton and L. E. Petrie 2

Effects of Corpuscular Emissions on the Polar Ionosphere Following Solar Flares
G. E. Hill 2

The Latitude Dependence of Radar Meteor Shower Observations
C. S. L. Keay and C. Ellyett 2

Theory of Electrostatic Fields in the Ionosphere at Equatorial Latitudes
John R. Spreiter and Benjamin R. Briggs 2

Measurement of Ionospheric Drift by Radio-Star Observations.....*Braulio Dueño* 2

Preliminary Data on Solar Extreme Ultraviolet Radiation in the Upper Atmosphere
H. E. Hinteregger 2

Frictional Effects and the Meridional Circulation in the Mesosphere
Bernhard Haurwitz 2

Adjustable Potential-Gradient-Measuring Apparatus for Airplane Use
B. Vonnegut, C. B. Moore, and F. J. Mallahan 2

The Diurnal Variation of *K* Indices of Geomagnetic Activity on Disturbed Days in 1940–1948.....*Seth B. Nicholson and Oliver R. Wulf* 2

On the Relation between the Spectrum of Turbulence and the Diabatic Wind Profile
J. A. Businger 2

Some Evidence on the Effect of Nonlinearity on the Position of the Equilibrium Range in Wind-Wave Spectra.....*Blair Kinsman* 2

Net Precipitation in a Northern Hardwood Forest.....*Raymond E. Leonard* 2

Projecting the Effect of Changed Stream Stages on the Water Table
J. E. Reed and M. S. Bedinger 2

Fluctuations of Ground-Water Levels Caused by Dispersion of Salts..*F. A. Kohout* 2

Ground-Water Investigations in a Saline Area of the Red River Valley, North Dakota
Leo C. Benz, Rome H. Mickelson, Fred M. Sandoval, and Carl W. Carlson 2

Some Implications of the Highly Saline Water off the Southwest Coast of Florida
Frank Chew 2

(*Continued inside back cover*)